Characterisation of Dendritic Cells in the Intestine

Charlotte Louise Scott

BSc., MRes.

A thesis submitted to the College of Veterinary, Medical and Life Sciences, University of Glasgow in fulfilment of the requirements for the degree of Doctor of Philosophy.

January 2014

Institute of Infection, Immunity and Inflammation
University of Glasgow
120 University Place
Glasgow, G12 8TA

Acknowledgments

Firstly, I would like to thank my supervisor, Allan Mowat for all his help, support and guidance throughout the last 3 years. Coming from a non-immunological background, I could not of done this without your help! Thanks for all the time you have devoted to reading and correcting this thesis and our manuscript. Also, for all of the non-scientific support you gave me, which I know is not part of the job description! Who knew when you took me on you would also end up taking on half of my family's zoo when they decided to emigrate to Australia last year!

I would also like to thank past and present members of 'Team Mowat'. First of all to Aude, who spent a lot of time optimising the protocols for isolating DCs from the small intestine and who has given me invaluable advice throughout my PhD. I also need to say a massive thank you to Calum who has been up at ridiculous hours of the morning (and evening!) to help with experiments, for reading this thesis and especially for all the banter over the last few years. I doubt I will find another team member like you, where together we have the ability to strike fear into the boss every time he had to ask "what are you two up to now?!". Also, a big thanks to Alberto and Tamsin for all their help in the lab and for making it so easy to come to work everyday!

To all the Millings, Simon, Vuk, Lotta, Pamela and Steph, thank you for making my time as a Mowling so enjoyable. You always made sure the office was a productive place to work and were careful to ensure my baking efforts never went to waste! A special thanks to Vuk and Steph for doing the cannulation and POI surgeries for me and to Pamela who spent a considerable proportion of time examining DC subsets in the human gut for CCR2.

I must also thank everyone on the 4th floor of the GBRC, there are too many of you to name, but you all made the lab such a fun place to work. A big thank you also goes to all the staff at the CRF, JRF and VRF and to Diane Vaughan. I would also like to thank all those who provided mice, advice and technical expertise for this project including Bill Agace, Simon Milling, Gill Douce, Andy Roe, Per-Arne Oldenborg, Takashi Matozaki, Rob Nibbs, Paul Garside, Fiona Powrie, Bernard

Malissen, Sandrine Henri, Toby Lawrence, Marc Dalod, Barry McColl, Bart Lambrecht and Martin Guilliams. I also need to thank Martin for giving me a post-doc job!

I would also like to thank the Wellcome Trust for funding my masters and PhD in Glasgow and Darren and Olwyn for all their support and advice over the last few years. I am also very grateful to the BSI who provided generous travel awards during my PhD.

Finally, the soppy bit! I probably should have written this before moving to Belgium as right now I am more of an emotional wreck than ever, so I have the tissues to hand writing this! I would like to thank my family and friends for all their support and encouragement during my PhD. Despite leaving me in the middle of it all to move to the other side of the world, I really appreciate the on-going support of my family, I know you think 8 years of university might have been a bit excessive but hopefully you will agree it was worthwhile! I am delighted that you are all so happy in Oz and will be over to visit you soon! I know it's a bit weird, but I should also thank Riddler, without whom I would have gone mad a long time ago! Thanks also to Janice, Laura and Eilidh for looking after my boy for me while I get settled in Belgium, I know he is in great hands! To all my friends back in Ireland, especially Ceara, Niamh and Brighid, thank you for always being there for me, I miss you all a lot and hope that you will still visit me even though I have not yet moved back to Ireland as was the deal four years ago when I left!

Last but not least to the Glasgow crew, I know I have already mentioned some of them above but you have made the last four years so enjoyable. David, thanks for being a great housemate, I have no doubt you will go on to be very successful, so don't forget me when you are a multi-millionaire and I am (hopefully) still in the lab! Vuk, thanks for all your advice and our random chats when walking back to Hyndland after the nights in the pub! Alberto, thanks for all your help and for sharing the pain of deciphering Allan's handwriting (sorry Allan!) during the last few months! Best of luck with everything in the future and remember to keep in touch. Tamsin, thank you for being a good laugh this last year and for rehoming Mac! I know the SIRP project is in good hands, and remember if you need anything you know where I am! Lotta and Steph, thanks for

the great nights out. Steph, I will never forget your face that night we HAD to leave Buff (after that unfortunate split!) and one day Lotta, we will be in a photo together where we both have our eyes open! Best of luck to you and Filippo, can't wait to see you get married next year! Calum and Michelle, thanks for all the laughs, the windows (Michelle) and for introducing me to the delta! Kate and Pamela, thank you for, well everything actually! You are both amazing and I couldn't have done this PhD without either of you. I can't believe I won't be seeing you everyday anymore, but I have no doubt that we will remain best friends for years to come. Ok that's it, no more tears! Just make sure you all keep in touch and come and visit me regularly, if not for me, just think of the beer and chocolates! Love you all xx

Table of Contents

List of Tables and Figures

Author's Declaration:

I declare that all the experimental data contained in this thesis are the result of my own work, with the exception of the human intestine data, which was generated in collaboration with Pamela Wright and as such has also been submitted as part of her PhD thesis at the University of Glasgow, the MLNx, cannulation and POI experiments which were performed in collaboration with Dr. Vuk Cerovic and Stephanie Houston, the parabiosis studies which were performed in collaboration with Dr. Sandrine Henri and Dr. Bernard Malissen at the CIML, Marseille and the WT:CCR2$^{-/-}$ bone marrow chimeras which were generated in collaboration with Dr. Calum Bain. With the exception of the human intestine data, no part of this thesis has been previously submitted for any other degree at the University of Glasgow or any other institution.

Signature……..

Printed name……

List of Publications

Scott, C.L.*, Aumeunier, A.M.*, and Mowat, A.M. (2011). Intestinal CD103+ dendritic cells:master regulators of tolerance? Trends Immunol. 32, 412-419.

Cerovic, V., Houston, S.A., **Scott, C.L.,** Aumeunier, A., Yrlid, U., Mowat, A.M., and Milling, S.W.F. (2013). Intestinal Cd103(-) dendritic cells migrate in lymph and prime effector T cells. Mucosal Immunol. 6(1), 104-113.

Bain, C.C., **Scott, C.L.,** Uronen-Hansson, H., Gudjonsson, S., Jansson, O., Grip, O., Guilliams, M., Malissen, B., Agace, W.W., and Mowat, A.M. (2013). Resident and pro-inflammatory macrophages in the colon represent alternative context-dependent fates of the same Ly6C(hi) monocyte precursors. Mucosal Immunol. 6(3), 498-510.

Persson, E.K.*, **Scott, C.L.*,** Mowat, A.M., Agace, W.W. (2013). Dendritic cell subsets in the intestinal lamina propria: ontogeny and function. Eur. J. Immunol. 43(12), 3098-3107.

Martin, J.C., Riou, G.B.E., Heslan, M., Chauvin, C., Utriainen, L., Aumeunier, A., **Scott, C.L.,** Mowat, A., Cerovic, V., Houston, S.A., et al. (2014). Interleukin-22 binding protein (IL-22BP) is constitutively expressed by a subset of conventional dendritic cells and is strongly induced by retinoic acid. Mucosal Immunol. 7(1), 101-113.

Scott, C.L., Bain, C.C., Wright, P.B., Beckham, K.S.H., Kotarsky, K., Guilliams, M., Lambrecht, B.N., Agace, W.W., Milling, S.W.F., and Mowat, A.M. (2014). CCR2-expressing CD103- intestinal dendritic cells develop from DC committed precursors and drive interleukin 17 production by T cells. Manuscript submitted.

* denotes co-authorship

List of Abbreviations

7-AAD	7-amino-actinomycin D
Abx	antibiotics
AF	alexa fluor
-APC	allophycocyanin
APC	antigen presenting cell
Avg	average
BatF	basic leucine zipper transcription factor, ATF-like
BLP	bacterial lipoprotein
BM	bone marrow
BrdU	bromodeoxyuridine
BV	brilliant violet
CD	cluster of differentiation
cDC	conventional dendritic cell
CLR	C-type lectin receptor
CDP	common dendritic cell progenitor
CFA	complete fruend's adjuvant
CFSE	caroboxyfluorescein succinimidyl ester
CFU	colony forming unit
CHS	contact hypersensitivity
CMP	common myeloid progenitor
CMF-HBSS	calcium/magnesium free Hank's buffered salt solution
CNS	central nervous system
CSF	colony stimulating factor
-Cy7	cyanine 7 dye
DC	dendritic cell
DEAB	diethylaminobenzaldehyde
DNA	deoxyribonucleic acid
DT	diphtheria toxin
DSS	dextran sulphate sodium
EAE	experimental autoimmune encephalitis
EDTA	ethylenediaminetetraacetic acid
FACS	fluorescence activated cell sorting
FCS	foetal calf serum
FITC	fluorescein isothiocyanate

flt3	*fms*-like tyrosine kinase 3
flt3L	*fms*-like tyrosine kinase 3 ligand
FoxP3	forkhead box P3
FSC	forward scatter
FTY720	fingolimod
GALT	gastrointestinal associated lymphoid tissue
GFP	green fluorescent protein
GM-CSF	granulocyte macrophage colony-stimulating factor
GMP	granulocyte/macrophage precursor
HAO	heat aggregated OVA
HBSS	Hank's buffered salt solution
HSC	haematopoietic stem cell
IBD	inflammatory bowel disease
ID	inhibitor of DNA binding
IDO	indoleamine-2,3-deoxygenase
IEL	intra-epithelial lymphocyte
IFN	interferon
Ig	immunoglobulin
IL	interleukin
ILC	innate lymphoid cell
ILF	isolated lymphoid follicle
i.p.	intraperitoneal
IRAK	IL1 receptor-associated kinase
IRF	interferon regulatory factor
i.v.	intravenous
KO	knock out
LHFP	left hind footpad
LP	lamina propria
LPS	lipopolysaccharide
LT	lymphotoxin
MAPK	mitogen-activated protein kinase
MDP	macrophage and dendritic cell precursor
Mϕ	macrophage
MFI	mean fluorescence intensity
MHC	major histocompatibility complex
MLN	mesenteric lymph node

MP	mononuclear phagocyte
MPS	mononuclear phagocyte system
Mt	mutant
MyD88	myeloid differentiation factor 88
NI	non-injected/non-infected
NK	natural killer
NLR	Nod-like receptor
NO	nitric oxide
NOD	nucleotide-binding oligomerisation domain
OVA	ovalbumin
PAMP	pathogen associated molecular pattern
PBS	phosphate buffered solution
PCR	polymerase chain reaction
pDC	plasmacytoid dendritic cell
PE	phycoerythrin
PG	prostaglandin
PFA	paraformaldehyde
PMA	phorbol 12-myristate 13-acetate
POI	post operative ileus
PP	Peyer's patches
PPAR	peroxisome proliferator-activated receptor
Pre-DC	DC-committed progenitor
PRR	pattern recognition receptor
RA	retinoic acid
RFP	red fluorescent protein
RHFP	right hind footpad
RPMI	Roswell Park Memorial Institute-1640 medium
RT-PCR	reverse transcriptase polymerase chain reaction
S1P	sphingosine-1-phosphate
SA	streptavidin
s.c.	subcutaneous
SD	standard deviation
SI LP	small intestine
SIRP	signal regulatory protein
SFB	segmented filamentous bacteria
SPF	specific pathogen free

SSC	side scatter
STAT	signal transducer and activator of transcription
TED	transepithelial dendrites
TGF	transforming growth factor
TRAF	TNF receptor activated factor
TREM	triggering receptor expressed by myeloid cells
T_h1	T helper 1
T_h2	T helper 2
T_h17	T helper 17
TLR	Toll-like receptor
TNF	tumour necrosis factor
TSLP	thymic stromal lymphopoietin
T_{Reg}	regulatory T cell
VEGF	vascular endothelial growth factor
VIP	vasoactive intestinal peptide
WT	wild type
Zbtb46	zinc finger and BTB containing 46

Summary

Due to the large surface area of the gut and its continual exposure to a wide variety of agents including dietary constituents, commensal bacteria and pathogens, the intestinal arm of the immune system has evolved to be the largest component of the immune system. It must be able to discriminate between harmless and harmful antigens, so that it can induce tolerance to harmless commensal, self or dietary antigens, but active immunity against pathogens. As the sentinels of the immune system, intestinal dendritic cells (DCs) are central to these processes, continually sampling antigen in the environment and migrating to the mesenteric lymph nodes (MLNs), where they present the antigen to naïve T cells and induce appropriate T cell responses. However the nature and functions of DCs in the intestine remains a topic of debate. Their characterisation has been hampered by the use of non-specific and overlapping markers which has led to intestinal DCs being confused with other cells of the mononuclear phagocyte system, especially macrophages (mϕs) which vastly outnumber DCs in the intestinal mucosa. While considerable progress has been made in recent years with the identification of CD103 and CX3CR1 as mutually exclusive markers of DCs and mϕs respectively, it has become assumed that $CD103^+$ DCs are intrinsically tolerogenic and thus it remains unclear how DCs contribute to active immunity in the intestine. Furthermore it is unknown whether CD103 is sufficient to define all intestinal DCs, or whether *bona fide* $CD103^-$ DCs may also exist. Thus a major aim of my project was to develop methods that allowed precise characterisation of the mononuclear phagocytes in the intestinal lamina propria (LP) and examine the functions of phenotypically defined subsets. As part of this, I also examined the contribution of the inhibitory signalling receptor, signal regulatory protein alpha (SIRPα) co-expressed by $CD11b^+$ DCs, in regulating intestinal DC function.

In Chapter 3, I set out to examine the phenotype of mononuclear phagocytes in the small intestine lamina propria (SI LP). Initially I confirmed previous studies that CD103 and CX3CR1 were mutually exclusive markers of DCs and mϕs respectively. This identified 2 populations of DCs separated on the basis of CD11b expression, together with two populations of mϕs distinguished by

their levels of CX3CR1. However, further experiments examining F4/80 expression in combination with the recently identified mϕ-specific marker CD64 showed that the CX3CR1^{int} CD103^{-} MPs were heterogeneous. Although the majority were F4/80^{+}CD64^{+}CD11b^{+} mϕs, I could also identify two additional populations that were F4/80^{-}CD64^{-} and could be separated on the basis of CD11b expression. I hypothesised these were DCs and this was supported by the fact that all 4 subsets of putative DCs could also be found amongst CD11c^{+}MHCII^{hi} migratory DCs in the MLNs and in pseudo-afferent intestinal lymph. All the subsets also expressed genes and markers of DCs but not mϕs and were dependent on Flt3L *in vivo*. Unlike CD64^{+} mϕs, the DC subsets had no ability to phagocytose *E. coli* particles. Four similar subsets were also identified in the colonic LP, however the proportions of the subsets in this location were distinct from those seen in the SI LP. While the CD103^{+}CD11b^{+} DCs were the main subset in the SI LP, in the colonic LP the CD103^{+}CD11b^{-} DCs dominated.

Having identified two novel populations of genuine CD103^{-} DCs in the intestinal LP, in Chapter 4 I went on to examine their origin. Previous reports had shown that CD103^{+} LP DCs were derived from DC-committed precursors (pre-DCs), whereas CD103^{-} MPs were reported to be of monocyte origin. However as I had shown the CD103^{-} MPs to include both DCs and mϕs, it was necessary to re-examine their origin using appropriate gating strategies. Adoptive transfer of pre-DCs from the BM into resting WT mice generated all subsets of DCs in the LP, including the two novel populations of CD103^{-} DCs I had identified. In contrast adoptive transfer of Ly6C^{hi} monocytes into monocytopenic CCR2$^{-/-}$ recipients generated mϕs exclusively. By comparing the small intestine, colon and spleen, I could show that the development of pre-DCs was determined by the tissue they entered, as the progeny took on the same subset profiles as seen in the endogenous DC populations. Thus the differentiation of pre-DCs appears to be driven by the local microenvironment. By tracking the appearance of donor-derived DCs over time, I could monitor their differentiation *in situ*. These studies and experiments using BrdU incorporation showed that all DC subsets turned over much more rapidly *in vivo* than mϕs and that a significant proportion were actively dividing *in situ*. No clear differences suggesting a precursor-product relationship between any of the DC subsets could be seen in these kinetic experiments. To

gain a better idea of how the DC subsets might develop, I also examined them in neonatal animals and examined the effects of administering broad-spectrum antibiotics. These studies demonstrated that the $CD103^+CD11b^+$ DCs were likely regulated by the presence of specific microbiota as they did not develop in the neonatal animals until day 7 after birth and were increased in proportion following administration of antibiotics.

In Chapter 5, I examined how the DC populations might behave during inflammation, using DSS colitis, post-operative ileus and infection with *Citrobacter rodentium* as models. DSS-colitis caused considerable inflammatory infiltrate and the number of DCs was increased, however there were no subset specific differences. Post-operative ileus also caused inflammation characterised by monocyte and neutrophil infiltration, but had few effects on the DC populations. Infection with *C. rodentium* resulted in a selective increase in the number of $CD103^-$ DCs in the colonic LP, suggesting these may be involved in modulating the T_h17 response which characterises the protective immune response in this infection. By transferring pre-DCs into colitic mice, I found that these still gave rise to all the DC subsets during inflammation.

In Chapter 6, I examined the functions of the phenotypically defined subsets of LP DCs by pulsing them with ovalbumin (OVA) protein *in vitro* and culturing them with OVA-specific $CD4^+$ or $CD8^+$ T cells. Consistent with their expression of $CD8\alpha$ and XCR1, I found the $CD103^+CD11b^-$ DCs to be the most efficient at cross-presenting antigen to naïve $CD8^+$ T cells and they were also the most efficient inducers of IFNγ-producing $CD4^+$ T cells. All populations of DCs could induce $FoxP3^+$ T_{Reg} cells, but consistent with their ability to produce retinoic acid as measured by the ALDEFLUOR assay, the $CD103^+$ DC subsets were most efficient at this. The $CD103^+CD11b^-$ subset also expressed the TGFβ-activating integrin $\alpha v\beta 8$. In contrast, induction of IL17a-producing $CD4^+$ T cells was a function of $CD103^+CD11b^+$ and $CD103^-CD11b^+$ DCs, with the latter being the most efficient.

In Chapters 7 and 8, I examined the role of the inhibitory molecule SIRPα in intestinal DC behaviour by examining the DC populations in SIRPα mutant (mt)

mice, which have a truncated cytoplasmic domain and hence cannot signal intracellularly. Despite being expressed by most myeloid cells including all $CD11b^+$ DC subsets and $CD64^+$ mϕs, SIRPα mt mice had a selective defect in the number of $CD103^+CD11b^+$ DCs in the LP and MLN. This correlated with a reduction in the number of T_h17 cells in the LP of steady state SIRPα mt mice and these mice showed reduced levels of T_h17 cell induction after antigen-specific immunisation and infection by *C. rodentium*. In parallel, SIRPα mt mice had impaired clearance of *C. rodentium* infection. T cells from SIRPα mt mice did not have an intrinsic defect in their ability to be polarised to the T_h17 phenotype and $CD103^+CD11b^+$ DCs from SIRPα mt LP were fully capable of priming T_h17 cells *in vitro*. They also produced normal amounts of the T_h17 inducing cytokines IL1β and IL6. As total DCs from SIRPα mt mice produced lower than normal levels of these cytokines, these findings suggest that the defective induction of T_h17 responses *in vivo* reflects the lower numbers of $CD103^+CD11b^+$ DC in these mice, rather than a defect in their function. However, preliminary studies investigating the role of $CD103^-CD11b^+$ DCs from these mice in the induction of T_h17 responses suggests that lack of SIRPα signalling in these cells may also contribute to the reduced T_h17 cell population observed in the LP.

Having identified these defects in Chapter 7, in Chapter 8 I went on to examine how the SIRPα mutation might be affecting the homeostasis of $CD103^+CD11b^+$ DCs. By competitively transferring pre-DCs from WT and SIRPα mt mice into WT recipients, I found that the SIRPα mt precursors generated $CD103^+CD11b^+$ DCs in the LP more rapidly than WT pre-DCs. Although this seemed to be at odds with the reduced numbers of these DCs in the SIRPα mt intestine, further work revealed that the $CD103^+CD11b^+$ DCs from SIRPα mt LP expressed higher basal levels of CD86 than their WT counterparts, while Annexin V staining suggested that these DCs were apoptosing more rapidly in SIRPα mt MLN. As these results suggested that the lack of $CD103^+CD11b^+$ DCs in SIRPα mt mice might reflect increased activation and susceptibility to death because of the absence of SIRPα's inhibitory signal, I examined whether this would also lead to more efficient migration into afferent lymph. However there were no differences in the proportions of $CD103^+CD11b^+$ DCs found in pseudo-afferent intestinal lymph from SIRPα mt and WT mice. Thus more rapid departure into lymph may be

sufficiently marked to counterbalance the decreased population in the mucosa. Further experiments are clearly needed to test the hypothesis that lack of SIRPα mediated inhibitory signalling allows hyperactivation of CD103$^+$CD11b$^+$ DCs and subsequent poor survival, as well as to determine why it is restricted to this subset.

Finally in Chapter 9, I examined the role of CCR2 in intestinal DC behaviour, aiming to follow up a recent report which had suggested that CD103$^-$ Zbtb46-expressing DCs in the LP were monocyte-derived based on their depletion following administration of an anti-CCR2 antibody. I found CCR2$^{-/-}$ mice had a selective reduction in the number of CD103$^-$CD11b$^+$ DCs in the LP and amongst migratory DCs in MLN, as well as amongst CD11b$^+$ DCs in the spleen. Competitive WT:CCR2$^{-/-}$ BM chimeras experiments demonstrated that the requirement for CCR2 in DC development was cell intrinsic. Although antibody staining, fluorescent CCL2-uptake and RFP expression in CCR2$^{+/RFP}$ mice revealed different levels of CCR2 expression, each method showed there was a proportion of CD103$^-$CD11b$^+$ DCs expressing CCR2. The CCR2$^+$ subset of CD103$^-$CD11b$^+$ DCs in LP expressed similar levels of the DC markers Zbtb46, CCR7 and Flt3 to the other *bona fide* intestinal DCs and were generated by adoptive transfer of pre-DCs, a proportion of which also expressed CCR2. A similar pattern of expression was found on CD103$^-$SIRPα^+ DCs isolated from the human colonic LP. The CCR2$^+$CD103$^-$CD11b$^+$ DCs were the most efficient inducers of T_h17 responses by naïve CD4$^+$ T cells *in vitro* and CCR2$^{-/-}$ mice had reduced generation of T_h17 responses after antigen specific immunisation and *C. rodentium* infection *in vivo.* This enhanced ability of CCR2$^+$CD103$^-$CD11b$^+$ DCs to induce T_h17 responses correlated with higher constitutive and LPS induced expression of IL12/IL23p40, which was presumed to be IL23. Together these findings reveal an entirely novel population of CCR2$^+$ and CCR2-dependent, genuine DCs which have a selective ability to drive T_h17 responses.

Taken together, the data in this thesis represent an important step forward in our understanding of intestinal dendritic cells. By developing rigorous gating strategies, I have been able to distinguish accurately between the various populations of intestinal mononuclear phagocytes and have identified two novel populations of CD103$^-$ conventional DCs that are derived from DC committed precursors rather than monocytes as previously assumed. Furthermore, by

showing there is a population of *bona fide* intestinal DC which expresses CCR2 and is dependent on this receptor *in vivo*, my project may help explain why previous studies have concluded that intestinal DCs may be derived from $Ly6C^{hi}CCR2^{+}$ monocytes. Importantly, the phenotypic subsets I identified appear to have functional consequences, although my work on SIRPα mt mice and on CCR2 expression have generated somewhat contradictory results on exactly how the different subsets of $CD11b^{+}$ DCs contribute to T_h17 polarisation. One explanation for this may be that these subsets are related members of a linear differentiation pathway, in which $CD103^{-}CD11b^{+}$ DCs precede the development of the $CD103^{+}CD11b^{+}$ subset. Further work on the nature of the precursors of these subsets at the single cell level will be required to shed light on this possibility, while it will also be important to investigate the nature of the local factors which determine the unique differentiation pathways of intestinal DCs.

Chapter 1 General Introduction

1.1 Introduction

The innate and adaptive arms of the immune system have evolved complex and distinct mechanisms to ensure that harmful agents are eradicated from the body, while preventing excessive damage and chronic inflammation in host tissues. The innate immune system provides a rapid non-specific response to pathogens and tissue damage, whereas the adaptive immune system responds in a delayed antigen-specific manner resulting in the generation of immunological memory that allows rapid and specific responses to be initiated upon re-exposure to the same harmful agents. Although the immune system must act to eliminate pathogens, it must also prevent unnecessary responses to both self and innocuous foreign antigens, such as dietary constituents, commensal and mutualistic bacteria. This crucial balance between immunity and tolerance is most apparent in the intestine, which encounters more foreign antigen than any other part of the immune system. The intestine represents one of the main routes of entry for pathogens, while also being home to an extensive and complex microbiota and being exposed continuously to an array of harmless dietary antigens. Dendritic cells (DCs) in the intestine are critical in this process, sampling the intestinal environment and subsequently migrating to the mesenteric lymph nodes (MLN) where they present antigen to naïve T cells. These T cells then proliferate and differentiate into gut homing effector or regulatory T cells allowing for active immunity or tolerance to be induced as required.

1.2 Dendritic Cells

Dendritic cells are myeloid cells named after their characteristic morphology, consisting of numerous long and dynamic finger-like cytoplasmic processes resembling the dendrites of nerve cells. They were first described by Ralph Steinman and Zanvil Cohn in 1973 (Steinman, 1973) and act as specialised sentinel cells that survey tissues, sampling the environment by ingesting large amounts of the extracellular fluid and its components through a process known as macropinocytosis. Like other innate immune cells such as macrophages and neutrophils, DCs can degrade any pathogens they engulf, but in contrast to these cells, the main role of DCs is not pathogen clearance, but rather to activate naïve T lymphocytes in the draining lymph nodes (LNs). By doing so, DCs form the

crucial link between the innate and adaptive arms of the immune system, with their importance recognised in 2011, when the late Ralph Steinman was awarded the Nobel Prize for their discovery. After sampling material from the environment, DCs process proteins into small peptides, which they then display on their cell surface in combination with major histocompatibility complex molecules (MHC) and migrate to the T cell zones of the lymph nodes (LNs). There they present the antigenic peptides to naïve T lymphocytes, inducing their proliferation and polarisation into antigen specific effector or regulatory T cells. The activated T lymphocytes subsequently home to the tissue of the DC origin and orchestrate the immune response through their production of a collection of immunomodulatory cytokines such as IL17, IFNγ, IL4, IL5, IL10 and others (Banchereau and Steinman, 1998).

1.2.1 Identifying Dendritic Cells

Given their role as linkers of the innate and adaptive immune systems, considerable research has gone into the accurate identification and characterisation of DCs. This is especially important given the significant phenotypic overlap between DCs and other mononuclear phagocytes such as macrophages (mϕs), which is described in detail below. DCs can be classified into two distinct groups, classical or conventional DCs (referred to here as DCs) as described originally by Ralph Steinman and Zanvil Cohn (Steinman, 1973; Steinman and Cohn, 1974; Steinman et al., 1974) and plasmacytoid DCs (pDCs), first identified by Lennert and Remmele (Lennert and Remmele, 1958), although these were not referred to as pDCs until later (Facchetti et al., 2003). Classical DCs of various subtypes in the intestine are the focus of this thesis.

In addition to their characteristic morphology, DCs, like other bone marrow (BM) derived leukocytes, express the haematopoietic marker CD45, while lacking expression of T and B cell, granulocyte, NK cell and erythrocyte lineage markers (Merad et al., 2013). Surface expression of the integrin CD11c and major histocompatibility complex class II molecules (MHCII) (Shortman and Liu, 2002) have been used extensively to identify DCs. However, despite its continued use to identify DCs, the discovery of the CD11c antigen (Metlay et al., 1990) has only served to complicate the specific identification of these cells. Although antibodies

raised against this molecule bound splenic DCs with high affinity, it was also found to bind peritoneal macrophages and T cells (Metlay et al., 1990; Rogler et al., 1998) (and reviewed in (Hume, 2008)). Despite this, CD11c still became the definitive 'DC' marker and the CD11c-DTR mice (Jung et al., 2002) and CD11c-cre mice (Caton et al., 2007) became popular tools for examining the *in vivo* role of DCs. Unfortunately, in reality, these tools only enable the examination of the role of CD11c-expressing cells and thus these tools have led to a number of functions being attributed incorrectly to DCs. Although DCs can be identified by their expression of CD11c and MHCII in lymphoid tissues, it is now clear that these markers alone are not sufficient for DC identification in most non-lymphoid tissues, as some mϕs, such as those in the intestine (P Pavli, 1990) and liver (Kupffer cells) (You et al., 2008) also express these molecules. Furthermore, alveolar mϕs in the lung (Plantinga et al., 2013), as well as plasma cells and T cells can also express CD11c (Caton et al., 2007; Postigo et al., 1991). The complexity involved in identifying *bona fide* DCs is further seen when Langerhans cells in the skin are considered. These cells express CD11c and MHCII and so are commonly referred to as DCs, but these also express the macrophage marker F4/80 and appear to derive independently from DC-committed precursors (discussed in detail below) (Ghigo et al., 2013; Ginhoux et al., 2006; Hoeffel et al., 2012).

Based on these findings, it has become clear that surface phenotyping alone may not be sufficient for the accurate identification of DCs and instead a combination of phenotypical and functional analysis is required to discriminate them from mϕs. While I was carrying out my work, a major advance came from the identification of a novel zinc finger transcription factor *Zbtb46* (herein referred to as zDC), whose expression is restricted to cells of the DC lineage within the immune system. Although also expressed by endothelial cells and erythroid progenitors, zDC is absent from mϕs, pDCs and all other $CD45^+$ cells (Meredith et al., 2012a; Satpathy et al., 2012). Thus zDC expression seems to provide a unique way for researchers to identify DCs accurately and with the generation of mice with cre recombinase or the human diphtheria toxin receptor (DTR) under the control of the zDC promoter, this will become the conventional way to assess the biology of *bona fide* DCs without contamination by other mononuclear phagocytes (MPs) such as mϕs. The accurate identification of DCs has also been aided by recent

studies in which the transcriptomes of DCs and mϕs in many different tissues have been compared, resulting in the identification of a provisional molecular signature for DCs (Gautier et al., 2012; Miller et al., 2012). In addition to zDC, these studies identified CD26 and CD272 as DC-specific markers (Miller et al., 2012), while CD64, CD14 and MerTK have been identified as monocyte/mϕ-specific markers (Bain et al., 2013; Gautier et al., 2012; Tamoutounour et al., 2012). Given the difficulties associated with the specific identification of DCs and the continued confusion surrounding what constitutes a DC in the intestine (discussed below), accurately identifying DC populations from mϕs in the intestine was a specific aim of this thesis.

While having a similar origin to classical DCs (discussed in detail below) pDCs lack the characteristic DC morphology and indeed as their name suggests, these rather resemble plasma cells. pDCs can be discriminated from classical DCs by their expression of a number of surface markers such as B220, Ly6C, CCR9 and Siglec-H. Furthermore, pDCs also express lower levels of CD11c and MHCII than classical DCs (Nakano et al., 2001). The principal function of pDCs is to produce large quantities of type 1 interferon (IFN)-α in response to viral infection. However, their ability to present viral antigens to naïve T cells and subsequently induce their proliferation remains controversial (Colonna et al., 2004).

1.2.2 Classical Dendritic Cell Function

1.2.2.1 Antigen Acquisition by DCs

Given the complications associated with identifying DCs on the basis of their surface phenotype, identification of DCs on the basis of their function has become crucial. In order to fulfil their function as antigen presenting cells, DCs must first acquire antigen from the tissue. When they first enter the tissues from the bloodstream, DCs are classified as immature and have a high ability to acquire material from their environment mainly by endocytosis and fluid phase macropinocytosis, with little or no phagocytic ability (Sallusto et al., 1995). Immature DCs are estimated to take up approximately 96 times their own volume each day and this material is delivered into the intracellular compartments of the endocytic pathway (Norbury, 2006; Sallusto et al., 1995). As immature DCs are

also constantly recycling MHCII molecules through this pathway, any antigenic peptides generated through the degradation of endocytosed material can be loaded onto these MHCII molecules, with the potential to be transported to the cell surface for presentation to naïve T lymphocytes (Pinet et al., 1995).

Table 1.1: Mammalian Pattern Recognition Receptors

Protein/domain family	PRR	Ligands
C-type Lectin	DC-SIGN	Mannose Oligosaccharides
	Dectin-1	b-glucans from fungi
	Mannose receptor	Terminal mannose residues
TLRs	TLRs	Lipopeptides, LPS, Flagellin, dsDNA, ssRNA, rRNA, CpG DNA, uropathogenic bacteria*
Caspase Recruiting Domain (CARD) Helicases	RIG1	dsRNA, Viral RNA
	MDA-5	Poly(I:C)
NODs	NOD1	Intestinal epithelial g-D-glutamyl-meso-diaminopimelic acid (DAP)
	NOD2	Muramyl dipeptide (MDP)
Scavenger Receptors	SRA	Modified low density lipoprotein (LDL), apoptotic cells
	MARCO	Modified LDL, gram+ and gram- bacteria

NOD, nucleotide-binding oligomerisation domain; SRA, scavenger receptor A; MARCO, macrophage receptor with collagenous structure; *Refer to Figure 1.1.

In the steady state, the generation of stable peptide-MHCII complexes by immature DCs is inefficient and these cells are thus thought to play a role in tolerance to self and innocuous antigen (Steinman et al., 2003). However, in the presence of pathogenic infection or tissue damage, DCs recognise conserved structures on microbes or damaged cells via a plethora of pattern recognition receptors (PRRs), such as Toll-like receptors (TLRs), lectins and Fc receptors (Table 1.1). The most extensively studied of these PRRs is the TLR family of receptors, which recognise microbial products. TLRs were first identified in *Drosophila* (Hashimoto et al., 1988) and to date ten human and thirteen murine TLRs have been identified (Kawai and Akira, 2009), each recognising distinct non-self microbial patterns (PAMPs; pathogen associated molecular patterns) found outside or inside the cell (Fig. 1.1) (Medzhitov, 2001; O'Neill et al., 2013).

Triggering of PRR on immature DCs causes them to become activated and mature, resulting in the stabilisation of peptide-MHCII complexes on the cell surface due to reduced MHCII recycling (Cella et al., 1997; Sallusto et al., 1995).

At the same time, the DCs become less able to sample the surrounding environment by endocytosis and upregulate their expression of co-stimulatory molecules, such as CD80 (Larsen et al., 1992) and CD86 (Lenschow et al., 1993), which are ligands for CD28 expressed by T cells. Additionally, activated DCs increase their locomotive activity and upregulate their expression of the chemokine receptor CCR7 (Dieu et al., 1998; Sallusto et al., 1998; Sozzani et al., 1998; Yanagihara et al., 1998), allowing them to enter afferent lymphatics and migrate to the draining LNs along a CCL19/CCL21 chemokine gradient (Forster et al., 1999; MartIn-Fontecha et al., 2003; Ohl et al., 2004).

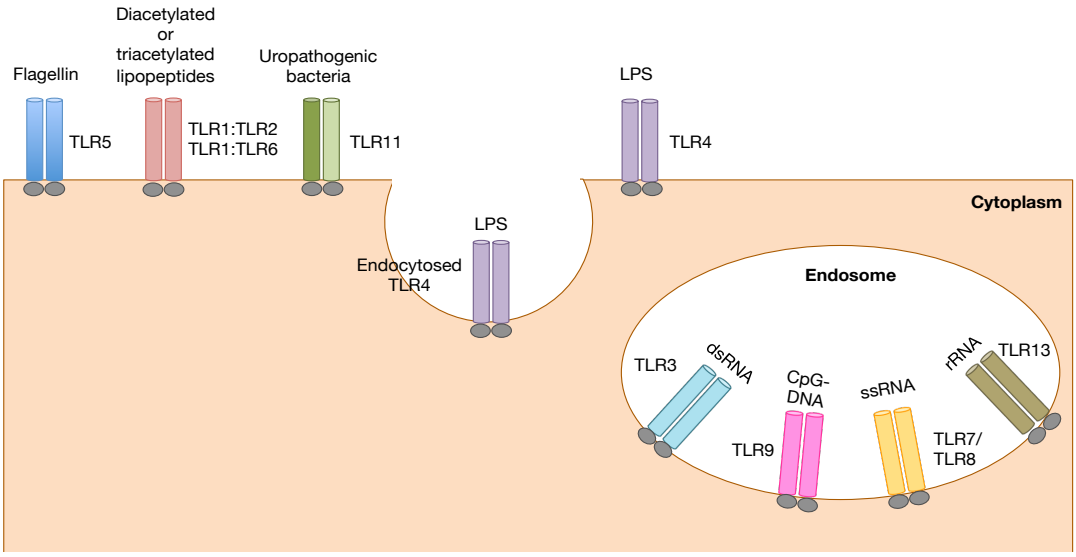

Figure 1.1: Ligand specificities of TLRs
TLRs recognise a variety of pathogen associated molecular patterns (PAMPs). TLR5, TLR11 and heterodimers of TLR1:TLR2 and TLR1:TLR6 bind their respective ligands at the cell surface. TLR3, TLR7, TLR8, TLR9 and TLR13 are localised in the endosome to allow binding of intracellular PAMPs. TLR4 localises at both the plasma membrane and endosomes. TLR1:TLR2, TLR1: TLR6 bind di- or tri-acetylated lipopeptides, TLR3 recognises double-stranded DNA (dsDNA), TLR4 binds LPS, TLR5 binds bacterial flagellin, TLR7 and TLR8 recognise single stranded RNA (ssRNA), TLR9 binds to unmethylated CpG motifs in DNA, TLR11 recognises uropathogenic bacteria while TLR13 is a receptor for ribosomal RNA (rRNA). Adapted from (O'Neill et al., 2013).

1.2.2.2 Priming of Naïve T Lymphocytes

Once DCs have migrated to the LNs, they move towards the T cell area in the paracortex. Here, DCs meet constantly recirculating naïve T cells which have entered via high endothelial venules (HEVs) and present antigen on MHCII molecules, inducing T cell proliferation and polarisation. DCs interact very efficiently with naïve T cells via several ligand receptor pairs such as ICAM-1/ICAM-2:LFA-1, CD58:CD2 and DC-SIGN:ICAM-3. In addition to presenting

antigen to $CD4^+$ T cells on MHCII molecules, DCs can also present antigens to naïve $CD8^+$ T cells on MHC class I molecules (MHCI), in a process known as cross-presentation. This is crucial for the generation of cytotoxic T lymphocytes (CTLs) against antigens not synthesised by the DCs themselves and appears to be a property of a particular subset of DCs (discussed below) (Bevan, 1995; Huang et al., 1994; Reis e Sousa and Germain, 1995; Shen et al., 1997). When a naïve T cell recognises a specific peptide antigen displayed on a DC expressing co-stimulatory molecules, it produces IL2 and enters cell cycle, a process known as clonal expansion (Guermonprez et al., 2002; Mellman and Steinman, 2001; Thery and Amigorena, 2001). After several rounds of cell division, the activated T cells differentiate into the effector cells needed to eliminate infectious organisms. $CD8^+$ T cells differentiate into cytotoxic T lymphocytes (CTLs), which kill cells infected with viruses and other intracellular pathogens, while $CD4^+$ T cells differentiate into T_h1, T_h2 or T_h17 cells, defined on the basis of the cytokines they secrete (Glimcher and Murphy, 2000; Harrington et al., 2005; Park et al., 2005). Effector T cell differentiation is driven by the expression of additional co-stimulatory molecules on activated DCs including CD40 and OX40, as well as cytokines such as IL12, IL6, IL1β, TGF-β and IL23 (Fig. 1.2). IL12 is a heterodimer composed of IL12p35 and IL12/IL23p40 subunits (Gubler et al., 1991), which is produced by DCs following TLR and/or CD40 ligation, leading to the generation of IFNγ-producing T_h1 cells (De Becker et al., 1998). DC production of IL6, TGFβ, IL1β and IL23, a heterodimer of IL12/IL23p40 and IL23p19 subunits (Oppmann et al., 2000), results in the induction of IL17-producing T_h17 cells (Aggarwal, 2002; Bettelli et al., 2006; Langrish et al., 2005; Mangan et al., 2006; Veldhoen et al., 2006). IL1β, IL6 and TGF-β act early in T_h17 cell differentiation, while IL23 acts once activated T cells express the IL23 receptor (IL23R) and is thought to be most important in maintaining T_h17 cells (Aggarwal, 2002; Oppmann et al., 2000; Parham et al., 2002). IL4 production is required to induce a T_h2 response from naïve T cells, but is produced by a number of other immune cells including T cells, eosinophils, NKT cells and basophils rather than DCs (O'Garra, 1998). These cytokines act by inducing lineage specific transcription factors (Fig. 1.2). T_h1 cells require the transcription factor T-bet (Szabo et al., 2000), T_h2 cells depend upon GATA-3, Stat-6 and c-Maf (Agarwal and Rao, 1998; Zhang et al., 1997; Zheng and Flavell, 1997), while T_h17 differentiation requires the transcription factor, RORγt

(Ivanov et al., 2006). The various T cell subsets play distinct roles in the immune response (Abbas et al., 1996) with T_h1 cells producing IFNγ that activates mϕs to kill intracellular pathogens, as well as stimulating the production of IgG2a antibodies by B cells (Snapper et al., 1988b). T_h2 cells produce IL4 which also activates naïve B cells and induces class switching, in this case generating IgE and IgG1 responses (Finkelman et al., 1988; Katona et al., 1991; Snapper et al., 1988a). The third, most recently described, effector T cell population, the IL17 and IL22 producing T_h17 cells, appear to function in the control of extracellular bacteria (Happel et al., 2005) but are also implicated in causing tissue inflammation (Park et al., 2005). Importantly, the largest population of T_h17 cells are found in the intestine, but their exact role in this location remains unclear (Maloy and Kullberg, 2008).

1.2.2.3 DCs in Tolerance

Although DCs are responsible for the initiation of active adaptive immunity (Hagnerud et al., 2006; Hildner et al., 2008; Jung et al., 2002; Lewis et al., 2011; Persson et al., 2013b; Satpathy et al., 2013; Schlitzer et al., 2013), they are also essential for the induction of both central and peripheral tolerance. DCs have been shown to be involved in the induction of central tolerance to self-antigens in the thymus, either by inducing clonal deletion of self-reactive T cells or by generating $FoxP3^+$ natural T_{Reg} cells (nT_{Reg}) (Derbinski and Kyewski, 2010; Hori et al., 2003; McCaughtry and Hogquist, 2008; Proietto et al., 2008). This may occur by antigen-loaded DCs from peripheral tissues migrating to the thymus (Bonasio et al., 2006) or alternatively thymic-resident DCs can acquire self-antigen from medullary thymic epithelial cells (mTECs) expressing the transcription factor autoimmune regulator (AIRE), which drives promiscuous expression of peripheral antigens in the thymus. The antigen acquired in this manner is then cross-presented to T cells (Gallegos and Bevan, 2004; Hubert et al., 2011) inducing negative selection or nT_{Reg} polarisation.

In addition to central tolerance, mechanisms exist to allow tolerance to also be induced in the periphery after T cells have left the thymus. Known as peripheral tolerance, this phenomenon involves the generation of suppressive induced regulatory $FoxP3^+$ T cells (iT_{Reg}) and specific immunological hyporesponsiveness

or anergy towards antigens. In addition to their role in central tolerance, DCs play a key role in peripheral tolerance. iT_{Reg} cell induction by DCs is mediated by TGFβ and the vitamin A metabolite, retinoic acid (RA) (Mucida et al., 2007) (Fig. 1.2). T cell anergy occurs when naïve T cells are presented with specific antigen by immature or semi-mature DCs, which lack effective levels of costimulatory molecules. Anergy can also occur when DCs present antigen in the presence of the anti-inflammatory cytokine IL-10 (Schwartz, 2003).

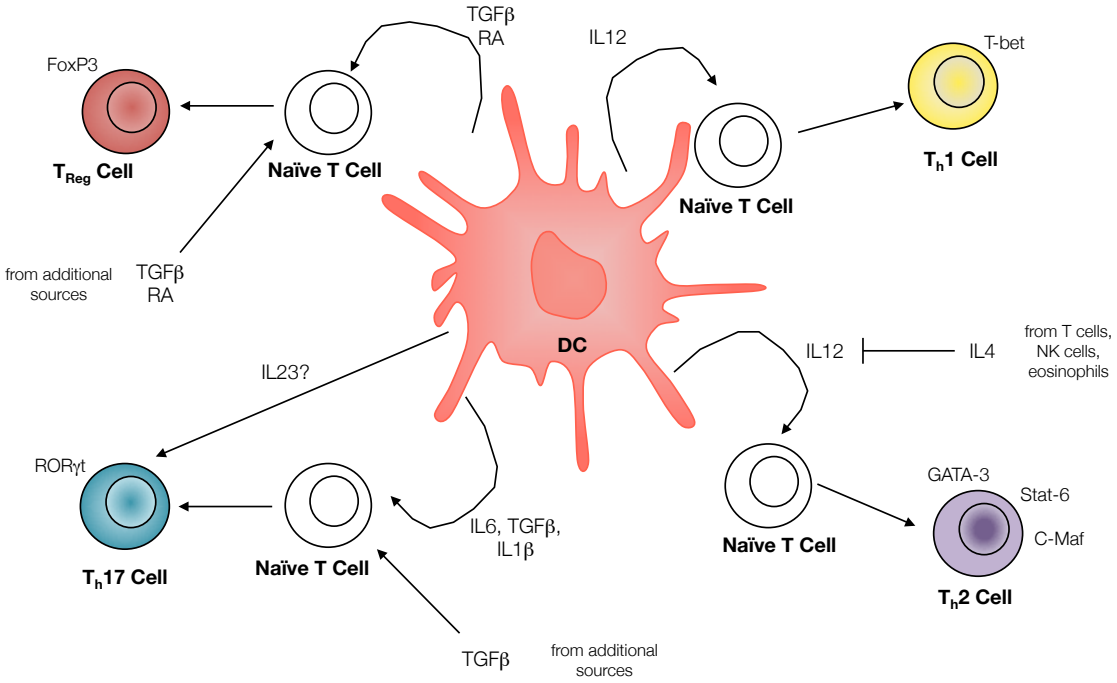

Figure 1.2: Outcomes of DC:T cell interactions
Depending on the signals received during antigen acquisition, DCs can be programmed to produce a variety of cytokines, which promote the polarisation of naïve T cells to distinct subsets of effector or regulatory T cells. Signals from outwith the DCs can also influence the outcomes of the DC:T cell interactions. Each distinct lineage of T cells is controlled by specific transcription factors.

1.2.3 Phenotypic subsets of DCs

It has long been an attractive idea that different DC subsets may exist to fulfil the different functions proposed for DCs. Early studies in mice indicated that there were two main populations, one expressing CD4 or CD11b, but lacking CD8α ($CD11b^+$ DCs) and a second, expressing CD8α but lacking CD4 and CD11b ($CD8^+$ DCs). These subsets were first identified in lymphoid organs, but similar subsets are also present in all non-lymphoid tissues, except the CNS, although this is currently being investigated further (M. Guilliams, personal communication).

In most tissues, expression of the α_E integrin CD103 overlaps with CD8α expression (Ginhoux et al., 2009), but as I will show, in the intestine a population of $CD103^+CD11b^+$ DCs is also present (Bogunovic et al., 2009; Denning et al., 2007; Varol et al., 2009) (Fig. 1.3). Initially these subsets, which were thought to be hard-wired to perform distinct functions, were also thought to derive from different lineages, with $CD8^+$ DCs being of lymphoid origin, while $CD11b^+$ DCs were thought to be of myeloid origin (Wu et al., 2001). However, as discussed below, it is now clear that both DC subsets arise from myeloid progenitors and that they are likely to show at least some functional overlap.

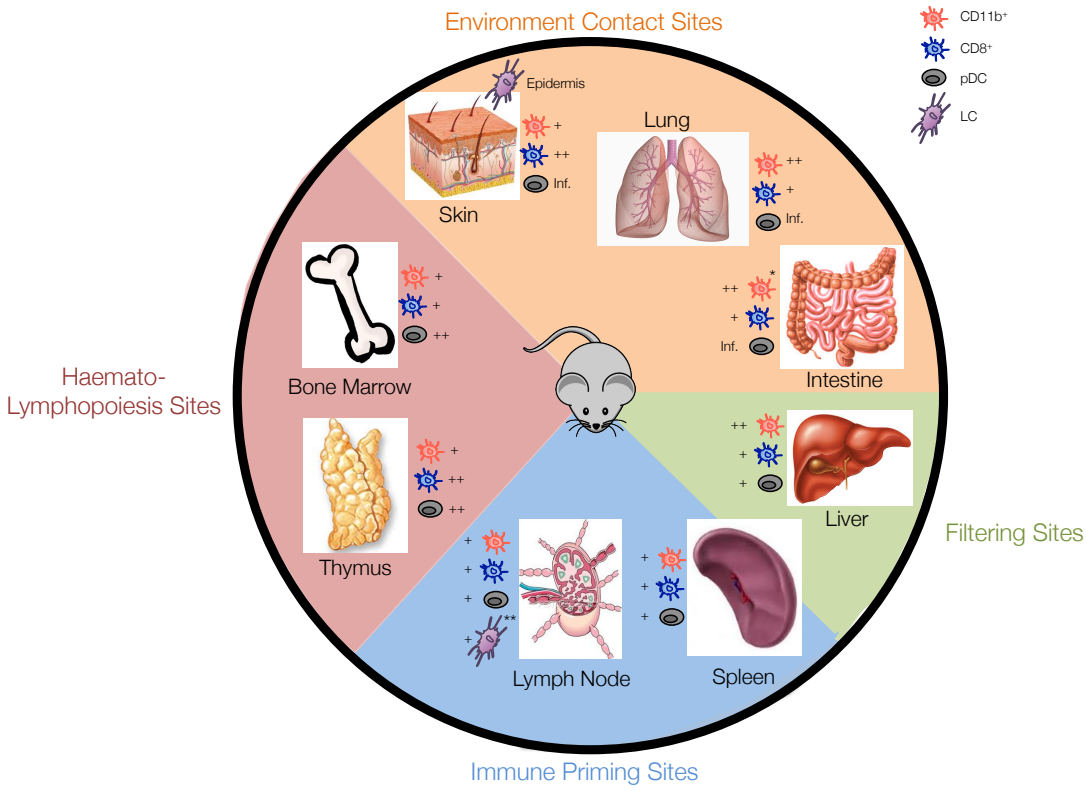

Figure 1.3: DC subsets in different locations in the mouse
$CD11b^+$ and $CD8\alpha^+$ (or $CD103^+$ equivalents in non-lymphoid tissue) DC subsets are present in each tissue in the mouse in varying proportions. + Denotes presence in tissue, while ++ marks the predominant DC population. pDCs are also present in each tissue however, in some tissues they only form a significant population during inflammation (Inf.). ** Langerhans cells (LC) are only found in the epidermis and the skin draining lymph node. * In the small intestine $CD11b^+$ DCs predominate while in the large intestine the main DC population is the $CD8\alpha^+$ DCs. Furthermore, throughout the intestine, a proportion of $CD11b^+$ DCs also express CD103. Adapted from (Merad and Manz, 2009).

These two DC subsets also differ in their expression of a number of other surface markers (Table 1.2), which have recently proved useful in defining

functional properties. SIRPα (CD172a) is a signalling transmembrane receptor expressed by myeloid cells that is found on $CD11b^+$ DCs (Adams et al., 1998). As is discussed below, its role on $CD11b^+$ DCs is currently unclear and thus one of the aims of this thesis was to address its role on intestinal $CD11b^+$ DCs. The chemokine receptor XCR1 and the lectin-like receptor Clec9A (DNGR-1) are expressed solely by $CD8^+$ DCs and appear to define those DCs capable of cross-presenting antigen to $CD8^+$ T cells (Bachem et al., 2010; 2012; Caminschi et al., 2008; Crozat et al., 2011; Huysamen et al., 2008; Poulin et al., 2012; 2010; Zelenay et al., 2012). However, more recently expression of DNGR-1 has been described on all DC-committed progenitors and has been used to track their fate *in vivo* (Schraml et al., 2013).

Table 1.2: Phenotype of murine DCs

Surface Marker	$CD8\alpha^+$	$CD11b^+$	pDCs
CD45	+	+	+
CD11c	++	++	+
MHCII	++	++	+
CD8α	+	-	+/-
CD11b	-	+	-
CD4	-	+/-	+
CD103	+	+/-*	-
F4/80	-	+/-*	-
SIRPα (CD172a)	-	+	+
B220	-	-	+
Ly6C	-	+/-	++
CD205	++	+/ND	-
CD209	-	+/-	++
Clec9A (DNGR1)	++	-	+
XCR1	+	-	-
CD24	++	+/-	ND
CX3CR1	-	+/-	-

* Expression amongst these cells are only reported in the intestine
ND; not determined

Much of what is known about DC subsets originates from murine studies and many of the markers are species-specific. However more recently, considerable progress has been made in identifying human DC subsets. Initially three main subsets were described in human blood on the basis of CD141, CD1c

and CD16 expression, with an additional population of $CD123^+CD303^+CD304^+$ pDCs being described (MacDonald et al., 2002). However, subsequent studies have demonstrated that $CD16^+$ DCs arise from distinct precursors to the others (Lindstedt et al., 2005) and in tissue, $CD16^+$ 'DCs' appear to be indistinguishable from mϕs. Thus, they are unlikely to represent *bona fide* DCs. Recent transcriptional studies suggest that the $CD141^+$ DCs may be the equivalent of the mouse $CD8^+$ DCs (Haniffa et al., 2012), while the $CD1c^+$ DCs are related to the $CD11b^+$ subset (Robbins et al., 2008). These computational studies have been confirmed by the finding that Clec9A and XCR1 are found on human $CD141^+$ DCs (Bachem et al., 2010; Caminschi et al., 2008; Huysamen et al., 2008; Poulin et al., 2010; Sancho et al., 2008) (Table 1.3), while SIRPα expression is found only on $CD1c^+$ DCs (Persson et al., 2013b; Schlitzer et al., 2013). CD103 expression has also been found on human DCs and as in the mouse, it is expressed by both CD1c and CD141 DCs in the gut (Beitnes et al., 2011; Jaensson et al., 2008; Persson et al., 2013b). Collectively, these studies suggest a high degree of evolutionary conservation of the DC populations between mice and men.

Table 1.3: Murine and Human DC subsets

DC Subset	Phenotype	
	Mice	**Human**
$CD8^+$ DCs	$CD11c^+$, $MHCII^+$, $CD8^+$, $XCR1^+$, $Clec9A^+$, $CD103^{+/-}$	$CD11c^+$, $MHCII^+$, $CD141^+$, $XCR1^+$, $Clec9A^+$, $CD103^{+/-}$
$CD11b^+$ DCs	$CD11c^+$, $MHCII^+$, $CD11b^+$, $CD103^{+/-*}$, $SIRP\alpha^+$	$CD11c^+$, $MHCII^+$, $CD11b^+$, $CD1c^+$, $CD103^{+/-*}$, $SIRP\alpha^+$
pDCs	$CD11c^{int}$, $MHCII^{int}$, $B220^+$, $Ly6C^+$, Siglec H^+	$CD11c^-$, $MHCII^{int}$, $CD123^+$, $CD303^+$, $CD304^+$

* Expression reported in intestine (Persson et al., 2013b).

1.2.4 Function of DC subsets

DCs are the only APCs which can prime naïve T cells. Initially it was proposed that the phenotypic subsets had distinct functions, with the $CD11b^+$ DCs

preferentially inducing $CD4^+$ effector T cell responses (Pooley et al., 2001) and the $CD8^+$ DCs inducing $CD8^+$ T cell responses or tolerance (Bonifaz et al., 2002; Haan et al., 2000; Hawiger et al., 2001; Kurts et al., 2001; 1996; Pooley et al., 2001). However it is now clear that both DC subsets can induce most T cell responses under different conditions, the exception to this being the selective ability of $CD8^+$ DC to cross-present antigen to $CD8^+$ T cells in the steady state (Bachem et al., 2010; Bedoui et al., 2009; Haan et al., 2000; Haniffa et al., 2012; Hildner et al., 2008; Pooley et al., 2001; Poulin et al., 2010; Zelenay et al., 2012), mainly because they have receptors like DNGR-1 which take antigen into the phagosomes and have appropriate processing machinery. $CD8^+$ DCs are also effective inducers of T_h1 responses, via an enhanced ability to produce the bioactive IL12p70 (Maldonado-López et al., 1999; Pulendran et al., 1999).

Whether the two DC subsets play distinct roles in inducing specific effector $CD4^+$ T cell responses or tolerance remains unclear. While much remains to be understood about the roles played by $CD11b^+$ DCs, their selective loss *in vivo* has recently been shown to affect T_h17 differentiation (Lewis et al., 2011; Persson et al., 2013b; Schlitzer et al., 2013). The nature of the DCs responsible for tolerance is not entirely clear. As mentioned above, $CD8^+$ DCs were originally thought to be the tolerogenic subset in both LNs and thymus, based on studies demonstrating that cross-presentation was crucial for tolerance to self-antigens (Kurts et al., 1996; 2001) and that targeting DEC-205 on $CD8^+$ DCs induced tolerance (Bonifaz et al., 2002; Hawiger et al., 2001). Given the link between $CD103^+$ and $CD8^+$ DCs, additional evidence that $CD8^+$ DCs may be involved in tolerance came from studies identifying intestinal $CD103^+$ DCs to be potent inducers of $FoxP3^+$ T_{Reg} cells (Coombes et al., 2007; Sun et al., 2007) (and reviewed in (Scott et al., 2011)). However, as previously mentioned $CD103^+$ DCs in the gut can be $CD11b^+$ or $CD8\alpha^+$ (Denning et al., 2011; Fujimoto et al., 2011). In addition, $SIRP\alpha^+$ DCs exist in the thymus and these along with $CD8^+$ DCs can induce central tolerance through the mechanisms described above (Hsieh et al., 2012; Klein et al., 2009). Furthermore, recent studies have shown that the selective depletion of $CD8^+$ or $CD11b^+$ DCs does not affect T_{Reg} cell populations (Edelson et al., 2010; Persson et al., 2013b; Welty et al., 2013). However, when both populations are simultaneously depleted a reduction in T_{Reg} cells is observed suggesting a degree of redundancy between the populations (Welty et al., 2013). Thus further studies

are required to assess the functionality of the distinct DC populations and investigating the specific functions of intestinal DC populations was one aim of this thesis. Additionally a number of studies have proposed that a specific population of TNF and iNOS producing inflammatory DCs (Tip-DCs) may be recruited during inflammation (Serbina et al., 2003). Whether these cells are indeed *bona fide* DCs remains to be determined. Tip-DCs are derived from distinct progenitors (monocytes) compared with the other DC populations (see below), their identification is controversial and furthermore it is yet unclear if they are capable of migrating in lymph to the draining lymph nodes.

1.3 DC Ontogeny and Development

DCs are classified along with macrophages and monocytes as mononuclear phagocytes. The mononuclear phagocyte system (MPS) was first described in 1972 by van Furth and colleagues as a system of phagocytic cells located in reticular connective tissue arising from a common bone marrow (BM) progenitor (van Furth et al., 1972). As discussed above, the surface phenotype of the cells of the MPS is overlapping despite the presence of a number of cell types (Table 1.4). Although arising from a common BM progenitor, DCs and mϕs follow distinct pathways of development ultimately deriving from distinct precursors (Liu et al., 2009). These distinct lineages will be used in this thesis, in combination with surface phenotype and functionality as an aid to definitively distinguish between DCs and mϕs in the intestine. Additionally, distinct cytokines and transcription factors have been implicated in the development of mϕs and DCs and a considerable degree of heterogeneity has also been reported regarding the transcriptional factor requirements of the DC subsets. This will also be investigated for the DC subsets in the intestine as part of this thesis.

Table 1.4: Cells of the Steady-State MPS

Cell	Tissue	Marker Expression			
		CD11c	MHCII	F4/80	CD11b
DCs	Intestine, Lung, Liver, Spleen, Blood, Kidney, Heart, Thymus	+	+	-	-/+
pDCs	Intestine, Lung, Liver, Spleen, Blood, Kidney, Heart, Thymus, BM	Int.	-	-	-
Intestinal mϕs	Intestine	+	+	+	+
Kupffer cells	Liver	Int.	+	+	-
Alveolar mϕs	Lung	+	-	+	-
Peritoneal mϕs	Peritoneum	+/-	-	+	+
Monocytes	Intestine, Lung, Liver, Spleen, Blood, Kidney, Heart, Thymus, BM	Int.	-/+	-/+	+
Langerhans cells	Skin	+	+	+	+

1.3.1 Bone Marrow Precursors for Cells of the MPS

In adult mice, progenitors of the MPS arise from haematopoietic stem cells (HSCs) through a series of intermediate stages in the BM. Each stage in development is accompanied by a progressive lineage commitment, in which cells lose the ability to generate certain cell types (Liu et al., 2009) (Fig. 1.4). The first stage results in the generation of the common myeloid progenitor (CMP) and the common lymphoid progenitor (CLP) from the HSC. CMPs have the potential to generate all myeloid cells, including DCs, mϕs, granulocytes, neutrophils and eosinophils (Akashi et al., 2000), whereas CLPs generate T cells, B cells and NK cells (Kondo et al., 1997). As discussed above, initial studies suggested that CLPs may also retain some potential to generate $CD8^+$ DCs but this remains controversial (Manz et al., 2001; Wu et al., 2001). CMPs then differentiate into mϕ/DC progenitors (MDPs) or granulocyte/mϕ progenitors (GMPs), the latter retaining the potential to generate DCs, but preferentially differentiating into granulocytes and monocytes/mϕs (Auffray et al., 2009; D'Amico and Wu, 2003). In contrast, MDPs have the potential to generate DCs and monocytes/mϕs only (Fogg et al., 2006). MDPs are characterised by their expression of CX3CR1, CD135, CD115 and CD117 while lacking expression of MHCII, T cell, B cell,

erythrocyte and NK cell lineage markers (Fogg et al., 2006). At the next stage of differentiation, the MDP generates either $CD117^{-}$ $CX3CR1^{+}$ $CD115^{+}$ $CD135^{-}$ $CD11b^{+}$ $Ly6C^{hi}$ monocytes or $CD117^{lo}$ $CX3CR1^{+}$ $CD135^{+}$ $CD115^{+}$ DC committed progenitors, termed common DC progenitors (CDPs) (Onai et al., 2007b) or pro-DCs (Naik et al., 2007). The $Ly6C^{hi}$ monocytes generated from MDPs are short-lived and have the ability to mature into $Ly6C^{lo}$ monocytes which circulate in the blood (Yona et al., 2013), or give rise to tissue-resident mϕs (Bain et al., 2013; Ginhoux et al., 2006; Tamoutounour et al., 2012). However, it is interesting to note that a number of recent studies have demonstrated that most tissue-resident mϕs are the progeny of primitive yolk-sac mϕs or foetal liver monocytes (Guilliams et al., 2013b; Hoeffel et al., 2012; Schulz et al., 2012; Yona et al., 2013) rather than being continually replenished by BM monocytes, the key exceptions to this being the gut (Bain et al., 2013; Tamoutounour et al., 2012) and skin (S. Tamoutounour, in press). Additionally during inflammation monocytes have been proposed to generate Tip-DCs (Serbina et al., 2003), although as discussed above the nature of these cells remains controversial. The CDPs generated from MDPs lose their potential to generate cells of the monocyte/mϕ lineage and then differentiate into either $CD117^{-}CX3CR1^{-}$ $CD135^{+}$ $CD115^{-}$ $CCR9^{+}$ $CD11c^{int}$ $B220^{+}$ $Ly6C^{+}$ pDCs or into $CD117^{-}CX3CR1^{+}$ $CD135^{+}$ $CD115^{-}$ $CD11c^{int}$ $CD11b^{-}$ precursors of conventional DCs (pre-DCs) (Naik et al., 2007). While mature pDCs develop from CDPs in the BM, pre-DCs exit the BM and traffic in blood to tissues before maturing into conventional DCs subsequently proliferating *in situ* (Liu et al., 2009). More recently, an additional stage of differentiation has been described in which CDPs may generate a $CCR9^{-}$ pDC-like progenitor (pDC progenitor) which retains both DC and pDC potential (Schlitzer et al., 2012; 2011).

It remains unclear if there are distinct subsets of pre-DCs that are pre-programmed to generate $CD8^{+}$ or $CD11b^{+}$ DCs, or if the same progenitors can differentiate into either DC subset once in the tissue. Recently it has been suggested that there is considerable heterogeneity in these cells, for instance Naik and colleagues demonstrated that pre-DCs could be divided into three populations based on CD24 expression, $CD24^{hi}$, $CD24^{int}$ and $CD24^{lo}$. They found that whereas the $CD24^{int}$ cells could generate both subsets, the $CD24^{hi}$ and $CD24^{lo}$ cells

preferentially generated $CD8^+$ or $CD11b^+$ DCs respectively, suggesting a degree of lineage commitment within the BM (Naik et al., 2007; 2006).

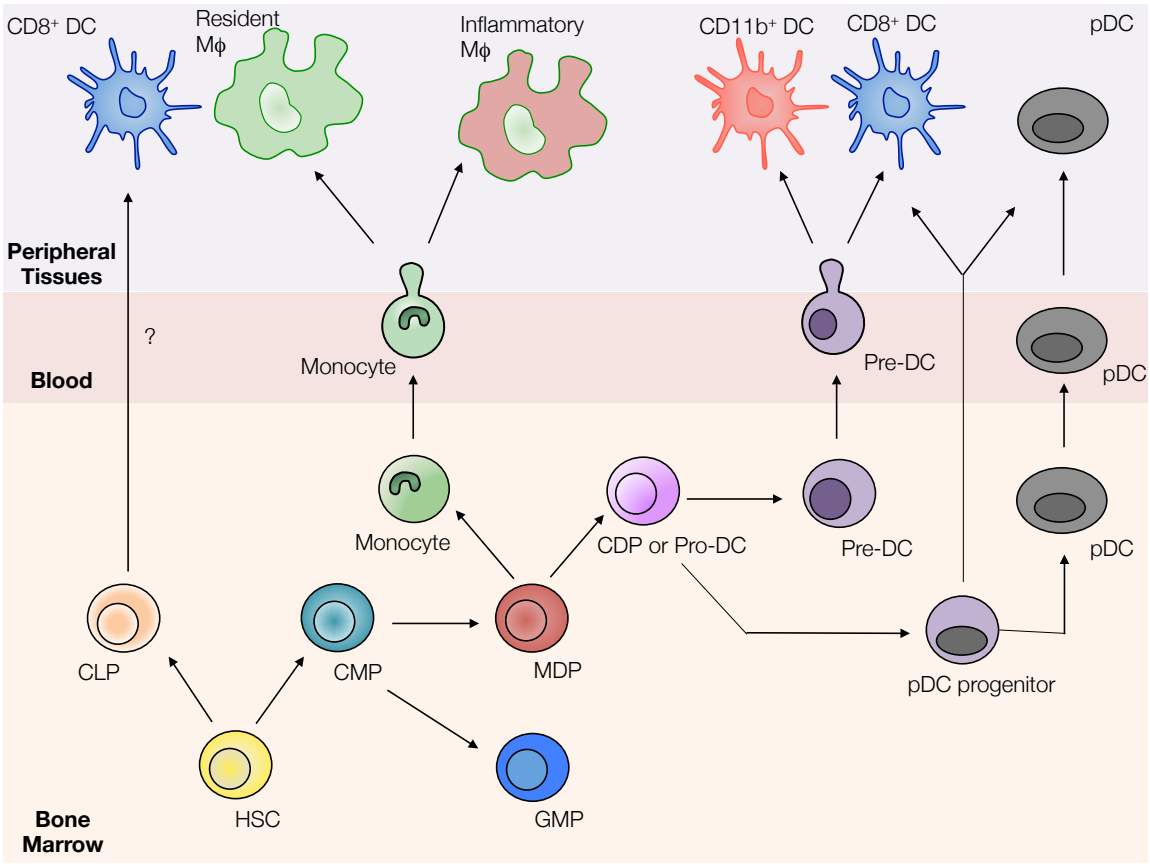

Figure 1.4: DCs develop from HSCs through a series of intermediate precursors stage in the BM

Progenitors restricted to the DC lineage arise in the bone marrow from HSCs. Firstly HSCs generate CMPs which in turn differentiate into MDPs and then into either monocytes or CDP/pro-DCs. Monocytes then enter the bloodstream and under inflammatory conditions eventually peripheral where they give rise to inflammatory mϕs. In the steady state, monocytes can also enter the skin and gut where they generate tissue resident mϕs. In other tissues, tissue-resident mϕs arise from foetal liver monocytes or primitive yolk-sac mϕs. The pro-DCs further differentiate in the bone marrow into pre-DCs or pDCs. pDCs then directly enter peripheral tissues through the bloodstream where they produce high levels of type 1 interferon in response to viral infections. Similarly pre-DCs also enter tissues but subsequently differentiate into both $CD11b^+$ and $CD8^+$ DCs. A pDC progenitor has also been reported, which lacks CCR9 expression that traffics to tissues retaining the potential to generate either DCs or pDCs depending on the environmental stimuli received. The HSCs also give rise to CLPs, which are reported to have the potential to generate $CD8^+$ DCs, however the intermediate stages in this process as well as the relative contribution of this pathway to the $CD8^+$ DC population remain unclear.

Additionally it is unclear if there are distinct subsets of pre-DCs which traffic to specific tissues. A recent study has identified a novel DC and pDC progenitor with apparent intestinal specificity (Zeng et al., 2013). However, how this $CCR9^-$ $B220^+$ $CD11c^{int}$ $\alpha4\beta7^+$ progenitor relates to the MDP:CDP:pre-DC system remains to be determined, but these may represent the plastic pDC-like progenitor recently described by Schlitzer and coworkers which retained the ability to generate pDCs

as well as DCs (Schlitzer et al., 2011; 2012; Zeng et al., 2013). Whether additional precursors exist with other tissue-specificities remains to be reported. However, it is important to note that in the Butcher study (Zeng et al., 2013) donor-derived cells could also be found in the spleen demonstrating that these are not completely imprinted with the decision to migrate to the intestine.

1.3.2 Role of Growth Factors in DC Development

The development of all haematopoietic cells is controlled by precursor and/or lineage-specific growth factors. Fms-like tyrosine kinase 3 (Flt3; also known as CD135, Flk-2 and STK-1) (Karsunky et al., 2003; Liu et al., 2009) is expressed by several haematopoietic progenitors, but unlike other lineages, DCs retain Flt3 expression throughout their maturation process. Mice lacking its ligand, Flt3L (Flt3L$^{-/-}$ mice), or mice receiving Flt3L inhibitors show a dramatic reduction of DCs and pDCs (McKenna et al., 2000; Tussiwand et al., 2005). In parallel, administration or conditional expression of Flt3L stimulates preferential expansion of DC-committed progenitors and both CD8^{+} and CD11b^{+} DCs (Björck, 2001; Karsunky et al., 2003; Maraskovsky et al., 1996). Flt3L can also be used to generate CDPs, pre-DCs and mature DCs from BM cells *in vitro*, providing a useful source of such cells for study (Brasel et al., 2000; Naik et al., 2007) and Flt3L has similar effects in humans (Pulendran et al., 2000). Importantly, expansion of DCs with Flt3L does not appear to alter their functionality, but simply increases their numbers (Shurin et al., 1997; Viney et al., 1998). Flt3L production is regulated in response to DC depletion *in vivo,* ensuring adequate replenishment of DCs in both the steady state and during inflammation (Birnberg et al., 2008). Thus it is clear that Flt3 and its ligand play a non-redundant role in DC development. Importantly and consistent with the confusion surrounding their identification, Langerhans cells and Tip-DCs are not dependent upon Flt3L. Thus I will use Flt3L dependence to identify *bona fide* DC populations in the intestine as part of this thesis.

Granulocyte/mϕ colony stimulating factor (GM-CSF or CSF-2), was the first growth factor used to generate DCs from murine haematopoietic progenitors and from human monocytes *in vitro* (Caux et al., 1992; Inaba et al., 1992; Sallusto and Lanzavecchia, 1994). Despite this, DC numbers are normal in the lymphoid organs

of mice lacking CSF-2 or its receptor and administration of exogenous CSF-2 or overexpression of CSF-2 in transgenic mice only marginally increases the DC populations in lymphoid organs (Maraskovsky et al., 1996; Vremec et al., 1997). CSF-2 appears to play a more important role in the development of DCs in non-lymphoid tissues, with the presence of $CD103^+CD11b^+$ DCs in the intestine and $CD103^+CD11b^-$ DCs in the lung, liver, kidney and dermis being dependent on CSF-2 (Bogunovic et al., 2009; Greter et al., 2012; King et al., 2010; Varol et al., 2009). Despite CD103 expression itself being regulated by CSF-2 (Zhan et al., 2011), the apparent role of CSF-2 in the development of $CD103^+$ DCs cannot be explained by its effects on CD103 expression because when CD24 is used as a surrogate marker for CD103 similar defects were observed (Greter et al., 2012). However, this approach remains to be validated and re-examining the role of CSF-2 in gut DC ontogeny was one aim of this thesis.

Mϕ colony stimulating factor (M-CSF or CSF-1) is a key cytokine involved in monocyte and mϕ differentiation and survival, with mice lacking CSF-1 or its receptor, CSF-1R (CD115) lacking most mϕ populations and developing osteopetrosis due to the lack of osteoclasts (Dai et al., 2002; Yoshida et al., 1990). Neither DCs nor pDCs appear to require CSF-1 for their development (Witmer-Pack et al., 1993) and the fact that it may be required for the development of Tip-DCs and Langerhans cells is further evidence against these being *bona fide* DCs (Ginhoux et al., 2006; Greter et al., 2012).

1.3.3 Transcription factors

A number of transcription factors have been associated with the development, homeostasis and function of murine and human DC subsets (Fig. 1.5). Interferon regulatory factor 4 (IRF4) is expressed by $CD11b^+$ but not by $CD8^+$ DCs and loss of this transcription factor leads to a selective defect in the ability to generate $CD11b^+$ DCs from BM cells *in vitro* as well as a reduction in the proportion and number of $CD4^+$ splenic DCs (Suzuki et al., 2004). More recently, it has been reported that absence of IRF4 leads to a reduced population of $CD11b^+$ DCs in the lung and $CD103^+CD11b^+$ DCs in the intestine (Persson et al., 2013b; Schlitzer et al., 2013). Although the role of IRF4 was initially assumed to be in DC development (Suzuki et al., 2004), more recently it has been implicated in

promoting CD11b$^+$ DC survival (Persson et al., 2013b). At this time no mechanism has been proposed, however as IRF4 functions as a negative regulator of pro-inflammatory cytokine production in response to TLR ligation (Honma, 2005), it is possible that absence of this transcription factor leads to aberrant activation contributing to the decreased survival of IRF4-deficient DCs. IRF4 is also expressed by mϕs and lymphocytes (Brüstle et al., 2007; Celada et al., 1996; Cretney et al., 2011; DeKoter et al., 1998; Henkel et al., 1996; Klein et al., 2009; McKercher et al., 1996; Mudter et al., 2011; Zheng et al., 2009). Thus studies of IRF4 function in DCs need to exclude potentially confounding effects on other leukocyte populations.

In addition to IRF4, CD11b$^+$ DCs are also regulated by Notch RBP-J, RelB and TRAF6 (Kobayashi et al., 2003; Lewis et al., 2011; Wu et al., 1998). Deletion of Notch, leads to a selective reduction in CD11b$^+$ DCs in the spleen and CD103$^+$CD11b$^+$ DCs in the intestine (Lewis et al., 2011; Satpathy et al., 2013), although its effects in the spleen are limited to the CD11b$^+$ DCs expressing the endothelial cell – selective adhesion molecule (ESAM). The relevance and functional implications of this remain unclear.

IRF8 (also known as IFN consensus sequence-binding protein, ICSBP) is expressed by CD8$^+$, but not CD11b$^+$ DCs, and has been implicated in the development and homeostasis of CD8$^+$ DCs and pDCs, in both lymphoid and non-lymphoid tissues (Edelson et al., 2010; Ginhoux et al., 2009; Schiavoni et al., 2002; Tamura et al., 2005; Tsujimura et al., 2003), however its role in the gut is yet to be examined. IRF8 has also been implicated in mϕ differentiation (Holtschke et al., 1996; Li et al., 2011). Although, basic leucine zipper ATF-like 3 (Batf3) is expressed by all DCs, it is specifically associated with the development of CD8$^+$ DCs, with Batf3$^{-/-}$ mice on the 129S6/SvEv background lacking CD8$^+$/CD103$^+$ DCs (Edelson et al., 2010; Hildner et al., 2008). The effect of this defect is strain-dependent and can be overcome in mice on the C57Bl/6 background by IL12/IFNγ production during infection driving compensatory Batf1 and/or Batf2 expression (Tussiwand et al., 2012). Inhibitor of DNA binding protein 2 (Id2) is another transcription factor associated with CD8$^+$ DC development and mice lacking Id2 display marked reductions in CD8$^+$/CD103$^+$ DCs in the lung, liver, kidney, spleen and intestine (Ginhoux et al., 2009; Hacker et al., 2003; Kusunoki et al., 2003).

The recently discovered zinc finger transcription factor, zDC, specifically marks all cells of the DC lineage (Meredith et al., 2012a; Satpathy et al., 2012), but its absence skews DC populations towards the $CD8^+$ DC phenotype suggesting its role may be lineage dependent (Meredith et al., 2012a; 2012b; Satpathy et al., 2012). zDC has also been shown to be a negative regulator of DC activation, thus perhaps its role in maintaining the $CD11b^+$ DCs may be liked to their activation status rather than being directly involved in their development (Meredith et al., 2012b).

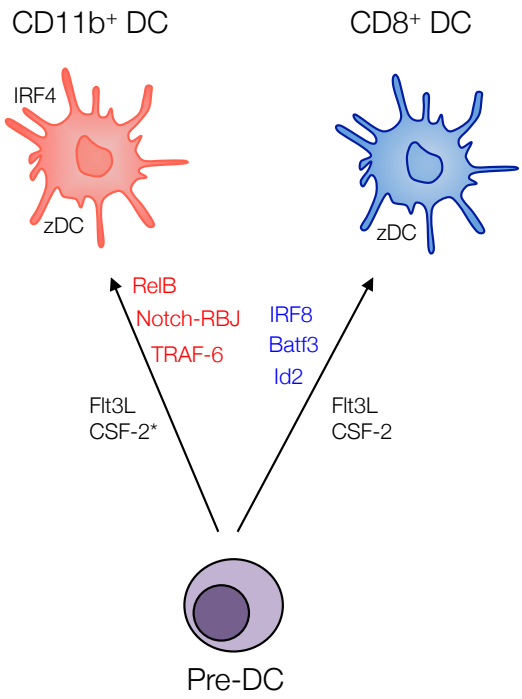

Figure 1.5: Expression and dependence of DC subsets on specific growth and transcription factors
$CD11b^+$ DCs develop from pre-DCs in peripheral tissues in an Flt3L dependent manner and has been shown to involve IRF4, Notch-RBJ, RelB and TRAF-6 signalling. * $CD11b^+$ DCs develop independently of CSF-2 apart from intestinal $CD103^+CD11b^+$ DCs, which similar to $CD8^+/CD103^+$ DCs in other tissues require CSF-2. $CD8^+/CD103^+$ DCs ($CD8^+$ DCs) develop from pre-DCs in an Flt3L and CSF-2 dependent manner. Their development is regulated by the transcription factors Batf3, Id2 and IRF8. Both classical DC subsets express the zinc finger transcription factor, zDC.

1.4 The Intestinal Immune System

The intestine represents a key immune site in the body. In order to allow for efficient absorption of water and nutrients, the single layer of intestinal epithelium

has to allow access by the contents of the lumen to the interior. As this renders it susceptible to invasion by pathogens, the intestinal immune system has to be able to mount protective responses against any harmful pathogens it encounters. At the same time, the gut is home to a large and diverse array of commensal bacteria, many of which are mutualistic symbionts (Sonnenburg et al., 2004), as well as being continuously exposed to a variety of foreign antigens in the diet. As it would be wasteful and dangerous to mount active immunity against these materials, the intestinal immune system induces a state of immunological hyporesponsiveness (tolerance) to such harmless antigens. This is no easy feat given the large surface area of the gut and that the intestinal microbiota outnumbers the total cells in the human body by 10-fold (Macpherson et al., 2009). Inappropriate responses to food proteins and commensal bacteria result in disorders such as coeliac disease and inflammatory bowel disease (IBD) respectively (Mowat, 2005). The decision making mechanisms that underlie this dichotomy are still to be elucidated fully, but DCs are likely to play a key role due to their ability to induce effector and regulatory T cells as well, as gut-specific IgA secreting plasma cells (Bergtold et al., 2005; Castigli et al., 2005; Massacand et al., 2008).

1.4.1 Components of the Intestinal Immune System

The gastrointestinal (GI) tract consists of the stomach, small intestine, caecum, large intestine (colon) and rectum and the largest compartment of the immune system has evolved in these tissues (Mowat, 2003). Immune cells are found in the mucosa itself, as well as in the organised lymphoid tissues associated with it. These organs are responsible for the induction of immune responses and they include the MLNs, Peyer's patches (PPs), which are scattered along the anti-mesenteric side of the small intestine, and the smaller isolated lymphoid follicles (ILFs), which have the appearance of microscopic PPs and are distributed throughout the walls of the small and large intestine (Mowat, 2003). The mucosa contains a large range of immune cells including lymphocytes, plasma cells, mϕs, DCs, ILCs and eosinophils, as well as a few mast cells.

1.4.1.1 Peyer's patches and ILFs

Peyer's patches (PPs) are macroscopic lymphoid aggregates found in the submucosa of the small intestine, particularly at the two ends. These consist of collections of large B cell follicles and intervening T-cell areas, together with the subepithelial dome (SED) which is the area directly below the epithelium. A single layer of columnar epithelial cells, known as the follicle-associated epithelium (FAE) separates the PPs from the intestinal lumen (Hamada et al., 2002; Mowat and Viney, 1997). The FAE contains specialised enterocytes called microfold (M) cells. As well as lacking a thick mucus layer immediately above them, M cells have distinct oligosaccharide epitopes on their surface, which allow the adhesion of invasive pathogens and other particulate antigens (Neutra et al., 1996). Antigen from these M cells is then delivered to DCs in the SED, which then interact with naïve T and B cells deeper in the PPs (Newberry and Lorenz, 2005). It is currently unclear if DCs in the PPs are solely responsible for priming T and B cells *in situ* or if these DCs can also migrate to the MLNs to carry out these functions. The exact need for the PPs remains unclear, as experiments using mice deficient in PPs and M cells have produced conflicting results with some groups reporting no effects on immunity and/or oral tolerance, while others suggest there are defects in these processes (Alpan et al., 2001; Fujihashi et al., 2001; Spahn et al., 2001). ILFs are microscopic lymphoid aggregates found throughout the length of both the small and large intestines. Similar to PPs, ILFs have both FAE and M cells, however consist of only 1 or 2 B cell follicles (Eberl and Lochner, 2009).

1.4.1.2 Mesenteric lymph nodes

In contrast to the discrepant findings on the role of PPs, the MLNs are clearly essential for the induction of all immune responses in the intestine. Just as the intestinal immune system is the largest component of the immune system, the mesenteric lymph nodes are the largest lymph nodes in the body. DCs from throughout the mucosa and possibly PPs and ILFs migrate to the MLNs via afferent lymphatics in a CCR7 dependent manner (Jang et al., 2006; Worbs et al., 2006). As in other LNs, migratory DCs in the MLNs can be identified as $MHCII^{hi}$ cells (Henri et al., 2001), while LN resident DCs (identified as $MHCII^{int}$) enter from bloodstream via high endothelial venules (HEVs). Both DC subsets can present

antigen to naïve T cells within the MLN allowing for a diverse array of responses to a variety of antigen. LN resident DCs acquire soluble antigen from afferent lymph draining the intestine in addition to blood for presentation to naïve T cells, which occurs more rapidly than when DC migration from the intestine is required (Sixt et al., 2005). In addition to the induction of protective immune responses, the MLNs play a critical role in the induction of oral tolerance as demonstrated by the loss of this phenomenon in mice that have had their MLNs surgically removed (Worbs et al., 2006), in lymphotoxin α ($LT\alpha$)$^{-/-}$ mice or in the progeny of pregnant mice treated with an anti-$LT\beta R$ antibody to block the formation of MLNs (Spahn et al., 2002).

Once T and B cells encounter antigen on migratory DCs, they become imprinted with the specific ability to return to the small intestinal mucosa due to expression of $\alpha 4\beta 7$ integrin and the chemokine receptor CCR9 (Agace, 2008; Johansson-Lindbom and Agace, 2007). The ligand for $\alpha 4\,\beta 7$ integrin mucosal addressin cell-adhesion molecule (MAdCAM)-1 which is expressed constitutively by postcapillary endothelial cells in mucosal tissues (Berlin et al., 1993; Hamann et al., 1994; Picarella et al., 1997). Consistent with its role as a gut homing receptor, mice lacking $\beta 7$ integrin lack mucosal T cells (Artis et al., 2000; Wagner et al., 1996). The ligand for CCR9 is CCL25, a chemokine expressed by small intestinal epithelial cells (Bowman et al., 2002; Kunkel et al., 2000; Pabst et al., 2004; Svensson et al., 2008) and as a result, the migration of activated T and B cells to the small intestine is highly dependent on CCR9, although this is more marked for $CD8^+$ T cells in the epithelium than $CD4^+$ T cells in the LP. Importantly, the CCL25-CCR9 axis is not needed for entry of lymphocytes to other parts of the gut such as the colon, where instead it has been proposed GPR15 may control T cell trafficking to this site (Kim et al., 2013). The imprinting of gut homing molecules on lymphocytes depends on the production of retinoic acid (RA) by DCs (Iwata et al., 2004; Jaensson-Gyllenbäck et al., 2011). RA is a metabolite of dietary vitamin A, generated through the action of two enzyme families, aldehyde dehydrogenases (ALDHs) and retinaldehyde dehydrogenases (RALDHs). Vitamin A is first oxidised to retinaldehyde by ALDHs, which is subsequently oxidised to RA by RALDHs (Duester, 2000; Maden, 2002). As discussed below, production of RA has been shown to be a function of $CD103^+$ DCs in the LP, PPs and MLNs.

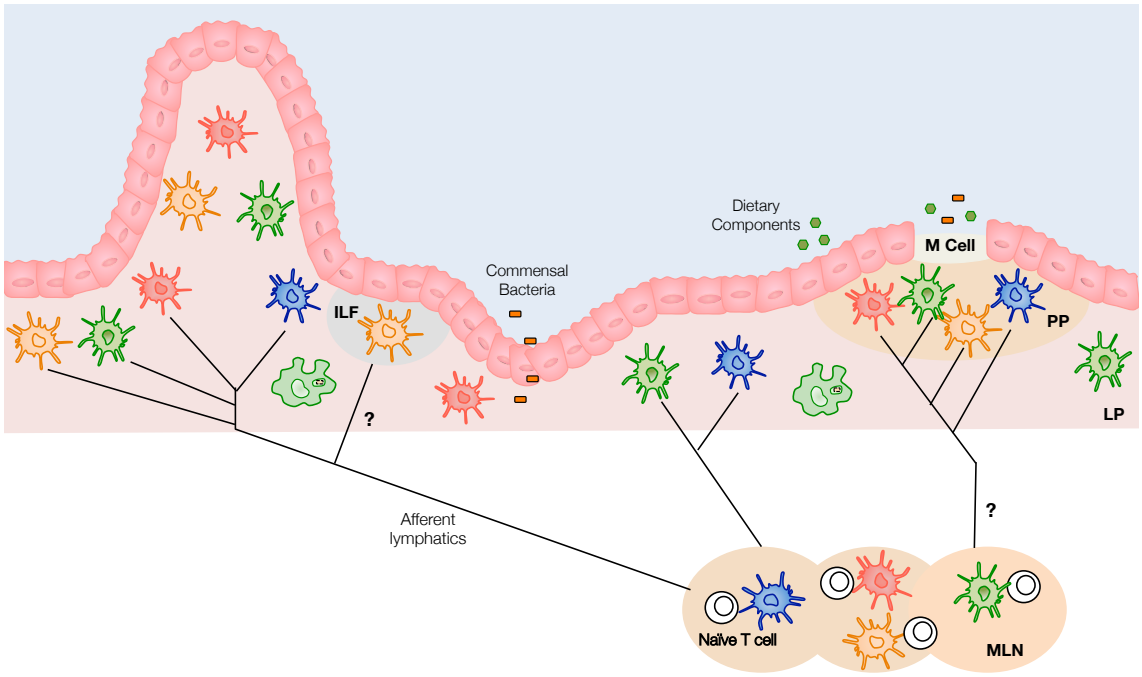

Figure 1.6: Schematic representation of intestine and gut-associated lymphoid tissues
DCs in the LP migrate through the afferent lymphatics to the MLNs, which are the crucial site for the induction of tolerance and immunity. PPs and ILFs represent additional priming sites and DCs in this location may also drain to the MLNs, although this remains to be shown.

1.4.1.3 Lamina propria

The lamina propria (LP) is a thin layer of loose connective tissue (Mowat, 2003) that together with its overlying epithelium, constitutes the mucosa. As mentioned above, the LP is home to a number of immune cells including lymphocytes, macrophages, DCs, eosinophils and ILCs. There are more lymphocytes in the mucosa than in any other part of the body, with the LP containing $CD4^+$ and $CD8^+$ T cells, NKT cells as well as a large population of plasma cells, which produce IgA, the dominant antibody isotype in the intestine. Following its transcytosis into the lumen, IgA functions to neutralise pathogens and their products (Cerutti and Rescigno, 2008). The majority of T cells in the LP are $CD4^+$ T cells and all subtypes of these can be found in the LP, including IFNγ-producing T_h1, cells, the suppressive $FoxP3^+$ T_{Reg} cells and T_h17 cells. A sizeable population of cytotoxic $CD8^+$ T cells is also present in the LP. The presence of T_h17 cells in the steady state LP has caused some confusion, as these cells are usually absent from the periphery in the absence of inflammation. Notably, T_h17 cells represent the majority of $CD4^+$ T cells in the steady state LP (Ivanov et al., 2006; Mangan et al., 2006). Several investigators have argued that their presence

in the absence of pathological inflammation suggests these may be protective. Consistent with this, IL17A$^{-/-}$ mice are more susceptible to dextran sodium sulphate (DSS) induced colitis (Yang et al., 2008). However, contrary to the idea that T_h17 cells are protective, similar to their roles in other tissues, T_h17 cells have also been associated with pathology. One explanation may come from the different effects of individual forms of the IL17 protein. Whereas IL17F has been implicated in the role of T_h17 cells in gut pathology, IL17A appears to play a more anti-inflammatory role (Yang et al., 2008). Nevertheless, additional studies are required to delineate the role of T_h17 cells in the steady state LP (Maloy and Kullberg, 2008). In addition to lymphocytes, the LP is home to a considerable number of mononuclear phagocytes such as DCs and mϕs. As alluded to earlier, the correct identification of these cells is the cause of continued debate and this is described in detail below.

1.4.2 Regulation of Tolerance vs. Immunity in the Intestine

Most individuals do not develop intestinal inflammation in response to the diverse array of harmless antigens encountered on a daily basis, yet are capable of clearing intestinal pathogens when necessary. In order to achieve this level of regulation, the intestinal immune system has evolved sophisticated processes which balance protective immunity and tolerance.

A number of mechanisms are designed to prevent the entry of pathogenic microbes into the intestine, including physical, biochemical and mechanical barriers, together with a diverse array of innate and adaptive immune cells at the mucosal surface. Despite only being one cell thick, the intestinal epithelium provides a physical barrier against the entry of potential pathogens. The barrier function of the intestinal epithelium is ensured by complex mechanisms acting on multiple levels. Commensal microbes themselves represent one arm of this defence, preventing potential pathogens from attaching and invading (Swidsinski et al., 2005). In addition to its barrier function, the epithelium can also initiate inflammatory responses as a result of intracellular and surface expression of PRR by enterocytes (Rakoff-Nahoum et al., 2004; Vaishnava et al., 2008). Furthermore, much of the epithelium is coated with a thick mucus layer, resulting from mucin production by goblet cells. This mucus layer is essential for host protection as

evidenced by the spontaneous development of colitis and impaired protection from DSS colitis in Muc2 knock out mice (van der Sluis and van Seuningen, 2006; van der Sluis et al., 2006; Van der Sluis et al., 2006). Trefoil factors are further agents produced by enterocytes which protect the barrier against invasion (Mashimo et al., 1996). Further protection against pathogenic bacteria comes from the MyD88-dependent production of anti-microbial peptides such as defensins and RegIIIγ by Paneth cells present in the crypts of the small intestine (Hooper et al., 2003; Ouellette and Bevins, 2001; Vaishnava et al., 2008).

Despite the presence of these surface defences, a number of microbes can breach the epithelium and communicate with the innate immune cells located in the lamina propria including the largest population of macrophages in the body, neutrophils, eosinophils, natural killer (NK) cells and innate lymphoid cells (ILCs). As well as producing pro-inflammatory mediators and being able to kill pathogens, some of these innate cells such as ILCs, produce mediators like IL22 which drives the production of anti-microbial peptides and enhances barrier integrity (Cella et al., 2009; Harrison and Maloy, 2011; Sanos et al., 2009; Sonnenberg et al., 2011; Zheng et al., 2008). If the innate response is overcome, uptake of invading microbes by DCs in LP or PPs leads to antigen specific immune responses via priming of T and B cells in PP or MLNs, as discussed in detail below.

A rather similar battery of innate and adaptive immune responses is now thought to also limit the uptake and penetration of commensal bacteria across the epithelium. However the main consequence in the adaptive immune system of exposure to harmless antigens such as commensal bacteria and food proteins is the induction of tolerance, which ensures that effector T cell responses are not generated inappropriately. In the case of food proteins, this tolerance affects both systemic and local immune responses, a phenomenon known as “oral tolerance” (Pabst and Mowat, 2012). The generalised effects of oral tolerance may reflect the fact that orally administered proteins may disseminate via the blood and lymph into systemic lymphoid tissue, as well as the liver, which receives blood from the intestine via the portal vein (Thomson and Knolle, 2010). In contrast, tolerance to commensal bacteria only affects mucosal immunity and the systemic immune system remains ignorant of the antigens. In addition, IgA production is stimulated in response to commensal bacteria, but not food proteins (Pabst and Mowat, 2012;

Pabst, 2012). The exact mechanisms of tolerance induced in the intestine remain unclear, with a number of different mechanisms being implicated, including the induction of T_{Reg} cells, clonal deletion and T cell anergy, with each mechanism possibly related to the nature and dose of the antigen (Chen and Weiner, 1996; Chen et al., 1995; Hadis et al., 2011; Pabst and Mowat, 2012).

When the intestinal immune system fails to induce tolerance, inappropriate inflammatory reactions against food proteins and commensal bacteria can lead to disorders such as coeliac disease, food allergies and inflammatory bowel diseases. There are two main forms of IBD, Crohn's disease (CD) and ulcerative colitis (UC), both of which are chronic, relapsing and remitting diseases which result in the loss of intestinal architecture and tissue destruction (Baumgart and Sandborn, 2007). Crohn's disease has become a major health problem in industrialised countries, being difficult to treat and with a rapidly increasing incidence in recent years (Lakatos, 2006; Molodecky et al., 2012). There is considerable evidence that IBD results from aberrant responses to the host microbiota in genetically susceptible individuals (Xavier and Podolsky, 2007). Many of the factors that underlie susceptibility to IBD are related to mechanisms of local bacterial defence, including barrier defects (Xavier and Podolsky, 2007), defects in Paneth cells and anti-microbial peptide production (Wehkamp et al., 2005), autophagy (Henry et al., 2009) and PRRs such as Nod2 (Kobayashi et al., 2005). These associations are underlined by the genetic linkage between Crohn's disease and polymorphism in the IL23R (Duerr et al., 2006; Kobayashi et al., 2008; Sarra et al., 2010), as well as the evidence that T_h17 responses are important for the pathology. Furthermore, murine models of IBD cannot be established in germ-free animals (Sellon et al., 1998) and can be transferred by microbes from the gut of an IBD mouse into a healthy animal (Garrett et al., 2007) and as a result both antibiotic and probiotic treatments have been used to treat IBD (Gionchetti et al., 2003; Khan et al., 2011). How the intestinal immune system decides between inducing tolerance or active immunity remains a matter of debate. However it seems very likely that dendritic cells play a central role, being the principal cells in the immune system which can distinguish between harmless and pathogenic antigens and translate this information into appropriate priming of naïve T cells. Which intestinal DCs are involved in these responses, whether different DC subsets are required for each

aspect of immunity and how they react to different kinds of antigen are among the questions I sought to address in my project.

1.4.3 Intestinal MPs

Mononuclear phagocytes play several important roles in maintaining the balance between tolerance and immunity in the intestine. DCs and mϕs are abundant in the mucosa, while PPs and ILFs also contain many DCs as well as some mϕs. As mentioned above, DCs are also present in the MLNs, where they either derive from the blood or have migrated to the MLNs from the intestine. Contrary to this, mϕs are absent from the steady state MLNs. Defining the exact roles of these cell types has been difficult especially in the mucosa where the use of overlapping markers has created many problems.

The intestinal LP was one of the first non-lymphoid tissues in which $MHCII^+$ cells with classical DC morphology were identified by immunohistochemistry (Mayrhofer et al., 1983). The idea that these may be involved with inducing antigen specific responses was supported by the identification of cells with a similar appearance in intestinal lymph from rats (Pugh et al., 1983). However it was soon realised that intestinal mϕs were also $MHCII^+$ (Janossy et al., 1986; Mayrhofer et al., 1983; Spencer et al., 1987), meaning that mere expression of MHCII could not discriminate between DC and mϕs.

When CD11c became established as the 'definitive' marker of DCs, this also became the convention for identifying these cells in the intestinal LP. Indeed from the late 1990s onwards, DCs were routinely identified solely on the basis of CD11c surface expression, with MHCII expression being largely ignored (Chirdo et al., 2005; Monteleone et al., 2008; Rescigno et al., 2001). Following the identification of $CD11b^+$ and $CD11b^-$ DC subsets, it became routine for co-expression of CD11c and CD11b to be used for the identification of LP DCs, and many groups have used this approach until fairly recently (Anjuère et al., 2004; Chirdo et al., 2005; Denning et al., 2007; 2011; Jang et al., 2006; Krajina et al., 2003). The development of more sophisticated multi-parameter flow cytometers has now shown that several other myeloid cells in the LP express CD11b, and many of these can co-express CD11c, such as mϕs and eosinophils (Bain et al.,

2013; Mowat and Bain, 2010; Pabst and Bernhardt, 2010). As discussed in more detail below, it is also now clear that the CD8α^+ DCs are present in the villous LP and not mere contaminants of intestinal lymphoid structures (Cerovic et al., 2013) as previously assumed (Anjuère et al., 1999; Bogunovic et al., 2009; Vremec et al., 1997; 2000; 1992).

A major advance in the identification of LP DCs came from the identification of CD103 (OX-62), which was suggested to be a specific marker of intestinal DCs. Although CD103 was first identified as a marker of intraepithelial lymphocytes (IELs), early work found CD103 to be expressed on DCs migrating in rat intestinal lymph (Brenan and Puklavec, 1992; Kilshaw, 1993). It was later shown to identify a proportion of CD11c$^+$ DCs in the LP and MLN, which induced gut homing receptors on interacting naïve T cells. Furthermore these DCs were also shown to play a role in the regulation of T cell mediated colitis (Annacker et al., 2005; Johansson-Lindbom et al., 2005), by driving T_{Reg} responses (Coombes et al., 2007; Sun et al., 2007). CD103$^+$ DCs in the intestine have been shown to consist of CD11b$^+$ and CD11b$^-$ fractions with the latter being outnumbered by CD103$^+$CD11b$^+$ DCs which appear to be specific to the intestine (Fujimoto et al., 2011; Sun et al., 2007).

The inadequacy of using CD11c and MHCII to specifically identify DCs was exemplified by reports that a population of LP 'DCs' could extend dendrites across the epithelium to sample antigen in the lumen (Rescigno et al., 2001). These MPs were shown to express the chemokine receptor CX3CR1 and CD11b, but not CD103, and as such were classified as CD103$^-$ DC (Niess et al., 2005; Vallon-Eberhard et al., 2006). Thus it was proposed that there were 3 distinct populations of intestinal DCs, CD103$^+$CD11b$^-$, CD103$^+$CD11b$^+$ and CD103$^-$CD11b$^+$ DCs (Table 1.5) (Bogunovic et al., 2009; Varol et al., 2009). Additional characterisation of these MP populations found the two CD103$^+$ MP populations to derive from pre-DCs in an Flt3L-dependent manner, with the CD103$^+$CD11b$^+$ DCs showing an additional dependence on CSF-2 (Bogunovic et al., 2009; Greter et al., 2012). Contrary to this, the CD103$^-$ DCs were reported to derived from Ly6C^{hi} monocytes in a CSF-1-dependent, Flt3L-independent manner (Bogunovic et al., 2009; Greter et al., 2012; Varol et al., 2009). However work published at the same time from the Pabst and Agace groups challenged the lineage designation of CX3CR1-

expressing cells (Schulz et al., 2009). Consistent with their derivation from pre-DCs and dependence upon Flt3L, Schulz et al. showed that the $CD103^+$ cells appeared to be genuine DCs, migrating in lymph and inducing proliferation of naïve T cells (Schulz et al., 2009), a finding confirmed by several groups since (Denning et al., 2011; Fujimoto et al., 2011; Uematsu et al., 2008). In direct contrast, the $CD103^-CX3CR1^+$ cells were not found in lymph and could not induce the proliferation of naïve T cells (Schulz et al., 2009). These findings coupled with their expression of F4/80 and CD115 resulted in these cells being redefined as a population of $CD11c^+MHCII^+$ mϕs (Schulz et al., 2009).

Interestingly, Schulz and colleagues also found that the $CD103^-CX3CR1^+$ MP population could be further divided on the basis of levels of CX3CR1 expression into a population of $CX3CR1^{int}$ and $CX3CR1^{hi}$ cells. Although they concluded that both these were likely to be tissue-resident mϕs, the $CD103^-CX3CR1^{int}$ cells, unlike their $CD103^-CX3CR1^{hi}$ counterparts were slightly increased following exogenous administration of Flt3L and were able to induce some proliferation of naïve T cells although at a much lower level than those induced by the genuine $CD103^+$ DCs (Schulz et al., 2009). These cells were not characterised further and several subsequent studies have grouped all $CD103^-CX3CR1$-expressing MPs together. Other studies, including those from our lab, have suggested that the $CX3CR1^{int}$ cells comprise monocytes maturing into tissue resident $CX3CR1^{hi}$ mϕs as well as a minor putative population of DCs (Bain et al., 2013; Rivollier et al., 2012; Tamoutounour et al., 2012). In addition, preliminary work from the Milling group had identified $CD103^-$ DCs in pseudo-afferent intestinal lymph. This was the position when I began my project, with considerable confusion over how to identify DCs and mϕs in the LP. In particular, there was no definitive evidence for a *bona fide* population of $CD103^-$ DCs, therefore this was the principal aim of my work. To do this, I adopted phenotyping strategies that had been used in our lab in conjunction with collaborators in Bernard Malissen's laboratory in Marseille which had found CD64 (FcγRI) and F4/80 expression to specifically mark mϕs amongst the $CD11c^+MHCII^+$ intestinal MPs (Bain et al., 2013; Tamoutounour et al., 2012).

Table 1.5: Intestinal Mononuclear Phagocyte Subsets as defined in 2009

MP Subset	Phenotype	Precursor	Growth Factor
$CD103^+CD11b^+$	$CD11c^+$, $MHCII^+$, $F4/80^-$, $CX3CR1^-$, $SIRP\alpha^+$, $XCR1^-$	Pre-DCs	Flt3L, CSF-2
$CD103^+CD11b^-$	$CD11c^+$, $MHCII^+$, $F4/80^-$, $CX3CR1^-$, $SIRP\alpha^-$, $XCR1^+$	Pre-DCs	Flt3L
$CD103^-CD11b^+$	$SIRP\alpha^+$, $XCR1^-$	Monocytes	CSF-1

1.4.4 Functions of Intestinal DCs

1.4.4.1 Antigen Acquisition by Intestinal DCs

As discussed above, DCs are involved in acquiring antigen from their local environment and transporting it to the draining lymph nodes, where they initiate adaptive immune responses. In the intestine, one way this could occur is that DCs in the SED of PPs may acquire antigen and subsequently migrate to the T cell areas of the PPs or potentially migrate in lymph to the MLNs (Mowat, 2003). However, the evidence discussed above that PPs may be dispensable for the induction of immunity and tolerance especially to soluble antigen suggests that additional antigen entry must occur across the villous epithelium into the LP. How this happens and what cells are involved are largely unknown. Pathogenic microbes may achieve this by invading the epithelium rendering them susceptible to engulfment by APCs in the LP. Additionally, M cells have been described in the villous epithelium (Jang et al., 2004), however these are likely to be rare occurrences. The suggestions that $CX3CR1^+CD11c^+MHCII^+$ cells could extend transepithelial dendrites (TEDs) through tight junctions in the epithelium to capture luminal bacteria seemed to offer one possible explanation (Chieppa et al., 2006; Niess et al., 2005; Rescigno et al., 2001). However, these TED-generating DCs were never shown to migrate to MLNs or present antigen and, as discussed above, most CX3CR1-expressing cells in the intestine are considered to be macrophages rather than DCs (Schulz et al., 2009). In addition, it is even uncertain if TEDs are

required because although Niess and coworkers demonstrated that CX3CR1-dependent TEDs were involved in the uptake of invasion-deficient Salmonella (Niess et al., 2005), invasive *Salmonella* usually gain entry to the intestine via M cells in PPs and ILFs (Carter et al., 1975; Halle et al., 2007; Jones et al., 1994) and CX3CR1-dependent TEDs were not required for uptake of such invasive strains. In the same vein, non-invasive *Aspergillus* spores were also found to gain access to the LP in a TED-independent fashion. However formation of TEDs has only been shown to occur in the terminal ileum and only in some strains of mice (Vallon-Eberhard et al., 2006).

More recently, two multi-photon *in vivo* microscopy studies attempted to address this issue using more rigorous approaches to identify the APCs involved. Using $CD11c^{+/YFP}$ x $CX3CR1^{+/GFP}$ mice in which $CX3CR1^{+}CD11c^{+}$ cells are assumed to be mϕs and $CX3CR1^{-}CD11c^{+}$ cells are assumed to be DCs, two studies failed to detect CX3CR1-expressing intestinal MPs extending TEDs into the lumen (Farache et al., 2013; McDole et al., 2012). Instead McDole and coworkers identified goblet cell associated antigen passages (GAPs) that appeared to pass soluble dextran and proteins from the lumen to underlying $GFP^{-}YFP^{hi}$ ($CD11c^{+}CX3CR1^{-}$) cells. This route is unlikely to be involved in the uptake of particulate antigen such as bacteria, as beads >0.02μm diameter could not transit through GAPs (McDole et al., 2012). In contrast, Farache and colleagues could not find a role for GAPs, but noted a small population of $CD103^{+}$ DCs present within the epithelium which could extend dendrites into the lumen. Notably this phenomenon was increased during *Salmonella* infection (Farache et al., 2013). Although these latter findings need to be confirmed, they are in agreement with previous reports suggesting that low numbers of $CD103^{+}$ DCs were present in the steady state epithelium and could increase during inflammation (Anjuère et al., 1999; Bogunovic et al., 2009; Cruickshank et al., 2009). Interestingly however, the idea that mϕs may be involved in the initial capture of soluble antigen from the lumen is supported by an earlier report suggesting $CX3CR1^{+}$ MPs preferentially take up orally administered soluble antigen (Schulz et al., 2009). Clearly more work is required to determine the nature of cells taking up antigen and how DCs acquire antigen for subsequent presentation to naïve T cells.

1.4.4.2 Migration of Intestinal DC to MLNs

After acquiring antigen, intestinal DCs migrate to the draining MLNs in a CCR7 dependent manner (Forster et al., 1999; Jang et al., 2006; Johansson-Lindbom et al., 2005; Worbs et al., 2006) carrying both soluble and particulate antigen (Bogunovic et al., 2009; Jaensson et al., 2008; Macpherson and Uhr, 2004). Antigen laden intestinal DCs were first demonstrated to be present in pseudo-afferent lymph of rats and pigs which had undergone mesenteric lymphadenectomy, followed by thoracic duct cannulation (Bimczok et al., 2005; Cerovic et al., 2009; Liu and MacPherson, 1991; Macpherson and Uhr, 2004; Mayrhofer et al., 1983; 1986; Milling et al., 2010; Pugh et al., 1983; Yrlid et al., 2006b) and more recently, these findings have been extended to mice (Bain et al., 2013; Cerovic et al., 2013; Schulz et al., 2009). The earliest studies of these in rats used CD103 to identify them, thus providing the first evidence that migration and APC activity were intrinsic properties of $CD103^+$ DCs in the gut (Brenan and Puklavec, 1992). Their importance was underlined by studies which showed similar DCs in the MLNs and that the generation of gut tropic T cells in the MLNs after oral administration of antigen was CCR7 dependent (Johansson-Lindbom et al., 2005). As $CD103^+$ DCs are selectively absent from $CCR7^{-/-}$ MLNs, these results indicate that migration of intestinal DCs is crucial in establishing immune responses (Worbs et al., 2006). Further studies using BrdU incorporation showed that the accumulation of $BrdU^+CD103^+$ DCs in the MLN was delayed compared with that in the LP, suggesting they were derived from the LP (Jaensson et al., 2008). *Ex vivo* confocal imaging of intestinal lymphatics and sampling of intestinal draining lymph then identified $CD103^+$ DCs directly as the major migratory DC population in intestinal lymph (Schulz et al., 2009). By adapting the lymph cannulation technique to mice, Cerovic and colleagues recently confirmed that $CD103^+$ DCs are the major population in intestinal lymph and that the $CX3CR1^{hi}$ MPs do not migrate, consistent with their lack of CCR7 expression and classification as tissue-resident mϕs (Cerovic et al., 2013). However, their work also showed a population of $CD103^-CX3CR1^{int}$ MPs which in addition to migrating in lymph, had APC capabilities and were Flt3L dependent demonstrating them to be *bona fide* DCs (Cerovic et al., 2013). This finding suggests a similar DC population should also be present in the LP and thus one aim of my project was to investigate their presence. Intriguingly, the migration of DCs from the LP appears

to be a constitutive process occurring in the absence of both overt inflammation and commensal bacteria and MyD88-signalling (Wilson et al., 2008). However, the number of DCs migrating can be increased following TLR ligation or TNFα (Turnbull et al., 2005; Yrlid et al., 2006b; 2006a).

1.4.4.3 Presentation of Antigen to T Cells

As discussed above the MLNs are essential for the development of both immunity and tolerance in the intestine (Mowat, 2003; Spahn et al., 2002; Worbs et al., 2006) and the ultimate fate of DCs migrating from the SI LP is the MLN, as few DCs are detectable in the thoracic duct without prior mesenteric lymphadenectomy (Cerovic et al., 2013). $CD103^+$ DCs are the only DC subset in the MLNs of mice fed soluble antigen that can induce antigen specific proliferation of $CD4^+$ and $CD8^+$ T cells *ex vivo* (Coombes et al., 2007; Jaensson et al., 2008). However as noted above, it has proved difficult to show these DCs taking up antigen directly from the lumen and it remains unclear how and where they first acquire antigen for presentation in the MLN.

One of the unique features of $CD103^+$ DCs in the intestine is their ability to generate RA from dietary vitamin A (Coombes et al., 2007; Iwata et al., 2004; Sun et al., 2007). This is most marked with $CD103^+$ DCs from the LP and MLNs, however it is also found with $CD103^+$ DCs isolated from the PPs and $CD103^+$ LP, MLN and PP DCs have been shown to express both *Aldh1a1* and *Aldh1a2* (Coombes et al., 2007; Yokota et al., 2009) and have considerable ALDH activity as assessed using the commercially available ALDEFLUOR assay (Schulz et al., 2009; Yokota et al., 2009). Importantly, $CD103^-$ MPs from the gut do not share this property and typically nor do $CD103^+$ DCs from other sites, however it can be upregulated in other DCs by CSF-2, IL4 and TLR signalling (Yokota et al., 2009). However, more recently, $CD103^+$ and $CD103^-$ DCs from the lung have also been reported to have ALDEFLUOR activity and be capable of inducing gut homing molecules on naïve T cells, suggesting some overlap between mucosal surfaces (Ruane et al., 2013). There also appears to be a feedback loop in which ALDH activity requires the presence of vitamin A, either directly from the diet or after excretion from the liver in bile (Jaensson-Gyllenbäck et al., 2011; Molenaar et al., 2011). Importantly, there may also be other sources of RA in the intestine,

including epithelial cells (Bhat, 1998; Lampen et al., 2000) and mesenteric stromal cells (Hammerschmidt et al., 2008; Molenaar et al., 2011). These cells themselves can induce gut homing molecule expression on naïve T cells (Agace and Persson, 2012; Annacker et al., 2005; Hammerschmidt et al., 2008; Jaensson et al., 2008; Jaensson-Gyllenbäck et al., 2011; Johansson-Lindbom et al., 2005; Svensson et al., 2008) and may cooperate with migratory DCs in this.

The other function of $CD103^+$ intestinal DCs, which was identified in early studies, was a preferential ability to drive the differentiation of $FoxP3^+$ T_{Reg} cells under steady state conditions. Again, this function was restricted to this subset from the gut and was related to the production of RA which cooperated with exogenous TGFβ (Coombes et al., 2007; Sun et al., 2007). Many cells in the intestine can produce TGFβ, including DCs. However, TGFβ is produced in an inactive form that has to be cleaved to allow it to mediate its biological effects (Annes et al., 2003). One molecule that can activate TGFβ is the integrin αvβ8 (Mu et al., 2002). Interestingly $CD103^+$ DCs express αvβ8 at high levels and mice that lack integrin αvβ8 expression on $CD11c^+$ or $CD11b^+$ cells have reduced numbers of $FoxP3^+$ T_{Reg} cells and develop intestinal pathology (Lacy-Hulbert et al., 2007; Travis et al., 2007; Worthington et al., 2011).

As a result of these studies, a paradigm has arisen that the principal function of $CD103^+$ DCs in the steady state intestine is the generation of gut homing T_{Reg} cells and that this is how tolerance is maintained. However, the contributions of each $CD103^+$ DC subset to T_{Reg} cell induction remain unclear. $Batf3^{-/-}$ mice, which lack intestinal $CD103^+CD11b^-$ DCs, have normal numbers of intestinal $FoxP3^+$ T_{Reg} cells (Edelson et al., 2010), as do mice with a severe and selective reduction in migratory MLN $CD103^+CD11b^+$ DCs (Lewis et al., 2011). Although this apparent contradiction could reflect that these studies did not distinguish natural thymus-derived T_{Reg} cells (nT_{Reg}) from intestinally induced T_{Reg} cells (iT_{Reg}) and the majority of T_{Reg} cells in the intestine represent nT_{Reg} cells (Cebula et al., 2013; Weiss et al., 2012), a recent study by the Agace lab, demonstrated that mice with a significant reduction in the $CD103^+CD11b^+$ DC population had normal proportions of both natural and induced T_{Reg} cells (Persson et al., 2013b). As I was finalising this thesis, a report came out demonstrating a

degree of redundancy between the $CD103^+$ intestinal DC subsets and effects on T_{Reg} populations were only apparent following deletion of both $CD103^+$ DC subsets (Welty et al., 2013). In direct contrast to these results implicating $CD103^+$ DCs as the tolerogenic APCs, two reports from Denning and colleagues have suggested that mϕs are responsible for priming T_{Reg} cells (Denning et al., 2007; 2011). However, given the inability of these cells to migrate to the draining MLN and the fact that the intestinal mucosa is devoid of naïve T cells, it is difficult to see where this would be physiologically relevant. One explanation for this apparent discrepancy could come from studies from the Pabst lab showing that IL10 producing mϕs in the LP are crucial for the *in situ* secondary expansion of $FoxP3^+$ T_{Reg} cells which were primed initially by DCs in the MLNs (Hadis et al., 2011). Thus this may be site-specific cooperation between intestinal MPs in immune regulation.

Considerable research effort has concentrated on intestinal $CD103^+$ DCs as mediators of tolerance, but the APCs involved in active immunity in the intestine are less well characterised. Because it was assumed that $CD103^+$ DCs were intrinsically tolerogenic, it was hypothesised that a separate population of $CD103^-$ pro-inflammatory DCs of monocyte-origin may exist in the LP (Rivollier et al., 2012; Siddiqui et al., 2010; Varol et al., 2009; 2007; Zigmond et al., 2012). However, these studies were carried out using phenotyping strategies which could not discriminate DCs from mϕs (Rivollier et al., 2012; Varol et al., 2007; 2009). Thus one aim of this thesis was to determine if a population of genuine $CD103^-$ DCs exist in the intestinal LP and explore their functions and origins. While the idea of distinct subsets of cells inducing either tolerance or active immunity is attractive, the presence of a $CD103^-$ DC population would not fit the current paradigm that only intestinal $CD103^+$ DCs can induce gut tropisms, as the generation of intestinal effector T cells would require the induction of the gut homing molecules CCR9 and $\alpha4\beta7$ expression on the T cells.

An alternative possibility is that the $CD103^+$ DCs are not inherently tolerogenic, but instead can adapt to the local environment to induce either tolerance or protective immunity as required. During T-cell mediated colitis, $CD103^+$ MLN DCs have reduced ability to drive the differentiation of T_{Reg} cells, a

finding that correlated with decreased ALDH expression and activity and instead $CD103^+$ DCs during inflammation induced T_h1 and T_h17 responses (Laffont et al., 2010). Moreover, it appears that the individual subsets of intestinal $CD103^+$ DCs may play distinct roles in promoting different arms of the adaptive immune response even in the steady state. *In vitro* studies indicate that both $CD103^+CD11b^+$ and $CD103^+CD11b^-$ DCs can drive IFNγ production from $CD4^+$ T cells (Fujimoto et al., 2011), while $CD103^+CD11b^-$ SI DCs excel at priming $CD8^+$ T cells (Cerovic et al., 2013; Fujimoto et al., 2011). Conversely $CD103^+CD11b^+$ DCs appear to be more efficient at inducing T_h17 polarization than their $CD103^+CD11b^-$ counterparts (Denning et al., 2011; Fujimoto et al., 2011; Lewis et al., 2011; Persson et al., 2013b; Schlitzer et al., 2013; Uematsu et al., 2008), and it is suggested that this reflects their production of IL6 (Persson et al., 2013b). Both properties are enhanced by ligation of TLRs including TLR2, TLR5 and TLR9 (Fujimoto et al., 2011; Persson et al., 2013b; Uematsu et al., 2008). Thus $CD103^+$ DCs may be able to become pro-inflammatory under some conditions and given that $CD103^+CD11b^+$ and $CD103^+CD11b^-$ DCs express a partially distinct array of TLRs (Fujimoto et al., 2011; Kinnebrew et al., 2012; Miller et al., 2012; Uematsu et al., 2008), they may react differently depending on the context of their immediate environment. In my project, I investigated the T cell priming properties of intestinal DC subsets *in vitro* and *in vivo*.

1.4.5 DC Conditioning Factors in the Gut

Intestinal DCs have many unusual properties including the expression of CD103 on $CD11b^+$ DCs and the production of retinoic acid (RA). Most evidence suggests that these properties result from the local 'conditioning' effect on DC precursors and mature DCs in the mucosa and a number of such factors have been identified. These include dietary constituents and neuroendocrine factors, as well as factors produced by intestinal epithelial cells (IECs), luminal bacteria, other leukocytes and stromal cells (Figure 1.7).

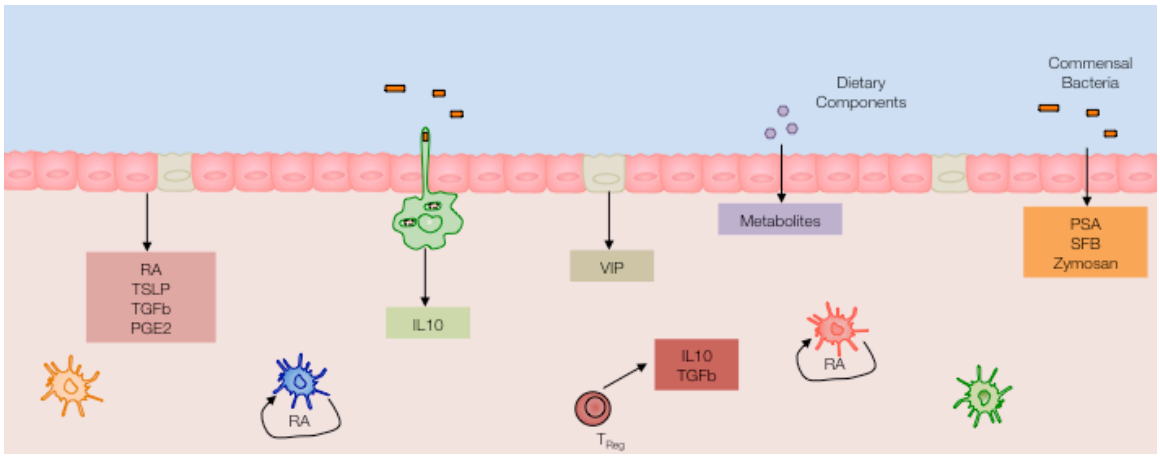

Figure 1.7: Conditioning of DCs by the intestinal environment
A number of different factors might act in concert to condition mucosal DCs with their unique properties. These include dietary metabolites, microbial-derived products, epithelial cell factors, neuropeptides produced by enteroendocrine cells, IL10 from $CX3CR1^{hi}$ mϕs and IL10 and TGFβ from gut-homing T_{Reg} cells. Adapted from (Scott et al., 2011).

1.4.5.1 Epithelial Cell Derived and Other Cytokines

DCs are situated close to IECs and the interaction between these two cell types is thought to be integral for the conditioning of DCs to their local environment. The first evidence for this came from co-culture studies with epithelial cells and human monocyte derived DCs (mo-DCs), whereby epithelial cells treated with different bacterial strains produced different pro-inflammatory mediators which modulated mo-DC function (Rimoldi et al., 2005a). Later, IEC-specific knock out (KO) of NF-kB signalling was reported to result in the dysregulated production of pro-inflammatory cytokines by DCs and the subsequent development of intestinal inflammation (Nenci et al., 2007; Zaph et al., 2007). Exactly how IECs modulate DCs is unclear but one mechanism is through their secretion of several immunoregulatory factors, such as thymic stromal lymphopoietin (TSLP), TGFβ and prostaglandin E2. Perhaps the best characterised of these is TSLP, which although constitutively expressed can be upregulated in response to infection, inflammation and tissue injury (Allakhverdi et al., 2007; Bogiatzi et al., 2007; Kato et al., 2007; Lee and Ziegler, 2007; Li et al., 2006; Rimoldi et al., 2005a; Zaph et al., 2007). TSLP appears to mediate its effects through modulating the expression of pro-inflammatory cytokines by DCs subsequently affecting their ability to induce naïve T cell polarisation. Consistent with the role of TSLP in the skin and lung (Holgate, 2007), IEC-derived TSLP has been shown to condition DCs to drive T_h2-like anti-inflammatory T cell differentiation, while limiting their production of IL12

(Rimoldi et al., 2005a; 2005b; Zeuthen et al., 2008), Furthermore, deletion of the TSLP receptor in mice leads to overexpression of IL12/IL23p40 and the inability to induce protective T_h2 responses to *Trichuris muris* infection (Zaph et al., 2007). Additionally, TSLP drives DC-dependent differentiation of nT_{Reg} cells in thymus (Watanabe et al., 2005), as well as inducing CD103 expression by monocyte-derived DCs, which then have enhanced ability to induce $FoxP3^+$ T_{Reg} differentiation (Iliev et al., 2009a; 2009b). Interestingly, DCs themselves may also produce TSLP in response to MyD88 signalling controlling T cell polarisation (Spadoni et al., 2012).

In addition to TSLP, TGFβ production by IECs contributes to the ability of these cells to condition DCs to drive $FoxP3^+$ T_{Reg} cell differentiation (Iliev et al., 2009a; 2009b). However, as mentioned above, several other cell types may also contribute to TGFβ production *in vivo*, including $CD4^+$ T cells (Fukaura et al., 1996; Gonnella et al., 1998) and macrophages (Gonnella et al., 1998; Weber et al., 2011).

1.4.5.2 Intestinal microbes

Although effects of the microbiota on immune function are well known and these can influence the differentiation of individual T cell subsets including T_{Reg} and T_h17 cells (Ivanov et al., 2009; 2008), very few of these studies have shown that this is the result of altered DC behaviour. Examples of direct effects on DCs come from studies where DCs isolated from mice sourced from different vendors, and therefore with distinct microbiota, induce differential T cell responses following *ex vivo* co-culture (Denning et al., 2011). Similarly, microbiota signals through TLR ligation can induce expression of the enzymes required for synthesis of RA (retinal dehydrogenases) by DCs, thus conferring upon the DC the ability to induce gut homing molecules on differentiating T cells (Johansson-Lindbom et al., 2005). This idea is supported by the fact that $MyD88^{-/-}$ mice express lower levels of retinal dehydrogenases compared with WT controls (Wang et al., 2011). Furthermore, several commensal *Bacteroides* and *Bifidobacteria* strains can directly induce a tolerogenic phenotype on monocyte-derived DCs (Baba et al., 2008). Zymosan, a component of yeast cell wall recognised through TLR2 and dectin-1, shapes the immune response by inducing DCs to produce IL10 and express *Aldh1a2*,

contributing to the ability of intestinal DCs to drive T_{Reg} cell differentiation (Dillon et al., 2006; Manicassamy et al., 2009; Zhou et al., 2004).

The presence of specific microbes can also contribute to the activation state of DCs. For example, polysaccharide A (PSA) from *Bacteroides fragilis*, associates with $CD11c^+$ cells in the MLN driving a mixture of T_h1 systemic responses and IL-10 producing T_{Reg} cells in the colonic LP (Mazmanian et al., 2005). Segmented filamentous bacteria (SFB) have recently been shown to induce T_h17 and inhibit $FoxP3^+$ T_{Reg} cell differentiation in the mucosa (Ivanov et al., 2009) presumably through its effects on DCs and mϕs in the LP which have been shown to regulate T_h17 differentiation and maintenance (Denning et al., 2011; Lewis et al., 2011; Persson et al., 2013b; Satpathy et al., 2013; Schlitzer et al., 2013; Shaw et al., 2012) although exactly how SFB affects the MPs remains to be determined.

1.4.5.3 Role of dietary constituents

Intestinal DCs are continuously exposed to foreign dietary constituents which may have immunomodulatory properties. As discussed earlier, vitamin A is perhaps the most studied of these, and its only source in mammals is from the diet. $CD103^+$ DCs themselves have the ability to metabolise vitamin A to RA and this has been linked to their ability to induce $FoxP3^+$ T_{Reg} cells (Coombes et al., 2007; Jaensson et al., 2008; Johansson-Lindbom and Agace, 2007; Johansson-Lindbom et al., 2005; Molenaar et al., 2011; Sun et al., 2007). Indeed, depletion of vitamin A from the diet impairs the ability of MLN $CD103^+$ DCs to induce T_{Reg} cell differentiation and imprint gut homing receptors on lymphocytes (Jaensson-Gyllenbäck et al., 2011; Molenaar et al., 2011). Interestingly, persistent infection with *T. muris* has recently been shown to abrogate the capacity of intestinal MPs to metabolise vitamin A until clearance of the infection, suggesting that the generation of RA is not required for the efficient clearance of this pathogen (Hurst and Else, 2013). Other cells including intestinal epithelial cells and MLN stromal cells are also likely to contribute to vitamin A metabolism (Agace and Persson, 2012).

Tryptophan, which is the substrate for indoleamine 2,3-dioxygenase (IDO), is also found in the diet. Removal of this hydrophobic amino acid from the

environment, through its metabolism into kyneurenines or tryptophan starvation can inhibit the generation of effector T cells instead promoting T_{Reg} cell differentiation (Belladonna et al., 2006; Fallarino et al., 2006b; 2006a). Similarly to retinal dehydrogenases, IDO is produced by $CD103^+$ DCs (Matteoli et al., 2010). Other dietary metabolites which have immunomodulatory effects, include prostaglandins, which are derived enzymatically from fatty acids. These lipid mediators activate the anti-inflammatory peroxisome-proliferative-activated receptor-γ (PPARγ) which is expressed by DCs, in addition to a variety of other cells types, augmenting RA production in the ligated DCs (Szatmari et al., 2006; Varga and Nagy, 2008). Additionally ligands of the aryl hydrocarbon receptor (AhR), including tryptophan, bilirubin, lipoxin A4 and prostaglandin G can induce IL6 production from $CD103^+$ DCs and promote T_h17 cell differentiation (Chmill et al., 2010). Furthermore, curcumin, a spice that has a long history of medical use in India and Southeast Asia has been shown to modulate immune responses. Curcumin-treated DCs acquire a tolerogenic phenotype, expressing *aldh1a2*, producing IL-10 and inducing the differentiation of $FoxP3^+$ T_{Reg} (Bereswill et al., 2010; Cong et al., 2009).

1.4.5.4 Neuroendocrine pathways and mucosal DC function

One of the best-described examples of neuropeptide-regulation of the immune system is vasoactive intestinal peptide (VIP). This product of intestinal enteroendocrine cells is a vasodilator and regulator of epithelial permeability. It is also produced by several immune cells and has anti-inflammatory properties (Bellinger et al., 1996). VIP suppresses LPS-induced CCR7 expression by DC, inducing IL10 production, preventing the establishment of an inflammatory immune response and promoting tolerance (Weng et al., 2007). Additionally, VIP-pulsed DCs preferentially induce naïve T cells to differentiate into T_{Reg} cells (Delgado et al., 2005a; 2005b) and in parallel VIP-treated DCs can prevent TNBS-induced colitis (Gonzalez-Rey and Delgado, 2006).

1.5 Signal Regulatory Protein α (SIRPα)

Many immune cells, including DCs, express inhibitory or activating receptors, which may determine or tune their functions. These include the signal inhibitory

regulatory protein family (SIRP) (Barclay and Brown, 2006), the CD200 receptor (CD200R) family (Gorczynski, 2012) and triggering receptors expressed by myeloid cells (TREM) (Colonna, 2003).

1.5.1 The SIRP Family

The SIRP family consists of three proteins, SIRPα, SIRPβ and SIRPγ, which all have similar extracellular regions, comprising three immunoglobulin superfamily (IgSF) domains (Nakaishi et al., 2008) (Fig.1.8). SIRPα, which is also known as CD172a, SHPS1, P84 or PTPNS1, was the first member of the family to be discovered. It is an inhibitory signalling receptor expressed predominantly by myeloid cells including $CD11b^+$ DCs, mϕs, eosinophils, monocytes and neutrophils. It is also found on neuronal cells (Adams et al., 1998; Fujioka et al., 1996; Kharitonenkov et al., 1997; Yamao et al., 1997). SIRPα is particularly relevant to intestinal DCs, since it can be used as a marker to distinguish between the two populations of $CD103^+$ DCs in the intestine of various species including mice, pigs and humans (Bimczok et al., 2005; Persson et al., 2013b; Saito et al., 2010).

SIRPα binds the ubiquitously expressed ligand, CD47, also known as integrin associated protein (IAP) (Vernon-Wilson et al., 2000), a transmembrane receptor with intracellular signalling capacity. The cytoplasmic region of SIRPα is highly conserved between mice, rats, pigs and humans, and contains an immunoreceptor tyrosine-based inhibition motif (ITIM), which is phosphorylated upon ligation of SIRPα. This leads to the recruitment of SH2-domain containing protein tyrosine phosphatase (SHP) 2 and SHP1, thereby inhibiting several tyrosine kinase dependent pathways (Barclay and Brown, 2006; Fujioka et al., 1996; Kharitonenkov et al., 1997; Ohnishi et al., 1996; Oshima et al., 2002; Veillette et al., 1998). SIRPβ does not bind CD47 and has the ability to relay a positive signal, as it associates with DAP12, a transmembrane adaptor protein containing an immunoreceptor tyrosine-based activation motif (ITAM) (Dietrich et al., 2000; Seiffert et al., 2001). The third member of the family, SIRPγ, is capable of binding CD47, but the strength of this binding is weaker than the SIRPα/CD47 interaction. In addition, SIRPγ also lacks an extensive cytoplasmic region and hence is unlikely to signal intracellularly (Brooke et al., 2004; Ichigotani et al.,

2000). As SIRPα expression is used to define DC populations in the gut, I concentrated on its potential role in regulating DC function in this thesis.

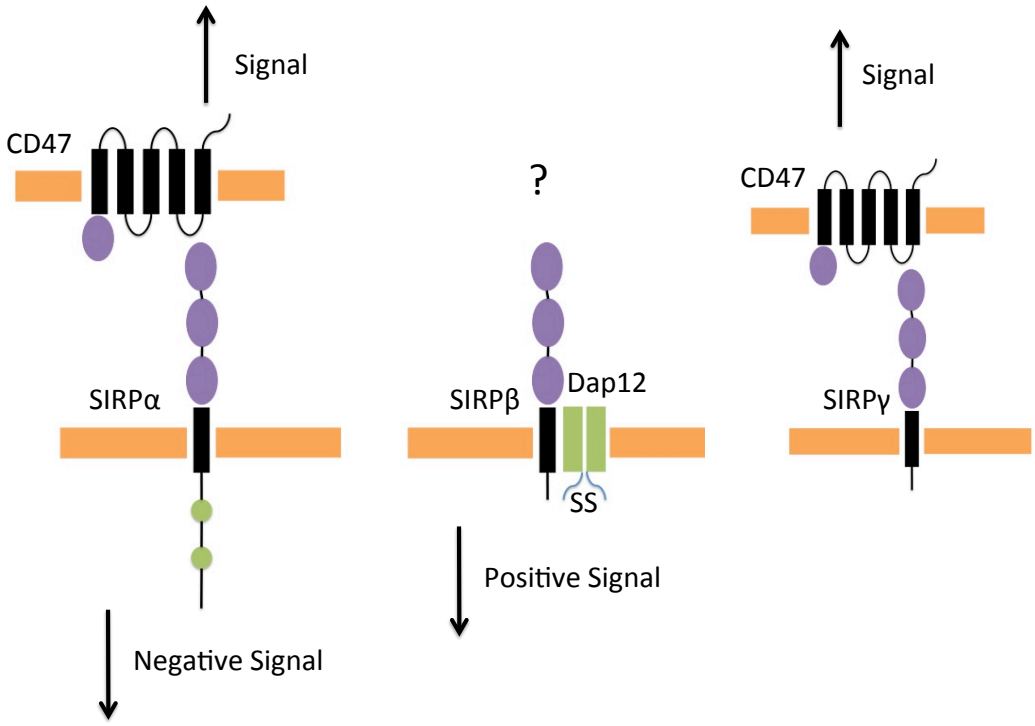

Figure 1.8: SIRP family of receptors with their associated ligands
Schematic representation of the SIRP family of signalling receptors depicting their extracellular regions and their signalling potentials. The IgSF domains are shown as purple ovals. CD47 contains one IgSF domains. Cartoon also demonstrates the bidirectional signalling of SIRPα through its interaction with CD47.

1.5.2 SIRPα Ligands

As detailed above, the predominant ligand for SIRPα is CD47, named for its ability to associate with integrins at the cell surface. CD47 is a transmembrane receptor, with five transmembrane regions and a single IgSF extracellular domain (Nakaishi et al., 2008) (Fig.1.8). As well as triggering SIRPα signalling, ligation of CD47 also activates an intracellular signalling cascade, although the details of this pathway remain be fully characterised. In neurons, ligation of CD47 by SIRPα activates a member of the Rho family of GTP-binding proteins, but whether this is involved in CD47 function in the immune system remains to be seen (Matozaki et al., 2009; Murata et al., 2006). As a result, the interaction between SIRPα and CD47 can lead to bidirectional signalling. CD47 is expressed by many cell types

including haematopoietic cells such as lymphocytes, red blood cells, endothelial and epithelial cells (Matozaki et al., 2009) in most tissues, although the exact pattern of expression in the intestine remains to be examined and this represents one aim of this thesis.

SIRPα also binds to the lung surfactant proteins SP-A and SP-D (Gardai et al., 2003; Janssen et al., 2008), which belong to the collectin family containing a C-type carbohydrate-recognition (lectin) domain coupled to a collagen-like tail (Håkansson and Reid, 2000). These ligands outcompete CD47 for binding to SIRPα in the lung and it is thought that they may hold SIRPα in a constitutively phosphorylated state which prevents immune activation until such time as an inflammatory response is required. Release of the cytoplasmic domain of SIRPα and surfactant protein binding to Calreticulin/CD91 subsequently inducing the p38 pathway and immune stimulation (Gardai et al., 2003). SP-D expression has been reported in the intestine (Akiyama et al., 2002; Lin and Floros, 2002; Madsen et al., 2000; Soerensen et al., 2005), but the roles of the surfactant proteins in the intestine have not been addressed.

1.5.3 Functions of the SIRPα/CD47 interaction

The SIRPα/CD47 axis has been proposed to influence a number of biological processes including phagocytosis and the functions of both the central nervous and immune systems. Perhaps the best characterised function of SIRPα/CD47 interaction is as a 'don't eat me' signal, whereby CD47-expressing cells are recognised as self by SIRPα$^+$ mφs and phagocytosis is inhibited (Oldenborg et al., 2000; Olsson et al., 2007; Wang et al., 2007). As a result, CD47-deficient red blood cells are cleared much more quickly from the bloodstream compared with wild-type cells (Oldenborg et al., 2000). This phenomenon also has important implications for organ transplantation as human SIRPα does not recognise porcine CD47 and thus the use of porcine organs for transplants may be limited (Subramanian et al., 2006).

In addition to inhibiting the phagocytic activity of mφs (Oldenborg et al., 2000; Olsson et al., 2007; Wang et al., 2007), ligation of SIRPα induces nitric

oxide production from mϕs (Alblas et al., 2005; Bogdan, 2001), although it has also been reported to prevent TNFα production from human peripheral blood mononuclear cells (PBMCs) in response to a variety of pathogen products (Smith et al., 2003). Ligation of SIRPα also prevents the upregulation of co-stimulatory molecules and cytokine production following exposure of human DCs to *Staphlococcus aureus* cowan I strain (SAC) (Latour et al., 2001), while pre-treatment with either an anti-SIRPα mAb or ligating CD47-Fc fusion protein prevented the maturation of Langerhans cells in response to 2,4-dinitro-1-fluorobenzene (DNFB) or TNFα (Fukunaga et al., 2006). Ligation of CD47 on human DCs also resulted in the inhibition of human DC maturation in response to SAC, confirming the bidirectional role of this interaction (Demeure et al., 2000).

Despite the evidence suggesting a predominantly inhibitory role of SIRPα on individual cells, mice with a non-signalling truncated form of the cytoplasmic domain of SIRPα (SIRPα mt mice) are less susceptible to a wide variety of autoimmune diseases, including experimental autoimmune encephalomyelitis (EAE) (Tomizawa et al., 2007), collagen-induced arthritis (CIA) (Okuzawa et al., 2008), contact hypersensitivity (CHS) (Fukunaga et al., 2006; Motegi et al., 2008) and colitis resulting from IL10 deficiency (Kanazawa et al., 2010). In parallel, CD47KO mice are less susceptible to trinitrobenzene sulfonic acid (TNBS) induced colitis (Fortin et al., 2009), although they are more susceptible to *Escherchia coli* peritonitis (Lindberg et al., 1996). Several early studies suggested that SIRPα on DCs acted as a co-stimulatory molecule in the induction of proliferation and differentiation of naïve T cells (Latour et al., 2001; Tomizawa et al., 2007; Waclavicek et al., 1997). This may be particularly important for the generation of T_h17 effector cells, given the paucity of these cells in SIRPα mt mice during the aforementioned diseases and the associated protection of these mice from autoimmunity (Fortin et al., 2009; Fukunaga et al., 2006; Kanazawa et al., 2010; Okuzawa et al., 2008; Tomizawa et al., 2007). SIRPα/CD47 signalling has also been suggested to be required for the migration of DCs to draining LNs (Hagnerud et al., 2006; Raymond et al., 2009; Van et al., 2006), with SIRPα mt mice having reduced numbers of $SIRP\alpha^+CD11b^+$ DCs in the LNs compared with WT controls (Iwamura et al., 2010). However, others have suggested that impaired

survival may explain the reduced numbers of SIRPα^+ DCs observed in the skin and spleen of SIRPα mutant mice (Iwamura et al., 2010; Saito et al., 2010).

The precise role of the SIRPα/CD47 axis in regulating immune responses remains unclear and very little is known about how it might affect the intestine. As discussed above, SIRPα mutant and CD47KO mice appear to be less susceptible to various models of IBD and this has been associated with a reduced number of T_h17 cells (Fortin et al., 2009; Kanazawa et al., 2010). A further study has shown that CD47KO mice have reduced levels of intestinal IgA in response to orally administered antigen, but this did not result in any defect in their ability to induce oral tolerance to the protein (Westlund et al., 2011). However, these studies have not shown how SIRPα and CD47 signalling contributes to these phenotypes. In addition, the reports which associated IBD with the reduced numbers of T_h17 cells simply implicated a role for SIRPα^+CD11c$^+$ MPs which were also reduced in SIRPα mutant and CD47KO mice, but did not identify these cells more precisely (Fortin et al., 2009; Kanazawa et al., 2010). As both SIRPα and CD11c are also expressed by eosinophils and mϕs in the intestine, clearly further investigation is required, especially as SIRPα signalling has recently been implicated in intestinal eosinophil homeostasis (Verjan Garcia et al., 2011). While the more recent study by Westlund and colleagues published during my PhD suggested that CD47 signalling was involved in the homeostasis of well-defined CD103$^+$CD11b$^+$ DCs in the intestine and MLN (Westlund et al., 2011), these authors did not study the functional consequences of CD47 ablation on DCs or on the generation of T_h17 cells. Thus one of the aims of this thesis was to investigate the role of SIRPα and CD47 signalling in DC homeostasis and function in the intestine using more precise analytical methods.

1.6 Thesis Aims

It is evident that DCs play a fundamental role in maintaining the balance between tolerance and immunity in the intestine. Despite this, there is still considerable confusion regarding the identification of DCs in the gut, including how they can be distinguished from other CD11c-expressing cells such as mϕs and eosinophils. As a result, it has been difficult to determine exactly which population

of intestinal DCs are responsible for inducing different aspects of the immune response.

Therefore the main aims of this thesis were to first develop a strategy using multi-parameter flow cytometry which would allow the accurate identification of DCs in the intestine LP and MLN in the steady state. Having identified putative DC populations, I then set out to examine the ontogeny, kinetics and growth factor dependence of these cells, focussing on a novel population of *bona fide* $CD103^-$ DCs that I discovered in the steady state LP. I then examined the functions of the various DC subsets in terms of their ability to induce naïve T cell proliferation and polarisation. I also explored the role of the chemokine receptor CCR2 and SIRPα in regulating DC development and function.

Chapter 3 of this thesis introduces the heterogeneity of the intestinal mononuclear phagocyte system and describes how $CD103^+$ and $CD103^-$ DCs can be discriminated accurately from $CD11c^+MHCII^+$ intestinal mϕs on the basis of CD64 and zDC expression, and growth factor dependence. Having identified *bona fide* DC populations in the LP and MLNs, Chapter 4 goes on to assess the ontogeny of these cells using adoptive transfer of pre-DC and monocyte precursors. In Chapter 5, the proportions and numbers of these DC populations are examined during active immune responses, including DSS-induced colitis, post-operative ileus and *Citrobacter rodentium* infection. The aim of Chapter 6 was to determine the ability of each DC population to present antigen to naïve $CD4^+$ and $CD8^+$ T cells and induce their differentiation into regulatory or effector cell populations. In Chapter 7, I explored the role of the SIRPα/CD47 axis in regulating intestinal DC function and in Chapter 8, I examined how SIRPα and CD47 signalling contributed to the homeostasis of $CD103^+CD11b^+$ intestinal DCs. Finally in Chapter 9, I describe the discovery of a novel subset of $CD103^-CD11b^+$ DCs which expresses CCR2 and is dependent on CCR2 for their development, but which are genuine DC, based on their expression of zDC and derivation from DC-committed progenitors.

Chapter 2 Materials and Methods

2.1 Mice

All mice were maintained under specific pathogen free (SPF) conditions at the Central Research Facility (CRF) or Veterinary Research Facility (VRF) at the University of Glasgow and were used between 6 and 12 weeks of age, unless otherwise specified. Table 2.1 details the mouse strains used throughout these studies. All strains were on the C57/Bl6 background. All procedures were carried out in accordance with UK Home Office regulations.

Table 2.1: Mice Strains

Strain	Source
C57Bl/6 (CD45.2)	Harlan Olac (Bicester, Oxfordshire)
C57Bl/6.SJL (CD45.1)	Kindly provided by Prof. W. Agace (Lund University, Sweden)
C57Bl/6 (CD45.1/CD45.2)	Generated by crossing C57Bl/6 with C57Bl/6.SJL
SIRPα Mutant (CD45.2)	Kindly provided by Prof. P.A. Oldenburg (Umeå University, Sweden) with kind permission from Prof. T. Matozaki (University of Tokyo, Japan) (Inagaki, Yamao et al. 2000)
CD47KO (CD45.2)	Jackson Laboratories (Maine, USA) (Lindberg et al., 1996)
$Flt3L^{-/-}$ (CD45.2)	Used in collaboration with Prof. B. Lambrecht (Ghent University, Belgium). Mice maintained at VIB, University of Ghent, Belgium with WT (C57Bl/6) controls (McKenna et al., 2000)
$Csf2rb^{-/-}$ (CD45.2)	Jackson Laboratories (Maine, USA). Used in collaboration with Fiona Powrie (University of Oxford, UK). Mice maintained in Oxford with WT (C57Bl/6) controls (Robb et al., 1995)
$CX3CR1^{gfp/gfp}$ ($B6.129P\text{-}CX3CR1^{tm1Litt/J}$) (CD45.2)	Kindly provided by Prof. W. Agace (Lund University, Sweden) (Jung et al., 2000)
$CX3CR1^{+/gfp}$ ($CD45.2^{+}$)	Generated by crossing $CX3CR1^{gfp/gfp}$ with C57Bl/6 mice.
$CX3CR1^{+/gfp}$ ($CD45.1^{+}/CD45.2^{+}$)	Generated by crossing $CX3CR1^{gfp/gfp}$ with C57Bl/6.SJL.
$CCR2^{-/-}$ (CD45.2)	Kindly provided by Dr Robert Nibbs (University of Glasgow) (Boring et al., 1997)
CD11c-DTR-GFP (CD45.2)	Kindly provided by Prof. Paul Garside (University of Glasgow) (Jung et al., 2002)
OT-I (CD45.2)	Jackson Laboratories (Maine USA) (Hogquist et al., 1995)
OT-II (CD45.2)	Jackson Laboratories (Maine USA) (Barnden et al., 1998)
OT-I (CD45.1/CD45.2)	Generated by crossing OT-I with C57Bl/6.SJL
OT-II (CD45.1/CD45.2)	Generated by crossing OT-II with C57Bl/6.SJL

$CCR2^{+/RFP}$	Jackson Laboratories, (Maine, USA) used in collaboration with Dr. Barry McColl, Roslin Institute, Edinburgh (Saederup et al., 2010)

2.2 Genotyping Mice

2.2.1 Genomic DNA Isolation

Tail tips were collected from mice to be genotyped and frozen at -20°C until use. DNA was isolated using the DNeasy Blood and Tissue Kit (Qiagen) as per the manufacturer's guidelines. Briefly, 25mg of each tail tip was digested overnight at 56°C with Proteinase K. The following day, DNA was purified by binding to the spin column membrane provided, washing and finally eluting in the elution buffer supplied. Genomic DNA was frozen and stored at -20°C until needed.

Table 2.2 Primers for Genotyping

Gene	Sense	Antisense
SIRP WT	ATACCATTGGCTGAGCCCACTGGGAAAGAA	TAGTACAGACCACAGCCCCATTCACTTCCT
SIRP MT	TCGTGCTTTACGGTATCGCCGCTCCCGAAT	TAGTACAGACCACAGCCCCATTCACTTCCT
CD47 WT	CAAGCATAAATGAACAGTTGCAG	CACGTTTCAAAACAGGCAAA
CD47 KO	CTTGGGTGGAGAGGCTATTC	AGGTGAGATGACAGGAGATC
CD11c-DTR	GCCACCATGAAGCTGCTGCGG	TCAGTGGGAATTAGTCATGCC

2.2.2 Genotyping

SIRPα mutant (mt), CD47KO and CD11c-DTR-GFP mice were genotyped before use in all experiments. Genomic DNA isolated from tail tips was diluted 1:2 prior to use in polymerase chain reaction (PCR). The primers (Integrated DNA Technologies, IDT) used for genotyping these strains are detailed in Table 2.2.

Each PCR mix had a final volume of 20μl and contained 1μl diluted genomic DNA, 0.2μl 10μM sense and anti-sense primers, 0.4μl 10μM dNTPs, 0.1μl 5U/μl Go Taq polymerase, 4μl 5X reaction buffer and 14.1μl nuclease free water (all Life Technologies, Paisley, UK). The PCR consisted of one cycle of denaturation at 95°C for 5 minutes, thirty-five cycles of denaturation at 95°C for 1 minute, annealing at the desired temperature (Table 2.3) and elongation at 72°C for 2 minutes, followed by one cycle of elongation at 72°C for 10 minutes.

Table 2.3: Annealing Temperatures

Primer Pair	Annealing Temperature (°C)
CD47 WT & KO	61
SIRP WT & MT	58
CD11c-DTR	58

Following PCR, the products were visualised using agarose gel electrophoresis on a 2% agarose gel (Sigma-Aldrich, Poole, UK) in 1X TAE with 3μl ethidium bromide (Life Technologies) per 100ml gel. 10μl of PCR reaction along with 2μl of 6X loading dye (Life Technologies) were loaded onto the gel with 5μl DNA ladder (Life Technologies) and 1μl 6X loading dye. Gels were run in 1X TAE for approximately 1 hour at 100mV. Gels were visualised by UV.

2.3 Isolation of Leukocytes from Tissue

2.3.1 Isolation of Lamina Propria Cells

Murine small intestines (SI) were excised and soaked in PBS (Gibco, Life Technologies). Peyer's patches and excess fat were removed and the intestines

opened longitudinally. Faeces were removed by washing in calcium/magnesium free (CMF) Hank's balanced salt solution (HBSS; Gibco) supplemented with 2% foetal calf serum (FCS; Gibco) and the intestines were cut into 0.5cm segments. Tissue was shaken vigorously in HBSS/2% FCS and the supernatant removed by pouring tissue and supernatant onto Nitex mesh (Cadisch and Sons, London, UK) and subsequently collecting the tissue sections. The epithelial layer was removed by incubating the tissue at 37°C with shaking in 10ml pre-warmed HBSS supplemented with 2mM EDTA (Sigma-Aldrich, Poole, UK) for 20 minutes. Following this the tubes were shaken vigorously, supernatants discarded and the tissue was washed in pre-warmed HBSS before a second incubation in HBSS/2mM EDTA for a further 20 minutes. Following repetition of the wash step, the tissue was digested in 10ml pre-warmed complete RPMI (RPMI 1640, 50μM 2-β-mercaptethanol, 2mM L-glutamine, 100μg/ml penicillin, 100μg/ml streptomycin, 1.25μg/ml Fungizone, and 10% FCS; all Gibco) supplemented with 1mg/ml collagenase VIII (Sigma), by incubation at 37°C with shaking for 20-30 minutes. To aid digestion, tubes were shaken vigorously every 5 minutes. Following digestion, the cell suspensions were passed through a 100μm filter (BD Falcon), followed by a 40μm filter (BD Falcon) washed twice in complete RPMI to remove any residual enzyme, resuspended in complete RPMI, counted and kept on ice until use.

Colonic LP cells were isolated in a similar fashion except that the HBSS/2mM EDTA incubations are 15 minutes and 30 minutes in duration, while the digestion step involved a 30-45 minute incubation in complete RPMI supplemented with an enzyme cocktail containing 1.25mg/ml collagenase D (Roche; Roche Diagnostics GmbH, Mannheim, Germany), 0.85mg/ml collagenase V (Sigma), 1mg/ml dispase (Gibco), and 30U/ml DNase (Roche).

2.3.2 Isolation of Lymph Node Cells and Splenocytes

Lymph nodes and/or spleens were excised from mice and excess fat was removed. The tissues were washed in HBSS and cut into small fragments. To isolate T and B lymphocytes, tissue was mashed between two pieces of Nitex mesh and filtered through a fresh piece of Nitex before being resuspended in complete RPMI, counted and left on ice until use. To isolate DCs, tissues were digested by incubating at 37°C with shaking in HBSS supplemented with 1mg/ml

collagenase D for 45 minutes. Following the digestion, any remaining tissue was passed through a 100μm filter, washed twice in complete RPMI to remove any residual enzyme, resuspended in complete RPMI, counted and left on ice until use. Red blood cells in the spleen preparations were lysed by incubation for 6 minutes on ice with ammonium chloride solution (0.8% NH_4Cl/0.1mM EDTA, Stem Cell Technologies, Grenoble, France) prior to resuspension in complete RPMI and counting.

2.3.3 Isolation of Liver Leukocytes

CO_2-euthanised mice were perfused through the heart with 10ml CMF PBS and the livers were excised. These were subsequently cut into small pieces (<2mm) and placed in HBSS supplemented with 2% FCS. Tissue was shaken vigorously in HBSS/2% FCS and the supernatant removed by pouring tissue and supernatant onto Nitex mesh and subsequently collecting the tissue sections. Livers were then digested in complete RPMI supplemented with an enzyme cocktail containing 0.75mg/ml collagenase D, 0.425mg/ml collagenase V, 1mg/ml dispase, and 30U/ml DNase at 37^oC with shaking for 20 minutes. Following digestion, the cell suspensions were passed through a 40μm filter washed twice in complete RPMI to remove any residual enzyme and red blood cells were lysed by incubation for 6 minutes on ice with ammonium chloride solution, before being resuspended in complete RPMI, counted and kept on ice until use.

2.3.4 Isolation of Lung Leukocytes

CO_2-euthanised mice were perfused with 10ml CMF PBS and the lungs were excised. These were subsequently cut into small pieces (<2mm) and digested in complete RPMI supplemented with 1mg/ml Collagenase D (Roche) at 37^oC with shaking for 45minutes. Following digestion, the cell suspensions were passed through a 40μm filter washed twice in complete RPMI to remove any residual enzyme and red blood cells were lysed by incubation for 6 minutes on ice with ammonium chloride solution before being resuspended in complete RPMI, counted and kept on ice until use.

2.3.5 Whole Blood Isolation

Whole blood was obtained from mice by cardiac puncture. Red blood cells (RBCs) were lysed by incubating heparinised blood on ice with ammonium chloride solution for 10 minutes and subsequently washed twice in PBS. Cells were counted and left on ice until use.

2.3.6 Isolation of Bone Marrow Cells

Femurs and tibiae were isolated from mice and the bone marrow was flushed out using RPMI 1640 and filtered through Nitex. If cells were to be used for flow cytometric analysis, RBCs were lysed as described above and cells were subsequently washed twice in RPMI 1640. If cells were to be used for culture, RBC lysis was omitted. Cells were then counted and left on ice until required.

2.4 Flow Cytometry

2.4.1 Cell Surface Staining:

Freshly isolated cells were resuspended in FACS buffer (CMF PBS, 2% FCS, 2mM EDTA) and 2.5-5x10^6 cells were added to 12x75mm polystyrene tubes (BD falcon). Non-specific binding of antibodies to Fc receptors was prevented by incubation of the cells with anti-CD16/CD32 ('Fc Block'; BD Biosciences) at 4°C for 15-20 minutes. Cells were then washed in FACS buffer and incubated with required antibodies or isotype controls at a dilution of 1:200 unless otherwise specified by manufacturer (Table 2.4) at 4°C for 20-30 minutes. Cells were then washed twice and incubated with streptavidin conjugates if biotinylated antibodies were used at 4°C for a further 20 minutes and washed twice more. Just prior to analysis, 15μl of 7-aminoactinomycin D (7-AAD; Biolegend) was added to the cells to allow dead cell exclusion. Cells were acquired on BD LSRII or BD FACSArial with Diva software. Cells were analysed using FlowJo Software (Treestar Inc., USA).

Table 2.4: Antibodies and Isotype Controls

Antibody	Clone	Isotype	Source
Annexin V	n/a	n/a	BD Biosciences
β7	M293	Rat IgG2a	BD Biosciences
CD3	145-2C11	Ham IgG	Biolegend
CD4	GK1.5	Rat IgG2b	Biolegend
CD8	53-6.7	Rat IgG2a	Biolegend
CD11b	M1/70	Rat IgG2b	Biolegend
CD11c	HL3	Ham IgG1	BD Biosciences
CD11c	N418*	Ham IgG	Biolegend
CD14	Sa2-8	Rat IgG2a	eBioscience
CD19	1D3	Rat IgG2a	BD Biosciences
CD25	7D4	Rat IgM	BD Biosciences
CD26 (DPP4)	H194-112	Rat IgG2a	Biolegend
CD40	3/23	Rat IgG2a	BD Biosciences
CD45	30-F11	Rat IgG2b	Biolegend
CD45.1	A20	Ms IgG2a	Biolegend
CD45.2	104	Ms IgG2a	Biolegend
CD45R (B220)	RA3-6B2	Rat IgG2a	Biolegend
CD47	B6H12	Ms IgG1	BD Biosciences
CD49b	DX5	Rat IgM	BD Biosciences
CD62L	MEL-14	Rat IgG2a	BD Biosciences
CD64	X54-5/7.1	Ms IgG1	Biolegend
CD80	16-10A1	Ham IgG1	BD Biosciences
CD86	GL1	Rat IgG2a	BD Biosciences
CD103	M2/90	Rat IgG2a	BD Biosciences
CD103	2E7	Ham IgG	Biolegend
CD115	AFS98	Rat IgG2a	eBioscience
CD117	2B8	Rat IgG2b	BD Biosciences
CD135	A2F10.1	Rat IgG2a	BD Biosciences
CD172a	P84	Rat IgG1	BD Biosciences

CD192 (CCR2)	475301	Rat IgG2b	R & D Systems
CD193 (CCR3)	83103	Rat IgG2a	BD Biosciences
CD197 (CCR7)	4B12	Rat IgG2b	Biolegend
CD199 (CCR9)	CW-1.2	Ms IgG2a	Biolegend
CD272	6F7	Ms IgG1	eBioscience
F4/80	BM8	Rat IgG2a	eBioscience
FoxP3	FJK-16s	Rat IgG2a	eBioscience
IFNg	XMG1.2	Rat IgG1	BD Biosciences
IL6	MP5-20F3	Rat IgG1	Biolegend
IL12/IL23p40	C15.6	Rat IgG1	Biolegend
IL17a	TC11-18H10.1	Rat IgG1	Biolegend
Ki67	B56	Ms IgG1	BD Biosciences
Ly6C	AL-21	Rat IgM	BD Biosciences
Ly6G	1A8	Rat IgG2a	BD Biosciences
MerTK	-	Goat IgG	R & D Systems
MHCII (IA-IE)	M5/114.15.2	Rat IgG2b	eBiosciences
Siglec F	E50-2440	Rat IgG2b	BD Biosciences
TNFa	MP-6XT22	Rat IgG1	BD Biosciences
XCR1	Marx10	Rat IgG2a	Kroczek lab
Streptavidin BV605			Biolegend
Streptavidin QDot 605			Molecular Probes

* N418 clone gave superior staining and was the only clone used after its introduction.

2.4.2 Intracellular Staining:

When staining for intracellular cytokines or transcription factors, the staining protocol was adapted slightly to be compatible with the fixable dead cell exclusion dyes used. $4x10^6$ cells were incubated in complete RPMI for 4.5hrs in 5ml polystyrene tubes in the presence of 1μM Monensin and 1μM Brefeldin A (both Biolegend) to prevent cytokine secretion. In most experiments stimulants such as phorbol 12-myristate 13-acetate (PMA) and ionomycin (Cell stimulation cocktail plus protein transport inhibitors, eBioscience) or the TLR4 ligand, LPS (100ng/ml; Sigma-Aldrich) were added to restimulate T cells or stimulate MP cells respectively.

Cells were washed in CMF PBS and then incubated for 20-30minutes protected from light at 4°C with LIVE/DEAD® fixable dead cell stain kits (eBioscience) as per the manufacturer's guidelines. Cells were then washed in FACS buffer, incubated with purified anti-CD16/CD32 and stained with the appropriate antibodies for cell surface antigens as described above, before being washed three times in FACS buffer. Cells were then fixed and permeabilised using the eBioscience Flow Kit according to manufacturer's instructions. Cells were subsequently incubated with purified anti CD16/CD32 and stained with appropriate antibodies to stain for intracellular cytokines or transcription factors in permeabilisation buffer for 20mins at 4°C protected from light, washed in permeabilisation buffer and subsequently resuspended in FACS buffer and analysed by flow cytometry.

2.4.3 CCL2 Uptake Assay

2-3x10^6 cells resuspended in complete RPMI were incubated, protected from light, in a 96-well polypropylene plate (Fischer Scientific, UK) with 25nM CCL2-AF647 (Almac) at 37°C for 60 minutes. Cells were washed in FACS buffer and stained for surface markers as indicated in section 2.4.1.

2.4.4 Fluorescence Activated Cell Sorting

Cells were prepared for FACS as described above but under sterile conditions, before being sorted using a BD FACSAria I cell sorter and were typically 94-99% pure.

2.5 *In Vitro* Cell Culture

2.5.1 *In Vitro* Stimulation of Isolated Leukocytes

Following isolation of leukocytes from tissues, cells were resuspended in complete RPMI and 5x10^6 cells in a final volume of 1ml complete RPMI were incubated in 5ml polystyrene tubes for 4.5 hours in the presence of absence of 100ng/ml lipopolysaccharide (LPS) from *Salmonella typhimurium* (Sigma-Aldrich), with 1μM Brefeldin A and 1μM Monensin to block protein secretion, before being stained for intracellular cytokines as indicated above.

2.5.2 DC:T Cell Co-cultures

To assess the ability of intestinal APC populations to prime naïve T cells, populations of DC and mϕ were FACS-purified from the LP as indicated above and co-cultured with FACS-purified naïve ($CD62L^+CD25^-$) $CD4^+$ or $CD8^+$ T cells from lymph nodes of OTII or OTI mice respectively. Prior to co-culture, T cells were labelled with 5mM Carboxyfluorescein diacetate succinimidyl ester (CFSE, Life Technologies) by incubating at room temperature for 10 minutes before washing in complete RPMI. The APC populations were pulsed with 1-2mg/ml Ovalbumin for 2 hours and then co-cultured at various ratios with 100,000 T cells for 3-4 days at 37°C with 5% CO_2. Following co-culture, supernatants were removed for CBA analysis described in section 2.7.1 and the cells were stimulated with fresh complete RPMI supplemented with 1X cell stimulation cocktail + protein transport inhibitors (eBioscience) for 4.5hrs. The cells were stained for expression of intracellular cytokines and FoxP3 by flow cytometry as described above. Dilution of CFSE dye on the T cells was also assessed.

2.5.3 T_h17 Differentiation *In Vitro*

24-well ultra low adherence plates were coated with 1.5μg/ml anti-CD3 and 1.5μg/ml anti-CD28 (BD Biosciences) in CMF PBS for 6 hours at 4°C. The plates were then washed once with CMF PBS and $8x10^5$ FACS-purified naïve $CD4^+$ $CD62L^{hi}$ $CD25^-$ T cells from mesenteric lymph nodes (MLN) were added in 1ml complete RPMI supplemented with 10μg/ml anti-IFNγ, 10μg/ml anti-IL4, 10μg/ml anti-IL2, 20ng/ml IL6, 20ng/ml IL23, 20ng/ml IL1β (all BD Biosciences) and 2.5ng/ml recombinant human TGFβ (Peprotech, London, UK). Cells were incubated at 37°C with 5% CO_2 for 4 days and supplemented with 500μl complete RPMI on day 3. On day 4 cells were harvested by flushing the wells before being washed in complete RPMI, resuspended in 1ml complete RPMI supplemented with 1X cell stimulation cocktail + protein transport inhibitors (eBioscience) containing Brefeldin A, Monensin, PMA and Ionomycin, in 12x75mm polystyrene tubes and incubated for 4.5 hours at 37°C with 5% CO_2. The cells were then harvested and stained for intracellular IL17A and RORγt as described above.

2.6 Transcriptional Analysis of Cell Populations

2.6.1 RNA Extraction

Single cell suspensions (FACS-sorted cells or BMDC/BMMϕ) were washed twice with PBS, spun down and the supernatant discarded. RNA was then isolated using the RNeasy Micro or Mini Kit (Qiagen) (depending on cell number) according to the manufacturer's guidelines. Contaminating genomic DNA was removed on-column during RNA isolation with the RNase-free DNase Set (Qiagen) according to the manufacturer's instructions. The RNA was quantified using a nanodrop spectrophotometer (Amersham Biosciences) and RNA was stored at –20^{o}C until use.

2.6.2 cDNA Synthesis

cDNA was reverse transcribed from DNase-treated RNA using Superscript III Reverse Transcriptase (RT) (Life Technologies) according to the manufacturer's instructions. Briefly, 10ng of RNA, 1µl Oligo(dT)$_{12\text{-}18}$ (500µg/ml; Life Technologies), 1µl dNTP mix (25mM each; Life Technologies), and nuclease-free water were added to a nuclease-free microcentrifuge tube (ABgene, Surrey, UK) in a total volume of 10µl. The mixture was heated at 65°C for 5 minutes, and then chilled on ice. 4µl 5X First-Strand Buffer, 2µl 0.1M DTT, and 1µl RNaseOUT (40 units/ml) were added and incubated at 42°C for 2 minutes. 1µl (200 units) Superscript III RT was then added and the RNA was reverse transcribed at 42°C for 50 minutes. The Superscript III RT was inactivated by heating at 70°C for 15 minutes and RNA was degraded using *Escherchia coli* RNase H (10units) at 37°C for 20 minutes. Negative control samples were incubated in the absence of Superscript III and all cDNA was stored at –20°C until use.

Table 2.5 Primers for qRT-PCR

Gene	Sense	Antisense
HPRT	GCTGACCTGCTGGATTACATTAA	TGATCATTACAGTAGCTCTTCAGTCTGA
Il1β	CTGGTGTGTGACGTTCCCATTA	CCGACAGCACGACGCTTT
Ccr2	ATCCACGGCATACTATCAACATC	CAAGGCTCACCATCATCGTAG
Il10	GCTCTTACTGACTGGCATGAG	CGCAGCTCTAGGAGCATGTG
Il6	CCAGTTGCCTTCTTGGGACT	GGTCTGTTGGGAGTGGTATCC
Caspase 3	ACGCGCACAAGCTAGAATTT	CTTTGCGTGGAAAGTGGAGT
Bcl2	TGTGTGTGGAGAGCGTCAACA	TGCCGGTTCAGGTACTCAGTC
Batf3	CAGACCCAGAAGGCTGACAAG	CTGCGCAGCACAGAGTTCTC
Id2	TCCTGTCCTTGCAGGCATCTGAAT	AACGTGTTCTCCTGGTGAAATGGC
Irf8	GAGCGAAGTTCCTGAGATGG	TGGGCTCCTCTTGGTCATAC
Zbtb46	TCACATACTGGAGAGCGGC	CCTCATCCTCATCCTCAACC
Irf4	TCTCTGAGGGTCTGGAAACT	GCCCAAGCTAGAAAG
Integrin β8	GGGTGTGGAAACGTGACAAGCAAT	TCTGTGGTTCTCACACTGGCAACT

Csf2RA	CGTGGCGCGATGCAT	TCACGACCAAGTAGGCCTCACT
Tlr1	TGGACACCCCTACAGAAACGT	AATTTGGTTTAGTCATTGTATGGCC
Tlr2	CTGGAGCATCCGAATTGCA	CATCCTCTGAGATTTGACTT
Tlr3	CCAGAAGAATCTAATCAAATTAGATTTGTC	TTTTGCTAAGAGCAGTTCTTGGAG
Tlr4	GGCAACTTGGACCTGAGGAG	CATGGGCTCTCGGTCCATAG
Tlr5	CACTCCCTCGGAGAACCCA	GGCCTTGAAAAACATCCCAAC
Tlr6	AAAGTCCCTCTGGGATAGCCTCT	TGCTTCCGACTATTAAGGCCA
Tlr7	ACAGAAATCCCTGAGGGCATT	CAGATGGTTCAGCCTACGGAAG
Tlr9	GGGCCCATTGTGATGAACC	CTTGGTCTGCACCTCCAACA
Il12p35	TACTAGAGAGACTTCTTCCACAACAAGAG	TCTGGTACATCTTCAAGTCCTCATAGA
Il12p40	GACCATCACTGTCAAAGAGTTTCTAGAT	AGGAAAGTCTTGTTTTTGAAATTTTTTAA
Il23p19	AGCGGGACATATGAATCTACTAAGAGA	GTCCTAGTAGGGAGGTGTGAAGTTG
Il17a	GCTCCAGAAGGCCCTCAG	CTTTCCCTCCGCATTGACA
Il22	CATGCAGGAGGTGGTGCCTT	CAGACGCAAGCATTTCTCAG
Cd115	GCATACAGCATTACAACTGGACCTACC	CAGGACATCAGAGCCATTCACAG

Ccr7	ATTGCTGCTGAGGGAAGAG	ACTTTTGGCTGTCGTTTTGG
Cd135	GGTTTAAAGCGTACCCACGA	GAACTGGGCGTCATCATTTT

2.6.3 Real-Time PCR

Gene expression was assayed by quantitative reverse transcription PCR (qRT-PCR) using Brilliant III Ultra Fast SYBR qPCR master mix (Agilient Technologies) on the 7900HT Fast system (Applied Biosystems). Primers (Table 2.5) were designed using Primer Express software (Applied Biosystems, Life Technologies) and purchased from IDT (Iowa, USA). cDNA samples were assayed in triplicate and gene expression levels were normalised to hypoxanthine phosphoribosyltransferase (HPRT) as a housekeeping gene. The mean relative gene expression was calculated using the $2^{-\Delta\Delta C(t)}$ method.

2.6.4 Microarray

Microarray analyses were performed in collaboration with the groups of Toby Lawrence, Bernard Malissen and Marc Dalod (Marseille, France). RNA was isolated from sorted SI LP cells as described above and sent for microarray analysis at the IGBMC facility in Strasbourg using the GeneChip Mouse Gene 1.0ST with single amplification using the Nugen Protocol. Analysis was performed at the CIML, Marseille, France by Marc Dalod.

2.7 Measurement of Proteins in Serum, Faeces and Culture Supernatants

2.7.1 Cytokine Bead Array

Cytokine bead array (CBA) assays were carried out by Knut Kotarsky, Biomedical Centre, University of Lund, Sweden. Culture supernatants were removed and frozen at -20^{o}C before being analysed using the CBA kit (BD Biosciences) as per manufacturers instructions.

2.7.2 Isolation and measurement of intestinal IgA by ELISA

Faeces were removed from the colon and transferred to eppendorfs containing ice cold CMF PBS with 0.1mg/ml soybean trypsin inhibitor type II (Sigma) and 50mM EDTA. Tubes were centrifuged at 1500g for 10 minutes at 4°C and the supernatants collected into fresh eppendorfs, to which 10μl of 100mM

phenylmethylsulfonyl (PMSF) (Sigma) in 95% ethanol solution was added before being centrifuged at 14000g for 30 minutes at 4°C. 10μl PMSF solution, 10μl of 1% sodium azide (Sigma) solution and 50μl FCS were then added to the resulting supernatants which were stored at –20°C until required. The total protein content was determined using the BCA assay kit (Pierce, Loughborough, UK) according to the manufacturer's guidelines and using two-fold dilutions of bovine serum albumin (BSA; Sigma) as standards. To measure total IgA, Immulon-4 ELISA plates (Corning) were coated overnight at 4°C with 50μl per well purified rat anti-mouse IgA (BD Biosciences) diluted at 1:500. The next day, the plates were washed a minimum of five times with PBS/0.05% Tween 20, before blocking with PBS/3% BSA for 1 hour at 37°C. Plates were washed and 50μl of neat faecal samples added in duplicate for 1 hour at 37°C. The plates were then washed and 75μl biotin conjugated rat anti-mouse IgA (BD Biosciences) diluted at 1:500 was added before being incubated at room temperature for 1 hour. Plates were then washed and incubated with 1:1000 extravidinperoxidase (Sigma) for 1 hour at room temperature before washing. The ELISA plates were then washed and subsequently developed using tetramethylbenzidine (TMB) substrate (Biolegend) before the reaction was stopped by adding 15-20μl stop solution (R & D Systems) and read at 450nm using a MRX II microplate reader (Dynex).

2.8 *In Vivo* Models of Inflammation, Infection, Priming and Tolerance

2.8.1 DSS Colitis

To induce acute colitis, mice received 1 or 2% dextran sodium sulphate (DSS) salt (reagent grade; MW 36,000-50,000 kDa; MP Biomedicals, Ohio, USA), *ad libitum* in sterile drinking water for up to 9 days. Mice were monitored daily for weight change, rectal bleeding and diarrhoea and a clinical score generated (Table 2.6). Mice that lost >20% of their initial bodyweight were sacrificed immediately in accordance with Home Office regulations. Water intake was measured daily for each group and the volume of water consumed per mouse was estimated by dividing the total volume of water consumed per cage by the number of animals in the cage.

Table 2.6: Clinical disease score criteria used during DSS-induced colitis studies

Score	Weight Loss	Rectal Bleeding	Stools
0	0%	None	Well-formed pellet
1	5-9.9%	Blood around anus	Pasty soft pellets
2	10-14.9%	Bleeding	Faeces around anus
3	15-19.9%	Gross Bleeding	Diarrhoea
4	>20%	N/A	N/A

2.8.2 Post-Operative Ileus

To induce transient inflammation of the SI, a model of post-operative Ileus (POI) was utilised. POI experiments were carried out in collaboration with Dr Simon Milling, University of Glasgow. Mice were anaesthetised, laparotomy performed to expose the SI and inflammation was induced by rubbing the length of the SI with a cotton bud. 24 hours after surgery mice were culled and SI LP MP populations were assessed by flow cytometry.

2.8.3 Citrobacter Rodentium Infection

Citrobacter rodentium infection was carried out in collaboration with Drs Gill Douce and Andrew Roe, University of Glasgow. Mice were infected with $10x10^7$ luminescent *Citrobacter Rodentium* by oral gavage. Infection was monitored by faecal colony forming unit (CFU) counts and by *in vivo* (IVIS) imaging. Mice were culled at various time points during infection and leukocyte populations in the colon were assessed by flow cytometry.

2.8.4 *In Vivo* T Cell Priming Following Oral Administration of Antigen

To assess antigen specific oral priming, $5x10^6$ CD45.1/CD45.2 OTII cells isolated from LNs were labelled with CSFE (Life Technologies) as described above and transferred into $CD45.1^+$ WT or $CD45.2^+$ SIRPα mt mice. 24 hours later mice received 10mg OVA protein by oral gavage in 200ml PBS. 3 days later mice were sacrificed and proliferation and polarisation of donor T cells were assessed by dilution of CSFE and IFNγ, IL17a and FoxP3 staining respectively in MLNs and SI LP as described above.

2.8.5 *In Vivo* T Cell Priming Following Systemic Administration of Antigen and Adjuvants

Mice were transferred with $5x10^6$ CFSE-labelled CD45.1/CD45.2 OTII cells isolated from LNs. 24 hours later mice received 25μg anti-CD40 (Biolegend, clone 1C10), 15μg LPS (Sigma) and 0.5mg OVA protein (Sigma) i.p in 100μL PBS (Sigma) and 1 and 3 days later received i.p. 1mg/kg bodyweight FTY720 (Cayman, Michigan, USA) in 0.9% NaCl (VWR, Leuven, Belgium). 5 days after T cell transfer mice were sacrificed and transferred T cells in MLN were examined for CSFE dilution and polarisation towards T_h17, T_h1 or T_{Reg} cell phenotypes as described above.

2.8.6 Induction of Oral Tolerance by Oral Administration of Antigen

To induce tolerance, mice were fed a single 25mg dose of OVA dissolved in 0.2ml sterile CMF PBS using a rigid steel curved gavage tube. Control mice received 0.2ml sterile CMF PBS alone. One week after feeding, all mice were immunized in the right hind footpad with 100μg OVA in complete Freund's adjuvant (CFA; Sigma) and 3 weeks later, OVA specific DTH responses were assessed by measuring the increase in thickness of the opposite footpad 24 hours after challenge with 100μg heat aggregated OVA (HAO) in 50μl sterile CMF PBS using calipers (Kroeplin, Hertfordshire, UK). HAO was prepared by heating a 2% solution of OVA in sterile PBS at 70°C for an hour. The precipitated OVA formed was then centrifuged for 10 minutes at 400G at 4°C and the supernatant discarded. HAO pellets were suspended in sterile PBS at a concentration of 20mg/ml until further use.

2.8.7 Antibiotic Treatment

Mice received 500mg/kg ampicillin, gentamycin, metranidazole, neomycin (Roche) and 250mg/kg vancomycin (Hospira, UK) for 2 weeks in their drinking water, which was sweetened (Swetex, Reckitt Benckiser Household, UK) to encourage drinking. Control mice received sweetened water only. Antibiotic solutions were made up immediately before administration and were replaced every other day.

2.9 Measurement of Cell Turnover by BrdU Incorporation

2.9.1 Short-Term Pulse-Chase

Mice were injected i.p. with 1mg 5-bromo-2'-deoxyuridine (BrdU; BD Biosciences) and then sacrificed at different time points thereafter. The incorporation of BrdU by isolated cells was assessed using the BD BrdU Flow Kit (BD Biosciences) as per manufacturers instructions.

2.9.2 Long-term BrdU Feeding

Mice were injected i.p. with 1mg BrdU and before receiving 0.8mg/ml BrdU (Sigma) in the drinking water for 3 days. Mice were culled immediately after cessation of feeding or at various time-points thereafter. As per section 2.9.1, BrdU incorporation was assessed using the BD BrdU Flow kit as per manufacturers instructions.

2.10 Adoptive Transfer of Progenitor Cells

2.10.1 Pre-DC Transfers

Donor mice were injected subcutaneously at the scruff of the neck with $2x10^6$ Flt3L secreting B16 tumour cells 10 days prior to pre-DC isolation to expand the number of pre-DC in the BM. On the day of the transfer, mice were culled and bone marrow was obtained as described in section 2.3.6, before red blood cells were lysed by incubation with ammonium chloride solution for 5 minutes on ice. The remaining cells were stained with efluor 450 violet proliferation dye (eBioscience) as per manufacturer's instructions and then stained for lineage markers (CD3, CD19, CD49b, CD11b and MHCII), CD11c, CCR9 and B220. Pre-DC ($Lineage^-$ $CD11c^+$ $CCR9^-$ $B220^{-/lo}$) were then sorted into complete RPMI. The purity was routinely >97%. Sorted pre-DC were washed twice in sterile PBS and $7x10^5$ were injected intravenously into congenic recipient mice in 0.1ml CMF PBS. The fate of donor cells was assessed by flow cytometry 1, 3, 5 and 7 days after transfer.

2.10.2 Transfer of Ly6C^{hi} Monocytes

Bone marrow was obtained as described in section 2.3.8 from CX3CR1$^{+/gfp}$ CD45.2^{+} mice, RBCs lysed and the remaining cells were stained for CD11b, CD117, Ly6G and Ly6C to allow the identification of Ly6C^{hi} monocytes (CD11b^{+} CD117^{-} Ly6G^{-} Ly6C^{hi} CX3CR1^{int}), which were then sorted into complete RPMI. The purity of these monocyte populations was routinely >97%. Sorted monocytes were washed twice in sterile PBS and then 1x10^{6} cells were transferred intravenously, in a volume of 0.1ml CMF PBS into congenic recipients. The fate of the donor cells was assessed 5 days after transfer by flow cytometry.

2.11 Generation of BM Chimeras

8 week old Ly5xC57Bl/6 (CD45.1/CD45.2) mice were irradiated with 2 doses of 5 Gy 2 hrs apart using the Cobalt source at the Beatson Institute, Glasgow, UK. Mice then received 1x10^{7} BM cells in a 50:50 ratio of WT (CD45.1^{+}) mice and either SIRP mutant (CD45.2^{+}) mice or CCR2null (CD45.2^{+}) mice. Recipient mice were left for 8 weeks to allow BM engraftment.

2.12 Parabiosis

WT:WT (CD45.1:CD45.2) and WT:CCR2null (CD45.1:CD45.2) parabiotic mice were generated by Sandrine Henri (Marseille-Luminy University, France). Briefly 8 week old male mice were surgically joined following exposure of the skin from the forearm to hindleg and left for 12 weeks to allow revascularisation. The mice were then culled and degree of chimersim determined by flow cytometry.

2.13 Administration of Growth Factors *in vivo*

2.13.1 Recombinant Human Flt3L

To assess DC expansion, CX3CR1$^{+/gfp}$ mice were injected i.p. with 10μg human recombinant CHO-derived flt3L (a kind gift of Amgen Corp, Seattle, USA) in 0.2ml sterile PBS for 8 consecutive days to achieve maximal cell expansion, as previously optimised in the Mowat lab. The extent of expansion was assessed by comparison with non-injected resting CX3CR1$^{+/gfp}$ mice.

2.13.2 B16 CSF-2 Secreting Melanoma Cells

To assess DC expansion, WT mice were injected subcutaneously in the scruff of the neck with $2x10^6$ B16 melanoma cells secreting CSF-2 (a kind gift from Dr. Oliver Pabst, Hannover Medical School, Hannover, Germany). 10 days later mice were culled and the extent of expansion assessed by comparison to non-injected resting mice.

2.14 Functional Analysis

2.14.1 Phagocytosis Assay

To measure the phagocytic activity, total SI LP cells were isolated and phagocytosis was assessed using the pHrodo assay according to the manufacturer's guidelines. Briefly, $3x10^6$ cells were incubated with 10µl pHrodo *E. coli* bioparticles (Molecular Probes) for 15mins at 37°C or at 4°C as a control, washed in Buffer C and analysed in Buffer C by flow cytometry. Results were expressed as ΔMFI (MFI 37^oC- MFI 4^oC).

2.14.2 DCs in Pseudo-Afferent Lymph

To assess the nature of the cells migrating from the SI LP to MLNs, pseudo-afferent lymph was collected by thoracic duct cannulation in mice, which had undergone mesenteric lymphadenectomy 6-8 weeks earlier. DCs in lymph were analysed by flow cytometry. These experiments were carried out in collaboration with Drs Simon Milling and Vuk Cerovic, University of Glasgow, UK

2.15 Statistical analysis

Results are presented as means ±1 standard deviation unless otherwise stated and groups were compared using a Student's t test, Mann Whitney or for multiple groups, a one-way or two-way ANOVA followed by a Bonferroni post test using Prism Software (GraphPad Software Inc., USA). Values of less than $p<0.05$ were considered significant.

Chapter 3 Phenotypic Characterisation of Intestinal Dendritic Cells

3.1 Introduction

As described in Chapter 1, the precise characterisation of intestinal DCs has been difficult. In part this has been due to the laborious processes required to isolate these cells from the intestinal LP. However, a major problem has been the use of traditional DC markers such as CD11c and MHCII, which do not discriminate between DCs and other cells such as mϕs in non-lymphoid tissues. Prior to starting my PhD, a post-doc in the lab had spent a considerable amount of time optimising protocols for isolating leukocytes from the small intestinal LP, while a PhD student had established multi-parameter flow cytometry techniques for characterising myeloid cells in the colonic LP. Thus when I began my project, the lab was ideally set up to start characterising intestinal DCs in more rigorous ways and this first chapter sets out my experiments designed to explore DC populations in the steady state intestinal LP.

3.2 Characterisation of intestinal DCs by surface phenotype

When I began, work in both our lab and others, was making it increasingly obvious that the use of the traditional markers such as CD11c, MHCII and F4/80 in isolation was insufficient to differentiate DCs from mϕs in the intestine. To begin to overcome these issues, a gating strategy had been developed in which mutually exclusive expression of CD103 and CX3CR1 defined DCs and mϕs respectively (Coombes et al., 2007; Jaensson et al., 2008; Schulz et al., 2009) and I adopted this strategy in my initial experiments. Using CX3CR1$^{+/GFP}$ mice, total mononuclear phagocytes (MPs) were identified amongst single live leukocytes (CD45^{+} 7AAD^{-}) as CD11c^{+} MHCII^{+} cells (Fig. 3.1A) and DCs and mϕs within these MPs were then distinguished on the basis of CD103 and CX3CR1 expression respectively (Fig. 3.1B). This showed the majority of MPs to be CX3CR1^{+}, all of which were CD103^{-} F4/80^{+}, consistent with them being mϕs. A much smaller population was CD103^{+}CX3CR1^{-} and did not express F4/80, suggesting they were DCs (Fig. 3.1C). Although my initial results supported the paradigm that these markers could be used to discriminate DCs and mϕs other experiments going on in the lab at the time were suggesting that CX3CR1 expression by intestinal MPs was heterogeneous and that CD103^{-} DCs may also exist. Furthermore, much of my project planned to use non-CX3CR1$^{+/GFP}$ mice and given that there was no anti-

CX3CR1 antibody commercially available, it was necessary to modify the gating strategy so that DC and mϕs could be discriminated in such mice.

To overcome these issues, I developed a new gating strategy in which no *a priori* assumptions were made regarding CD103 and CX3CR1 expression. At this time, a PhD student in the lab investigating mϕs in the colonic lamina propria in collaboration with the lab of Bernard Malissen in Marseille found that expression of CD64 (FcγRI) appeared to be specific for mϕs (Bain et al., 2013; Tamoutounour et al., 2012). Therefore, I decided to investigate this marker in combination with the pan mϕ marker F4/80, as a potential means of discriminating intestinal DCs and mϕs. To this end, total MPs were first identified amongst single live leukocytes as $CD11c^{+}MHCII^{+}$ and contaminating B cells were excluded as $B220^{+}$ cells (Fig. 3.2A). The remaining MPs were analysed for expression of CD103 and CD11b. This analysis revealed the presence of 4 discrete subsets of MPs ($CD103^{+}CD11b^{+}$, $CD103^{+}CD11b^{-}$, $CD103^{-}CD11b^{+}$ and $CD103^{-}CD11b^{-}$) (Fig. 3.2B). To determine if these subsets were likely to represent DCs or mϕs, I next analysed expression of F4/80 and CD64 on each of the populations. Consistent with their previous identification as genuine DCs, neither the $CD103^{+}CD11b^{+}$ nor $CD103^{+}CD11b^{-}$ populations expressed either F4/80 or CD64. Additionally, the novel $CD103^{-}CD11b^{-}$ MP population lacked both F4/80 and CD64 expression suggesting these to also be a *bona fide* DC population (Fig. 3.2C). In contrast, the $CD103^{-}CD11b^{+}$ MPs consisted of two distinct populations, with the overwhelming majority (~80%) expressing both CD64 and F4/80, suggesting they were mϕs. The remaining ~20% were negative for both these markers and I hypothesised that these may also be a novel population of genuine DCs (Fig. 3.2C). By applying this analysis to multiple mice, I found that the $CD64^{+}F4/80^{+}CD103^{-}CD11b^{+}$ mϕ population was clearly the largest subset of MPs in the small intestinal LP, representing 73.85 ± 2.01% of MPs. $CD103^{+}CD11b^{+}$ MPs were the most abundant $CD64^{-}F4/80^{-}$ MP population comprising 6.07 ± 0.52%, while there were similar proportions of $CD103^{+}CD11b^{-}$ MPs and $CD64^{-}F4/80^{-}CD103^{-}CD11b^{+}$ MPs (~2.5 ± 0.25% and ~3.28 ± 0.15% respectively). The $CD103^{-}CD11b^{-}$ MPs comprised a small minority population at 0.84 ± 0.24% of all MPs (Fig. 3.2D).

My identification of novel putative $CD103^{-}$ DCs suggested that the current convention of discriminating DCs and mϕs on the basis of CD103 and CX3CR1

expression was insufficient. To explore this in more detail, I next examined CX3CR1 expression by the various populations I had defined by applying the phenotyping strategy to CX3CR1$^{+/GFP}$ mice. To reflect the above finding that CD64 and F4/80 are either co-expressed or both absent from the MP populations defined above, I modified the gating strategy slightly. Thus, total MPs were examined for CD64 expression prior to analysis of CD103 and CD11b expression on the CD64^{-}B220^{-} MPs (Fig. 3.3A). This analysis revealed the same subsets of CD64^{-} MPs based on CD103 and CD11b expression (Fig. 3.3A). As expected, the two CD103^{+} DC populations were negative for CX3CR1, while the CD64^{+} mϕ population mostly expressed high levels of this chemokine receptor. However, the CD64^{-}CD103^{-} putative DCs were heterogeneous for CX3CR1. Whereas the CD64^{-}CD103^{-}CD11b^{+} MPs expressed intermediate levels, some of the CD64^{-}CD103^{-}CD11b^{-} MPs lacked CX3CR1 expression while others expressed intermediate levels (Fig 3.3B). Thus, neither CD103 nor CX3CR1 are completely reliable for distinguishing DCs from mϕs in the LP. I next went on to examine the expression of other DC and myeloid markers on the various MP populations. As described previously and consistent with this population in other tissues, the CD103^{+}CD11b^{-} DCs expressed CD8α, whereas neither the CD103^{+}CD11b^{+} DCs, the CD103^{-}CD11b^{+} putative DCs nor the CD103^{-}CD11b^{+} mϕs were CD8α^{+}. The CD103^{-}CD11b^{-} putative DCs expressed heterogeneous levels of CD8α (Fig. 3.3C). The myeloid cell marker, signal regulatory protein α (SIRPα) was expressed by all intestinal MP populations except for the CD103^{+}CD11b^{-} DCs and a proportion of the CD103^{-}CD11b^{-} putative DCs (Fig. 3.3D).

Previous studies have suggested that the relative proportions of CD103^{+}CD11b^{+} and CD103^{+}CD11b^{-} DCs depend on the part of the gastrointestinal (GI) tract examined, with CD103^{+}CD11b^{+} DCs predominating in the SI duodenum and CD103^{+}CD11b^{-} predominating in the colon (Denning et al., 2011). Having identified two novel populations of CD103^{-} putative DCs in the whole SI LP, I next investigated if the frequencies of these cells were also dependent upon location throughout the GI tract. To do this, I examined the proportions of CD64^{-} DC subsets in the duodenum, jejunum, ileum and colon. This analysis revealed a marked and progressive decrease in the proportion of CD103^{+}CD11b^{+} DCs going down the length of the intestine from the duodenum to the colon, with significantly fewer in the colon (~4%) compared with the duodenum

(~15%). The other CD64$^-$ MP populations examined remained constant throughout the length of the small intestine but were significantly increased in proportion in the colon, this being most apparent for the CD103$^+$CD11b$^-$ DCs which constituted ~14% in the colon and only ~3% in the duodenum of the SI (Fig. 3.4A). Total mϕs were also examined throughout the length of the intestine. However, as the level of CD11c on intestinal mϕs is not uniform, to ensure all mϕs were included in this analysis, they were identified amongst live leukocytes as CD11b$^+$ and CD64$^+$ cells (Fig. 3.4B) rather than pre-gating on CD11c and MHCII. The proportion of mϕs was shown to increase progressively from the duodenum (~38%) to the colon (~50%) (Fig. 3.4C).

As the ability to migrate to the draining lymph node is a definitive property of DCs, I next examined whether the putative DC subsets I had identified in the gut could be found in the mesenteric lymph nodes (MLNs). To do this, live leukocytes were first identified and then B cells were excluded as B220$^+$ cells (Fig. 3.5A). Analysis of the remaining cells for CD11c and MHCII expression revealed two distinct populations, a CD11c$^+$MHCII^{int} population and a CD11c$^+$MHCII^{hi} population (Fig. 3.5B). Recent work on DCs in the skin and lung draining lymph nodes, as well as in pseudo-afferent intestinal lymph (Cerovic et al., 2013; Guilliams et al., 2010b; Plantinga et al., 2013) has concluded that the CD11c$^+$MHCII^{hi} cells are migratory DCs which have entered lymph nodes from tissues via lymph. In contrast, the CD11c$^+$MHCII^{int} population is thought to be blood-derived, lymph node resident DCs. Consistent with the non-migratory nature of mϕs, very few of the cells in the migratory gate identified in the MLNs expressed CD64 (Fig. 3.6A) and CD64$^+$ cells were also rare amongst the resident DC gate (Fig. 3.6B). Analysis of CD103 and CD11b expression by the CD64$^-$ cells amongst the migratory DC gate revealed four populations that were phenotypically similar to those I found in the LP (Fig. 3.6A). While phenotypically similar, the proportions of the CD103$^+$CD11b$^-$ and CD103$^-$CD11b$^+$ DC subsets differed slightly to those seen in LP (compare Fig. 3.3B with Fig. 3.6A). Consistently, the frequency of CD103$^+$CD11b$^-$ DCs tended to be higher in the MLNs than in the LP (~20-30% of migratory DC compared with ~15-18% in the SI LP) and this was coupled with a trend towards a lower frequency of CD103$^-$CD11b$^+$ DCs in the MLNs compared with the LP (~10-12% in the MLNs and ~15-18% in the SI LP). In contrast there were only three populations of CD64$^-$ MPs amongst the resident DC gate, with the

$CD103^+CD11b^+$ subset being absent (Fig. 3.6B). This is consistent with the designation of the DCs within the $CD11c^+MHCII^{int}$ gate as LN resident, as the $CD103^+CD11b^+$ DCs have, to date, only been described in the intestine. Indeed, I could not find any $CD103^+CD11b^+$ DCs outwith the intestinal mucosa in either lymphoid tissues such as the spleen (Fig. 3.7A), or non-lymphoid tissues such as the lung, liver or kidney (Fig. 3.7B-D).

The expression of CD11c and MHCII, but not CD64 or F4/80, coupled with the presence of phenotypically similar cells in the migratory subset of MLN DCs, suggested that the four populations of MP I had identified in the LP are indeed genuine DCs. To confirm this, I next set out to determine if the MP populations conformed to the core gene signatures recently identified by the Immunological Genome Consortium as being typical of DCs and mϕs (Gautier et al., 2012; Miller et al., 2012). First I examined expression of CD26 and CD272 as DC-specific markers and CD14 and MerTK as mϕ–specific. Consistent with their designation as DCs, all $CD11c^+CD64^-$ populations expressed CD26 and CD272, but lacked MerTK and CD14 (Fig. 3.8). On the other hand, the $CD11c^+CD64^+$ MPs lacked expression of the DC-specific markers, but expressed both CD14 and MerTK, confirming their identification as mϕs (Fig. 3.8).

3.3 Transcription factor expression by intestinal MP subsets

To explore further the nature of the MP populations I had identified, I next FACS-purified the individual subsets (Fig. 3.9) and examined the expression of the transcription factors associated with the development and differentiation of DCs and mϕs.

I first examined the expression of Zbtb46, the recently reported DC-specific transcription factor (Meredith et al., 2012a; Satpathy et al., 2012). Confirming my earlier phenotypic analysis all four populations of $CD64^-$ putative DCs expressed mRNA for *Zbtb46* at equivalent levels, while the $CD64^+$ mϕs did not (Fig. 3.10A). The other transcription factors I analysed were Batf3, IRF4, IRF8 and Id2. Batf3 is considered to be specific for $CD8\alpha^+$ DCs and $Batf3^{-/-}$ mice have been shown to lack $CD103^+CD11b^-$ DCs in the intestine (Edelson et al., 2010). Despite this, similar levels of Batf3 mRNA were observed in all intestinal DC subsets, as well as

in the mϕ population (Fig. 3.10B). IRF4 and IRF8 are interferon regulatory factors associated with the development of $CD11b^+$ and $CD11b^-$ DCs respectively (Edelson et al., 2010; Ginhoux et al., 2009; Persson et al., 2013b; Schlitzer et al., 2013). Consistent with this, IRF4 mRNA was detected at similar levels in $CD103^+CD11b^+$ and $CD103^-CD11b^+$ DCs, as well as in mϕs. IRF4 mRNA was also detected in the $CD103^-CD11b^-$ DCs (Fig. 3.10C). On the other hand, IRF8 mRNA was detected at the highest level in $CD103^+CD11b^-$ DCs, with very little being found in $CD103^+CD11b^+$ DCs. The $CD103^-CD11b^+$ and $CD103^-CD11b^-$ DCs also expressed IRF8 mRNA; although at levels about 10-fold lower than seen in the $CD103^+CD11b^-$ DC (Fig. 3.10D). Interestingly, mϕs expressed similar levels of IRF8 to the $CD103^+CD11b^-$ DCs, but the relevance of this remains unclear. Id2 was originally thought to control the differentiation of $CD8\alpha^+$ lineage of DCs, but it has since been shown to be expressed by both $CD11b^+$ and $CD11b^-CD8\alpha^+$ DCs (Jackson et al., 2011). Consistent with this, all intestinal DC subsets expressed Id2 mRNA, although this was approximately 2-fold lower in the two subsets of $CD103^-$ DCs compared with the $CD103^+$ subsets. Mϕs also expressed Id2 at levels equivalent to $CD103^+$ DCs (Fig. 3.10E).

3.4 Transcriptional profile of intestinal MP populations

I next set out to determine how similar or otherwise these cells were in terms of their complete transcriptional profiles. For this, I FACS-purified the MP populations from the SI LP and sent RNA samples for microarray. The analysis of the microarray data is currently being performed in collaboration with Drs. Toby Lawrence, Bernard Malissen and Marc Dalod (CIML, Marseille, France).

3.5 Growth factor dependence of intestinal MP subsets

So far my data suggest that all four populations of $CD11c^+CD64^-$ MP are *bona fide* DCs, while the $CD11c^+CD64^+$ MP are mϕs. As DCs and mϕs require distinct growth factors for their development, I next investigated the dependency of each intestinal MP population on Flt3L, CSF-1 and CSF-2. DC development has been shown to require Flt3L and CSF-2, while mϕ development is known to depend on CSF-1 (Helft et al., 2010; MacDonald et al., 2010; Merad and Manz, 2009; Waskow et al., 2008). To investigate the role of these growth factors, I first

examined the expression of their receptors on sorted populations of intestinal MPs (Fig. 3.11). Consistent with their designation as DCs, all four populations of $CD11c^+CD64^-$ cells expressed high levels of mRNA for CD135 (Flt3), the receptor for Flt3L, while the mϕs lacked expression of this receptor (Fig. 3.11A). Interestingly all intestinal MP subsets expressed similar levels of mRNA for CD116, the α chain of the receptor for CSF-2 (Fig. 3.11B). Conversely and consistent with their known requirement for CSF-1R signalling, the mϕs expressed the highest levels of the receptor for this factor, CD115 (CSF-1R). In comparison, both subsets of $CD103^+$ DCs expressed very low levels of CD115 and although the two $CD103^-$ DC subsets expressed intermediate amounts of CD115 mRNA, this was at a level about 10-fold lower than that of the mϕs (Fig. 3.11C).

Given these results, I next decided to investigate how the intestinal MP populations were affected in mice lacking growth factors or their receptors. Although I did not have access to any of these mice in Glasgow, I was able to establish collaborations that allowed me to investigate $Flt3L^{-/-}$ mice (in collaboration with Prof. Bart Lambrecht and Dr. Martin Guilliams, University of Ghent) and $CSF\text{-}2R2b^{-/-}$ mice (in collaboration with Prof. Fiona Powrie and Dr. Thibault Griseri, University of Oxford). In both cases I travelled to their labs and compared MP populations in the SI LP of the KO mice with co-housed WT mice as controls. Importantly, I found the same populations of DCs and mϕs in both groups of WT mice that I had identified in Glasgow.

As reported previously (Tamoutounour et al., 2012), the proportion of total $CD64^-CD11c^+MHCII^+$ DCs was severely reduced in the SI LP of $Flt3L^{-/-}$ mice (Fig. 3.12A). Subsequent analysis of the remaining DCs in these mice for expression of CD103 and CD11b demonstrated that there was no selective effect of Flt3L deficiency and that all four putative DC populations were virtually absent in the $Flt3L^{-/-}$ mice (Fig. 3.12B). In contrast, the relative proportion of mϕs was unchanged in these mice indicating their independence of Flt3L (Fig. 3.12C).

To complement these studies I examined the effects of exogenous recombinant murine Flt3L on the numbers of MP subsets in the intestine of WT mice in Glasgow. For this, mice received 10μg Flt3L i.p. for 8 days, or PBS as a control. Flt3L administration led to a dramatic expansion in the numbers of $CD11c^+MHCII^+$ MPs, which now comprised 40-45% of live leukocytes, compared

with 12-16% in the PBS treated controls (Fig. 3.13A). Upon examination of CD11c and F4/80 expression, it was clear that this expansion was due to a preferential increase in $CD11c^{+}F4/80^{-}$ DCs (Fig. 3.13B). This was most marked in the $CD103^{+}CD11b^{-}$ DC population, but the relative increases in numbers of $CD103^{-}CD11b^{+}$ and $CD103^{-}CD11b^{-}$ DCs were almost as marked and the numbers of $CD103^{+}CD11b^{+}$ DCs were also significantly increased compared with controls (Fig. 3.13C-E). Although the numbers of $CD64^{+}$ mϕs were not altered by administration of Flt3L, there was a slight but significant reduction in the proportion of mϕs (Fig. 3.13C-F).

There were no differences in the relative proportion of $CD11c^{+}CD64^{-}$ DCs and $CD11c^{+}CD64^{+}$ mϕs in the SI LP of CSF-2R2b$^{-/-}$ mice compared with WT mice (Fig. 3.14A), but, there was a significant defect in the proportion of $CD103^{+}CD11b^{+}$ DCs in CSF-2R2b$^{-/-}$ mice compared with controls. However, it should be noted that a number of cells in the KO mice fell outside the CD103 gate set using WT controls, suggesting generally lower levels of CD103 expression. This is consistent with previous suggestions that CSF-2 is needed for CD103 expression (Edelson et al., 2010; Greter et al., 2012; Zhan et al., 2011). As a result, it is difficult to make conclusions about the involvement of CSF-2 in intestinal DC development when using CD103 as a marker. There were no significant differences in the other MP populations in the CSF-2R2b$^{-/-}$ mice (Fig. 3.14B,C).

As with Flt3L, I attempted to complement the studies in the CSF-2R2b$^{-/-}$ mice by giving WT mice in Glasgow exogenous CSF-2. Initially, I attempted to do this by administration of recombinant CSF-2, but this was unsuccessful due to the limited amounts available. Therefore I used an alternative approach, in which mice were inoculated with CSF-2 secreting B16 melanoma cells for 10 days. This led to a dramatic increase in the proportion of $CD11c^{+}MHCII^{+}$ cells, with a marked upregulation of CD11c expression so that almost all of the cells within the $CD11c^{+}MHCII^{+}$ gate expressed high levels of CD11c (Fig. 3.15A). CD64 expression was also upregulated on $CD11c^{+}MHCII^{+}$ cells from CSF-2 treated animals compared with those from WT controls (Fig. 3.15B), although expression of F4/80 was not affected by the administration of CSF-2 (Fig. 3.15B). As a result of their high expression of CD11c and lack of F4/80, for the purposes of this analysis, I assumed the $F4/80^{+}$ cells to be mϕs while the $F4/80^{-}CD64^{int}$ cells were analysed as DCs. On this basis CSF-2 administration resulted in an expansion of

all DC populations, while F4/80$^+$ mϕs were unaffected (Fig. 3.15C-E). The greatest increase in DC number was observed amongst the CD103$^-$CD11b$^+$ DC population (Fig. 3.15E) with decreases in the proportion of the other DC subsets (Fig. 3.15C.D). Unfortunately I did not have time to repeat this experiment or to confirm the nature of these cells induced by CSF-2 by more detailed analysis. Thus further investigation is required to determine the role of CSF-2 in intestinal DC development.

3.6 Population kinetics of intestinal MP populations *in vivo*

As intestinal DCs are short-lived cells that sample antigen in the LP and migrate constitutively to the MLNs, I hypothesised that they would have distinct kinetics to intestinal mϕs, which are long-lived and sessile in the LP. Therefore as a final means of distinguishing DCs and mϕs amongst intestinal MPs, I examined their kinetics *in vivo* using BrdU pulse-chase, in which mice were given a single dose of BrdU i.p. and then fed BrdU in the drinking water for 3 days. BrdU$^+$ cells amongst the MP in the SI LP were then assessed immediately after cessation of BrdU feeding and again at 3, 6 and 9 days after withdrawing BrdU. I also examined BrdU incorporation by DCs in the MLNs to determine if any of the LP DCs had migrated to the MLNs.

After 3 days of BrdU feeding, all the CD64$^-$ DC populations in the SI LP were ~65-80% BrdU$^+$, whereas only ~20% of the CD64$^+$ mϕs were BrdU$^+$ (Fig. 3.16A,B). After withdrawal of BrdU, the proportion of BrdU$^+$ DCs in the LP decreased over time, until few BrdU$^+$ cells remained in any DC population 9 days after cessation of BrdU feeding (Fig. 3.16B). No differences were observed in the rate of BrdU$^+$ cell loss between the different subsets of DCs. The loss of BrdU$^+$ cells from the LP correlated with an increase in the proportion of BrdU$^+$ cells amongst the migratory CD11c$^+$MHCII^{hi} DCs within the MLNs which rose from ~40% immediately after BrdU administration to 60-70% 3 days after BrdU withdrawal (Fig. 3.16C). This increase was observed for all DC populations except for the CD103$^-$CD11b$^-$ DCs, where the proportion of BrdU$^+$ cells fell progressively from ~40% after cessation of BrdU feeding. The proportion of BrdU$^+$ cells amongst the other migratory DC subsets in the MLNs fell slightly from 3-6 days after BrdU withdrawal and decreased further by day 9 (Fig. 3.16C). Conversely, the number of BrdU$^+$ cells

amongst the CD64$^+$ mϕs remained at similar levels throughout the study with the exception of 3 days after cessation of BrdU, which likely represents a technical issue as all MP populations had a slightly lower than expected proportion of BrdU$^+$ cells (Fig. 3.16B). This analysis thus confirms the extended half-life of the mϕs and their inability to migrate to the MLNs compared with the DCs.

3.7 Summary

In this chapter I set out to characterise intestinal DCs using multi-parameter flow cytometry, transcriptional analysis, growth factor dependence and kinetic studies. I first made use of recent developments in our lab and elsewhere in which CD64 was found to be a useful means of distinguishing DCs and mϕs (Bain et al., 2013; Tamoutounour et al., 2012). By exploiting this, I was able to characterise total CD11c$^+$MHCII$^+$ MPs in the small intestinal LP without relying on CD103 and CX3CR1, two markers which had become the convention in the field for distinguishing between DCs and mϕs in the intestinal lamina propria. This analysis allowed me to define mϕs as CD64$^+$ and to identify four subsets of CD64$^-$ MPs, based on the expression of CD103 and CD11b, which I proposed to be genuine DCs. In addition to the well-characterised populations of CD103$^+$CD11b$^+$ and CD103$^+$CD11b$^-$ DCs, I also found equivalent subsets of CD103$^-$ DCs whose existence had been contentious, often resulting in their inclusion amongst mϕs. All these CD64$^-$ DC subsets could also be found in the colonic LP and amongst migratory populations of DCs in the MLNs.

I went on to demonstrate definitively that the novel CD103$^-$CD64$^-$ MPs were indeed DCs, as they expressed CD26, CD272 and the recently defined DC-specific transcription factor, Zbtb46, but lacked expression of the mϕ markers; MerTk and CD14. Additionally, all the CD103$^-$ and CD103$^+$ DCs expressed similar levels of the transcription factors and growth factor receptors associated with DC development, which was were quite distinct from the CD64$^+$ mϕs. In parallel, all the DC subsets but not mϕs were absent in Flt3L$^{-/-}$ mice and their numbers increased in response to *in vivo* administration of Flt3L. Additionally, all CD64$^-$ DCs were shown to expand in response to exogenous CSF-2 *in vivo* with apparent preferential increase in the numbers of CD103$^-$CD11b$^+$ DCs, although the effects of CD11c and CD64 expression made these results more difficult to interpret. *In*

vivo kinetic studies demonstrated similar BrdU incorporation by the $CD103^+$ and $CD103^-$ DC subsets in the SI LP, all of which showed rapid turnover from precursors and efficient migration to the MLNs. In contrast the $CD64^+$ mϕs were comparatively long-lived and sessile.

Together these experiments allowed me to establish reliable techniques for distinguishing DCs and mϕs in the steady state intestine and to identify two novel *bona fide* populations of $CD103^-$ DCs. In the next chapter, I set out to examine the ontogeny of these cells, and more specifically to determine whether they were the progeny of common DC precursors or if monocytes also played a role in their replenishment.

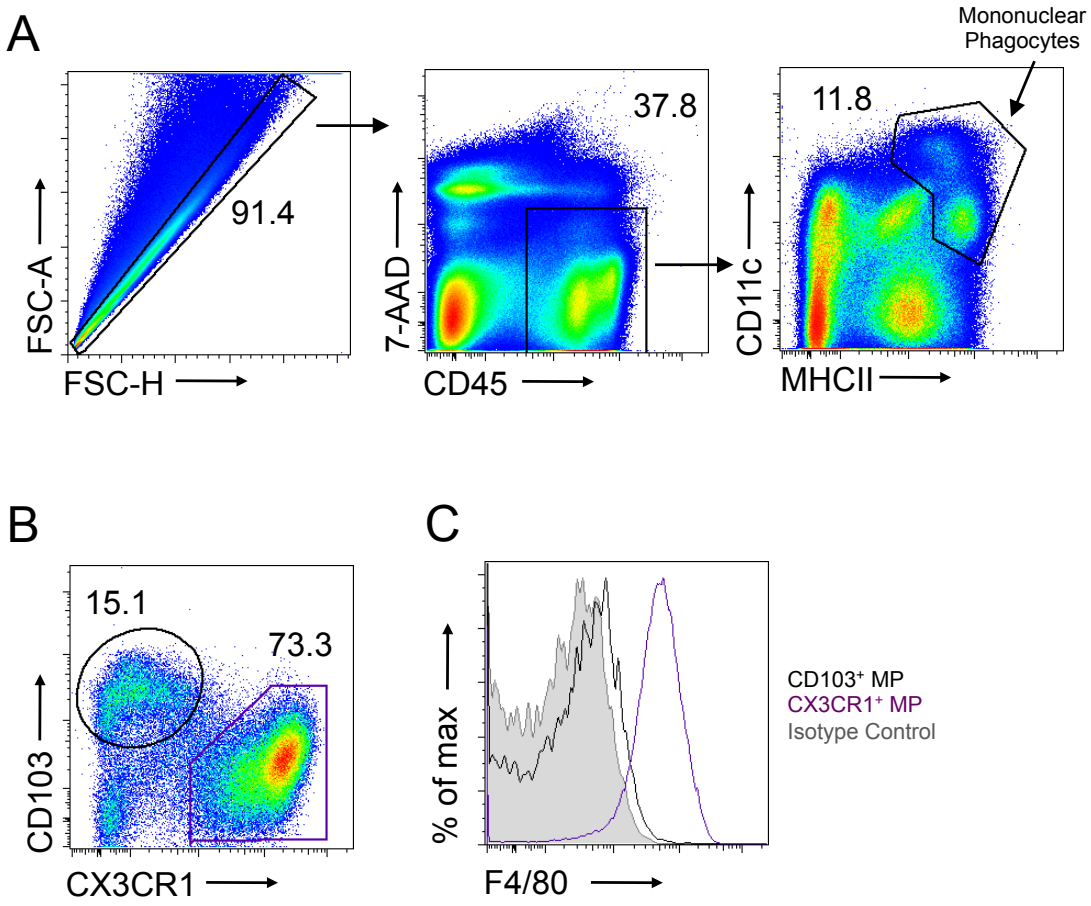

Figure 3.1: Initial gating strategy for identification of SI mononuclear phagocytes
SI LP cells were isolated from CX3CR1$^{+/GFP}$ mice and analysed for CD103 and CX3CR1-GFP expression by flow cytometry. **A.** Representative dot plots showing the identification of single cells based on FSC-A and FSC-H profiles. Live leukocytes were identified amongst single cells as CD45^{+}7-AAD^{-} cells and mononuclear phagocytes identified as CD11c^{+}MHCII^{+} cells. **B.** Representative dot plots showing expression of CD103 and CX3CR1-GFP by mononuclear phagocytes as gated in A. **C.** Expression of the pan mϕ marker F4/80 by CD103^{+} MP (black line) and CX3CR1^{+} MP (purple line) compared with isotype control (shaded grey line). Results are representative of at least 10 individual experiments.

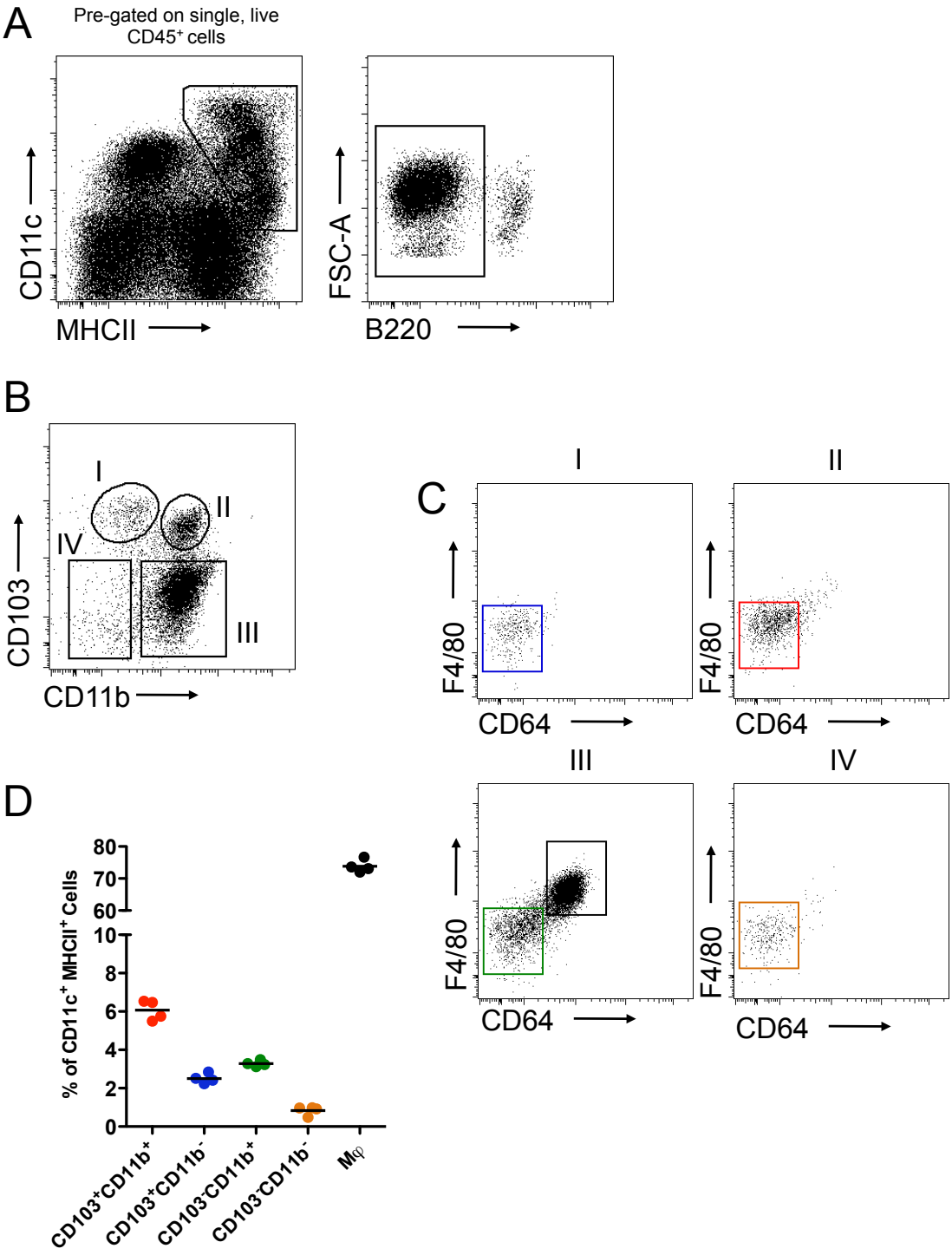

Figure 3.2: Characterisation of intestinal MP populations in non CX3CR1$^{+/GFP}$ mice

A. Representative dot and contour plots showing the gating used to define MPs in SI LP digests. After selection of single, live (7-AAD^{-}) leukocytes (CD45^{+}) as shown in Fig 3.1, MPs were identified as CD11c^{+}MHCII^{+} and any contaminating B cells were excluded as B220^{+} cells. **B.** Representative dot plots showing expression of CD103 and CD11b on B220^{-} MPs. **C.** Expression of F4/80 and CD64 on the four populations of MPs identified in B. **D.** Proportion of each MP subset as a percentage of total CD11c^{+}MHCII^{+} cells. Data are representative of at least 20 independent experiments with n =3/4 per experiment.

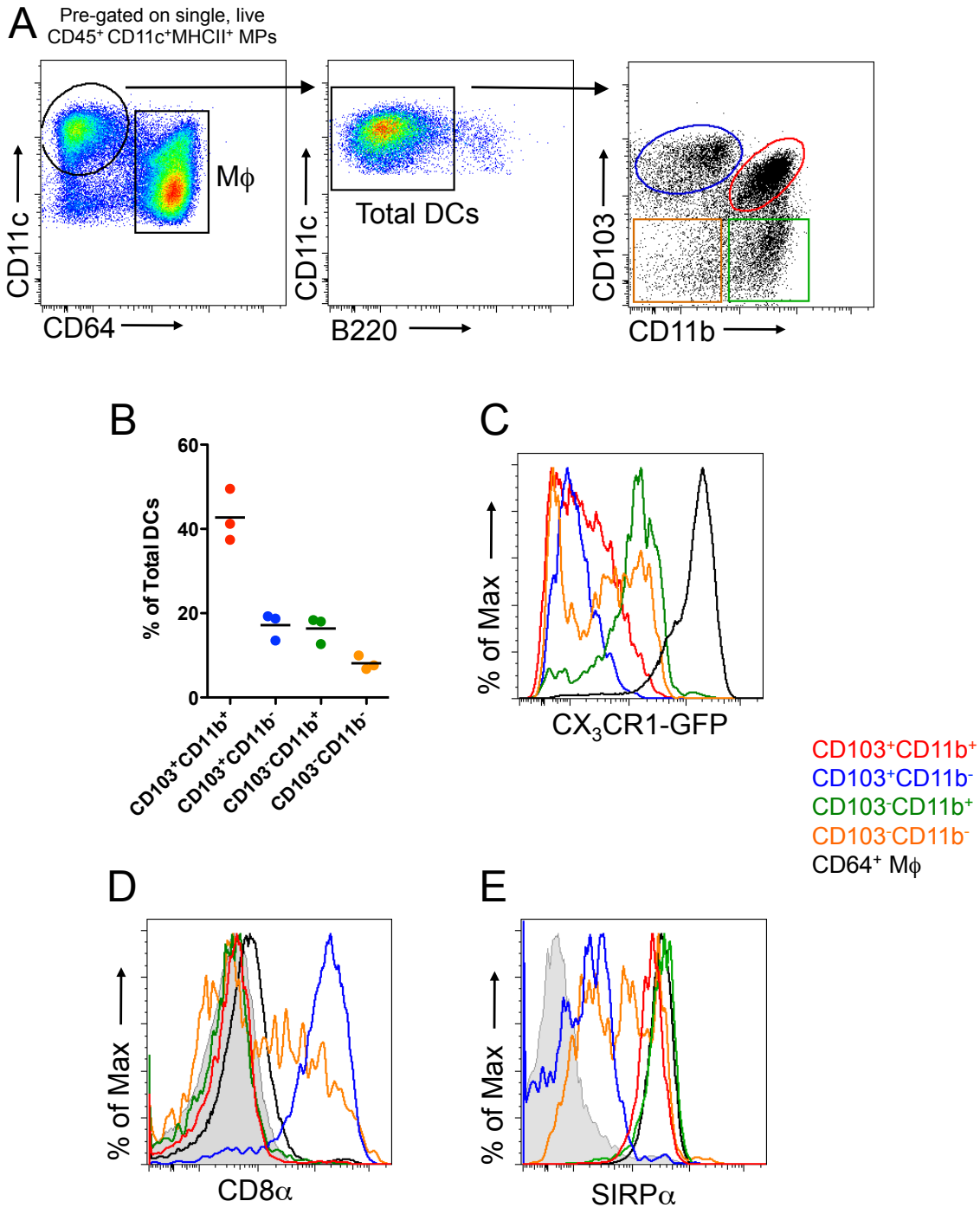

Figure 3.3: Expression of CX3CR1, CD8α and SIRPα by intestinal MPs

A. Representative dot plot showing identification of total DCs as CD64^{-}CD11c^{hi}B220^{-} cells and mϕs as CD11c^{+}CD64^{+} cells amongst single live CD45^{+}CD11c^{+}MHCII^{+} MPs in SI LP digests from CX3CR1$^{+/GFP}$ mice. Total DCs were divided into four distinct subsets on the basis of their expression of CD103 and CD11b. **B.** Proportion of each DC subset as a percentage of total DCs as gated in A. **C-E.** Representative histogram showing expression of CX3CR1-GFP (B), CD8α (C) and SIRPα (D) on the four DC subsets and CD64^{+} mϕs with isotype controls shown in grey. Data are representative of at least 10 independent experiments with n =3/4 per experiment.

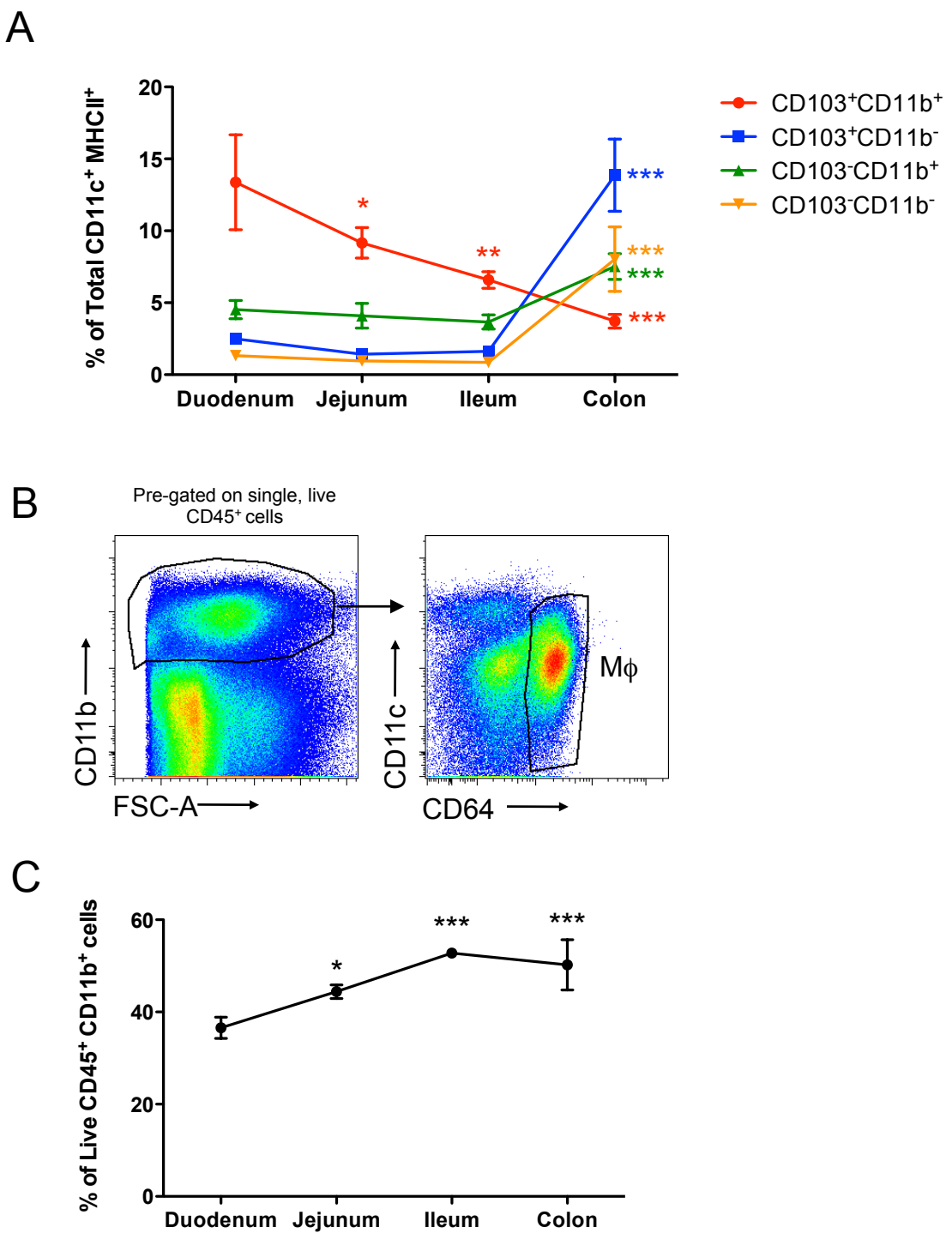

Figure 3.4: MP populations throughout the GI tract

A. DC populations were identified in the duodenum, jejunum and ileum of the small intestine LP and colonic LP as shown in Fig. 3.3. The results shown are the frequencies of each DC subset as a percentage of total CD11c$^+$MHCII$^+$ cells. **B.** Total mϕs were identified in the different parts of the GI tract as CD11b$^+$CD64$^+$ amongst single live CD45$^+$ cells as shown in Fig. 3.1. Data shown is from Ileum. **C.** Mϕs were identified in the duodenum, jejunum and ileum of the small intestine LP and colonic LP as shown in B. The results shown are the frequencies of mϕs as a percentage of live CD45$^+$CD11b$^+$ cells. Data are from a single experiment with n=3/4 *p<0.05, **p<0.01, ***p<0.005, versus equivalent population in duodenum. One way ANOVA with Bonferroni post-test.

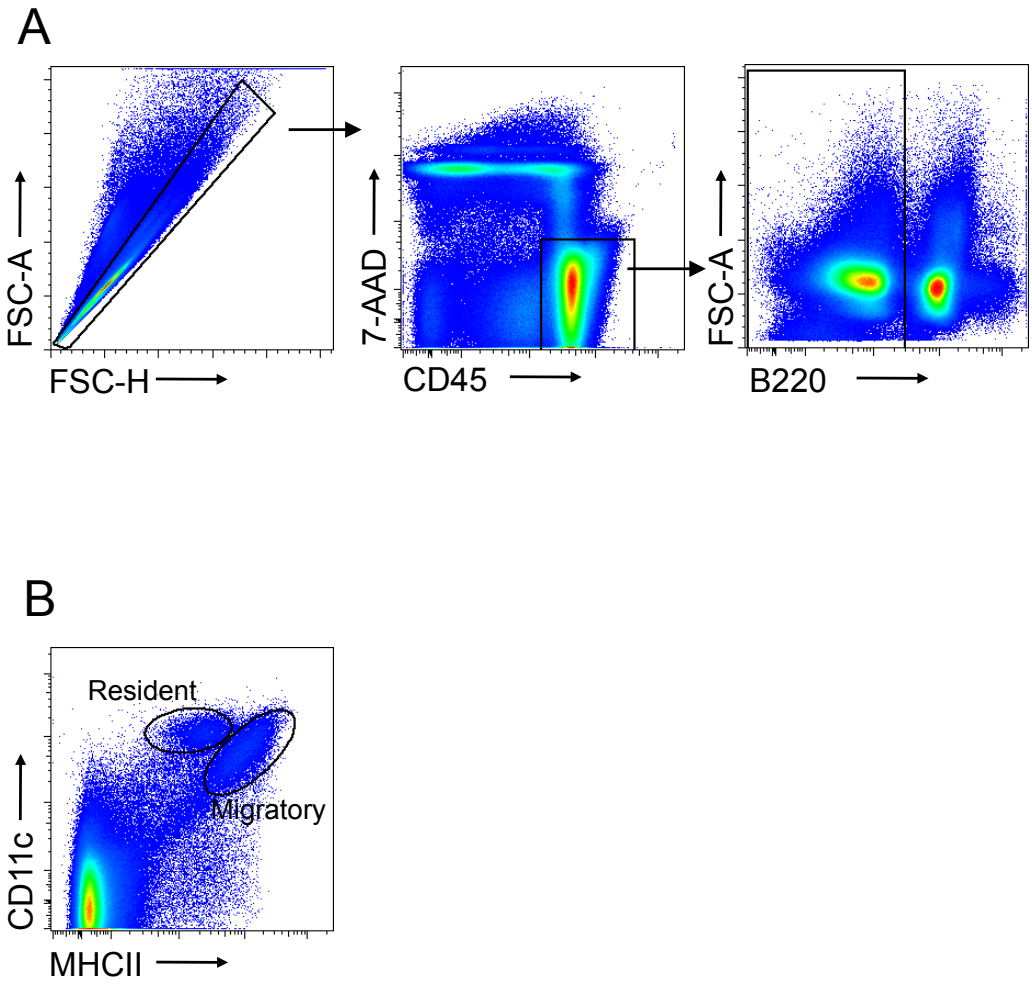

Figure 3.5: Migratory and resident DCs in the MLN

A. Representative dot plots showing the gating strategy used to define single live $B220^{-}$ $CD45^{+}$ cells amongst MLN cells. **B.** Expression of CD11c and MHCII by live-gated $B220^{-}$ $CD45^{+}$ cells defining migratory and resident DCs as $CD11c^{+}MHCII^{hi}$ and $CD11c^{+}MHCII^{int}$ respectively. Data are representative of at least 20 independent experiments with n =3/4 per experiment.

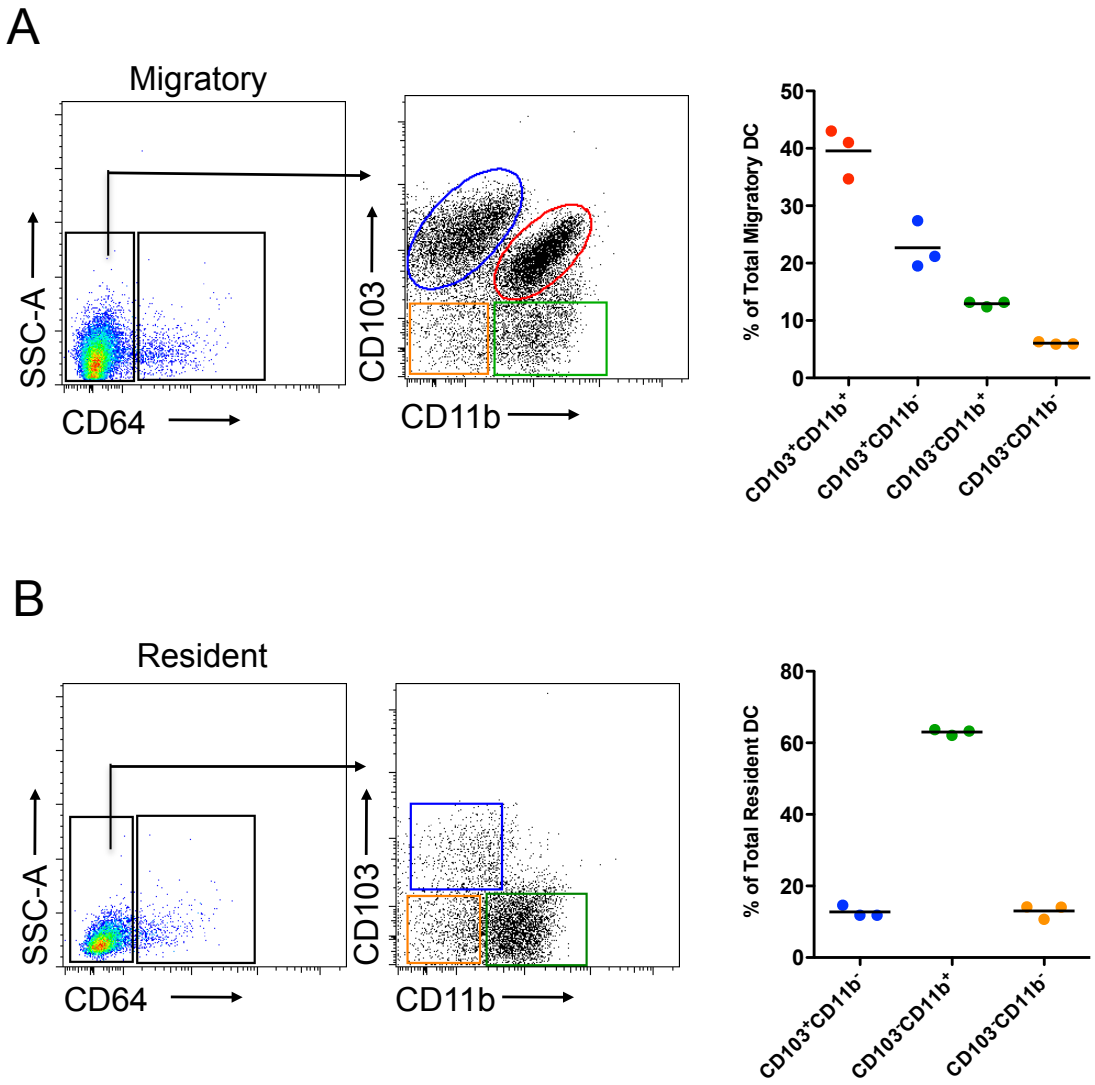

Figure 3.6: Subsets of migratory and resident DCs in the MLN

Migratory ($CD11c^{+}MHCII^{hi}$) and resident ($CD11c^{+}MHCII^{int}$) cells were identified in the MLN amongst live $B220^{-}$ $CD45^{+}$ cells and analysed for expression of CD64, CD103 and CD11b. **A.** Representative dot plots showing expression of CD64, CD103 and CD11b by migratory DCs in MLN gated as in Fig. 3.5. Scatter plot shows proportion of each DC subset as a percentage of total migratory DCs. **B.** Representative dot plots showing expression of CD64, CD103 and CD11b by resident MLN DCs gated as in Fig 3.5. Scatter plot shows proportion of each DC subset as a percentage of total resident DC. Data are representative of at least 20 independent experiments with n =3/4 per experiment.

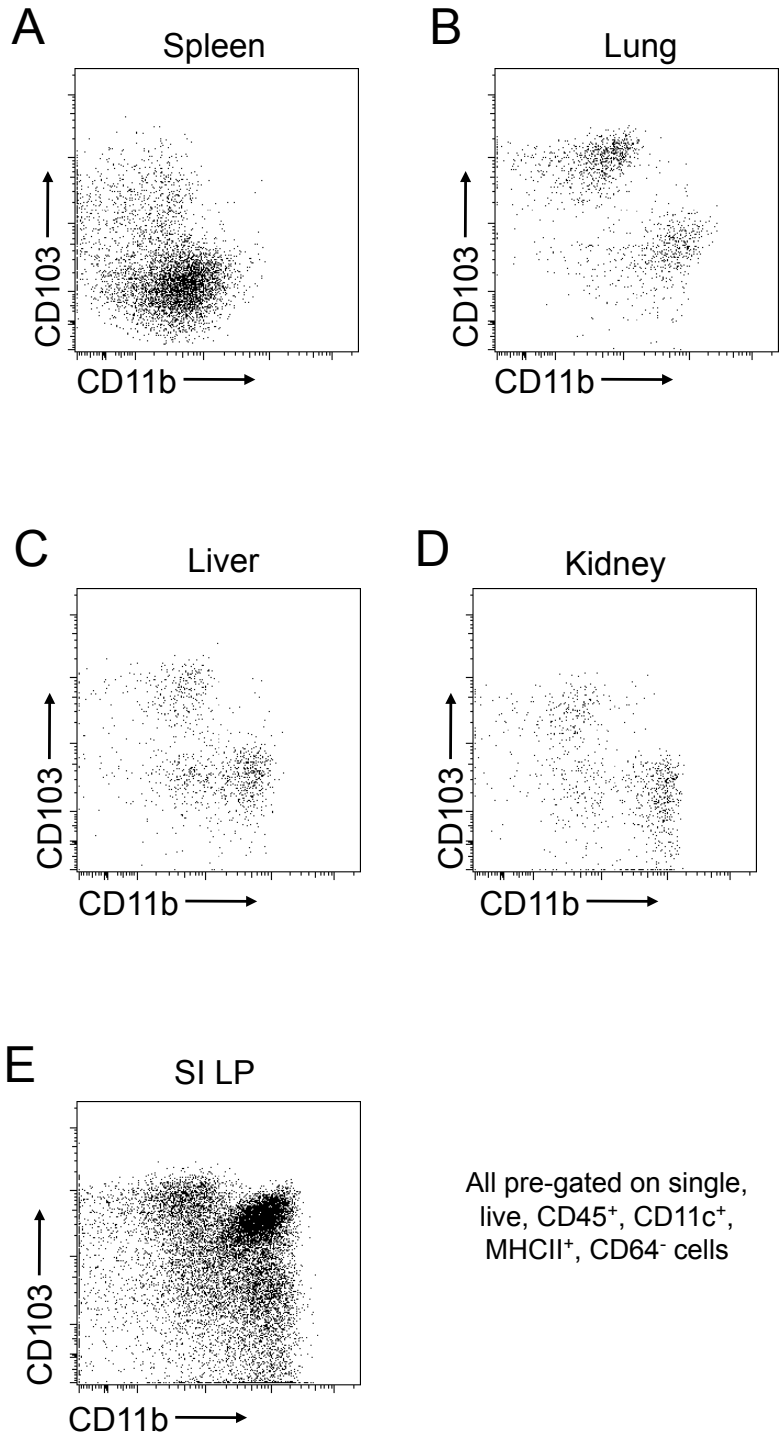

Figure 3.7: DC populations in non-intestinal tissues

Non-intestinal tissues were digested, DCs were identified as live $CD45^+$ $CD11c^+$ $MHCII^+$ $CD64^-$ cells and analysed for CD103 and CD11b expression compared with the SI LP. **A-E.** Representative dot plots showing expression of CD103 and CD11b by DCs in (A) spleen, (B) lung, (C) liver, (D) kidney and (E) SI LP. Data are from 1-2 independent experiments with n =2/3 per experiment.

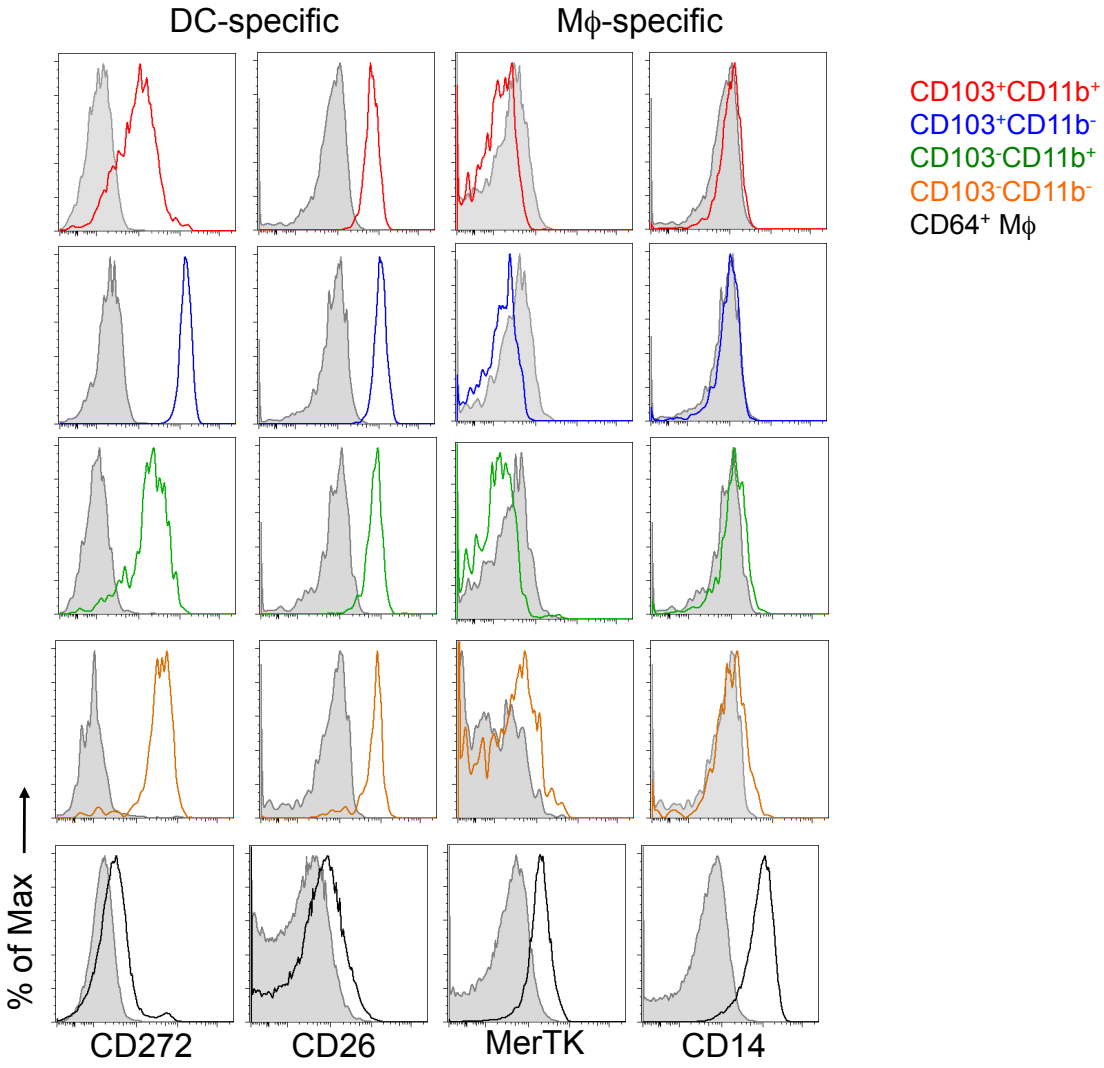

Figure 3.8: Expression of DC and mϕ specific markers by intestinal MPs

The subsets of DCs and mϕs from SI LP were identified as described in Fig. 3.3 and analysed for expression of DC and mϕ specific markers. Representative histograms shows the expression of CD272, CD26, MerTK and CD14 compared with isotype (CD272, CD26, CD14) or streptavidin only controls (MerTK) (shaded grey histograms).

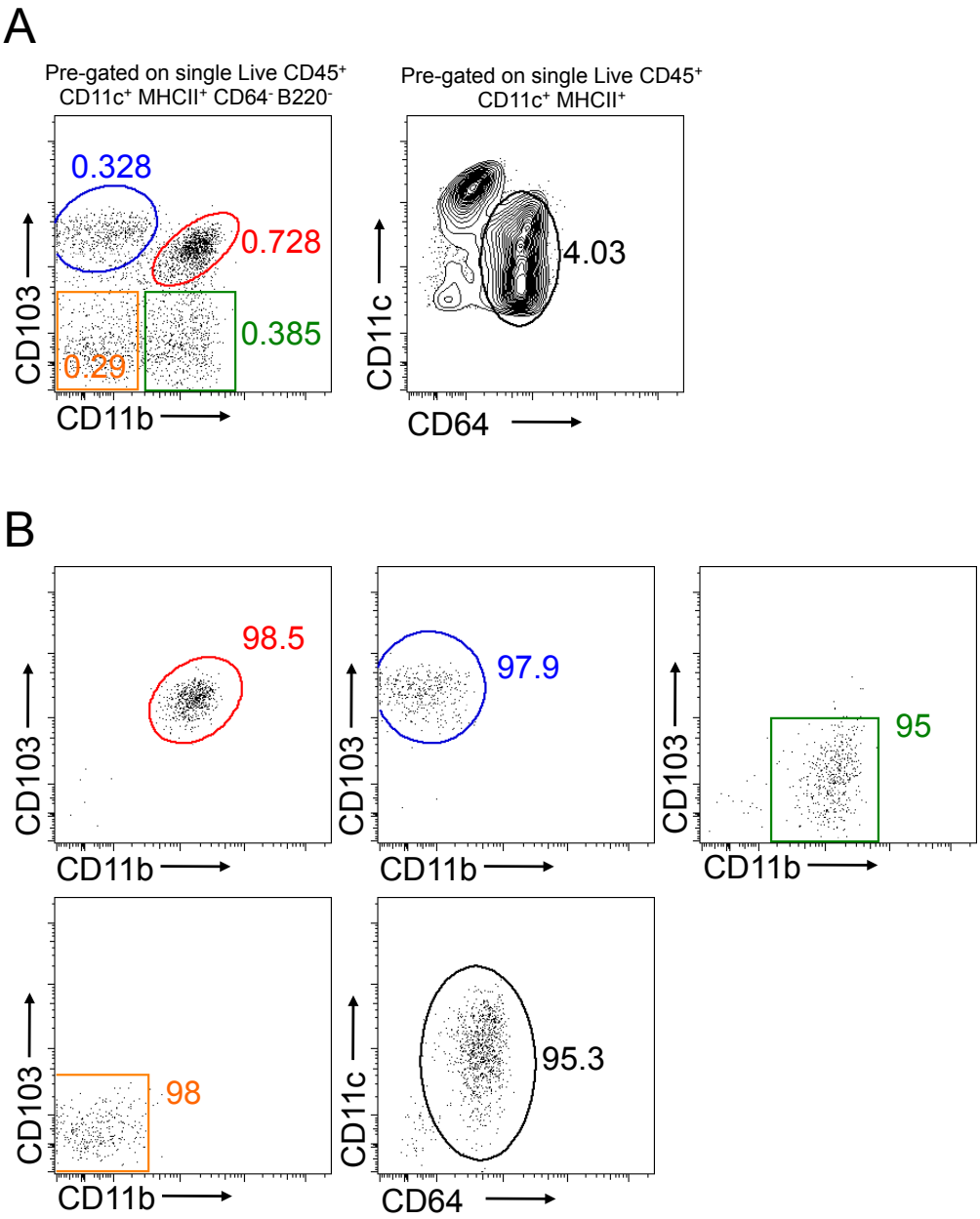

Figure 3.9: Purification of intestinal MP subsets by FACS

Subsets of CD64$^-$ DCs and CD64$^+$ mϕs were identified amongst live gated single CD45$^+$CD11c$^+$MHCI$^+$B220$^-$ in SI LP digests as shown in Fig. 3.3. **A.** Representative plots showing the proportion of each DC subset (left panel) and mϕs (right panel) as a percentage of total cells prior to sorting. **B.** Representative plots showing the proportion of each cell type as a percentage of sorted cells. Data are representative of at least 20 independent experiments with 9-12 mice pooled per experiment.

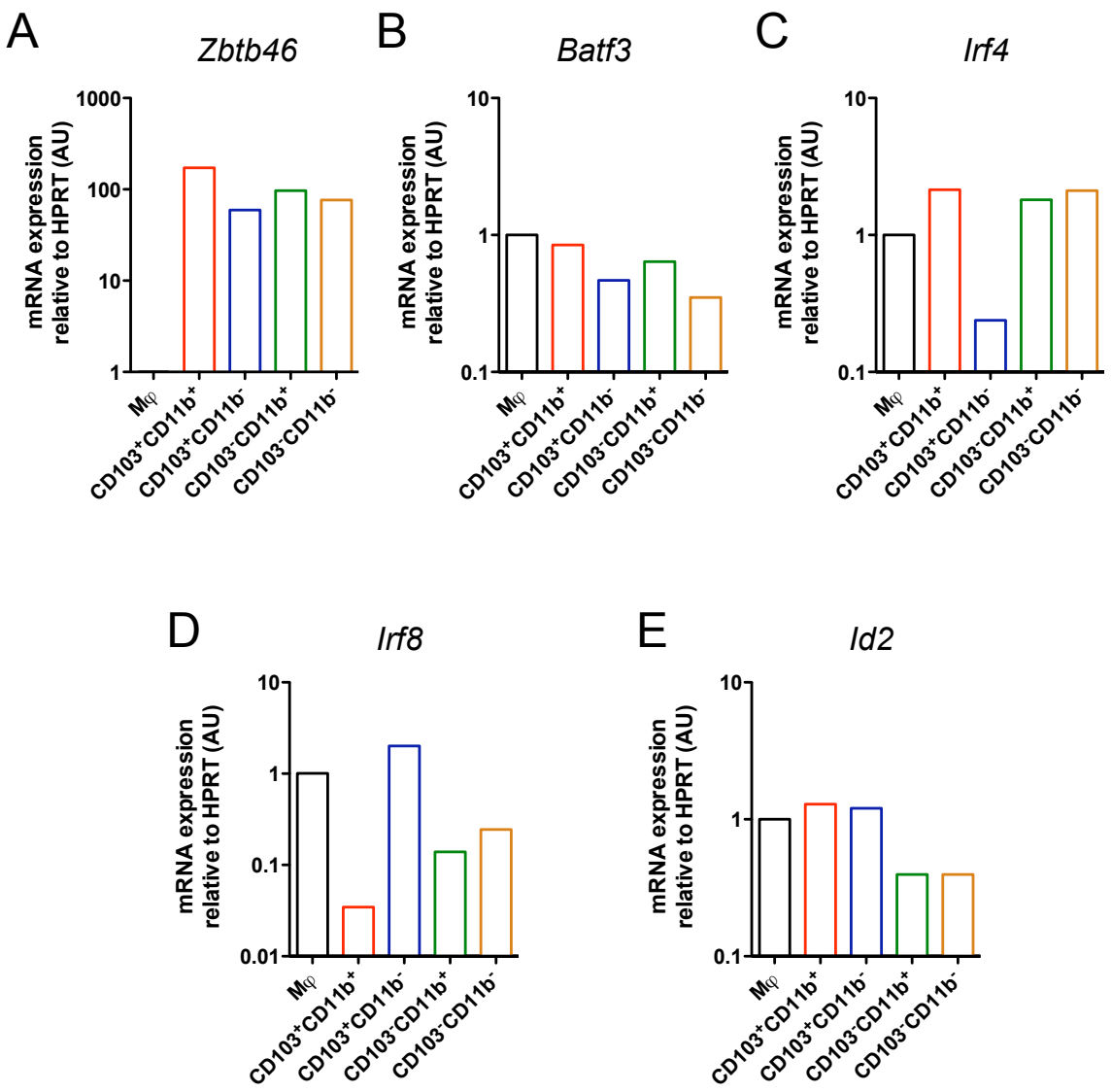

Figure 3.10: Transcription factor expression by intestinal MP subsets

A-E. SI LP DCs and mϕs were FACS-purified from whole digests as described in Fig. 3.9 and analysed by qRT-PCR for expression of mRNA for (A) *Zbtb46,* (B) *Batf3,* (C) *Irf4,* (D) *Irf8* and (E) *Id2*. Results shown are relative to HPRT using the $2^{-\Delta\Delta ct}$ method with mϕs set to 1. Data are pooled from 2 independent experiments with cells pooled from 9-12 mice per experiment.

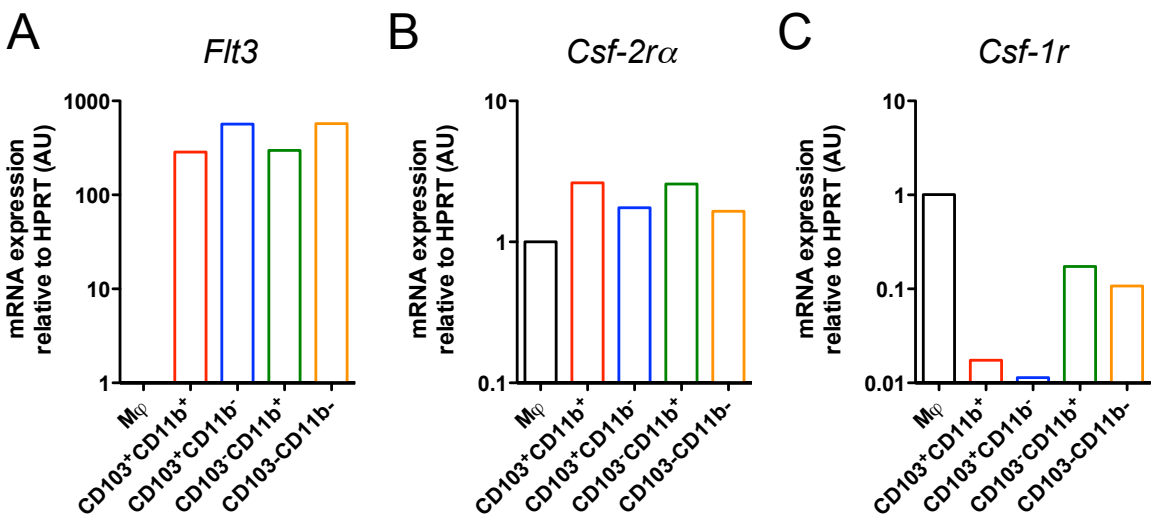

Figure 3.11: Growth factor receptor expression by intestinal MP subsets

A-C. SI LP DCs and mϕs were FACS-purified from whole digests as described in Fig. 3.9 and analysed by qRT-PCR for expression of mRNA for (A) *Flt3,* (B) *Csf-2Ra* and (C) *Csf-1R.* Results shown are relative to HPRT using the $2^{-\Delta\Delta ct}$ method with mϕs set to 1. Data are pooled from 1/2 independent experiments with cells pooled from 9-12 mice per experiment.

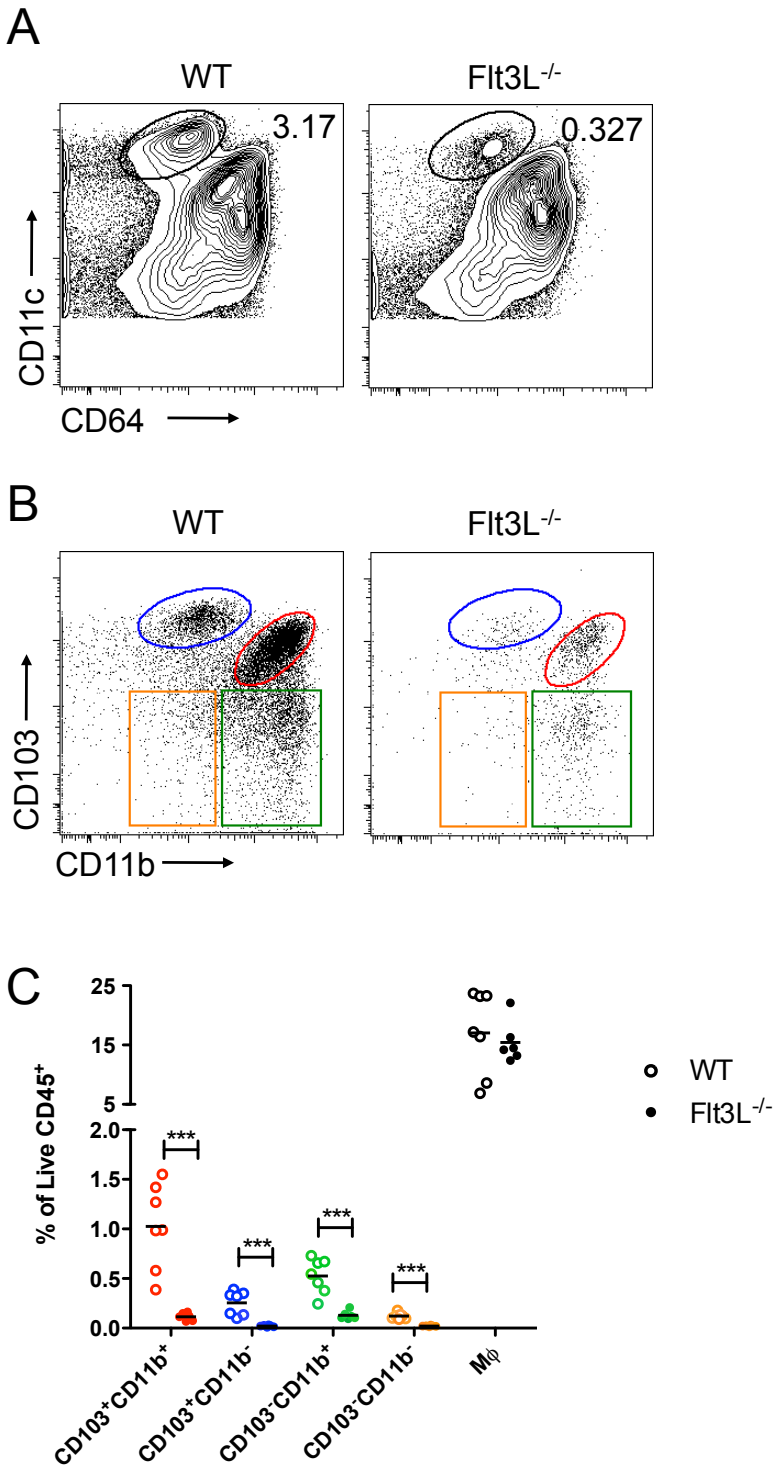

Figure 3.12: Role of Flt3L in development of intestinal MPs

A. Representative plots showing CD11c and CD64 expression on live gated $CD45^+CD11c^+MHCII^+$ in SI LP digests from $Flt3L^{-/-}$ and WT control mice. Numbers indicate percentage of live $CD45^+$ cells. **B.** Representative dot plots showing CD103 and CD11b expression on $CD11c^{hi}CD64^-$ DCs in $Flt3L^{-/-}$ and WT mice gated in A. **C.** Proportion of each MP subtype as a percentage of total live leukocytes in LP of $Flt3L^{-/-}$ and WT controls. Data are from two independent experiments with n=3/4 per group per experiment. ***p<0.001 Student's t test.

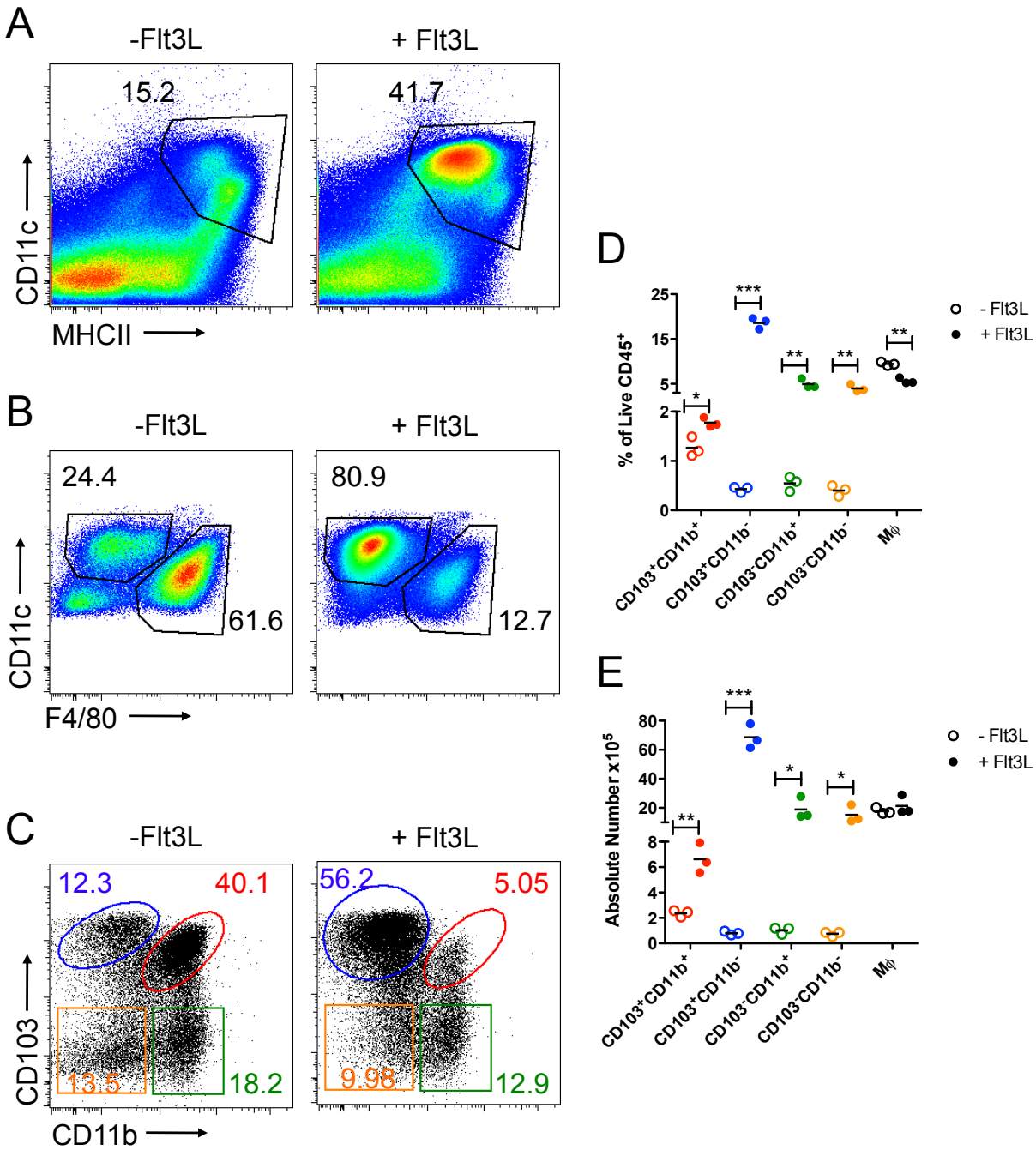

Figure 3.13: Effects of recombinant Flt3L on intestinal MP populations *in vivo*

Mice received PBS or 10μg of recombinant Flt3L i.p. daily for 8 days and DC and mϕ populations were analysed in SI LP. **A.** Representative dot plots showing CD11c and MHCII expression by live gated CD45$^+$ single cells in control and Flt3L-treated mice. **B.** Representative dot plots showing CD11c and F4/80 expression on total MPs in control and Flt3L-treated mice. **C.** Representative dot plots showing CD103 and CD11b expression on CD11c$^+$F4/80$^-$ DCs in control and Flt3L-treated mice. **D.** Proportion of each MP subtype as a percentage of total live CD45$^+$ cells in control and Flt3L-treated mice. **E.** Absolute number of each MP subset in control and Flt3L-treated mice. Data are representative of three independent experiments with n=3 per group. *p,0.05, **p<0.005, ***p<0.001 Student's t test.

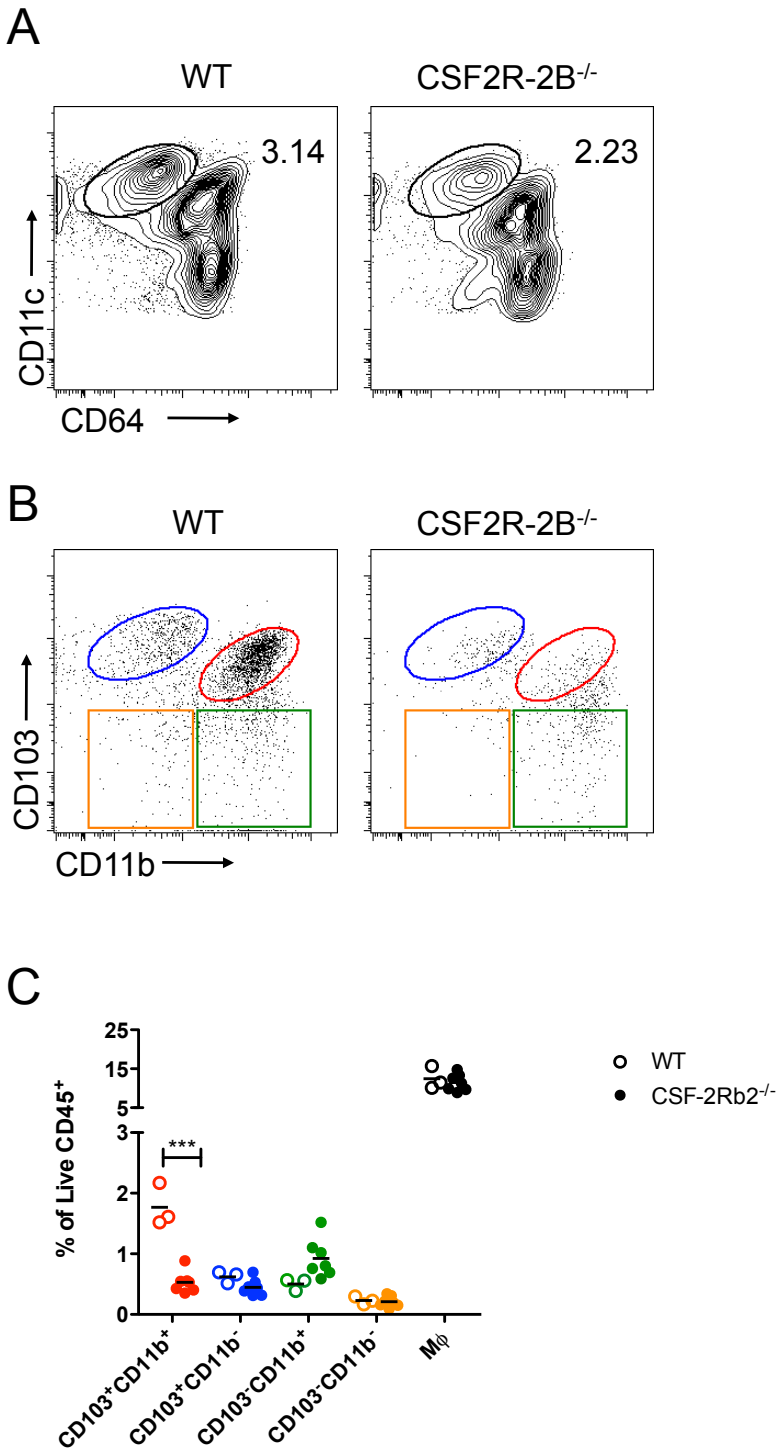

Figure 3.14: Role of CSF-2 in development of intestinal MPs

A. Representative plots showing CD11c and CD64 expression on live gated $CD45^+CD11c^+MHCII^+$ in SI LP digests from CSF-2R2b$^{-/-}$ and WT control mice. Numbers indicate percentage of live $CD45^+$ cells. **B.** Representative dot plots showing CD103 and CD11b expression on $CD11c^{hi}CD64^-$ DCs in CSF-2R2b$^{-/-}$ and WT mice. **C.** Proportion of each MP subtype as a percentage of total live leukocytes in LP of CSF-2R2b$^{-/-}$ and WT controls. Data are from a single experiment with n=3/6 per group per experiment. ***p<0.001 Student's t test.

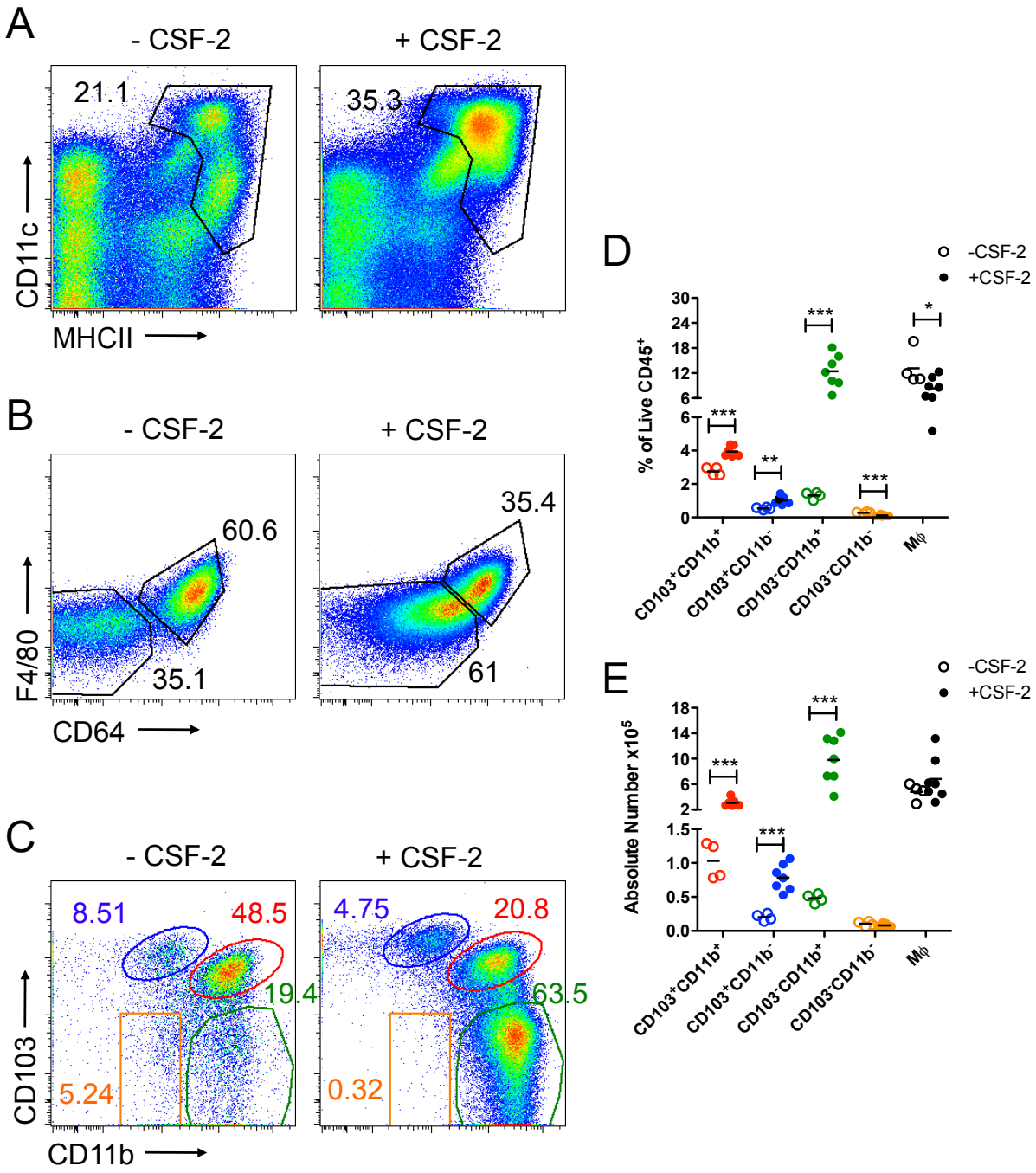

Figure 3.15: Effects of B16 melanoma-derived CSF-2 on intestinal MP populations
Mice received 2x10^6 CSF-2 secreting B16 melanoma cells s.c. and SI LP DC and mϕ populations were analysed 10 days later. **A.** Representative contour plots showing CD11c and MHCII expression by live gated CD45$^+$ single cells in resting control and CSF-2 tumour inoculated mice. **B.** Representative plots showing CD64 and F4/80 expression on live gated CD45$^+$B220$^-$CD11c$^+$ MHCII$^+$ MPs in control and CSF-2 tumour bearing mice. **C.** Representative dot plots showing CD103 and CD11b expression on CD64$^-$F4/80$^-$ DCs in control and CSF-2 tumour inoculated mice. **D.** Proportion of each MP subtype as a percentage of total live CD45$^+$ cells in control and CSF-2 tumour mice. **E.** Absolute number of each MP subset in control and CSF-2 tumour inoculated mice. Data are from a single experiment with n=4-7. *p,0.05, **p<0.005, ***p<0.001 Student's t test.

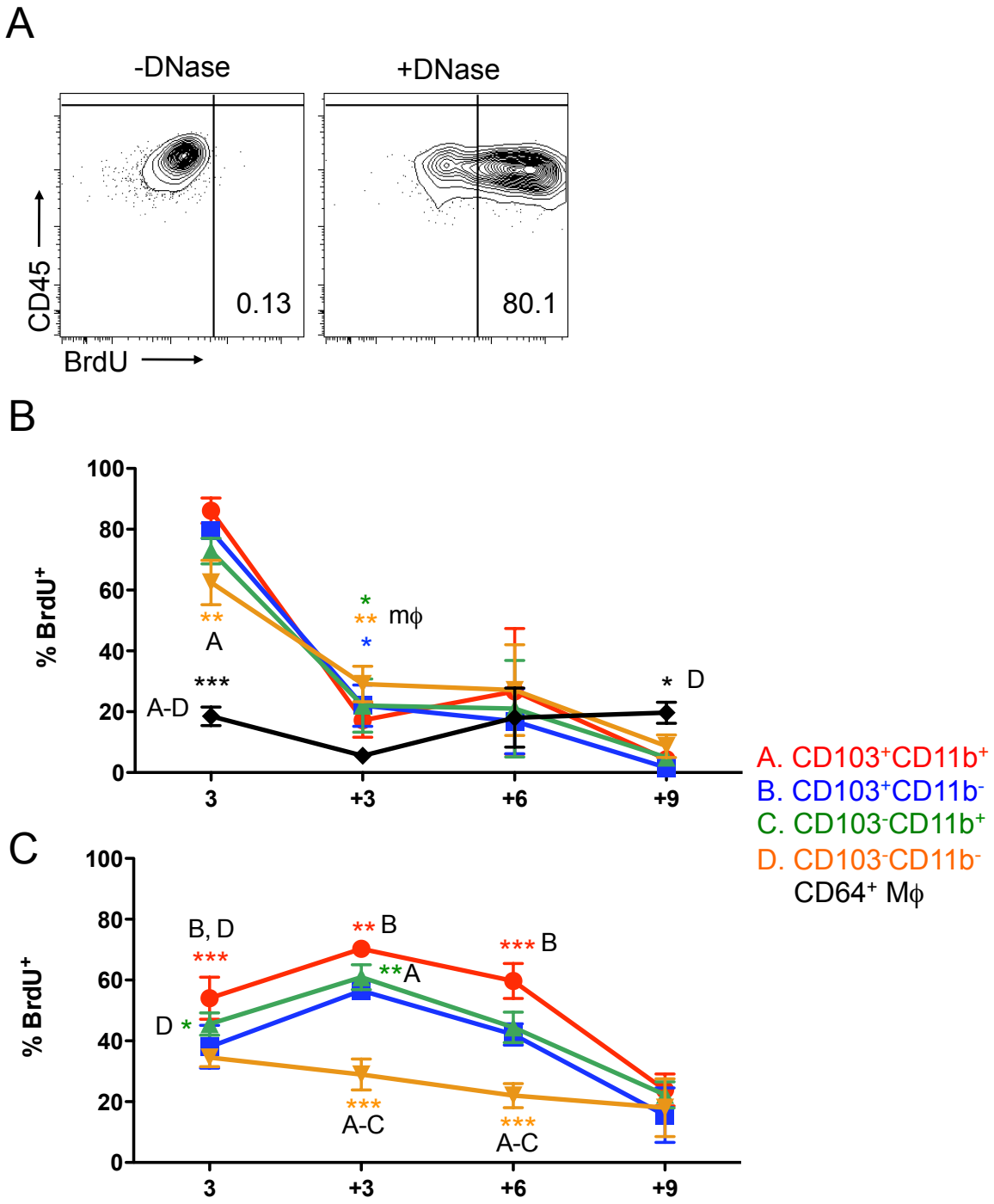

Figure 3.16: Differential Kinetics of DC and mϕ populations in the SI LP and MLN

Mice were given a single i.p. injection of 1mg BrdU and fed 0.8mg/ml BrdU in the drinking water for 3 days. **A.** Representative contour plots showing CD45 and BrdU staining on single live CD45$^+$ CD11c$^+$MHCII$^+$CD64$^-$ DCs from SI LP gated as shown in Fig. 3.3 in the presence or absence of DNase to expose incorporated BrdU. **B.** Percentage of BrdU$^+$ cells amongst DC and mϕ populations at day 3 after feeding and again 3, 6 and 9 days after withdrawal of BrdU. **C.** Percentage of BrdU$^+$ cells amongst MLN migratory DC populations gated as in Fig. 3.6 at day 3 after feeding and again 3, 6 and 9 days thereafter. Data are from 2 independent experiments with n=3/4 per time point per experiment. *p<0.05, **p<0.01 and ***p<0.005. Colour of * indicates which DC populations are significantly different compared with listed populations. Two-way ANOVA with Bonferroni post-test.

Chapter 4 Ontogeny and Development of Intestinal DCs

4.1 Introduction

In the previous chapter I identified four distinct subsets of $CD64^-$ intestinal DCs based on CD103 and CD11b expression ($CD103^+CD11b^+$, $CD103^+CD11b^-$, $CD103^-CD11b^+$ and $CD103^-CD11b^-$), which were clearly distinct from $CD64^+$ intestinal mϕs. While the two $CD103^+$ DC populations were expected (Bogunovic et al., 2009; Varol et al., 2009) genuine $CD103^-$ DCs of this kind had not been identified previously, as earlier studies had used phenotyping strategies that could not distinguish $CD103^-$ DCs from mϕs. In these earlier reports, it was also suggested that the $CD103^-$ "DCs" were derived from $Ly6C^{hi}$ monocytes rather than DC-committed precursors that give rise to DCs in other tissues (Geissmann et al., 2010; Liu et al., 2009; Naik et al., 2006; 2007) and the $CD103^+$ genuine DC populations in the intestine (Bogunovic et al., 2009; Varol et al., 2009). However, as the results in my previous chapter emphasised that intestinal $CD103^-$ MPs are in fact a heterogeneous population consisting of both DCs and mϕs, it became clear that the findings of these previous studies clearly required re-examination. Therefore, in this chapter I set out to determine the nature of the precursors of the various MP populations I had identified.

4.2 DC progenitors in the BM

4.2.1 Defining pre-DCs in the BM

The current theory of DC development is that common DC progenitors (CDPs or pro-DCs) first differentiate into either precursors of DCs (pre-DCs) or fully differentiated pDCs in the BM which then home to the tissues (Liu et al., 2009; Naik et al., 2006; 2007; Onai et al., 2007a). In order to determine if the novel $CD103^-$ DCs I had described in Chapter 3 are derived from a DC committed precursor, I set out to examine the fate of adoptively transferred pre-DCs *in vivo.* First, I had to establish methods for identifying and isolating these precursors from the BM, basing this on previous studies. Therefore after excluding cell aggregates and lineage-bearing cells (CD3, CD19, CD49b, CD11b and MHCII), I examined the remaining $CD11c^+$ cells for their expression of CCR9 and B220, with pre-DCs being identified as $CCR9^-B220^-CD135^+SIRP\alpha^{int}$ and pDCs as $CCR9^+B220^+$ cells (Fig. 4.1A). Consistent with previous reports (Liu et al., 2009), these pre-DCs

expressed intermediate levels of CX3CR1-GFP and lacked CD8α (Fig. 4.1B,C). I also examined the expression of β7 integrin, which has been shown to mark a population of DC progenitors which home preferentially to the intestine (Zeng et al., 2013). A small proportion (~15%) of pre-DCs expressed this marker (Fig. 4.1D).

4.2.2 Expansion of pre-DCs in the BM with Flt3L

As pre-DCs constitute a very minor population (<0.1%) of cells in the BM, it was necessary to expand their numbers to generate sufficient numbers for adoptive transfer experiments. To do this, I employed a frequently used approach, in which WT mice were inoculated subcutaneously with B16 melanoma cells secreting Flt3L, the principal growth factor for DC *in vivo* (Karsunky et al., 2003; Merad and Manz, 2009; Viney et al., 1998). 10 days later, Flt3L secreting tumours had formed and this resulted in a dramatic increase in both the proportion and absolute number of pre-DCs in the BM (Fig. 4.2).

4.3 Adoptive transfer of DC progenitors

I next set about developing a protocol for tracking pre-DC migration and fate in recipient mice. As previous studies involving adoptive transfer of pre-DCs used recipient mice that had either been irradiated or depleted of all $CD11c^+$ cells using CD11c-DTR mice, so that donor cells could be visualised more easily, this was the first approach I considered. Although the four populations of DCs identified in the previous chapter were depleted by administration of DT to CD11c-DTR mice, there was actually a much more intense depletion of $CD11c^{int}$ mϕs (Fig. 4.3). As this result raised issues over the suitability of this approach, I decided to try to transfer pre-DCs into unmanipulated steady state recipients. Although I could not find previous reports of this, I reasoned it would be the most physiological way of exploring DC development without the artefacts produced by severe population depletion or irradiation. To this end, FACS-purified pre-DCs isolated from CD45.2 WT donors that had been inoculated with Flt3L secreting B16 melanoma cells 10 days prior to harvest were transferred into resting CD45.1 congenic WT recipient mice (Fig. 4.4A,B). To aid the identification of donor cells in recipient mice, pre-DCs were also labelled with a CellTrace violet dye prior to transfer (Fig. 4.4B). Importantly, the transferred pre-DCs lacked expression of CD11b, MHCII and CD103 markers found at high levels on live leukocytes in the SI LP (Fig. 4.4C).

4.3.1 Identification and fate of donor-derived cells in the blood

24 hours after transfer, CD45.2$^+$violet$^+$ donor cells could be identified in the bloodstream of recipient mice (Fig. 4.5A). At this time, these donor cells retained the CD11c^{int}MHCII$^-$ phenotype of the pre-DCs, in contrast to the CD11c^{hi}MHCII$^+$ phenotype of endogenous tissue DCs (Fig. 4.5B). Very few CD45.2$^+$violet$^+$ donor cells could be seen in the bloodstream 3, 5 or 7 days after transfer (Fig. 4.5C) suggesting that most surviving pre-DCs had left the bloodstream by this time.

4.3.2 Identification and fate of donor-derived cells in the spleen

Donor-derived cells could be detected in the spleen by 24 hours after transfer and were most numerous between 1 and 5 days after transfer, before decreasing dramatically by day 7 (Fig. 4.6A). Over this time period the donor-derived cells showed progressively lower levels of violet dye (Fig. 4.6B) suggesting these cells might be proliferating, as this label halves in intensity with each cell division. In parallel, donor-derived cells in the spleen showed progressive upregulation of CD11c and MHCII to levels comparable with the endogenous splenic DCs. This could be seen as soon as 24 hours after transfer, although a true population of cells with the phenotype of mature DCs was not observed until 3 days after transfer (Fig. 4.7). At all time points, a population of CD11c$^+$MHCII$^-$ donor-derived cells remained detectable, suggesting that not all transferred pre-DCs could differentiate into mature DCs even after 7 days (Fig. 4.7). I then analysed the phenotype of the mature progeny of the pre-DCs, using the expression of CD103 and CD8α as markers. As described previously, this revealed two distinct DC populations amongst endogenous DCs (CD103$^-$CD8α^- DCs and CD103$^{-/int}$CD8α^+ DCs) (Fig. 4.8A). Although CD4 and CD11b are often used to define DC subsets in the spleen, I found that the combination of CD103 and CD8α gave better separation in FACS analysis than CD103 and CD11b, while my staining panel did not allow for incorporation of an appropriate CD4 antibody. Analysis of the donor-derived CD11c$^+$MHCII$^+$ DCs showed that these also acquired CD103 and CD8α expression, with CD8α^+ DCs appearing 24-72 hours after transfer and CD103 being first detectable by 72 hours and becoming more apparent on days 5 and 7 (Fig. 4.8). As with the endogenous subsets, the CD103$^+$ donor-derived DCs were also CD8α^+ (Fig. 4.8A) and the transferred pre-DCs

could also generate the $CD103^{-}CD8\alpha^{-}$ DC subset normally seen in the spleen (Fig. 4.8).

4.3.3 Identification and fate of donor-derived cells in the SI LP

$CD45.2^{+}violet^{+}$ donor-derived cells could also be identified in the SI LP as soon as 24 hours after transfer and clear populations were seen from 3-7 days after transfer (Fig. 4.9A). As in the spleen, there was a progressive decrease in the intensity of the violet dye over the time course, suggesting that donor-derived cells in the SILP may be proliferating *in situ*. The donor-derived cells began to upregulate CD11c and MHCII expression as soon as 24 hours after transfer and by day 3, approximately 30% expressed CD11c and MHCII at levels comparable to endogenous SI LP DCs. This population then increased steadily from day 3 to day 7 (Fig. 4.10). In parallel with their acquisition of the mature DC phenotype, the donor-derived DCs acquired expression of CD103 and CD11b, with both markers appearing by day 3 after transfer and by day 7, all four subsets of DCs normally seen amongst endogenous cells in the LP could be seen at similar proportions to those seen in the resting LP (Fig. 4.11). Notably, this included the $CD103^{+}CD11b^{+}$ DCs, in contrast to what was observed when the transferred pre-DCs differentiated in the spleen. Interestingly, the $CD103^{+}CD11b^{+}$ DCs appeared to take longer to accumulate in the LP than the other DC subsets, potentially suggesting these develop through a $CD11b^{+}CD103^{-}$ intermediary, although this remains to be directly investigated.

Similar to the spleen, a population of $CD11c^{int}MHCII^{-}$ donor-derived cells remained in the SI LP throughout the duration of the analysis (Fig. 4.10) thus I next set out to investigate what these cells might be. First I examined the possibility that the transferred pre-DCs were contaminated with other precursor cells. To do this I examined the expression of CD115 which is expressed by more primitive progenitors (Liu et al., 2009). This revealed that a minority of these cells (<0.2%) expressed low levels of CD115 (Fig. 4.12A). To rule out the possibility that the pre-DCs were contaminated with cells not committed to the DC lineage, which also express CD115, although usually at higher levels, I examined the ability of the transferred cells to give rise to mϕs. As none of the donor cells generated $F4/80^{+}$ mϕs (Fig. 4.12B), no cells of the monocyte/mϕ lineage or with the potential to generate monocytes/mϕs such as CMPs or MDPs could be present amongst

the transferred cells. Thus we reasoned that these contaminating cells were due to the presence of a minor population of contaminating $CD115^+$ CDPs. To test this hypothesis, I next examined if the donor-derived $CD11c^{int}MHCII^-$ cells in the LP were pDCs. As pDCs express Ly6C and B220, I examined the expression of these markers on all on all donor-derived cells at day 7 and compared levels to those seen on endogenous live SI LP cells. Unfortunately due to constraints of antibody and fluorochrome combinations, it was not possible to co-stain for MHCII for this analysis. Despite this shortcoming, this analysis demonstrated that the donor-derived cells, which had upregulated CD11c expression and hence became DCs lacked expression of both Ly6C and B220. Contrary to this the donor cells, which remained $CD11c^{int}$ did express these markers suggesting that these cells were likely to be pDCs (Fig. 4.12C,D). Interestingly, those cells that did not acquire high levels of MHCII did not dilute the cell-trace dye to the same extent as the $MHCII^+$ donor-derived cells (Fig. 4.12E), suggesting that pDCs do not share the ability of mature DCs to proliferate *in situ*.

4.3.4 Identification and fate of adoptively transferred pre-DCs in the colonic LP

Pre-DC derived cells were also found in the colonic LP from day 1 until day 7 after transfer and there was a similar progressive dilution of the violet dye (Fig. 4.13A,B). The time course of acquisition of CD11c and MHCII by donor-derived cells was also similar in the colonic LP, first being seen on day 3 (Fig. 4.14). As in the SI, CD103 and CD11b expression increased progressively on donor-derived DCs in the colon, again generating all four DC populations (Fig. 4.15). However, the relative proportions of the different DC subsets amongst donor-derived cells differed to those observed in the SI LP (compare Fig. 4.11B-E with Fig. 4.15B-E), but were similar to those found among endogenous DCs in the colonic LP, with $CD103^+CD11b^-$ DCs predominating. Similar to the SI LP the development of the $CD103^+CD11b^+$ DCs was slower than that of the other subsets (Fig. 4.15B). Fewer donor-derived pDCs appeared to be present in the colon compared with the SI, which may reflect of the number of pDCs in the colonic LP versus the SI LP, which I have not examined in this thesis. Alternatively, this may be a technical issue as I identified donor cells in the colon based on co-expression of CD11c and CD45.2, rather than violet dye, and as such $CD11c^{lo}$ cells may be missed using this approach.

4.3.5 Identification and fate of adoptively transferred pre-DCs in the MLN

I next investigated the fate of donor-derived pre-DCs in the MLNs, with the aim of exploring whether resident and migratory DCs could be identified amongst the progeny. As in the other tissues, donor-derived cells were present in the MLN from 24 hours after transfer and could still be identified 7 days later (Fig. 4.16A). By day 7 there was a considerable reduction in the levels of violet dye on the donor-derived cells suggesting that these cells had proliferated (Fig. 4.16B). Unlike other tissues, MHCII expression was not acquired until day 3, but similar to the LP this increased progressively from day 3 to day 7 after transfer (Fig. 4.17A). Interestingly, however, virtually all donor-derived cells expressing MHCII remained in the $CD11c^{+}MHCII^{int}$ resident DC population at early time points (day 3), with donor-derived cells only appearing in the $CD11c^{+}MHCII^{hi}$ migratory gate by day 5. By day 7 after transfer the majority of donor-derived DCs were present in the migratory DC gate (Fig. 4.17). This relative delay in the appearance of pre-DC progeny within the migratory DC gate in the MLN would be consistent with them having matured in the LP for a few days before migrating to the MLN. This is supported by the fact that few cells expressing CD103 and/or CD11b could be seen amongst the migratory gate in the MLN 5 days after transfer, when they are at a peak in the LP, but became abundant by day 7 (Fig. 4.18). As in other tissues, the donor-derived cells in the migratory DC gate adopted the subsets in similar proportions as found for the endogenous migratory DC populations (Fig. 4.18B-E). In contrast and consistent with their designation as lymph node resident DCs, the $CD11c^{+}MHCII^{int}$ donor-derived DC population contained only $CD103^{+}CD11b^{-}$, $CD103^{-}CD11b^{+}$ and $CD103^{-}CD11b^{-}$ DCs at similar proportions to the endogenous resident DCs (Fig. 4.19).

4.4 Fate of $Ly6C^{hi}$ monocytes *in vivo*

The results of these transfer studies indicate that all intestinal subsets including the novel $CD103^{-}$ DCs I had identified could be generated by precursors committed to the DC lineage. However, I thought it important to examine directly whether $Ly6C^{hi}$ monocytes could give rise to any of the DC subsets I had identified, as had been suggested by the previous studies using less rigorously characterised $CD103^{-}$ MPs (Bogunovic et al., 2009; Varol et al., 2007; 2009). To do this, $Ly6C^{hi}$ monocytes were FACS-purified from the BM of unmanipulated $CX3CR1^{+/GFP}$ mice

as CD11b^{+} Ly6G^{-} Ly6C^{hi} CD117^{-} and CX3CR1-GFP^{int} (Fig. 4.20) and transferred into CD45.2 monocytopenic CCR2$^{-/-}$ recipients (Fig. 4.21 A,B) (Kurihara et al., 1997; Serbina and Pamer, 2006). These recipients were chosen as they have considerably fewer circulating blood monocytes and as a result have fewer monocytes and mϕs in the intestine (Bain et al., 2013). Thus, they represent a model in which some space has been created in the myeloid compartment without the need for depletion or irradiation and this model had been used successfully in our lab to track intestinal mϕ development *in vivo.* Importantly the transferred monocytes did not express CD11c, MHCII or CD103 (Fig. 4.21C).

To identify the progeny of the transferred monocytes in the SI LP, I used the gating strategy I described in Chapter 3, in which DCs and mϕs, were discriminated on the basis of their expression of CD11c, MHCII and F4/80. Donor cells were then identified amongst the DC or mϕ populations by their expression of CX3CR1-GFP and CD45.1 This showed that donor monocytes could give rise to CD11c^{int} MHCII^{+} F4/80^{+} mϕs, but not to CD11c^{hi} MHCII^{+} F4/80^{-} DCs (Fig. 4.22). These results indicate *bona fide* intestinal DCs, including the CD103^{-} DCs, are the progeny of pre-DC precursors and not Ly6C^{hi} monocytes as previously suggested. Conversely, intestinal mϕs are derived exclusively from Ly6C^{hi} monocytes.

4.5 SI LP DCs proliferate in situ

As described above, the dilution of the violet dye in the mature progeny of transferred pre-DCs suggested that these cells were dividing *in situ.* Although this had been shown previously in a number of other non-lymphoid tissues including the dermis, lung and kidney (Ginhoux et al., 2009), to my knowledge this had not been shown for DCs in the intestine. Therefore, I next to set out to confirm whether SI LP DCs were dividing using a pulse-chase BrdU protocol, in which mice received a single i.p. injection of BrdU and were sacrificed 3 hours later. BrdU labelling was then assessed in conjunction with Ki67 expression as a marker of cells in active division. This approach was validated by the fact that a considerable proportion (~40%) of pre-DCs in the BM were BrdU^{+}Ki67^{+} 3 hours after injection of BrdU (Fig. 4.23). No BrdU^{+}Ki67^{+} pre-DCs could be found in the blood at this time (Fig. 4.23) and the small number of cells phenotypically resembling pre-DCs in the LP (Fig. 4.24) were also BrdU^{-}Ki-67^{-} (Fig. 4.23). In contrast, small numbers of

$BrdU^+Ki\text{-}67^+$ cells were clearly detectable amongst the $CD103^+CD11b^+$, $CD103^+CD11b^-$ and $CD103^-CD11b^+$ DC subsets in the SI LP confirming their cell division *in situ* (Fig. 4.23). Notably neither the $CD103^-CD11b^-$ DCs nor the $F4/80^+CD64^+$ mϕ population contained any $BrdU^+Ki67^+$ cells above background staining, demonstrating these to be non-proliferative (Fig. 4.23). Although some $BrdU^-Ki\text{-}67^+$ cells were detected amongst intestinal mϕs, similar Ki-67 staining was seen in the isotype control suggesting this to be an artefact of staining protocol.

4.6 Development of intestinal DCs in neonatal mice

Having examined the development of the intestinal DC populations from their precursors in adult mice, I next investigated how this might relate to their appearance in the SI LP after birth. Using the gating strategies I employed for adult mice, all four subsets of DCs could already be identified in the SI LP of newborn mice, although there were very few $CD103^+CD11b^+$ DCs at this time (Figs. 4.25-4.27). There were also fewer $CD103^-CD11b^-$ DCs in the newborn intestine, while the proportions of the $CD103^+CD11b^-$ and $CD103^-CD11b^-$ DC populations were increased compared with adult mice (Figs. 4.25-4.26). The proportion of $CD103^+CD11b^+$ DCs had increased markedly by 7 days of age and from 11 days onwards, they attained adult levels. The proportions of $CD103^+CD11b^-$ DCs fell markedly from birth to 7 days of age, perhaps reflecting the increased numbers of $CD103^+CD11b^+$ DC, but then rose again on days 11 and 14 before falling towards adult levels by day 21. The proportions of $CD103^-CD11b^+$ DCs fell slightly from day 0 to day 7, before falling more dramatically by day 11 to mirror the proportions seen in adulthood. The proportions of $CD103^-CD11b^-$ DCs rose after birth to above adult levels, where they remained until 21 days of age (Figs. 4.25-4.26). As expected, the absolute numbers of each DC population increased incrementally with age (Fig. 4.27A-D), which mirrored the accumulation of other leukocytes in the mucosa (Fig. 4.27E).

4.7 Intestinal DC populations in antibiotic treated mice

One possible explanation for the low numbers of $CD103^+CD11b^+$ DCs in the neonatal intestine could be the lack of microbiota, which only begins to colonise the intestine after birth. To investigate whether this might also influence DC populations in adult mice, I analysed the SI LP and MLN after 2 weeks of

administering a well-established broad-spectrum antibiotic cocktail (Abt et al., 2012). In contrast to what was seen in newborn mice, antibiotic treatment increased both the proportion and absolute number of $CD103^+CD11b^+$ DCs in the SI LP (Fig. 4.28). In parallel, the proportions of the $CD103^-CD11b^+$ DCs were reduced, although the absolute number of these DCs was not altered (Fig. 4.28). There were also no effects of the antibiotics on the numbers or proportions of either the $CD103^+CD11b^-$ or $CD103^-CD11b^-$ DCs in the LP (Fig. 4.28).

The increased number of $CD103^+CD11b^+$ DCs in the SI LP of antibiotic treated mice was paralleled by a significant increase in the proportion of this subset amongst migratory DCs in the MLNs, together with a trend towards an increase in their absolute numbers (Fig. 4.29). As in the LP, this was accompanied by a decrease in the proportion of $CD103^+CD11b^-$ DCs, with no change in the proportions or numbers of the other subsets of migratory DC apart from a small but significant decrease in the proportion of $CD103^-CD11b^-$ DCs (Fig. 4.29). Together these results provide evidence that the development of $CD103^+CD11b^+$ intestinal DC may be regulated by the microbiota, but that treatment of adult mice with antibiotics may not recapitulate the state of the newborn intestine.

4.8 Summary

In this chapter I set out to explore directly the origin of the DC subsets I had identified in the previous chapter. By developing protocols which allowed me to track the fate of adoptively transferred DC-committed precursors in tissues of unmanipulated recipients, I showed that these gave rise to all four populations of intestinal DCs defined on the basis of CD103 and CD11b expression and obtained evidence that these migrated from the LP to the MLNs after maturation. Following their arrival in the LP, the transferred precursors first acquired MHCII and upregulated CD11c expression, before acquiring CD103 and/or CD11b expression. Approximately 5 days after transfer, the precursors had given rise to the various DC subsets in similar proportions to the endogenous populations. Although donor-derived cells could also be found in the spleen, they acquired the phenotypes characteristic of endogenous splenic DC populations with $CD103^+CD11b^+$ DCs being absent from this location. A similar phenomenon was seen in the colonic LP, where the $CD103^+CD11b^-$ DC phenotype predominated amongst donor-derived cells. Together these results suggest that local conditioning by the environment

may determine the fate of pre-DCs in tissue, although the possibility of distinct populations of precursors cannot be ruled out. In contrast to previous reports, using less rigorously characterised MPs, transferred Ly6C^{hi} monocytes could not generate any of the *bona fide* subsets of mucosal DC including the CD103^{-} DC populations I had defined, indicating that these are all derived exclusively from DC committed precursors. This was in direct contrast with mϕs, which could only be generated from Ly6C^{hi} monocytes and not pre-DCs. Taken together these studies confirm and extend my findings from Chapter 3, by showing that the identification of mucosal MPs on the basis of CD64 expression defines distinct lineages of cells.

By using pre-DCs labelled with a violet dye which dilutes following cell division and a short-term BrdU pulse in combination with Ki67 staining, I was also able to demonstrate that most subsets of mature DCs in the SI LP proliferate *in situ.* In contrast, the rare putative pre-DCs in the LP did not divide *in situ* and nor did mϕs. Interestingly, the CD103^{-}CD11b^{-} DCs also did not proliferate *in situ*, perhaps reflecting their derivation from isolated lymphoid follicles rather than the LP (Cerovic et al., 2013) or because they comprise more primitive cells as these are the first subset to appear in the LP after pre-DC transfer. Together, these findings allowed me to track the fate of LP DCs from their arrival as pre-DCs, through their progressive acquisition of the different subset markers and a number of cell divisions, before their emigration to the MLN. Overall, these processes appear to take place within 7 days, emphasising the short lifespan of these cells.

Having established that all four intestinal DC populations were derived from pre-DCs, I next investigated how these developed after birth. This showed that the CD103^{+}CD11b^{+} DC subset was much reduced at birth and only gradually increased to adult levels over the first 2-3 weeks of life. This lag in CD103^{+}CD11b^{+} DC development could be consistent with the fact that this population took the longest to appear after the transfer of pre-DCs. This progressive increase in this population after birth correlated with a progressive decrease in CD103^{-}CD11b^{+} DCs, while the proportion of CD103^{+}CD11b^{-} DCs varied throughout the first 3 weeks of life until reaching levels seen in the adult LP thereafter. The proportions of the CD103^{-}CD11b^{-} DCs increased dramatically between day 0 and 7 and then fell progressively to the levels observed in adulthood 21 days after birth. To determine if these changes in the proportions of each DC population were driven by the microbiota, I administered a cocktail of broad-spectrum antibiotics for 2

weeks before examining the DC populations in the SI LP and MLNs. This caused an increase in the proportions and numbers of $CD103^+CD11b^+$ DCs, suggesting that these $CD103^+CD11b^+$ DCs might be regulated by the microbiota. The increase in $CD103^+CD11b^+$ DCs correlated with a decrease in the population of $CD103^-CD11b^+$ DCs perhaps suggesting a developmental relationship between these DC subsets.

Having defined four distinct DC subsets originating from DC committed precursors in the steady state intestine, in the next chapter I went on to characterise these DC populations during inflammation and infection.

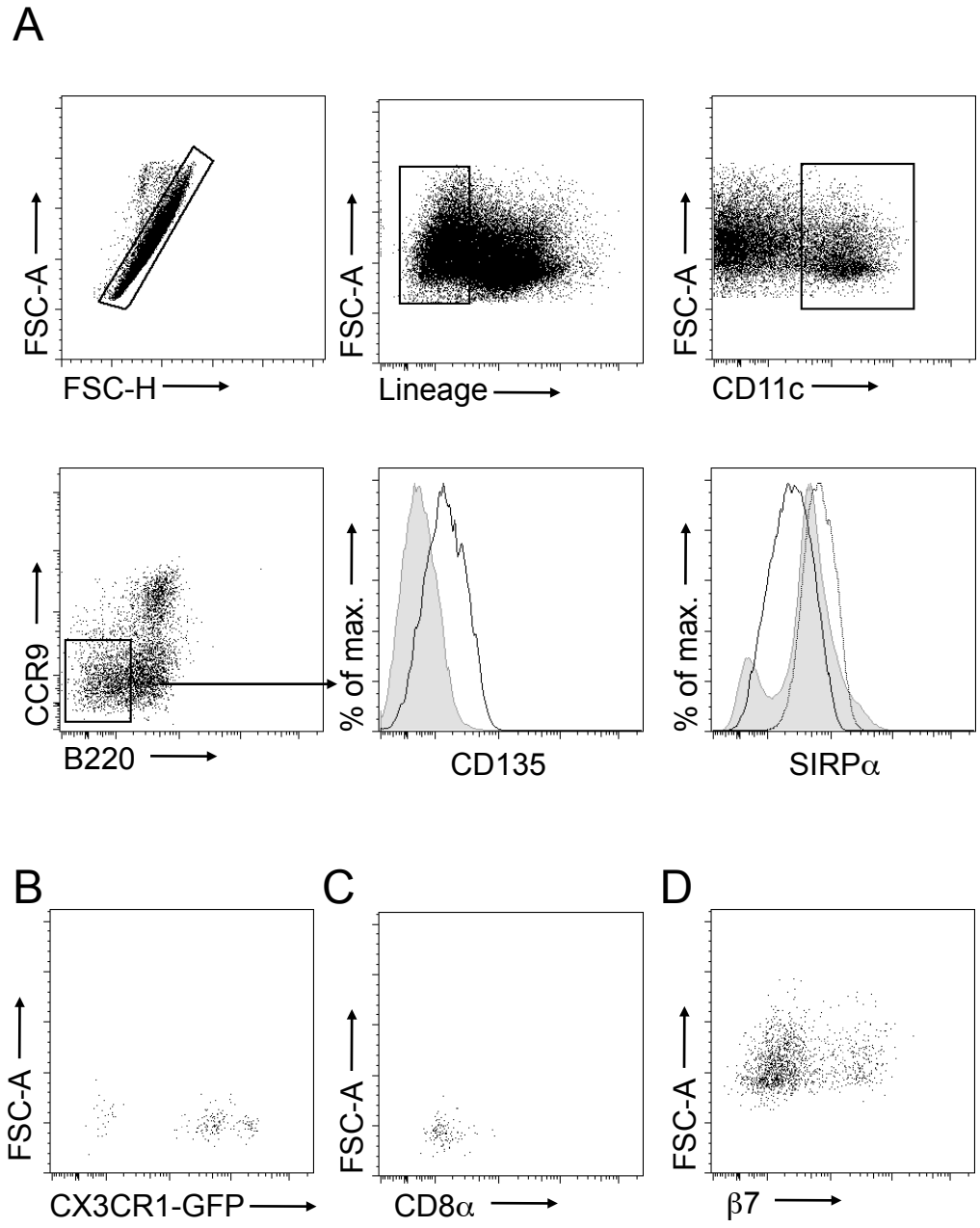

Figure 4.1: Identification of pre-DCs in the BM

A. Lineage$^-$ cells (CD3, CD19, CD49b, CD11b and MHCII) were identified amongst single cells in BM isolates and CDPs were identified as CD11c$^+$ cells. Pre-DCs were then identified amongst these as CCR9$^-$B220$^{-/int}$ cells. Pre-DCs uniformly expressed CD135 (black line) compared with isotype control (shaded grey) and were SIRPα^{int} (black line) compared with Ly6C^{hi} monocytes (dotted line) and Lineage$^+$ cells (shaded grey). **B-D.** Representative dot plots showing expression of CX3CR1-GFP (B), CD8α (C) and **β**7 (D) by pre-DCs in BM. Data are representative of at least 10 independent experiments.

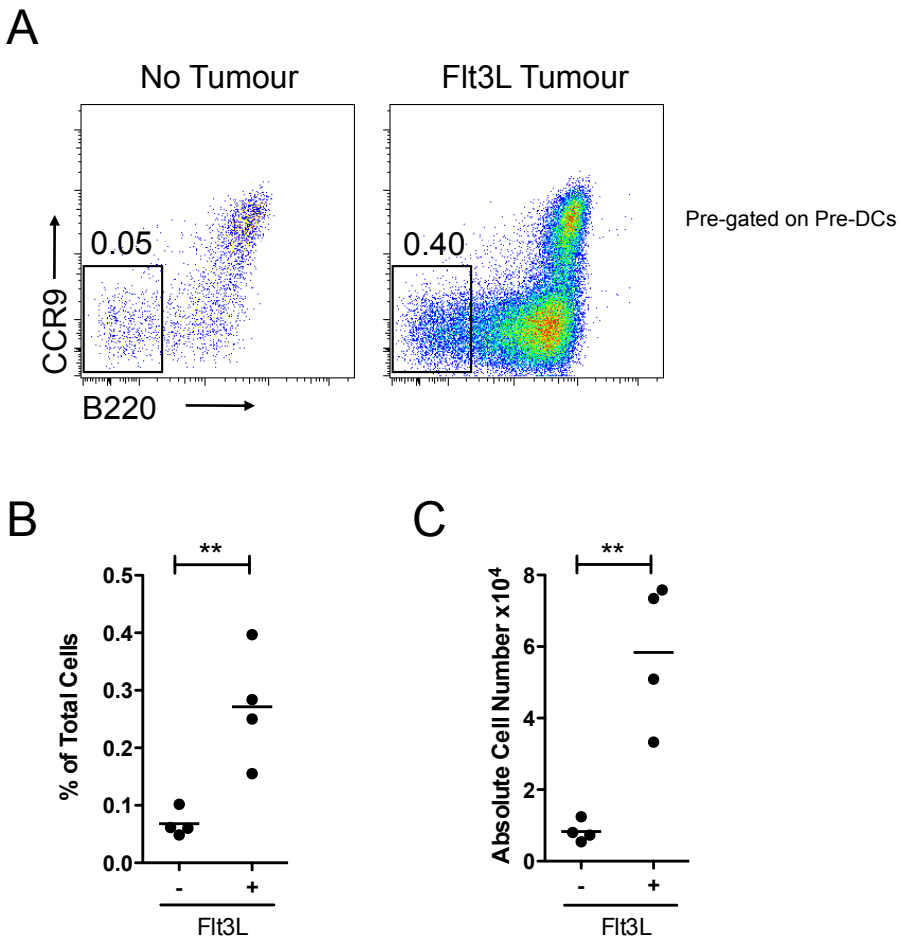

Figure 4.2: Expansion of pre-DCs by Flt3L *in vivo*

Mice were inoculated with $2x10^6$ B16 Flt3L secreting tumour cells subcutaneously and 10 days later BM was analysed to determine expansion of pre-DCs. **A.** Representative dot plots showing the proportions of pre-DCs in BM from mice with Flt3L secreting B16 tumours, compared with resting controls. Number indicates percentage of pre-DCs amongst single, live, lineage$^-$ (CD3, CD19, CD49b, MHCII, CD11b), CD11c$^+$ CDPs. **B.** Proportion of pre-DCs as a percentage of total BM cells in the presence (+) or absence (-) of Flt3L secreting B16 tumours. **C.** Absolute number of pre-DCs/femur in the presence (+) or absence (-) of Flt3L secreting B16 tumours. Data are from a single experiment with n=4. **p<0.01 Student's t test.

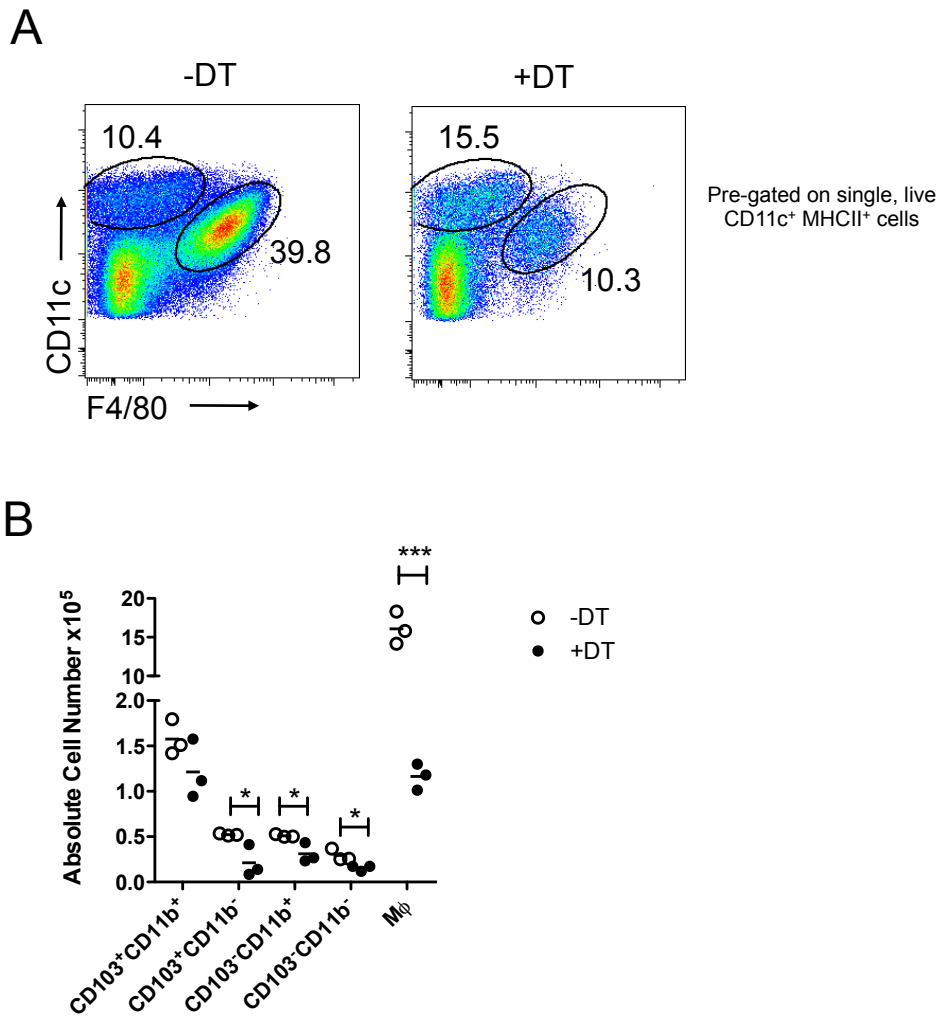

Figure 4.3: Depletion of CD11c⁺ cells in CD11c-DTR mice

CD11c-DTR mice were given a single injection of 4ng/g bodyweight DT and 24 hours later, SI LP mononuclear phagocyte populations were examined. **A.** Representative dot plots showing expression of CD11c and F4/80 on single live CD45⁺CD11c⁺MHCII⁺ cells in DT-treated (+DT) or PBS-treated (-DT) mice. Numbers indicate percentage of each population amongst total MPs. **B.** Absolute number of DC subsets and mϕs in the SI LP of mice receiving DT or PBS. Data are from a single experiment with n=3 per group. *p<005, ***p<0.001 Student's t test.

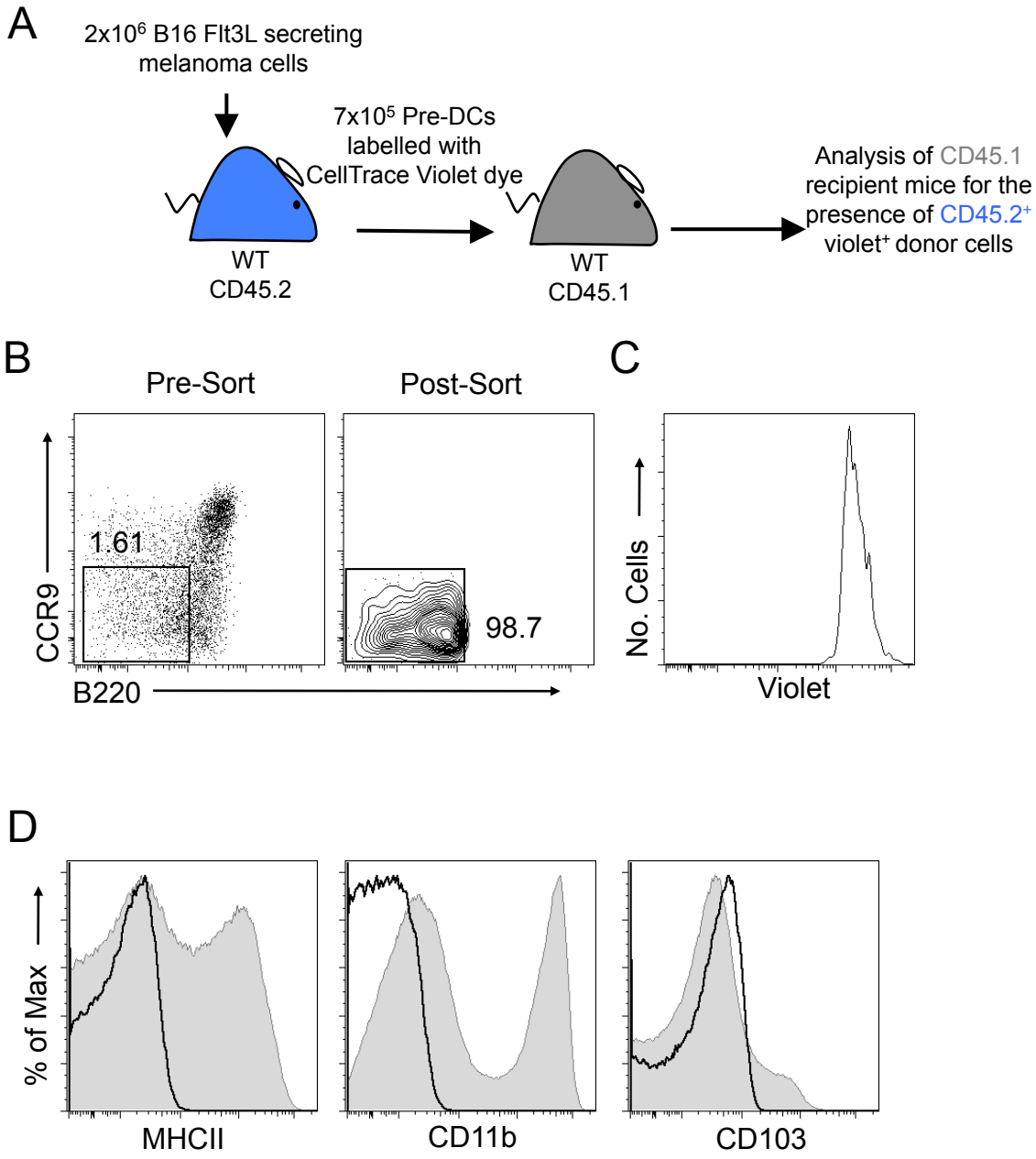

Figure 4.4: Purification of pre-DCs for adoptive transfer

A. CD45.2$^+$ WT mice were injected with 2x10^6 B16 Flt3L secreting tumour cells and 10 days later BM was harvested and 7x10^5 FACS-purified pre-DCs were transferred into CD45.1$^+$ WT mice. **B** Pre-DCs were identified as shown in Fig 4.1 and sorted to high purity. Numbers indicate the proportions of pre-DCs as a percentage of total BM cells before and after FACS-purification. **C.** Levels of CellTrace Violet dye on the sorted pre-DCs prior to transfer. **D.** Expression of MHCII, CD11b and CD103 on sorted pre-cDCs (black line) compared with levels on live CD45$^+$ SI LP cells (shaded grey). Data are representative of at least 4 independent experiments.

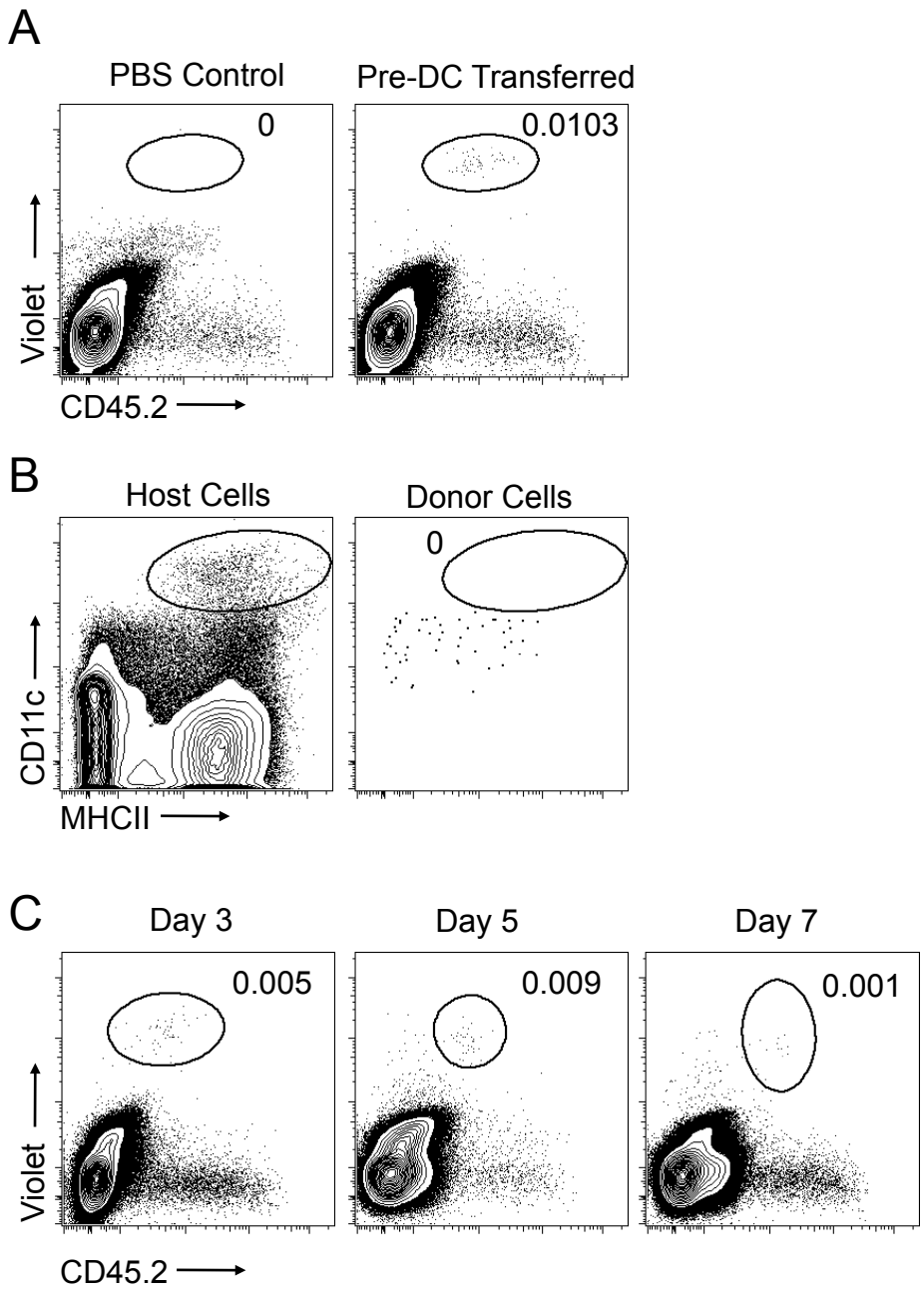

Figure 4.5: Identification of donor-derived cells in the bloodstream of recipients

$7x10^5$ CD45.2$^+$Violet$^+$ pre-DCs were transferred into resting WT CD45.1$^+$ mice and 1, 3, 5 or 7 days later, recipient mice were examined for the presence of donor-derived cells. **A.** Representative contour plots of CD45.2 expression and Violet dye labelling on live-gated cells in the blood of mice receiving pre-DCs or PBS 1 day after transfer. Numbers indicate the proportion of donor-derived cells as a percentage of total live cells. **B.** Expression of CD11c and MHCII on live-gated host blood DCs or donor-derived cells 1 day after transfer. Number indicates the frequency of CD11c$^+$MHCII$^+$ as a percentage of CD45.2$^+$Violet$^+$ donor-derived cells. **C.** Identification of CD45.2$^+$Violet$^+$ donor-derived cells amongst live-gated cells 3, 5 and 7 days after transfer. Numbers indicate the frequency of CD45.2$^+$Violet$^+$ donor-derived cells as a percentage of total live cells. Data are representative of either a single experiment (1 & 3 days) or 3 independent experiments (5 & 7 days) with 2-4 recipient mice per time point per experiment.

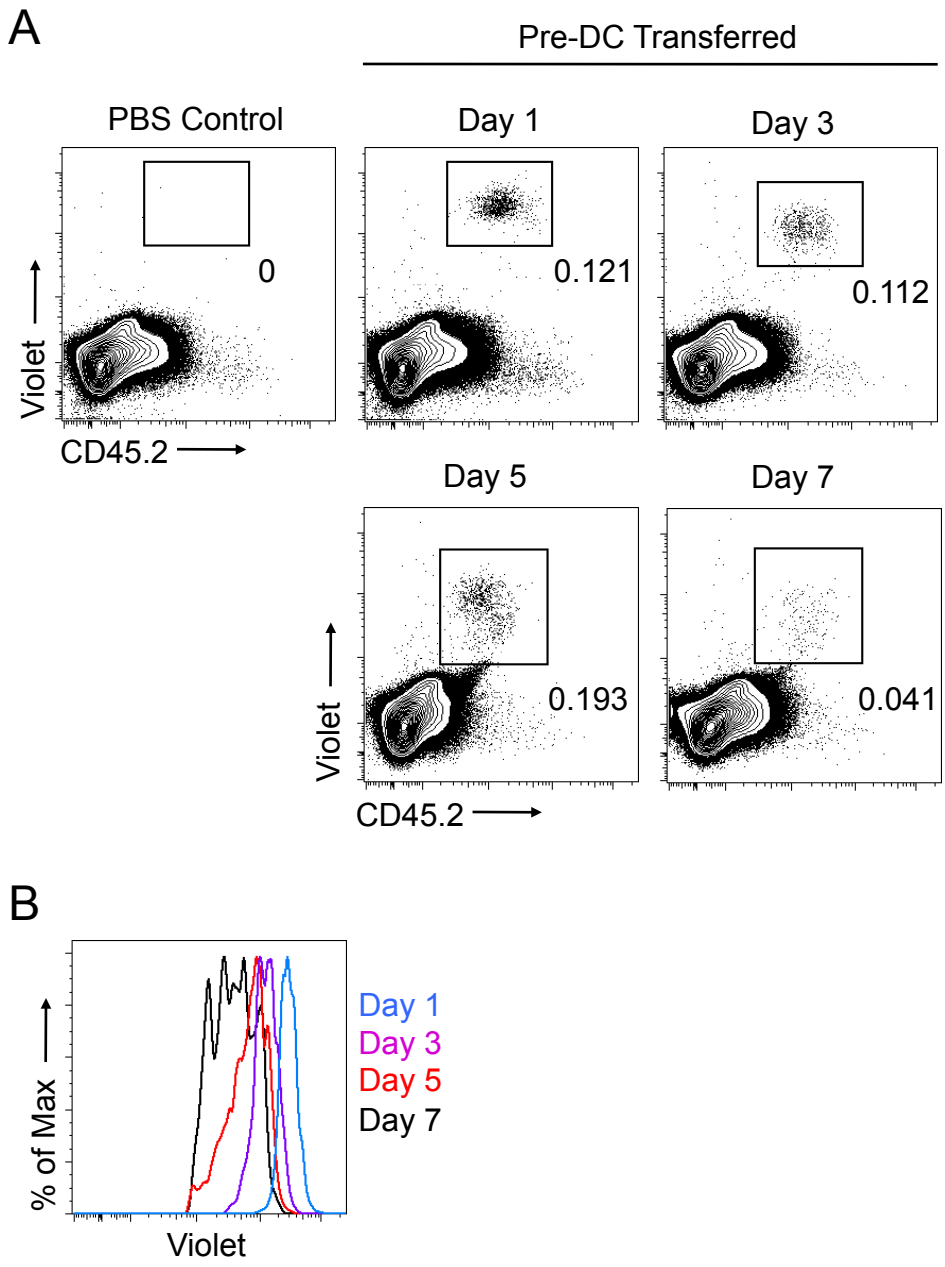

Figure 4.6: Identification of donor-derived cells in the spleen

$7x10^5$ CD45.2$^+$Violet$^+$ pre-DCs were transferred into resting WT CD45.1$^+$ mice and 1, 3, 5 or 7 days later, recipient mice were examined for the presence of donor-derived cells. **A.** Representative contour plots of CD45.2 expression and Violet dye labelling on live-gated CD3$^-$ CD19$^-$ cells in the spleen of mice receiving pre-DCs or PBS 1, 3, 5 and 7 days after transfer. Numbers indicate the proportion of donor-derived cells as a percentage of live-gated CD3$^-$CD19$^-$ cells. **B.** Levels of Violet dye were assessed on donor-derived cells 1, 3, 5 and 7 days after transfer. Data are representative of either a single experiment (1 & 3 days) or 3 independent experiments (5 & 7 days) with 2-4 recipient mice per time point per experiment.

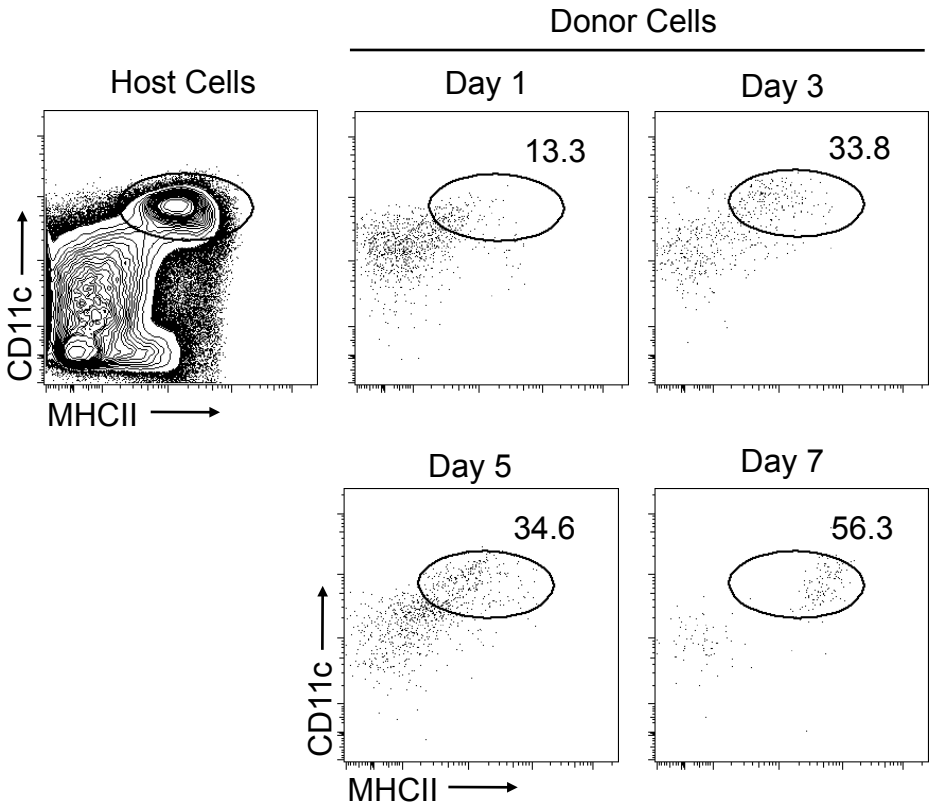

Figure 4.7: Acquisition of CD11c and MHCII on progeny of transferred pre-DCs in the spleen

$7x10^5$ CD45.2$^+$Violet$^+$ pre-DCs were transferred into resting WT CD45.1$^+$ mice and 1, 3, 5 or 7 days later, recipient mice were examined for the presence of donor-derived cells. Representative contour and dot plots of CD11c and MHCII expression on live-gated CD3$^-$ CD19$^-$ host cells or CD45.2$^+$Violet$^+$ donor-derived cells (gated as shown in Fig. 4.6), 1, 3, 5 and 7 days after transfer. Numbers indicate the frequencies of CD11c$^+$MHCII$^+$ cells as a percentage of total donor-derived cells. Data are representative of either a single experiment (1 & 3 days) or 3 independent experiments (5 & 7 days) with 2-4 recipient mice per time point per experiment.

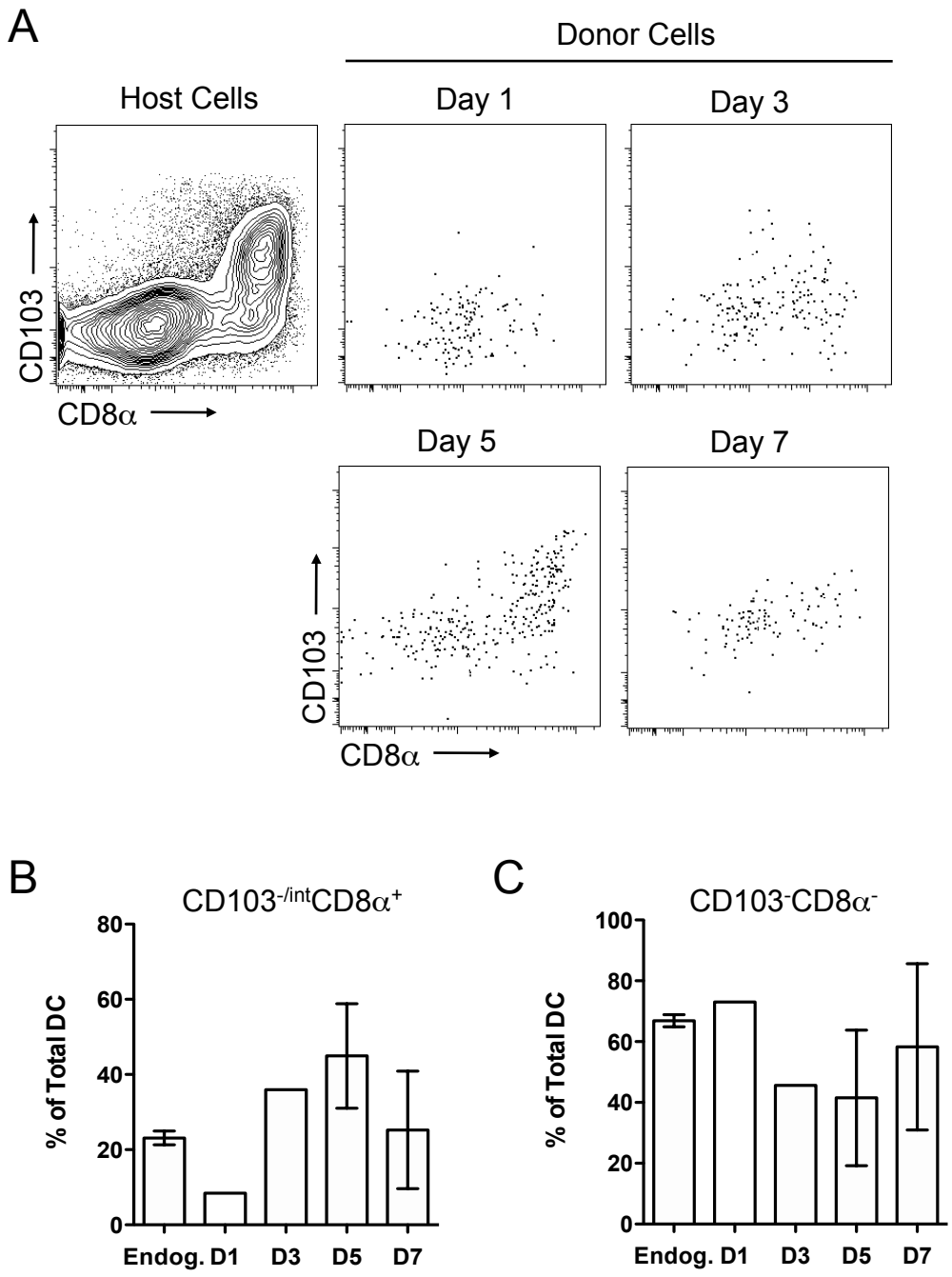

Figure 4.8: Development of DC subsets in spleen after transfer of pre-DCs

$7x10^5$ CD45.2$^+$Violet$^+$ pre-DCs were transferred into resting WT CD45.1$^+$ mice and 1, 3, 5 or 7 days later, spleens of recipient mice were examined for the presence of donor-derived cells. **A.** Representative contour and dot plots of CD103 and CD8α expression on live-gated host DCs or CD11c$^+$ MHCII$^+$ donor-derived DCs (gated as shown in Fig. 4.7), 1, 3, 5 and 7 days after transfer. **B,C.** Frequencies of donor-derived and endogenous DCs 1, 3, 5 and 7 days after transfer amongst CD103$^{-/int}$CD8α^+ DCs (B) and CD103$^-$CD8α^- DCs (C). Data are shown as means (±1SD) of either a single experiment (1 & 3 days) or 3 independent experiments (5 & 7 days) with 2-4 recipient mice per time point per experiment.

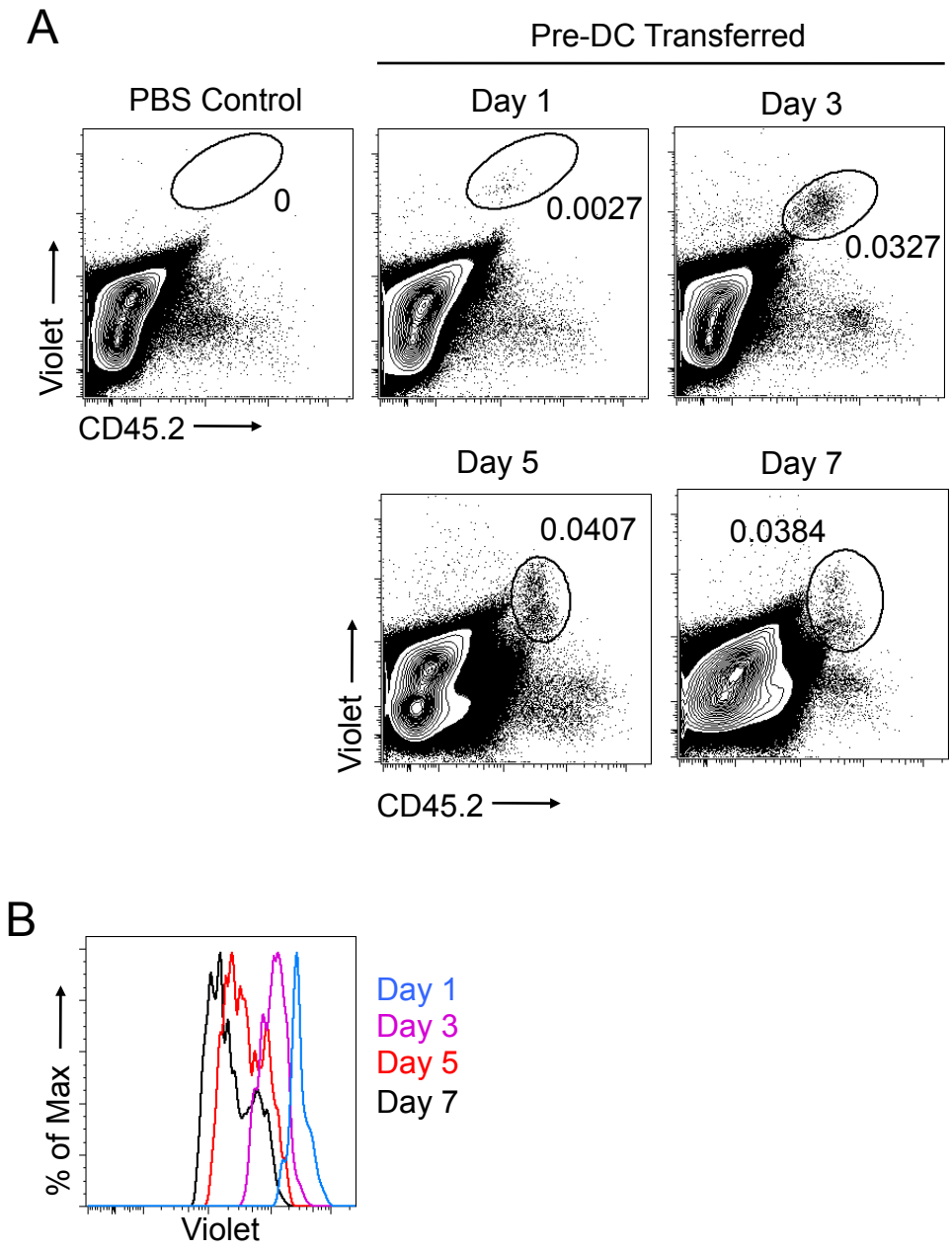

Figure 4.9: Identification of donor-derived cells in the SI LP

$7x10^5$ $CD45.2^+Violet^+$ pre-DCs were transferred into resting WT $CD45.1^+$ mice and 1, 3, 5 or 7 days later, the SI LP of recipient mice was examined for the presence of donor-derived cells. **A.** Representative contour plots of CD45.2 expression and Violet dye labelling on live-gated cells in mice receiving pre-DCs or PBS, 1, 3, 5 and 7 days after transfer. Numbers indicate the proportion of donor-derived cells as a percentage of live-gated cells. **B.** Levels of Violet dye were assessed on donor-derived cells 1, 3, 5 and 7 days after transfer. Data are representative of either a single experiment (1 & 3 days) or 3 independent experiments (5 & 7 days) with 2-4 recipient mice per time point per experiment.

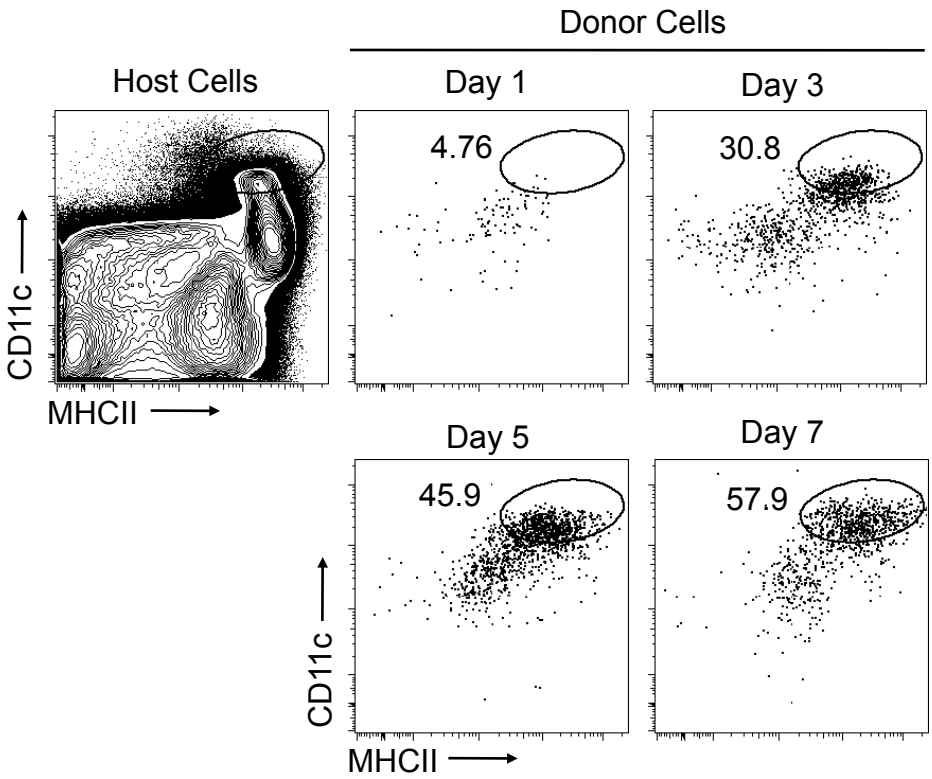

Figure 4.10: Acquisition of CD11c and MHCII by donor-derived cells in the SI LP

$7x10^5$ CD45.2$^+$Violet$^+$ pre-DCs were transferred into resting WT CD45.1$^+$ mice and 1, 3, 5 or 7 days later, the SI LP of recipient mice was examined for the presence of donor-derived cells. Representative contour and dot plots of CD11c and MHCII expression on live-gated host cells or donor-derived cells (gated as shown in Fig. 4.9), 1, 3, 5 and 7 days after transfer. Numbers indicate the frequencies of CD11c$^+$MHCII$^+$ cells as a percentage of total donor-derived cells (as gated in Fig. 4.9A). Data are representative of either a single experiment (1 & 3 days) or 3 independent experiments (5 & 7 days) with 2-4 recipient mice per time point per experiment.

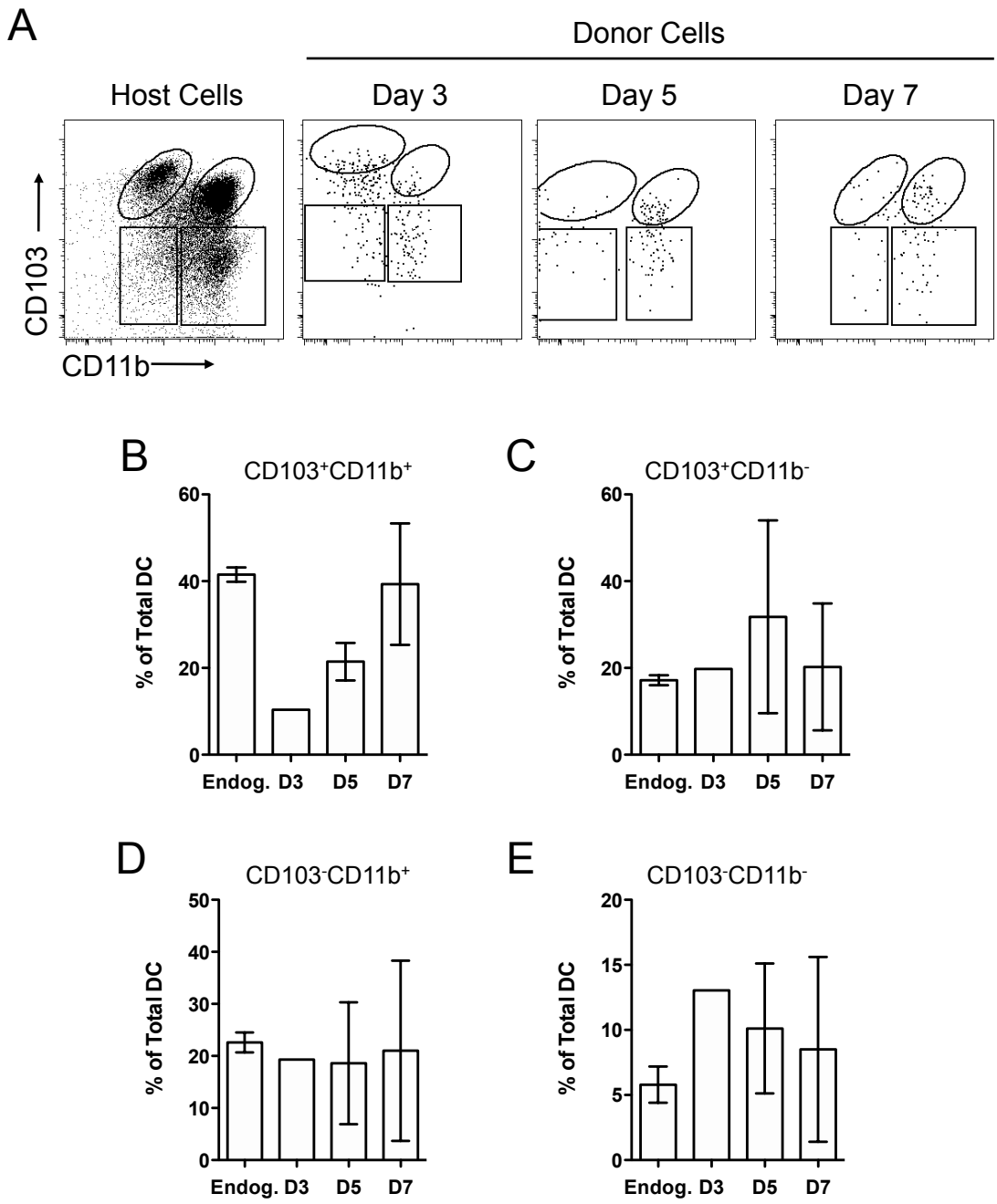

Figure 4.11: Development of DC subsets in SI LP after transfer of pre-DCs

$7x10^5$ CD45.2$^+$Violet$^+$ pre-DCs were transferred into resting WT CD45.1$^+$ mice and 1, 3, 5 or 7 days later, the SI LP of recipient mice was examined for the presence of donor-derived cells. **A.** Representative dot plots of CD103 and CD11b expression by live-gated host DCs or CD11c$^+$ MHCII$^+$ donor-derived DCs. **B-E.** Frequencies of donor-derived and endogenous DCs on days 3 ,5 and 7 after transfer in each DC population defined by CD103 and CD11b expression, CD103$^+$CD11b$^+$ DCs (B), CD103$^+$CD11b$^-$ DCs (C), CD103$^-$CD11b$^+$ DCs (D) or CD103$^-$CD11b$^-$ DCs (E). Data are shown as means (±1SD) of either a single experiment (3 days) or 3 independent experiments (5 & 7 days) with 2-4 recipient mice per time point per experiment.

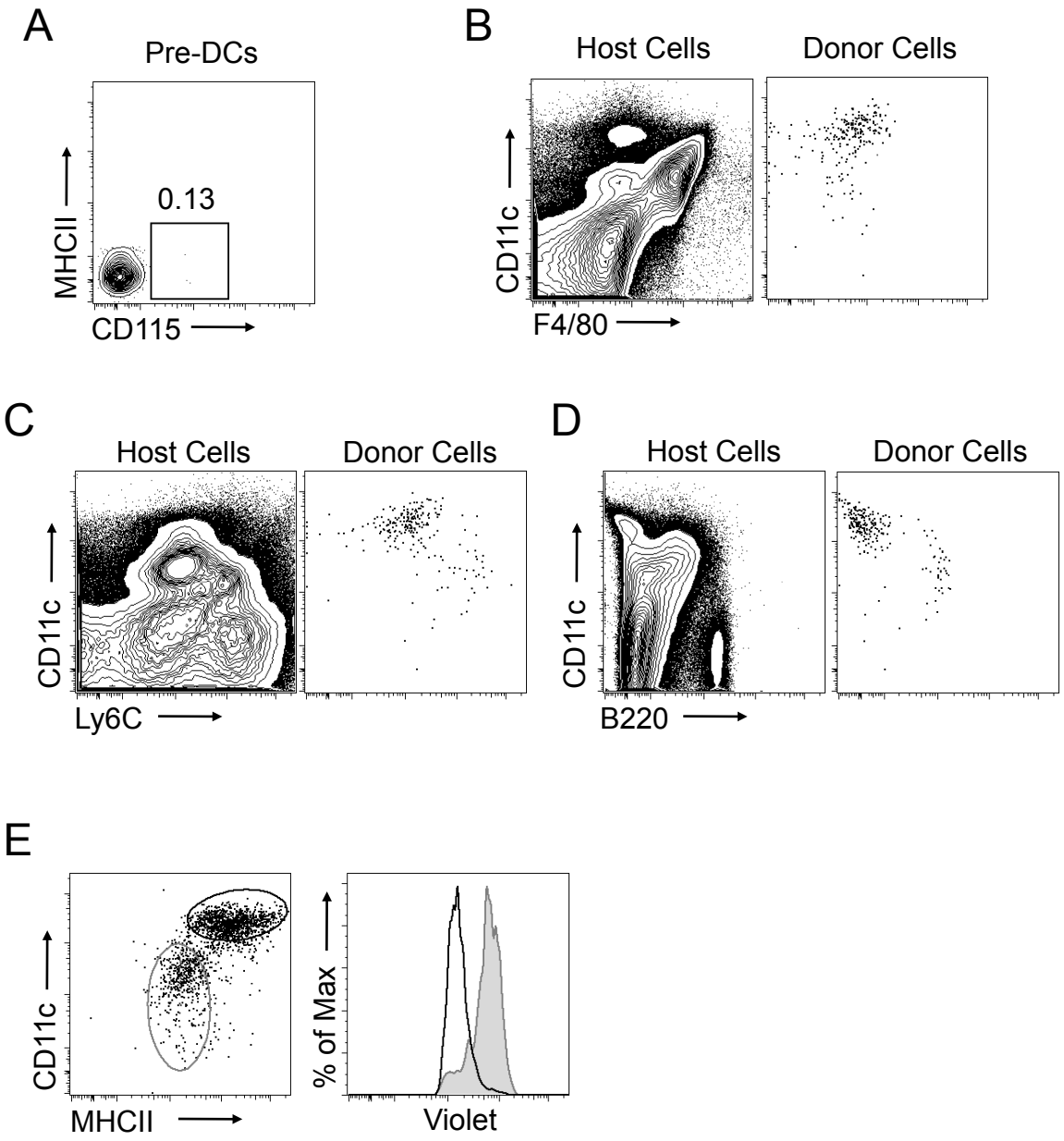

Figure 4.12 Transferred cells also give rise to pDCs but not mϕs in LP

7x10^5 CD45.2$^+$Violet$^+$ pre-DCs were transferred into resting WT CD45.1$^+$ mice. **A.** Representative contour plot showing expression of CD115 by pre-DCs in BM isolates from WT mice with Flt3L secreting B16 tumours. Number indicates percentage of CD115$^+$ pre-DCs. **B-D.** Live-gated host cells and total CD45.2$^+$Violet$^+$ donor-derived cells were examined for expression of F4/80 (B), Ly6C (C) and B220 (D) 7 days after transfer. **E.** Total donor-derived cells were examined for MHCII expression and violet dye levels were assessed on MHCII$^+$ (black line) and MHCII$^-$ (shaded grey) cells. Data are representative of 3 independent experiments with 2-4 recipient mice per experiment.

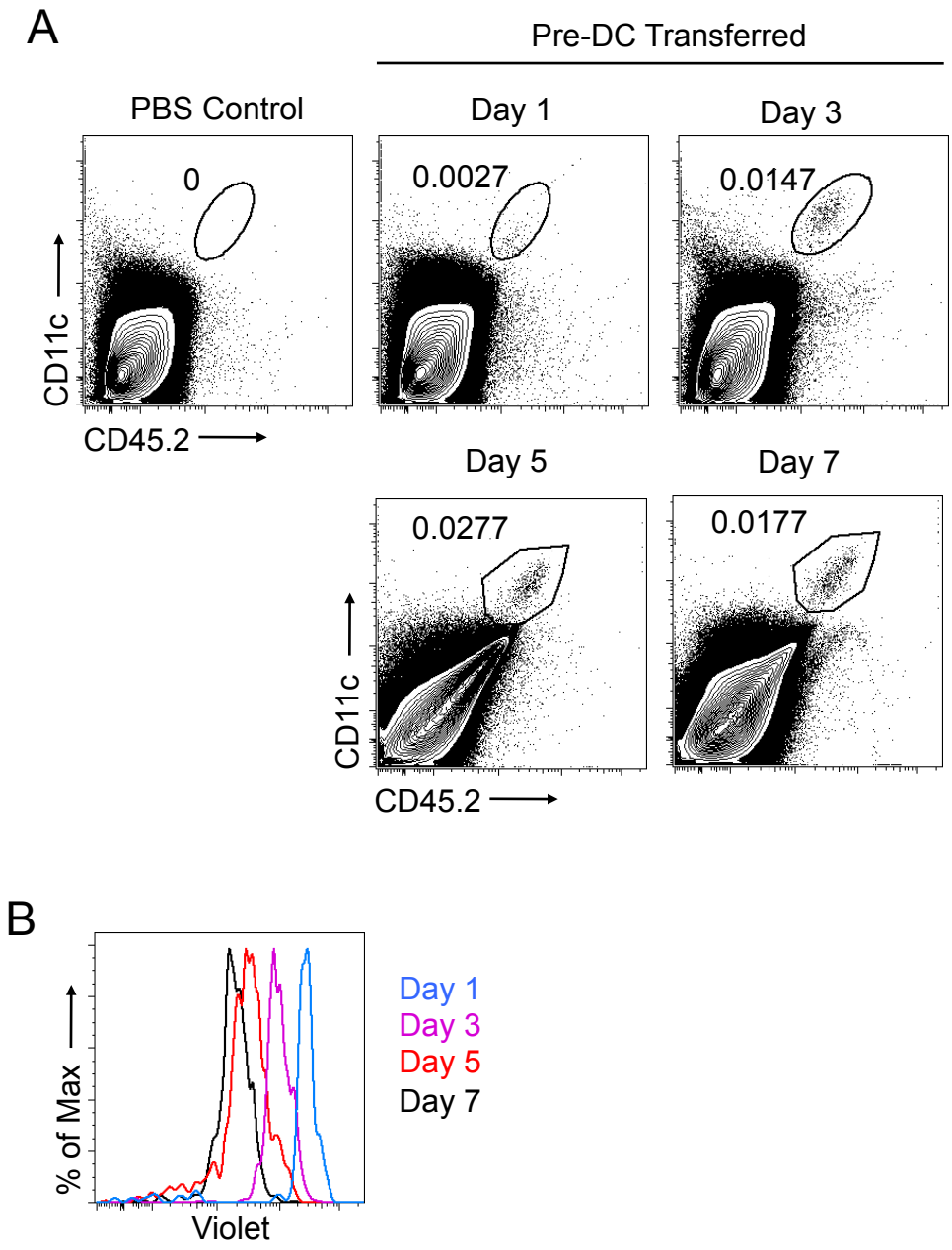

Figure 4.13: Identification of donor-derived cells in the colonic LP

$7x10^5$ CD45.2$^+$Violet$^+$ pre-DCs were transferred into resting WT CD45.1$^+$ mice and 1, 3, 5 or 7 days later, the colonic LP of recipient mice was examined for the presence of donor-derived cells. **A.** Representative contour plots of CD45.2 and CD11c expression on live-gated CD45.1$^-$ cells in mice receiving pre-DCs or PBS 1, 3, 5 and 7 days after transfer. Numbers indicate the proportion of donor-derived cells as a percentage of live-gated CD45.1$^-$ cells. **B.** Violet dye levels on donor-derived cells at day 1, 3, 5 and 7 after transfer. Data are representative of either a single experiment (1 & 3 days) or 3 independent experiments (5 & 7 days) with 2-4 recipient mice per time point per experiment.

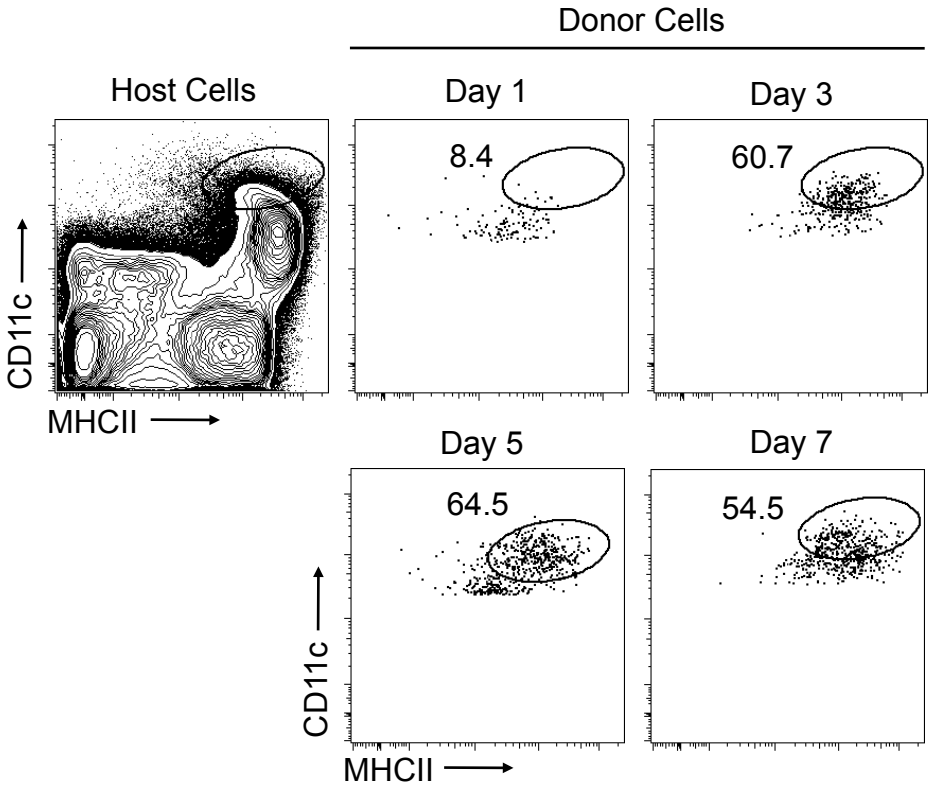

Figure 4.14: Acquisition of MHCII by donor-derived cells in the colonic LP

$7x10^5$ CD45.2$^+$Violet$^+$ pre-DCs were transferred into resting WT CD45.1$^+$ mice and 1, 3, 5 or 7 days later, the colonic LP of recipient mice was examined for the presence of donor-derived cells. Representative contour and dot plots of CD11c and MHCII expression by live-gated host cells or donor-derived cells (gated as shown in Fig. 4.13), 1, 3, 5 and 7 days after transfer. Numbers indicate proportions of MHCII$^+$ cells as a percentage of total donor-derived DCs. Data are representative of either a single experiment (1 & 3 days) or 3 independent experiments (5 & 7 days) with 2-4 recipient mice per time point per experiment.

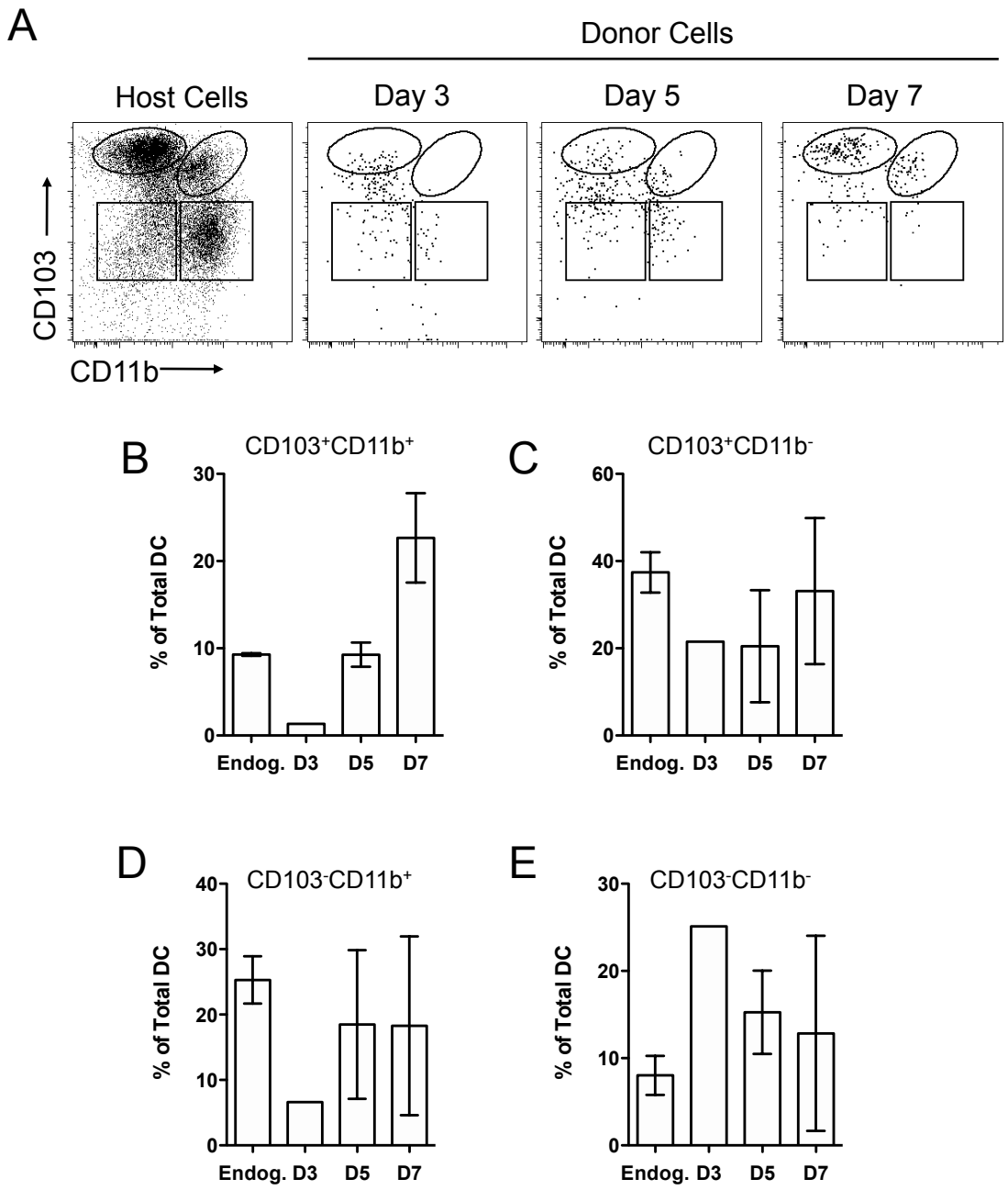

Figure 4.15: Development of DC subsets in colonic LP after transfer of pre-DCs

$7x10^5$ CD45.2$^+$Violet$^+$ pre-DCs were transferred into resting WT CD45.1$^+$ mice and 1, 3, 5 or 7 days later, recipient mice were examined for the presence of donor-derived cells. **A.** Representative dot plots of CD103 and CD11b expression by live-gated host DCs or CD11c $^+$MHCII$^+$ donor-derived DCs. **B-E.** Frequencies of donor-derived and endogenous DCs on days 3 , 5 and 7 after transfer in each DC population defined by CD103 and CD11b expression, CD103$^+$CD11b$^+$ DCs (B), CD103$^+$CD11b$^-$ DCs (C), CD103$^-$CD11b$^+$ DCs (D) or CD103$^-$CD11b$^-$ DCs (E). Data are shown as means (±1SD) of either a single experiment (3 days) or 3 independent experiments (5 & 7 days) with 2-4 recipient mice per time point per experiment.

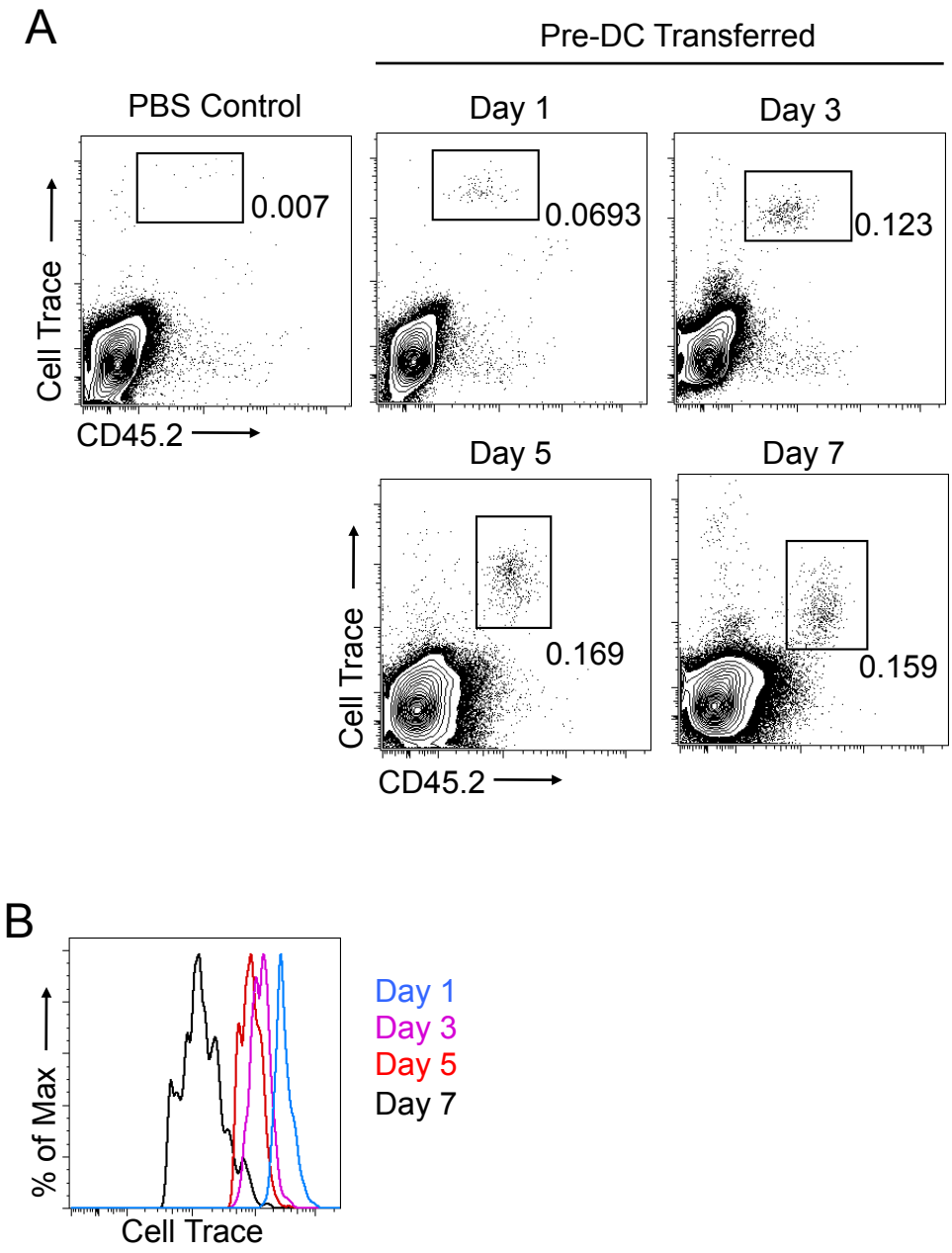

Figure 4.16: Identification of donor-derived cells in the MLNs

$7x10^5$ $CD45.2^+Violet^+$ pre-DCs were transferred into resting WT $CD45.1^+$ mice and 1, 3, 5 or 7 days later, recipient mice were examined for the presence of donor-derived cells. **A.** Representative contour plots of CD45.2 expression and Violet dye labelling on live-gated $CD3^-CD19^-$ cells in the MLNs of mice receiving pre-DCs or PBS 1, 3, 5 and 7 days after transfer. Numbers indicate the proportion of donor-derived cells as a percentage of live-gated $CD3^-CD19^-$ cells. **B.** Dilution of Violet dye on donor-derived cells 1, 3, 5 and 7 days after transfer. Data are representative of either a single experiment (1 & 3 days) or 3 independent experiments (5 & 7 days) with 2-4 recipient mice per time point per experiment.

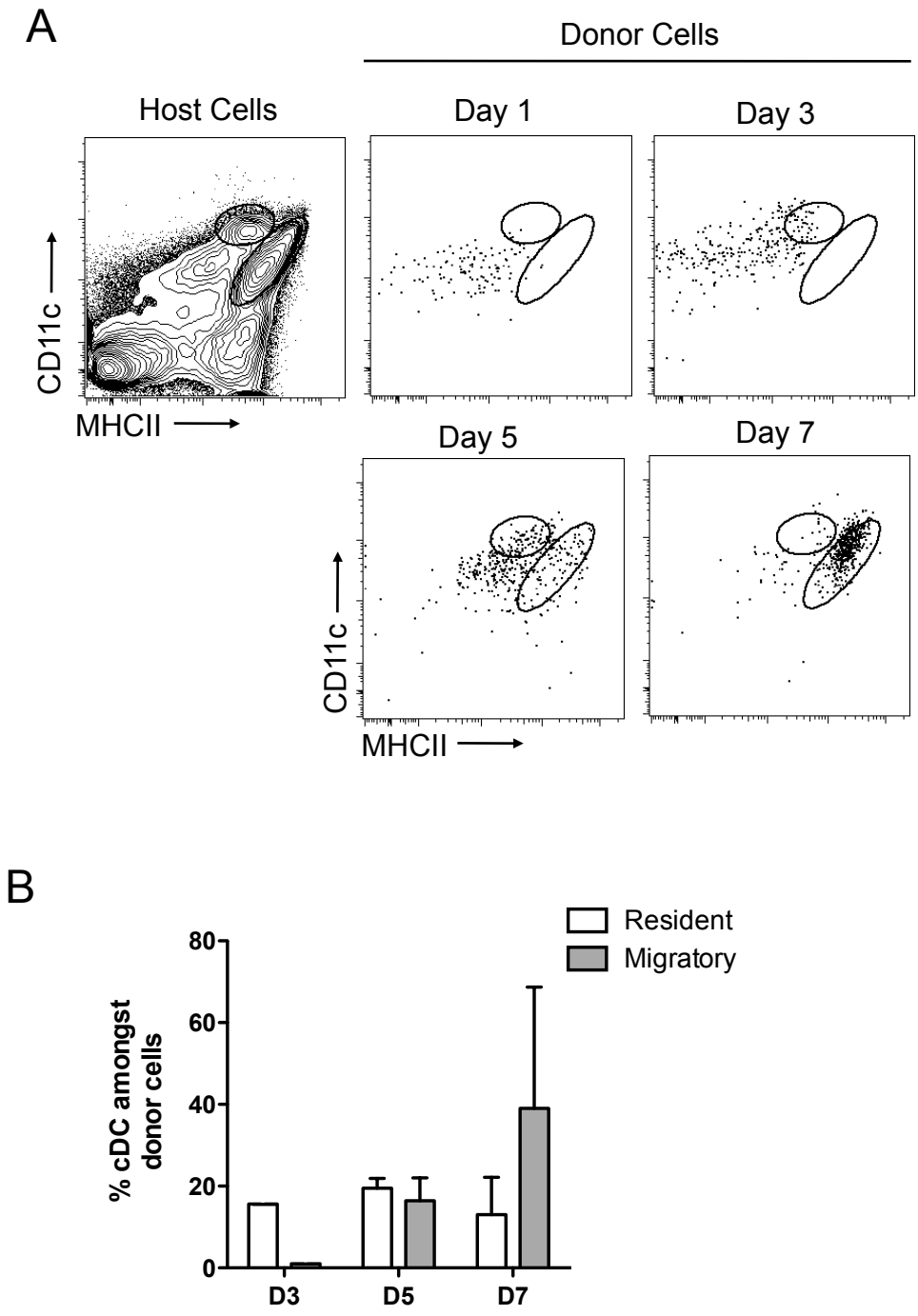

Figure 4.17: Acquisition of MHCII donor-derived cells in the MLNs

$7x10^5$ $CD45.2^+Violet^+$ pre-DCs were transferred into resting WT $CD45.1^+$ mice and 1, 3, 5 or 7 days later, MLNs of recipient mice were examined for the presence of donor-derived cells. **A.** Representative contour and dot plots of CD11c and MHCII expression by live-gated host cells or donor-derived cells (gated as shown in Fig. 4.16), 1, 3, 5 or 7 days after transfer **B.** Proportions of donor-derived DC adopting the phenotype of migratory ($CD11c^+MHCII^{hi}$) or LN resident ($CD11c^+$ $MHCII^{int}$) DCs 3, 5 and 7 days after transfer as a percentage of total donor-derived DCs. Data are shown as the mean (+1SD) of either a single experiment (3 days) or 3 independent experiments (5 & 7 days) with 2-4 recipient mice per time point per experiment.

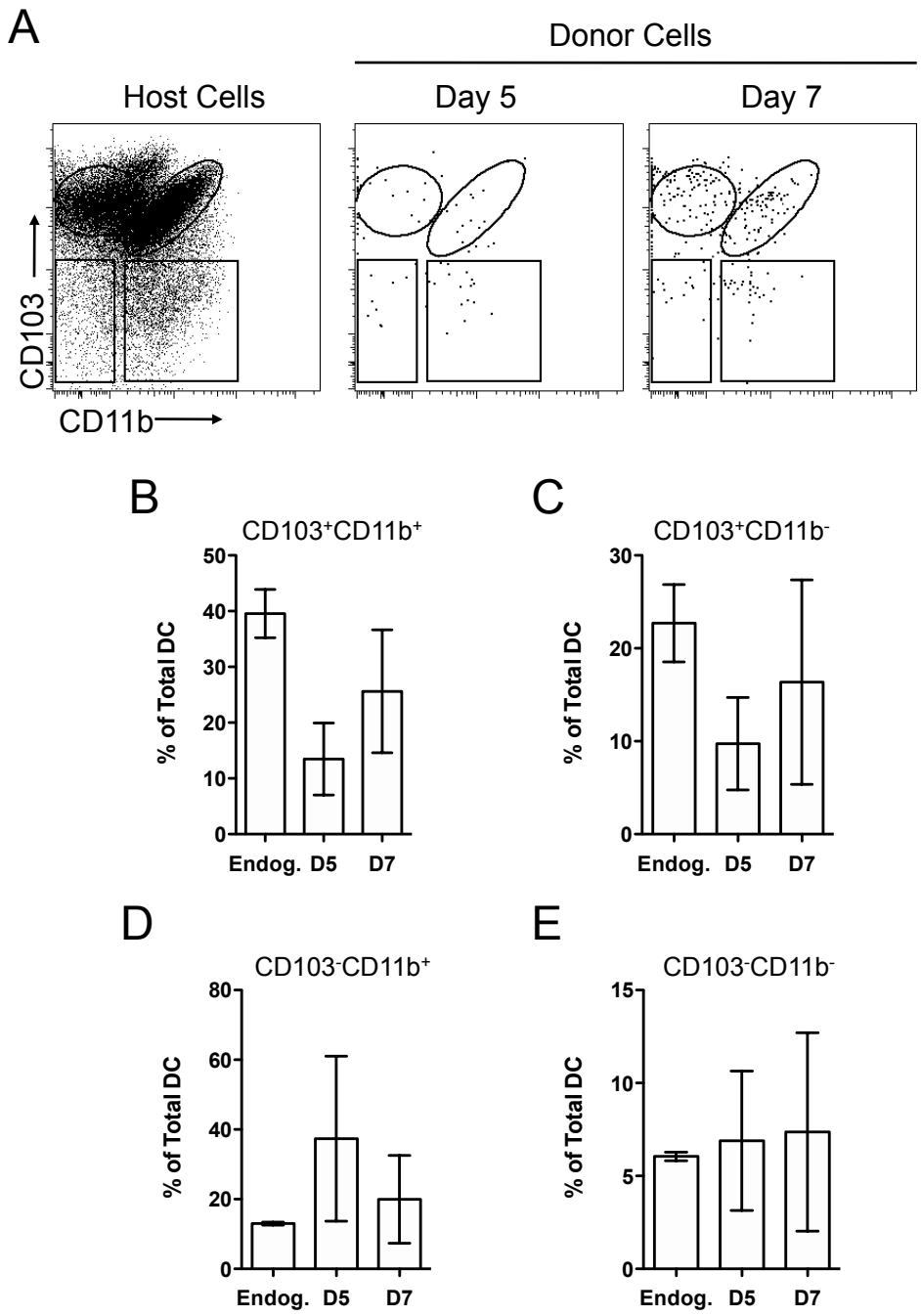

Figure 4.18: Phenotypes of donor-derived cells amongst migratory DCs in MLN

$7x10^5$ CD45.2$^+$Violet$^+$ pre-DCs were transferred into resting WT CD45.1$^+$ mice and the MLNs of recipient mice were examined for the presence of donor-derived cells 5 or 7 days later. **A.** Representative contour plots of CD103 and CD11b expression by live-gated migratory host DCs or CD11c$^+$MHCII^{hi} donor-derived DCs. **B-E.** Frequencies of donor-derived DCs in each DC population as defined by CD103 and CD11b expression compared with endogenous DCs 5 and 7 days after transfer, CD103$^+$CD11b$^+$ (B), CD103$^+$CD11b$^-$ (C), CD103$^-$CD11b$^+$ (D) or CD103$^-$CD11b$^-$ (E). Data are shown as mean ±1SD of 2 independent experiments with 2-4 recipient mice per time point per experiment.

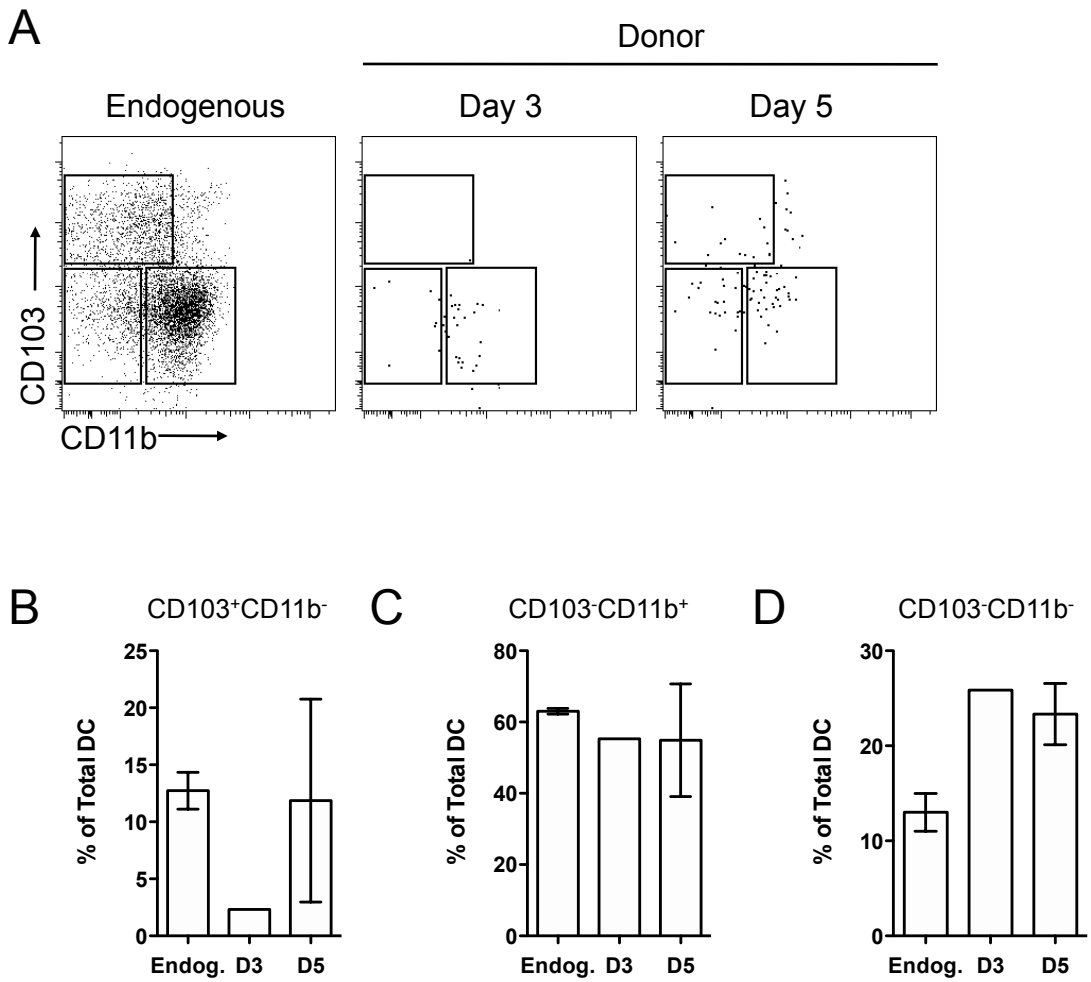

Figure 4.19: Phenotypes of donor-derived cells amongst resident DCs in MLN

$7x10^5$ CD45.2$^+$Violet$^+$ pre-DCs were transferred into resting WT CD45.1$^+$ mice and the MLNs of recipient mice were examined for the presence of donor-derived cells 5 or 7 days later. **A.** Representative dot plots of CD103 and CD11b expression by live-gated migratory host DCs or CD11c$^+$MHCII^{int} donor-derived DCs. **B-D.** Frequencies of donor-derived DCs in each DC population as defined by CD103 and CD11b expression compared with endogenous DCs 5 and 7 days after transfer, CD103$^+$CD11b$^-$ (B), CD103$^-$CD11b$^+$ (C) or CD103$^-$CD11b$^-$ (D). Data are shown as mean (±1SD) of either a single experiment (3 days) or 2 independent experiments (5 days) with 2-4 recipient mice per time point per experiment.

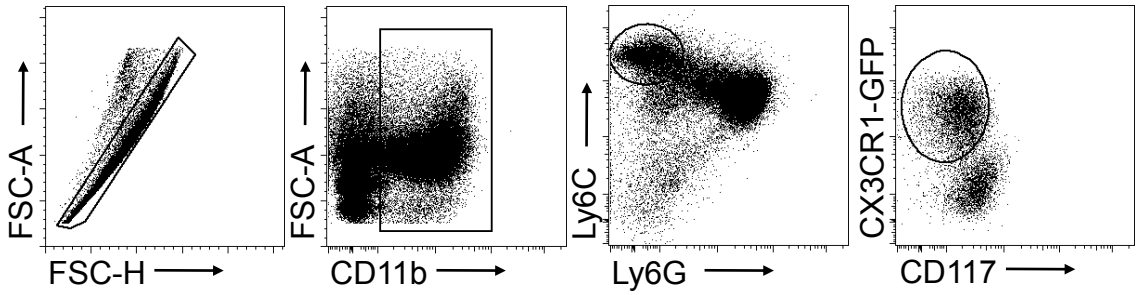

Figure 4.20: Identification of Ly6C^{hi} monocytes in the BM

Doublets were excluded from BM from CX3CR1$^{+/GFP}$ mice and Ly6C^{hi} monocytes were identified amongst remaining cells as CD11b^{+} Ly6G^{-} Ly6C^{hi} CX3CR1-GFP^{int} and CD117^{-} cells. Data are representative of at least 5 independent experiments.

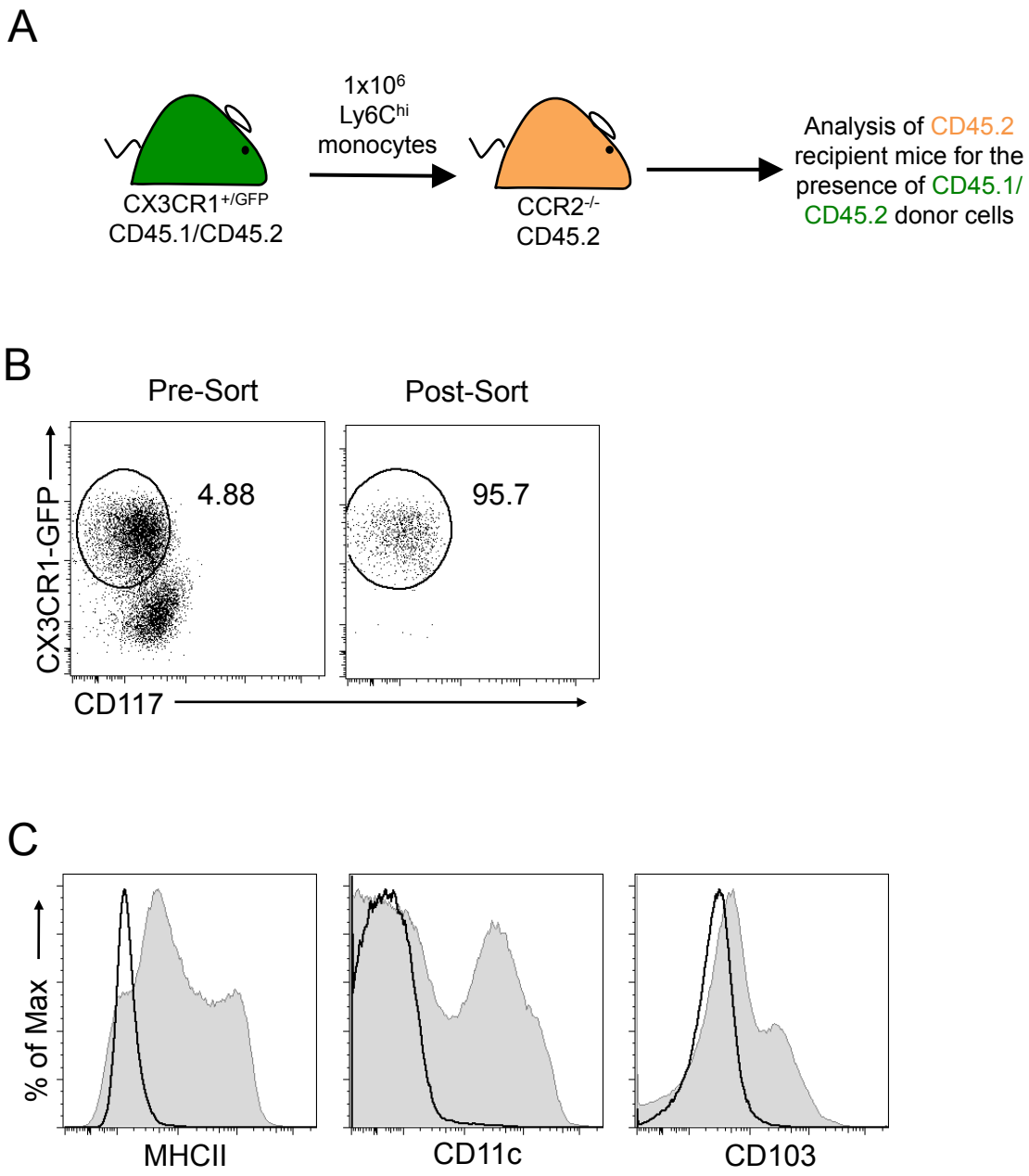

Figure 4.21: Purification of Ly6C^{hi} monocytes for adoptive transfer

A. BM was harvested from CD45.1^{+}/CD45.2^{+} CX3CR1$^{+/GFP}$ mice, Ly6C^{hi} monocytes were FACS-purified and 1x10^{6} were transferred into CD45.2^{+} CCR2$^{-/-}$ mice. **B.** Ly6C^{hi} monocytes were identified as in Fig. 4.20 and sorted to high purity. Numbers indicate proportion of Ly6C^{hi} monocytes a percentage of total BM cells. **C.** Expression of MHCII, CD11b and CD103 on Ly6C^{hi} monocytes (black line) compared with levels on endogenous SI LP live CD45^{+} cells (shaded grey). Data are from a single experiment in which Ly6C^{hi} monocytes were sorted from 6 pooled mice.

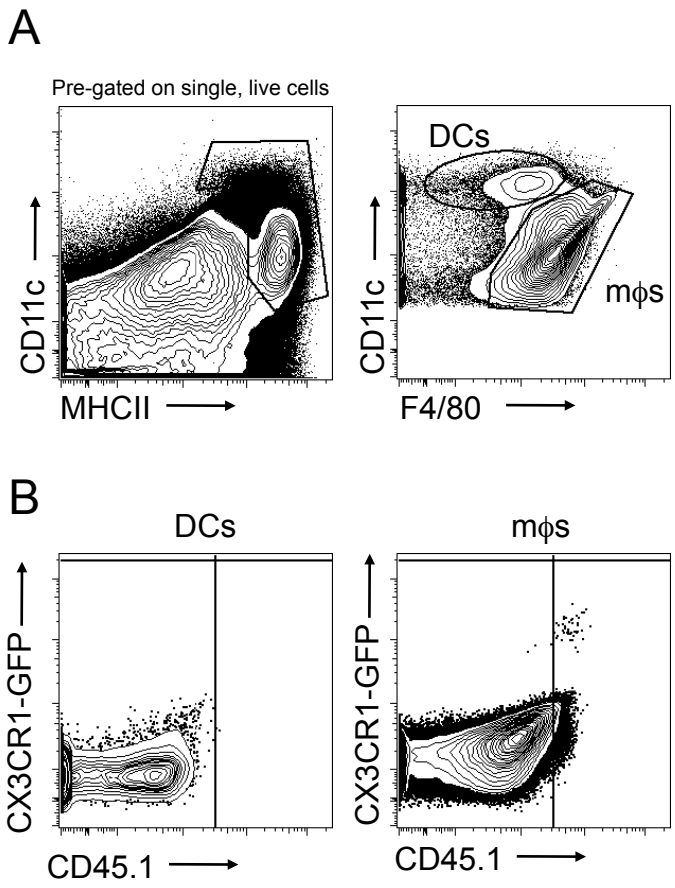

Figure 4.22: Progeny of adoptively transferred Ly6C^{hi} donor monocytes in SI LP
1x10^6 Ly6C^{hi} monocytes from CD45.1/CD45.2$^+$ CX3CR1$^{+/GFP}$ mice were FACS-purified and adoptively transferred into CD45.2$^+$ CCR2$^{-/-}$ recipients. Recipient mice were analysed for the presence of donor cells in the SI LP 5 days after transfer. **A.** CD11c$^+$MHCII$^+$ MPs were identified in recipient mice amongst single, live CD45$^+$ cells and DCs and mϕs were identified based on CD11c and F4/80 expression respectively. **B.** Donor-derived CD11c^{hi}F4/80$^-$ DCs and CD11c^{int}F4/80$^+$ mϕs were identified by their expression of CX3CR1-GFP and CD45.1 expression. Data are from a single experiment with 3 recipient mice.

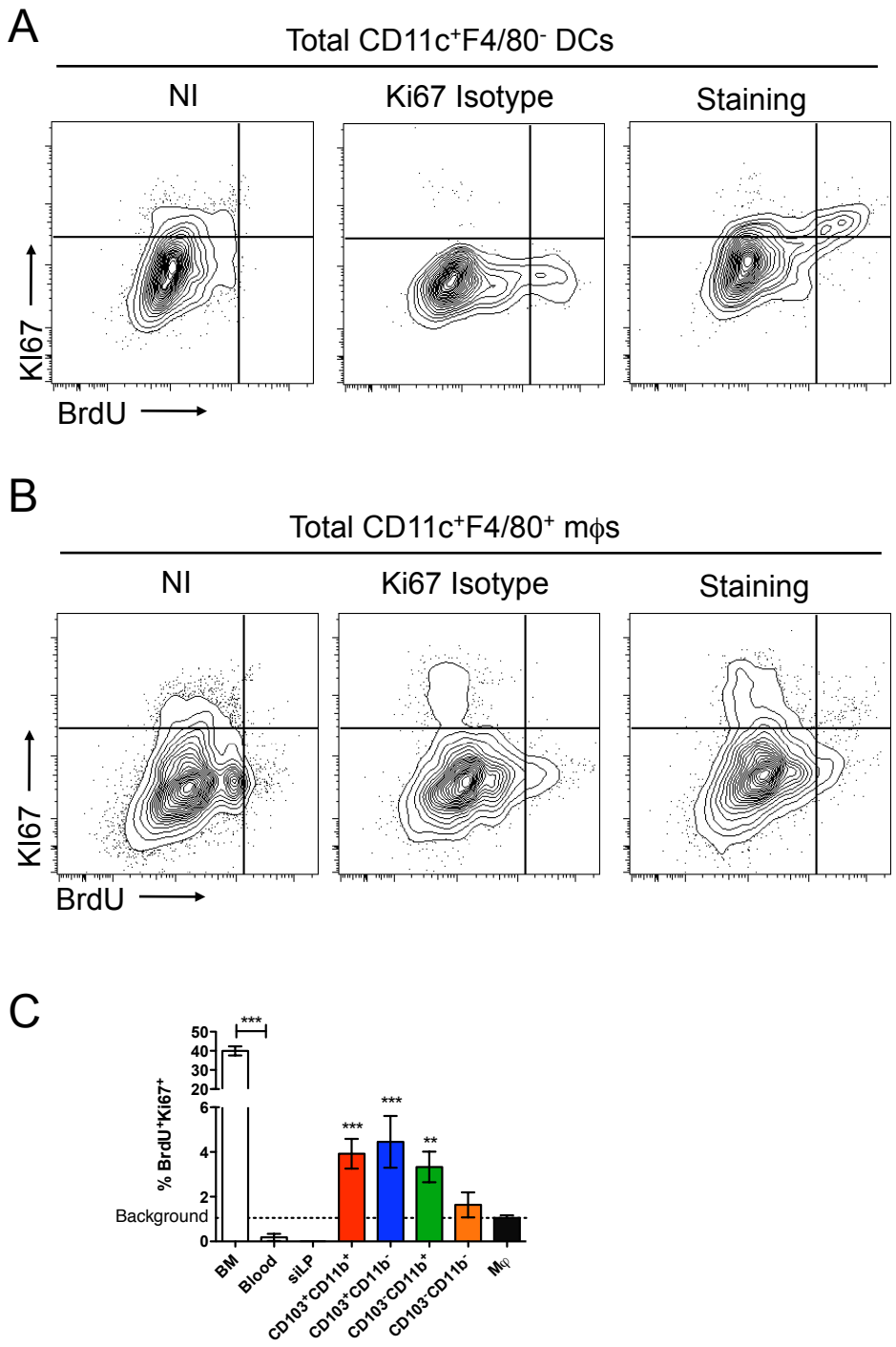

Figure 4.23: Mature DCs but not pre-DCs or mϕs proliferate *in situ* in SI LP

Mice received a single i.p. injection of 1mg BrdU and 3 hours later BrdU incorporation and Ki67 expression was assessed in BM, blood and SI LP. **A,B.** Representative contour plots showing BrdU and Ki67 staining on CD11c$^+$F4/80$^-$ DCs (A) and CD11c$^+$F4/80$^+$ mϕs (B) in the SI LP of BrdU injected mice compared with non-injected (NI) BrdU and Ki67 isotype controls. **C.** Proportion of BrdU$^+$Ki67$^+$ cells amongst pre-DCs in BM, blood and SILP and amongst SI LP DC subsets and mϕs. Data are representative of 3 independent experiments with n=3/4 per experiment, **p<0.01, ***p<0.001 Asterisks denote significant differences between each SI LP DC population and mϕs, unless otherwise marked. One way ANOVA with Bonferroni post test.

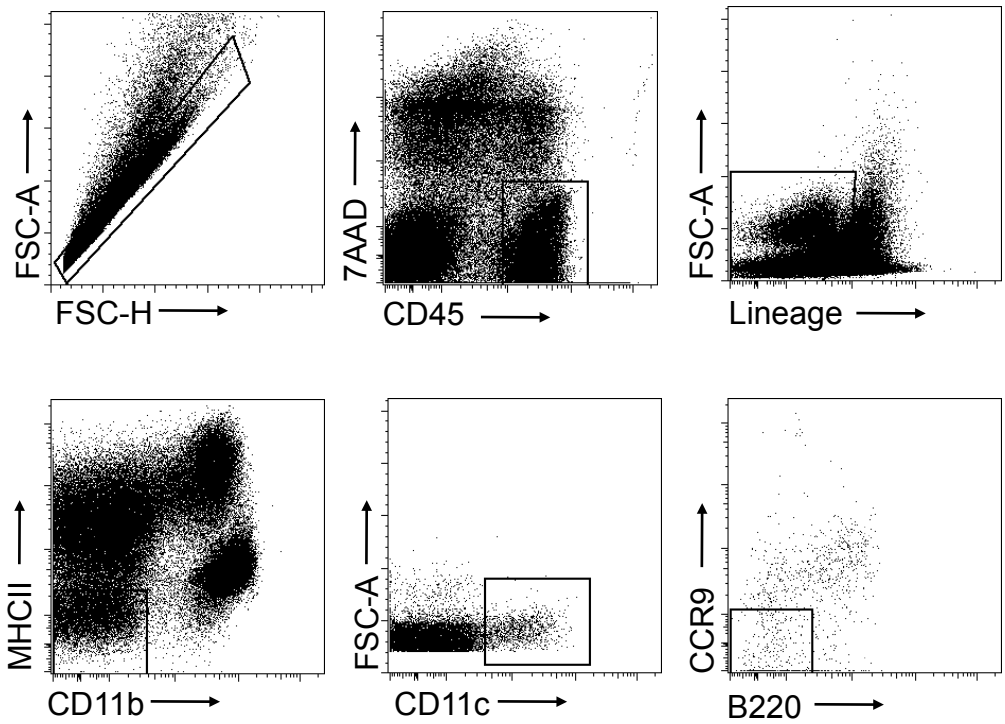

Figure 4.24: Identification of putative pre-DCs in the SI LP

Putative pre-DCs were identified as single live, $CD45^{+}$, $lineage^{-}$ (CD3, CD19, CD49b) $MHCII^{-}$ $CD11b^{-}$ $CD11c^{+}$ $B220^{-}$ and $CCR9^{-}$ cells. Data are representative of at least 5 independent experiments.

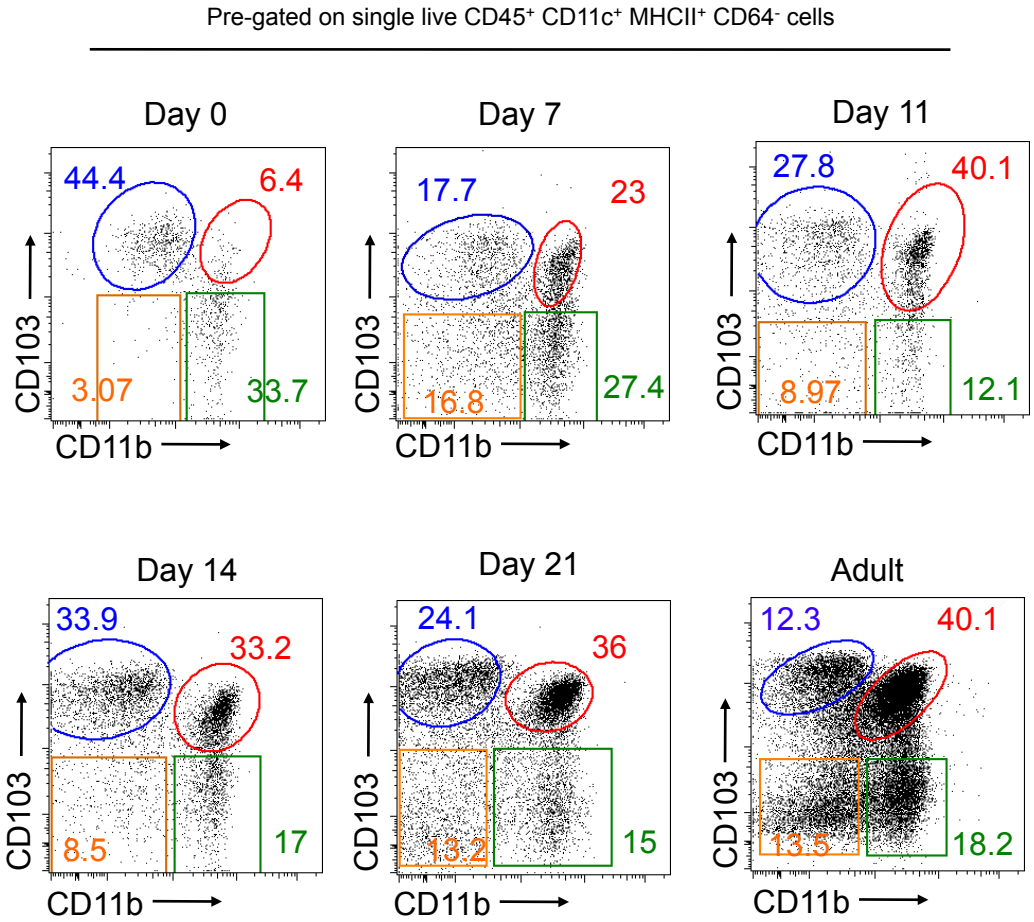

Figure 4.25: Development of DC subsets in SI LP after birth

$CD11c^+MHCII^+CD64^-$ DCs in SI LP digests were examined for their expression of CD103 and CD11b. Representative dot plots showing CD103 and CD11b expression by total DCs in SI LP of newborn, 7 day old, 11 day old, 14 day old, 21 day old or 7 week old adult mice. Numbers indicate the frequencies of each DC population as a percentage of total DCs. Data are representative from 1 or 2 experiments with n =3/4 per time point per experiment.

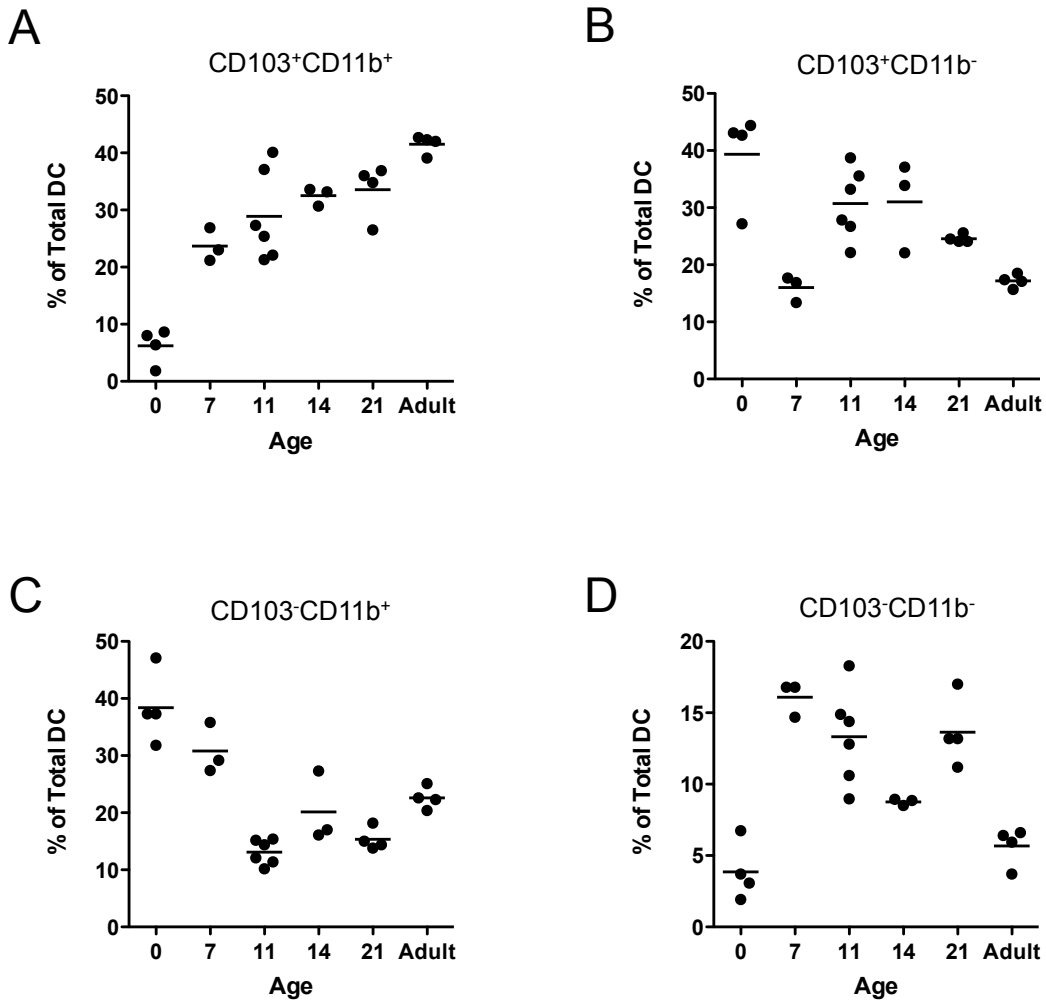

Figure 4.26: Development of DC subsets in SI LP after birth

$CD11c^+MHCII^+CD64^-$ DCs in SI LP digests were examined for their expression of CD103 and CD11b. **A-D.** Proportions of $CD103^+CD11b^+$ (A), $CD103^+CD11b^-$ (B), $CD103^-CD11b^+$ (C) and $CD103^-CD11b^-$ (D) DCs as a percentage of total DCs in newborn, 7 day old, 11 day old, 14 day old, 21 day old and 7 week old adult mice. Data are pooled from 1 or 2 experiments with n =3/4 per time point per experiment.

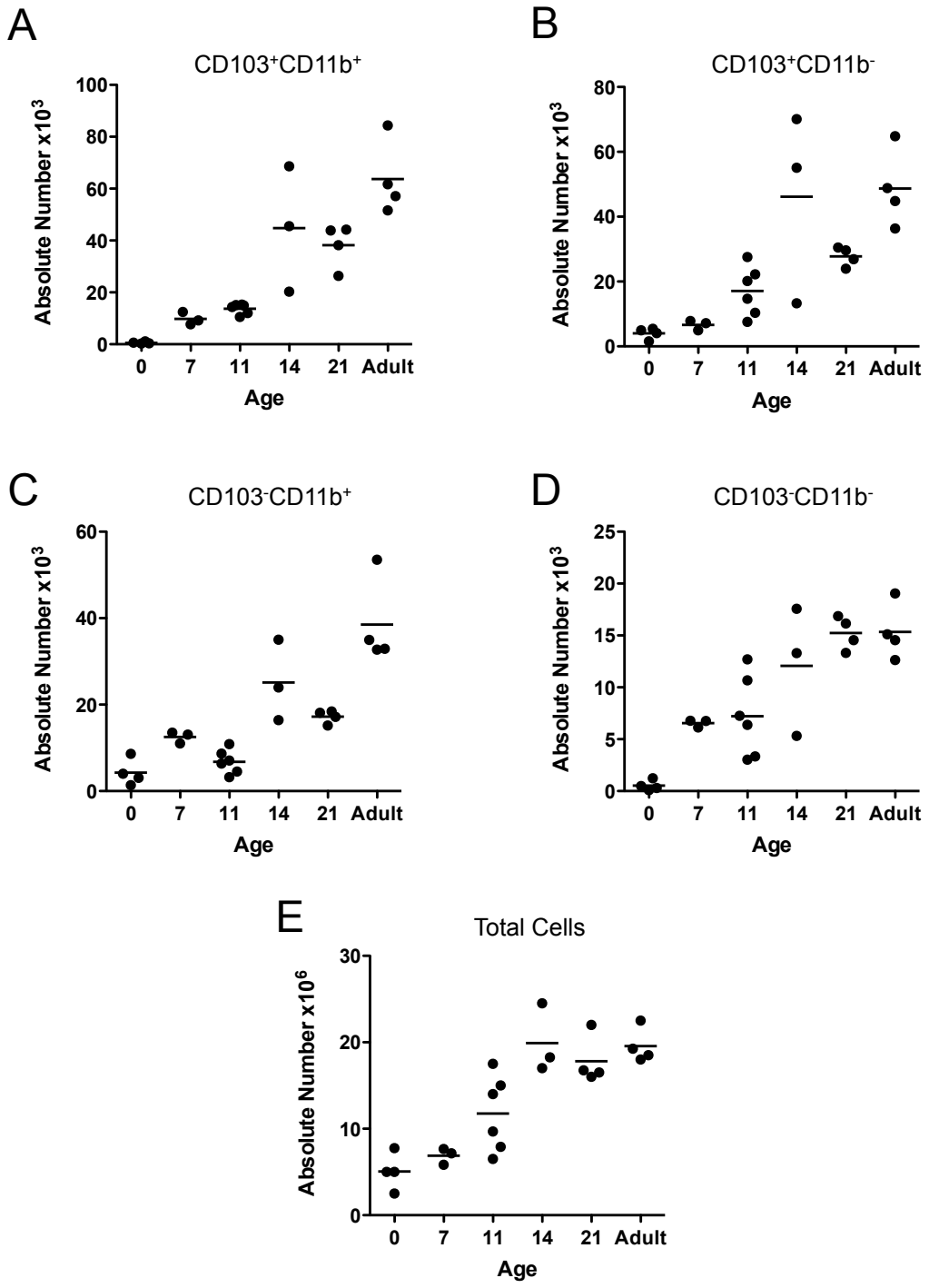

Figure 4.27: Development of DC subsets in SI LP after birth

$CD11c^+MHCII^+CD64^-$ DCs in SI LP digests were examined for their expression of CD103 and CD11b. **A-D.** Absolute numbers of $CD103^+CD11b^+$ (A), $CD103^+CD11b^-$ (B), $CD103^-CD11b^+$ (C) and $CD103^-CD11b^-$ (D) DCs in newborn, 7 day old, 11 day old, 14 day old, 21 day old and 7 week old adult SI LP. **E.** Absolute number of total cells isolated from SI LP of newborn, 7 day old, 11 day old, 14 day old, 21 day old and 7 week old adult mice. Data are pooled from 1 or 2 experiments with n =3/4 per time point per experiment.

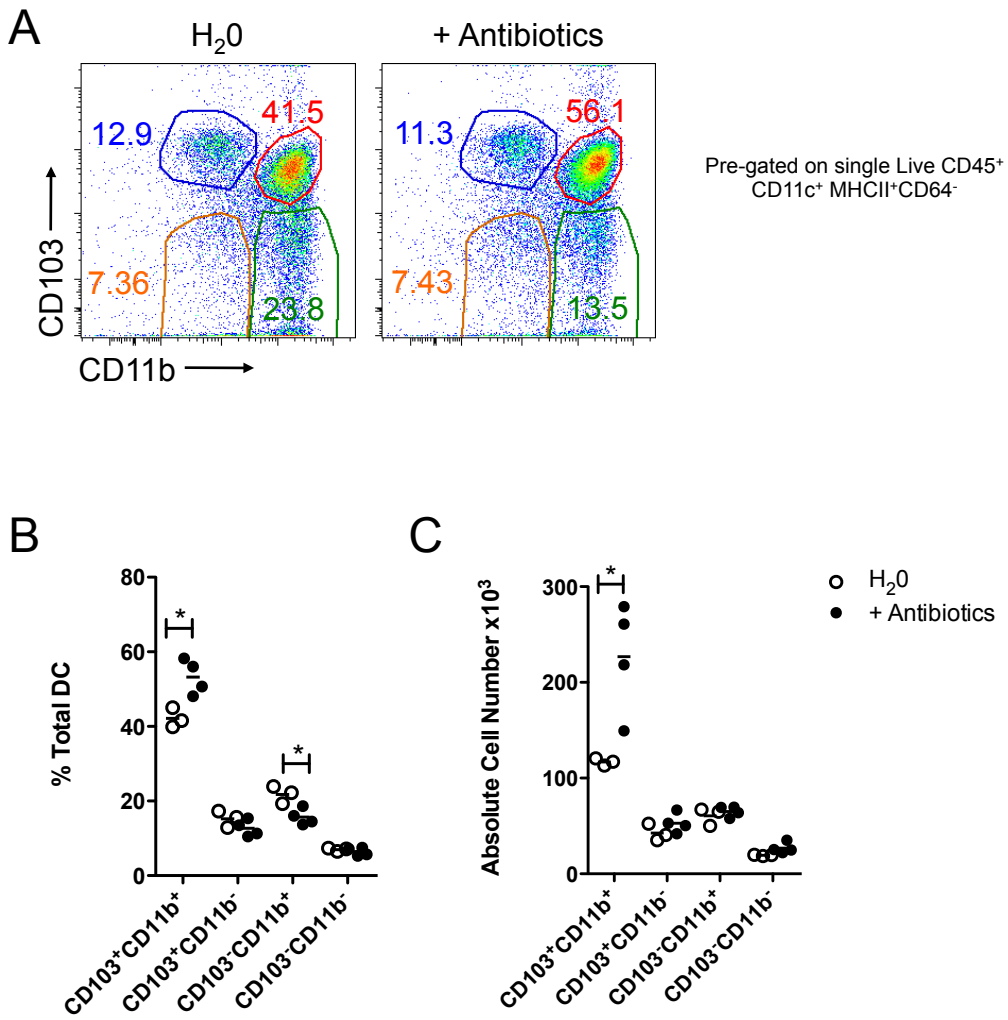

Figure 4.28: Effects of antibiotic treatment on intestinal DC subsets

Mice received vancomycin, metronidazole, ampicillin, neomycin and gentamycin in their drinking water for 2 weeks. **A.** Representative dot plots showing CD103 and CD11b expression by $CD11c^+$ $MHCII^+CD64^-$ DCs in antibiotic treated mice compared with mice receiving water alone. Numbers represent proportion of each DC subset as a percentage of total DCs. **B.** Proportion of each DC subset as a percentage of total DCs in antibiotic treated and control mice. **C.** Absolute number of each DC subset in antibiotic treated and control mice. Data are from a single experiment with n =3-6 per group per experiment. *$p<0.05$ Student's t test.

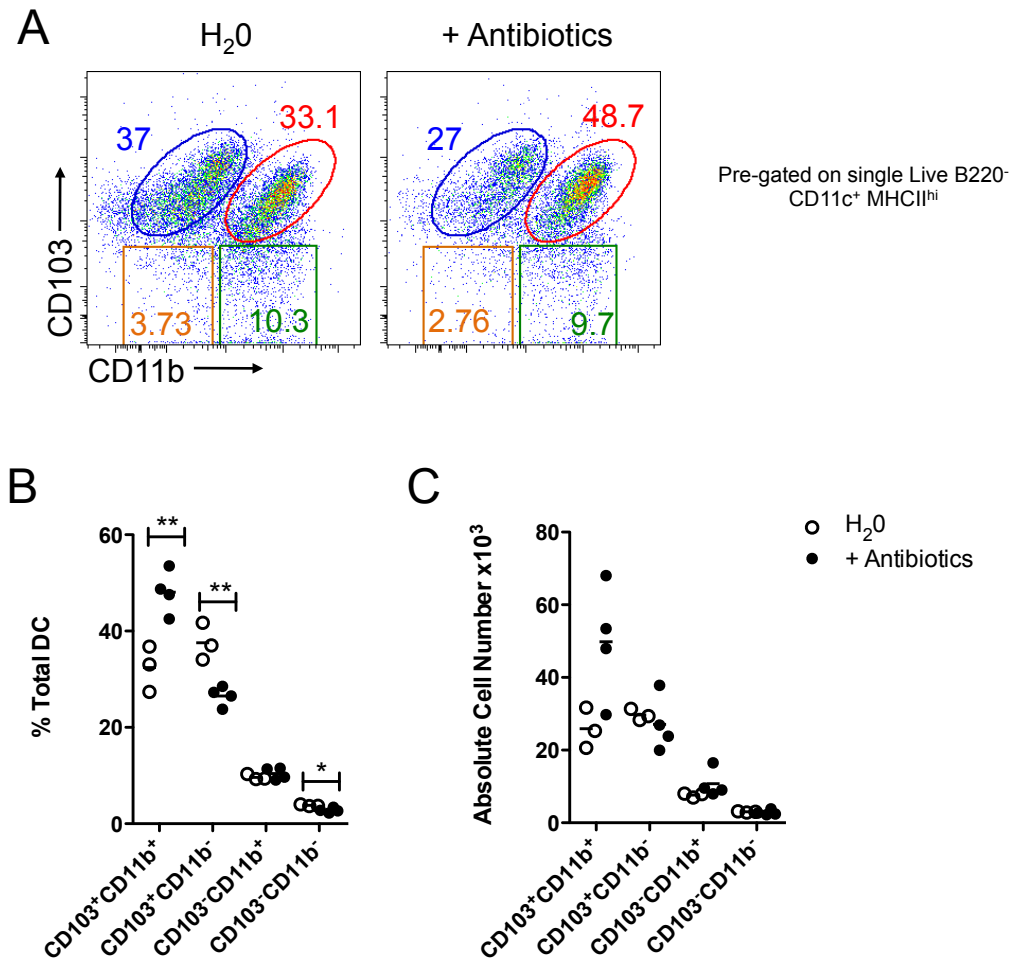

Figure 4.29: Effects of antibiotics on migratory DC subsets in MLN

Mice received vancomycin, metronidazole, ampicillin, neomycin and gentamycin in their drinking water for 2 weeks. **A.** Representative dot plots showing CD103 and CD11b staining amongst $CD11c^{+}MHCII^{hi}B220^{-}$ migratory DC in antibiotic treated and control mice. Numbers represent proportion of each DC subset as a percentage of total migratory DCs. **B.** Proportion of each DC subset as a percentage of total migratory DCs in antibiotic treated and control mice. **C.** Absolute numbers of each DC subset in antibiotic treated and control mice. Data are from a single experiment with n =3-6 per group per experiment. *p<0.05, **p<0.01 Student's t test.

Chapter 5 Characterisation of intestinal DC populations during inflammation and infection

5.1 Introduction

In the previous two chapters, I characterised the DC populations present in the steady state intestinal LP and examined their development from committed DC precursors. I identified four distinct subsets of DCs, two of which did not express the prototypical gut DC marker CD103 and which had not been investigated thoroughly in the past due to their phenotypic overlap with intestinal mϕs. As previous studies using less rigorous identification strategies had suggested that $CD103^-$ MPs were associated with intestinal inflammation, in this chapter, I set out to examine the DC populations during non-steady state conditions. To do this I used two models of sterile inflammation; dextran-sodium sulphate induced colitis (DSS colitis) and post-operative ileus (POI), while *Citrobacter rodentium* infection was used as a model of protective immunity similar to that seen in enteropathogenic (EPEC) *Escherichia coli* infection.

5.2 Dextran sodium sulphate induced colitis

DSS colitis is a model of acute intestinal inflammation and had been characterised extensively by previous work in the lab. Within 3 days of administering 2% DSS *ad libitum* in the drinking water, there is a rapid infiltration of the colonic LP by neutrophils and monocytes. This precedes clinical signs of disease such as rectal bleeding, diarrhoea and weight loss, which typically appear after 4-6 days of DSS administration. Although the previous studies in the lab had investigated the myeloid compartment of the colonic LP (Bain et al., 2013), these analyses had been carried out before I had established the methods for characterising DCs properly. Therefore this well-defined model of intestinal inflammation was the first I decided to utilise.

5.2.1 Characterisation of DC populations during DSS colitis

I first examined the DC populations present in the colonic LP after 4 days of 2% DSS administration. I chose this time because there are few clinical symptoms at this stage, allowing me to examine the behaviour of the DC populations during the initiation of the disease and before mucosal destruction occurred. To ensure that the LP was inflamed at this time, I assessed the numbers of inflammatory $Ly6C^{hi}$ monocytes and their mϕ progeny using the phenotyping scheme that had

been developed in the lab (Bain et al., 2013). This revealed a trend towards increased total cellularity in the colitic LP compared with resting controls (Fig. 5.1A), consistent with the presence of inflammation. To investigate this further, I examined total myeloid ($CD45^+CD11b^+$) cells for their expression of Ly6C and MHCII. This revealed there to be significant increases in both the proportions and numbers of $Ly6C^{hi}MHCII^-$ (P1) and $Ly6C^{hi}MHCII^+$ (P2) inflammatory monocytes in the colitic mice, clearly demonstrating that the colons were inflamed (Fig. 5.1B-E). Based on these results, I next set out to examine the DC populations. However as my DC identification strategy relies upon CD64 and/or F4/80 expression being restricted to mϕs, it was first necessary to examine if CD64 discriminated between DCs and mϕs in this inflammatory setting. Analysis of total $CD11c^+MHCII^+$ MPs at this time point demonstrated that CD64 expression continued to define two distinct populations of intestinal MPs (Fig. 5.2A), suggesting it was an appropriate marker for distinguishing DCs and mϕs in this model. While this gating strategy remains to be definitively demonstrated by examining the ability of these populations to migrate in lymph and to function as APCs, this analysis found the proportion of $CD64^+$ mϕs to be slightly but significantly reduced in colitic mice compared with controls, which correlated with a slight but non-significant increase in the proportion of total DCs (Fig. 5.2A). Further analysis of the $CD11c^{hi}CD64^-$ DCs for CD103 and CD11b expression revealed that all four populations of DCs found in the steady state colonic LP were also present during inflammation (Fig. 5.2B). Interestingly, despite previous studies suggesting the $CD103^-$ 'DCs' to be preferentially involved in inflammation (Siddiqui et al., 2010), the proportions of $CD64^-$ genuine DCs were not altered in this model of inflammation. In contrast, the proportion of $CD103^+CD11b^+$ DCs was significantly reduced in the colitic LP compared with controls, whereas the proportion of $CD103^+CD11b^-$ DCs was slightly increased (Fig. 5.2C). There was a significant increase in the absolute numbers of all DC populations during colitis (Fig. 5.2D).

5.2.2 DC development during inflammation

Previous studies had suggested that the $CD103^-$ MPs that were associated with inflammation were derived from $Ly6C^{hi}$ monocytes (Bogunovic et al., 2009; Rivollier et al., 2012; Varol et al., 2009), which form a substantial part of the infiltrate in colitis, as I showed above. However, as this work did not identify $CD103^-$ DCs precisely, I thought it important to exploit my adoptive transfer

protocol to examine whether the genuine DCs I found in inflamed mucosa were derived from pre-DCs as they were in steady state. To do this, I had to modify the DSS protocol to give sufficient time for pre-DCs to mature into all subsets after transfer, which I found previously to be five days. As the use of 2% DSS for the length of time required by this protocol would result in fatal disease, I reduced the concentration of DSS to 1.2% and planned to transfer pre-DCs after 3 days of DSS administration, before continuing DSS for an additional 5 days. Before doing this, I examined if 3 days of feeding 1.2% DSS was sufficient to induce intestinal inflammation. 3 days administration of 1.2% DSS was indeed sufficient to induce inflammation, as there was considerable expansion of the $Ly6C^{hi}MHCII^{-}$ (P1) and $Ly6C^{hi}MHCII^{+}$ (P2) populations of monocytes compared with control colon, although this was not always statistically significant (Fig. 5.3). I next examined if this model of disease could be maintained for 8 days without requiring these mice to be culled. Using this protocol, mice progressively lost weight up to 8 days, but remained above 80% of their starting weight, which is the limit permissible under the UK Home Office guidelines (Fig. 5.4A). In parallel, mice showed increasing signs of disease including diarrhoea and rectal bleeding, and again, the total clinical score remained within the prescribed limit of 10 (Fig. 5.4B).

Having established that this prolonged regime was effective for generating inflammation, I next transferred $CD45.1/CD45.2^{+}$ pre-DCs into mice that had been receiving 1.2% DSS for 3 days. I then continued to administer 1.2% DSS for a further 5 days before examining the fate of the transferred cells. As described in the previous chapter, pre-DCs were FACS-purified from the BM of WT mice inoculated with Flt3L secreting melanoma cells 10 days earlier and donor-derived DCs were identified in the colonic LP as $CD45.2^{+}violet^{+}CD11c^{+}MHCII^{+}$ cells (Fig. 5.5A). Analysis of these cells demonstrated that all four populations of intestinal DCs developed from pre-DCs under conditions of inflammation in the same way as they did in the steady state colon (Fig. 5.5B,C). However it appeared that donor-derived DCs contained fewer $CD103^{+}CD11b^{-}$ DCs and slightly more $CD103^{+}CD11b^{+}$ DCs than the equivalent populations present amongst endogenous DCs in the inflamed colon. The significance of this finding is unclear, but these results, together with earlier work in the lab showing that $Ly6C^{hi}$ monocytes do not give rise to *bona fide* DCs in DSS colitis (Bain et al., 2013), indicate that pre-DCs are the only source of DCs regardless of the presence or absence of inflammation.

5.3 Characterisation of DCs during post-operative ileus

As DSS colitis affects the colonic LP exclusively, I next wanted to characterise the DC populations in the small intestine during inflammation. There are few experimental models of inflammation in this tissue, but one such model is post-operative ileus (POI), in which transient inflammation occurs after mechanical manipulation of the gut during surgery. To induce POI, the gut was exposed by laparotomy and the length of the SI was rubbed with a cotton bud (Wehner et al., 2007). Due to the rapid and transient nature of this model, it allowed me to examine DC populations in the SI during the early stages of inflammation, which I did 24 hours after surgery. The presence of inflammation was verified by a significant increase in both the proportion and number of $Ly6C^{hi}MHCII^{+}$ monocytes (P2) in mice having undergone surgery compared with resting controls (Fig. 5.6). There was also a trend towards increased proportions and numbers of $Ly6C^{hi}MHCII^{-}$ monocytes (P1) (Fig. 5.6).

Next I confirmed that as in DSS colitis, CD64 expression remained a valid means of distinguishing two populations assumed to be DCs and mϕs amongst total $CD11c^{+}MHCII^{+}$ MPs in POI (Fig. 5.7A), again functional analysis remains to be performed to further demonstrate this. Using the gating strategy I had developed in my earlier analysis, I found significant reductions in the proportions of both $CD103^{-}$ DC subsets in the SI LP of mice with POI compared with resting controls (Fig. 5.7B,C). However, these results did not translate into significant differences in the absolute number of any of the DC populations (Fig. 5.7D). Whether this procedure would have any effect on the DC populations at different time points remains to be determined.

5.4 Characterisation of DCs during *Citrobacter rodentium* infection

Having investigated the intestinal DC populations in two models of sterile inflammation, I next investigated these populations during infection with *C. rodentium.* This natural murine pathogen produces a self-limiting infection restricted to the caecum and colon and is used as a model of EPEC and EHEC *Escherichia coli* infection. Its resolution is associated with the generation of protective T_h17 cells (Geddes et al., 2011). WT mice were infected with *C.*

rodentium and the DC populations in the colonic LP were examined 9 days later. As the strain of *C. rodentium* used is bioluminescent, infection levels were monitored during this time using *in vivo* imaging (IVIS) in conjunction with faecal colony counts. These analyses confirmed that the mice were infected and revealed the peak of infection to be around day 6, with resolution already beginning by day 9 (Fig. 5.8A,B). Faecal counts were not taken on day 9, as time did not allow this to be done at the same time as isolating colonic LP. As these studies clearly demonstrated that the mice were infected, I did not examine for the presence of monocytes and other inflammatory cells in this model.

As with the other models of inflammation, I first confirmed that CD64 could be used to distinguish between DCs and mϕs, with DCs being identified as $CD64^-$ $CD11c^+MHCII^+$ (Fig. 5.9A). Further analysis revealed there to be a significant decrease in the proportion of total DCs amongst $CD11c^+MHCII^+$ MPs in *Citrobacter* infected mice, paralleled by a slight increase in the proportion of mϕs (Fig. 5.9A). The decrease in total DCs was associated with significant decreases in the proportions of $CD103^+CD11b^+$ and $CD103^+CD11b^-$ DCs, together with a significant increase in the proportion of $CD103^-CD11b^-$ DCs; the proportion of $CD103^-CD11b^+$ DCs was unaffected in infected mice (Fig. 5.9B,C). Despite the decreased proportions of the two $CD103^+$ DC populations in infected mice, there were no significant differences in their absolute numbers. In contrast, there were significant increases in the numbers of $CD103^-CD11b^+$ and $CD103^-CD11b^-$ DCs (Fig. 5.9D). These discrepancies between the proportions and absolute numbers can be reconciled by the overall increase in the absolute number of DCs, which overcame the effects of the proportional decreases in individual subsets (Fig. 5.9E).

5.5 Summary

Having previously characterised intestinal DC populations in the steady state intestine, in this chapter I set out to examine these populations during non-steady state conditions, specifically in two models of sterile inflammation, DSS colitis and post-operative ileus, and during infection with a natural pathogen *C. rodentium*.

Administration of 2% DSS for four days resulted in an increase in the overall cellularity of the colonic LP, mostly due to inflammatory monocytes as reported

previously (Bain et al., 2013). Importantly, during disease it remained possible to distinguish between DCs and mϕs amongst total $CD11c^{+}MHCII^{+}$ intestinal MPs using CD64 expression and thus I was able to examine the four DC populations using the gating strategy I had developed in the steady state. Analysis of the four DC populations on the basis of CD103 and CD11b expression revealed all four populations to be present during disease. Overall, I found the increased cellularity in the colonic LP to translate into an increase in the absolute number of all DC subsets. However, in terms of proportion, I observed a decrease in $CD103^{+}CD11b^{+}$ DCs with a parallel increase in the proportion of $CD103^{+}CD11b^{-}$ DCs. Despite previous studies suggesting the $CD103^{-}$ MPs to be specifically involved in inflammation (Siddiqui et al., 2010), I did not observe any selective changes in the $CD103^{-}$ DC populations.

It has been suggested that $Ly6C^{hi}$ monocytes have the potential to differentiate into 'inflammatory $CD103^{-}$ DCs' during conditions of inflammation (Bogunovic et al., 2009; Rivollier et al., 2012; Varol et al., 2009). While previous studies in the lab have shown that $Ly6C^{hi}$ monocytes remain faithful to the monocyte/mϕ lineage during DSS (Bain et al., 2013), I thought it important to verify that pre-DCs continue to generate all four DC populations under these conditions. By altering the concentration of DSS, I was able to administer it for 8 continuous days thereby allowing me to assess the differentiation of pre-DCs in the inflamed setting. Analysis of CD103 and CD11b expression by donor cells and their progeny revealed that the pre-DCs remained capable of generating all DC populations seen in the steady state. Overall the pre-DCs seemed to generate fewer $CD103^{+}CD11b^{-}$ DCs and more $CD103^{+}CD11b^{+}$ DCs compared with the endogenous populations, which could suggest differences in *in situ* proliferation or migration of these subsets during DSS colitis. However this remains to be investigated.

Induction of post-operative ileus resulted in inflammation in the small intestinal LP, consisting mainly of $Ly6C^{hi}MHCII^{+}$ monocytes, suggesting that the immediate infiltration of $Ly6C^{hi}MHCII^{-}$ monocytes (P1) had already ceased by the time I looked at 24 hours. Again CD64 expression distinguished clearly between DCs and mϕs in this inflammatory model, revealing that all four DC populations were present in the SI LP 24 hours after induction POI. However, no major changes were observed in the absolute numbers of the four DC populations,

although there was a slight reduction in the proportions of both $CD103^-$ DC subsets, while the proportions of the $CD103^+$ subsets were unaffected.

Finally, having investigated the DC populations during sterile inflammation, I next sought to examine whether the DC populations were altered during infection with a natural pathogen. The infection was monitored using bioluminescence and IVIS in conjunction with faecal colony counts and I examined the DC populations in the colonic LP just after infection had begun to resolve. In this model, there were increases in the absolute numbers of $CD103^-CD11b^+$ and $CD103^-CD11b^-$ DCs, while the numbers of the two $CD103^+$ DC populations were not significantly altered. Despite no overall change in their absolute numbers, these $CD103^+$ DC populations were both significantly reduced in terms of proportion in the *C. rodentium* infected mice. In parallel there was an increase in the proportion of $CD103^-CD11b^-$ DCs, while the proportion of $CD103^-CD11b^+$ DCs was unaffected.

Together these results show that the populations of *bona fide* DCs change in terms of both frequency and number during intestinal inflammation and infection. However the exact pattern of DC behaviour varies dependent on the model, perhaps reflecting the nature of the inflammatory stimulus, as well as the anatomical location of each DC populations and their specific roles in the immune response. Thus in the next chapter I set out to examine the specific functions of each intestinal DC subset, by examining their ability to drive T cell responses both *in vitro* and *in vivo*.

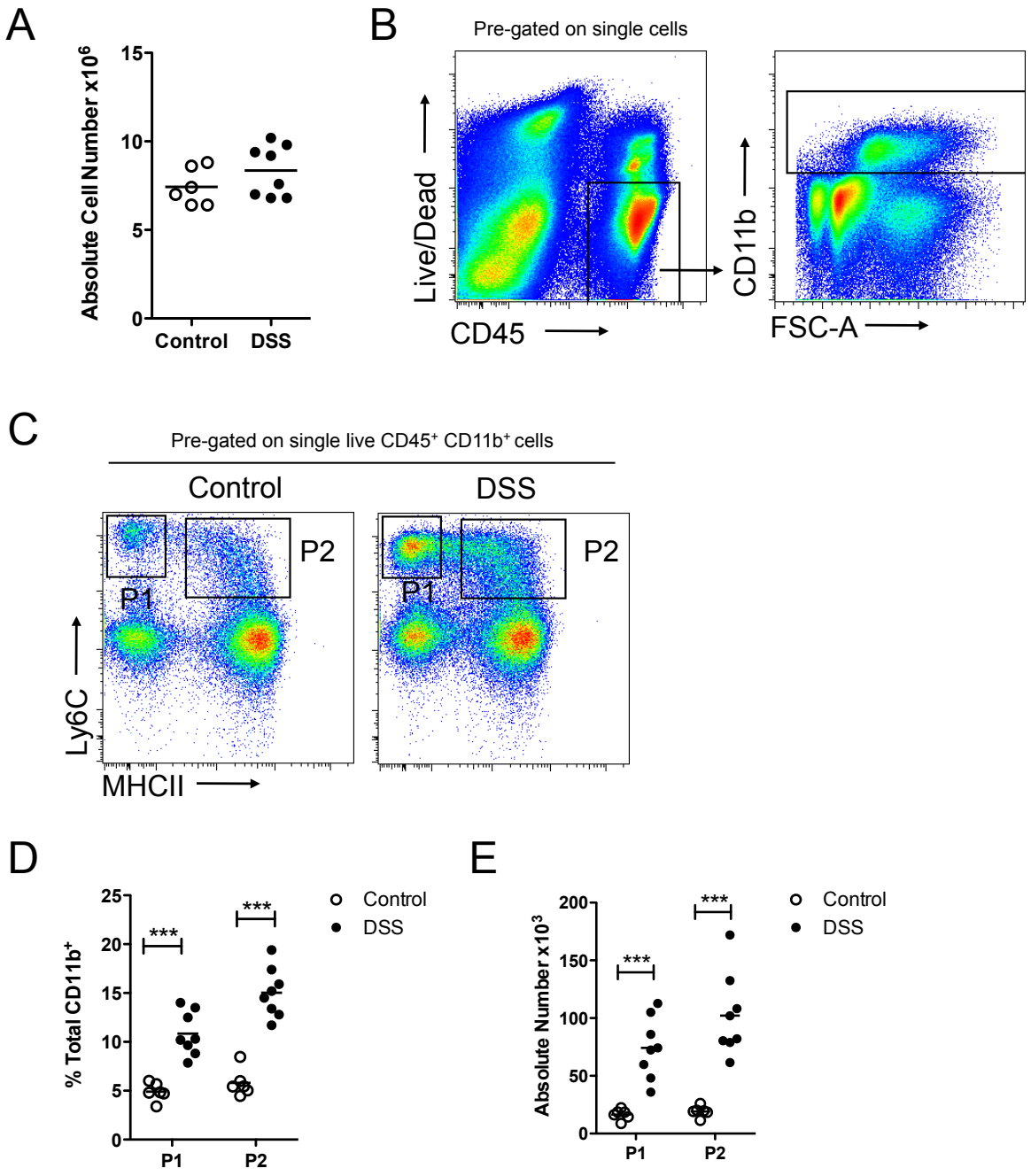

Figure 5.1: Induction of colitis by feeding 2% DSS

Mice received 2% DSS *ad libitum* in the drinking water for four days or normal water as a control and inflammation was assessed by enumerating monocytes in the colonic LP. **A.** Scatter plots show total cellularity in colonic LP of mice receiving DSS compared with controls. **B.** Representative dot plots showing identification of $CD11b^+$ myeloid cells amongst single live $CD45^+$ cells. **C.** Representative dot plots showing Ly6C and MHCII staining on $CD11b^+$ live leukocytes in the colonic LP of mice receiving DSS compared with controls. **D.** Scatter plot shows proportions of P1 ($Ly6C^{hi}MHCII^-$ monocytes) and P2 ($Ly6C^{hi}MHCII^+$ monocytes) as a percentage of $CD11b^+$ cells in mice receiving DSS compared with controls. **D.** Scatter plot shows absolute cell number of P1 and P2 in mice receiving DSS compared with controls. Data are representative of 2-3 independent experiments with n=4-8 per group per experiment. ***p<0.001 Student's t test.

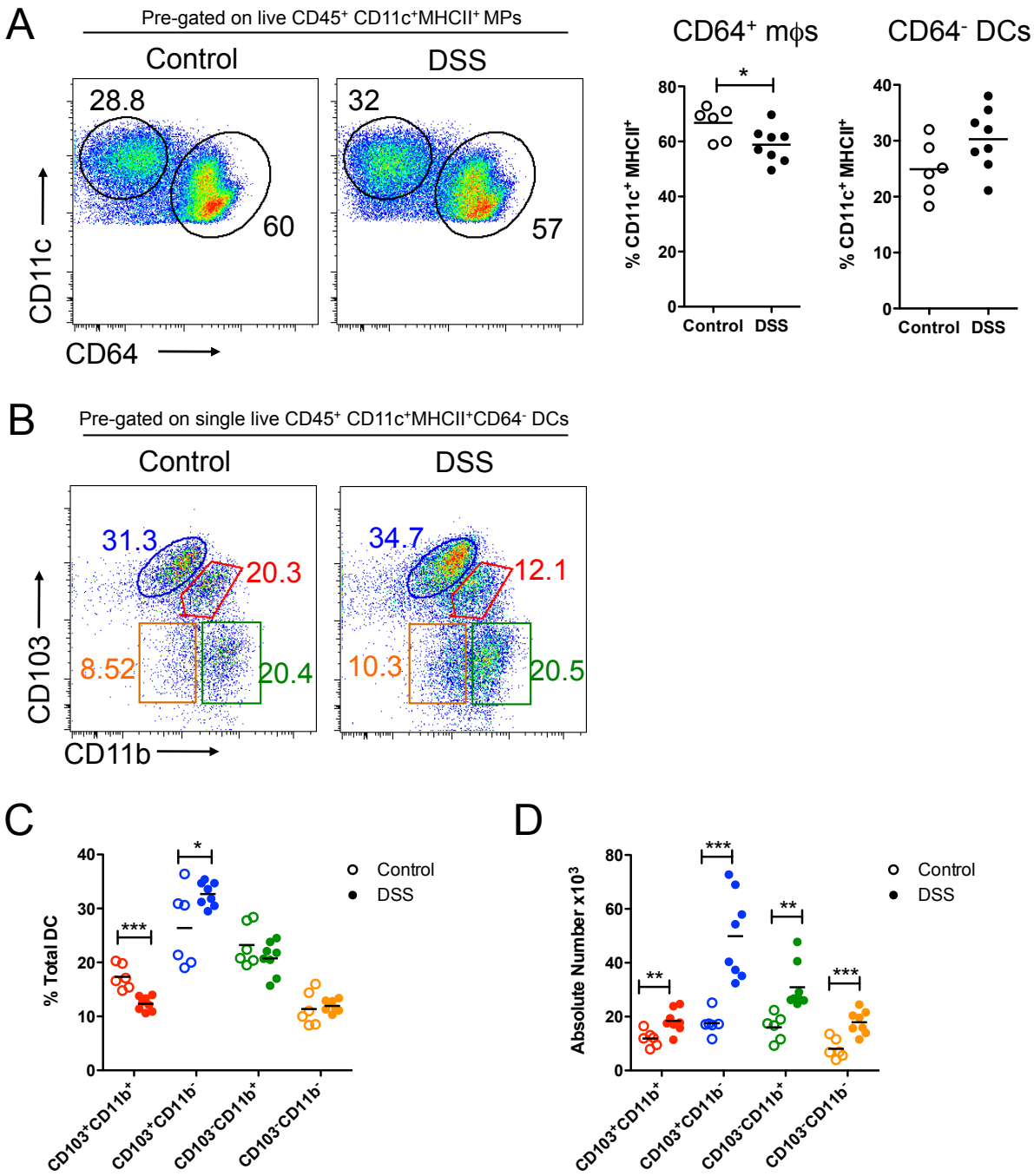

Figure 5.2: DC populations in the colonic LP following administration of DSS

Mice received 2% DSS *ad libitum* in the drinking water for four days or normal water as a control and DC populations in the colonic LP were assessed. **A.** Representative dot plots showing CD11c and CD64 expression on total CD11c$^+$MHCII$^+$ MPs in mice receiving DSS compared with controls. Scatter plots show proportion of CD64$^+$ mϕs and CD64$^-$ DCs as a percentage of total CD11c$^+$ MHCII$^+$ MPs. **B.** Representative dot plots showing CD103 and CD11b expression on total CD11c$^+$ MHCII$^+$CD64$^-$ DCs in the colonic LP of mice receiving DSS compared with controls. **C.** Scatter plot shows proportions of each DC population as a percentage of total DCs in mice receiving DSS compared with controls. **D.** Scatter plot shows absolute cell number of each DC population in mice receiving DSS compared with controls. Data are representative of 2-3 independent experiments with n=4-8 per group per experiment. *p<0.05, **p<0.01, ***p<0.001 Student's t test.

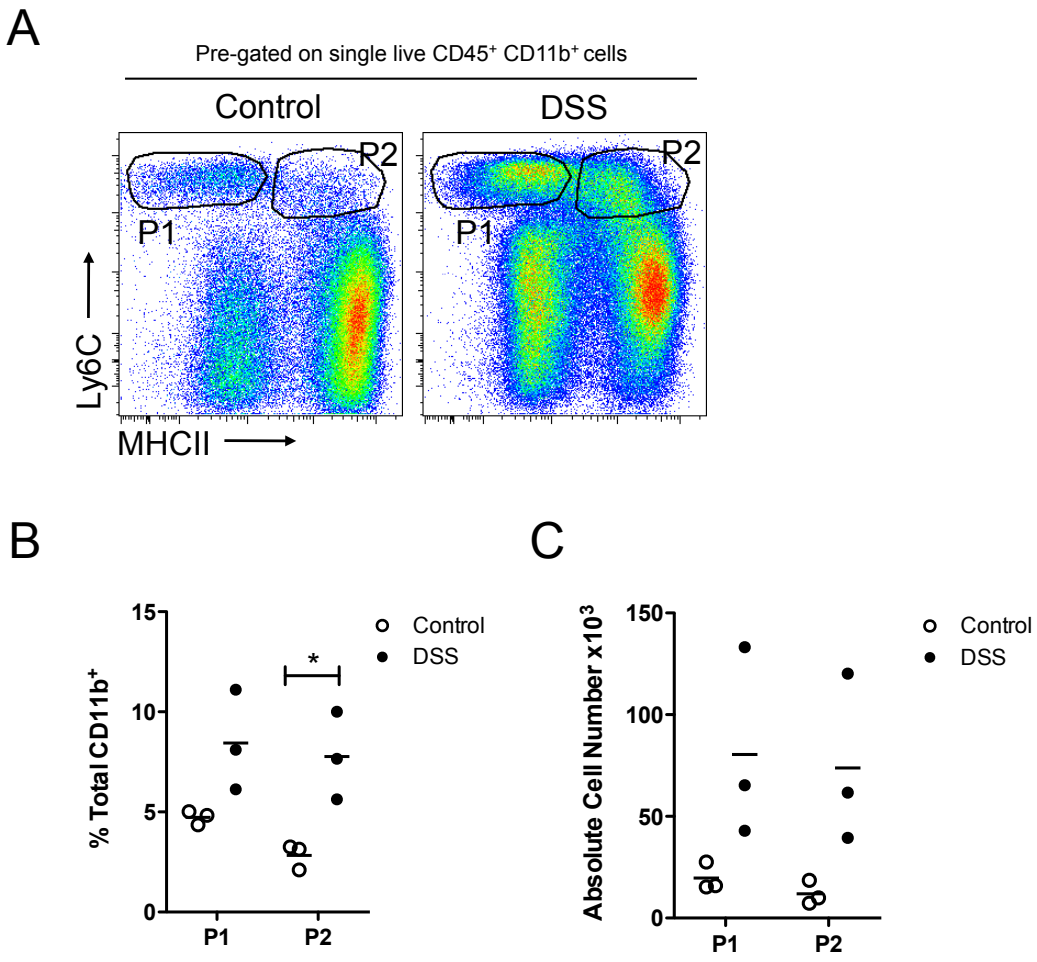

Figure 5.3: Induction of colitis by administration of 1.2% DSS

Mice received 1.2% DSS *ad libitum* in the drinking water for three days or normal water as a control and inflammation was assessed by enumerating monocytes in the colonic LP. **A.** Representative dot plots showing Ly6C and MHCII staining on CD11b$^+$ live leukocytes in the colonic LP of mice receiving DSS compared with controls. **B.** Scatter plot shows proportions of P1 (Ly6C^{hi}MHCII$^-$ monocytes) and P2 (Ly6C^{hi}MHCII$^+$ monocytes) as a percentage of CD11b$^+$ cells in mice receiving DSS compared with controls. **C.** Scatter plot shows absolute cell number of P1 and P2 in mice receiving DSS compared with controls. Data are from a single experiment with n=3 per group. *p<0.05 Student's t test.

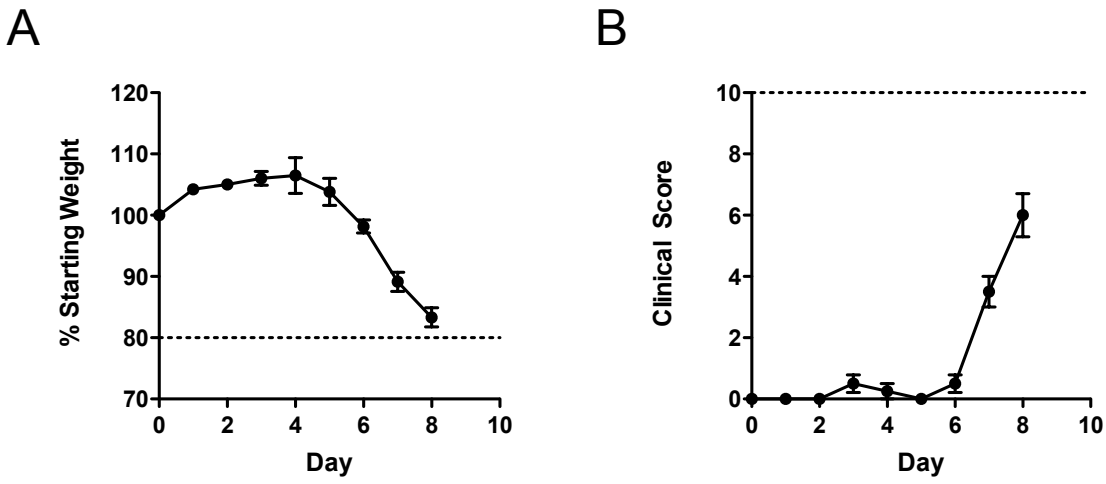

Figure 5.4: Induction of clinical disease by administration of 1.2% DSS

Mice received 1.2% DSS *ad libitum* in the drinking water for eight days and disease was assessed. **A.** Weight loss as a percentage of original starting weight in mice receiving DSS. **B.** Clinical scores of mice receiving DSS. Dashed lines represent UK Home Office prescribed limits. Data are from a single experiment with n=3.

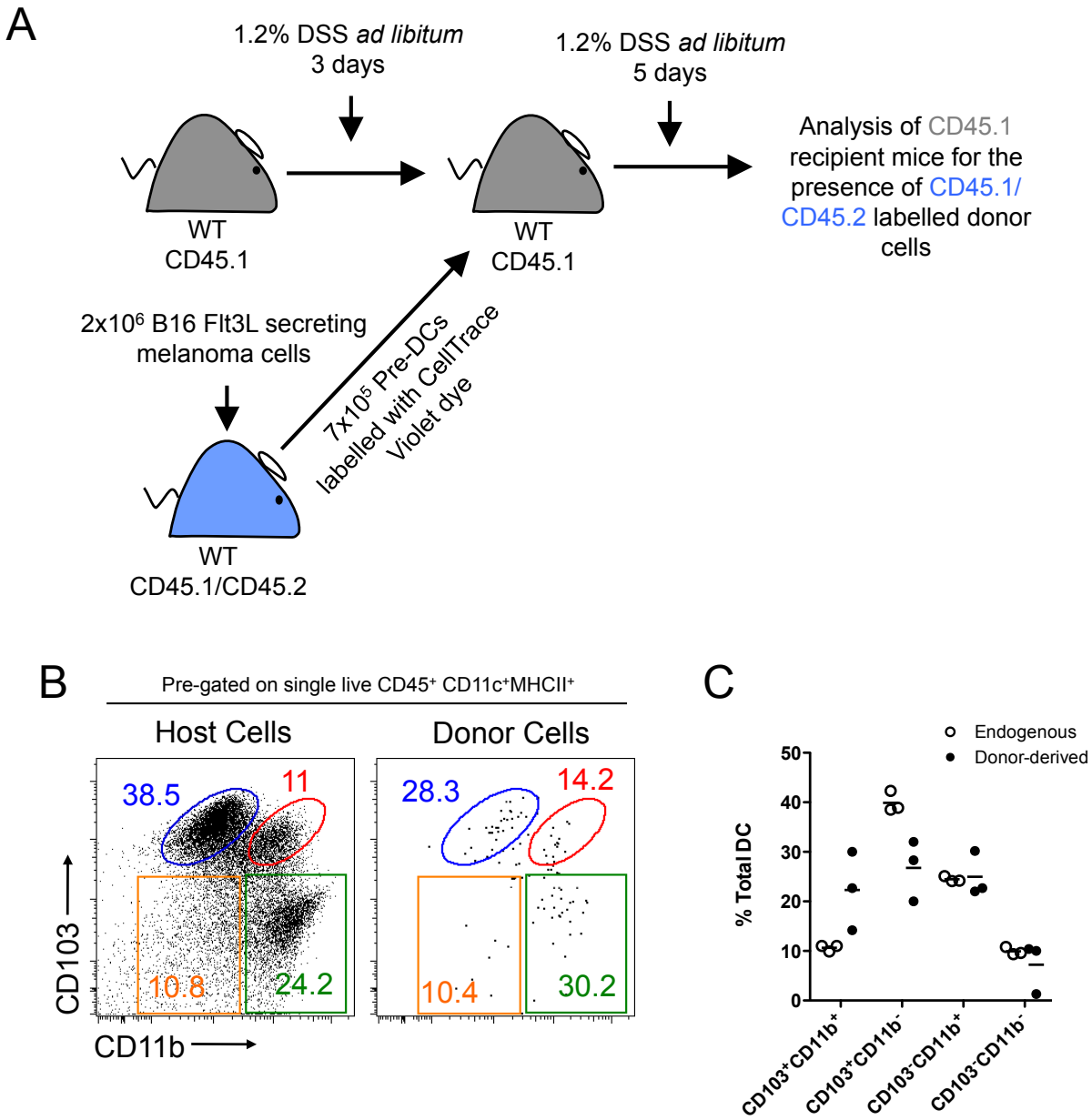

Figure 5.5: Fate of pre-DCs in the colonic LP of mice with DSS colitis

A. CD45.1⁺ mice received 1.2% DSS *ad libitum* in the drinking water for 8 days. On day 3 of DSS administration, mice received 7x10^5 pre-DCs i.v., FACS-purified from the BM of Flt3L treated CD45.1/CD45.2⁺ WT mice. 5 days after transfer, CD45.2⁺violet⁺CD11c⁺MHCII⁺ donor-derived DCs in the colonic LP were assessed for CD103 and CD11b expression. **B.** Representative dot plots showing CD103 and CD11b staining on CD11c⁺MHCII⁺ live leukocytes in the colonic LP amongst donor-derived CD45.2⁺violet⁺ cells compared with host CD11c⁺MHCII⁺F4/80⁻ cells. **C.** Scatter plot shows proportion of each DC population as a percentage of total donor-derived or host DCs. Data are from a single experiment with 3 recipients.

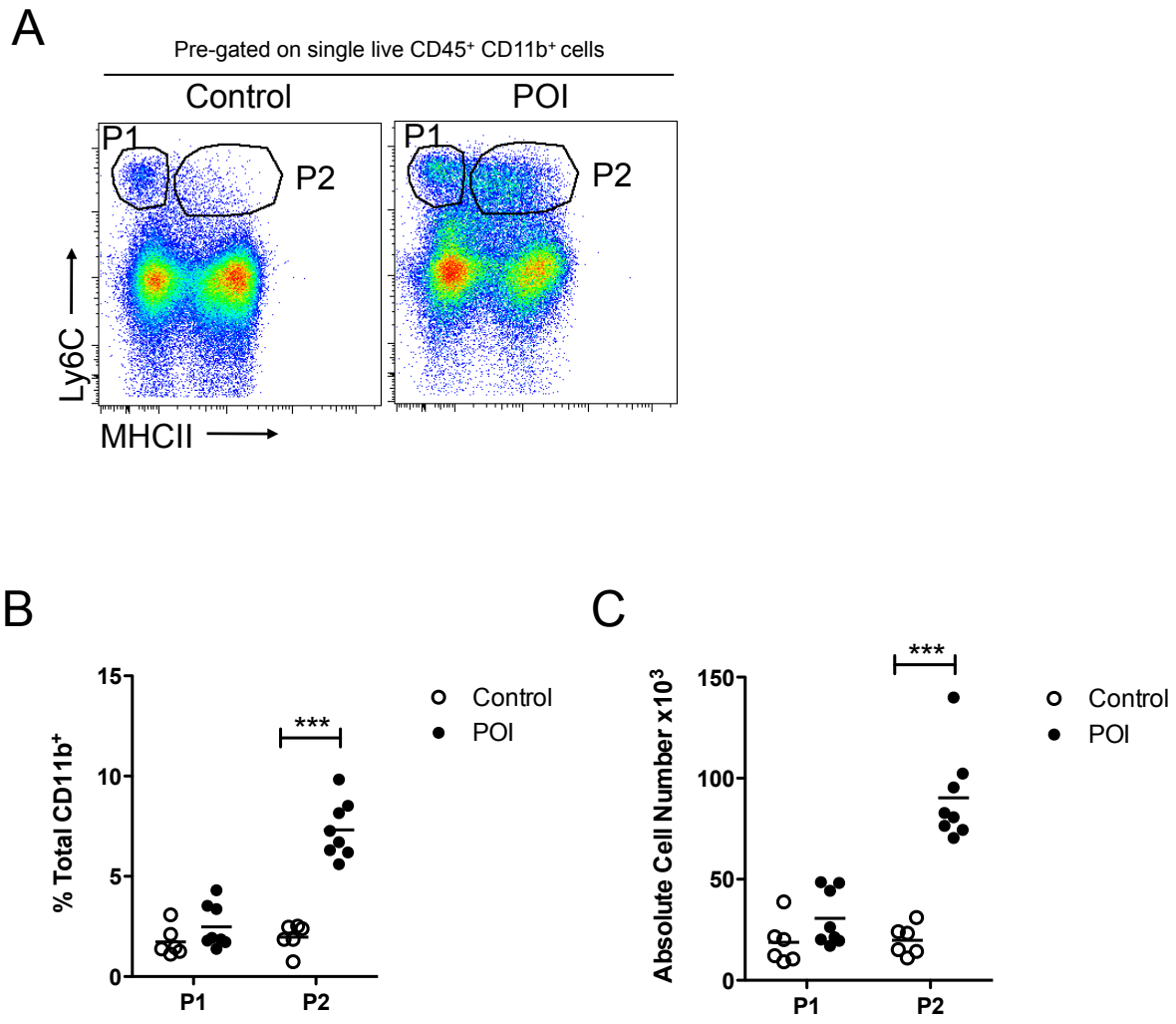

Figure 5.6: Inflammation induced by post-operative ileus

POI was induced by exposing intestines by laparotomy and rubbing the length of the SI with a cotton bud. Control animals were not subjected to surgery. 24 hours later inflammatory infiltrates in the SI LP was characterised by flow cytometry. **A.** Representative dot plots showing Ly6C and MHCII staining on $CD11b^+$ live leukocytes in the colonic LP of mice with POI compared with controls. **B.** Scatter plot shows proportions of P1 ($Ly6C^{hi}MHCII^-$ monocytes) and P2 ($Ly6C^{hi}MHCII^+$ monocytes) as a percentage of $CD11b^+$ cells in mice with POI compared with controls. **C.** Scatter plot shows absolute cell number of P1 and P2 in mice with POI compared with controls. Data are from a single experiment with n=6-8 per group per experiment. ***p<0.001 Student's t test.

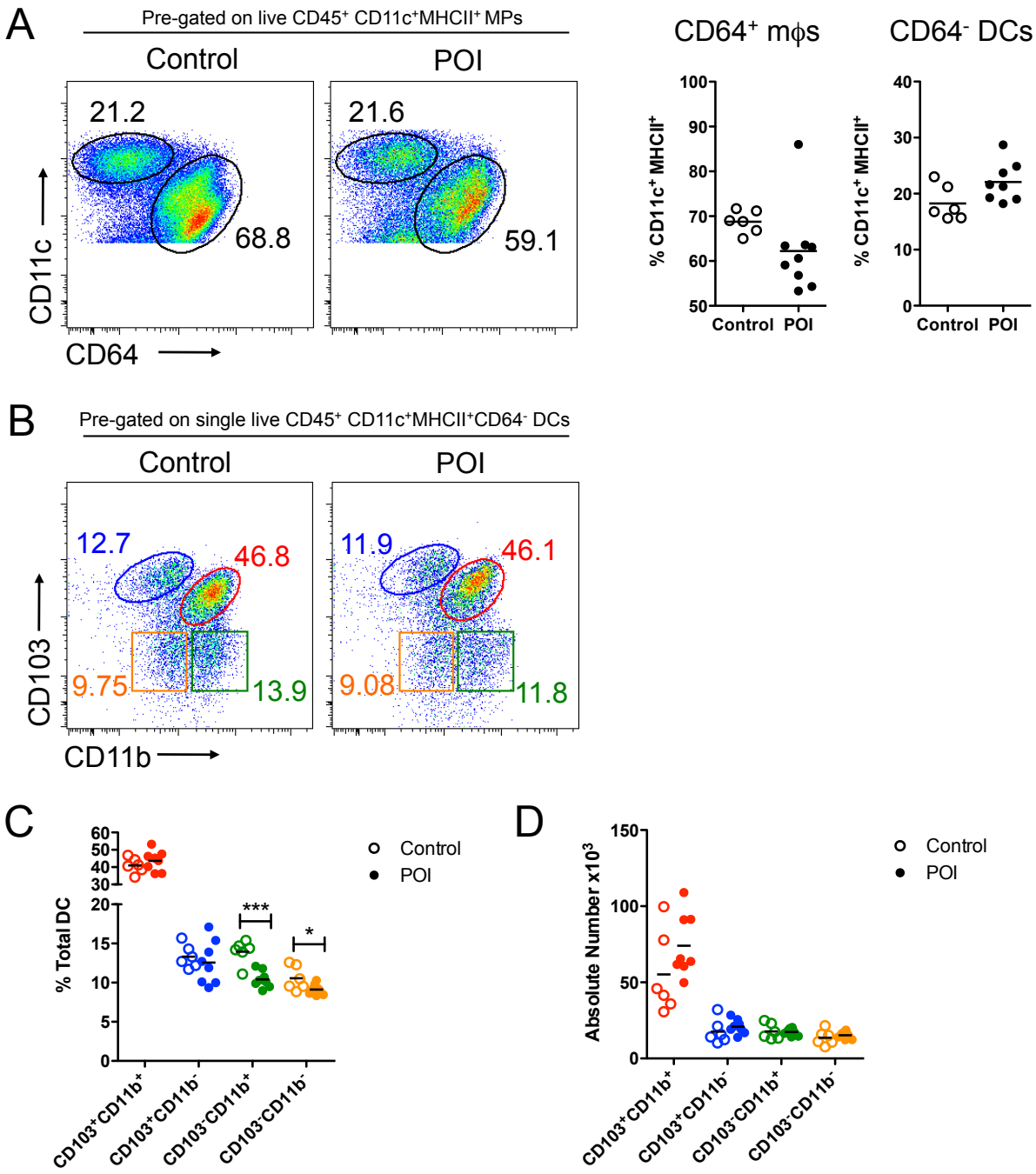

Figure 5.7: DC populations in colonic LP during post operative ileus

POI was induced by exposing intestines by laparotomy and rubbing the length of the SI with a cotton bud. Controls animals were not subjected to surgery. 24 hours later DC populations in the SI LP were characterised by flow cytometry. **A.** Representative dot plots showing CD11c and CD64 expression on total CD11c$^+$MHCII$^+$ MPs in the SI LP of mice with POI compared with controls. Scatter plots show proportion of CD64$^+$ mϕs and CD64$^-$ DCs as a percentage of total CD11c$^+$MHCII$^+$ MPs. **B.** Representative dot plots showing CD103 and CD11b expression on total CD11c$^+$ MHCII$^+$CD64$^-$ DCs in the SI LP of mice with POI compared with controls. **C.** Scatter plot shows proportions of each DC population as a percentage of total DCs in mice with POI compared with controls. **D.** Scatter plot shows absolute cell number of each DC population in mice with POI compared with controls. Data are from a single experiment with n=6-8. *p<0.05, ***p<0.001 Student's t test.

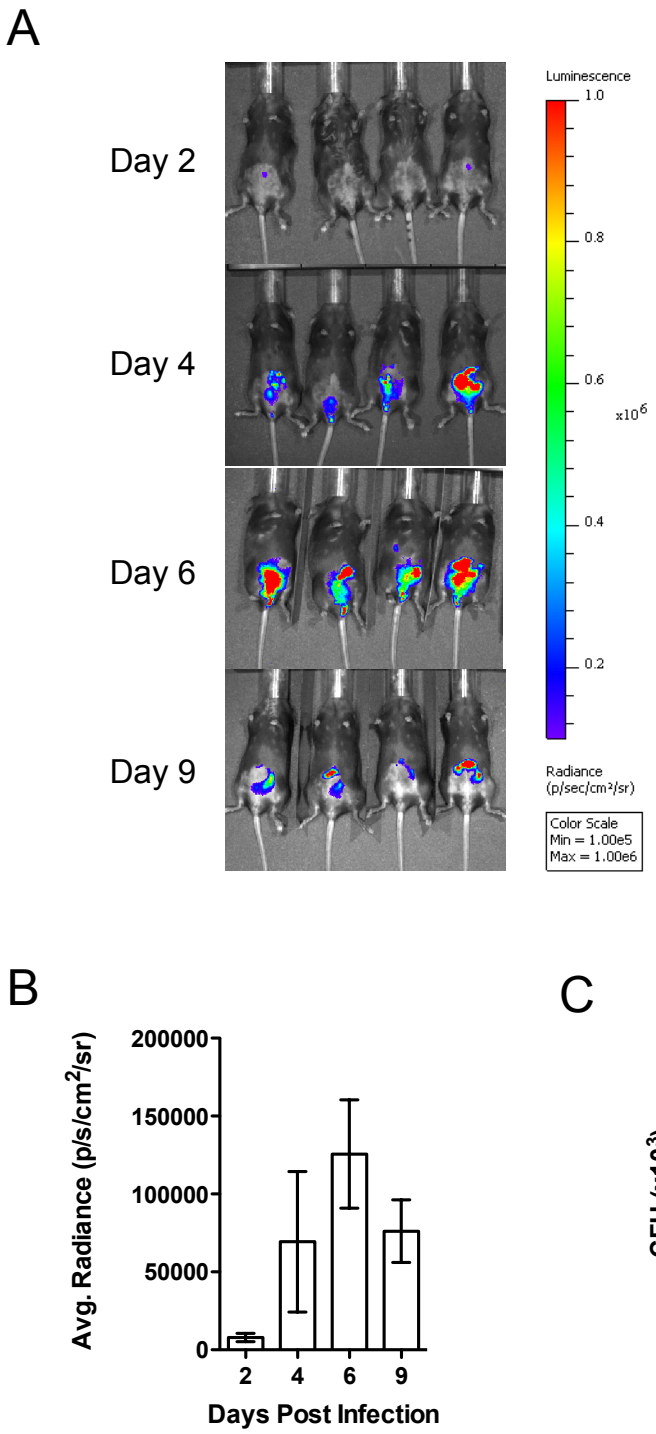

Figure 5.8: Infection with *Citrobacter rodentium*

Mice were gavaged with 1x10^9 *Citrobacter rodentium* organisms and infection levels were monitored over a 9 day period. **A.** Infected mice were anaesthetised and the bioluminescence activity of the *C. rodentium* was assessed by IVIS on day 2, 4, 6 and 9 of infection. Representative images from one group of infected mice. **B.** Bar chart shows average radiance in photons/ second/cm^2 in infected mice as measured by IVIS on days 2, 4, 6 and 9 post infection. **C.** Bar chart shows CFU per gram of faeces on days 2, 4 and 6 post infection with *C. rodentium* as measured by bacterial growth on erythromycin supplemented LB agar plates. Data are from a single experiment with n=6-10 per group.

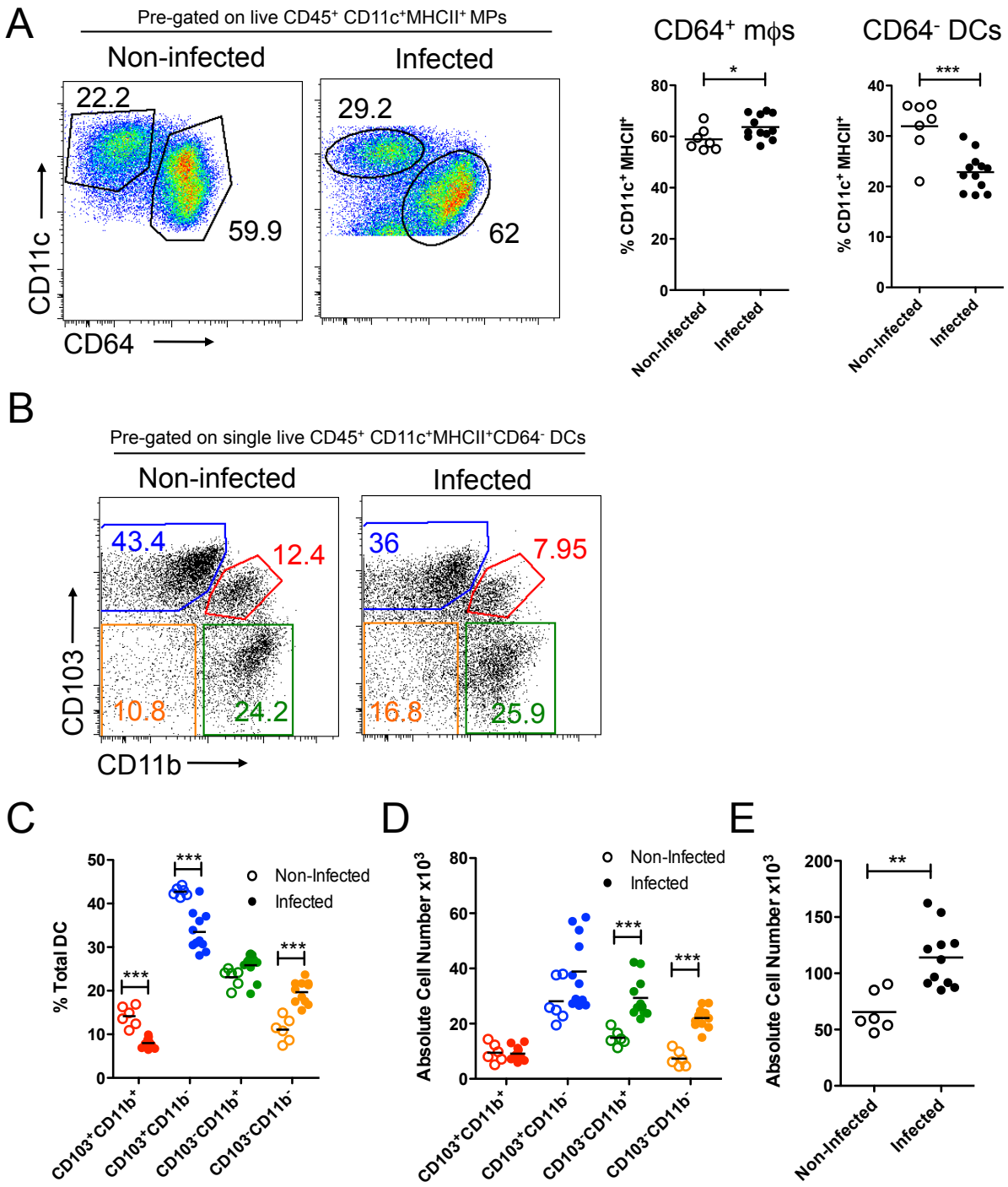

Figure 5.9: DC populations in colonic LP during *Citrobacter rodentium* infection

Mice were gavaged with 1x10^9 *C. rodentium* and colonic LP DC populations were examined on day 9 of infection by flow cytometry. **A.** Representative dot plots showing CD11c and CD64 expression on total CD11c$^+$MHCII$^+$ MPs in the colonic LP of infected mice compared with controls. Scatter plots show the proportions of CD64$^+$ mϕs and CD64$^-$ DCs as percentages of total CD11c$^+$MHCII$^+$ MPs. **B.** Representative dot plots showing CD103 and CD11b expression on total CD11c$^+$MHCII$^+$CD64$^-$ DCs in the colonic LP of infected mice compared with controls. **C.** Scatter plot shows proportions of each DC population as a percentage of total DCs in infected mice compared with controls. **D.** Scatter plot shows absolute cell number of each DC population in infected mice compared with controls. Data are from a single experiment with n=6-10. *p<0.05, **p<0.01, ***p<0.001, Student's t test.

Chapter 6 Functions of Intestinal Dendritic Cells

6.1 Introduction

Having established that there are four distinct subsets of CD64$^-$ intestinal dendritic cells and that their proportions change during inflammation and infection, I next wanted to investigate their specific roles in the induction of adaptive immune responses. Although previous studies have shown distinct functions for the two subsets of CD103$^+$ DCs (Denning et al., 2011; Fujimoto et al., 2011; Uematsu et al., 2008), the novel CD103$^-$ DCs I identified in Chapter 3 have usually been included with mϕs for functional analyses and thus their roles in initiating adaptive immunity remain uncertain. Now able to accurately distinguish CD103$^-$ DCs from mϕs, in this chapter I set out to examine the specific functions of each DC subset.

6.2 Co-stimulatory Molecule Expression

I first used flow cytometry to assess expression of the co-stimulatory molecules CD80 and CD86 on the four intestinal DC subsets. This revealed that none of the DCs expressed CD80 (Fig. 6.1A), while all DCs expressed CD86 at low levels and this was slightly higher on CD103$^+$CD11b$^-$ DCs (Fig. 6.1B,C). The exact relevance of these findings is unclear but it is interesting to note that in lymph all DC subsets express CD80 and CD86, with the CD103$^+$CD11b$^-$ DCs expressing slightly elevated levels compared with the other DC subsets (Cerovic et al., 2013).

6.3 SI LP DCs are Functional Antigen Presenting Cells

As the ability to present antigen to naïve T cells is a defining characteristic of DCs, I first determined if all four intestinal DC populations I had identified were functional antigen presenting cells (APCs). To this end, DCs were FACS-purified from the SI LP, pulsed with 2mg/ml ovalbumin protein and co-cultured with naïve OVA-specific TcR transgenic CD4$^+$ (OTII) or CD8$^+$ (OTI) T cells. Ovalbumin protein was used in these studies rather than peptide to ensure the DCs were able to both take up and process the antigen, as well as present it to T cells.

6.3.1 Antigen Presentation to $CD4^+$ T Cells

Naïve $CD4^+$ T cells were FACS-purified from pooled LNs from OTII transgenic mice as live $CD4^+$ $CD62L^+$ $CD25^-$ cells (Fig. 6.2). To assess T cell proliferation, they were labelled with CFSE and cultured with FACS-purified antigen-loaded DCs. To determine how efficient each SI LP DC subset was at antigen presentation, co-cultures were set up at a number of DC:T cell ratios ranging from 1:2 to 1:80. At a ratio of 1:2, all DC subsets were able to induce the proliferation of naïve $CD4^+$ T cells equally. As expected, the amount of proliferation decreased progressively with decreasing DC to T cell ratios and this occurred with all the DC subsets (Fig. 6.3). However as the numbers of DCs were decreased, the $CD103^+CD11b^-$ and $CD103^-CD11b^+$ DC subsets appeared to be slightly less efficient than the other subsets (Fig. 6.3).

6.3.2 Cross-presentation to $CD8^+$ T Cells

I next investigated the ability of the DC subsets to cross-present antigen to naïve $CD8^+$ T cells. When high numbers of DCs were used, all four DC subsets were able to induce $CD8^+$ T cell proliferation as assessed by CFSE dilution (Fig. 6.4A,B). However, when the number of DCs in the co-cultures was titrated down, the $CD103^+CD11b^-$ DCs were clearly the most efficient at cross-presenting antigen (Fig. 6.4A,B). In addition only these DCs were able to induce IFNγ production by $CD8^+$ T cells as assessed by cytokine bead array (CBA) analysis of the co-culture supernatants. Recently XCR1 expression has been suggested to identify cross-presenting DCs in different species (Bachem et al., 2010; 2012; Crozat et al., 2011) and in agreement with both these studies and my findings from the co-cultures, only the $CD103^+CD11b^-$ DCs from SI LP expressed XCR1 (Fig. 6.4D).

6.4 $CD4^+$ T Cell Polarisation

These findings confirmed that all the DC subsets I had identified in the SI LP could act as APCs and I next examined their ability to induce functional polarisation of the proliferating $CD4^+$ T cells. First I attempted to gain some idea of how this might be operating *in situ*, by examining the nature of the $CD4^+$ T cells present in the steady state LP, by assessing the intracellular expression of FoxP3, IL17 and IFNγ. $CD4^+$ T cells were identified amongst whole SI LP digests as live

$CD45^+$ $CD3^+$ $CD4^+$ single cells (Fig. 6.5A). Analysis of IL17, FoxP3 and IFNγ expression revealed the majority of $CD4^+$ T cells in the SI LP to be either $IL17a^+$ T_h17 or $FoxP3^+$ T_{Reg} cells, with a smaller population of $IFN\gamma^+$ T_h1 cells (Fig. 6.5B,C).

6.4.1 Induction of FoxP3 Expression in Naïve $CD4^+$ T Cells by LP DC Subsets

I next examined the ability of the DC subsets to induce the polarisation of these phenotypes from naïve $CD4^+$ T cells *in vivo*. Although all subsets were able to induce FoxP3 expression by a proportion of proliferating T cells as assessed by intracellular staining, the two subsets of $CD103^+$ DCs were generally more effective at this than the other subsets. However, although this pattern was seen in repeat experiments, the differences were not statistically significant when the data were pooled (Fig. 6.6A,B). To try to assess the mechanisms that might be used by the DC subsets, I examined the expression of factors implicated in the generation of T_{Reg} cells by DCs, including the production of TGFβ (Coombes et al., 2007; Sun et al., 2007; Worthington et al., 2011), the expression of the TGFβ activating integrin αvβ8 (Travis et al., 2007) and the production of retinoic acid (Elias et al., 2008; Mucida et al., 2007). All four DC populations expressed equal levels of mRNA for TGFβ, but only the $CD103^+CD11b^-$ DCs expressed mRNA for the β8 integrin (Fig. 6.6C,D). Using the commercially available ALDEFLUOR assay to examine the DC subsets aldehyde dehydrogenase (ALDH) activity, I found that the two $CD103^+$ DC subsets and $CD103^-CD11b^+$ DCs had high levels of ALDEFLUOR activity, while the $CD103^-CD11b^-$ showed little expression of ALDEFLUOR (Fig. 6.7). Interestingly, the $CD103^+CD11b^-$ DCs had significantly higher ALDEFLUOR activity than the other subsets. Together with their unique expression of the β8 integrin, this result may explain the trend towards these DC being particularly efficient at driving the generation of $FoxP3^+$ T_{Reg} cells

6.4.2 Induction of IL17 Expression by Naïve $CD4^+$ T Cells by LP DC Subsets

I next examined the ability of the FACS-purified DC populations to induce IL17a production by proliferating $CD4^+$ T cells. In contrast to their ability to induce $FoxP3^+$ T_{Reg} cells, the $CD103^+CD11b^-$ DCs failed to induce IL17 production from

the T cells, whereas the other three populations could all induce T_h17 priming, with the $CD103^-CD11b^+$ population appearing more effective than the others, including $CD103^+CD11b^+$ DCs (Fig. 6.8A,B). I next assessed the production of the T_h17 polarising cytokines, IL6, IL1β and IL23p19, by the DC subsets. All subsets except for the $CD103^+CD11b^-$ DCs expressed similar levels of IL1β mRNA, paralleling their relative abilities to drive T_h17 cell differentiation (Fig. 6.8C). Analysis of IL6 mRNA expression suggested that there was a trend towards increased expression by the $CD103^-$ DC subsets compared with the $CD103^+$ DCs (Fig. 6.8D), although these differences need to be confirmed by further experiments. I was unable to detect IL23p19 mRNA in any of the DC subsets sorted from steady state WT mice.

6.4.3 Induction of IFNγ Expression by Naïve $CD4^+$ T Cells by LP DC Subsets

I next investigated the generation of T_h1 cells. While the $CD103^+CD11b^-$, $CD103^-CD11b^+$ and $CD103^-CD11b^-$ DCs could all drive IFNγ production in proliferating $CD4^+$ T cells, the $CD103^+CD11b^+$ DCs did not induce any IFNγ production (Fig. 6.9). IL12 is the main cytokine thought to be involved in the differentiation of T_H1 cells, however I was unable to detect any mRNA for IL12p35 or IL12p40 in any of the SI LP DCs when FACS-purified from the steady state gut.

6.5 Intestinal DCs are Non-phagocytic

I next investigated the phagocytic potential of the individual intestinal DC subsets and compared this with $CD64^+$ mϕ as a positive control. Total cells isolated from SI LP digests were incubated with pHrodo *E. coli* bioparticles which fluoresce when taken into acidified vesicles, allowing phagocytosis to be assessed by flow cytometry. As shown in Figure 6.10 and consistent with their definition as DCs (Steinman, 1973), all four DC populations were poorly phagocytic compared with the $CD64^+$ mϕs.

6.6 TLR Expression by Intestinal DC Subsets

To further investigate functional differences between the four intestinal DC populations, I next examined if they might respond differently to distinct microbial signals, by exploring their expression of different TLRs. Although most subsets

expressed mRNA for most TLRs, there were some differences in the expression levels of the individual TLRs (Fig. 6.11). For instance, the $CD103^-CD11b^+$ DCs expressed 2-fold less TLR2 compared with the $CD103^+CD11b^+$ DCs and ~10-fold lower TLR2 than the $CD103^+CD11b^-$ DCs. The inverse pattern was observed for TLR3, where the $CD103^-CD11b^+$ DCs expressed the lowest levels, while the $CD103^+CD11b^-$ DCs expressed ~50-fold more mRNA for TLR3 compared with the $CD103^+CD11b^+$ and $CD103^-CD11b^-$ DCs. TLR4 mRNA was expressed by all DC subsets, but was lowest in $CD103^+CD11b^+$ DCs. TLR5 was expressed at the highest levels by the $CD103^-CD11b^-$ DCs, which were ~5-fold higher than those seen in $CD103^+CD11b^+$ and $CD103^-CD11b^+$ DCs; the $CD103^+CD11b^-$ DCs expressed very little mRNA for TLR5. $CD103^+CD11b^+$ DCs were the main DC population found to express mRNA for TLR6, at levels ~5-fold higher than the $CD103^+CD11b^-$ and $CD103^-CD11b^+$ DCs, and no mRNA for TLR6 was detected in the $CD103^-CD11b^-$ DCs. Consistent with a report that was published during my PhD (Fujimoto et al., 2011), the $CD103^+CD11b^-$ DCs expressed higher levels of TLR7 and TLR9 than the $CD103^+CD11b^+$ DCs. Interestingly however, the $CD103^-$ DC populations, which had not been investigated previously, both expressed similar levels of mRNA for TLR7 to the $CD103^+CD11b^-$ DCs, and equivalent levels of TLR9 mRNA to the $CD103^+CD11b^+$ DCs. Finally, TLR1 mRNA expression was comparable amongst all the DC populations (Fig. 6.11).

6.7 Effects of Antibiotic Treatment on SI LP T Cells

To further explore the potential of the DC subsets to react to microbial stimuli, I next examined how the antibiotic regime that had increased the number of $CD103^+CD11b^+$ DCs in Chapter 4 might affect the populations of $CD4^+$ T cells in steady state mucosa. Mice receiving the antibiotic cocktail for 2 weeks showed a significant reduction in the proportion and number of T_h17 cells in the SI LP, but this had no effect on the T_{Reg} cell population (Fig. 6.12). Due to antibody constraints at the time of this experiment, I was unable to examine T_h1 cells on this occasion, but these will be examined in the future.

6.8 Summary

In this chapter, I set out to investigate the functions of each of the DC subsets in the initiation of adaptive immunity. First I found that all the subsets

expressed the CD86 co-stimulatory molecule, although this was highest on $CD103^+CD11b^-$ DCs. In contrast, none of the DCs were found to express CD80. This is in contrast with DCs in intestinal lymph, suggesting that acquisition of CD80 may correlate with their decision to migrate to the MLN. However all DC subsets were capable of functioning as APCs, priming and cross-priming proliferation by CD4 and CD8 T cells respectively, especially when high numbers of DCs were used. Although all DCs were able to induce $CD4^+$ T cell proliferation to similar extents, the $CD103^+CD11b^-$ DCs excelled at cross-presentation to $CD8^+$ T cells, a finding that correlated with their expression of XCR1.

As T_{Reg}, T_h17 and to a lesser extent, T_h1 cells were all present in steady state LP, I examined the ability of each SI LP DC subset to drive the differentiation of these populations from naïve $CD4^+$ T cells *in vitro*. The $CD103^+CD11b^-$ DCs were the most efficient at inducing T_{Reg} cell differentiation and this was associated with enhanced ALDEFLUOR activity and unique expression of the TGFβ activating β8 integrin. These DCs also were the main inducers of T_h1 cells, although the two $CD103^-$ DC populations were also capable of inducing some IFNγ production from $CD4^+$ T cells. In contrast, the $CD103^+CD11b^-$ DCs did not induce IL17a production, which was found to be particularly a property of $CD103^-CD11b^+$ DCs. $CD103^+CD11b^+$ DCs also induced some T_h17 cells, however following antibiotic treatment mice displayed an inverse correlation between the proportion of T_h17 cells and $CD103^+CD11b^+$ DCs, suggesting these DCs may not be the main T_h17 cell inducers. The ability to induce T_h17 cells correlated with the production of IL1β, although most subsets also produced the IL17-inducing cytokine IL6. I was unable to determine whether differential production of IL12 or IL23 might explain the induction of T_h17 or T_h1 cells.

Consistent with their classical definition, none of the DC subsets were highly phagocytic, but they all expressed most TLRs. However there were differences in the pattern of TLR expression, with the $CD103^+CD11b^-$ DCs expressing considerable amounts of TLR3, 4, 7 and 9, while the $CD103^+CD11b^+$ DCs expressed the most TLR4 and TLR7, and the $CD103^-CD11b^-$ DCs expressed the most TLR5. In general, the $CD103^+CD11b^+$ DCs expressed the lowest levels of TLRs, with particularly low amounts of TLR4, 7 and 9, suggesting these may have very distinct abilities to respond to microbial stimuli.

Taken together these studies suggested that the distinct DC subsets I had identified are likely to play distinct roles in the induction of specific immune responses. In the next chapter, I went on to try to understand the mechanisms regulating DC behaviour, focusing on the potential role of the CD47-SIRPα regulatory axis.

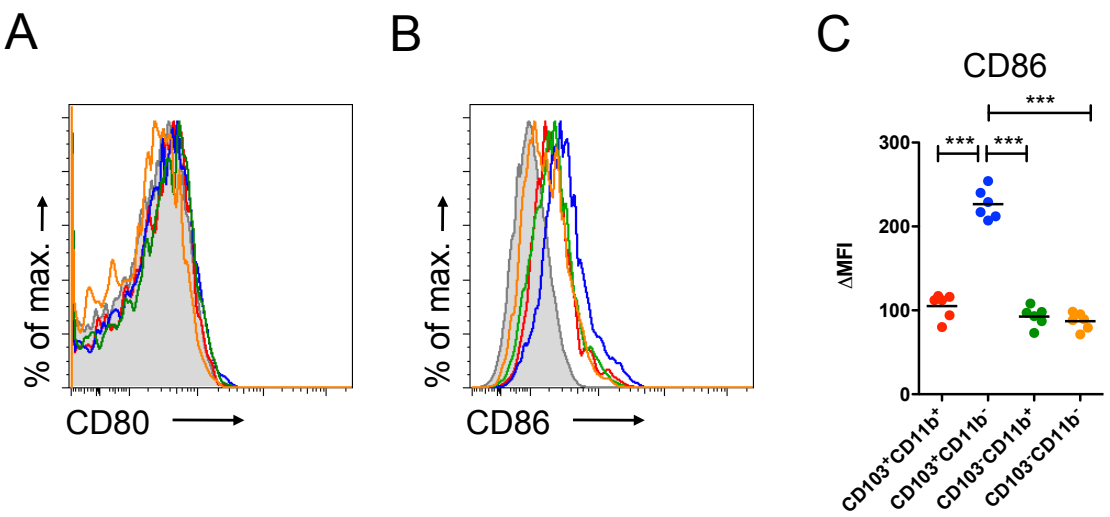

Figure 6.1: Costimulatory molecule expression by SI LP DCs

SI LP DCs were examined for expression of costimulatory molecules (A) CD80 and (B) CD86 by flow cytometry. **C.** ΔMFI (MFI of DC subset minus the MFI for the isotype control) for CD86 expression by the DC subsets. ***p<0.001 One way ANOVA with Bonferroni post-test. Data are from a single experiment with n=6.

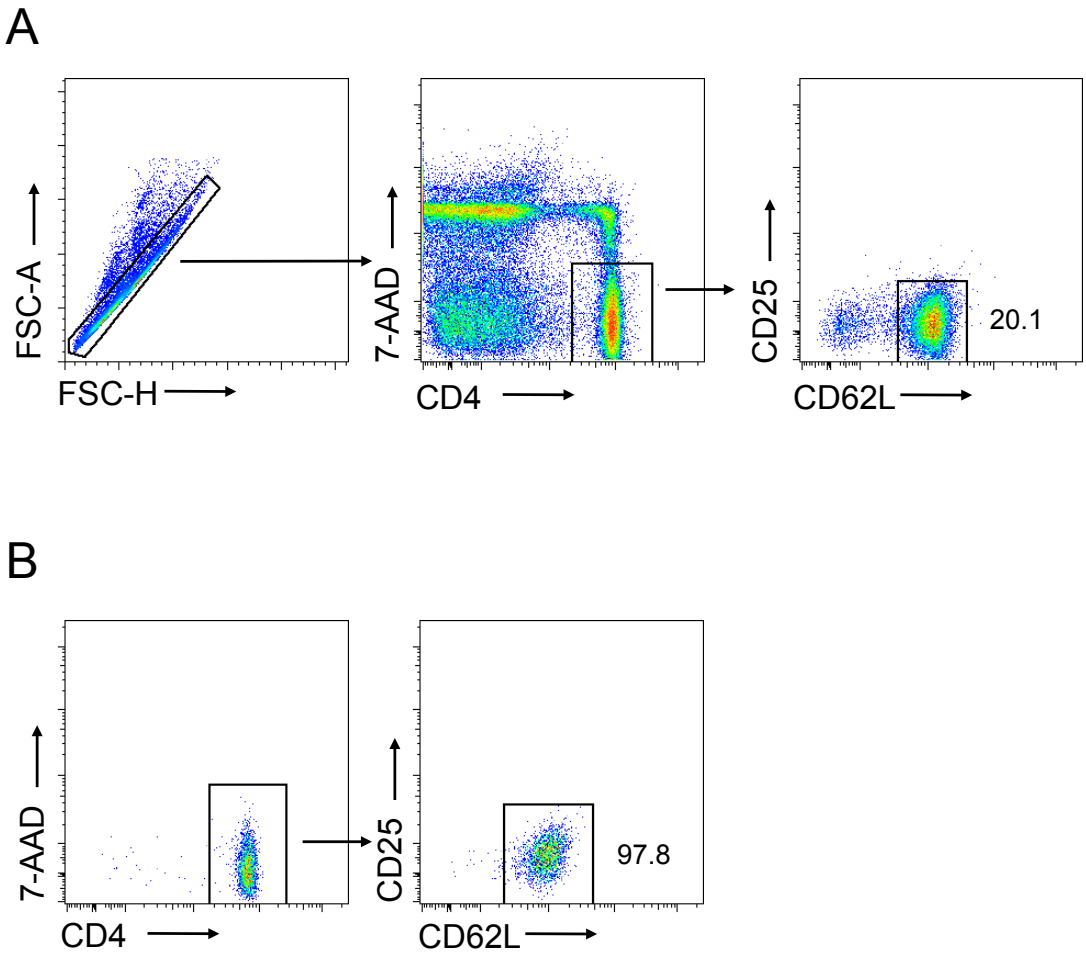

Figure 6.2: FACS-purification of naïve CD4⁺ T cells

CD4⁺ naïve T cells were FACS-purified from pooled LNs from OTII TcR mice. **A.** Representative dot plots showing gating strategy to sort naïve CD4⁺ T cells as single, live, CD4⁺ CD62L⁺ CD25⁻ cells. Number represents pre-sort purity of naïve CD4⁺ T cells as a percentage of total cells. **B.** Representative dot plots showing post-sort purity of naïve CD4⁺ T cells as a percentage of total cells.

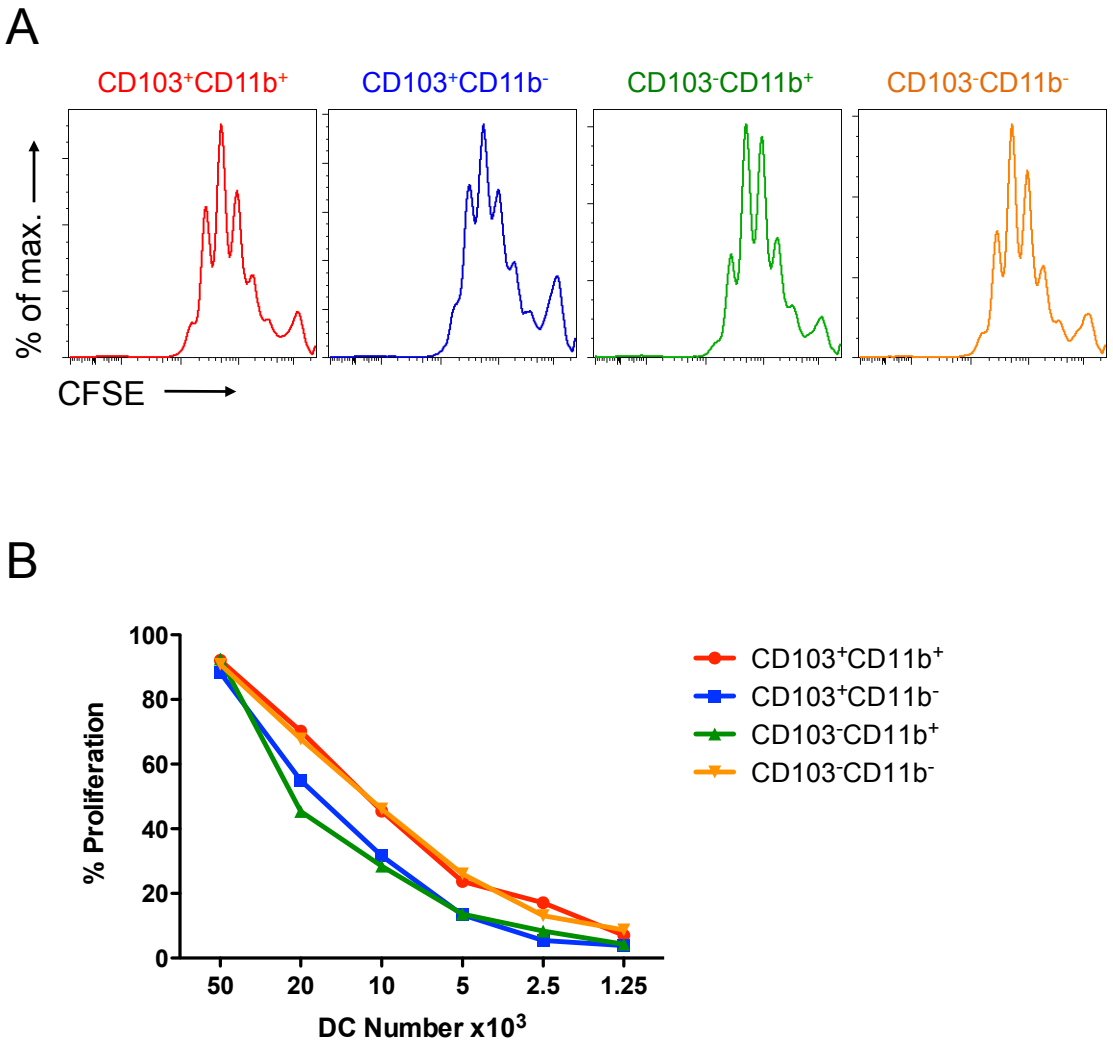

Figure 6.3: SI LP DCs prime proliferation of naïve antigen-specific CD4⁺ T cells *in vitro*

SI LP DCs were FACS-purified from whole digests as shown in Fig. 3.9, pulsed with 2mg/ml ovalbumin protein and co-cultured with FACS-purified naïve CFSE-labelled CD4⁺ (OTII) T cells for 4 days. **A.** Representative histograms showing dilution of CFSE dye in T cells following 4 days of culture of 50,000 DCs with 100,000 T cells. **B.** Percentage of naïve CD4⁺ T cells that have undergone at least one round of cell division after co-culture of 100,000 T cells with decreasing numbers of each DC subset. Data are shown as the mean of two independent experiments with n=1 per experiment, using DC subsets pooled from 9-12 mice per experiment. Naïve CD4⁺ T cells were pooled from LNs of 2-3 mice per experiment.

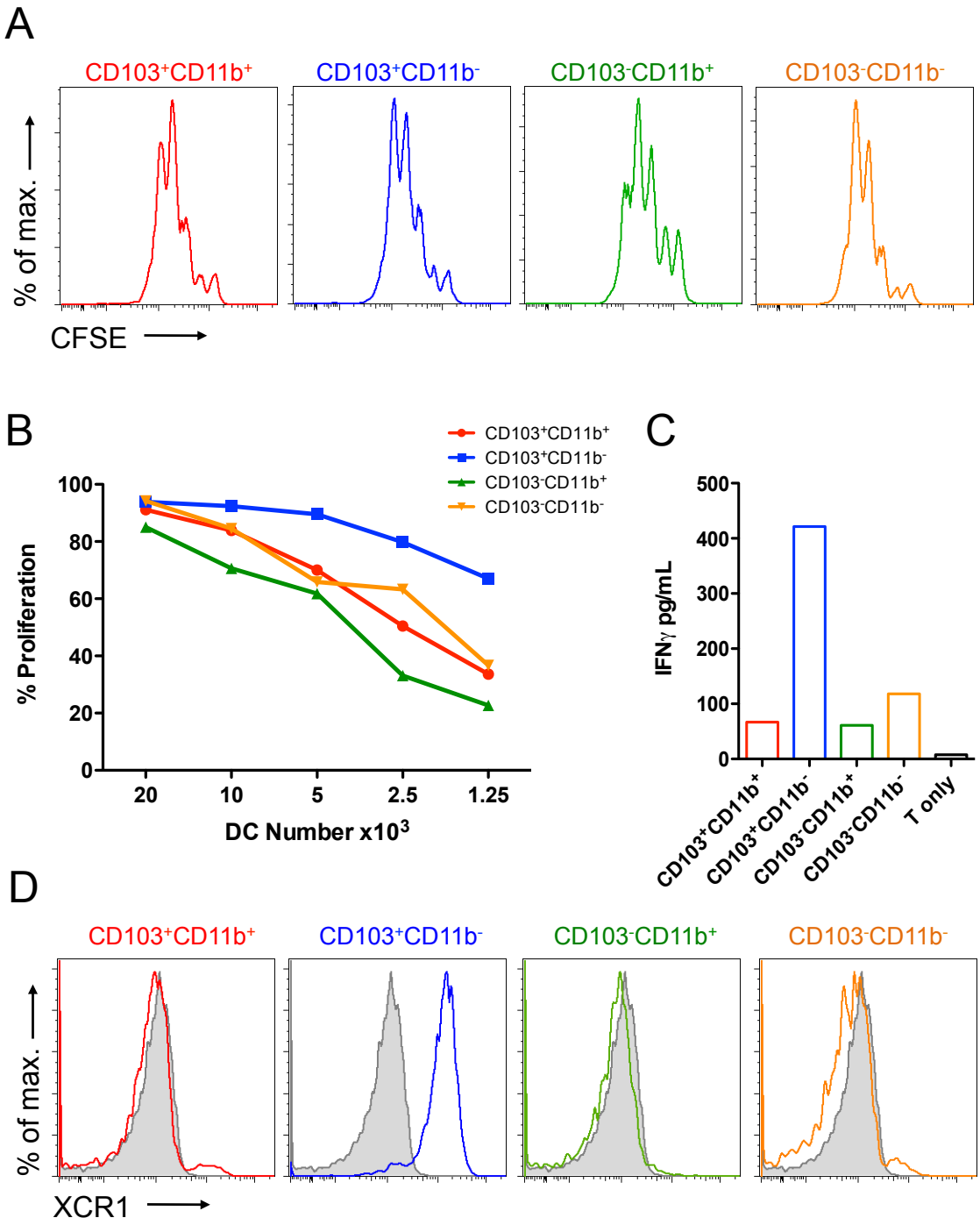

Figure 6.4: Priming of naïve antigen-specific CD8⁺ T cells by SI LP DCs *in vitro*

SI LP DCs were FACS-purified from whole digests as shown in Fig. 3.9, pulsed with 2mg/ml ovalbumin protein and co-cultured with FACS-purified CFSE-labelled naive CD8⁺ (OTI) T cells for 3 days. **A.** Representative histograms showing dilution of CFSE dye in T cells following 3 days of culture of 20,000 DCs with 100,000 T cells. **B.** Percentage of naïve CD8⁺ T cells that have undergone at least one round of cell division after co-culture with decreasing numbers of each DC subset. **C.** IFNγ levels in co-culture supernatants assessed by cytokine bead array. **D.** XCR1 expression by SI LP DC subsets compared to isotype control (shaded grey). Data are from two independent experiments at each DC:T cell ratio with n=1 per experiment. DC subsets were sorted from 9-12 mice pooled per experiment. Naïve CD8⁺ T cells were sorted from LNs of 2-3 mice pooled per experiment.

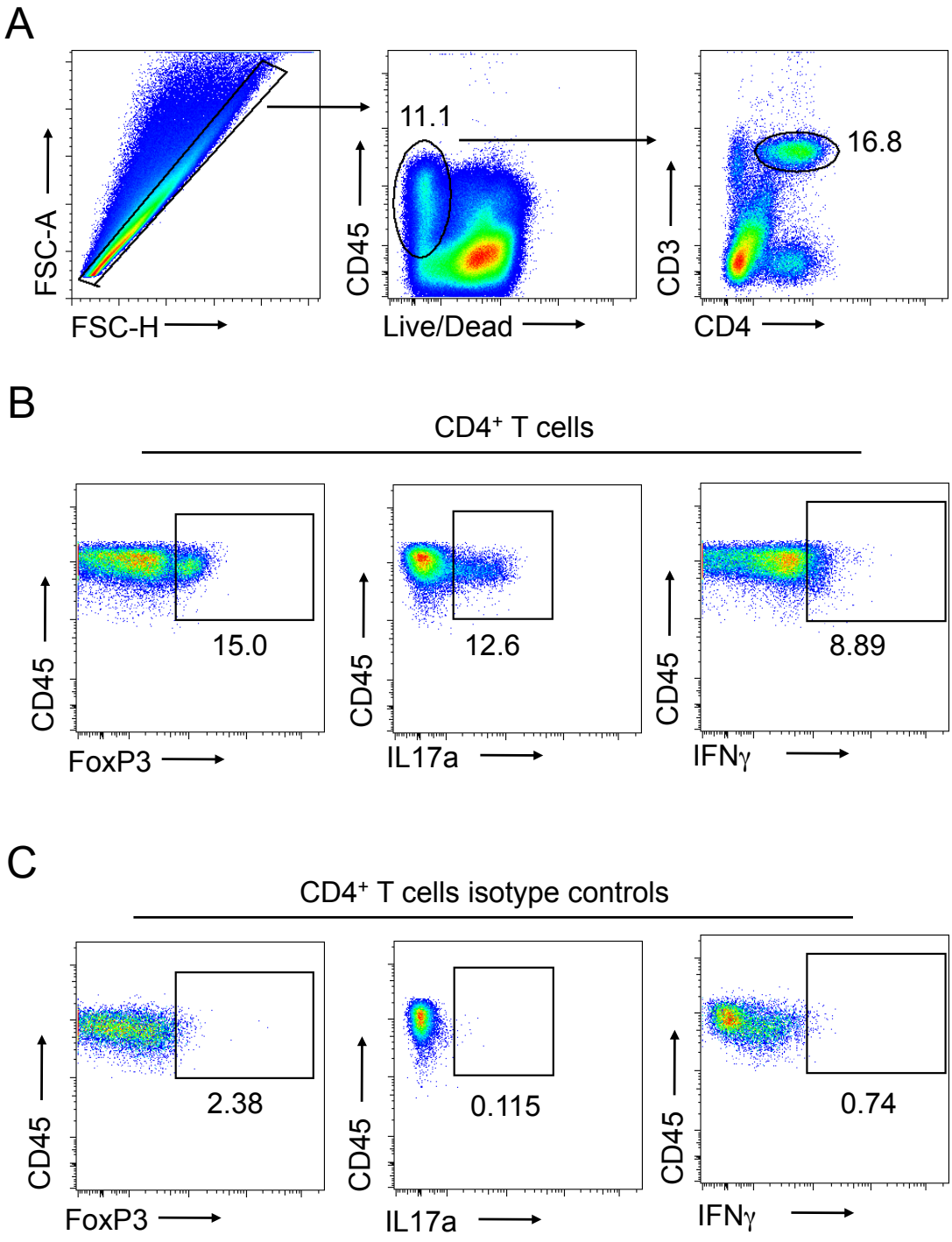

Figure 6.5: CD4⁺ T cell populations in steady state SI LP

A. CD4⁺ T cells were identified in the SI LP as single live CD45⁺ CD3⁺ CD4⁺ cells. Numbers represent frequency of parent gate. **B,C.** SI LP whole digests were stimulated for 4.5 hours with PMA and ionomycin in the presence of protein transport inhibitors Brefeldin A and Monensin and live CD45⁺ CD3⁺ CD4⁺ T cells in SI LP were stained for intracellular FoxP3, IL17 and IFNγ (B) or appropriate isotype controls (C). Numbers represent frequency of CD4⁺ T Cells. Data are representative of at least 5 independent experiments with n =3/4 per experiment.

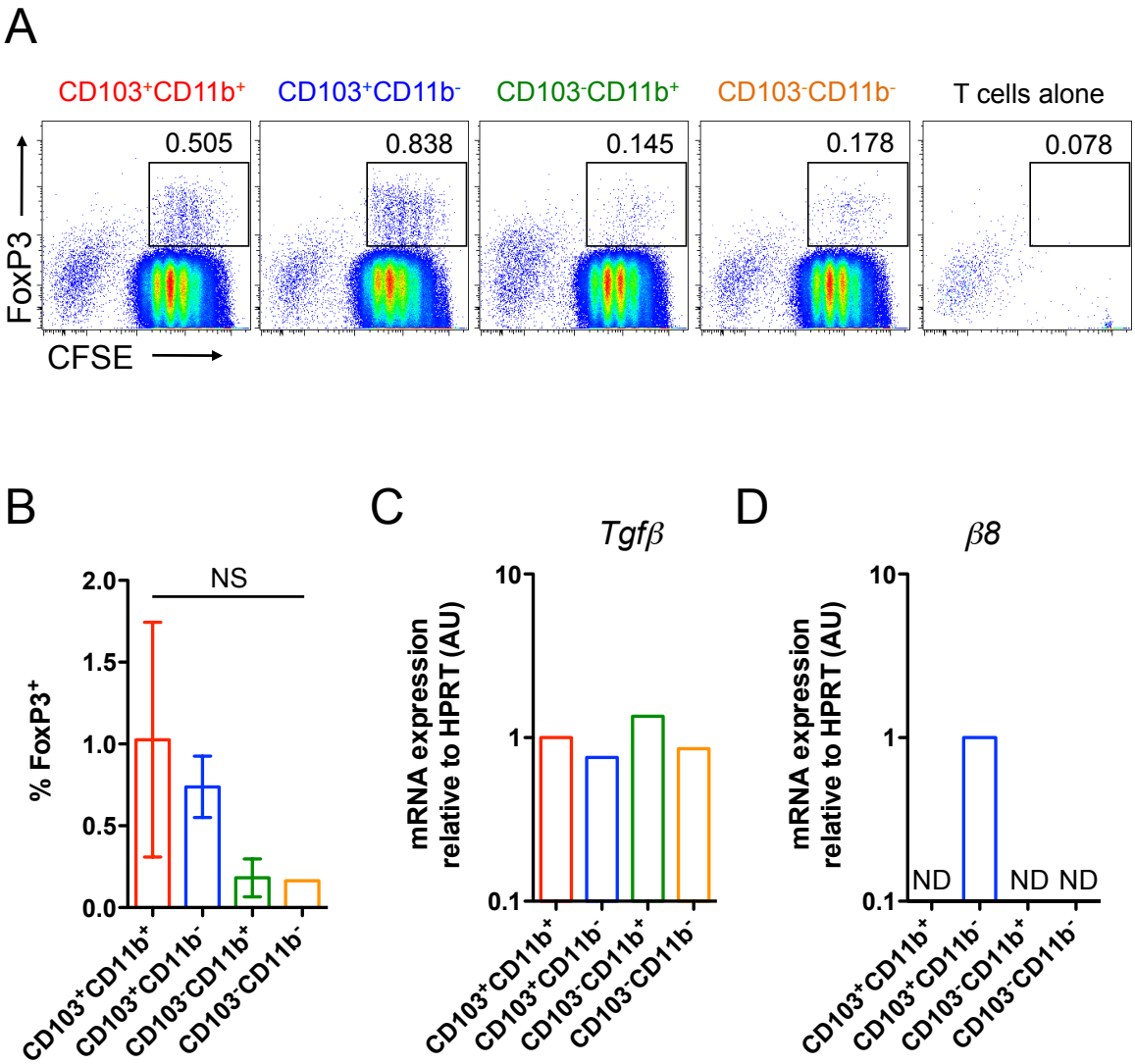

Figure 6.6: FoxP3 induction in naïve CD4⁺ T cells by SI LP DCs *in vitro*

SI LP DCs were FACS-purified from whole digests as per Fig. 3.9, pulsed with 2mg/ml ovalbumin protein and co-cultured with CFSE-labelled naive CD4⁺ (OTII) T cells as shown in Fig. 6.1 for 4 days. **A.** Representative dot plots showing dilution of CFSE dye in T cells and expression of FoxP3 following 4 days of culture of 50,000 DCs with 100,000 T cells or T cells alone. **B.** Mean percentage of FoxP3⁺ T cells as a proportion of total live T cells ±1SD. Data are from two (CD103⁻CD11b⁻), three (CD103⁻CD11b⁺) or four (CD103⁺CD11b⁺ & CD103⁺CD11b⁻) independent experiments with n=1 per experiment. NS; not significant, One way ANOVA with Bonferroni post test. DC subsets were sorted from 9-12 mice pooled per experiment. **C,D.** Naïve CD4⁺ T cells were sorted from LNs of 2-3 mice pooled per experiment. Expression of mRNA for TGFβ (C) and β8 (D) by FACS-purified SI LP DCs. Results shown are relative to HPRT using the $2^{-\Delta\Delta ct}$ method with CD103⁺CD11b⁻ DCs set to 1. Data shown are means from 2 independent experiment with cells pooled from 9-12 mice in each case. ND; not detected.

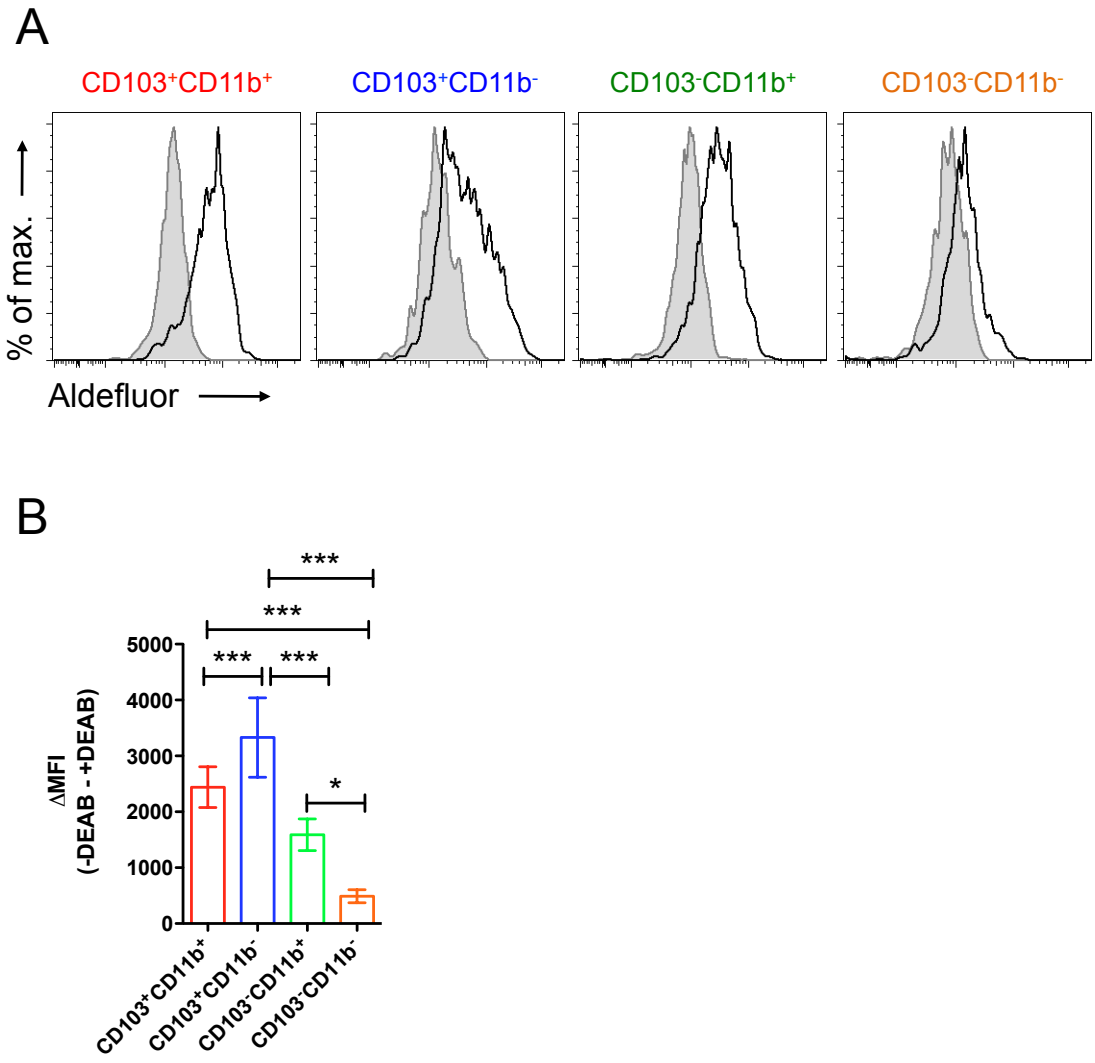

Figure 6.7: ALDH function in SI LP DCs

Whole SI LP digests were incubated with the fluorescent ALDH substrate ALDEFLUOR in the presence or absence of the ALDH inhibitor diethylaminobenzoaldehyde (DEAB) and subsequently stained for flow cytometry. **A.** Representative histograms showing ALDEFLUOR fluorescence in each DC subset in the presence (grey line) or absence (black line) of DEAB **B.** Δ Mean fluorescence intensity (MFI) for ALDEFLUOR activity (MFI in absence of DEAB – MFI in presence of DEAB) ±1SD for each DC subset. Data are representative of two independent experiments with n=4 per experiment. *p<0.05, ***p<0.001. One way ANOVA with Bonferroni post-test.

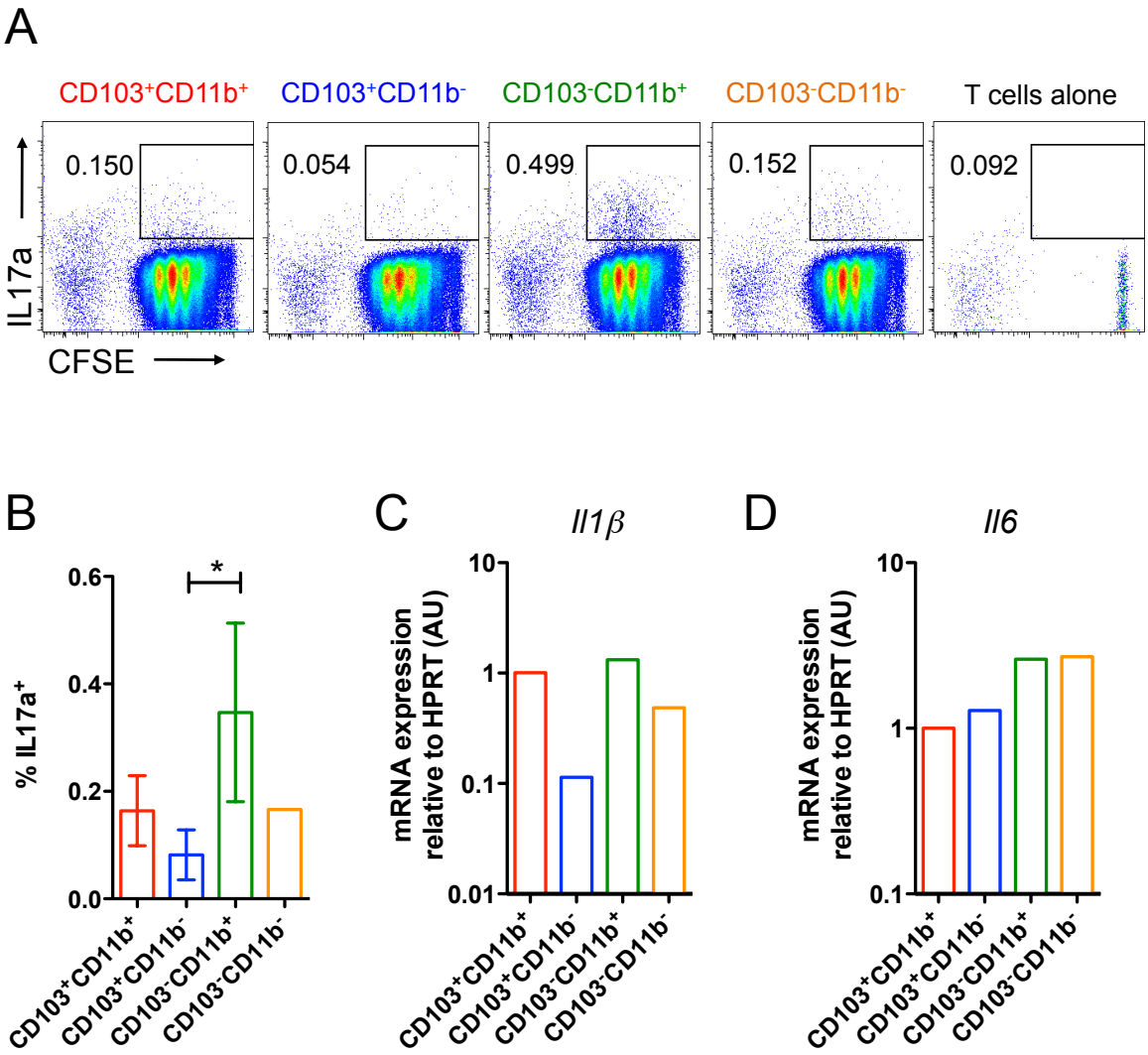

Figure 6.8: IL17a induction in naïve CD4⁺ T cells by SI LP DCs *in vitro*

SI LP DCs were FACS-purified from whole digests as per Fig. 3.9, pulsed with 2mg/ml ovalbumin protein and co-cultured with CFSE-labelled naive CD4⁺ (OTII) T cells as shown in Fig. 6.1 for 4 days before being restimulated with PMA and ionomycin in the presence of Brefeldin A and Monensin for 4.5 hours. **A.** Representative dot plots showing dilution of CFSE dye in T cells and expression of IL17a following 4 days of culture of 50,000 DCs with 100,000 T cells or T cells alone. **B.** Mean percentage of IL17a⁺ T cells as a proportion of total live T cells ±1SD. Data are from two (CD103⁻CD11b⁻), three (CD103⁻CD11b⁺) or four (CD103⁺CD11b⁺ & CD103⁺CD11b⁻) independent experiments with n=1 per experiment. *p<0.05, One way ANOVA with Bonferroni post test. DC subsets were sorted from 9-12 mice pooled per experiment. **C,D.** Naïve CD4⁺ T cells were sorted from LNs of 2-3 mice pooled per experiment. Expression of mRNA for IL1β (C) and IL6 (D) by FACS-purified SI LP DCs. Results shown are relative to HPRT using the $2^{-\Delta\Delta ct}$ method with CD103⁺CD11b⁻ DCs set to 1. Data are shown as mean from 2 independent experiment with cells pooled from 9-12 mice in each case. ND; not detected.

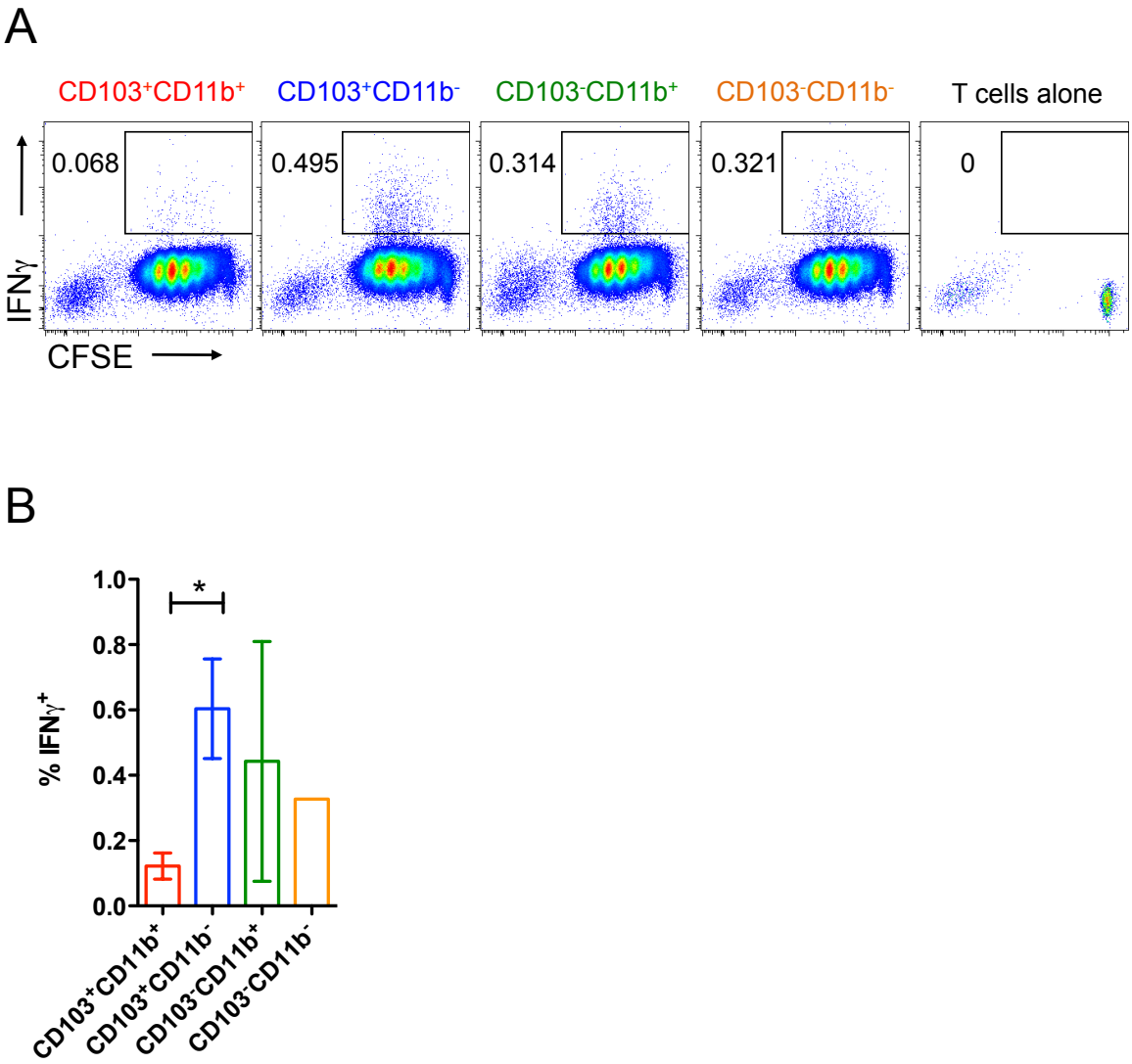

Figure 6.9: IFNγ induction in naïve CD4⁺ T cells by SI LP DCs *in vitro*

SI LP DCs were FACS-purified from whole digests as per Fig. 3.9, pulsed with 2mg/ml ovalbumin protein and co-cultured with CFSE-labelled naive CD4⁺ (OTII) T cells as shown in Fig. 6.1 for 4 days before being restimulated with PMA and ionomycin in the presence of Brefeldin A and Monensin for 4.5 hours. **A.** Representative dot plots showing dilution of CFSE dye in T cells and expression of IFNγ following 4 days of culture of 50,000 DCs with 100,000 T cells or T cells alone. **B.** Mean percentage of IFNγ⁺ T cells as a proportion of total live T cells ±1SD. Data are from two (CD103⁻CD11b⁻), three (CD103⁻CD11b⁺) or four (CD103⁺CD11b⁺ & CD103⁺CD11b⁻) independent experiments with n=1 per experiment. *p<0.05, One way ANOVA with Bonferroni post test. DC subsets were sorted from 9-12 mice pooled per experiment. Naïve CD4⁺ T cells were sorted from LNs of 2-3 mice pooled per experiment.

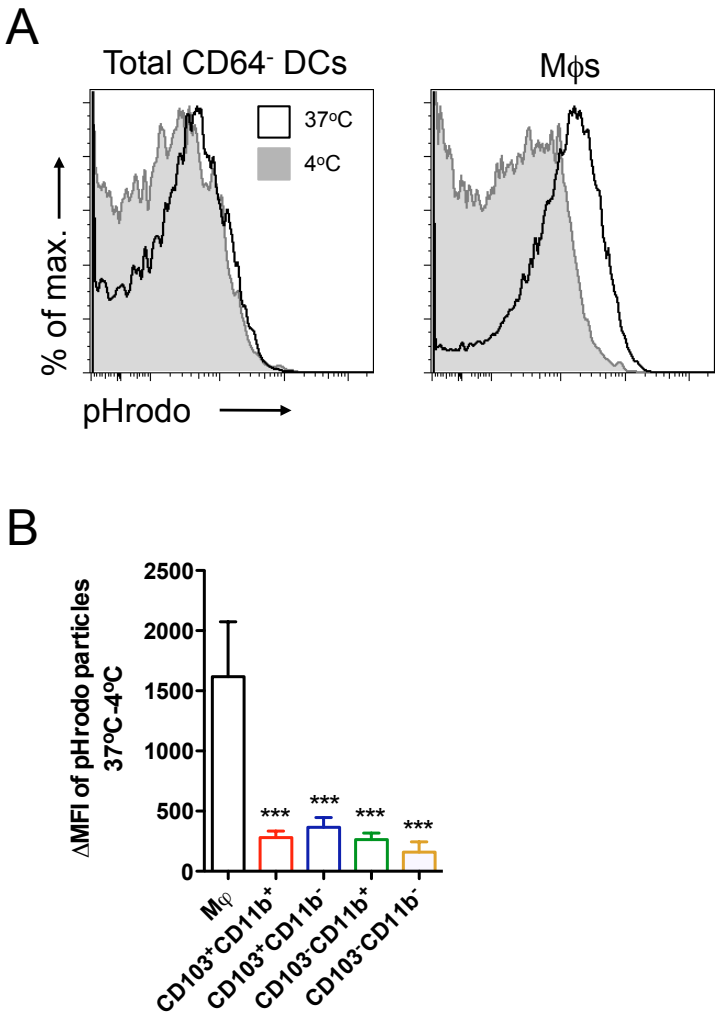

Figure 6.10: Phagocytic activity of MPs from SI LP

Whole SI LP digests were incubated with pHrodo *E.* coli bioparticles for 15 mins at 37°C (black line) or at 4°C as a control (grey shaded line). **A.** Representative histograms of pHrodo dye fluorescence of total CD64$^-$ DCs or CD64$^+$ mϕs. **B**. ΔMFI (MFI at 37°C-MFI at 4°C control) +1SD for mϕs and each DC population. Data are representative of 2 individual experiments with n=4/5. ***p<0.001 vs. mϕs. One-way ANOVA with Bonferroni post-test.

A

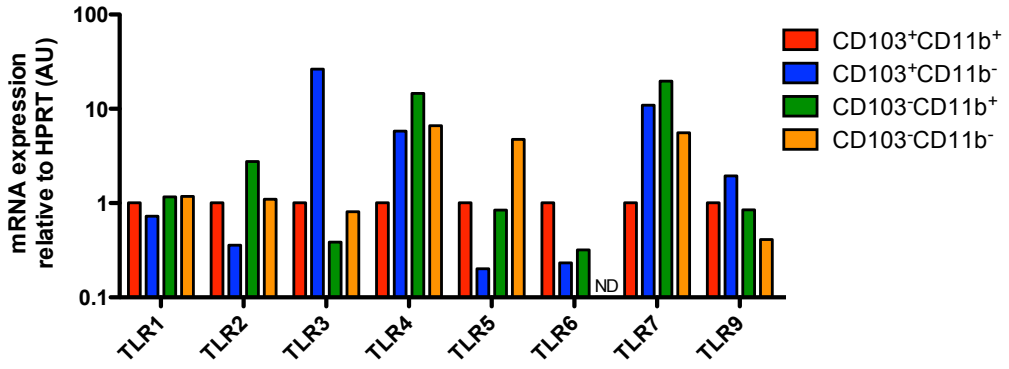

Figure 6.11: TLR and costimulatory molecule expression by SI LP DCs

SI LP DCs were FACS-purified from whole digests as described in Fig. 3.9 and analysed by qRT-PCR for expression of TLRs. Results shown are relative to HPRT using the $2^{-\Delta\Delta ct}$ method with $CD103^{+}CD11b^{+}$ DCs set to 1. Data are from a single experiment with cells pooled from 12 mice.

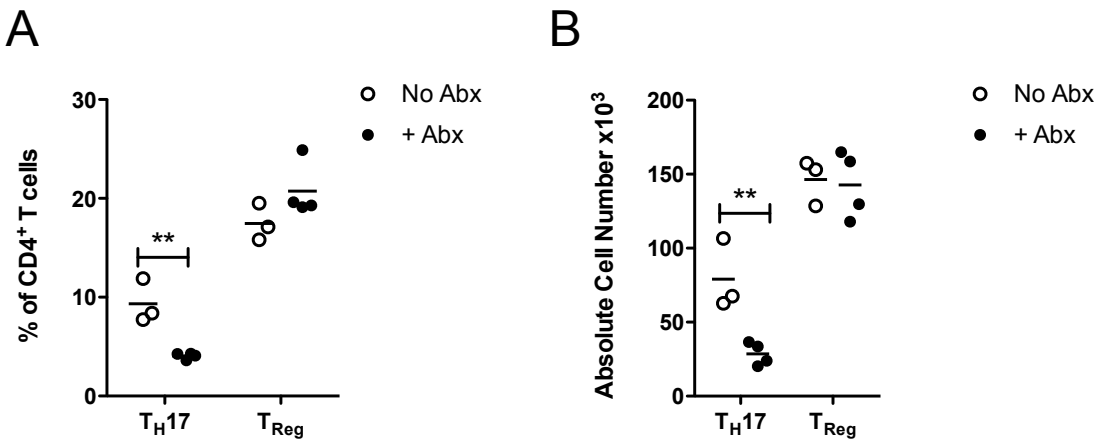

Figure 6.12: Effects of antibiotic treatment on SI LP CD4⁺ T cells

Mice received an antibiotic cocktail containing vancomycin, metronidazole, ampicillin, neomycin and gentamycin in sweetened drinking water for 2 weeks. Control mice received sweetened water only. Whole SI LP digests were restimulated with PMA and ionomycin in the presence of Brefeldin A and Monensin for 4.5 hours before analysis of IL17 and FoxP3 by intracellular staining. **A.** Proportion of $CD4^+$ T cells expressing IL17a or FoxP3 in antibiotic treated mice compared with mice receiving control water. **B.** Absolute numbers of $CD4^+$ T cells expressing IL17a or FoxP3 in antibiotic treated mice compared with mice receiving control water. Data are from a single experiment with n=3-4 per group. **p<0.01. Student's t test.

Chapter 7 SIRPα Signalling Regulates Intestinal $CD103^+CD11b^+$ DC Homeostasis

7.1 Introduction

Signal regulatory protein α (SIRP α) is an inhibitory receptor expressed by a number of myeloid cells, whose function has been implicated in controlling the behaviour of $CD11b^+$ DCs in the spleen and skin (Iwamura et al., 2010; Saito et al., 2010). When I began my PhD, we were only aware of two intestinal DC subsets which differentially expressed SIRPα, thus one aim of this thesis was to examine the role played by this signalling protein in modulating the behaviour of the $SIRP\alpha^+CD103^+CD11b^+$ DCs. However in Chapter 3, I showed that there were two additional $CD103^-$ DC subsets both of which also expressed SIRPα, therefore, I instead investigated the role of SIRPα on multiple intestinal DC subsets, using mice with a point mutation that results in a truncated, inactive form of the cytoplasmic signalling domain, herein referred to as SIRPα mutant (mt) mice.

7.2 $CD103^+CD11b^+$ Intestinal DCs are Reduced in SIRPα Mutant Mice

I first examined the DC populations present in the SI LP of SIRPα mt mice compared with WT controls. Rather unexpectedly, given the expression pattern of SIRPα, there was a selective reduction of approximately 50% in $CD103^+CD11b^+$ DCs in SIRPα mt mice compared with WT mice, whereas the other DC populations, as well as SIRPα-expressing mϕs were unaffected (Fig. 7.1). A defect of similar magnitude was seen in the proportion of $CD103^+CD11b^+$ DCs amongst migratory DCs in the MLNs, with compensatory increases in the proportion of the $CD103^+CD11b^-$ and $CD103^-CD11b^-$ DCs (Fig. 7.2A). As there was a reduction in the proportion of total migratory ($CD11c^+MHCII^{hi}$) DCs as a percentage of live leukocytes in the MLNs of SIRPα mt mice compared with WT controls, all migratory DC subsets were reduced in numbers. However this was most marked for the $CD103^+CD11b^+$ DC subset (Fig. 7.2B). Despite the much reduced population of $CD103^+CD11b^+$ DCs in the colon compared with the SI LP in WT mice, the defect in this population was replicated in the colonic LP of SIRPα mt mice (Fig. 7.3A), while the other DC populations and mϕs were unaffected (Fig. 7.3A,B). Confirming the previous reports and in contrast to the intestine, I found that SIRPα mutant mice had a selective reduction in $CD103^-CD11b^+$ DCs in the

spleen and amongst resident DCs in MLN (Fig. 7.3C,D). Thus SIRPα signalling appears to be selectively involved in the homeostasis of $CD103^+CD11b^+$ DCs in the intestine.

7.3 CD47KO Mice Phenocopy SIRPα Mutant Mice

As the only reported ligand for SIRPα in the gut is CD47, I next examined the MP populations in the SI LP of CD47KO mice. As in SIRPα mt mice, CD47KO mice had reduced proportions and numbers of $CD103^+CD11b^+$ DCs in the SI LP. This was associated with increases in the proportions of the $CD103^+CD11b^-$ and $CD103^-CD11b^-$ DCs and a small but significant decrease in the numbers of $CD103^-CD11b^+$ DCs (Fig. 7.4A,). However, these latter features were not consistent between experiments and indeed I often had problems with cells dying when isolating cells from CD47KO intestine, leading to lower yields of viable cells. This appeared to be a consequence of increased mucus levels in the CD47KO small intestine, although this is merely an observation that requires further examination. No significant differences in the proportions or numbers of $CD64^+$ intestinal mϕs were found in the SI LP of CD47KO mice compared with WT controls (Fig. 7.4B). As in SIRPα mt mice, there was a reduced proportion of $CD103^+CD11b^+$ DCs amongst migratory DCs in the MLNs of CD47KO mice and again, all migratory DC populations were reduced in number due to a marked reduction in the total cell numbers in CD47KO MLNs (Fig. 7.4C,D).

7.4 T Cell Responses in SIRPα Mutant Mice

Given the role of DCs in priming the adaptive immune response and previous reports that SIRPα mt mice had defective T_h17 cell responses in experimental autoimmune encephalomyelitis, contact hypersensitivity and collagen-induced arthritis (Motegi et al., 2008; Okuzawa et al., 2008; Tomizawa et al., 2007), I next investigated $CD4^+$ T cell populations in steady state mucosa. As shown in Chapter 6, the normal SI LP $CD4^+$ T cell pool comprises $FoxP3^+$ T_{Reg} cells, IFNγ-producing T_h1 cells and IL17a-producing T_h17 cells, and I first studied these populations in the SI LP of SIRPα mt mice. This revealed a marked reduction in both the proportion and number of IL17a-producing T_h17 cells in SIRPα mt mice compared with WT controls, whereas the populations of T_h1 and T_{Reg} cells were unaffected

(Fig. 7.5A). To verify these findings, I FACS-purified total $CD4^+$ T cells from the SI LP of WT and SIRPα mt mice and assessed mRNA expression of two T_h17 cell associated cytokines, IL17a and IL22. This revealed a slight reduction in the levels of IL17 and approximately a 2-fold reduction in IL22 mRNA expression in $CD4^+$ T cells from SIRPα mt mice compared with WT SI LP (Fig. 7.5B). A similar trend towards fewer T_h17 cells was also shown by intracellular cytokine analysis of colonic LP $CD4^+$ T cells, although this did not reach statistical significance, possibly because of the low numbers of IL17-producing T cells in the steady state colon (Fig. 7.5C). CD47KO mice also had reduced proportions and numbers of T_h17 cells in SI LP, but normal populations of T_{Reg} and T_h1 cells (Fig. 7.6). Together these results suggest that the SIRPα-CD47 axis is involved in the homeostasis of the $CD103^+CD11b^+$ DCs and that these DCs play a role in the generation of T_h17 cells *in vivo.*

To explore further the defect in T_h17 cells in SIRPα mt mice, I next examined the priming of antigen-specific $CD4^+$ T cells *in vivo.* First I used a model in which no T cell polarising conditions were used. WT and SIRPα mt mice received CSFE-labelled total $CD45.1^+/CD45.2^+$ OTII LN cells isolated 1 day before feeding 10mg ovalbumin and T cell clonal expansion and differentiation was assessed in MLNs four days later (Fig. 7.7). Similar numbers of donor $CD4^+$ T cells could be found in MLNs in WT and SIRPα mt mice at this time point (Fig. 7.7B), but analysis of CSFE levels showed that these had proliferated less in the SIRPα mt MLNs compared with that in WT MLNs (Fig. 7.7C). In both cases, donor cells in the MLNs differentiated into T_h1, T_h17 and T_{Reg} cells, as shown by intracellular expression of IFNγ, IL17a and FoxP3 respectively. Although there was a trend towards a decrease in the proportion of donor cells expressing IL17a in SIRPα mt MLNs compared with WT MLNs, this did not attain statistical significance. As in the endogenous LP T cell populations, there were no differences in the generation of antigen specific T_h1 and T_{Reg} cells in response to OVA feeding in SIRPα mt MLNs (Fig. 7.7D-F).

Next I examined a model of antigen-specific immunisation which is known to favour the polarisation of T_h17 cells in MLNs (Persson et al., 2013b). In addition, I included a step which prevents these cells emigrating from the MLNs as a means of ensuring I could detect maximal polarisation of antigen specific $CD4^+$ T cells. To

do this, I immunised SIRPα mt and WT mice with OVA i.p., together with α-CD40 and LPS as adjuvants and administered the S1P inhibitor FTY720, to block T cell migration from the MLNs (Fig. 7.8). Under these conditions, there was a significant reduction in the proportion of donor $CD4^+$ T cells in the MLNs of SIRPα mt mice compared with WT MLNs (Fig. 7.8B), although similar proportions of these cells had undergone at least one division as assessed by CFSE dilution in both cases (Fig. 7.8C). Furthermore, while the proportion of $IL17a^+$ cells amongst donor cells was the same in the two strains (Fig. 7.8D), the absolute number of T_h17 cells was significantly reduced in the MLNs of SIRPα mt mice compared with WT (Fig. 7.8E). Interestingly, despite the reduced population of donor cells, there was an increase in the number of T_h1 and T_{Reg} cells induced in the MLNs of SIRPα mt mice (Fig. 7.8F,G). To rule out the possibility that there was an intrinsic defect in the ability of SIRPα mt T cells to generate T_h17 cells, I cultured FACS-purified naïve $CD4^+$ T cells from the MLNs of WT and SIRPα mt mice *in vitro* with TGFβ, IL6, IL1β, IL23, anti-IL2, anti-IL4 and anti-IFNγ, a protocol used routinely within the department to induce T_h17 cell polarisation *in vitro.* Using this approach, SIRPα mt T cells generated entirely normal proportions and numbers of $CD4^+$ T cells expressing IL17a and the T_h17 cell transcription factor RORγt (Fig. 7.9). Together these experiments are further evidence that the defect in $CD103^+CD11b^+$ DCs in SIRPα mt mice leads to a selective defect in T_h17 priming.

7.5 DC Function in SIRPα Mutant Mice

I next thought it important to examine whether the reduced population of T_h17 cells in the SI LP of SIRPα mt mice could reflect abnormalities in the function of the DCs remaining in these mice. Examination of mRNA expression of the T_h17 inducing cytokines IL6, IL1β and IL23p19 by total SI LP DCs revealed a ~2-fold reduction in the levels of *Il6* and a slight reduction in *Il1b* expression compared with WT controls (Fig. 7.10A). As in previous experiments, I could not detect mRNA for IL23p19 in either WT or SIRPα mt SI LP DCs. To determine if this reduced cytokine expression by total DCs was due to the $CD103^+CD11b^+$ DC defect, I next examined mRNA expression of IL6 and IL1β by FACS-purified $CD103^+CD11b^+$ DCs. This demonstrated the remaining DCs in the SIRPα mt mice expressed slightly more *Il6* and slightly less *Il1β* than WT controls (Fig. 7.10B). Although I was unable to obtain sufficient mice to repeat these experiments, these

results support the idea that the apparent defect in IL6 production amongst total DCs from SIRPα mt mice may be explained by the reduced number of $CD103^+CD11b^+$ DCs in these mice.

To extend the analysis of DC function, I performed a preliminary experiment in which FACS-purified $CD103^+CD11b^+$ and $CD103^-CD11b^+$ DCs from WT and SIRPα mt mice were pulsed with OVA and used to prime naïve $CD4^+$ T cells *in vitro.* To avoid any potential bias, in terms of cell viability due to the time required to sort each strain individually, I mixed $CD45.1^+$ WT and $CD45.2^+$ SIRPα mt SI LP isolates prior sorting to ensure WT and SIRPα mt DCs were treated in the same manner before co-culture. Because I could only sort four ways using the FACSAria cell sorter, I could only examine two DC populations from each strain. In addition to the $CD103^+CD11b^+$ DCs, I chose to examine $CD103^-CD11b^+$ DCs, as my experiments in Chapter 6 had shown this subset to be proficient at inducing T_h17 cell polarisation. As I found before, these two subsets induced identical levels of proliferation by naïve $CD4^+$ T cells and there were no differences between DCs from WT and SIRPα mt SI LP (Fig. 7.11A). Furthermore, $CD103^+CD11b^+$ DCs from WT and SIRPα mt mice induced equivalent levels of T_h17, T_h1 and T_{Reg} cell differentiation (Fig. 7.11B). Interestingly however, the $CD103^-CD11b^+$ DCs from SIRPα mt mice appeared to induce fewer T_h17 cells, more T_h1 cells and equal proportions of T_{Reg} cells compared with WT controls (Fig. 7.11C). As I was only able to perform this experiment once, more studies are required to assess the significance of these findings.

7.5.1 Effects of SIRPα Mutation on Immune Function *in vivo*

7.5.1.1 *C. rodentium* Infection

Having established that SIRPα mt mice have reduced numbers of T_h17 cells, I next wanted to investigate the consequences of this defect and to do this, I first used the mouse model of *C. rodentium* infection, in which T_h17 cells play an important protective role (Ishigame et al., 2009; Ivanov et al., 2009; Mangan et al., 2006). SIRPα mt and WT mice were infected with *C. rodentium* and infection was monitored by faecal colony forming units (CFU) counts. This revealed that while the initial colonisation of *C. rodentium* was similar in both strains, by day 11 of infection the WT mice had begun to clear the infection, whereas the SIRPα mt

mice did not do so until day 14 (Fig. 7.12A). To investigate if this reduced clearance was due to an impaired ability to induce T_h17 cells, I examined T_h17 cells in the MLNs and colonic LP at day 8 of infection, a time point where both strains had similar levels of colonisation (Fig. 7.12B). This revealed a marked reduction in the number of IL17a producing $CD4^+$ T cells in the MLNs of SIRPα mt mice compared with WT controls. In contrast, the proportions of T_h17 cells in the colonic LP at this time point were similar in the two strains, perhaps because this was too early to see maximal localisation of effector T cells in this site (Fig. 7.12C).

7.5.1.2 DSS-Induced Colitis

As discussed in Chapter 5, DSS-colitis is a model of IBD routinely used in the lab. As our previous studies have demonstrated this model of IBD to be dependent on myeloid innate cells (Bain et al., 2013; Bain and Mowat, 2012; Platt et al., 2010), the majority of which express SIRPα, I next examined the susceptibility of the SIRPα mt mice to DSS colitis. Both WT and SIRPα mt mice developed clinical signs of disease after 5 days of receiving 2% DSS *ad libitum* in their drinking water and no significant differences were observed between the two groups in terms of weight loss or total clinical score during the 8 days of DSS administration (Fig. 7.13).

7.5.1.3 Induction of Oral Tolerance

Although my results from SIRPα mt mice had emphasised a role for $CD103^+CD11b^+$ DCs in driving T_h17 cells, I had also shown earlier that this DC subset could also induce $FoxP3^+$ T_{Reg} cells *in vitro.* Furthermore, $CD103^+$ DCs have often been assumed to be crucial for tolerance induction *in vivo.* Therefore, I decided to examine whether oral tolerance could be induced normally by feeding antigen to SIRPα mt mice. Mice were gavaged with a single dose of 25mg OVA or PBS as a control and 7 days later were immunised with OVA/CFA subcutaneously. The induction of tolerance was assessed by measuring the DTH response to a challenge injection of heat aggregated OVA (HAO). Although PBS fed SIRPα controls showed a trend towards increased DTH responses compared with WT controls, both strains showed similar levels of suppression of DTH responses after feeding OVA compared with PBS controls (Fig. 7.14). Thus tolerance can be

induced normally in the absence of SIRPα signalling and despite the defect in $CD103^+CD11b^+$ DCs.

7.6 Lack of Spontaneous Disease and Restoration of DC Defect in Ageing SIRPα Mutant Mice

In view of the defects in DCs and T cells I found in young adult SIRPα mt mice, I thought it important to monitor if these animals developed overt disease such as increased susceptibility to infection or IBD as they aged. No difference in weight loss or any other clinical signs of disease were seen in either WT or SIRPα mt mice left to age for 11 months. Interestingly however, the $CD103^+CD11b^+$ DC defect in the SI LP was absent in the aged SIRPα mt mice, which showed an increased proportion of these DCs compared with young mice (Fig. 7.15). In addition there was now a significant decrease in the proportions of $CD103^-CD11b^+$ and $CD103^-CD11b^-$ DCs in the aged SIRPα mt compared with aged matched WT controls (Fig. 7.15), although this seemed to be due to a trend towards increased proportions of these subsets in ageing WT mice compared with their younger counterparts. A similar restoration of T_h17 cells was also seen in the SI LP of aged SIRPα mt mice and these cells were now present in identical proportions to aged matched WT controls and at significantly higher levels than in young SIRPα mt mice (Fig. 7.16). In contrast, there were no effects of ageing on the DC defect in the spleen of SIRPα mt mice, where a severe reduction in $CD4^+$ DCs was seen in both young and old mice, even though this population also decreased in aged WT mice compared with their young controls. There was no effect of SIRPα mutation on $CD4^-$ DCs in the spleen at any age (Fig. 7.17).

7.7 Summary

In this chapter, I set out to investigate the role of the inhibitory receptor SIRPα on intestinal DC function. Despite the fact that SIRPα is expressed by most intestinal DC subsets, as well as resident macrophages, I found SIRPα mt mice to have a selective reduction in the proportions and numbers of $CD103^+CD11b^+$ DCs in LP and amongst migratory DCs in the MLNs. Consistent with previous reports, I also found a reduction in the proportion and numbers of $CD4^+/CD11b^+$ splenic and LN resident DCs in these mice (Saito et al., 2010). The requirement for a

functional SIRPα signal in the homeostasis of these DCs was confirmed using mice in which the only known ligand for SIRPα in the gut, CD47, was knocked out, as these CD47KO mice phenocopied the DC defects observed in the SIRPα mt mice.

This intestinal $CD103^+CD11b^+$ DC defect correlated with a selective reduction in the local population of T_h17 cells in the LP, while T_h1 and T_{Reg} cells were present in normal numbers. The normal populations of $FoxP3^+$ T_{Reg} cells correlated with the normal induction of oral tolerance to fed antigen by the SIRPα mt mice. Antigen specific $CD4^+$ T cells transferred into SIRPα mt mice also showed defective proliferation and generation of T_h17 cells in the MLNs following oral and systemic administration of antigen, particularly when LPS and anti-CD40 were used as adjuvants. SIRPα mt mice exhibited delayed clearance of *C. rodentium* and this was associated with defective priming of T_h17 cells in MLNs. The defects in T_h17 cells were not due to an intrinsic inability to generate these cells, as T_h17 cells could be generated from naïve SIRPα mt $CD4^+$ T cells normally under polarising conditions *in vitro*. Moreover, the lack of SIRPα signalling on the remaining $CD103^+CD11b^+$ DCs in the LP, did not appear to be responsible for the T_h17 defect, as the remaining DCs expressed the cytokines required to generate T_h17 cells and could drive T_h17 polarisation *in vitro.* Thus the defect in T_h17 cells in SIRPα mt mice appears to be a consequence of the SIRPα mt mice having fewer $CD103^+CD11b^+$ DCs. This hypothesis was supported by the correlation I and others have found between this DC population and T_h17 cells in the SI compared with the colon (Denning et al., 2011). Interestingly however, I obtained preliminary evidence that despite being present in normal numbers, $CD103^-CD11b^+$ DCs from SIRPα mt mice may have a may have a reduced ability to drive T_h17 cell generation *in vitro*. As this could be consistent with my earlier findings that this subset is efficient at inducing T_h17 cells, the contribution of $CD103^-CD11b^+$ DCs to the T cell phenotype in SIRPα mt mice requires further investigation.

Despite being expressed by most myeloid innate cells, the lack of SIRPα signalling in SIRPα mt mice did not affect disease progression in animals receiving DSS. I found weight loss and colitis scores to be consistent between WT and SIRPα mt animals. Furthermore, despite their proposed involvement in IBD, the

reduced population of T_h17 cells did not alter the susceptibility of SIRPα mt mice to chemically-induced colitis, although this may not be the best model to evaluate the deficit in T_h17 cells as DSS colitis has been shown to develop normally in SCID animals, suggesting a minimal involvement for T cells in this IBD model (Axelsson et al., 1996). Moreover, the defect in T_h17 cells was less pronounced in the colon compared with the SI LP.

Finally, examination of aged SIRPα mt mice revealed that these mice appear to overcome the selective reduction in intestinal $CD103^+CD11b^+$ DCs and T_h17 cells with time, again underlining the association between these cells *in vivo*, but in direct contrast with the splenic $CD4^+$ DC defect, which did not recover with age.

Together these results show that the abrogation of the SIRPα-CD47 axis has a transient, yet selective effect on the homeostasis intestinal $CD103^+CD11b^+$ DCs and in the next chapter, I set out to explore the possible mechanisms governing this.

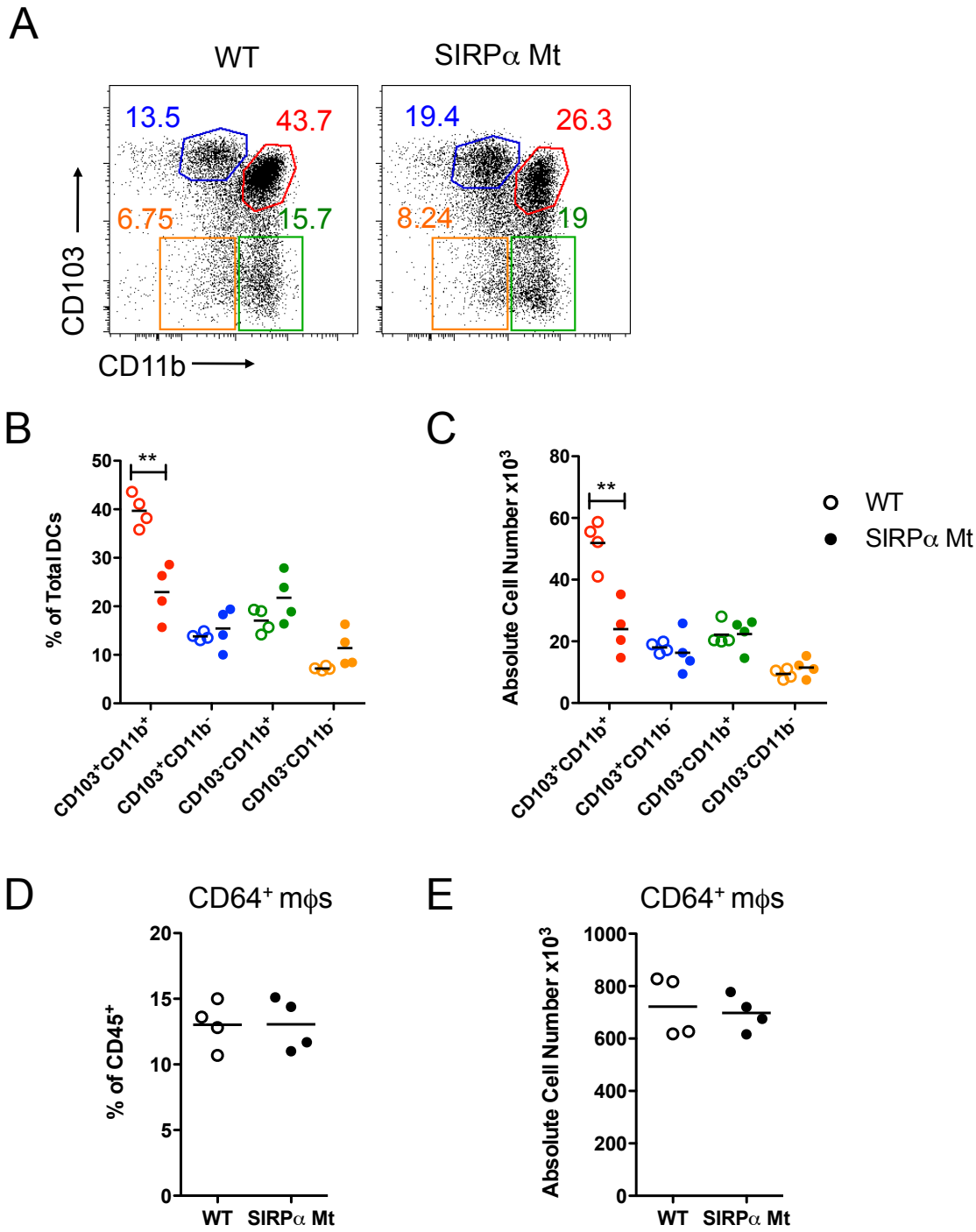

Figure 7.1: Effects of SIRPα mutation on MPs in SI LP

A. Representative dot plots showing identification of total DCs as CD64$^-$CD11c^{hi}B220$^-$ cells and mϕs as CD11c$^+$CD64$^+$ cells amongst single live CD45$^+$CD11c$^+$MHCII$^+$ MPs in SI LP digests from SIRPα mt or control WT mice. Total DCs were divided into four subsets on the basis of their expression of CD103 and CD11b. **B.** Proportion of each DC subset as a percentage of total DCs in SIRPα mt and control mice as gated in A. **C.** Absolute number of of each DC population in SIRPα mt mice compared with WT controls. **D.** Proportion of CD64$^+$ mϕs as a percentage of live CD45$^+$ cells in SIRPα mt and control mice. **E.** Absolute number of CD64$^+$ mϕs in SIRPα mt mice compared with controls. Data are representative of at least 10 independent experiments with n =3/4 per experiment. **p<0.01. Student's t test.

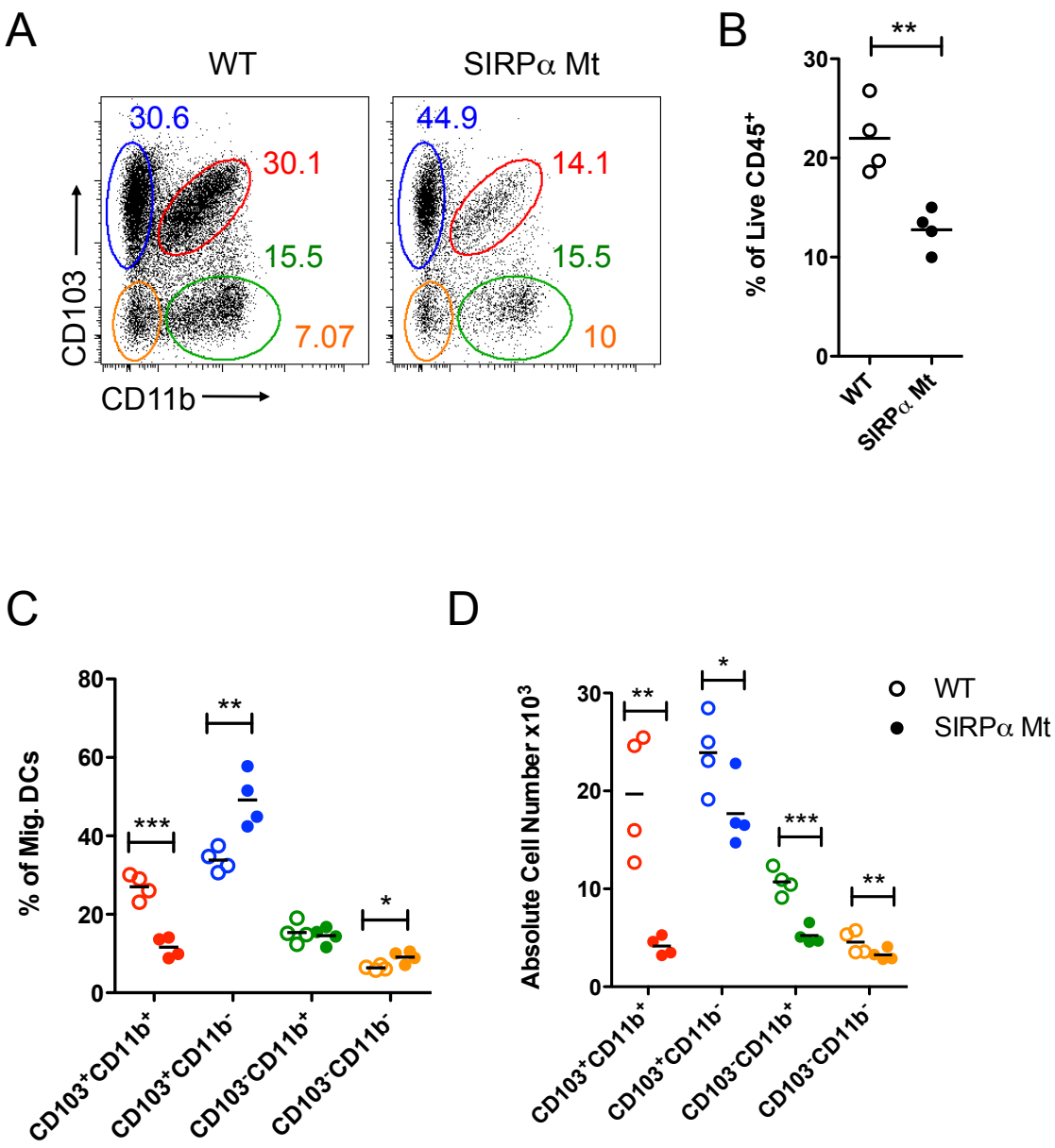

Figure 7.2: Effects of SIRPα mutation on migratory DCs in MLNs

A. Representative dot plots showing CD103 and CD11b expression on CD11c^{+}MHCII^{hi} migratory MLN DCs in SIRPα mt mice compared with WT controls. **B.** Proportion of CD11c^{+}MHCII^{hi} migratory DCs as a percentage of total DCs in MLNs of SIRPα mt and control mice. **C.** Proportion of each DC subset as a percentage of total migratory DCs as gated in A in MLNs of SIRPα mt and control mice**. D.** Absolute number of of each DC population in MLNs of SIRPα mt mice compared with WT controls. Data are representative of at least 10 independent experiments with n =3/4 per experiment. *p<0.05, **p<0.01, ***p<0.001. Student's t test.

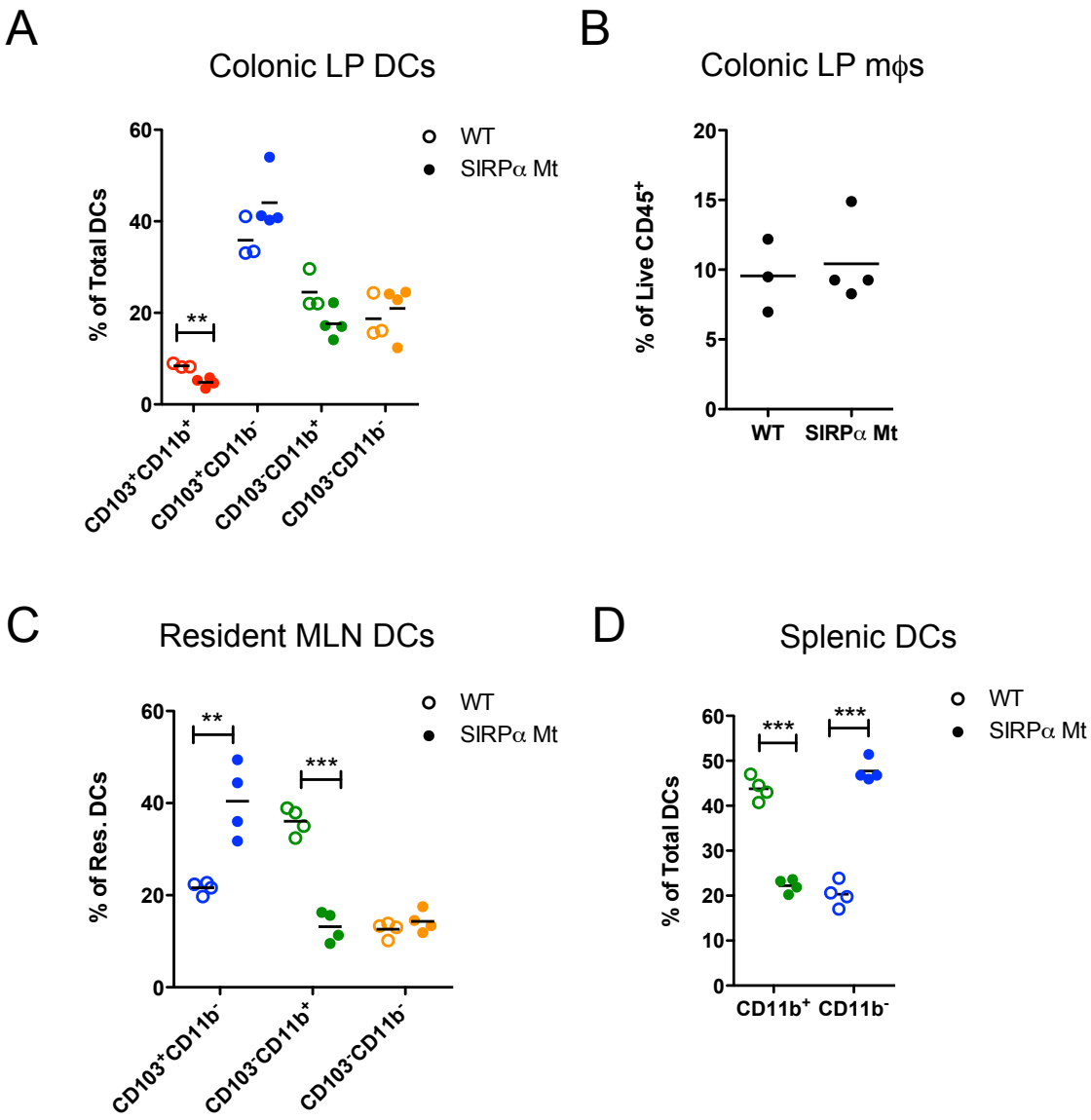

Figure 7.3: Effects of SIRPα mutation on colonic LP MPs and lymphoid tissue DCs
A. Proportion of each DC subset as a percentage of total DCs in colonic LP of SIRPα mt and control mice**. B.** Proportion of mϕs as a percentage of live CD45⁺ cells in colonic LP of SIRPα mt mice compared with controls. **C.** Proportion of each DC subset as a percentage of total resident DCs in MLNs of SIRPα mt mice compared with WT controls. **D.** Proportion of each DC subset as a percentage of total splenic DCs in SIRPα mt mice compared with WT controls. Data are representative of at least 3 independent experiments with n =3/4 per experiment. **p<0.01, ***p<0.001, Student's t test.

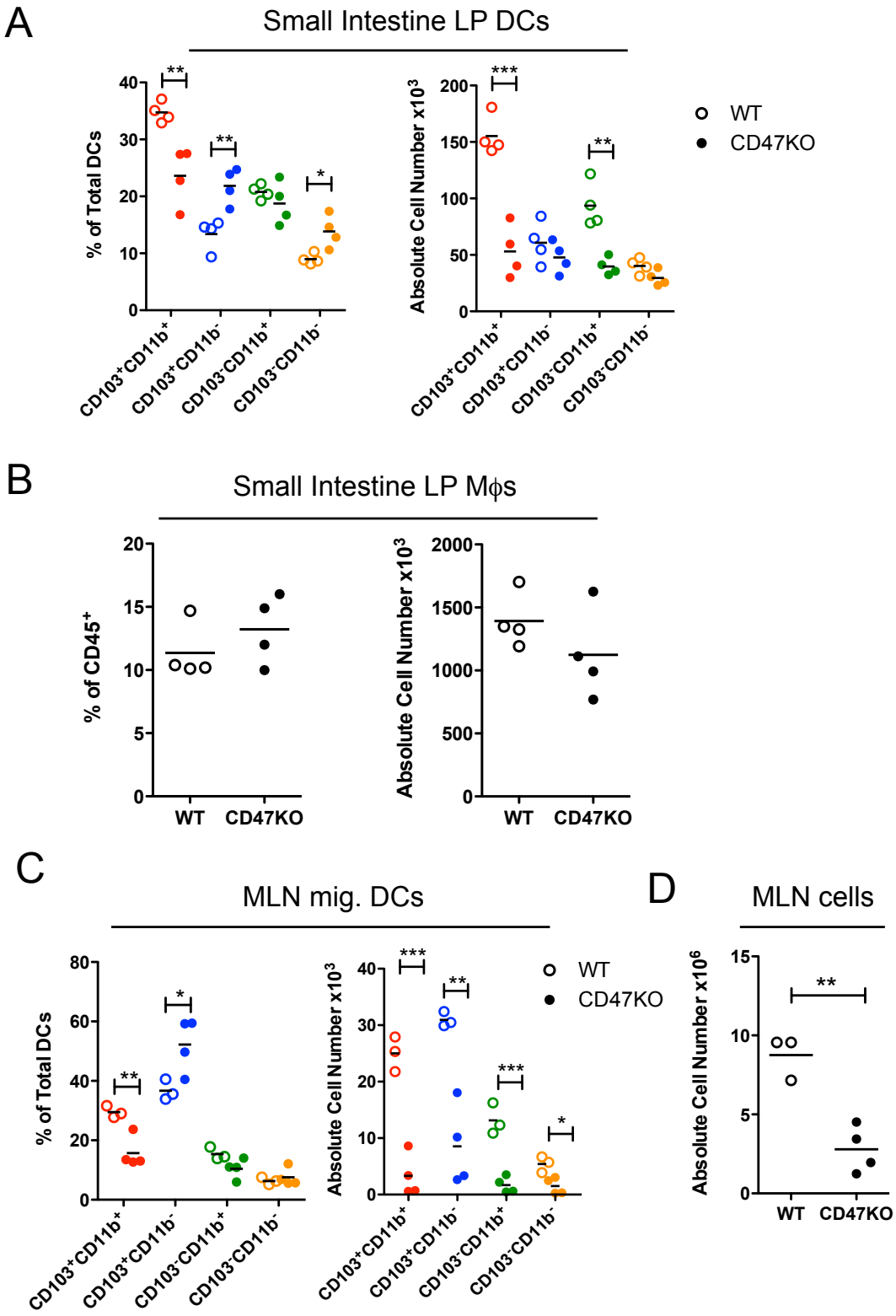

Figure 7.4: Effects of loss of CD47 on SI LP MPs and migratory MLN DCs

A. Proportion and absolute number of each DC subset as a percentage of total DCs in the SI LP of CD47KO and control WT mice. **B.** Proportion and absolute number of CD64⁺ mϕs as a percentage of live CD45⁺ cells in the SI LP of CD47KO and control mice. **C.** Proportion and absolute number of each DC subset as a percentage of total migratory DCs in MLNs of CD47KO and control mice. **D.** Absolute number of cells in MLNs of CD47KO mice compared with WT controls. Data are representative of at least 5 independent experiments with n =3/4 per experiment. *p<0.05, **p<0.01, ***p<0.001. Student's t test.

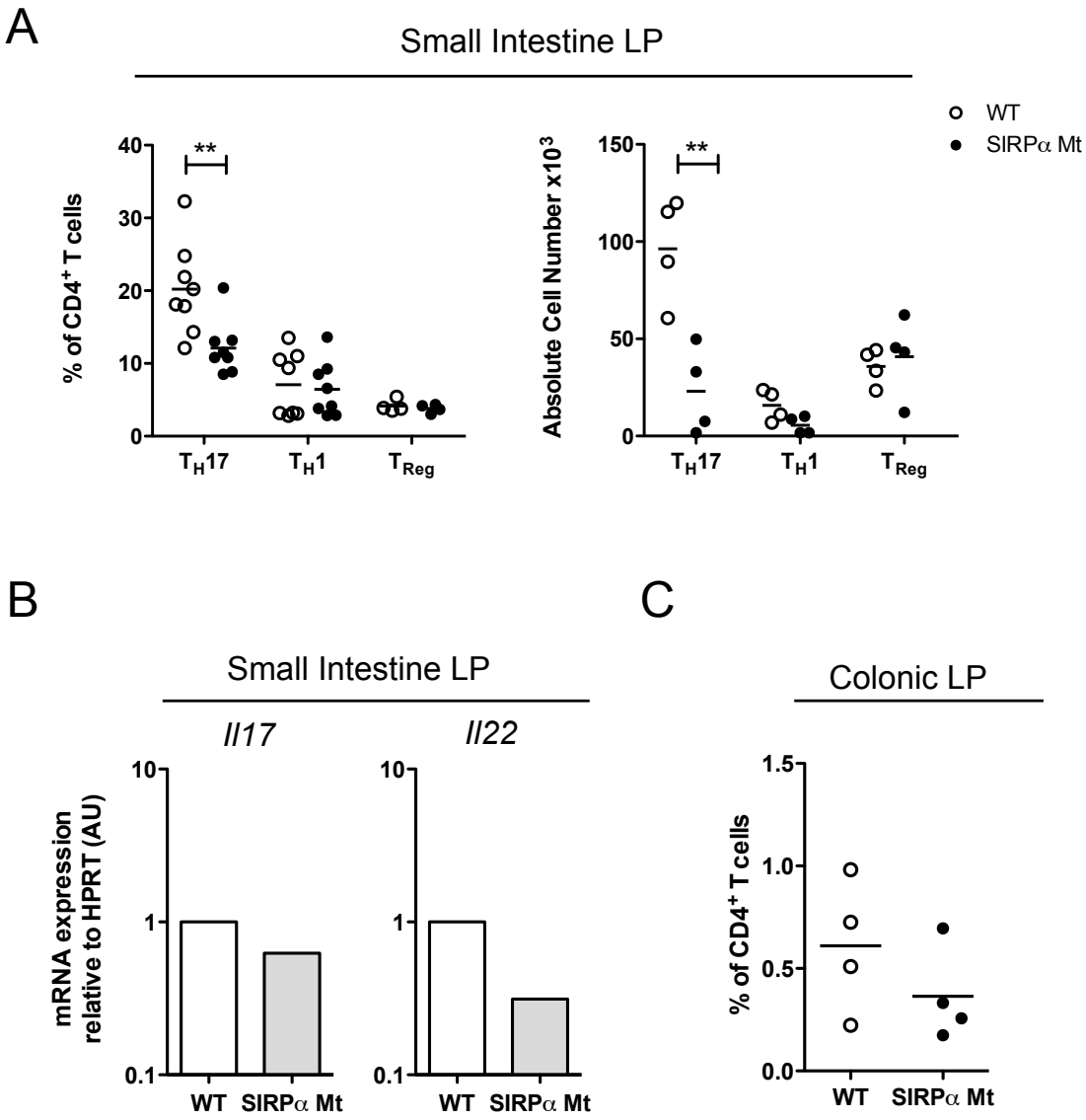

Figure 7.5: Effects of SIRPα mutation on CD4⁺ T cells in steady state intestine

A. Whole SI LP digests were restimulated with PMA and ionomycin in the presence of brefeldin A and monensin for 4.5 hours and CD4⁺ T cells were assessed for expression of IL17a, IFNγ and FoxP3 by intracellular staining. Frequencies and absolute numbers of T_h17, T_h1 and T_{Regs} amongst total live CD4⁺ T cells in the SI LP of SIRPα mt mice compared with WT controls. Data are representative of 2 independent experiments with n=4 per experiment. **p<0.01. Student's t test. **B.** Total CD4⁺ T cells were FACS-purified from SI LP of SIRPα mt mice and analysed by qRT-PCR for mRNA expression of *Il17* and *Il22.* Results shown are relative to HPRT using the $2^{-\Delta\Delta ct}$ method with WT T cells set to 1. Data are pooled from 2 independent experiments with 9 mice per experiment. **C.** Whole colonic LP digests were restimulated with PMA and ionomycin in the presence of brefeldin A and monensin for 4.5 hours and CD4⁺ T cells were assessed for expression of IL17a by intracellular staining. Frequencies of T_h17 cells amongst total live CD4⁺ T cells in the colonic LP of SIRPα mt mice compared with WT controls. Data are representative of 2 independent experiments with n=4 per experiment.

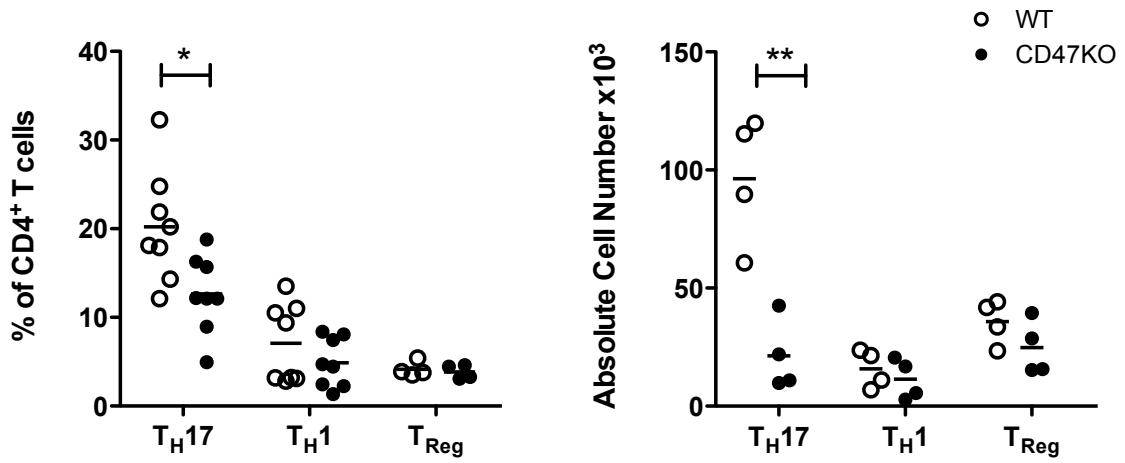

Figure 7.6: Effects of loss of CD47 on CD4⁺ T cell populations in steady state SI LP
Whole SI LP digests were restimulated with PMA and ionomycin in the presence of brefeldin A and monensin for 4.5 hours and CD4⁺ T cells were assessed for expression of IL17a, IFNγ and FoxP3 by intracellular staining. Frequencies and absolute numbers of T_h17, T_h1 and T_{Regs} amongst total live CD4⁺ T cells in the SI LP of CD47KO mice compared with WT controls. Data are representative of 2 independent experiments with n=4 per experiment. *p<0.05, **p<0.01. Student's t test.

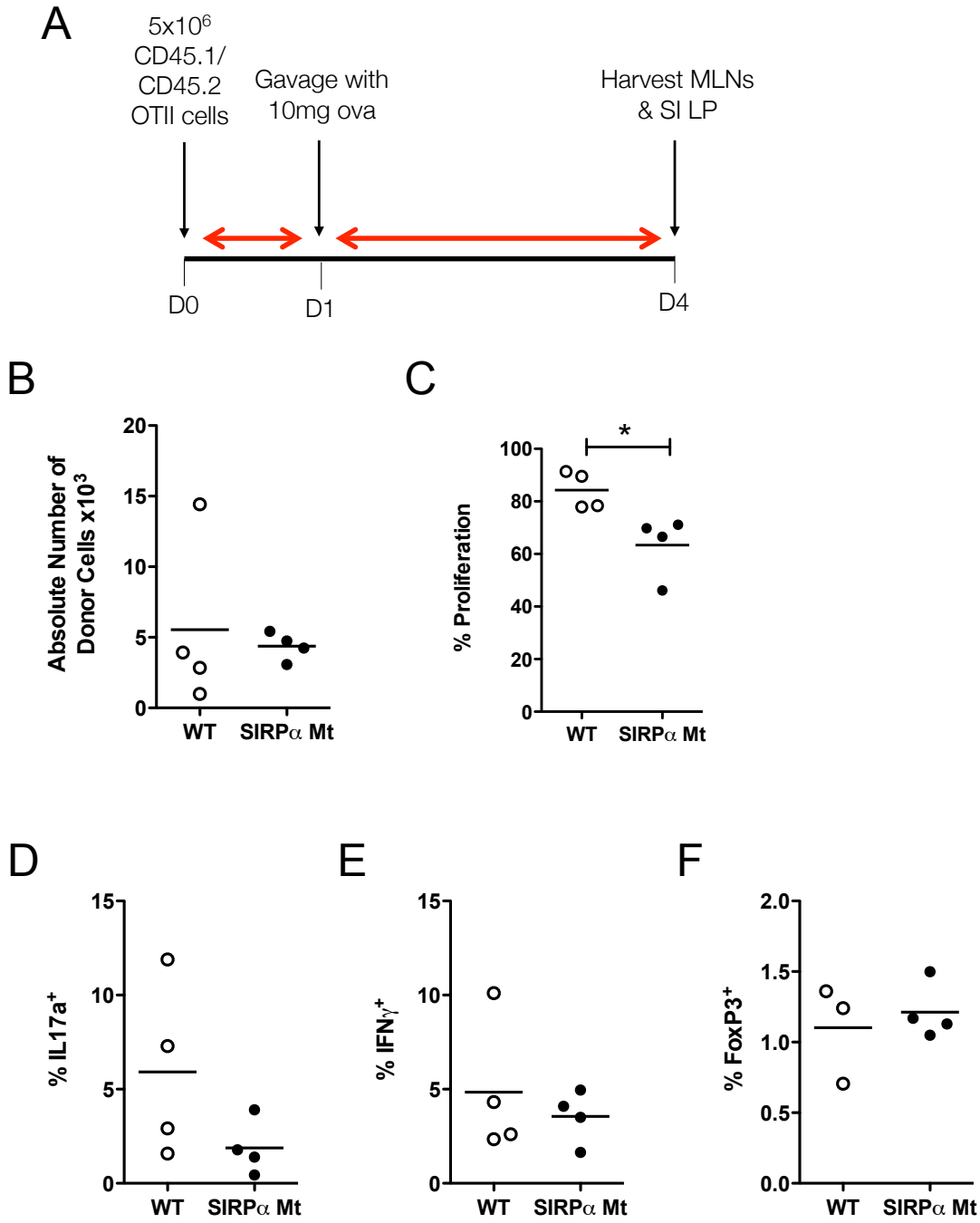

Figure 7.7: Priming of antigen-specific CD4⁺ T cells in SIRPα mt mice by oral administration of OVA

A. 5x10⁶ cells from the LNs of CD45.1/CD45.2 OTII mice were adoptively transferred into CD45.1⁺ WT or CD45.2⁺ SIRPα mt mice. 24 hours later mice received a single gavage of 10mg ovalbumin and 3 days later donor T cells were identified as CD45.2⁺ or CD45.1⁺ in the MLNs of WT or SIRPα mt mice respectively. **B.** Absolute number of OTII CD4⁺ T cells in MLNs of WT and SIRPα mt mice. **C.** Proliferation of OTII cells in the MLNs of WT and SIRPα mt mice as assessed by CFSE dilution. Results show the proportion of donor cells that had gone through at least one round of division as a percentage of total donor cells. **D-F.** Percentage of donor cells in MLN polarized to express (D) IL17a, (E) IFNγ or (F) FoxP3. Data are representative of 2 independent experiments with n=4 per experiment.

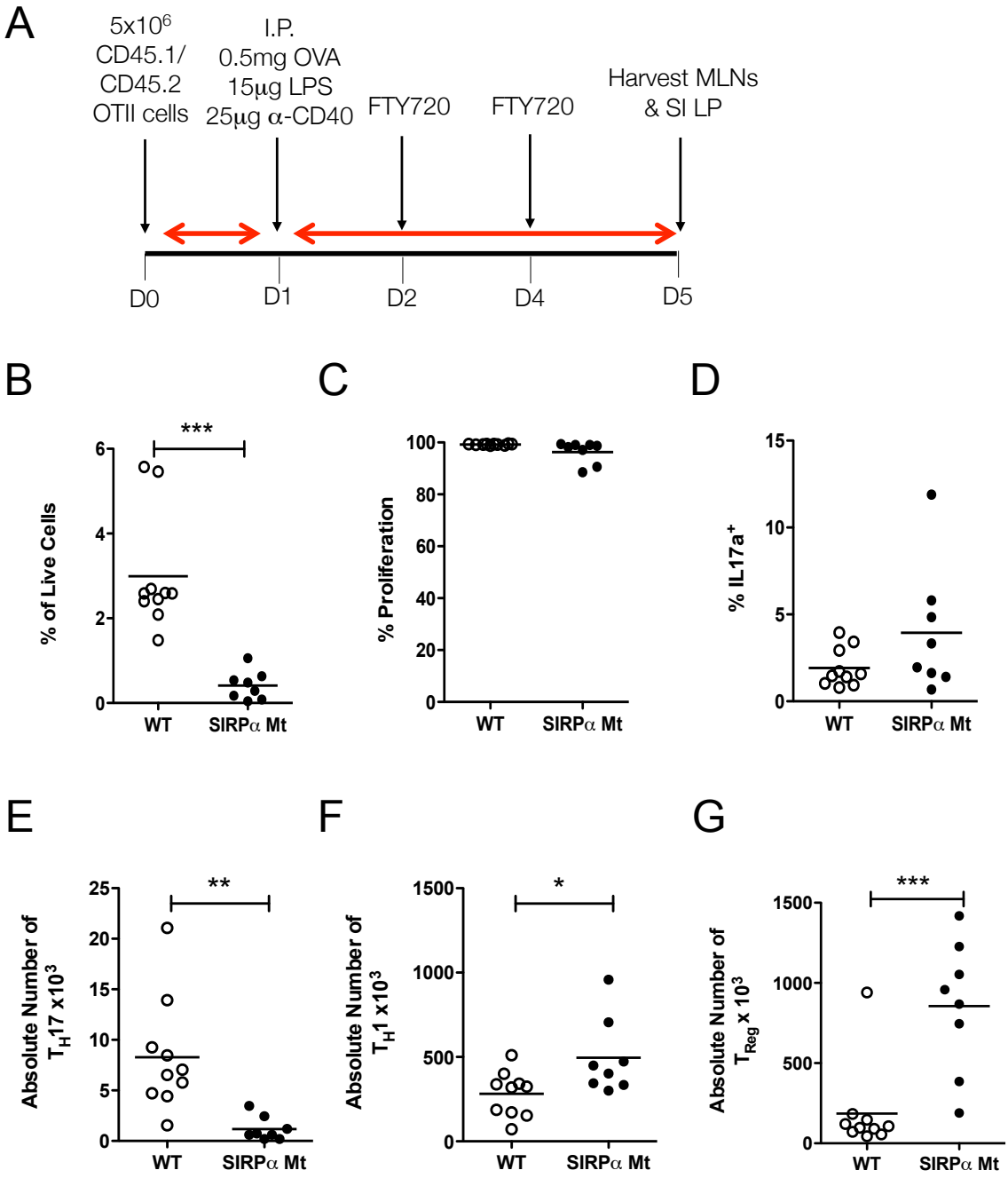

Figure 7.8: Priming of antigen-specific CD4⁺ T cells in SIRPα mt mice by i.p. administration of OVA, LPS and α-CD40

A. 5x10^6 cells from LNs of CD45.1/CD45.2 OTII mice were adoptively transferred into CD45.1$^+$ WT or CD45.2$^+$ SIRPα mt mice. 24 hours later mice received an i.p. injection of 0.5mg OVA together with 25μg α-CD40 and 15μg LPS, and 1 and 3 days later, mice were received 1mg/kg FTY720 i.p. On day 6 donor T cell proliferation was assessed in the MLNs. **B.** Proportion of OTII CD4$^+$ T cells in the MLNs of WT and SIRPα mt mice shown as a percentage of live cells. **C.** Proliferation of OTII cells in the MLNs of WT and SIRPα mt mice as assessed by CFSE dilution. Results show the proportion of donor cells that had gone through at least one round of division as a percentage of total donor cells. **D.** Percentage of donor cells in MLN polarized to express IL17a. **E-G.** Absolute number of donor cells in MLN polarized to induce (E) T_h17, (F) T_h1 or (G) T_{Reg} cells. Data are from a single experiment with n=8-10. *p<0.05, **p<0.01, ***p<0.001 Student's t test or Mann Whitney.

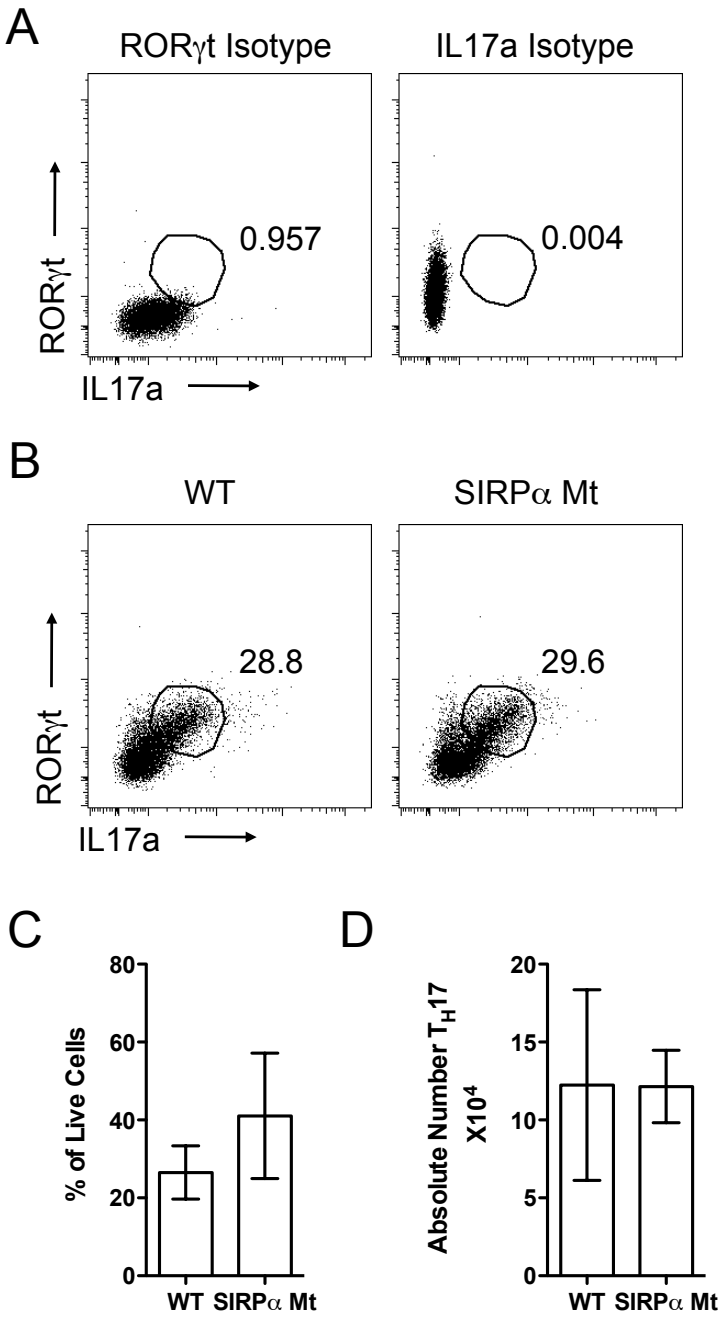

Figure 7.9: SIRPα mt mice have no intrinsic defect in ability to generate T_h17 cells
Naïve CD4$^+$ T cells were FACS-purified from MLNs of WT or SIRPα mt mice and cultured *in vitro* for 4 days with a T_h17 inducing cytokine cocktail, containing IL6, IL1β, IL23, TGFβ, anti-IL2, anti-IL4 and anti-IFNγ restimulated with PMA and ionomycin in the presence of brefeldin A and monensin for 4.5 hours and examined for expression of IL17a and RORγt by intracellular staining. **A.** Representative dot plots showing IL17a and RORγt isotype controls on cultured T cells from WT mice. Numbers indicate percentage of live cells. **B.** Representative dot plots showing IL17a and RORγt staining in WT and SIRPα mt cultures. Numbers indicate percentage of live cells. **C,D.** Mean frequencies (C) and absolute numbers (D) of RORγt$^+$ IL17a$^+$ T_h17 cells ±1SD amongst total live cells. Data are from a single experiment with n=3.

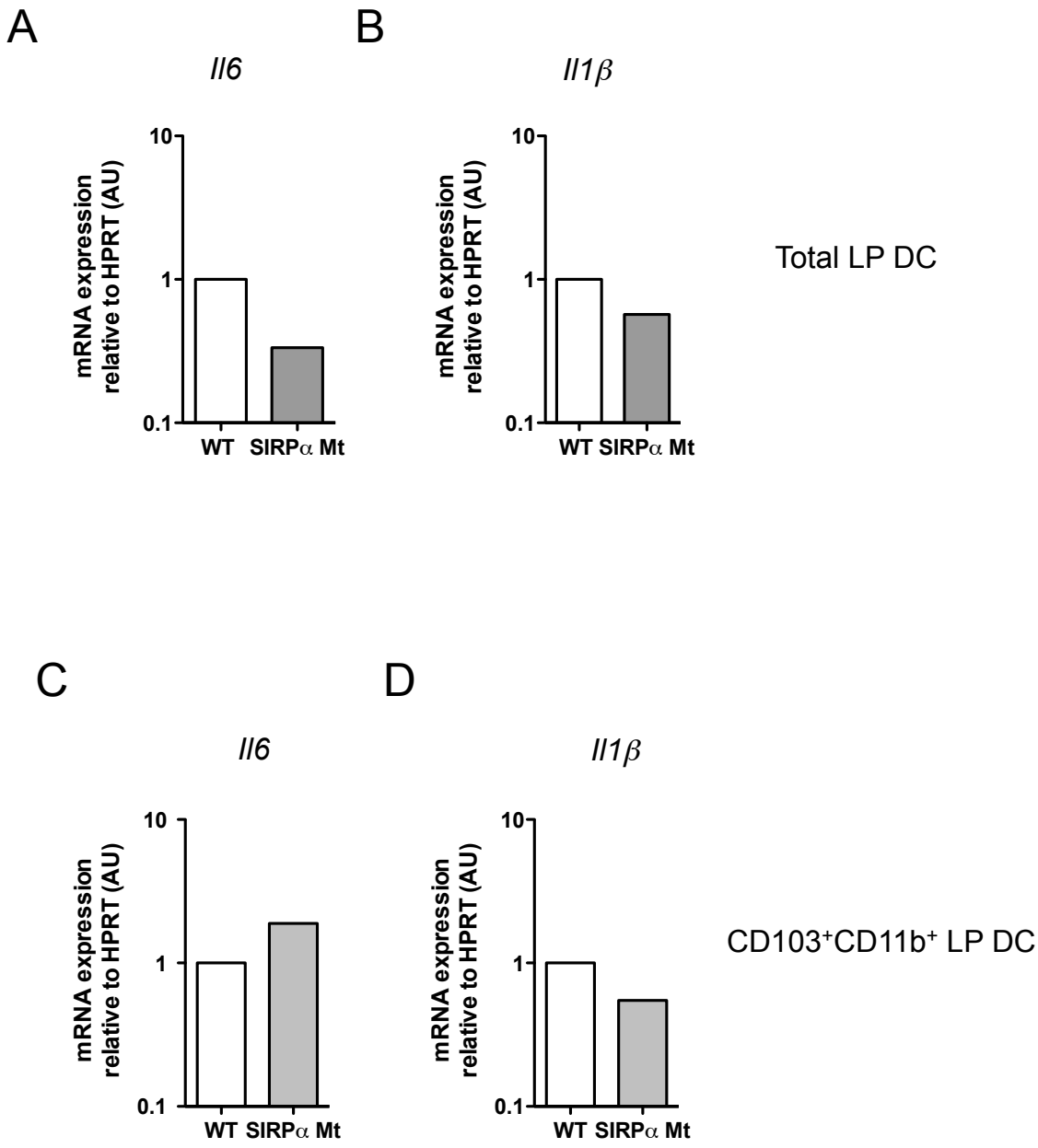

Figure 7.10: IL6 and IL1β expression by total and sorted CD103$^+$CD11b$^+$ DCs from SI LP from SIRPα mt mice

A-B. Total CD64$^-$ CD11c$^+$MHCII$^+$ DCs were FACS-purified from the SI LP of WT or SIRPα mt mice and analysed by qRT-PCR for expression of mRNA for (C) *Il6* and (D) *Il1β*. **C-D**. CD103$^+$CD11b$^+$ were FACS-purified from the SI LP of WT or SIRPα mt mice and analysed by qRT-PCR for expression of mRNA for (A) *Il6* and (B) *Il1β*. Results shown are relative to HPRT using the $2^{-\Delta\Delta ct}$ method with WT DCs set to 1. Data are pooled from 2 independent experiments with cells pooled from 9-12 mice per experiment.

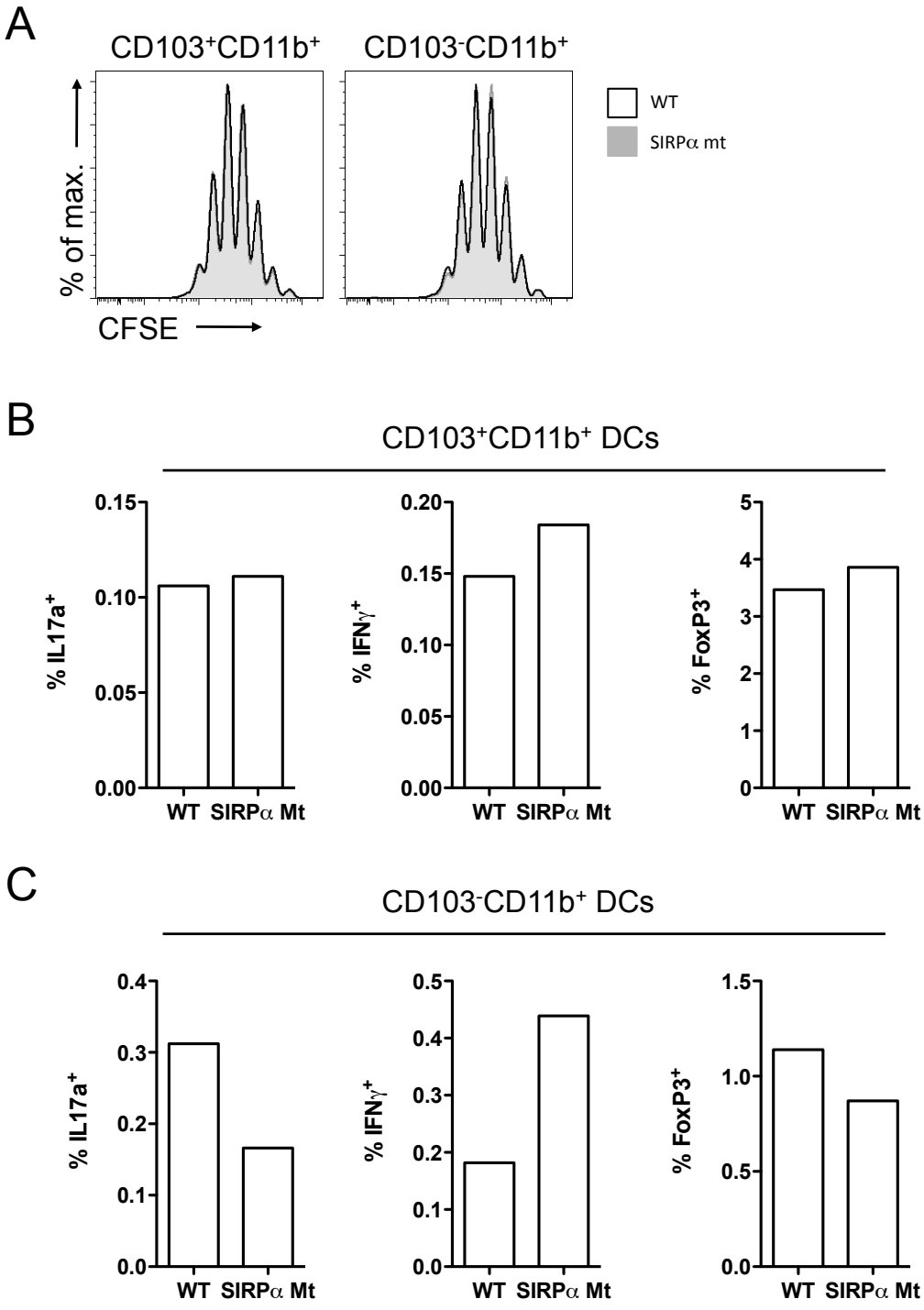

Figure 7.11: T_h17 polarising ability of CD103$^+$CD11b$^+$ and CD103$^-$CD11b$^+$ DCs from WT and SIRPα mt mice

3x10^4 SI LP CD103$^+$CD11b$^+$ and CD103$^-$CD11b$^+$ DCs from SIRPα mt or WT mice were pulsed with 2mg/ml OVA and co-cultured with 1x10^5 naïve CD4$^+$ T cells for 4 days. **A.** Proliferation of total live OTII cells co-cultured with WT (black line) or SIRPα mt (shaded grey) DCs as assessed by CFSE dilution. **B.** Percentage of IL17a$^+$, IFNγ$^+$ and FoxP3$^+$ T cells as a proportion of total live T cells from co-cultures of naïve CD4$^+$ T cells with CD103$^+$CD11b$^+$ DCs from WT and SIRPα mt mice. **B.** Percentage of IL17a$^+$, IFNγ$^+$ and FoxP3$^+$ T cells as a proportion of total live T cells from co-cultures of naïve CD4$^+$ T cells with CD103$^-$CD11b$^+$ DCs from WT and SIRPα mt mice. Data are from a single experiment.

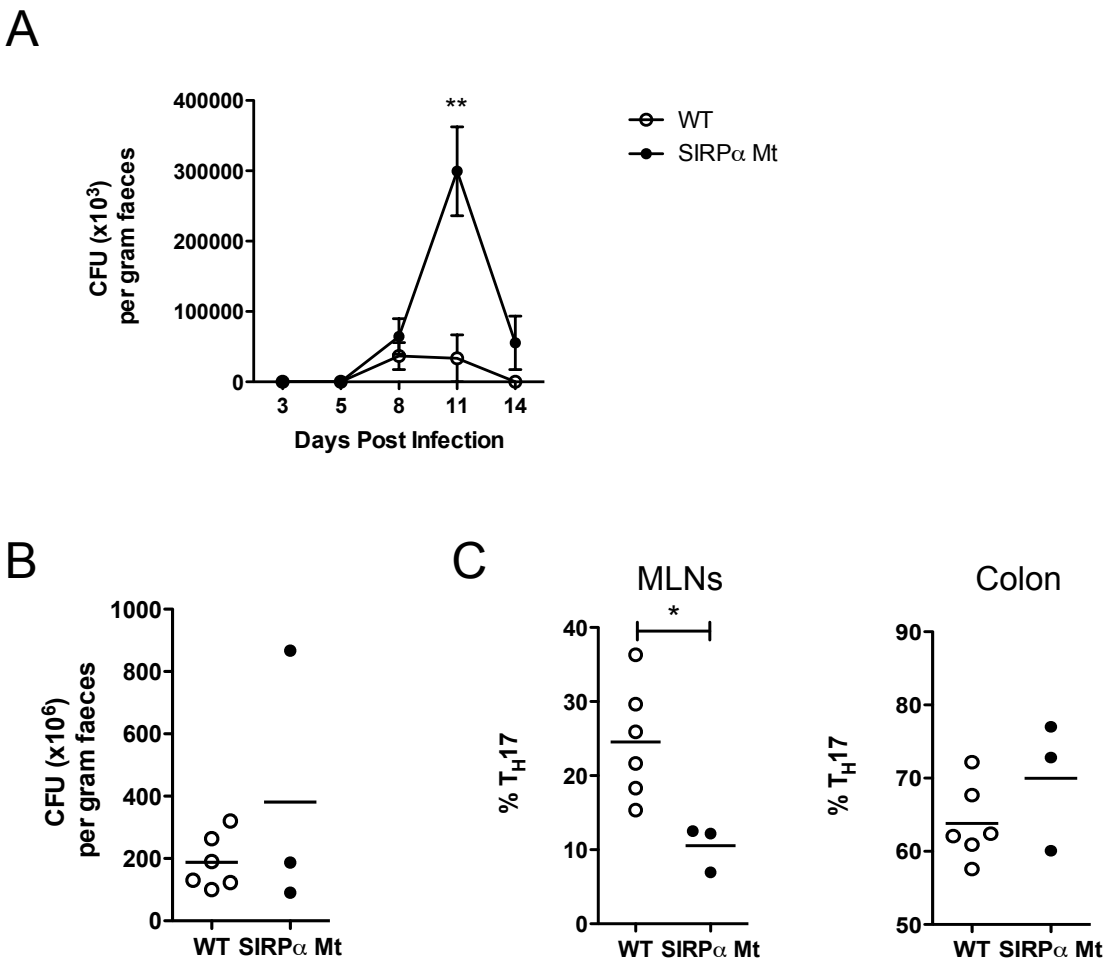

Figure 7.12: *Citrobacter rodentium* infection in SIRPα mt mice

WT and SIRPα mt mice were gavaged with 1x10^9 *C. rodentium* and infection was monitored by faecal CFU counts. **A.** Bacterial counts in faceces enumerated as CFU/gram of faeces. Data are from a single experiment with 10 WT and 8 SIRPα mt mice. **B.** CFU counts of *C. rodentium* per gram of faeces in SIRPα mt mice compared with WT controls on day 8 of infection. **C.** Following restimulation with PMA and ionomycin in the presence of brefeldin A and monensin, MLN and colonic LP isolates were examined for IL17a producing CD4$^+$ T cells by intracellular cytokine staining. Results show proportion of T_h17 cells as a percentage of total CD4$^+$ T cells in the MLN and colonic LP of SIRPα mt mice compared with WT controls on day 8 of infection. Data are from a single experiment with 6 WT and 3 SIRPα mt mice. *p<0.05, **p<0.01, Student's t test.

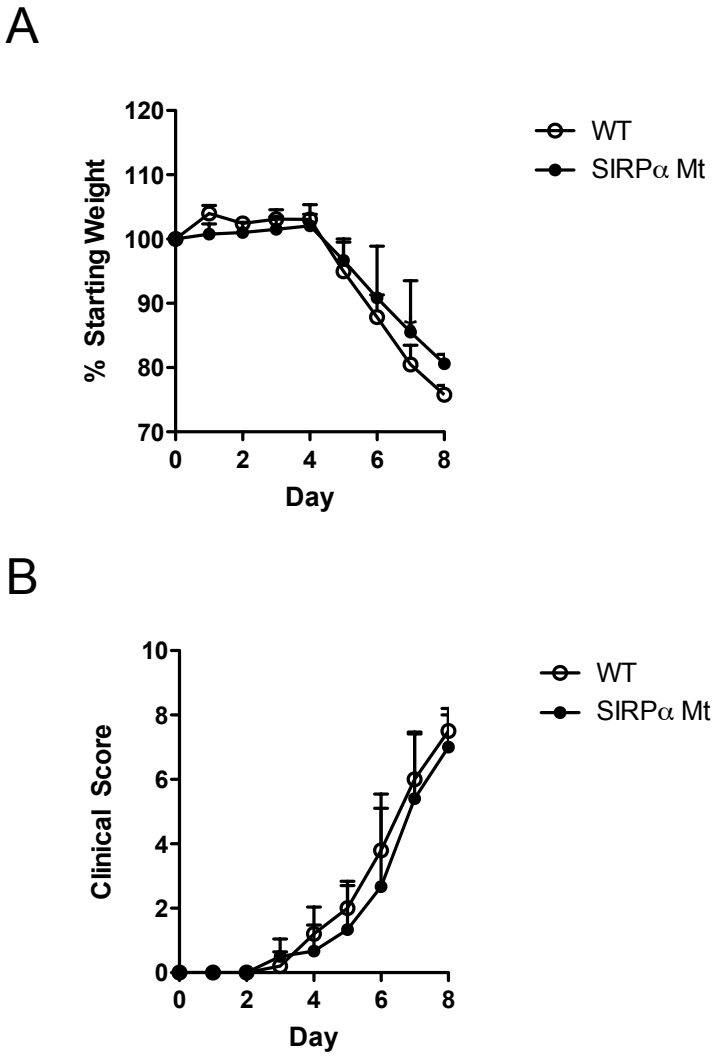

Figure 7.13: DSS colitis in SIRPα mt mice

WT or SIRPα mt mice received 2% DSS *ad libitum* in the drinking water for eight days. **A.** Weight loss was assessed daily and expressed as percentage of starting weight +1SD. **B.** Clinical scores +1SD calculated as described in Materials and Methods. Data are representative of 2 independent experiment with n=4-8 per experiment.

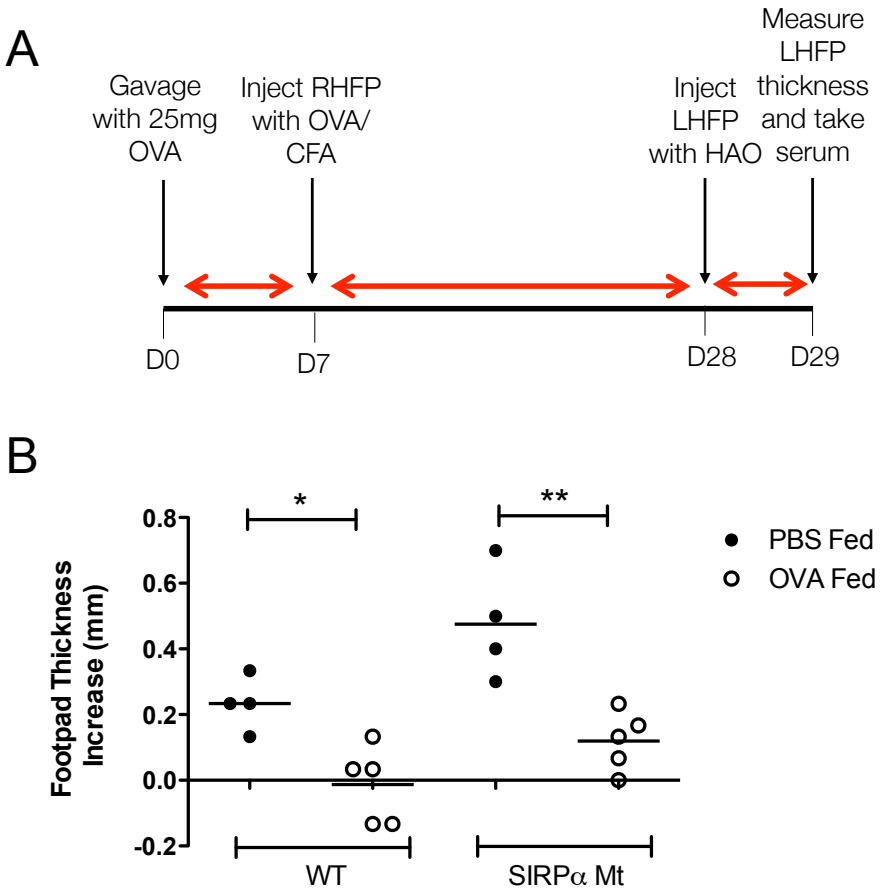

Figure 7.14: Induction of oral tolerance in SIRPα mt mice

A. WT or SIRPα mt mice were fed a single dose of 25mg OVA or PBS and immunized in the right hind footpad with OVA emulsified in CFA 7 days later. 21 days later, mice were challenged in the contralateral footpad with HAO and 24 hours later, OVA specific DTH responses were assessed by measuring the increase in footpad size. **A.** Schematic of oral tolerance protocol. **B.** OVA specific DTH responses are shown as the mean increase in footpad measurement of 4-5 mice per group and are representative of two independent experiments. *p<0.05, **p<0.01. One Way ANOVA with Bonferroni post-test.

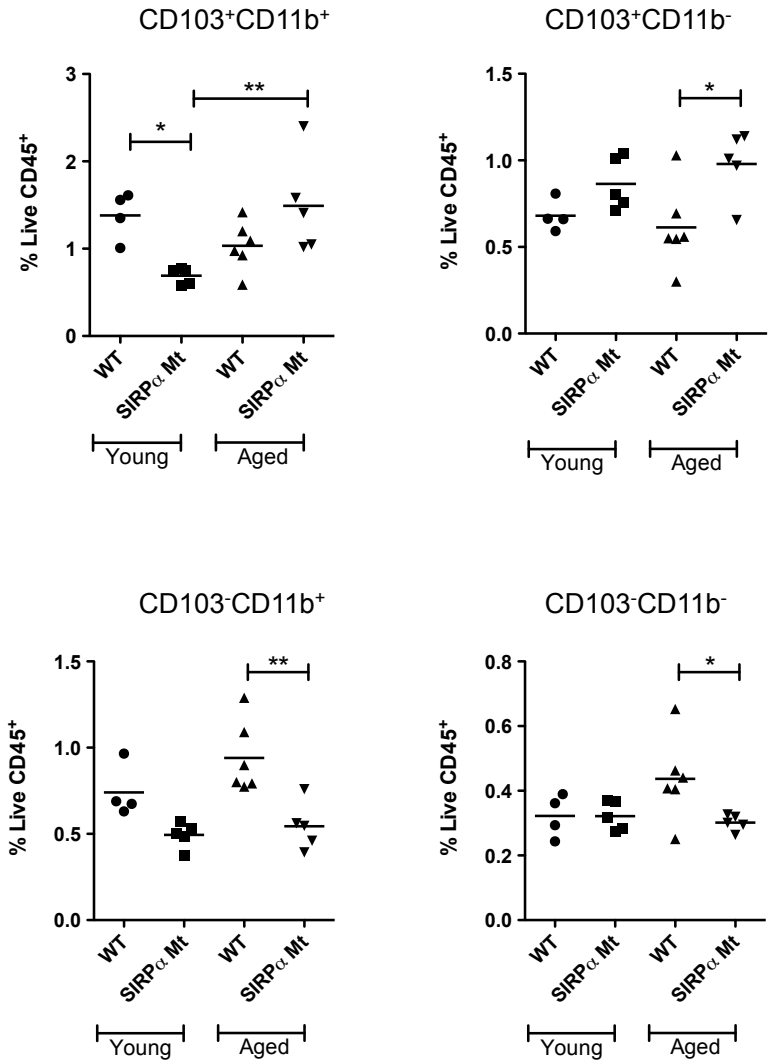

Figure 7.15: Effects of ageing on DC populations in SI LP of SIRPα mt mice

LP cells were isolated from the SI of 11 month old (aged) and 6-8 week old (young) WT and SIRPα mt mice and total DCs amongst live $CD45^+$ $CD11c^+$ $MHCII^+$ $CD64^-$ cells were divided into four subsets on the basis of their expression of CD103 and CD11b, by flow cytometry as shown in Fig. 7.1**.** Proportion of each DC subset as a percentage of live $CD45^+$ cells in young and aged WT and SIRPα mt mice**.** Data are from a single experiment with n=4-6 per group. *p<0.05, **p<0.01, two way ANOVA with Bonferroni post-test.

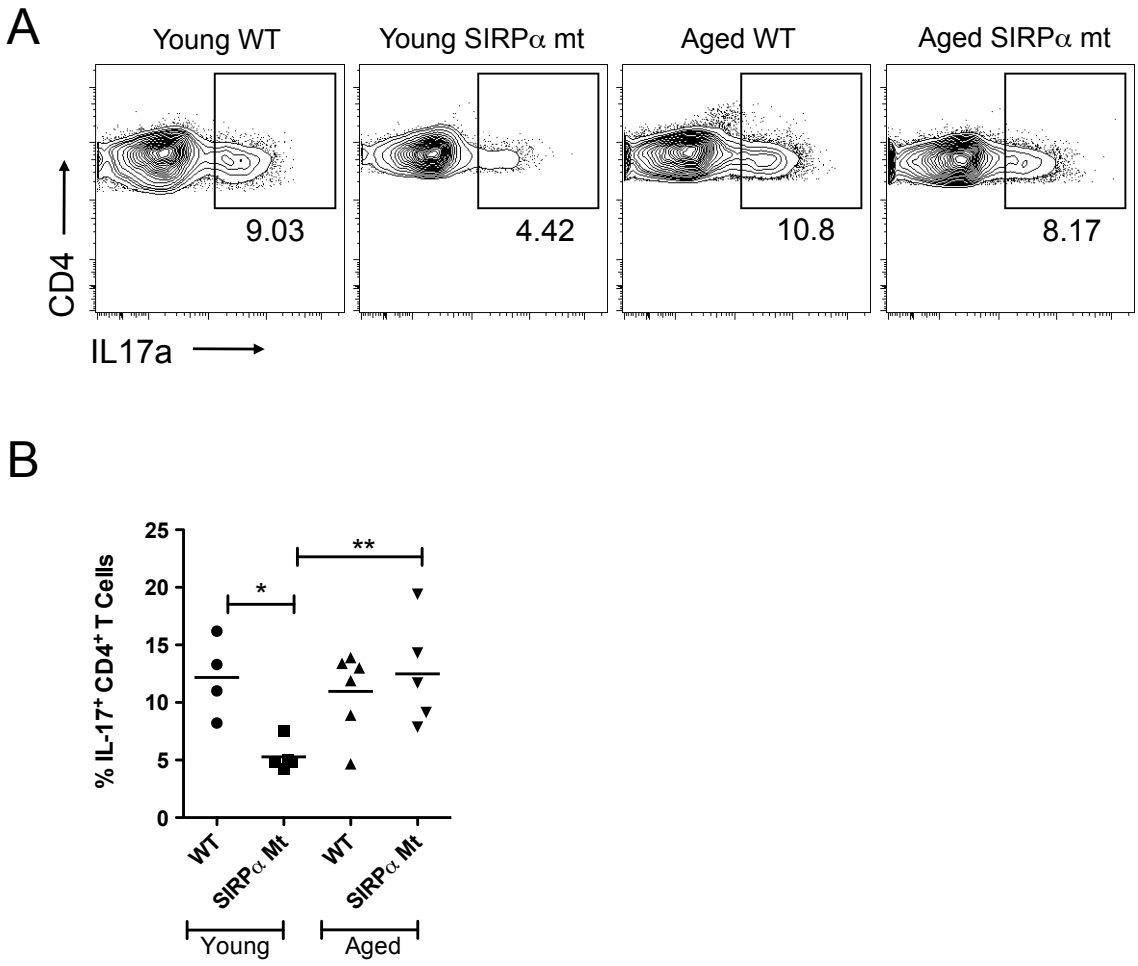

Figure 7.16: Effects of ageing on T_h17 cells in SI LP of SIRPα mt mice

LP cells were isolated from the SI of 11 month old (aged) and 6-8week old (young) WT and SIRPα mt mice, restimulated for 4.5hours with PMA and ionomycin in the presence of brefeldin A and monensin and IL17a-producing $CD4^+$ T cells were assessed by intracellular cytokine staining. **A.** Representative contour plots showing CD4 and IL17a staining on $CD4^+$ T cells in SI LP of young and aged WT and SIRPα mt mice. **B.** Proportion of $IL17^+$ $CD4^+$ T cells as a percentage of total $CD4^+$ T cells. Data are from a single experiment with n=4-6 per group. *p<0.05, **p<0.01, two way ANOVA with Bonferroni post-test.

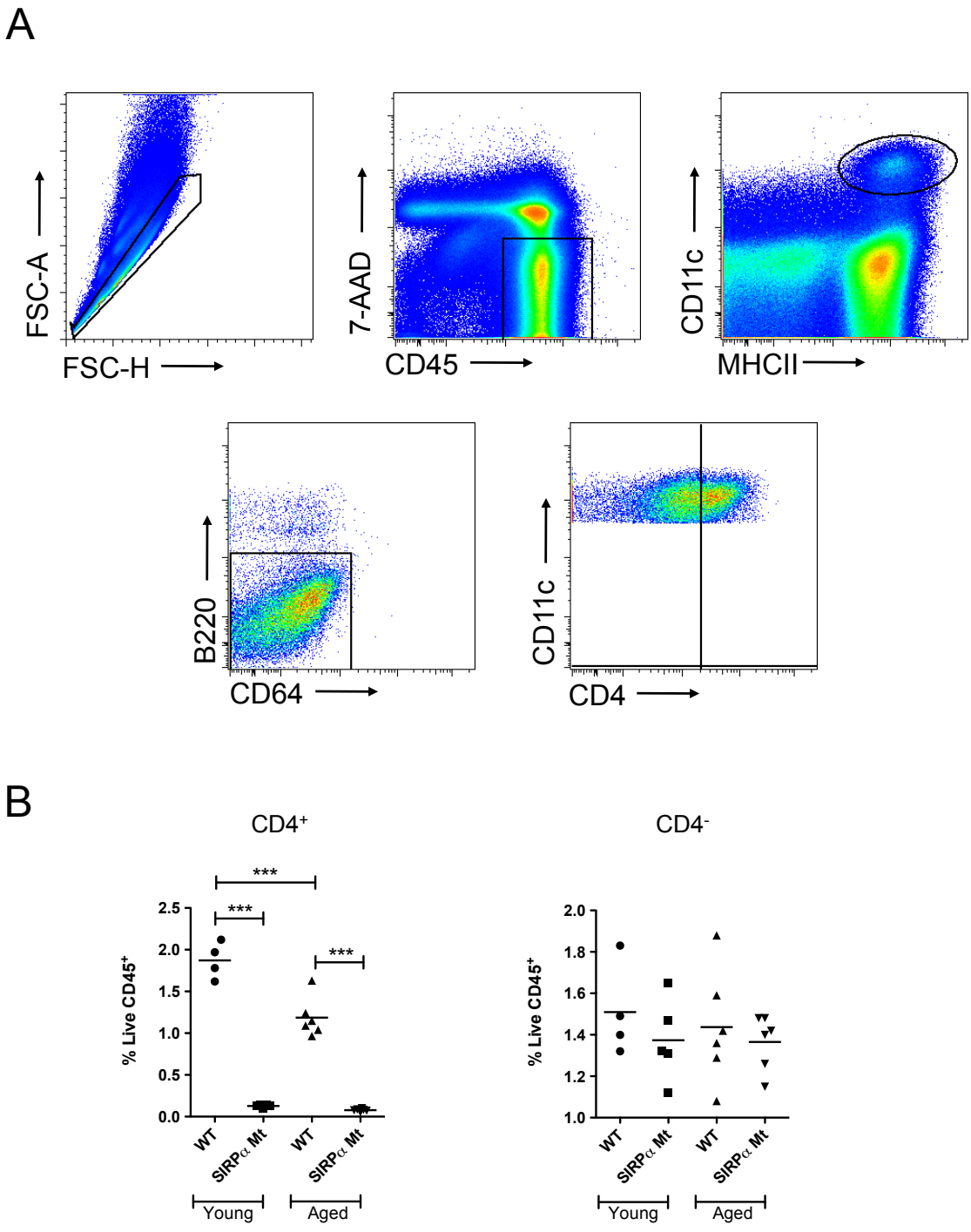

Figure 7.17: Effects of ageing on splenic DC populations in SIRPα mt mice

Splenocytes were isolated from resting 11 month old (aged) and 6-8week old (young) WT and SIRPα mt mice and DC populations were assessed by flow cytometry. **A.** DCs were identified as $CD11c^{+}MHCII^{+}$ cells amongst live $CD45^{+}$ cells and analysed for expression of CD4. **B.** Proportion of each DC subset as a percentage of total live $CD45^{+}$ cells. Data are from a single experiment with n=4-6 per group. ***p<0.001, two way ANOVA with Bonferroni post-test.

Chapter 8 Basis of Intestinal DC Defect in SIRPα Mutant Mice

8.1 Introduction

In the previous chapter I identified a selective defect in the proportion and number of $CD103^+CD11b^+$ DCs in the LP and MLNs of SIRPα mt and CD47KO mice. In this chapter, I set out to explore the basis of this defect by investigating the development, *in situ* proliferation, migration and survival of $CD103^+CD11b^+$ DCs in SIRPα mt mice compared with WT controls. In addition, I examined whether the SIRPα-dependent DC defect was cell intrinsic by generating WT:SIRPα mt mixed BM chimeras and tried to identify the $CD47^+$ cells in the LP which could be interacting with the $SIRP\alpha^+CD103^+CD11b^+$ DCs.

8.2 Expression of CD47 in the Intestinal Mucosa

Although CD47 is reported to be expressed ubiquitously (Barclay and Brown, 2006; Brown and Frazier, 2001), there is little information available regarding exactly which cells in which tissues express this receptor and to the best of my knowledge this has not been rigorously explored in the intestine. Therefore I decided to investigate which cells may be interacting with the $SIRP\alpha^+CD103^+CD11b^+$ DCs in the intestine, by identifying $CD47^+$ cells in the LP. Flow cytometric analysis of isolated cells revealed that both haematopoietic and non-haematopoietic cells expressed CD47, although at variable levels (Fig. 8.1A). Examination of the intestinal MP populations identified in Chapter 3 showed that most of the DC subsets expressed CD47 at similar levels, with the $CD103^+CD11b^+$ DCs perhaps expressing slightly lower levels that the other populations (Fig. 8.1B). $CD11c^+MHCII^+$ $F4/80^+$ mϕs also expressed similar levels of CD47 (Fig. 8.1C). This widespread expression of CD47 made it unlikely that I would be able to determine which specific cell types were interacting with $SIRP\alpha^+CD103^+CD11b^+$ DCs on the basis of CD47 expression alone. As multi-colour microscopy techniques that might allow interacting $CD47^+$ cells to be identified precisely were not yet established in our lab, I did not take this analysis any further. Instead this will be a focus for a new PhD student in the lab.

8.3 DC Development in the Absence of SIRPα Signalling

I hypothesised that SIRPα might affect the homeostasis of $CD103^+CD11b^+$ DCs at one or more of the different phases of DC lifespan: generation or migration of precursors to the intestinal mucosa, subsequent differentiation and/or proliferation in the mucosa, survival of mature DC, or their migration out of the LP into the MLN. First I examined the role of SIRPα in the development of $CD103^+CD11b^+$ DCs from their precursors. SIRPα mt and WT mice had similar proportions and numbers of pre-DCs in the BM (Fig. 8.2A). Similar results were obtained when pre-DCs when examined in blood (Fig. 8.2B). Next, I performed competitive adoptive transfers in which a 50:50 mix of pre-DCs from $CD45.1^+$ WT and $CD45.2^+$ SIRPα mt BM was transferred into unmanipulated CD45.1/CD45.2 WT recipients (Fig. 8.3A). Because of difficulties in obtaining sufficient cells from both strains simultaneously, I had to use separate adoptive transfer experiments to examine pre-DC development at each time point after transfer.

As I showed in Chapter 4, 3 days after transfer all four DC populations could be seen amongst the progeny of transferred pre-DCs in the SI LP, although there were few donor-derived $CD103^+CD11b^+$ DCs at this time (Fig. 8.3B). Interestingly, approximately 80% of donor-derived $CD103^+CD11b^+$ DCs were from the SIRPα mt pre-DCs at this time (Fig. 8.3C), whereas the other DC populations retained the approximately 50:50 ratio of WT:SIRPα mt found in the original transfer mix (Fig. 8.3D). A similar pattern was observed 5 days after transfer, where although all DC populations were present amongst donor-derived cells (Fig. 8.4B), the majority (~70%) of $CD103^+CD11b^+$ DCs was derived from SIRPα mt pre-DCs (Fig. 8.4C). At this time, there was also a slight bias towards $CD103^+CD11b^-$ DCs being derived from SIRPα mt pre-DCs, whereas both $CD103^-$ DC populations were derived from WT and SIRPα mt pre-DCs in equal ratios (Fig.8.4D). By day 7, the SIRPα mt pre-DCs no longer had an advantage over the WT pre-DCs in terms of generating $CD103^+CD11b^+$ DCs, with the proportions of each now being almost identical to the transferred population (Fig. 8.5B,D). The other DC populations also showed no preference towards WT or SIRPα mt origin at this time (Fig. 8.5D).

Having established that SIRPα mt pre-DCs appear to generate $CD103^+CD11b^+$ DCs in the LP more rapidly than their WT counterparts, I

hypothesised that these should then be detected sooner in the MLNs of recipient mice. As my previous adoptive transfer using WT pre-DCs and BrdU incorporation studies had indicated that DCs take approximately 48 hours to transit from the SI LP to the MLNs, I examined the fate of the mixed pre-DCs in the MLNs 5 and 7 days after transfer. Due to the fact that only small numbers of donor cells could be found in the recipient MLNs, I could only analyse total $CD11c^+MHCII^+$ DCs rather than defining resident and migratory DCs separately. However this should not affect the identification of LP-derived $CD103^+CD11b^+$ DCs, as these can only be found within the migratory DC population of the MLNs (Fig. 3.6). 5 days after transfer, I found the same bias towards the $CD103^+CD11b^+$ DCs in MLN being derived from $CD45.2^+$ SIRPα mt pre-DCs as I had seen in the LP (Fig. 8.6B). This was paralleled by a decrease in the proportion of $CD103^+CD11b^-$ derived from SIRPα mt pre-DCs, while all $CD103^-$ DCs showed same ratio as in injected mixture (Fig. 8.6B). These differences were not seen 7 days after transfer, when all DC subsets showed same ratio of WT:SIRPα derived cells as in the transferred pre-DCs (Fig. 8.6C). Together these results suggest SIRPα mt pre-DCs may generate $CD103^+CD11b^+$ DCs more efficiently than WT pre-DCs in LP and as a result of this increased maturation, these migrate to the MLN more quickly than WT DCs. As these experiments were done with small numbers of mice, repeat studies are required to verify these results. However it is clear that these results cannot explain the selective $CD103^+CD11b^+$ DC defect observed in the LP and MLNs of SIRPα mt mice. Indeed they indicate that an increased ability to generate $CD103^+CD11b^+$ DCs in these mice must be counteracted by even more potent mechanism which depletes these cells.

8.4 *In Situ* Proliferation of DCs in SIRPα Mt Mice

To explore this, I first examined if the lower numbers of $CD103^+CD11b^+$ DCs in SIRPα mt LP might reflect reduced proliferation of this DC population *in situ.* To investigate this, WT and SIRPα mt mice were given a single i.p. injection of BrdU and DCs in the SI LP were assessed for BrdU incorporation 3 hours later. This time was chosen on the basis of my results in Chapter 4, which had shown that no $BrdU^+$ pre-DCs were present in the blood at this time point and hence any $BrdU^+$ cells in the LP would be the result of *in situ* proliferation. Approximately 2% of $CD103^+CD11b^+$ DCs in both SIRPα mt and WT LP were $BrdU^+$ at this time and

there were also no differences in the levels of BrdU incorporation by the other DC subsets in SIRPα mt SI LP compared with WT controls (Fig. 8.7). Thus *in situ* proliferation does not appear to account for the differences in the number of $CD103^+CD11b^+$ DCs in SIRPα mt mice.

8.5 Activation Status of DCs in SIRPα Mt Mice

As SIRPα is primarily thought to be an inhibitory receptor, I next investigated if the lack of functional SIRPα signalling increased the activation status of $CD103^+CD11b^+$ DCs, with the hypothesis that over-activation of the DCs may be detrimental to the viability of $CD103^+CD11b^+$ DCs and thus contribute potentially explain the defect observed in these DCs in SIRPα mt mice. Therefore I assessed the expression of the co-stimulatory molecules, CD40, CD80 and CD86 on SI LP DCs from WT and SIRPα mt mice. This showed that $CD103^+CD11b^+$ DCs from SIRPα mt mice expressed similar levels of CD40 and CD80 as WT controls, but expressed significantly more CD86 (Fig. 8.8A,B). This increase in CD86 expression was not seen with the other subsets of DCs in SIRPα mt LP, although SIRPα mt $CD103^-CD11b^-$ DCs had decreased expression of CD80 and SIRPα mt $CD103^+CD11b^-$ DCs had decreased CD40 expression compared with WT controls (Fig. 8.8C). However, it should be noted that these differences in co-stimulatory molecule expression were all minor compared with the ~50% increase in CD86 expression seen with SIRPα mt $CD103^+CD11b^+$ DCs. All other co-stimulatory molecule expression patterns were identical in WT and SIRPα mt LP DCs.

8.6 Migration of DCs to MLNs

As my competitive adoptive transfer studies suggested that SIRPα mt $CD103^+CD11b^+$ SI LP DCs might transit to the MLNs more quickly than WT counterparts, I next examined this directly. To do this, I collaborated with Dr. Simon Milling's lab to investigate DC subsets in pseudo-afferent intestinal lymph. For this, WT and SIRPα mt mice underwent mesenteric lymphadenectomy (MLNx) and were left for 6 weeks to allow reanastomosis of the lymphatics before lymph was collected by cannulation of the thoracic duct. The collected lymph thus consists mostly of lymph that drains the intestine, containing the DCs that would have previously drained to the MLNs (Cerovic et al., 2013). DCs were identified in

lymph as single, live $CD45^+$, $B220^-$, $CD64^-$, $CD11c^+$ and $MHCII^+$ cells (Fig. 8.9A) and as with both SI LP and migratory DCs in the MLNs, lymph DCs could be divided into four distinct subsets based on CD103 and CD11b expression (Fig. 8.9B). Consistent with recent work from the Milling lab (Cerovic et al., 2013), the proportions of DCs in lymph mirrored those found amongst migratory MLN DCs, with the $CD103^+CD11b^+$ DCs dominating, followed by the $CD103^+CD11b^-$ and finally the two smaller populations of $CD103^-$ DCs, the majority of these being $CD11b^+$. Somewhat unexpectedly, all these subsets were found in similar proportions in SIRPα mt and WT lymph, apart from $CD103^+CD11b^-$ DCs, which were increased in proportion in SIRPα mt lymph compared with WT lymph (Fig. 8.9C). Unfortunately this technique does not allow quantitation of DC numbers in lymph, but the apparently normal proportions of $CD103^+CD11b^+$ DCs in SIRPα mt lymph could reflect the increased efficiency of migration to the MLNs, counterbalancing the reduced numbers of these cells in the LP. Alternatively, it may be because the mice used in this experiment had to be relatively old due to the need to wait for lymphatic re-anastomosis and as I showed earlier, the DC defect in SIRPα mt may be reduced with age. Further investigation is required to determine if the SIRPα mt $CD103^+CD11b^+$ DCs do indeed migrate more efficiently than WT counterparts.

8.7 DC Survival in SIRPα Mt Mice

Next I investigated if survival of the $CD103^+CD11b^+$ DCs was impaired in SIRPα mt mice. For this, I started by examining MLNs, reasoning that as the digestion process used to isolate the DCs from this tissue was less extensive, the isolated DCs would be in better condition for analysis. Total cell isolates were stained with Annexin V and 7-AAD to identify apoptotic (Annexin V^+ 7-AAD^-) and dead (Annexin V^+ 7-AAD^+) cells. Although there was considerable variability, this showed significantly more apoptotic cells amongst the $CD103^+CD11b^+$ subset of migratory DCs in SIRPα mt MLNs compared with WT controls (Fig. 8.10). There were no differences in apoptosis amongst the other migratory DC populations in SIRPα mt and WT MLNs (Fig. 8.10). I next attempted to study apoptosis amongst freshly isolated SI LP DCs, but no differences could be detected in any of the DC populations between WT and SIRPα mt mice (Fig. 8.11A). However the overall levels of apoptosis were much lower in this experiment than I had observed in the

MLNs and I reasoned that many cells that might have been undergoing apoptosis *in situ* may have been killed during the lengthy digestion process needed to obtain LP cells. In an attempt to overcome this, I isolated cells from the SI LP of WT and SIRPα mt mice and cultured them for 3 hours at 37°C *ex vivo* before examining Annexin V and 7-AAD staining on the DC populations. Again, no differences were observed between any of the DC subsets in WT and SIRPα mt mice (Fig. 8.11B) and the proportions of apoptotic cells remained low, except for $CD103^+CD11b^-$ DCs from both strains.

With the ongoing difficulties with the Annexin V assay, I sought to find another method for examining apoptosis in intestinal DCs. Tunel staining *in situ* was not feasible as it would not allow the identification of $CD103^+CD11b^+$ DCs. Therefore I decided to examine the expression of the pro-apoptotic gene *Caspase 3* in $CD103^+CD11b^+$ DCs FACS-purified from the SI LP of WT and SIRPα mt mice. This showed a 2-fold increase in the expression of *Caspase 3* in $CD103^+CD11b^+$ DCs isolated from SIRPα mt mice compared with the WT subset (Fig. 8.12). However SIRPα mt $CD103^+CD11b^+$ DCs also showed a similar increase in the anti-apoptotic *Bcl2* gene (Fig. 8.12,) making it difficult to assess the significance of the Caspase 3 results and thus further experiments are required to clarify the relative expression of pro- and anti-apoptotic genes. Furthermore, as I did not have RNA from the other DC subsets, it is not clear if these changes in gene expression are specific to the $CD103^+CD11b^+$ DC subset. In the future, protein levels will be also be investigated, as this may be more relevant, especially given the presence of inactive pro-caspase 3.

At the time I was carrying out these studies, our collaborators in Lund found a similar survival defect in $CD103^+CD11b^+$ DCs in mice with a DC-specific deletion of the transcription factor IRF4 (Persson et al., 2013b). Therefore, I decided to examine if the SIRPα mutation might be acting by downregulating this pathway by assessing the expression of *Irf4* in the $CD103^+CD11b^+$ DCs FACS-purified from the SI LP of WT and SIRPα mt mice. However, this revealed a 5-fold increase in expression of *Irf4* in the $CD103^+CD11b^+$ DCs isolated from the SIRPα mt mice compared with their WT counterparts (Fig. 8.12), indicating that the reduction in $CD103^+CD11b^+$ DCs in SIRPα mutant mice is not due to defective IRF4

expression and suggesting that IRF4 may actually be upregulated to compensate for the lack of SIRPα signalling.

In a further attempt to examine the survival of $CD103^+CD11b^+$ DCs in the SI LP of SIRPα mt mice, I next FACS-purified these DCs from the SI LP of $CD45.1^+$ WT and $CD45.2^+$ SIRPα mt mice, mixed them in a 50:50 ratio and cultured them for 16 hours before analysing cell death by 7-AAD staining. In this study I digested the SI from the two strains in the same tube, thus avoiding any bias at the digestion stage. The pooled $CD103^+CD11b^+$ DCs were then separated by FACS-purification on the basis of CD45.1 and CD45.2 expression, before being mixed back together at a 50:50 ratio for culture. After 16 hours of culture, there were more dead cells amongst the SIRPα mt DCs, with only ~30% being alive, while 36% of the WT $CD103^+CD11b^+$ DCs were alive at this time (Fig. 8.13A). As mentioned previously, due to the set up of our FACS-Aria, I could only sort one other population of DCs from WT and SIRPα mt SI LP isolates simultaneously. I chose to use the $CD103^-CD11b^+$ DCs as a control population, as they also express SIRPα, but are unaffected in the SIRPα mt mice. In this case the proportion of live DCs after culture was similar amongst the WT and SIRPα cells and I also noted that this subset showed better overall viability after culture than the $CD103^+CD11b^+$ DCs (Fig. 8.13B). Taken together these results suggest that $CD103^+CD11b^+$ DCs might be generally more prone to dying and that this is enhanced in SIRPα mt mice. However, as I was only able to do the experiment once with a single replicate, these results need to be repeated.

8.8 Is the $CD103^+CD11b^+$ DC Defect Cell Intrinsic?

Finally, I examined if the selective defect in $CD103^+CD11b^+$ DCs was cell intrinsic or could be overcome in an environment where functional SIRPα was expressed normally by stromal and haematopoietic cells. To investigate this, I generated mixed bone marrow chimeras, in which CD45.1/CD45.2 WT recipients were reconstituted with a 50:50 mix of $CD45.1^+$ WT and $CD45.2^+$ SIRPα mt BM (Fig. 8.14A,B). Importantly, all subsets of intestinal DC were present at the expected frequencies 8 weeks after reconstitution (Fig. 8.14D). However it should be noted that only ~40% of non-host cells derived from SIRPα mt BM, suggesting that SIRPα mt BM was slightly defective in its ability to repopulate $CD45^+$

leukocytes in general (Fig. 8.14C-E). $CD103^+CD11b^+$ DCs were not affected to any greater extent than the other subsets in LP and similar results were seen for all subsets of migratory DCs in recipient MLNs, although in this case, the $CD103^+$ DC subsets showed slightly lower reconstitution by SIRPα mt BM (~30%) (Fig. 8.14F). A different pattern was seen in the spleen, where $CD11b^+$ DCs were clearly skewed towards WT reconstitution, with only 20% of these being of SIRPα mt origin (Fig. 8.15). In contrast, the $CD11b^-$ DCs mirrored the reconstitution ratio seen amongst the total leukocyte populations. Together these results indicate a slight cell intrinsic defect in the ability of SIRPα mt BM to generate DCs and other leukocytes, but that this is not different for the $CD103^+CD11b^+$ DCs in LP and so does not seem to account for the selective defect in this subset in the intact SIRPα mt mouse. However, this may be different for the splenic $CD11b^+$ population. Again it is important to note that because these BM chimeric mice were older than the mice I normally used, it will be important to ensure that this does not account for any apparent differences between the steady state and chimeric SIRPα mt animals.

8.9 Summary

In this chapter I set out to examine the cause of the SIRPα-mediated reduction in intestinal $CD103^+CD11b^+$ DCs in SIRPα mt mice that I had identified in Chapter 7. Initially I examined the cellular distribution of the SIRPα ligand CD47 in the intestine, as I hoped this would aid the identification of which $CD47^+$ cells might be interacting with $SIRP\alpha^+CD103^+CD11b^+$ DCs *in situ*. However, this showed that many different intestinal cells expressed CD47, including the DCs themselves, meaning it was going to be difficult to identify interacting cells by CD47 expression alone.

I next examined the ability of SIRPα mt mice to generate pre-DCs. As their proportions were normal in both the BM and blood, I went on to compare the ability of SIRPα mt and WT pre-DCs to give rise to $CD103^+CD11b^+$ DCs. When transferred into resting WT recipients, SIRPα mt pre-DCs generated $CD103^+CD11b^+$ SI LP DCs more efficiently than their WT counterparts and this did not affect the other DC subsets. This was mirrored by a more rapid appearance of SIRPα mt-derived $CD103^+CD11b^+$ DCs in MLNs. No differences were seen in the

levels of *in situ* proliferation by any of the mature DC subsets in SIRPα mt and WT LP, but $CD103^+CD11b^+$ DCs from SIRPα mt LP showed increased expression of CD86 compared with WT counterparts, and this was not seen with other DC subsets. These results could suggest that the absence of SIRPα signalling leads to more efficient differentiation and/or activation of $CD103^+CD11b^+$ DCs in the gut environment. To determine if this might be reflected in more rapid emigration from the LP, I next examined DCs in pseudo-afferent lymph from MLNx mice. This showed no differences in the proportions of the DC subsets between WT and SIRPα mt lymph, with the exception of $CD103^+CD11b^-$ DCs being slightly increased in SIRPα mt mice. This finding was surprising given the absence of SIRPα expression by these DCs and could indicate the secondary effects of subtle changes in the other, SIRPα expressing DCs which were not evident in the original analysis. The equal proportions of $CD103^+CD11b^+$ DCs in lymph contrasts with their decreased numbers in the LP and could indicate these cells have an increased ability to migrate out of the LP. However, as these mice were quite old by the time they were cannulated and I found earlier that the DC defect in SIRPα mt mice reduces with age, these results need more detailed follow up.

Studies comparing DC survival between WT and SIRPα mt mice were inconclusive. Although Annexin V staining suggested enhanced and selective cell death amongst $CD103^+CD11b^+$ DCs in SIRPα mt MLNs, this was not seen in the LP, possibly as a consequence of the extensive enzymatic digestion used to isolate the DCs. Furthermore, although the $CD103^+CD11b^+$ DCs from SIRPα mt SI LP expressed approximately 2-fold more mRNA for the pro-apoptotic gene *Caspase 3,* a similar increase was seen for the anti-apoptotic gene *Bcl2.* However, studies using $CD103^+CD11b^+$ DCs that had been isolated and sorted together from WT and SIRPα mt mice did suggest that the SIRPα mt $CD103^+CD11b^+$ SI LP DCs were slightly more susceptible to death following culture overnight, although these differences were minor. Interestingly all my studies suggested that the $CD103^-CD11b^+$ DCs survive better than the $CD103^+CD11b^+$ DCs. $CD103^+CD11b^+$ DCs from SIRPα mt mice SI LP had increased expression of IRF4, whose deletion in DCs leads to a similar selective reduction in $CD103^+CD11b^+$ intestinal DCs *in vivo.* Thus, while impaired survival may account for the selective defect in $CD103^+CD11b^+$ DCs in SIRPα mt MLNs, more work is required to assess whether

this accounts for the effects of the lack of SIRPα signalling on $CD103^+CD11b^+$ DC homeostasis in the LP.

Finally, mixed WT:SIRPα mt BM chimeras showed there was a slight cell intrinsic defect in the ability of SIRPα mt BM to generate DCs and other leukocytes in the intestine and elsewhere. However there was no additional defect in the generation of $CD103^+CD11b^+$ intestinal DCs by SIRPα mt BM, although $CD4^+CD11b^+$ splenic DCs did appear to show a cell intrinsic defect of greater magnitude.

Overall my studies suggest that a lack of SIRPα signalling on pre-DCs causes them to differentiate locally into $CD103^+CD11b^+$ DCs more efficiently. In turn, these DCs express higher levels of the co-stimulatory molecule CD86 compared with WT controls suggesting they may be more activated. Possibly as a consequence of this increased activation, the SIRPα mt $CD103^+CD11b^+$ DCs appear to exit the LP more rapidly and at least in the MLN, appear more prone to apoptosis. Together these effects may account for the defect in these DCs in the LP and MLNs of SIRPα mt mice. However, the lack of a selective inability of SIRPα mt BM to reconstitute irradiated mice compared with WT BM suggests the role of this signalling molecule may be more complex. Alternatively, this apparent lack of a cell intrinsic defect may also be due to the age of the animals and this remains to be examined directly.

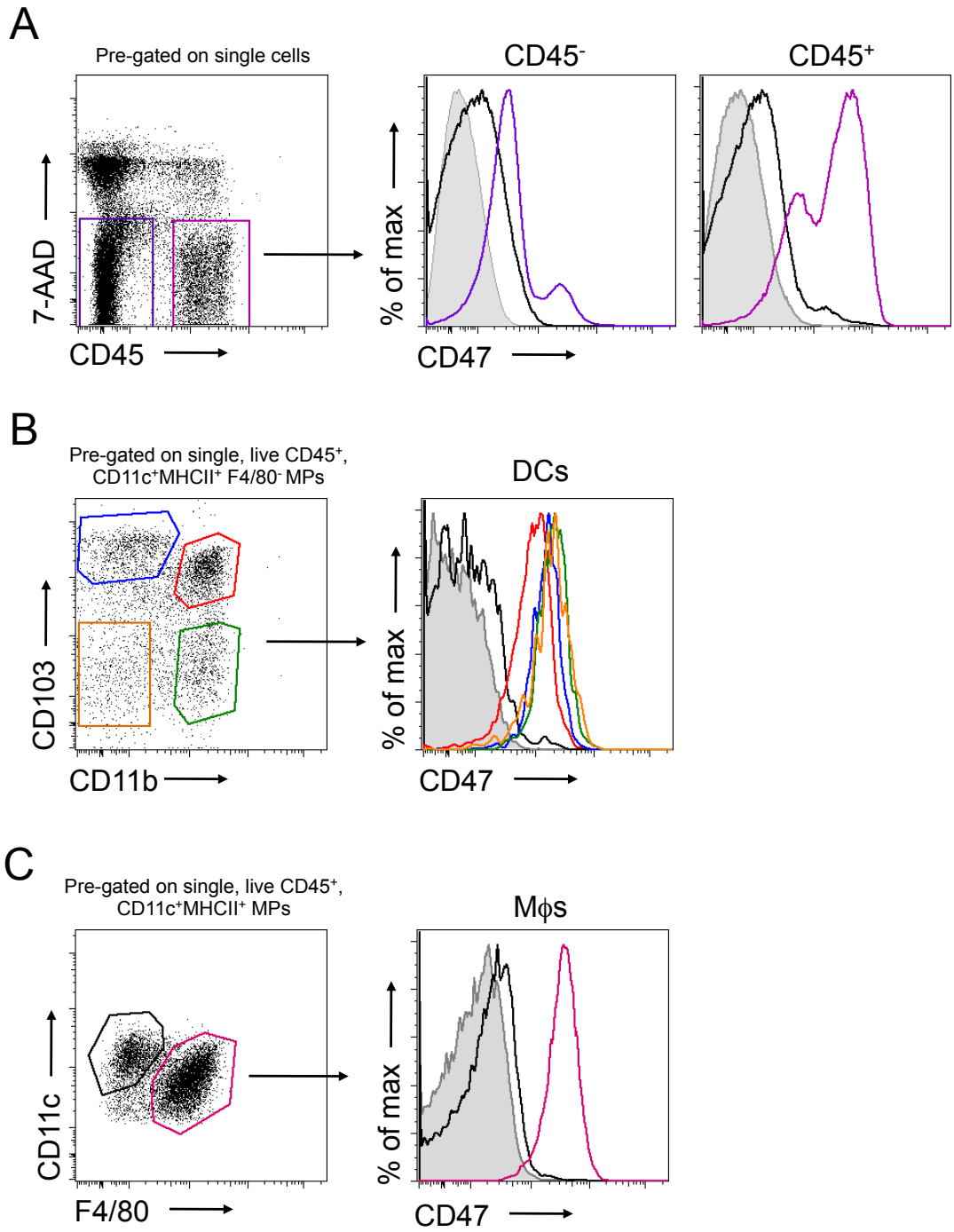

Figure 8.1: Expression of CD47 by intestinal cells

Whole SI LP digests from WT (coloured histograms) and CD47KO mice (black histograms) were assessed for CD47 expression and compared with isotype controls (shaded grey histograms). **A.** Representative plots showing CD45 expression and 7-AAD staining on single cells (left panel) and histograms showing CD47 expression on live $CD45^-$ and $CD45^+$ cells. **B.** Representative plots showing CD103 and CD11b expression on total $CD11c^+MHCII^+F4/80^-$ DCs showing CD47 expression on each DC population. **C.** Representative plots showing CD11c and F4/80 expression on total $CD11c^+MHCII^+$ MPs and histogram showing CD47 expression on $CD11c^+F4/80^+$ mϕs. Data are representative of 2-5 independent experiments with n =3/4 per experiment.

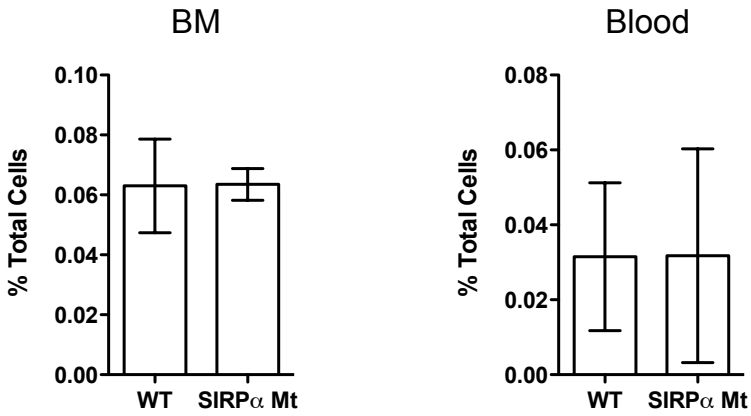

Figure 8.2: Pre-DCs in BM and blood of SIRPα mt mice.

Pre-DCs were identified in BM and blood amongst total donor cells as live lin^-, $CD11c^+$, $B220^-$, $CCR9^-$, $CD135^+$ cells as described in Fig. 4.1 in WT and SIRPa mt mice. Data are shown as mean proportion of pre-DCs as a percentage of total cells ±1SD. Data are representative of 2-5 independent experiments with n =3/4 per experiment.

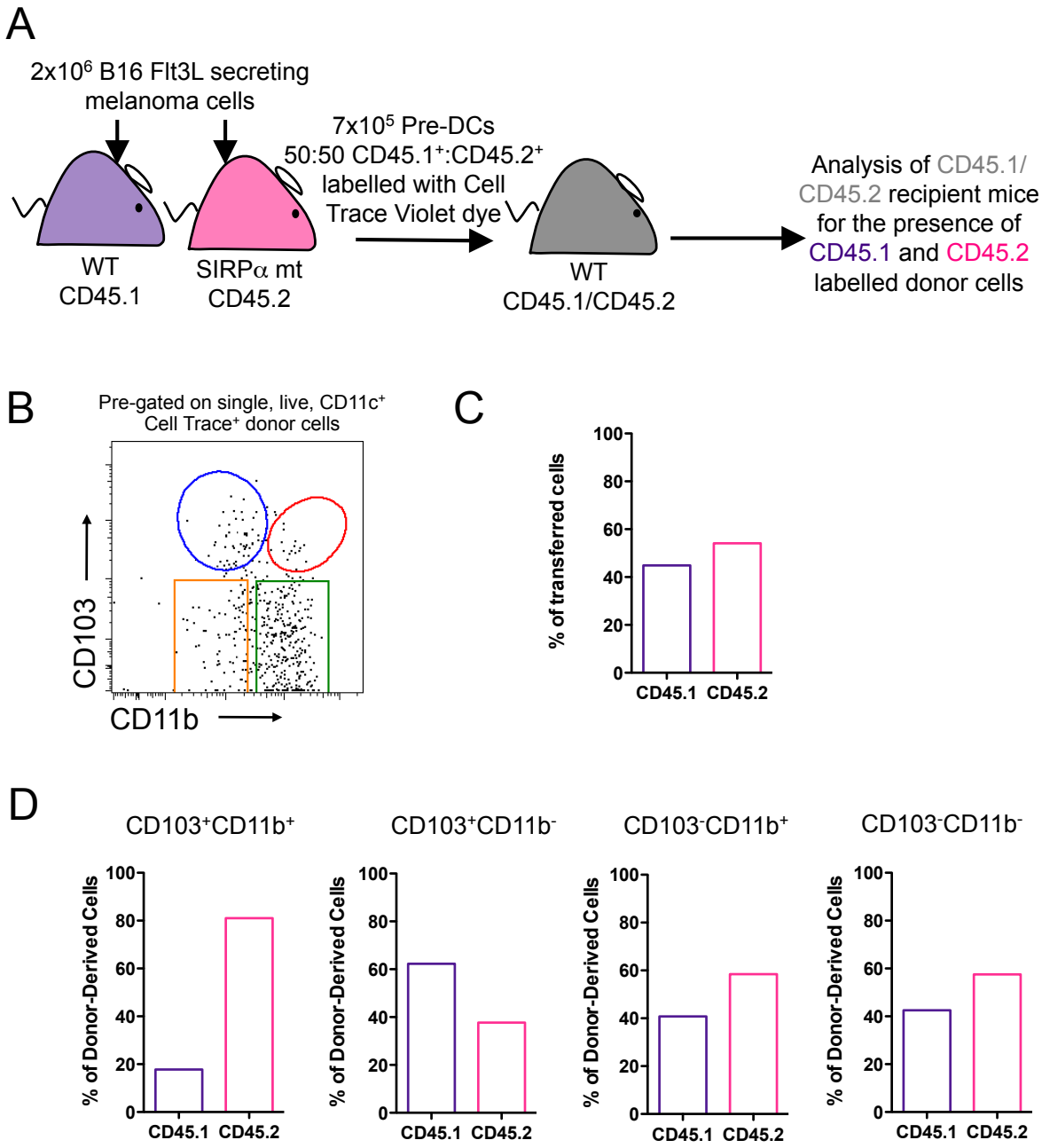

Figure 8.3: Generation of DC subsets in LP 3 days after competitive transfer of WT and SIRPα mt pre-DCs

A. CD45.1⁺ WT and CD45.2⁺ SIRPα mt mice were injected with 2x10⁶ B16 melanoma cells secreting Flt3L. 10 days later BM was harvested, pre-DCs sorted as described in Fig. 4.4, mixed in a 50:50 ratio and 7x10⁵ total pre-DCs were transferred into resting CD45.1/CD45.2 WT recipients. 3 days later recipient mice were examined for the presence of donor cells. **B.** Representative plot showing CD103 and CD11b expression by donor-derived CD11c⁺MHCII⁺ DCs in the SI LP. **C.** Proportion of CD45.1 WT and CD45.2 SIRPα mt pre-DCs amongst total transferred cells in SI LP. **D.** Percentages of CD45.1⁺ and CD45.2⁺ cells amongst CD103⁺CD11b⁺, CD103⁺CD11b⁻, CD103⁻CD11b⁺ and CD103⁻CD11b⁻ donor-derived DCs. Data are shown as means from a single experiment with n=2.

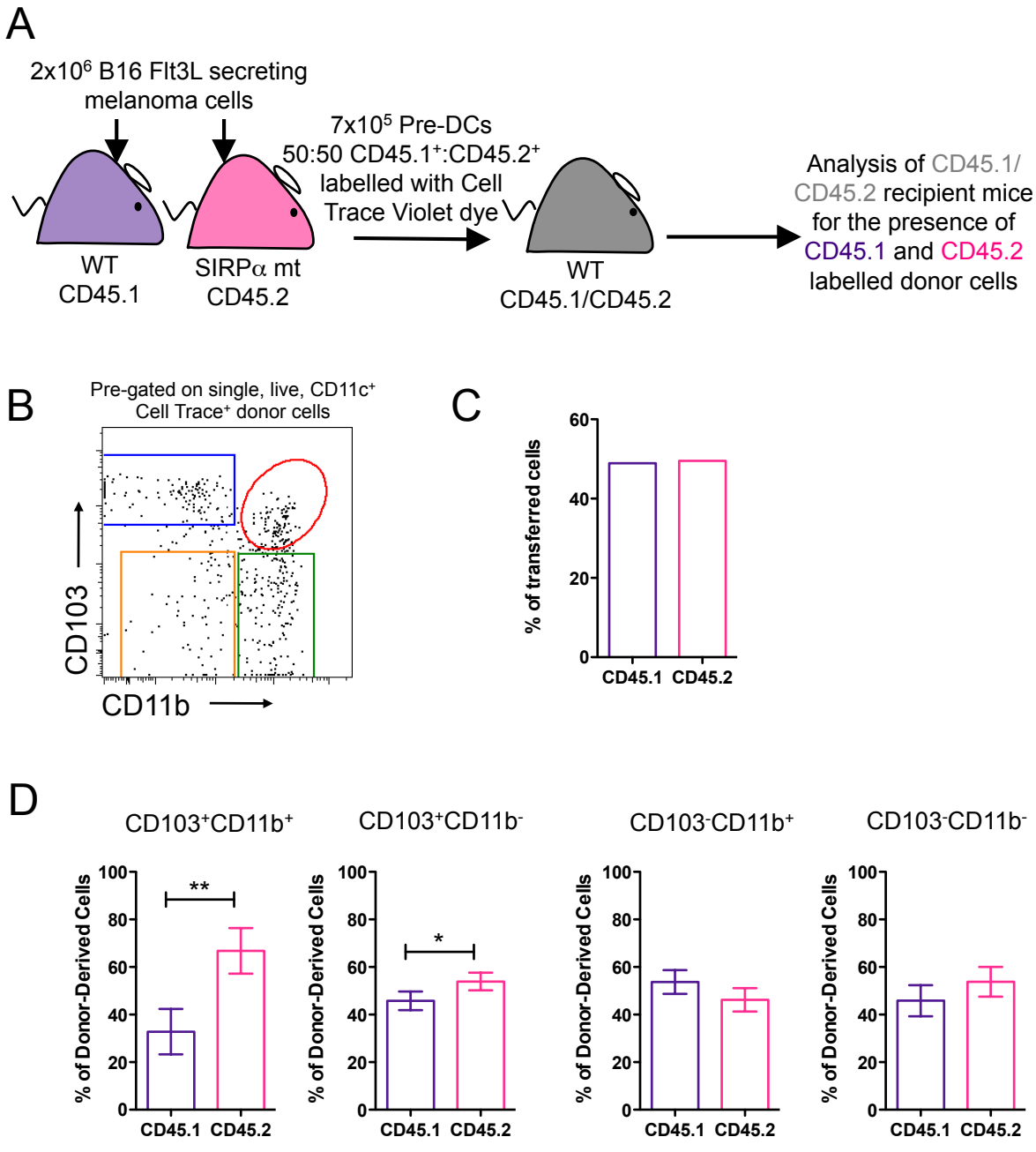

Figure 8.4: Generation of DC subsets in LP 5 days after competitive transfer of WT and SIRPα mt pre-DCs

A. CD45.1⁺ WT and CD45.2⁺ SIRPα mt mice were injected with 2x10⁶ B16 melanoma cells secreting Flt3L. 10 days later BM was harvested, pre-DCs sorted as described in Fig. 4.4, mixed in a 50:50 ratio and 7x10⁵ total pre-DCs were transferred into resting CD45.1/CD45.2 WT recipients. 5 days later recipient mice were examined for the presence of donor cells. **B.** Representative plot showing CD103 and CD11b expression by donor-derived CD11c⁺MHCII⁺ DCs in the SI LP. **C.** Proportion of CD45.1 WT and CD45.2 SIRPα mt pre-DCs amongst total transferred cells in SI LP. **D.** Percentages of CD45.1⁺ and CD45.2⁺ cells amongst CD103⁺CD11b⁺, CD103⁺CD11b⁻, CD103⁻CD11b⁺ and CD103⁻CD11b⁻ donor-derived DCs. Data are shown as mean ±1SD from 2 independent experiments pooled with n=4. *p<0.05, **p<0.01.

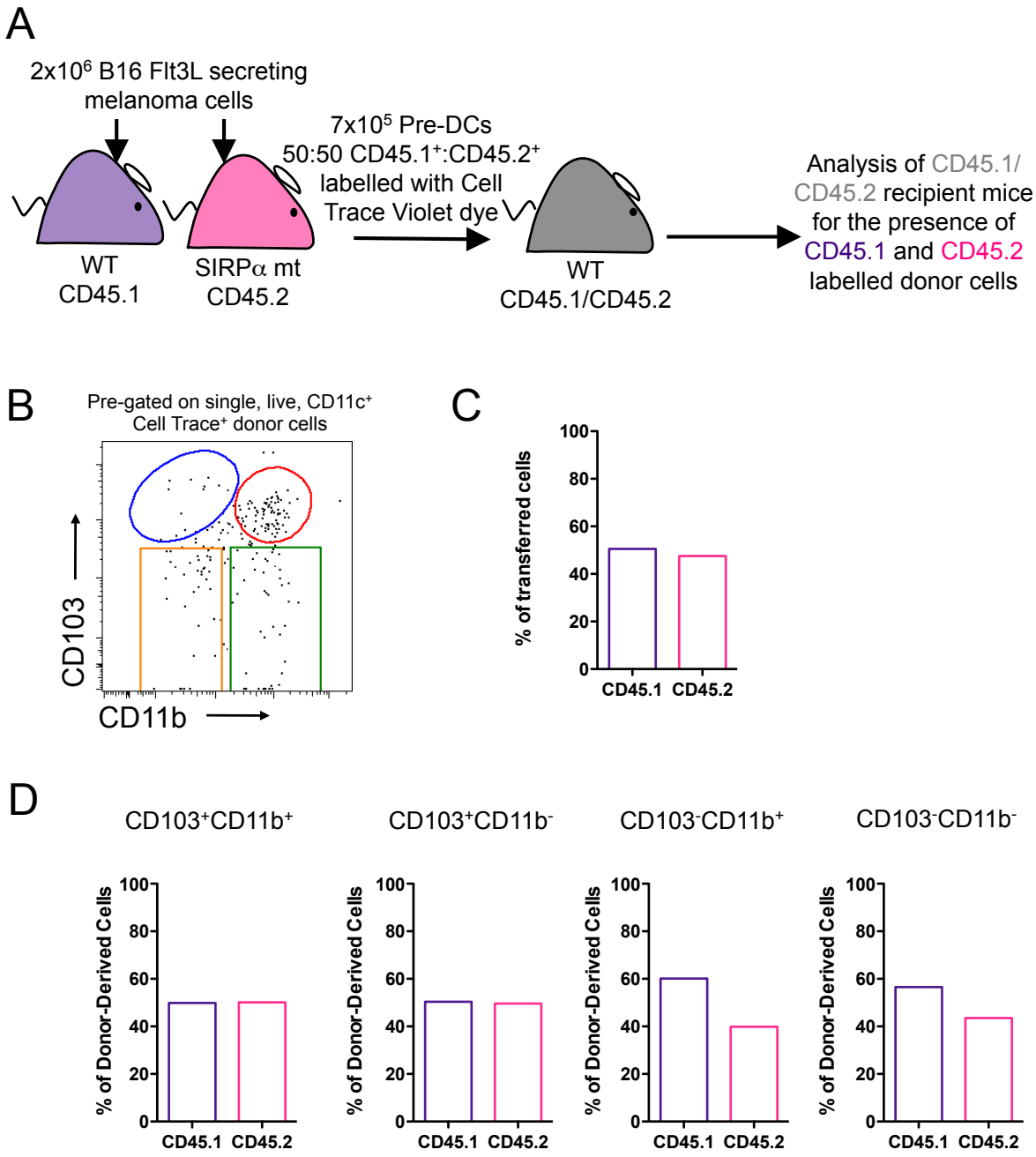

Figure 8.5: Generation of DC subsets in LP 7 days after competitive transfer of WT and SIRPα mt pre-DCs

A. CD45.1⁺ WT and CD45.2⁺ SIRPα mt mice were injected with 2x10⁶ B16 melanoma cells secreting Flt3L. 10 days later BM was harvested, pre-DCs sorted as described in Fig. 4.4, mixed in a 50:50 ratio and 7x10⁵ total pre-DCs were transferred into resting CD45.1/CD45.2 WT recipients. 7 days later recipient mice were examined for the presence of donor cells. **B.** Representative plot showing CD103 and CD11b expression by donor-derived CD11c⁺MHCII⁺ DCs in the SI LP. **C.** Proportion of CD45.1 WT and CD45.2 SIRPα mt pre-DCs amongst total transferred cells in SI LP. **D.** Percentages of CD45.1⁺ and CD45.2⁺ cells amongst CD103⁺CD11b⁺, CD103⁺CD11b⁻, CD103⁻CD11b⁺ and CD103⁻CD11b⁻ donor-derived DCs. Data are shown as means from a single experiment with n=2.

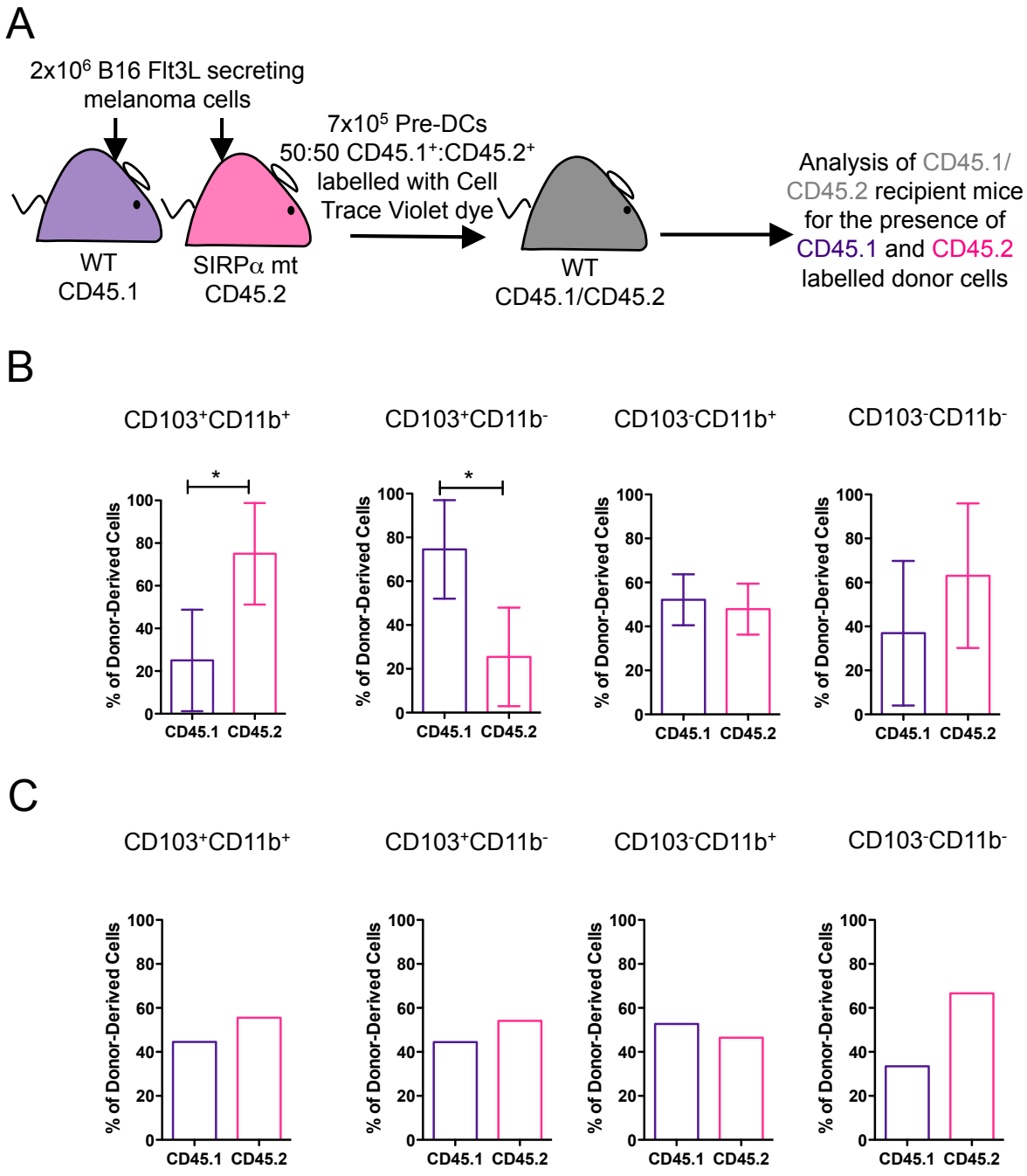

Figure 8.6: Generation of DC subsets in MLN after competitive transfer of WT and SIRPα mt pre-DCs

A. CD45.1⁺ WT and CD45.2⁺ SIRPα mt mice were injected with 2x10⁶ B16 melanoma cells secreting Flt3L. 10 days later BM was harvested, pre-DCs sorted as described in Fig. 4.4, mixed in a 50:50 ratio and 7x10⁵ total pre-DCs were transferred into resting CD45.1/CD45.2 WT recipients. 5 and 7 days later recipient mice MLNs were examined for the presence of donor cells. **B.** Percentages of CD45.1⁺ and CD45.2⁺ cells amongst CD103⁺CD11b⁺, CD103⁺CD11b⁻, CD103⁻CD11b⁺ and CD103⁻CD11b⁻ donor-derived DCs 5 days after transfer. Data are pooled from 2 independent experiments with n=2 per experiment and results shown as means ±1SD. **C.** Percentages of CD45.1⁺ and CD45.2⁺ cells amongst CD103⁺CD11b⁺, CD103⁺CD11b⁻, CD103⁻CD11b⁺ and CD103⁻CD11b⁻ CD11c⁺MHCII⁺ donor-derived DCs 7 days after transfer. Data are shown as mean from a single experiment with n=2. *p<0.05 Student's t test.

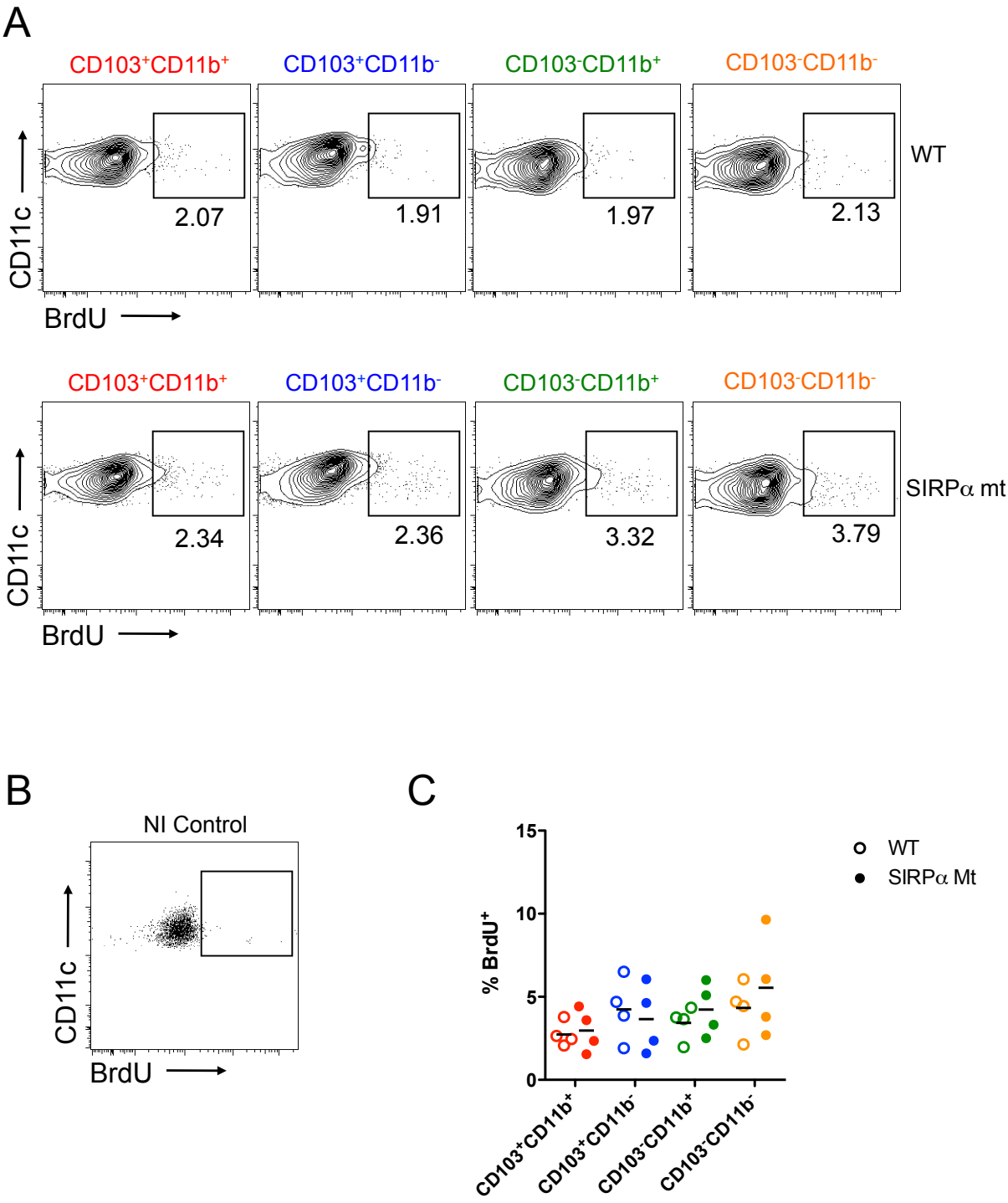

Figure 8.7: *In situ* proliferation of DC subsets in LP of SIRPα mt mice

WT and SIRPα mt mice received 1mg BrdU i.p. and BrdU$^+$ cells amongst SI LP DCs were assessed 3 hours later. **A.** Representative plots showing BrdU staining in each DC population in WT (top panel) and SIRPα mt mice (lower panel). Number represents percentage of BrdU$^+$ cells. **B.** Representative plot showing BrdU staining amongst total CD11c$^+$ MHCII$^+$CD64$^-$ DCs from a non-BrdU injected control (NI). **C.** Proportions of BrdU$^+$ cells as a percentage of each DC population in SI LP of WT and SIRPα mt mice. Data are from a single experiment with n=4 per group.

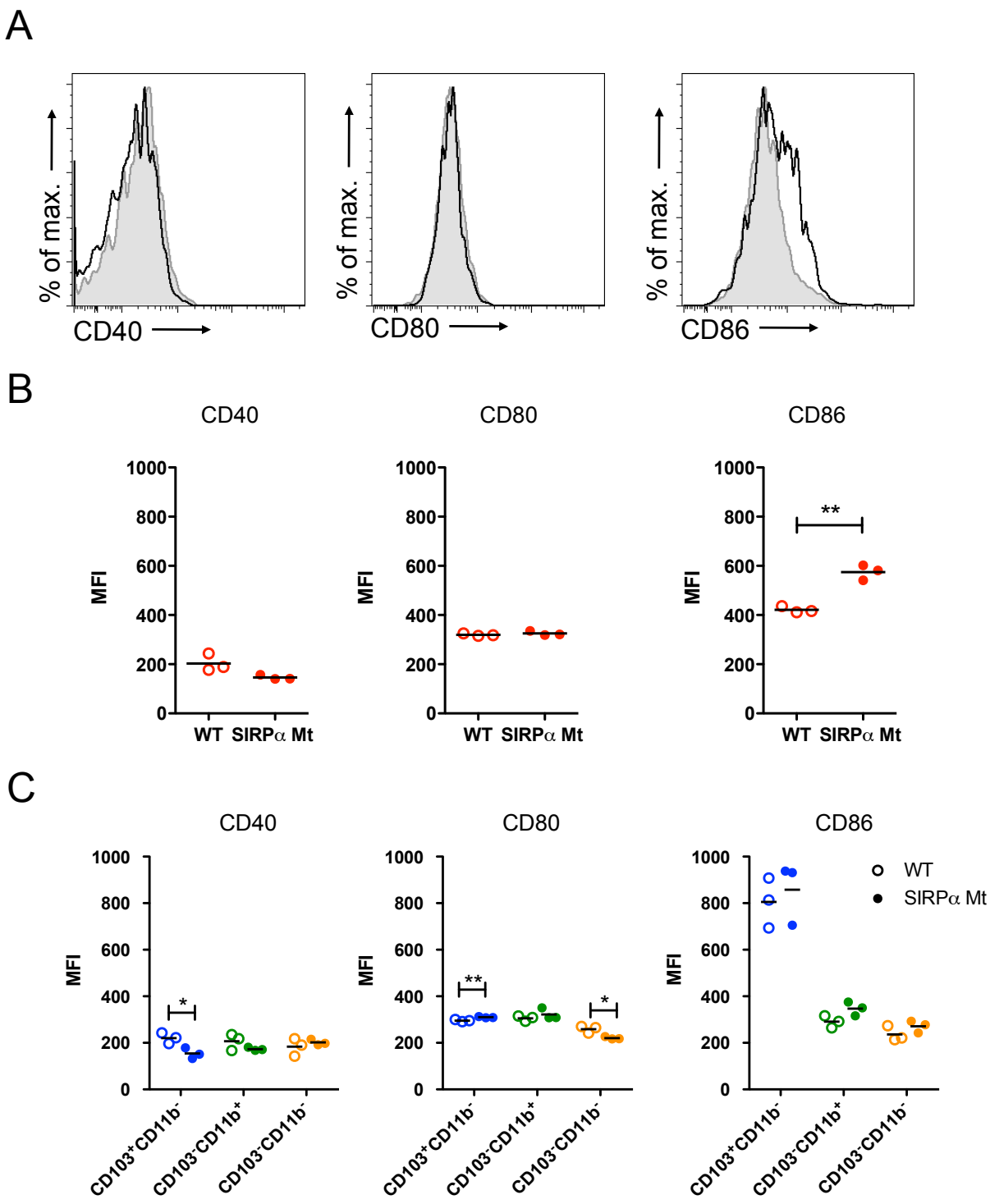

Figure 8.8: Expression of co-stimulatory molecules by SI LP DCs from SIRPα mt mice
LP DC subsets from WT and SIRPα mt mice were examined for their expression of the co-stimulatory molecules CD40, CD80 and CD86. **A.** Representative histograms showing CD40, CD80 and CD86 expression $CD103^+CD11b^+$ DCs from SIRPα mt mice (black line) compared with WT controls (shaded grey histogram). **B.** Mean fluorescence intensity (MFI) for CD40, CD80 and CD86 expression by SIRPα mt and WT $CD103^+CD11b^+$ SI LP DCs. **C.** Mean fluorescence intensity (MFI) for CD40, CD80 and CD86 expression by $CD103^+CD11b^-$, $CD103^-CD11b^+$ and $CD103^-CD11b^-$ DCs from WT and SIRPα mt SI LP. Data are from a single experiment with n=3 per group. *p<0.05, **p<0.01, Student's t test.

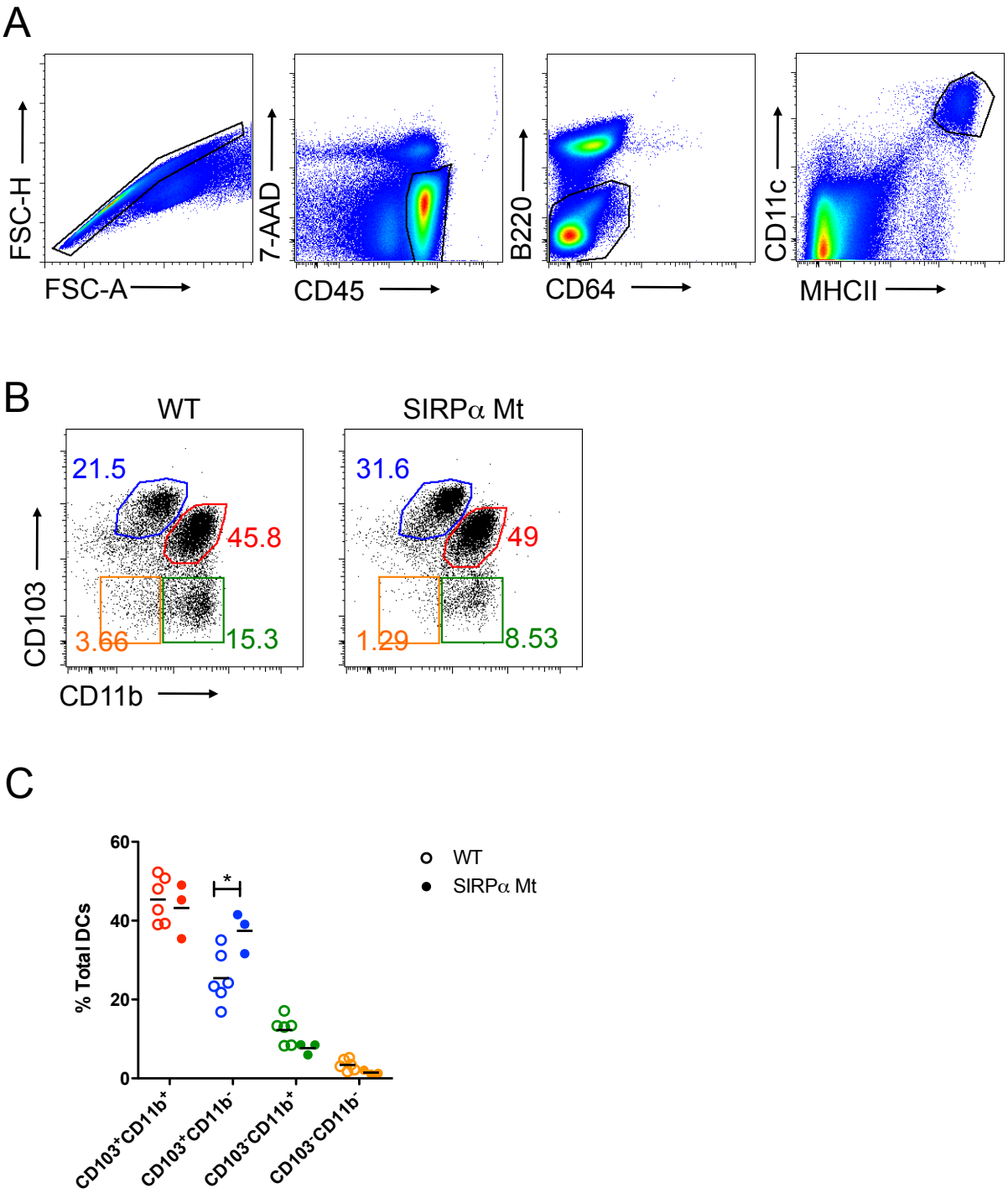

Figure 8.9: DC subsets in pseudo-afferent intestinal lymph of SIRPα mt mice

MLNs of WT and SIRPα mt mice were removed and lymphatics allowed to reanastamose. 6 weeks later the thoracic ducts were cannulated and lymph collected overnight. **A.** DCs were identified in lymph as single, live $CD45^+$ $B220^-$ $CD11c^+$ $MHCII^+$ cells. **B.** Representative dot plots showing CD103 and CD11b expression on lymph DCs and DC subsets in the lymph of WT and SIRPα mt mice. Numbers represent proportion of total DCs. **C.** Proportions of each DC subset as a percentage of total DCs in lymph of WT and SIRPα mt mice. Data are from a single experiment with n=3-6 per group. *p<0.05 Student's t test.

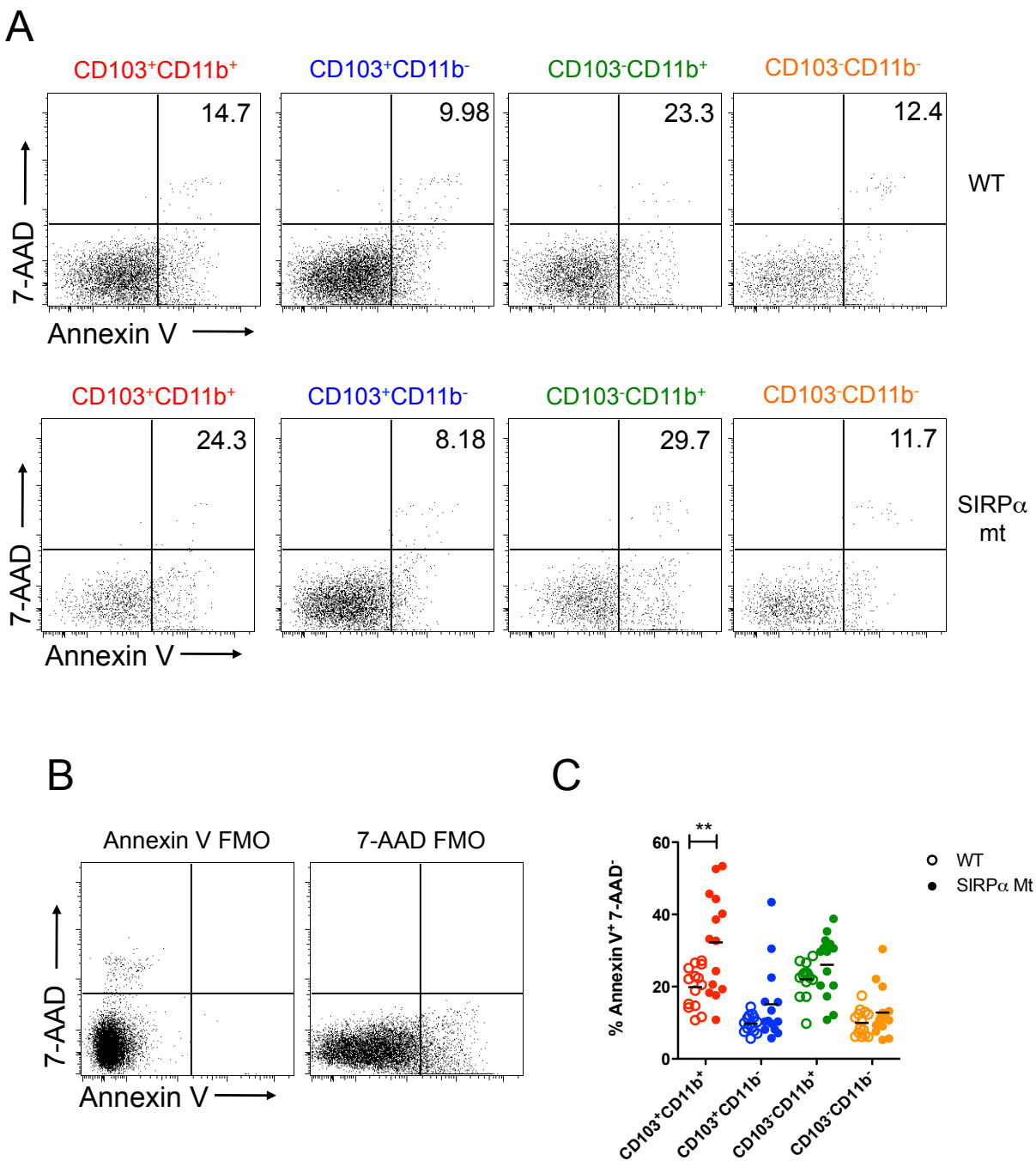

Figure 8.10: Apoptosis of CD103⁺CD11b⁺ DCs from MLNs of SIRPα mt mice

DC subsets were identified amongst migratory DCs in whole MLN isolates from WT and SIRPα mt mice and stained for Annexin V and 7-AAD. **A.** Representative plots showing Annexin V and 7-AAD staining in each DC population in WT (top panel) and SIRPα mt mice (lower panel). Numbers represent proportions of apoptotic (Annexin V⁺ 7-AAD⁻) cells. **B.** Representative plot showing Annexin V and 7-AAD staining in fluorescence minus one (FMO) controls used to set gates amongst total migratory (CD11c⁺ MHCII^{hi}) DCs. **C.** Proportions of apoptotic (Annexin V⁺ 7-AAD⁻) cells as a percentage of each DC subset in WT and SIRPα mt MLNs. Data are pooled from four independent experiments with n=3-4 per group per experiment. **p<0.01 Student's t test.

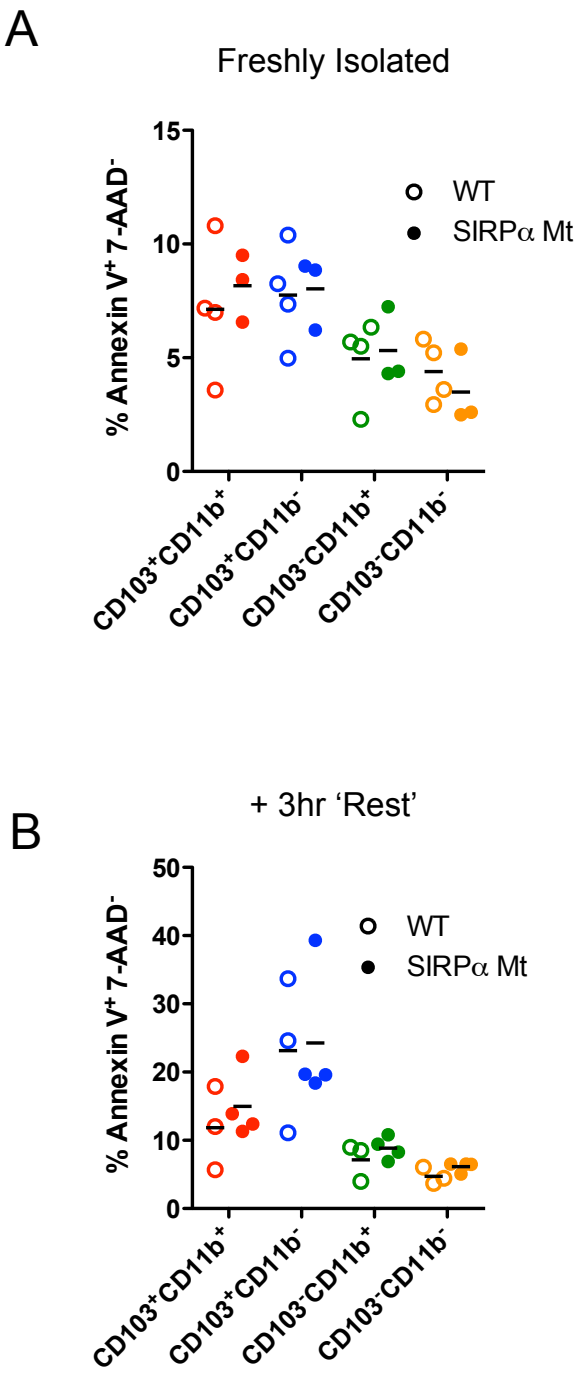

Figure 8.11: Apoptosis of SI LP DCs from SIRPα mt mice

DC subsets were identified amongst DCs in SI LP isolates from WT and SIRPα mt mice and stained for Annexin V and 7-AAD. **A.** Proportions of apoptotic (Annexin V^+ 7-AAD^-) cells as a percentage of each DC subset in WT and SIRPα mt SI LP. **B.** Proportions of apoptotic (Annexin V^+ 7-AAD^-) cells as a percentage of each DC subset in WT and SIRPα mt SI LP following 3 hours of culture at 37°C. Data are from a single experiment with n=3/4 per group.

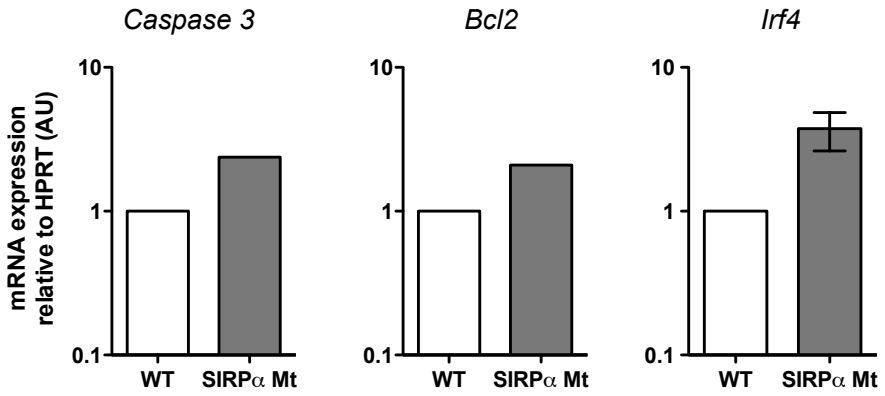

Figure 8.12: Expression of apoptosis associated genes by CD103$^+$CD11b$^+$ SI LP DCs from SIRPα mt mice

CD103$^+$CD11b$^+$ DCs were FACS-purified from SI LP of WT and SIRPα mt mice as described in Fig. 3.10 and analysed by qRT-PCR for expression of mRNA for *Caspase 3, Bcl2* and *Irf4*. Results shown are relative to HPRT using the $2^{-\Delta\Delta ct}$ method with WT set to 1. Data are from two (*Caspase 3* and *Bcl2*) or three (*Irf4*) independent experiments and are shown as means ±1SD. Cells were pooled from 6-9 mice per group per experiment.

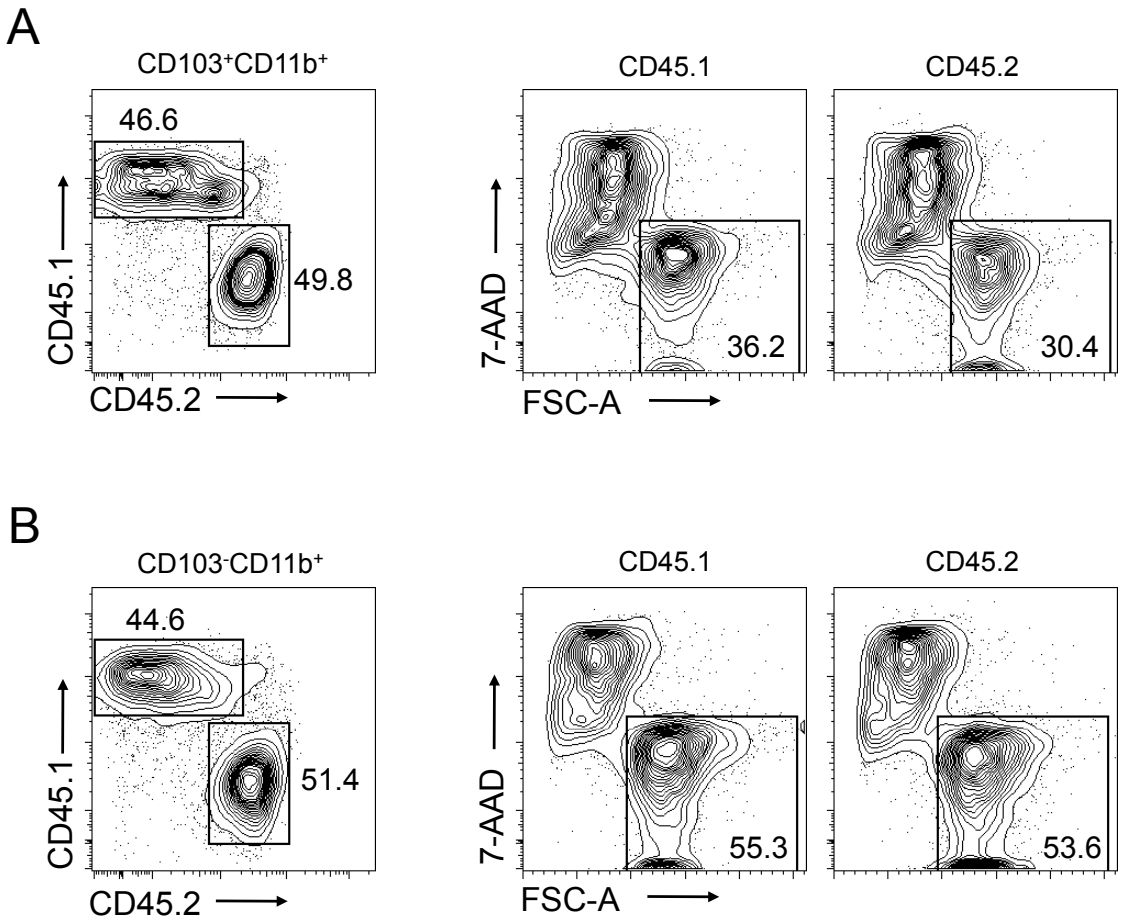

Figure 8.13: Survival of SI LP DCs in SIRPα mt mice

SI from CD45.1$^+$ WT and CD45.2$^+$ SIRPα mt mice were pooled, digested together and CD103$^+$CD11b$^+$ and CD103$^-$CD11b$^+$ DCs FACS-purified as described in Fig. 3.1. After sorting, 30,000 CD45.1$^+$ and CD45.2$^+$ cells were mixed together in a 50:50 ratio and cultured for 16 hours before their viability was assessed. **A.** Representative plots showing CD45.1 and CD45.2 staining on CD103$^+$CD11b$^+$ DCs after culture and 7-AAD staining and FSC-A profiles of CD45.1$^+$ WT and CD45.2$^+$ SIRPα mt DCs. Numbers represent proportions of parent population. **B.** Representative plots showing CD45.1 and CD45.2 staining on CD103$^-$CD11b$^+$ DCs after culture and 7-AAD staining and FSC-A profiles of CD45.1 WT and CD45.2 SIRPα mt DCs. Numbers represent proportions of parent population. Data are from a single experiment with n=1. Cells were pooled from 6 mice per group.

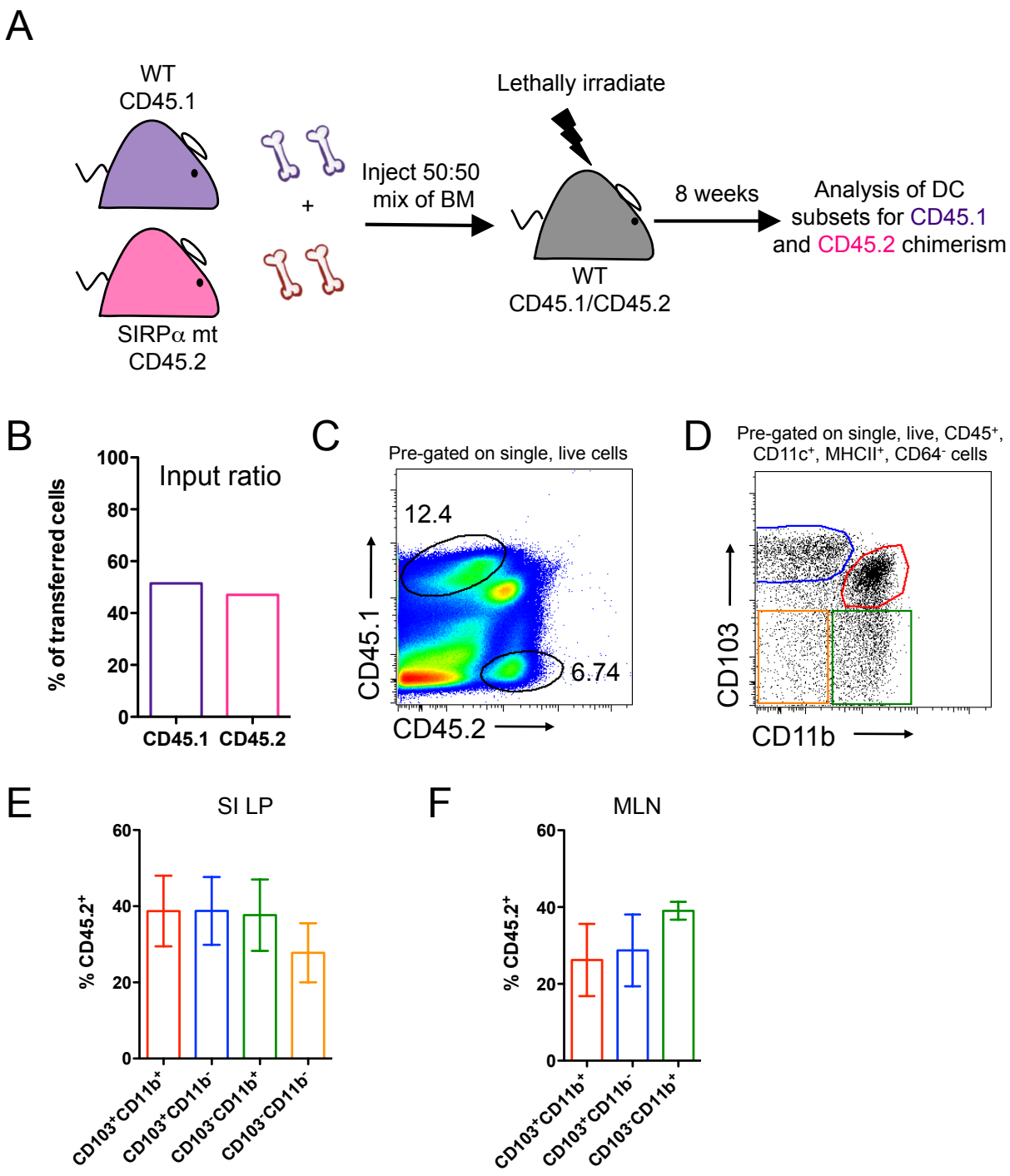

Figure 8.14: DCs in SI LP and MLNs of mixed WT:SIRPα mt BM chimeras

A. Mixed BM chimeras were generated by lethally irradiating CD45.1/CD45.2 WT mice and reconstituting with a 50:50 mix of CD45.1$^+$ WT and CD45.2$^+$ SIRPα mt BM. Mice were left for 8 weeks to allow reconstitution of all populations. **B.** Proportions of CD45.1$^+$ WT and CD45.2$^+$ SIRPα mt BM used for reconstitution. **C.** Representative dot plot showing expression of CD45.1 and CD45.2 by total live SI LP cells 8 weeks after reconstitution. Numbers represent proportions of live cells. **D.** Representative plot showing CD103 and CD11b expression by CD11c$^+$MHCII$^+$CD64$^-$ DCs in the SI LP 8 weeks after reconstitution. **E.** Proportions of CD45.2$^+$ SIRPα mt BM-derived cells shown as a percentage of each DC population in the SI LP 8 weeks after reconstitution. **F.** Proportions of CD45.2$^+$ SIRPα mt BM-derived cells shown as a percentage of CD11c$^+$MHCII^{hi} migratory DCs in the MLNs 8 weeks after reconstitution. Data are shown as mean ±1SD from 2 independent experiments pooled with n=8. ***p<0.001 Student's t test.

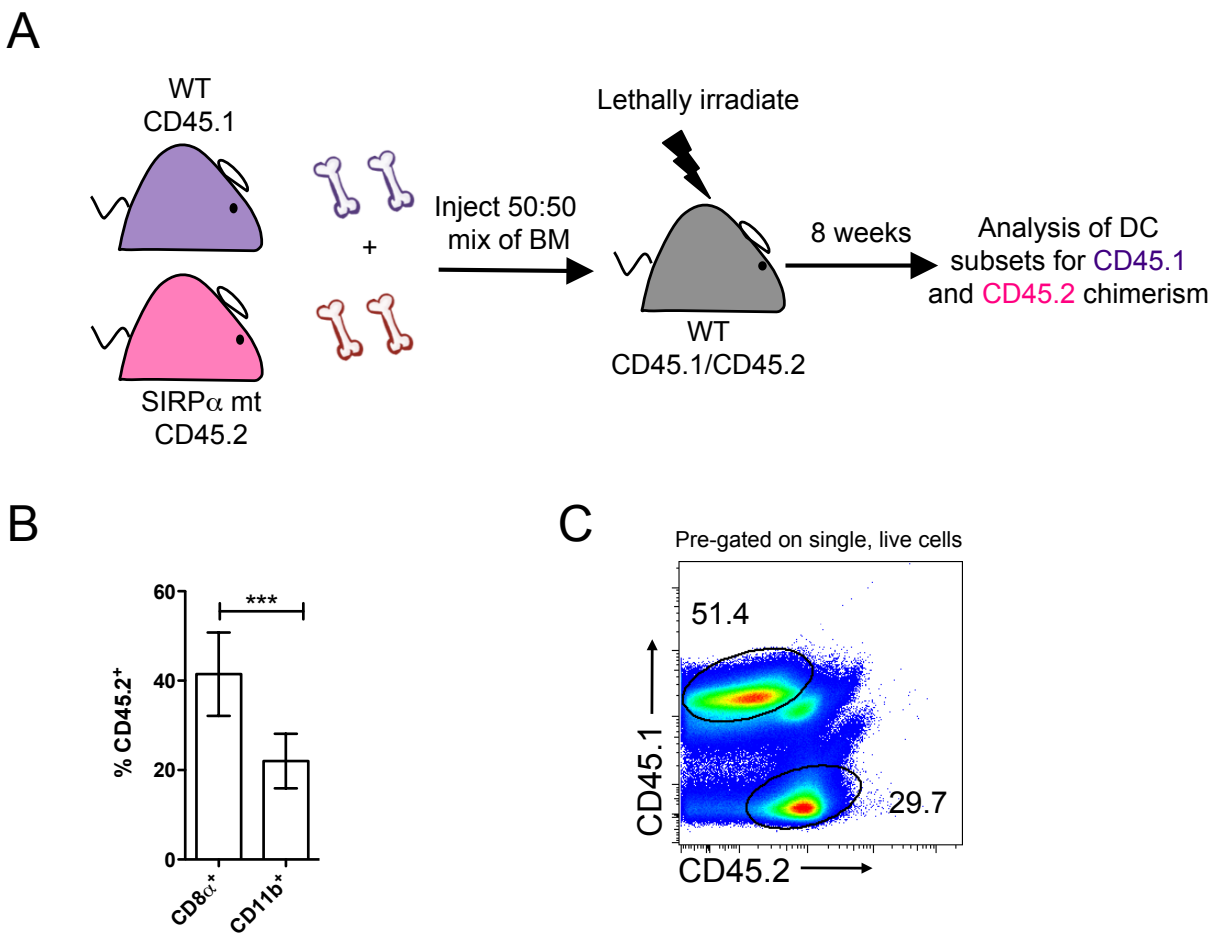

Figure 8.15: DCs in spleen of mixed WT:SIRPα mt BM chimeras

A. Mixed BM chimeras were generated by lethally irradiating CD45.1/CD45.2 WT mice and reconstituting with a 50:50 mix of CD45.1$^+$ WT and CD45.2$^+$ SIRPα mt BM. Mice were left for 8 weeks to allow reconstitution of all populations. **B.** Proportions of CD45.2$^+$ SIRPα mt BM-derived cells shown as a percentage of each DC population in the spleen 8 weeks after reconstitution. **C.** Representative dot plot showing expression of CD45.1 and CD45.2 by total live splenocytes 8 weeks after reconstitution. Numbers represent proportions of live cells. Data are shown as mean ±1SD of 2 independent experiments, n=8. ***p<0.001, Student's t test.

Chapter 9 CCR2^{+} Intestinal Dendritic Cells

9.1 Introduction

In the previous chapters I demonstrated that CD103$^-$CD11b$^+$CD64$^-$ intestinal MPs were genuine DCs derived from committed DC precursors (pre-DCs). However towards the end of my PhD, a CCR2-dependent Zbtb46$^+$ Ly6C^{lo} MP population was identified that was proposed to comprise monocyte-derived DCs (mo-DCs) (Zigmond et al., 2012) based on the known dependence of monocytes on CCR2 for BM egress (Kurihara et al., 1997; Serbina and Pamer, 2006). As I could find no evidence of a population of mo-DCs in my previous adoptive transfer studies, in this chapter I set out to investigate if I had overlooked this mo-DC population in my previous analyses.

9.2 CD103$^-$CD11b$^+$ DCs are Reduced in CCR2$^{-/-}$ Intestine

I first examined whether deletion of CCR2 affected the abundance of DCs in the steady state mucosa by comparing the four populations of intestinal DCs in CCR2$^{-/-}$ mice and WT controls. This revealed a partial reduction in both the proportion and number of CD103$^-$CD11b$^+$ DCs in the SI LP of CCR2$^{-/-}$ mice compared with WT controls (Fig. 9.1). In parallel there was a slight increase in CD103$^+$CD11b$^+$ DCs in terms of proportion, but this did not translate into a change in their absolute number (Fig. 9.1B,C). There was also a slight but significant reduction in the absolute number of CD103$^-$CD11b$^-$ DCs in the CCR2$^{-/-}$ LP (Fig. 9.1C). Consistent with our previous report in the colonic LP (Bain et al., 2013), the absolute number of mϕs in the SI LP was also reduced in CCR2$^{-/-}$ mice compared with WT controls (Fig. 9.1D) consistent with these being monocyte-derived cells.

There was an even more profound reduction in the proportion and absolute number of CD103$^-$CD11b$^+$ DCs amongst migratory DCs in CCR2$^{-/-}$ MLNs, where there was also a slight increase in the proportion of CD103$^+$CD11b$^+$ DCs. Again there was a slight decrease in the numbers of CD103$^-$CD11b$^-$ DCs (Fig. 9.2). Unlike LP, the number of CD103$^+$CD11b$^-$ migratory DCs was also decreased in CCR2$^{-/-}$ MLNs, despite an increase in their proportion compared with WT control MLNs (Fig. 9.2B,C). These decreases in the numbers of the DC subsets reflected a significant decrease in the total number of migratory DCs in CCR2$^{-/-}$ MLNs (Fig. 9.2D). In contrast the total cellularity of their MLNs was normal (Fig. 9.2E), as were all subsets of resident DCs, apart from a small but significant decrease in the

proportion of $CD103^-CD11b^-$ DCs (Fig. 9.3). Together these results could suggest that some intestinal DCs are dependent upon CCR2 and that this chemokine receptor may play an additional role in DC migration to the MLNs.

There was also a significant reduction in the numbers of both $CD4^+$ ($CD11b^+$) and $CD4^-$ ($CD11b^-$) DC populations in the spleen of $CCR2^{-/-}$ mice, although their proportions were normal (Fig. 9.4A-C). In parallel, total DC numbers were reduced in the spleen compared with WT controls, while total cell numbers were normal (Fig. 9.4D,E). Thus although CCR2 may have more widespread effects on DCs in general, it appears to play a particularly important role in the homeostasis of $CD103^-CD11b^+$ DCs in the intestine.

9.3 The Defect in $CD103^-CD11b^+$ DCs in $CCR2^{-/-}$ Mice is Cell Intrinsic

To examine if this defect in $CD103^-CD11b^+$ DCs in $CCR2^{-/-}$ mice was cell intrinsic, I generated mixed BM chimeras, in which lethally irradiated CD45.1/CD45.2 WT mice were reconstituted with a 50:50 mix of $CD45.1^+$ WT and $CD45.2^+$ $CCR2^{-/-}$ BM (Fig. 9.5A). 8 weeks after reconstitution, mϕs in the SI LP were derived almost exclusively from WT BM (Fig. 9.5B,C), confirming the known requirement for CCR2-dependent monocytes in replenishing this population (Bain et al., 2013; Tamoutounour et al., 2012). All the DC populations in chimeric SI LP also showed slightly skewed reconstitution in favour of WT origin, suggesting that CCR2 may also play a cell intrinsic role in the development and/or recruitment of these cells. However, a similar bias was seen when eosinophils were examined, a population with no known requirement for CCR2 in their development or recruitment, suggesting that the overall reconstitution by KO BM was less efficient. The only exception to this were the $CD103^-CD11b^+$ DCs, which had a WT:KO ratio of ~3, which was greater than the other DC subsets and eosinophils, although less than for mϕ. This finding would be consistent with the idea that a cell intrinsic defect in $CD103^-CD11b^+$ DCs accounts for at least part of their selective reduction in $CCR2^{-/-}$ mice (Fig. 9.5B,C). There was a similar and significant skewing towards WT origin amongst $CD103^-CD11b^+$ migratory DCs in the MLNs of chimeric mice, with a WT:KO ratio of ~2.5 , compared with the other DC subsets which had a ratio of 1-1.8 (Fig. 9.6). In this case, the $CD103^+CD11b^+$ DCs had a WT:KO ratio approaching 1, which was significantly higher than that of the $CD103^+CD11b^-$ and

$CD103^-CD11b^-$ DC subsets (Fig. 9.6). In contrast, there was no skewing to WT origin amongst MLN resident or splenic DCs (Fig. 9.7 and Fig. 9.8). Together these findings indicate that the partial reduction of $CD103^-CD11b^+$ DCs in the intestine of $CCR2^{-/-}$ mice is cell intrinsic, whereas the effects of CCR2 deficiency on other DCs in the MLN and spleen are secondary to effects on other cell types.

9.4 $CD103^-CD11b^+$ DCs in WT:$CCR2^{-/-}$ Parabiotic Mice

To verify further the partial dependence of $CD103^-CD11b^+$ DCs on CCR2, I had the opportunity to examine WT:$CCR2^{-/-}$ parabiotic mice in collaboration with Bernard Malissen's lab in Marseille. These were created by surgically joining $CD45.1^+$ WT mice with $CD45.2^+$ $CCR2^{-/-}$ mice and they were compared to $CD45.1^+$ WT partnered with $CD45.2^+$ WT controls (Fig. 9.9). The parabiotic mice were left for 12 weeks after the procedure to allow blood vessels to fuse and chimerism to be established. The level of chimerism for $CD45.1^+$-derived DCs in the SI LP of the $CD45.2^+$ WT partners in the WT:WT parabionts varied slightly between the subsets, but was generally in the region of 10-20% (Fig. 9.10A,C). Identical levels of chimerism were found for $CD45.1^+$ WT-derived $CD103^+CD11b^+$, $CD103^+CD11b^-$ and $CD103^-CD11b^-$ DCs in the $CD45.2^+$ $CCR2^{-/-}$ partners in the WT:$CCR2^{-/-}$ parabionts. However considerably more $CD45.1^+$ WT-derived cells (~30%) were present amongst the $CD103^-CD11b^+$ DCs in WT:$CCR2^{-/-}$ parabionts than in the WT:WT parabionts (Fig. 9.10B,C). Unfortunately, the small group size meant that I could not conduct statistical analysis of these differences and we were also unable to obtain sufficient blood cells as a baseline control for the levels of chimerism for pre-DCs in the parabionts. Therefore these findings need to be verified with larger sample numbers and appropriate blood controls.

Analysis of the opposite ($CD45.1^+$) partners suggested that $CD45.2^+$ blood-derived cells were generally more efficient at reconstituting the CD45.1 host, as 15-30% of SI LP DCs were of non-host origin in these mice (Fig. 9.11A,C). Under these conditions, all DC subsets showed a defective chimerism when derived from $CCR2^{-/-}$ origin, with only 5-10% being of non-host ($CCR2^{-/-}$) origin (Fig. 9.11B,C). The reasons for this discrepancy between partners is unclear, but it seems to confirm my findings in competitive chimeras, where all DC populations and CCR2-independent eosinophils showed a slight bias towards WT reconstitution.

9.5 CCR2 Expression by Intestinal DCs

9.5.1 Anti-CCR2 Antibody Reactivity

Having established that the $CD103^-CD11b^+$ DCs were partially dependent upon CCR2, I hypothesised that this may reflect heterogeneity of CCR2 expression within this population. Therefore, I examined the levels of CCR2 on the various DC subsets, first using a commercially available anti-CCR2 antibody. Because of previous problems in the laboratory with non-specific staining using anti-CCR2 antibodies, I used total $CD11c^+MHCII^+CD64^-$ LP DCs from $CCR2^{-/-}$ mice as controls. This revealed the presence of two distinct populations of $CD103^-CD11b^+$ DCs, the majority of which were $CCR2^-$ and 15-30% were $CCR2^+$ (Fig. 9.12). While some CCR2 expression was also detected amongst $CD103^+CD11b^-$ DCs, this was considerably lower than that on $CD103^-CD11b^+$ DCs and a clear positive population was not observed (Fig. 9.12). $CD103^+CD11b^+$ DCs did not express CCR2 above background levels, but somewhat surprisingly given their normal levels in $CCR2^{-/-}$ LP, the $CD103^-CD11b^-$ DCs expressed similar levels of CCR2 to $CD103^-CD11b^+$ DCs (Fig. 9.12). $CCR2^+CD103^-CD11b^+$ DCs were also present amongst total migratory DCs in the MLN, whereas none of the other migratory DC populations expressed CCR2, including the $CD103^-CD11b^-$ DCs which were $CCR2^+$ in LP (Fig. 9.13). Interestingly, similar populations of $CCR2^+$ cells could be identified amongst $CD103^-CD11b^+$ DCs in the lung and amongst $CD11b^+$ ($CD4^+$) DCs in the spleen (Fig. 9.14).

9.5.2 CCL2-AF647 Uptake Assay

Due to the problems we and others had encountered with the anti-CCR2 antibody, I decided to try and confirm my results using a new assay developed by Professor Rob Nibbs' group in our department in which $CCR2^+$ cells are identified by the uptake of fluorescently labelled CCL2. This had already been used successfully for analysis of spleen and lymph nodes (Ford et al., 2013; McKimmie et al., 2008), but not in the intestine. This approach validated the results I obtained in the MLN using anti-CCR2 antibody staining, with only the $CD103^-CD11b^+$ migratory DCs showing uptake of CCL2 (Fig. 9.15). The specificity of this assay was confirmed by the absence of uptake by any DCs from $CCR2^{-/-}$ MLNs.

Rather different results were obtained when DC from SI LP were examined using this assay, as all the populations of DCs showed significant and similar levels of CCL2 uptake, apart from $CD103^+CD11b^+$ DCs which were negative (Fig. 9.16). As this assay has not yet been compared exhaustively with antibody staining for a wide range of cells and tissues, the reasons for these discrepancies are unclear and require further investigation.

9.5.3 $CCR2^{+/RFP}$ Mice

To attempt to address the discrepancies between the anti-CCR2 antibody and CCL2 uptake assay, I had the opportunity to examine $CCR2^{+/RFP}$ mice in collaboration with Dr. Barry McColl in Edinburgh. These mice revealed yet another pattern of CCR2 expression amongst DCs. Consistent with the results I had obtained using antibody staining, the $CD103^-CD11b^+$ LP DCs were the major CCR2-expressing DC population in the SI LP of $CCR2^{+/RFP}$ mice (Fig. 9.17). However ~70% of these were $CCR2^+$ using this approach, compared with only ~20% using antibody staining. In parallel, the $CD103^+CD11b^+$, $CD103^+CD11b^-$ and $CD103^-CD11b^-$ LP DCs also appeared to contain more $CCR2^+$ cells using the RFP mice (~20%, 20% or 50% respectively), whereas antibody staining had suggested that these populations were largely negative for CCR2 expression (Fig. 9.17). Analysis of the migratory DC populations in the MLNs of these mice revealed a similar pattern to that seen in the LP (Fig. 9.18). It is possible that the additional $CCR2^+$ cells revealed in the $CCR2^{+/RFP}$ mice may represent intracellular expression of CCR2 that was not detected by the antibody. Alternatively, it is not known how long RFP expression is maintained after downregulation of CCR2 surface expression, nor at what stage(s) of development this may occur. Thus CCR2-RFP^+ cells in these mice may have expressed CCR2 earlier in development but fail to maintain expression.

Together these results appear to confirm the findings in $CCR2^{-/-}$ mice that intestinal $CD103^-CD11b^+$ DCs show a selective association with expression of this receptor. However further investigation is required to explore the reasons for the discrepant results obtained using different methods for detecting CCR2 expression.

9.6 Putative CCR2$^+$CD103$^-$CD11b$^+$ Equivalent DCs Exist in the Healthy Human Colonic LP

Around the time I had identified CCR2$^+$ DCs in the murine intestine, Dr Simon Milling's group were establishing methods for characterising DCs in human intestine and I decided it would be of interest to examine if CCR2 expression might also define heterogeneity in humans. DCs were identified in healthy human colonic LP as live CD45$^+$ CD14$^-$ CD64$^-$ CD11c$^+$ HLA-DR$^+$ cells (Bain et al., 2013; Jaensson et al., 2008; Persson et al., 2013b; Schlitzer et al., 2013) and then divided into three populations on the basis of CD103 and SIRPα expression (Fig. 9.19A,B). The latter was used as a surrogate marker for CD11b, which is not a useful marker of human DCs, but its expression in many species appears to identify the DC subsets homologous to CD11b$^+$ DCs in mice (Persson et al., 2013b; Schlitzer et al., 2013). Using this approach, clear populations of CD103$^+$SIRPα^+, CD103$^+$SIRPα^- and CD103$^-$SIRPα^+ DCs could be identified. Interestingly, a significant proportion of CD103$^-$SIRPα^+ DCs, the putative equivalents of murine CD103$^-$CD11b$^+$ DCs, expressed CCR2, indicating that this population may be heterogeneous in both species. However, in contrast to mice, humans CD103$^-$SIRPα^+ DCs contained approximately equal proportions of CCR2$^+$ and CCR2$^-$ cells (Fig. 9.19C). A smaller proportion of human CD103$^+$SIRPα^+ DCs also expressed CCR2, while the CD103$^+$SIRPα^- DCs did not (Fig. 9.19C). However, it should be noted that it was more difficult to resolve clearly between CD103$^+$ and CD103$^-$ DCs in humans than in mice. Thus the apparent expression of CCR2 by CD103$^+$SIRPα^+ DCs needs further confirmation using better-optimised staining methods.

9.7 CCR2$^+$CD103$^-$CD11b$^+$ MPs are genuine DCs

As noted above, CCR2 dependency has usually been interpreted to mean that MPs are derived from monocytes. Therefore I thought it important to rule out the possibility that the CCR2$^+$ subset of CD103$^-$CD11b$^+$ I had found represented a population of monocyte derived cells that might have had been overlooked in my earlier analyses in which I had assumed the CD103$^-$CD11b$^+$ DCs to be a homogenous population. First, I FACS-purified the CCR2$^-$ and CCR2$^+$ subsets of CD103$^-$CD11b$^+$ SI LP DCs and compared their expression of mRNA for the DC-

specific genes, *Zbtb46* and *Flt3* with the other LP populations of DCs and mϕs. This showed that both the CCR2^{+} and CCR2^{-} subsets of CD103^{-}CD11b^{+} DCs expressed *Zbtb46* and *Flt3* at identical levels to the CD103^{+} DC subsets (Fig. 9.20). In addition and consistent with their presence in the migratory population of DCs in the MLNs, the CCR2^{+}CD103^{-}CD11b^{+} DCs also expressed mRNA for *Ccr7* at similar levels to the CCR2^{-}CD103^{-}CD11b^{+} and CD103^{+} DC subsets (Fig. 9.20). These results contrasted markedly with the lack of expression of any of these genes by the CD64^{+} mϕs which are the progeny of CCR2-dependent Ly6C^{hi} monocytes (Bain et al., 2013; Tamoutounour et al., 2012).

As these results suggested that pre-DCs were likely to give rise to CCR2^{+} DCs, I next examined this directly by investigating CCR2 expression by donor-derived DCs in the SI LP 5 days after transfer of FACS-purified pre-DCs. Under these conditions, 15-20% of donor-derived CD103^{-}CD11b^{+} and CD103^{-}CD11b^{-} DCs in the SI LP expressed CCR2, clearly demonstrating that CCR2^{+}CD103^{-} DCs arise from pre-DCs (Fig. 9.21). Small numbers of donor-derived CD103^{+}CD11b^{+} and CD103^{+}CD11b^{-} DCs SI LP DCs also expressed CCR2, although these were far lower than with the CD103^{-} subsets (Fig. 9.21).

9.8 Development of all SI LP DC Subsets is Partially Dependent on CCR2

I next investigated whether CCR2 expression by pre-DCs might account for the expression of and dependence on CCR2 by some LP DCs. Anti-CCR2 antibody staining showed that a proportion of pre-DCs (~25%) in normal BM expressed this receptor and this was specific, as no staining was found using CCR2$^{-/-}$ BM as controls (Fig. 9.22A,B). In comparison, ~80% of Ly6C^{hi} monocytes were CCR2^{+} in the same experiment (Fig. 9.22A,B). This expression of CCR2 did not appear to correlate with a dependence of pre-DCs on CCR2, as WT and CCR2$^{-/-}$ mice had identical proportions of pre-DCs in the BM and blood. In contrast and as expected, Ly6C^{hi} monocytes were virtually absent from the blood of CCR2$^{-/-}$ mice, confirming the requirement for this receptor in the export of these cells from the BM (Fig. 9.22C,D).

As I was unable to purify enough CCR2^{+} pre-DCs to determine whether CCR2 expression defined the function of pre-DCs using an adoptive transfer

approach, I decided to examine this by competitively transferring pre-DCs from CD45.1$^+$/CD45.2$^+$ WT and CD45.2$^+$ CCR2$^{-/-}$ BM into CD45.1 resting WT recipients. Interestingly, 7 days after transfer, I found that all DC subsets were derived preferentially from WT pre-DCs, with only 25-35% being derived from the CCR2$^{-/-}$ pre-DCs. No significant differences in CCR2 dependence were seen between the DC subsets under these conditions (Fig. 9.23). Thus CCR2 plays a role in the generation of all DC subsets, suggesting that it may be required for the recruitment of pre-DCs into tissues and/or their subsequent development into mature DCs. Further studies are required to investigate this phenomenon.

9.9 Functions of CCR2$^+$CD103$^-$CD11b$^+$ Intestinal DCs

Having identified CCR2$^+$ DCs in SI LP, I wanted to examine if these were functionally distinct from their CCR2$^-$ counterparts.

9.9.1 *In Vitro* Functions

Due to the limitations on sorting multiple populations simultaneously, I decided to focus on the CCR2$^+$CD103$^-$CD11b$^+$ DCs, as these were the subset which consistently showed the highest expression of CCR2 and dependence on its presence. Furthermore, these were the only CCR2$^+$ DCs found in the MLNs, the tissue where any immune priming activity by mucosa-derived DCs will take place. Thus I FACS-purified CCR2$^+$ and CCR2$^-$ CD103$^-$CD11b$^+$ DCs from SI LP of WT mice, pulsed them with OVA-protein and examined their ability to induce proliferation and functional differentiation of FACS-purified, naïve, CFSE-labelled OTII CD4$^+$ T cells *in vitro*. As controls, I compared the APC activity of sorted CD103$^+$CD11b$^+$ and CD103$^+$CD11b$^-$ DCs from the same mice.

These studies showed that the CCR2$^+$CD103$^-$CD11b$^+$ LP DCs (herein referred to as CCR2$^+$ DCs) were as capable as the other SI LP DC populations at inducing antigen-specific CD4$^+$ T cell proliferation, as assessed by dilution of the CSFE dye (Fig. 9.24A). The CCR2$^+$ and CCR2$^-$ subsets of CD103$^-$CD11b$^+$ DCs induced similar levels of FoxP3 expression by the CD4$^+$ T cells, with both being less efficient at this than either of the CD103$^+$ DC populations, consistent with my previous findings (Fig. 9.24). The CCR2$^+$ subset also induced similar proportions of IFNγ production by co-cultured CD4$^+$ T cells as the CCR2$^-$CD103$^-$CD11b$^+$ and

$CD103^+CD11b^+$ DCs. As before, the $CD103^+CD11b^-$ DCs were the most effective inducers of IFNγ (Fig. 9.25). In contrast, the $CCR2^+$ DCs were the most efficient at driving T_h17 cell polarisation, inducing 2-fold more $IL17a^+$ $CD4^+$ T cells than either their $CCR2^-$ counterparts or the $CD103^+CD11b^+$ DCs and approximately 5-fold more $IL17a^+$ T cells than the $CD103^+CD11b^-$ DCs (Fig. 9.26).

As these results suggested that the $CCR2^+CD103^-CD11b^+$ DCs had a superior ability to prime T_h17 cells *in vitro,* I next investigated if the absence of CCR2 dependent DCs in $CCR2^{-/-}$ mice influenced the ability of LP DCs to induce T cell priming *in vitro.* To do this, I cultured naïve $CD4^+$ T cells with OVA pulsed $CD103^-CD11b^+$ DCs from the SI LP of WT and $CCR2^{-/-}$ mice. These experiments showed that $CD103^-CD11b^+$ DCs from WT and $CCR2^{-/-}$ mice induced similar levels of proliferation and T_h1 differentiation *in vitro*, but the $CCR2^{-/-}$ DCs were significantly less effective at inducing T_h17 differentiation than their WT counterparts (Fig. 9.27).

Together these results suggest that the CCR2 expressing/dependent subset of $CD103^-CD11b^+$ DCs has a preferential ability to drive the generation of T_h17 cells *in vitro*.

9.9.2 *In Vivo* Functions

I next examined the *in vivo* consequences of these findings by comparing T cell priming in WT and $CCR2^{-/-}$ mice using a protocol known to induce T_h17 differentiation in MLNs (Persson et al., 2013b). Naïve OTII cells were transferred into WT and $CCR2^{-/-}$ mice, which were immunised i.p. 1 day later with OVA together with anti-CD40 and LPS as adjuvants. Immunised mice also received the S1P agonist FTY720 1 and 3 days after immunisation to prevent the activated T cells from leaving the MLNs. Four days after immunisation, intracellular cytokine staining revealed there were significantly fewer $IL17a^+$ cells in the MLNs of immunised $CCR2^{-/-}$ mice compared with WT controls, whereas $IFN\gamma^+$ cells were identical (Fig. 9.28A).

To investigate further the role of CCR2-dependent $CD103^-CD11b^+$ DCs in priming T_h17 cells *in vivo,* I next infected WT and $CCR2^{-/-}$ mice with *Citrobacter rodentium.* 6 days later, the two strains showed similar levels of infection as

assessed counts of colony forming units in faeces (Fig. 9.28B). However on day 7, the CCR2$^{-/-}$ mice had significantly fewer T_h17 cells in the MLNs than seen in WT mice, whereas T_h1 cell priming was unaffected (Fig. 9.28C). Together these results support the idea that CCR2-dependent CD103$^-$CD11b$^+$ DCs play a selective role in the priming of T_h17 cells.

9.9.3 Enhanced T_h17 Induction by CCR2$^+$CD103$^-$CD11b$^+$ DCs Correlates with Increased IL12/IL23p40 Production

In an attempt to understand why CCR2$^+$CD103$^-$CD11b$^+$ DCs had a preferential ability to prime T_h17 cells, I compared the CCR2$^-$ and CCR2$^+$ CD103$^-$ CD11b$^+$ DCs, as well as the CD103$^+$ DC populations for their expression of T_h17 polarising cytokines. First I examined IL6 production by the DC subsets in the presence and absence of exogenous TLR4 stimulation. Intracellular cytokine staining revealed that a slightly lower proportion of resting CCR2$^+$CD103$^-$CD11b$^+$ DCs produced IL6 than the other subsets and a similar pattern was seen when the DCs were stimulated with LPS, which had no significant effects on IL6 production by any subset (Fig. 9.29). Thus IL6 production is unlikely to account for the increased propensity of CCR2$^+$ DCs to induce T_h17 cell differentiation. In contrast, ~3-fold more CCR2$^+$CD103$^-$CD11b$^+$ DCs expressed IL12/IL23p40 in the steady state than either the CCR2$^-$CD103$^-$CD11b$^+$ or CD103$^+$CD11b$^+$ DC subsets (Fig. 9.30). Interestingly the preferential ability of steady state CD103$^+$CD11b$^-$ DCs to prime T_h1 cells *in vitro* was associated with the presence of similar numbers of IL12/IL23p40 producing cells to those seen amongst CCR2$^+$CD103$^-$CD11b$^+$ DCs, perhaps reflecting IL12 production by the CD103$^+$CD11b$^-$ DCs. LPS stimulation led to increases in the proportion of IL12/IL23p40 producing cells amongst all the DC subsets except for the CD103$^+$CD11b$^-$ DCs, but this was much more marked with CCR2$^+$CD103$^-$CD11b$^+$ DCs, with ~30% of these now producing the cytokine (Fig. 9.30). As I was unable to detect IL23p19 using either commercially available antibodies or qPCR analysis of steady state DCs, or develop a protocol in which LPS stimulated DCs could be analysed by qPCR, it is not possible to conclude definitively that these findings reflect enhanced IL23 production by the CCR2$^+$CD103$^-$CD11b$^+$ DCs. However, their selective effect on T_h17 cell differentiation and the lack of correlation between their ability to produce IL12/IL23p40 and prime T_h1 cells would suggest that IL23 accounts for the difference in IL12/IL23p40 production by these cells.

9.10 Summary

In the previous chapters, I had defined DC populations in the intestine based on their phenotype, kinetics, Flt3L dependence, ontogeny and function. These studies revealed four distinct subsets of DCs, including two novel $CD103^-$ DC populations, which were derived from DC-committed precursors and not from the $Ly6C^{hi}$ monocytes, which gave rise solely to $CD64^+F4/80^+$ mϕs. However recent work from the Jung lab proposed that a genuine population of CCR2-dependent, $Zbtb46^+$ monocyte-derived DC exists, albeit during inflammation (Zigmond et al., 2012). Thus in order to align these results with my own, in this chapter I examined the CCR2 dependence of the DC populations I had identified earlier.

Initially I found that $CCR2^{-/-}$ mice had reduced numbers of $CD103^-CD11b^+$ DCs in the SI LP and amongst migratory DCs in the MLNs. This partial reduction was cell intrinsic, as these DC populations were also reduced in WT:$CCR2^{-/-}$ mixed BM chimeras. A population of CCR2-dependent $CD11b^+$ DCs was also found in lung and spleen and I hypothesised that these DCs may correspond to steady state equivalents of those identified by Zigmond et al. (Zigmond et al., 2012).

I next investigated if the partial dependence on CCR2 reflected heterogeneity in the $CD103^-CD11b^+$ DC subset and examined their expression of CCR2, using antibody staining, a CCL2 uptake assay and $CCR2^{+/RFP}$ reporter mice. All these methods showed that the intestinal $CD103^-CD11b^+$ DC population was consistently heterogeneous for CCR2 expression, with the majority of the population being $CCR2^-$ while 15-25% were $CCR2^+$, consistent with these being reduced in $CCR2^{-/-}$ mice. However the exact levels of CCR2 and the pattern of CCR2 expression by the different DC subsets varied depending on the assay used and it appeared that CCR2 may also be expressed by other intestinal DC at least at some stages of their development. This requires further investigation in the future.

Although I had not been able to find $Ly6C^{hi}$ monocytes giving rise to any of my original DC subsets in Chapter 4, to rule out the possibility that the newly discovered small subset of $CCR2^+CD103^-CD11b^+$ DCs might have been overlooked in my previous analyses, I first showed that this subset expressed the

DC specific genes *Zbtb46*, *Flt3* and *CCR7* at the same levels as the other, previously defined subsets in SI LP. I next found that adoptively transferred pre-DC gave rise to both $CCR2^+$ and $CCR2^-$ $CD103^-CD11b^+$ DCs. Interestingly a small population of pre-DCs also expressed CCR2 and although pre-DC numbers were normal in CCR2-deficient mice, WT precursors outcompeted $CCR2^{-/-}$ pre-DCs in their ability to generate all DC subsets *in vivo.* Thus CCR2 may play a wider role in DC development than is suggested by the small and selective defect in the KO mice.

I next determined the functional characteristics of this previously unrecognised population of $CCR2^+CD103^-CD11b^+$ DCs. The $CCR2^+$ DCs were equally capable of inducing naïve $CD4^+$ T cells to proliferate and acquire FoxP3 expression or IFNγ production *in vitro* as the $CCR2^-CD103^-CD11b^+$ DC subset However the $CCR2^+$ DCs were superior at inducing IL17a production by proliferating T cells to any other DC subset, including the $CD103^+CD11b^+$ DCs recently proposed to be the main inducers of mucosal T_h17 responses *in vivo* (Denning et al., 2011; Lewis et al., 2011; Persson et al., 2013b; Schlitzer et al., 2013). Importantly, total $CD103^-CD11b^+$ DCs from $CCR2^{-/-}$ mice were also less able to induce T_h17 cells compared with WT $CD103^-CD11b^+$ DC *ex vivo* and $CCR2^{-/-}$ mice had defective induction of T_h17 cells in the MLNs *in vivo* after immunisation with specific antigen plus adjuvant, and during infection with *Citrobacter rodentium*. The enhanced ability of $CCR2^+CD103^-CD11b^+$ DCs to drive T_h17 responses correlated with high levels of production of IL12/IL23 and this appeared to reflect IL23 rather than IL12. As I was able to identify a population of $CCR2^+CD103^-SIRP\alpha^+$ DCs in the healthy human colonic LP, this heterogeneity may be of clinical relevance.

Overall, these studies have identified a novel population of $CCR2^+$ $CD103^-$ $CD11b^+$ DCs that are derived from DC-committed precursors and that are involved in driving T_h17 responses both *in vitro* and *in vivo*. However it has to be noted that this conclusion appears to contradict my earlier findings in Chapters 7 and 8, where I found that a lack of $CD103^+CD11b^+$ DCs was associated with decreased T_h17 responses *in vivo* and these discrepant results require further exploration.

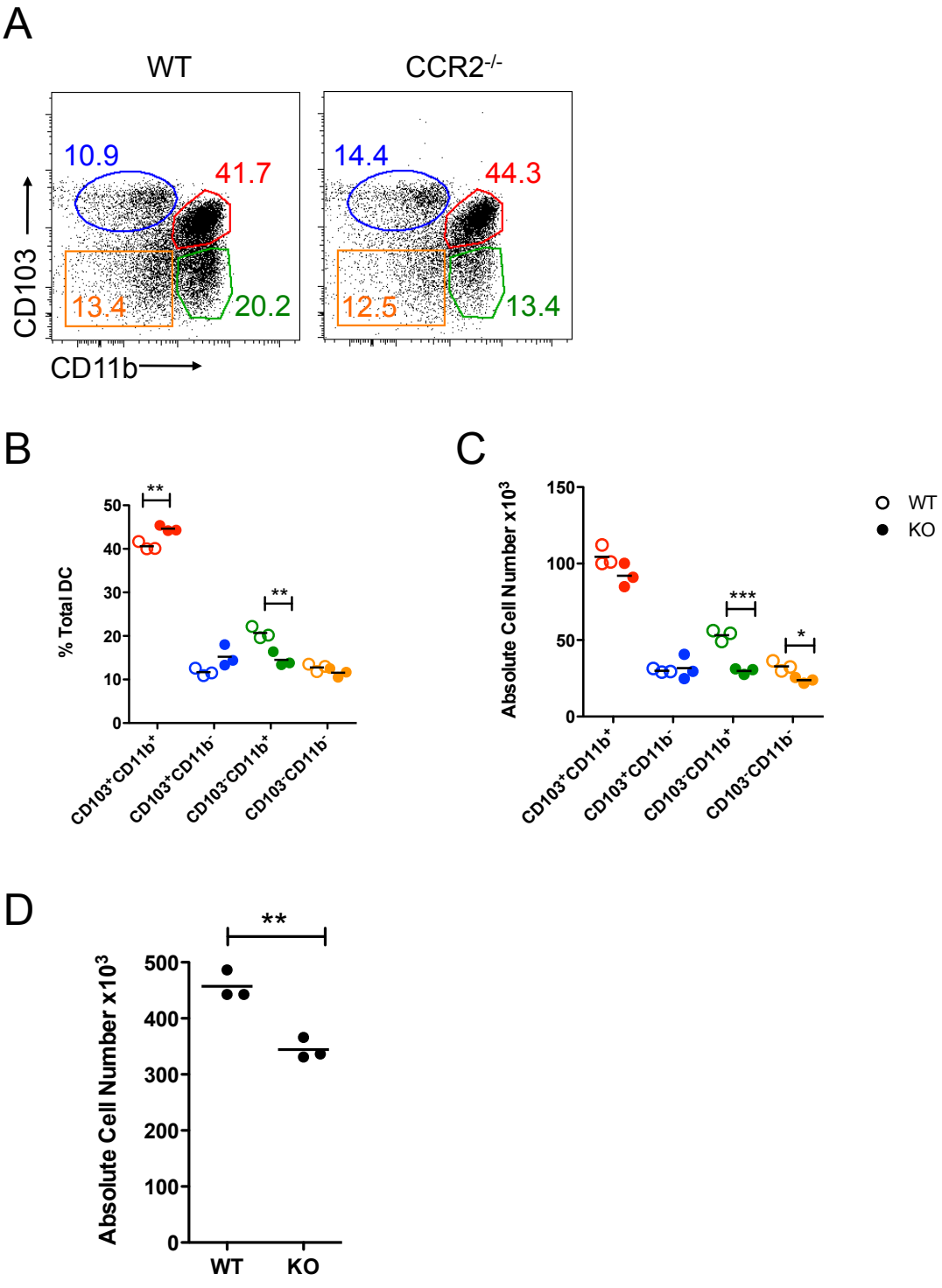

Figure 9.1: DC subsets in SI LP of CCR2$^{-/-}$ mice

SI LP cells were isolated from WT and CCR2$^{-/-}$ mice and total DC (live CD45^{+} CD11c^{+} MHCII^{+} CD64^{-}) were analysed for expression of CD103 and CD11b. **A.** Representative dot plots of CD103 and CD11b expression by WT and CCR2$^{-/-}$ mice. **B.** Proportion of each SI LP DC population as a percentage of total DC in WT and CCR2$^{-/-}$ (KO) mice. **C.** Absolute number of each DC population in SI LP of WT and CCR2$^{-/-}$ (KO) mice. **D.** Absolute number of CD64^{+} mϕs in the SI LP of CCR2$^{-/-}$ mice compared with WT controls. Data are representative of 2 independent experiments with n=3-4 per group per experiment. *p<0.05, **p<0.01, ***p<0.001, Student's t test.

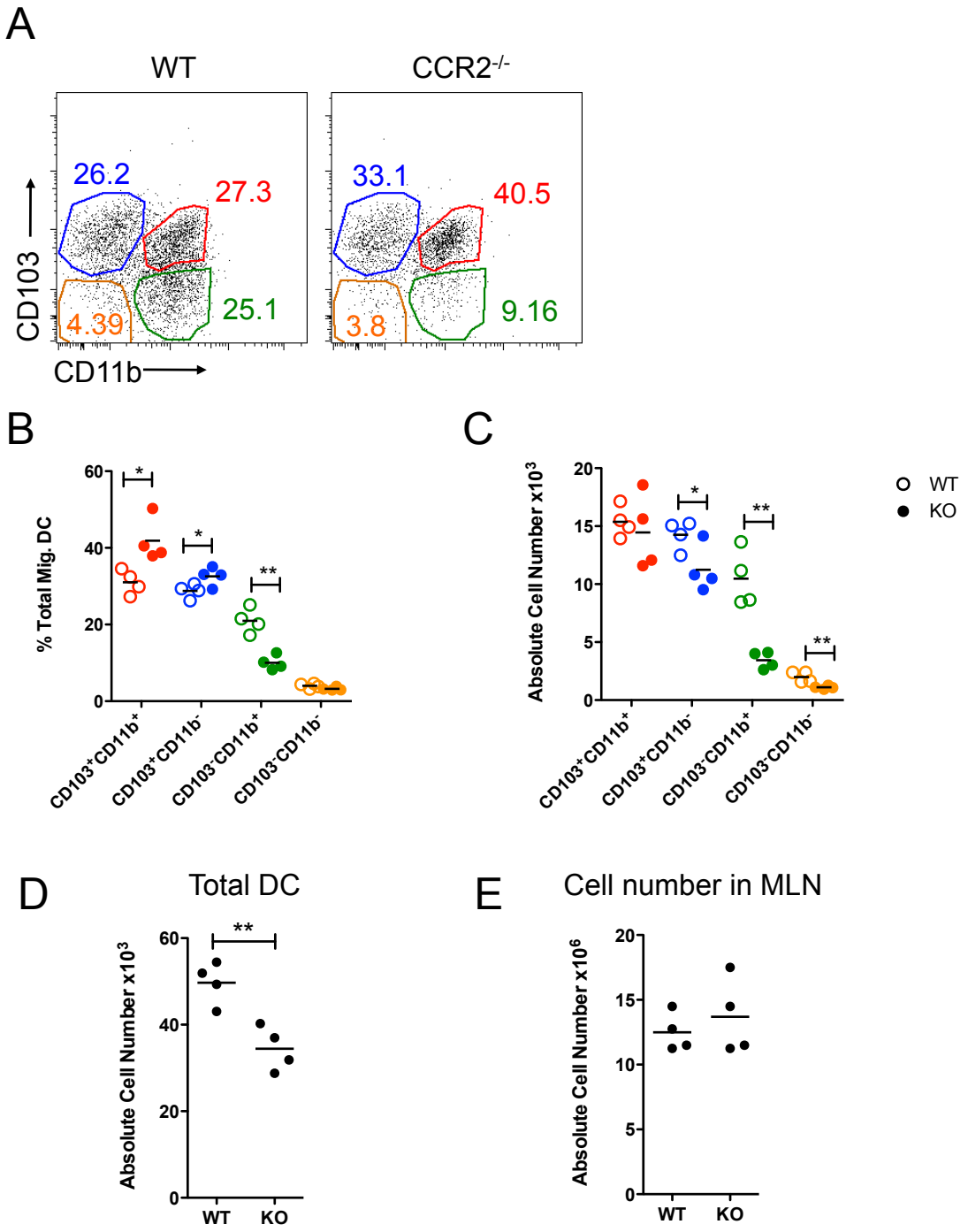

Figure 9.2: DC subsets amongst migratory DC in MLNs of CCR2$^{-/-}$ mice

MLN cells were isolated from WT and CCR2$^{-/-}$ mice and CD11c^{+}MHCII^{hi} migratory DCs were examined for expression of CD103 and CD11b. **A.** Representative CD103 and CD11b expression by migratory DCs in WT and CCR2$^{-/-}$ mice. **B.** Proportion of each migratory DC subset as a percentage of total migratory DC in the MLNs of WT and CCR2$^{-/-}$ (KO) mice. **C.** Absolute numbers of each migratory DC population in WT and CCR2$^{-/-}$ (KO) mice. **D.** Absolute numbers of total migratory DCs in WT and CCR2$^{-/-}$ (KO) mice. **E.** Total cell number in MLNs of WT and CCR2$^{-/-}$ (KO) mice. Data are from a single experiment with n=4. *p<0.05, **p<0.01, Student's t test.

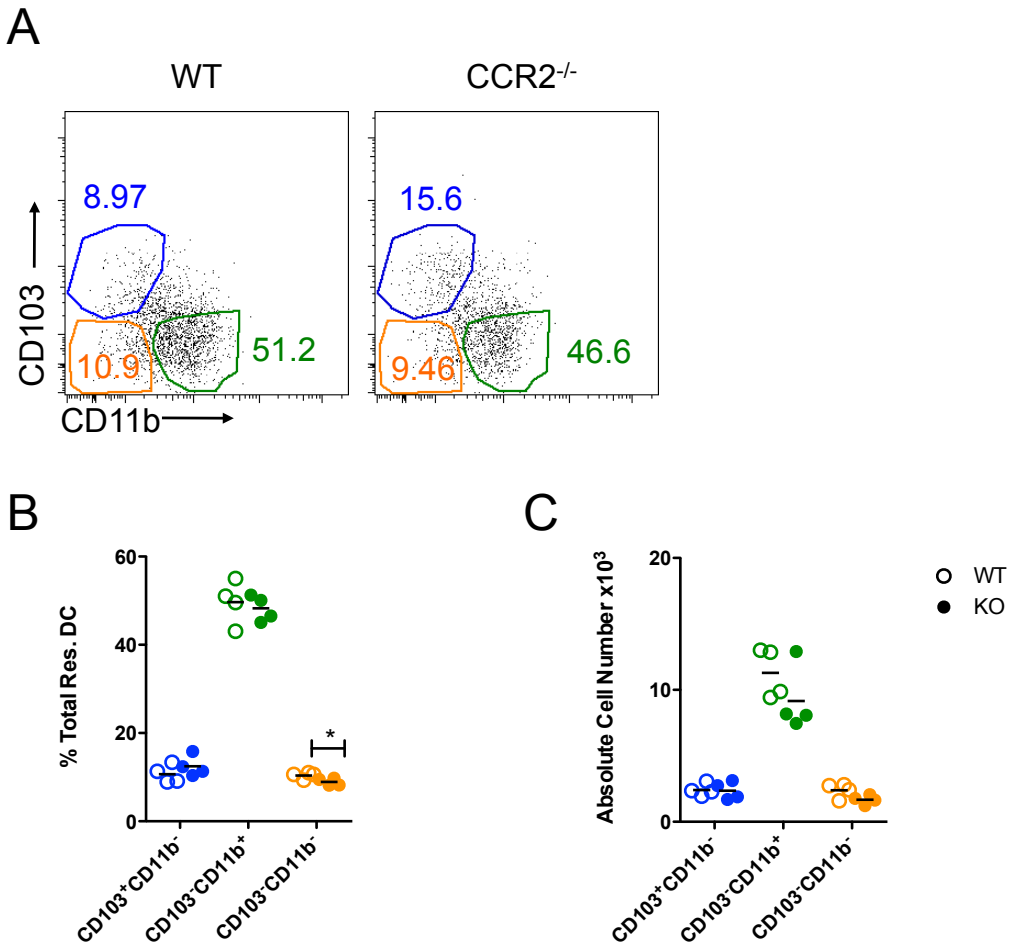

Figure 9.3: DC subsets amongst resident DCs in MLN of CCR2$^{-/-}$ mice

MLN cells were isolated from WT and CCR2$^{-/-}$ mice and CD11c^{+}MHCII^{int} resident DCs were examined for expression of CD103 and CD11b. **A.** Representative CD103 and CD11b expression by resident DCs in WT and CCR2$^{-/-}$ mice. **B.** Proportion of each resident DC subset as a percentage of total resident DCs in the MLN of WT and CCR2$^{-/-}$ (KO) mice. **C.** Absolute numbers of each resident DC population in WT and CCR2$^{-/-}$ (KO) mice. Data are from a single experiment with n=4. *p<0.05, Student's t test.

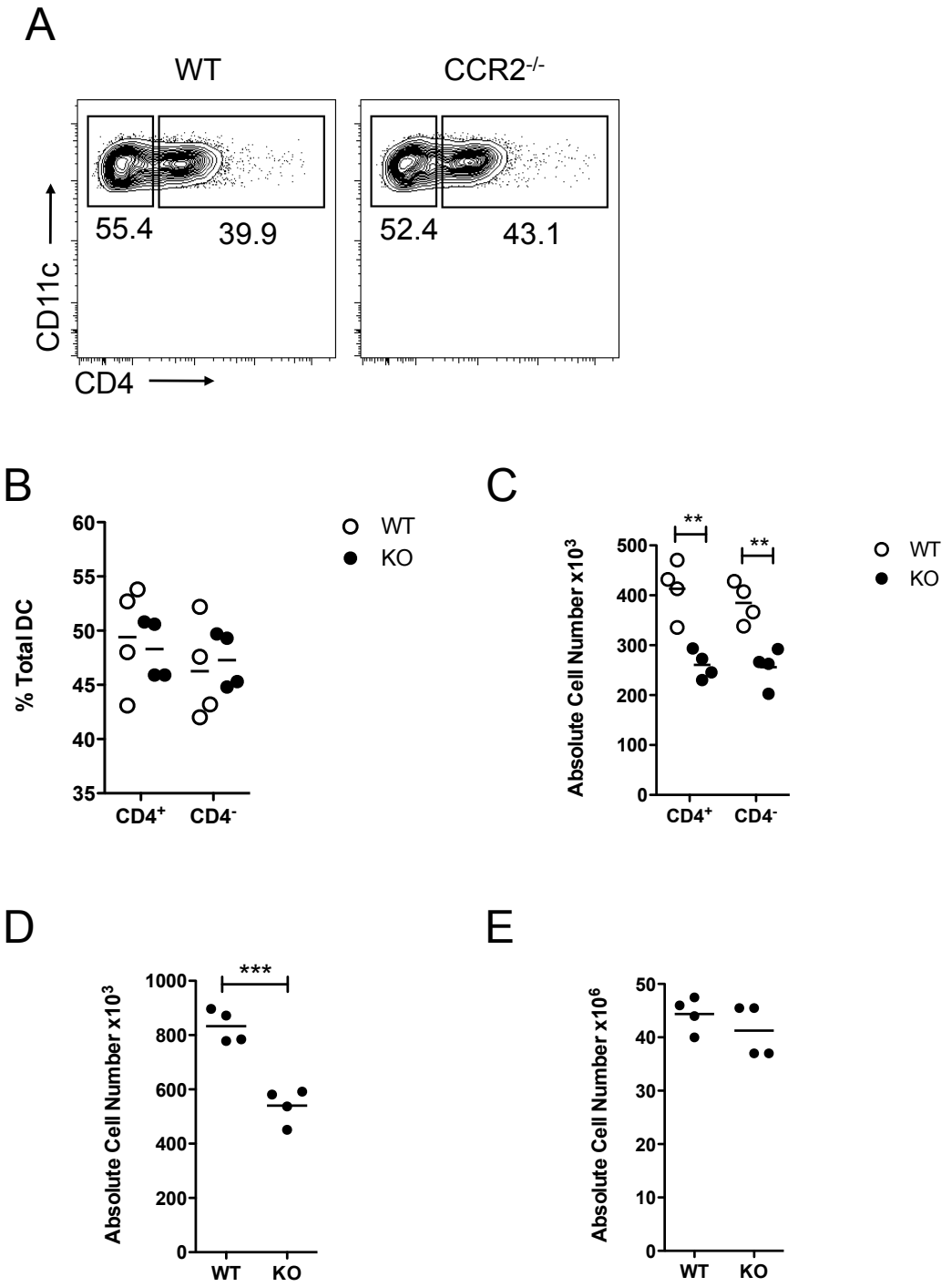

Figure 9.4: DC subsets in spleen of CCR2$^{-/-}$ mice

Splenocytes were isolated from WT and CCR2$^{-/-}$ mice and total CD11c^{+}MHCII^{+}CD64^{-} DCs were examined for expression of CD4. **A.** Representative staining of CD11c and CD4 expression by total DC in WT and CCR2$^{-/-}$ mice. **B.** Proportion of CD4^{+} and CD4^{-} DC as a percentage of total DC in WT and CCR2$^{-/-}$ (KO) mice. **C.** Absolute numbers of CD4^{+} and CD4^{-} DC in WT and CCR2$^{-/-}$ (KO) mice. **D.** Absolute numbers of total DCs in spleens of WT and CCR2$^{-/-}$ (KO) mice. **E.** Total cell numbers in spleens of WT and CCR2$^{-/-}$ (KO) mice. Data are from a single experiment with n=4.**p<0.01, ***p<0.001, Student's t test.

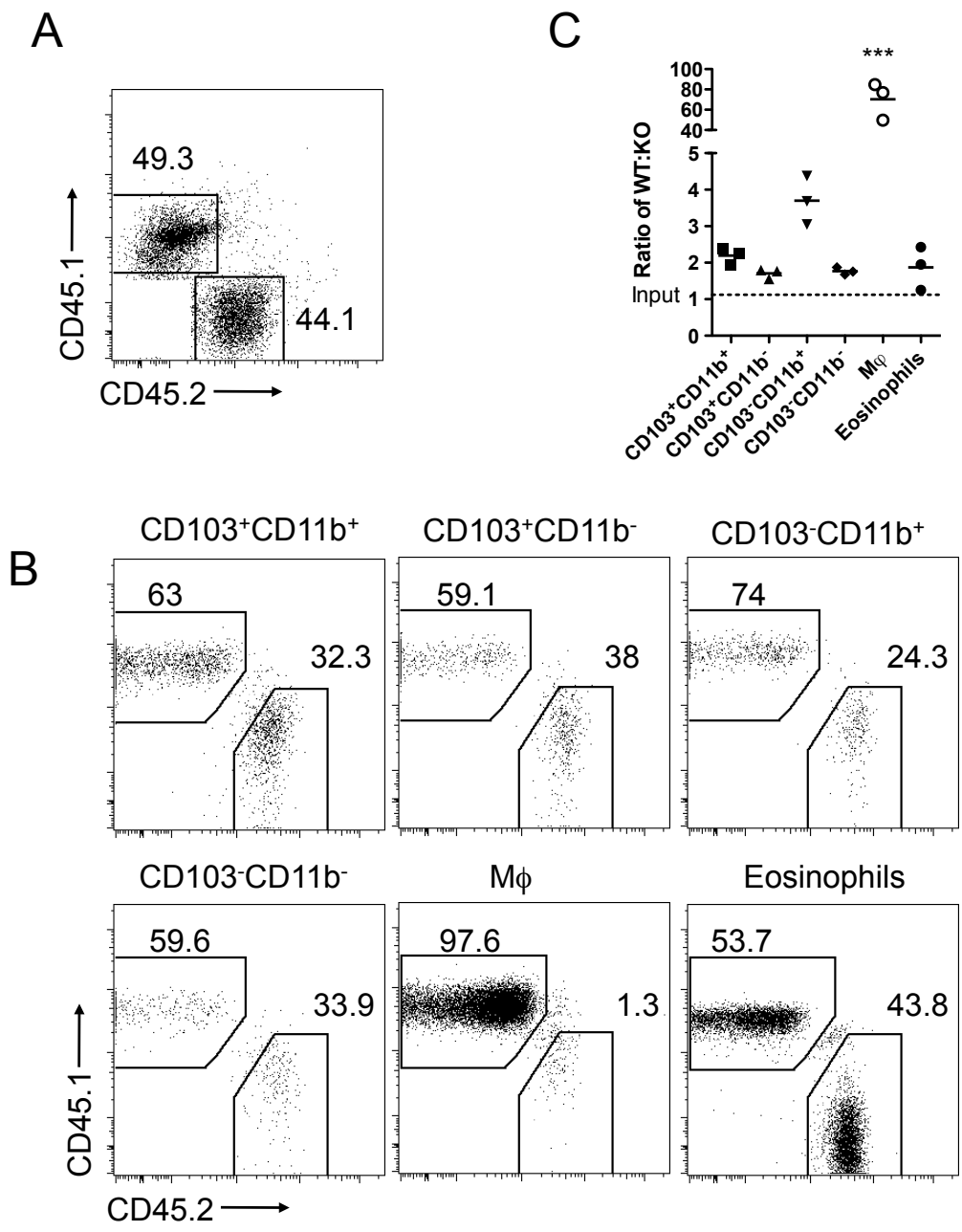

Figure 9.5: Myeloid Populations in SI LP of WT:CCR2$^{-/-}$ competitive BM chimeras

Mixed WT:CCR2$^{-/-}$ BM chimeras were generated by lethally irradiating CD45.1/CD45.2 WT mice and reconstituting with a 50:50 mix of CD45.1^{+} WT and CD45.2^{+} CCR2$^{-/-}$ BM. The level of chimerism was assessed 8 weeks after reconstitution. **A.** CD45.1 and CD45.2 expression by the BM leukocyte mixture used to reconstitute irradiated recipients. **B.** Live CD45^{+} CD11c^{+} MHCII^{+} MP populations as defined in Fig. 3.3 and live CD45^{+} CD11b^{+} MHCII^{-} SSC^{hi} eosinophils in SI LP were analysed for CD45.1^{+} and CD45.2^{+} expression. Numbers represent percentage of CD45.1 or CD45.2 cells amongst each population. **C.** Ratio of WT:CCR2$^{-/-}$ derived cells amongst the populations of MPs and eosinophils from SI LP of chimeric mice. ***p<0.001, one way ANOVA with Bonferroni post-test between mϕs and all other SI LP MP populations. Data are from a single experiment with n=3.

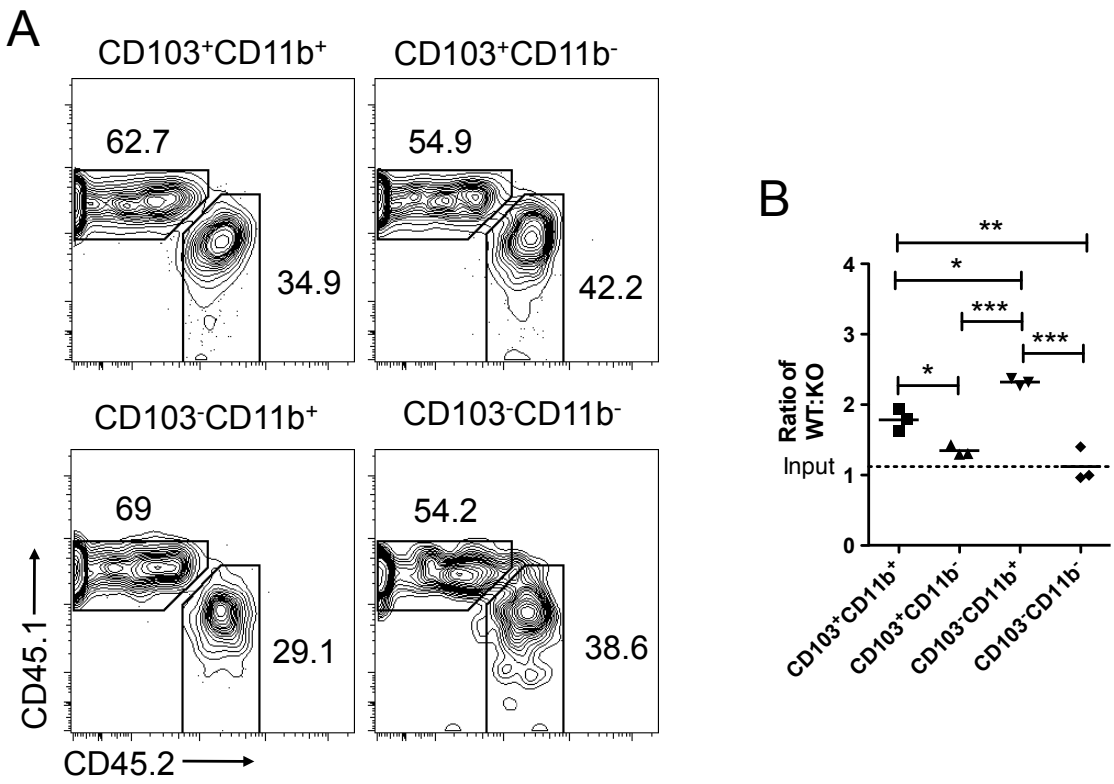

Figure 9.6: Migratory DCs in MLNs of WT:CCR2$^{-/-}$ competitive BM chimeras

Mixed WT:CCR2$^{-/-}$ BM chimeras were generated by lethally irradiating CD45.1/CD45.2 WT mice and reconstituting with a 50:50 mix of CD45.1^{+} WT and CD45.2^{+} CCR2$^{-/-}$ BM. The level of chimerism was assessed 8 weeks after reconstitution. **A.** Migratory MLN CD11c^{+}MHCII^{hi} DCs were analysed for CD45.1 and CD45.2 expression. Numbers represent percentage of CD45.1^{+} or CD45.2^{+} cells amongst each DC population. **B.** Ratio of WT:CCR2$^{-/-}$ derived cells amongst the populations of migratory DCs in MLNs of chimeric mice. *p<0.05, **p<0.01, ***p<0.001, one way ANOVA with Bonferroni post-test. Data are from a single experiment with n=3.

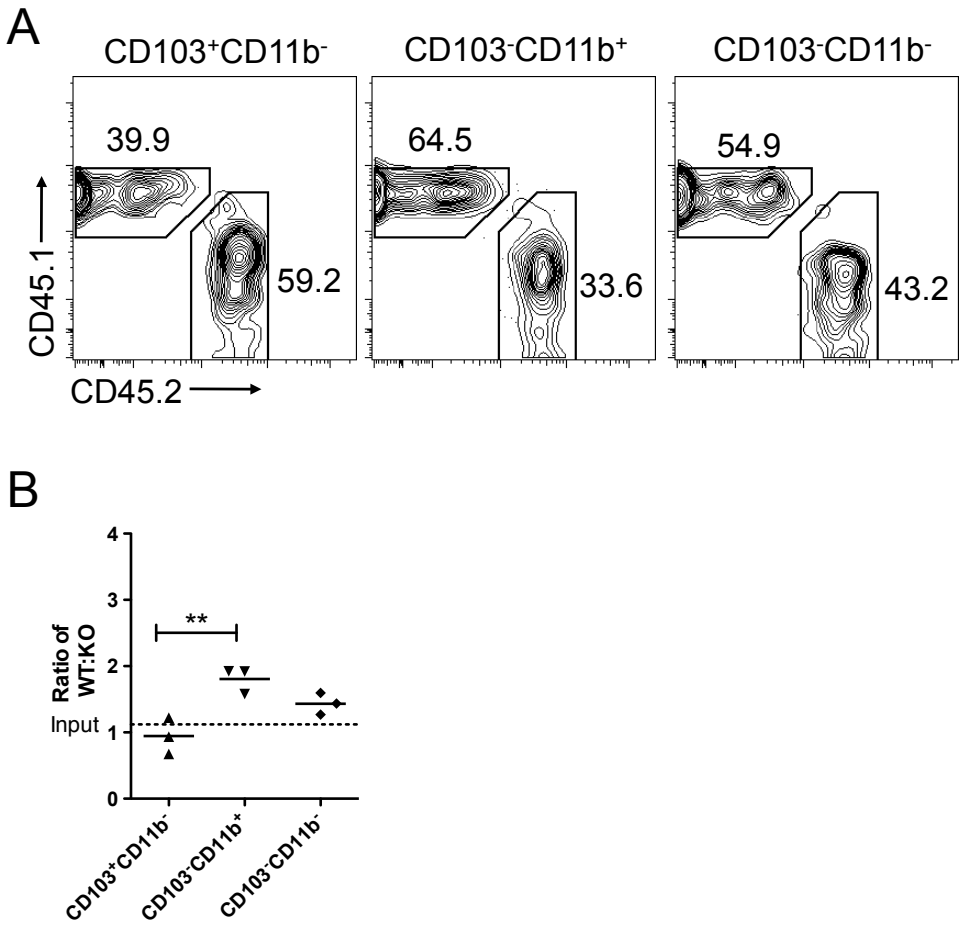

Figure 9.7: Resident DCs in MLNs of WT:CCR2$^{-/-}$ competitive BM chimeras

Mixed WT:CCR2$^{-/-}$ BM chimeras were generated by lethally irradiating CD45.1/CD45.2 WT mice and reconstituting with a 50:50 mix of CD45.1^{+} WT and CD45.2^{+} CCR2$^{-/-}$ BM. The level of chimerism was assessed 8 weeks after reconstitution. **A.** Resident MLN CD11c^{+}MHCII^{int} DCs were analysed for CD45.1 and CD45.2 expression. Numbers represent percentage of CD45.1^{+} or CD45.2^{+} cells amongst each DC population. **B.** Ratio of WT:CCR2$^{-/-}$ derived cells amongst the populations of resident DCs in MLNs of chimeric mice. **p<0.01, one way ANOVA with Bonferroni post-test. Data are from a single experiment with n=3.

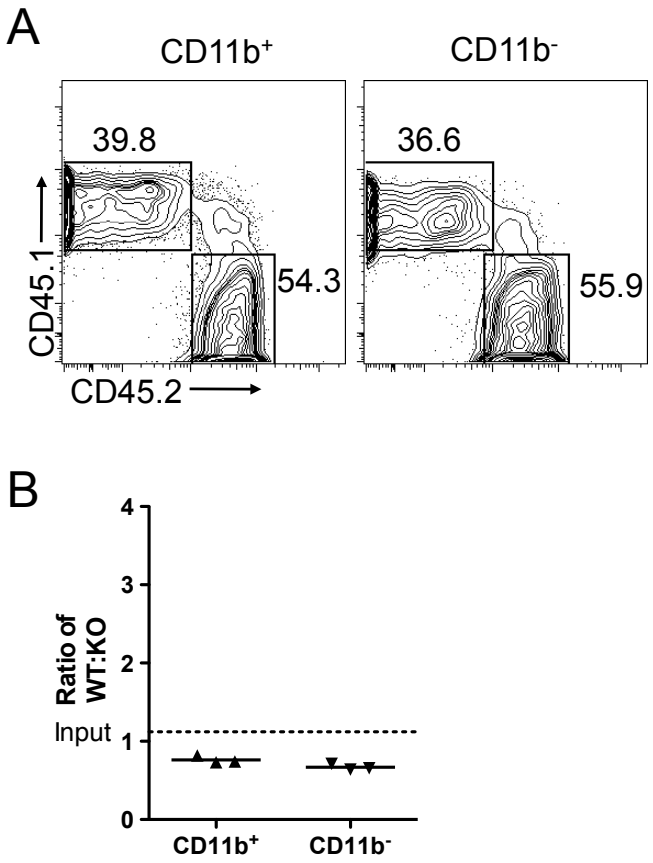

Figure 9.8: Splenic DC populations in WT:CCR2$^{-/-}$ competitive BM chimeras

Mixed WT:CCR2$^{-/-}$ BM chimeras were generated by lethally irradiating CD45.1/CD45.2 WT mice and reconstituting with a 50:50 mix of CD45.1^{+} WT and CD45.2^{+} CCR2$^{-/-}$ BM. The level of chimerism was assessed 8 weeks after reconstitution. **A.** Splenic CD11c^{+}MHCII^{+}CD64^{-} DCs were analysed for CD45.1 and CD45.2 expression. Numbers represent percentage of CD45.1^{+} or CD45.2^{+} cells amongst each DC population. **B.** Ratio of WT:CCR2$^{-/-}$ derived cells amongst the populations of splenic DCs of chimeric mice. Data are from a single experiment with n=3.

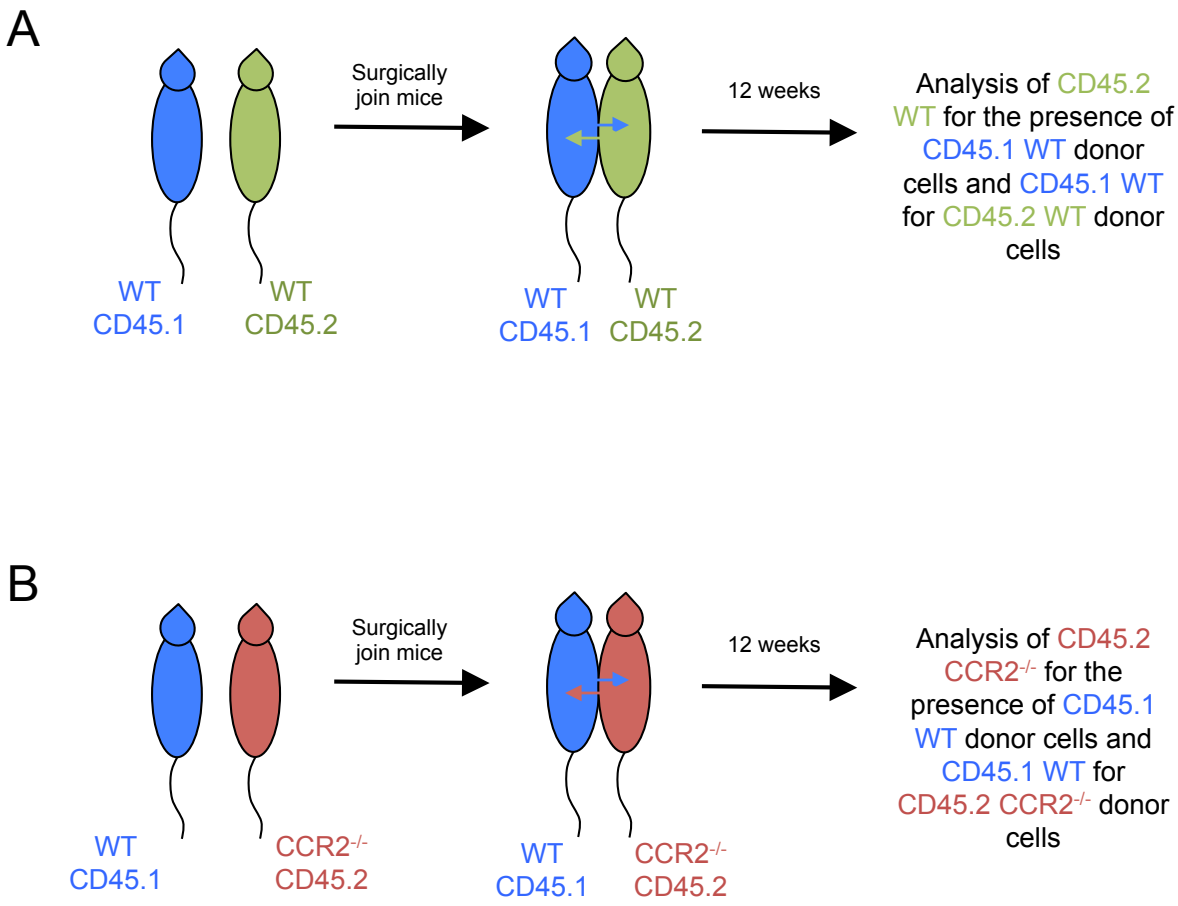

Figure 9.9: Generation of WT:WT and WT:CCR2$^{-/-}$ parabiotic mice

Parabiotic mice were generated in Bernard Malissen's group in Marseille, France by Dr. Sandrine Henri. **A,B.** WT:WT parabionts (A) and WT:CCR2$^{-/-}$ parabionts (B) were surgically and left for 12 weeks to allow exchange of blood leukocytes, before the SI LP was analysed for the level of chimerism in each partner.

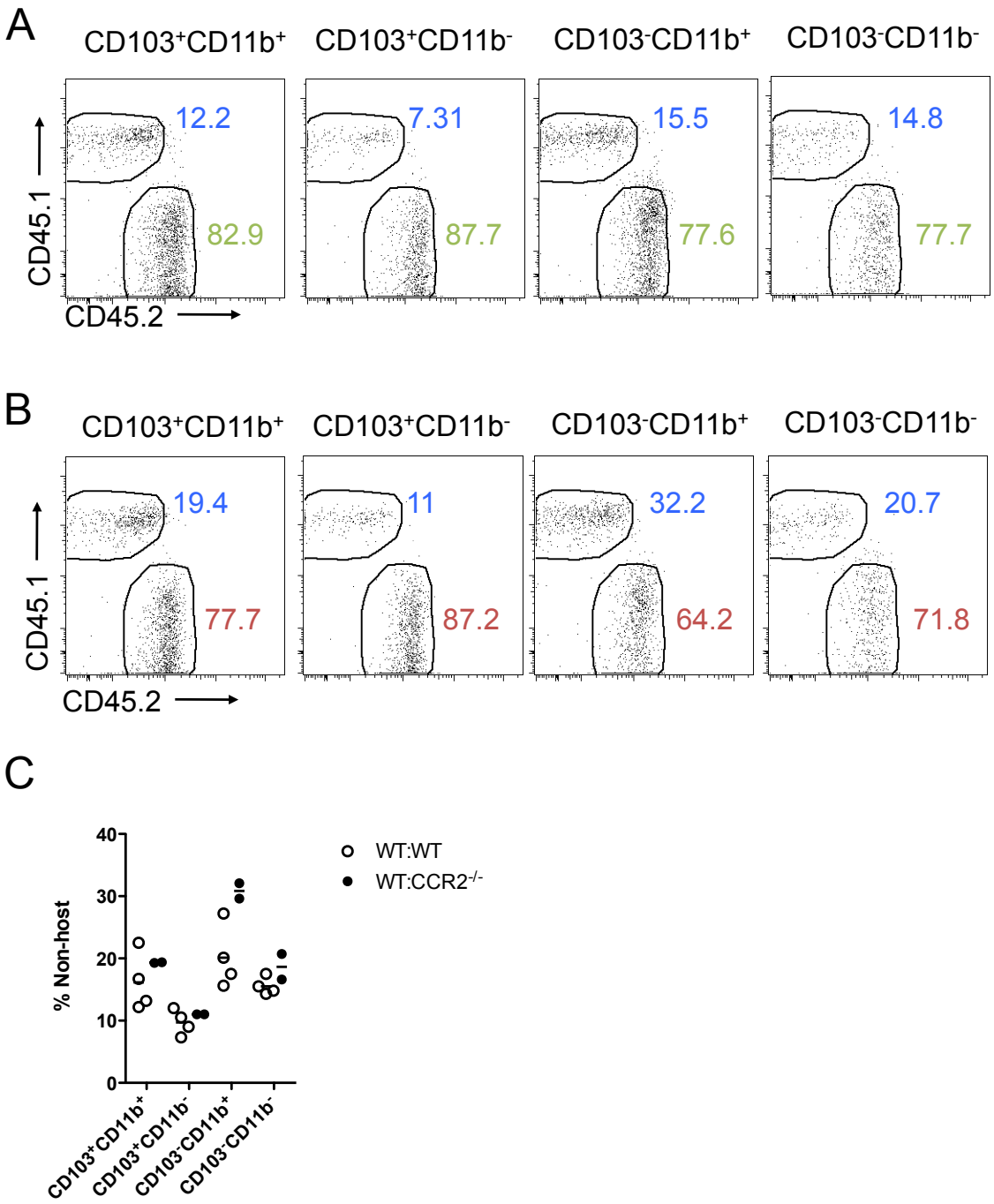

Figure 9.10: CD45.1$^+$ DC populations in SI LP of CD45.2$^+$ parabiont partner

WT:WT (CD45.1:CD45.2) and WT:CCR2$^{-/-}$ (CD45.1:CD45.2) parabiotic mice were generated as shown in Fig. 9.9 and left for 12 weeks before tissues were harvested and the level of chimerism examined. **A**. Representative CD45.1 and CD45.2 staining amongst populations of CD11c$^+$MHCII$^+$CD64$^-$ DCs in SI LP of the CD45.2$^+$ WT partner of WT:WT parabionts. Numbers represent percentage of CD45.1$^+$ or CD45.2$^+$ cells in each DC population. **B.** Representative CD45.1 and CD45.2 staining amongst populations of CD11c$^+$MHCII$^+$CD64$^-$ DCs in SI LP of the CD45.2$^+$ CCR2$^{-/-}$ partner of WT:CCR2$^{-/-}$ parabionts. Numbers represent percentages of CD45.1$^+$ or CD45.2$^+$ cells in each DC population. **C.** Percentage of non-host (CD45.1$^+$) cells in CD45.2$^+$ parabiotic partners. Data are from a single experiment with 4 WT:WT parabionts and 2 WT:CCR2$^{-/-}$ parabionts.

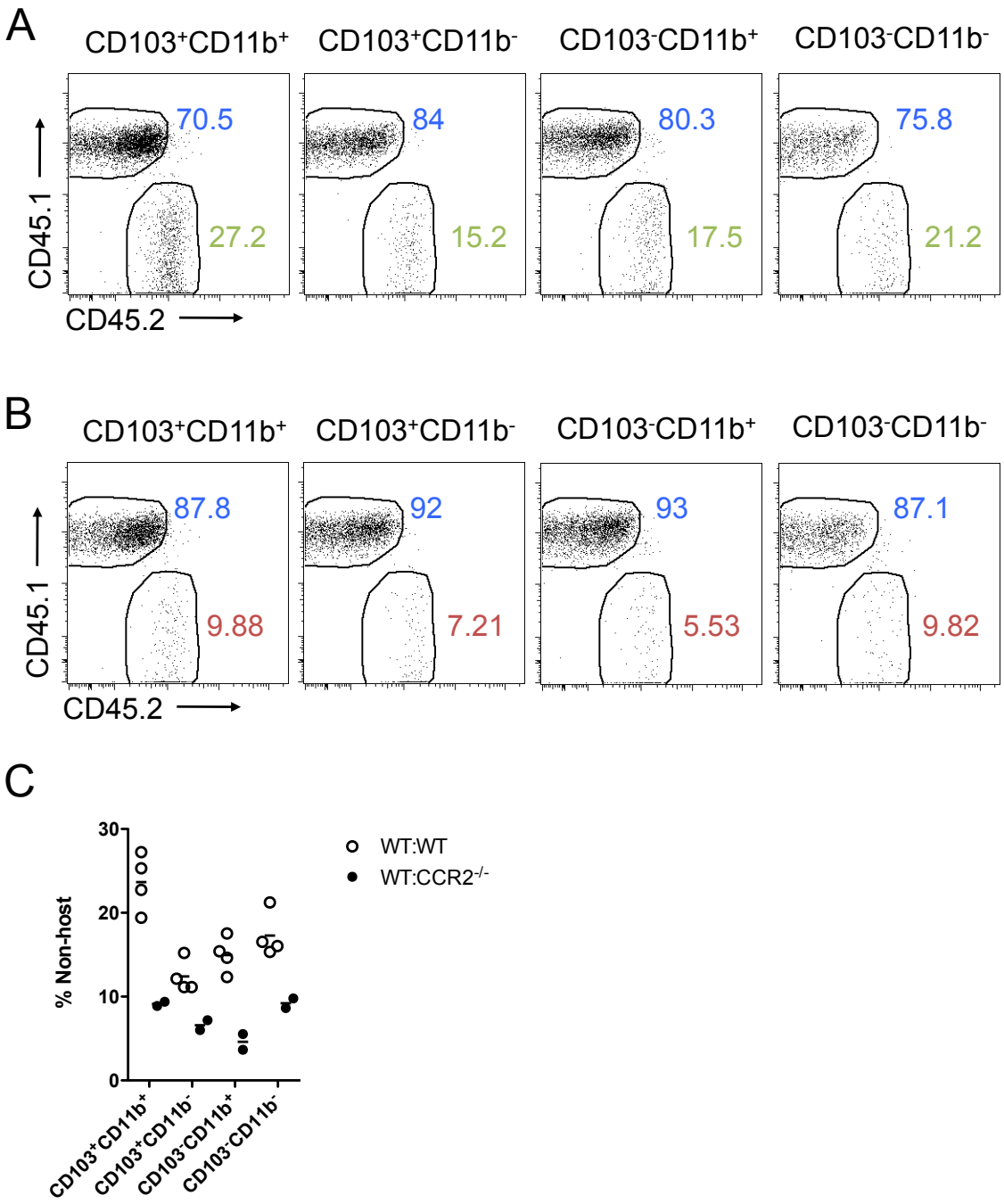

Figure 9.11: CD45.2⁺ DC populations in SI LP of CD45.1⁺ parabiotic mice

WT:WT (CD45.1:CD45.2) and WT:CCR2$^{-/-}$ (CD45.1:CD45.2) parabiotic mice were generated as shown in Fig. 9.9 and left for 12 weeks before tissues were harvested and the level of chimerism examined. **A**. Representative CD45.1 and CD45.2 staining amongst populations of CD11c^{+}MHCII^{+}CD64^{-} DCs in SI LP of the CD45.1^{+} WT partner of WT:WT parabionts. Numbers represent percentage of CD45.1^{+} or CD45.2^{+} cells in each DC population. **B.** Representative CD45.1 and CD45.2 staining amongst populations of CD11c^{+}MHCII^{+}CD64^{-} DCs in SI LP of the CD45.1^{+} CCR2$^{-/-}$ partner of WT:CCR2$^{-/-}$ parabionts. Numbers represent percentages of CD45.1^{+} or CD45.2^{+} cells in each DC population. **C.** Percentage of non-host (CD45.2^{+}) cells in CD45.1^{+} parabiotic partners. Data are from a single experiment with 4 WT:WT parabionts and 2 WT:CCR2$^{-/-}$ parabionts.

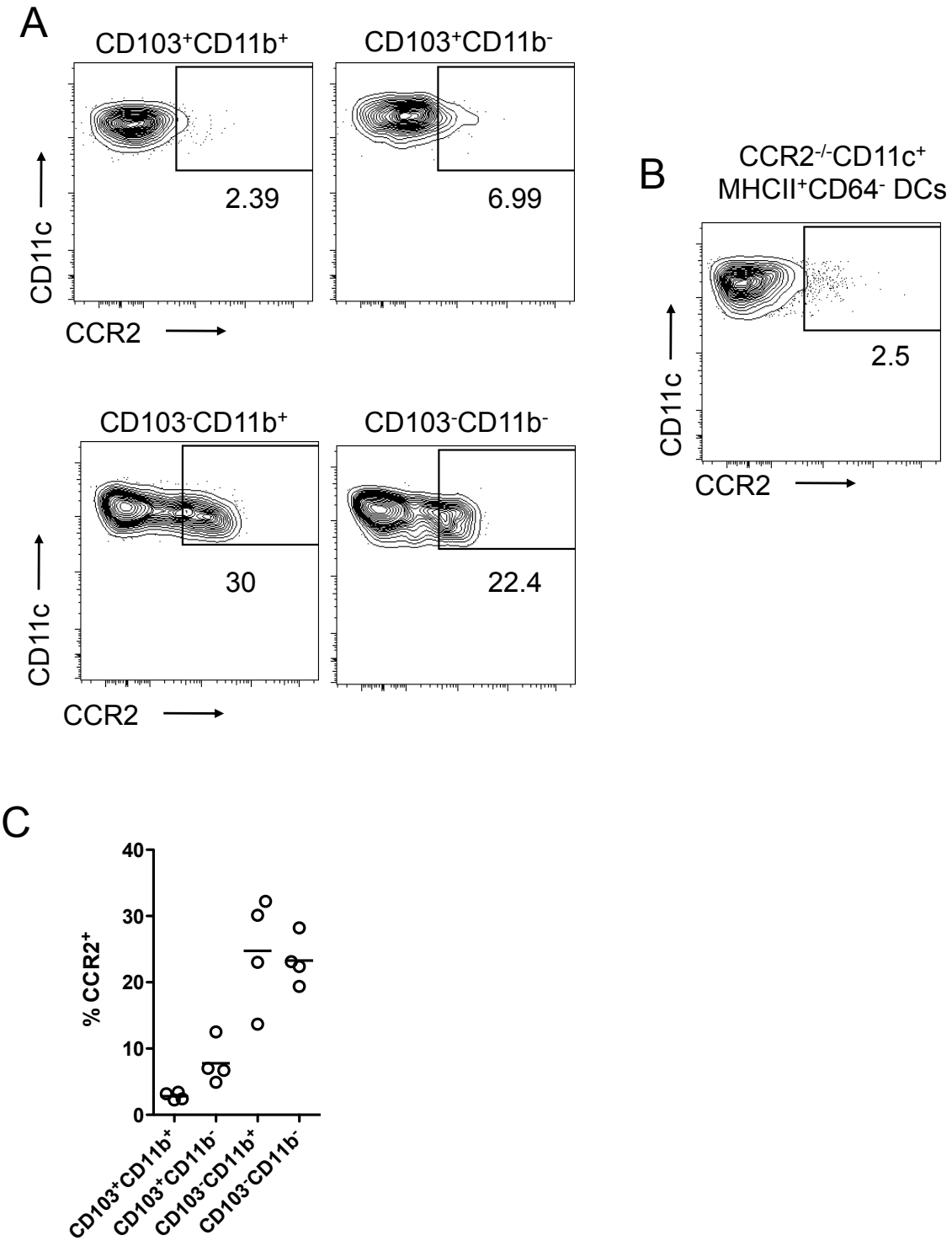

Figure 9.12: CCR2 expression by SI LP DCs

SI LP DC populations were identified as $CD11c^{+}MHCII^{+}CD64^{-}$ and examined for expression of CCR2 by flow cytometry. **A.** Representative CCR2 expression on each SI LP DC population from WT mice. **B.** CCR2 expression by total $CD11c^{+}MHCII^{+}CD64^{-}$ DCs from $CCR2^{-/-}$ mice as control. Numbers represent percentage of $CCR2^{+}$ DCs. **C.** Proportion of $CCR2^{+}$ cells as a percentage of each DC population. Data are representative of at least 7 independent experiments with n=3-5 per experiment.

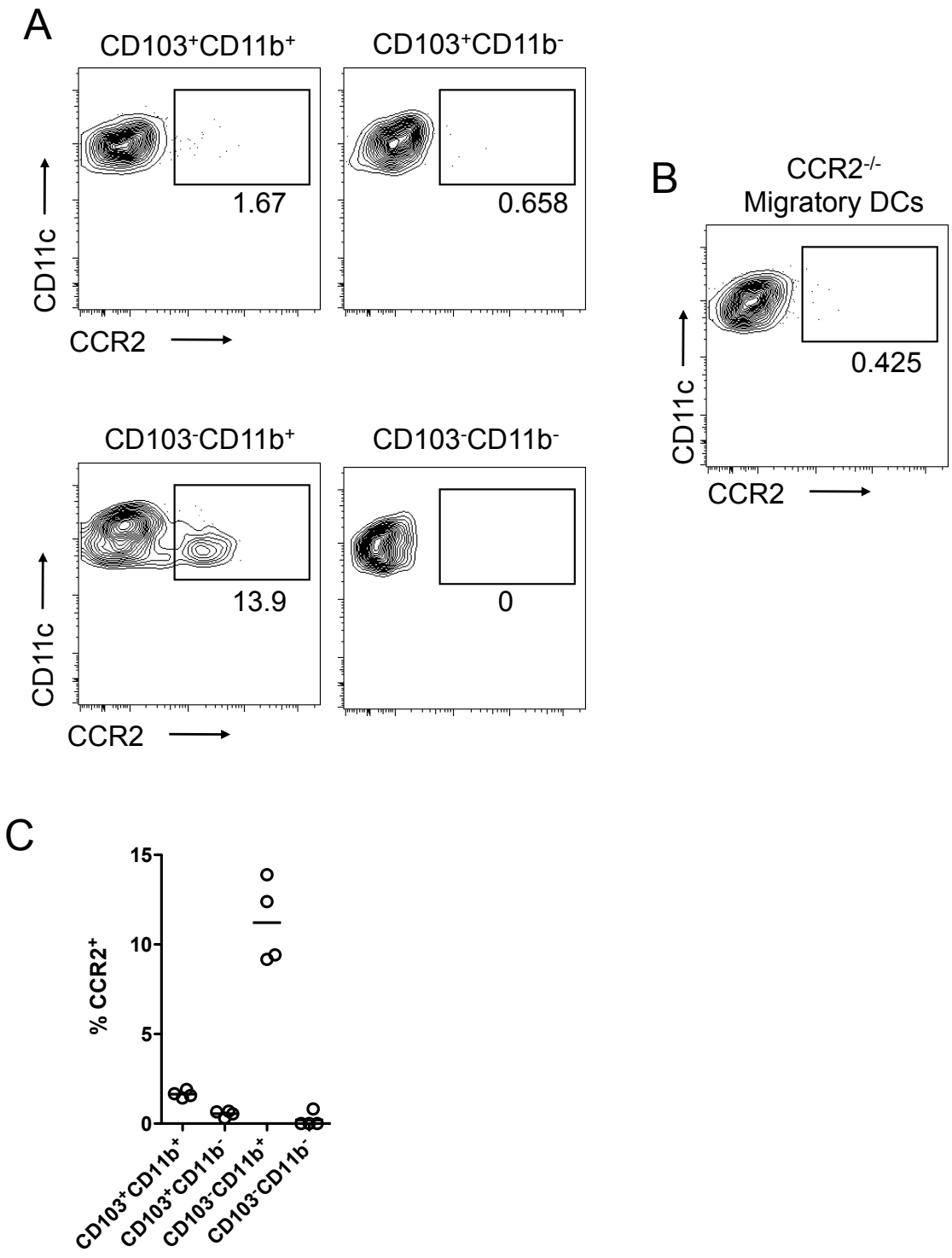

Figure 9.13: CCR2 expression by migratory DCs in MLN

DC populations amongst CD11c^{+}MHCII^{hi} migratory MLN DCs were identified and examined for expression of CCR2 by flow cytometry. **A.** Representative CCR2 expression on each DC population from WT mice. **B.** CCR2 expression by total migratory CD11c^{+}MHCII^{hi} DCs from CCR2$^{-/-}$ mice as control. Numbers represent percentage of CCR2^{+} DCs. **C.** Proportion of CCR2^{+} cells as a percentage of each DC population. Data are representative of at least 2 independent experiments with n=4 per experiment.

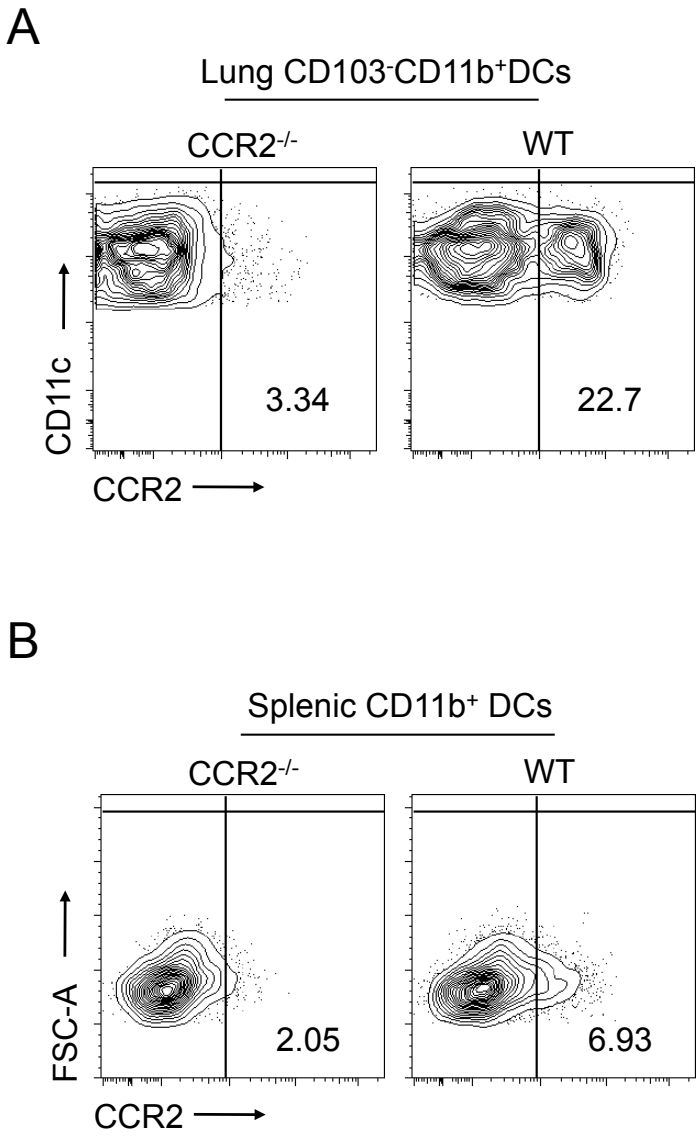

Figure 9.14: CCR2 expression by DCS from lung and spleen

A. CD103^{-}CD11b^{+} DC were identified amongst live CD45^{+} CD11c^{+} MHCII^{+} CD64^{-} non-autofluorescent cells in lung digests of WT mice as and examined for expression of CCR2 and compared with CD103^{-}CD11b^{+} DC from lungs of CCR2$^{-/-}$ mice. **B.** CD11b^{+} DCs were identified amongst live CD45^{+} CD11c^{+} MHCII^{+} cells in spleen digests of WT mice as and examined for expression of CCR2 and compared with CD11b^{+} DCs from spleen of CCR2$^{-/-}$ mice. Data are from a single experiment with 4 WT mice and 1 CCR2$^{-/-}$ mouse.

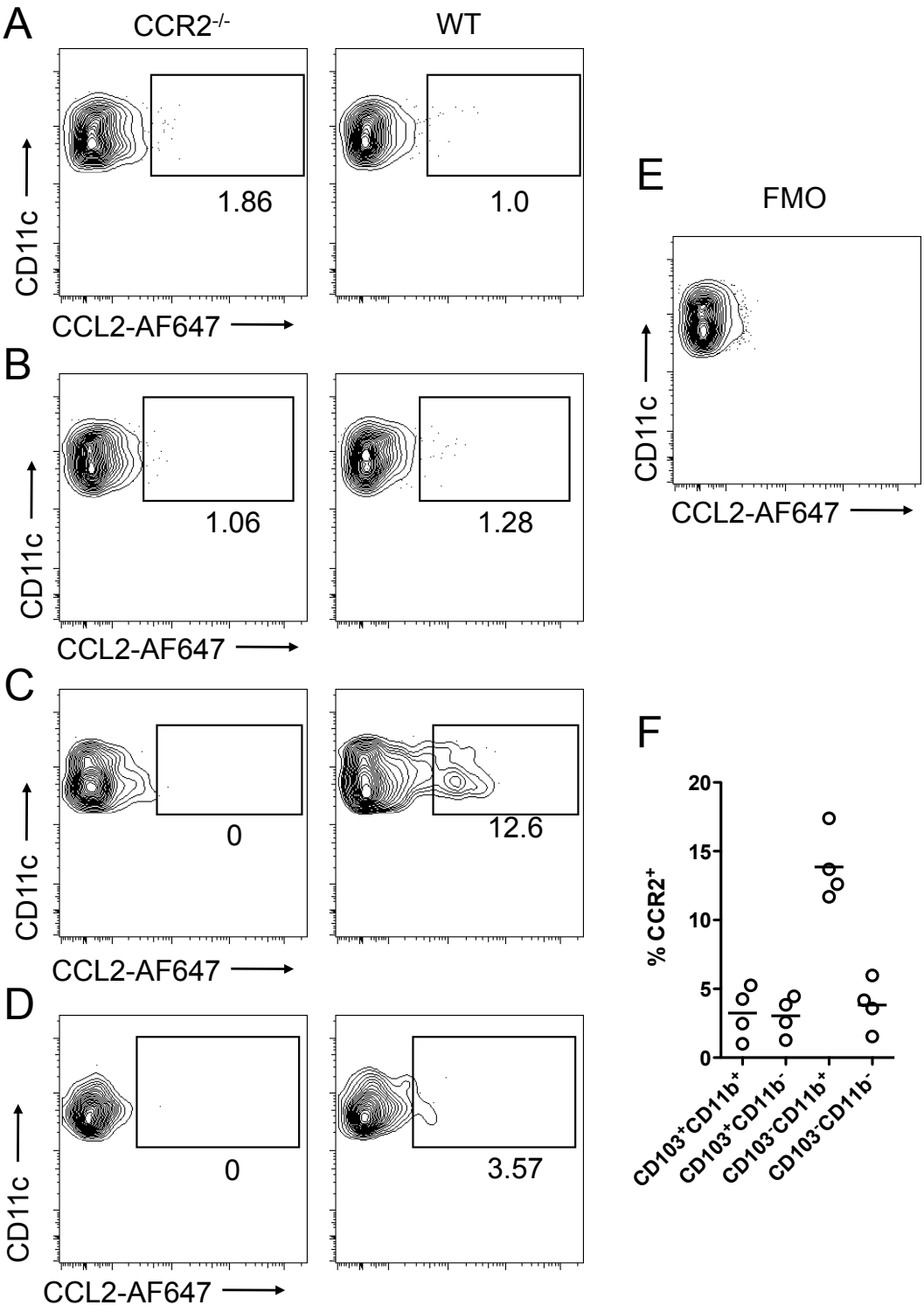

Figure 9.15: CCL2-AF647 uptake by migratory DCs in the MLN

Populations of migratory CD11c^{+}MHCII^{hi} DCs from WT and CCR2$^{-/-}$ MLNs were examined for their ability to bind AF647-labelled CCL2 by flow cytometry. **A-D.** AF647 fluorescence of (A) CD103^{+}CD11b^{+}, (B) CD103^{+}CD11b^{-}, (C) CD103^{-}CD11b^{+} and (D) CD103^{-}CD11b^{-} migratory MLN DCs in WT mice compared with CCR2$^{-/-}$ controls. Numbers represent percentages of CCL2-AF647^{+} DCs in each population. **E.** Background AF647 fluorescence by total migratory DCs in WT mice in the absence of AF647-CCL2 in fluorescence minus one (FMO) control. **F.** Proportion of CCR2^{+} DCs binding AF647-CCL2 as a percentage of each DC subset. Data are from a single experiment with n=4.

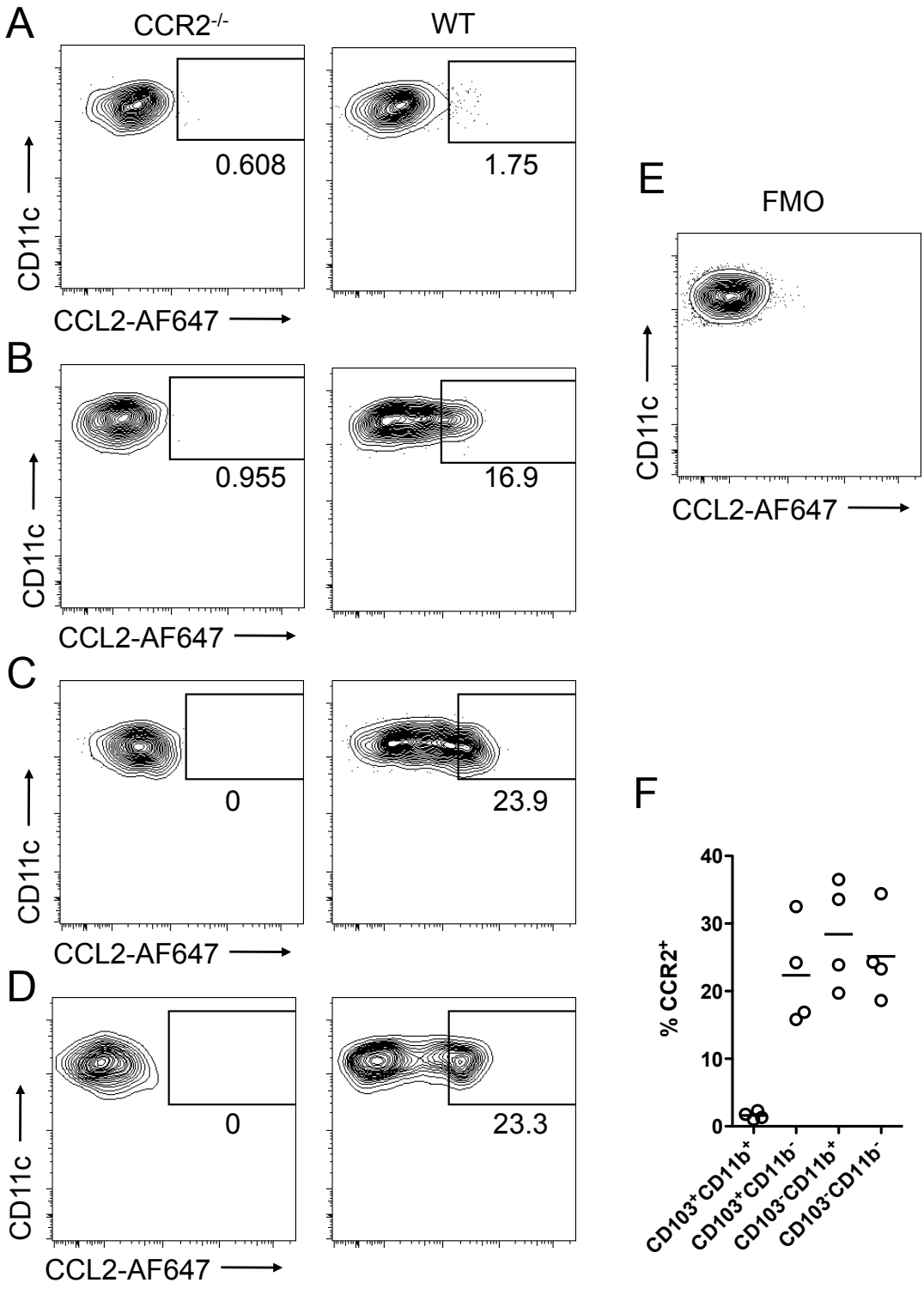

Figure 9.16: CCL2-AF647 uptake by SI LP DC.

Populations of CD11c^{+}MHCII^{+}CD64^{-} DCs from WT and CCR2$^{-/-}$ SI LP were examined for their ability to bind AF647-labelled CCL2 by flow cytometry. **A-D.** AF647 fluorescence of (A) CD103^{+}CD11b^{+}, (B) CD103^{+}CD11b^{-}, (C) CD103^{-}CD11b^{+} and (D) CD103^{-}CD11b^{-} SI LP DCs in WT mice compared with CCR2$^{-/-}$ controls. Numbers represent percentages of CCL2-AF647^{+} DCs in each population. **E.** Background AF647 fluorescence by total migratory DCs in WT mice in the absence of AF647-CCL2 in fluorescence minus one (FMO) control. **F.** Proportion of CCR2^{+} DCs binding AF647-CCL2 as a percentage of each DC subset. Data are from a single experiment with n=4.

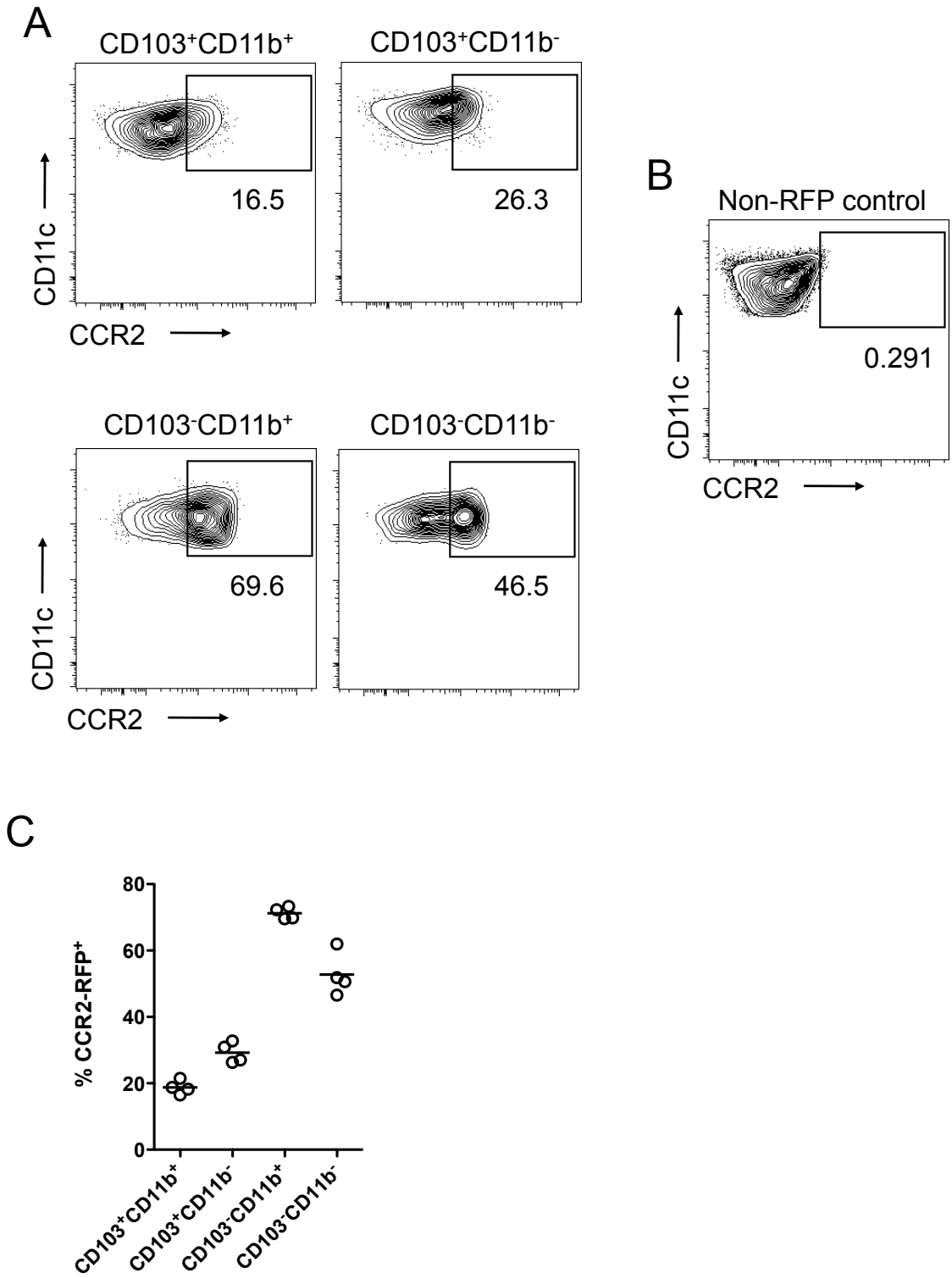

Figure 9.17: CCR2-RFP expression by SI LP DCs

Populations of CD11c^{+}MHCII^{+}F4/80^{-} DCs from CCR2$^{+/RFP}$ SI LP were examined for RFP expression by flow cytometry. **A.** RFP expression by each DC population. **B.** Background RFP expression in total DCs from WT SI LP. **C.** Proportion of CCR2-RFP^{+} DCs as a percentage of each DC subset. Data are from a single experiment with n=4.

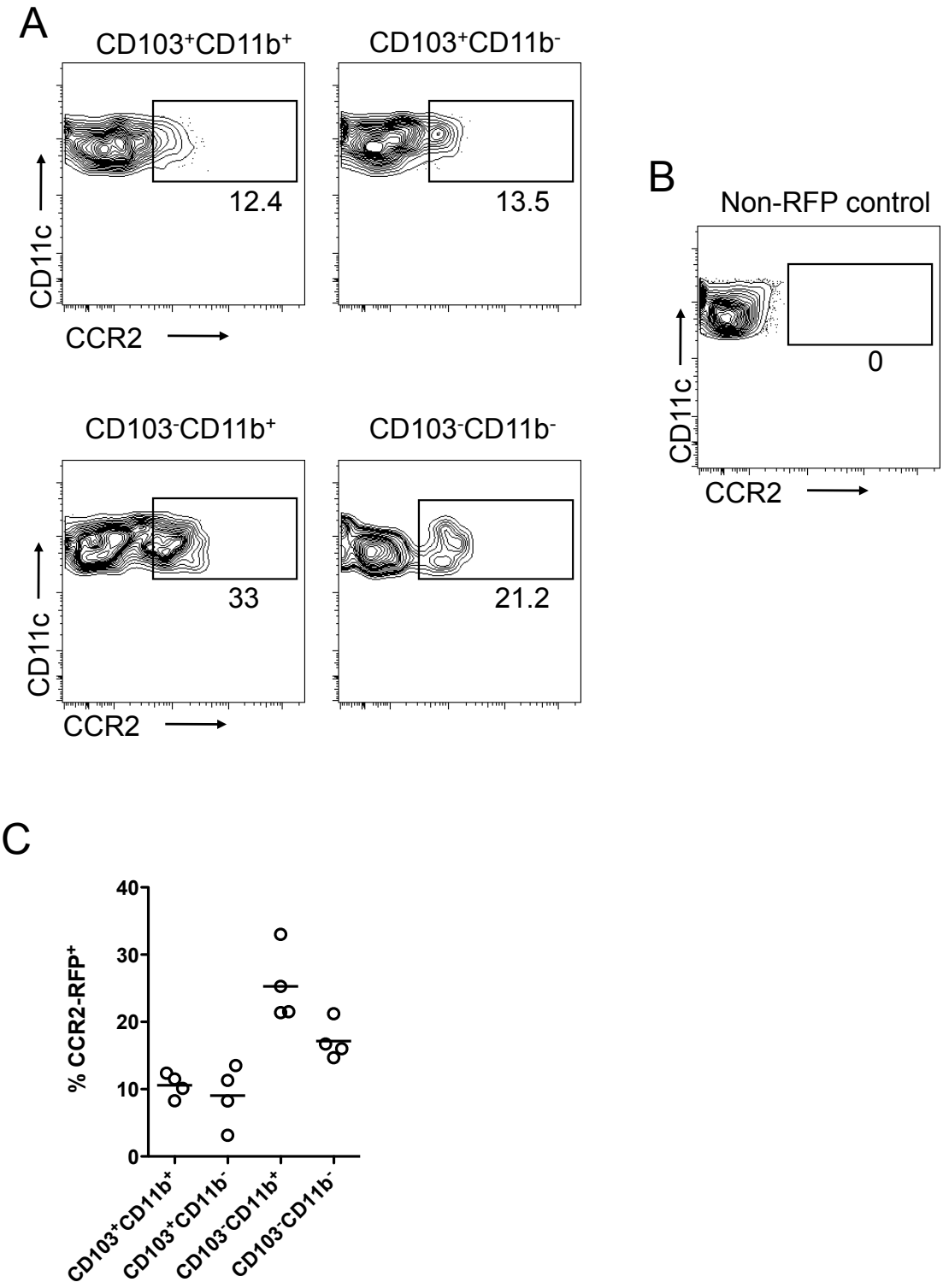

Figure 9.18: CCR2-RFP expression by migratory MLN DCs

Populations of migratory CD11c^{+}MHCII^{hi} DCs from CCR2$^{+/RFP}$ MLNs were examined for RFP expression by flow cytometry. **A.** RFP expression by each migratory DC population. **B.** Background RFP expression in total migratory DCs from WT MLNs. **C.** Proportion of CCR2-RFP^{+} DCs as a percentage of each DC subset. Data are from a single experiment with n=4.

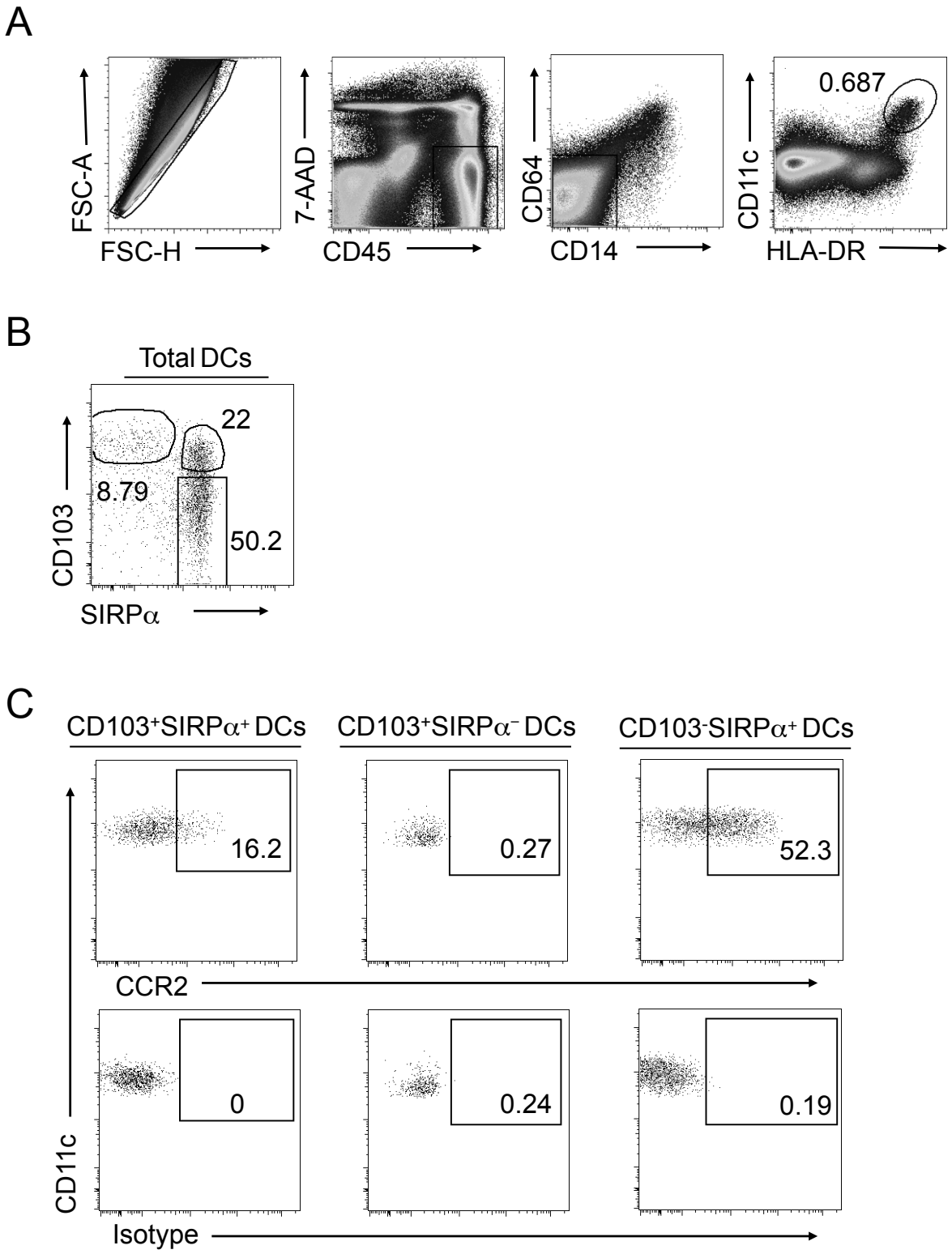

Figure 9.19: Putative CCR2$^+$CD103$^-$CD11b$^+$ DC equivalents exist in healthy human colonic lamina propria.

A. DCs were identified in resected samples of healthy human colon as live CD45$^+$ CD14$^-$ CD64$^-$ CD11c$^+$ HLA-DR$^+$ cells. **B.** Expression of CD103 and SIRPα was assessed on total human colonic LP DCs. **C.** Each DC population was assessed for CCR2 expression compared with CCR2 isotype control by flow cytometry. Numbers represent the proportions of CCR2$^+$ cells as a percentage of each DC population. Data are representative of 2 independent experiments.

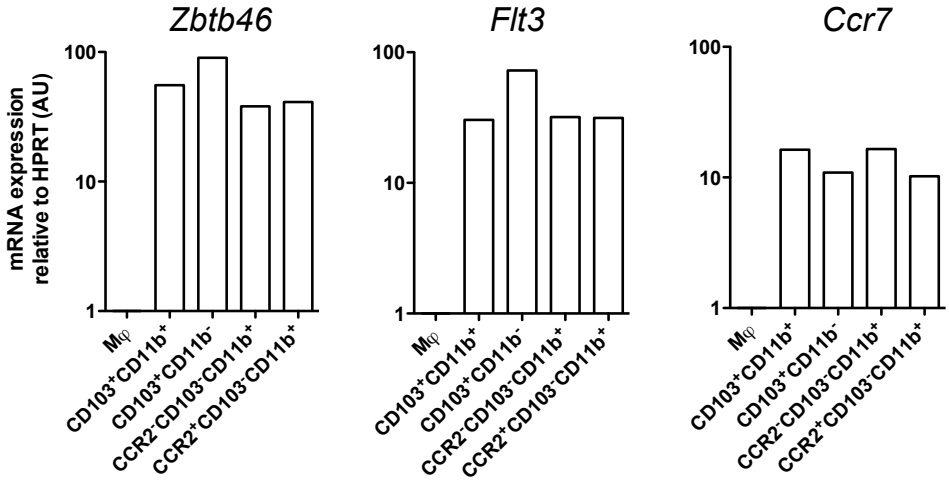

Figure 9.20: Expression of DC related genes by CCR2$^+$CD103$^-$CD11b$^+$ DCs from SI LP

CCR2$^+$ and CCR2$^-$ subsets of CD103$^-$CD11b$^+$ DC were FACS-purified from SI LP digests of WT mice as shown in Fig. 9.12, together with CD103$^+$CD11b$^+$ DCs, CD103$^+$CD11b$^-$ DCs and CD64$^+$ mϕs. **A-C.** qRT-PCR analysis of expression of (A) *Zbtb46,* (B) *Flt3* and (C) *Ccr7* mRNA expression by each subsets. Results shown are relative to HPRT using the $2^{-\Delta\Delta ct}$ method with mϕ set to 1. Data are from a single experiment with cells pooled from 9-12 mice.

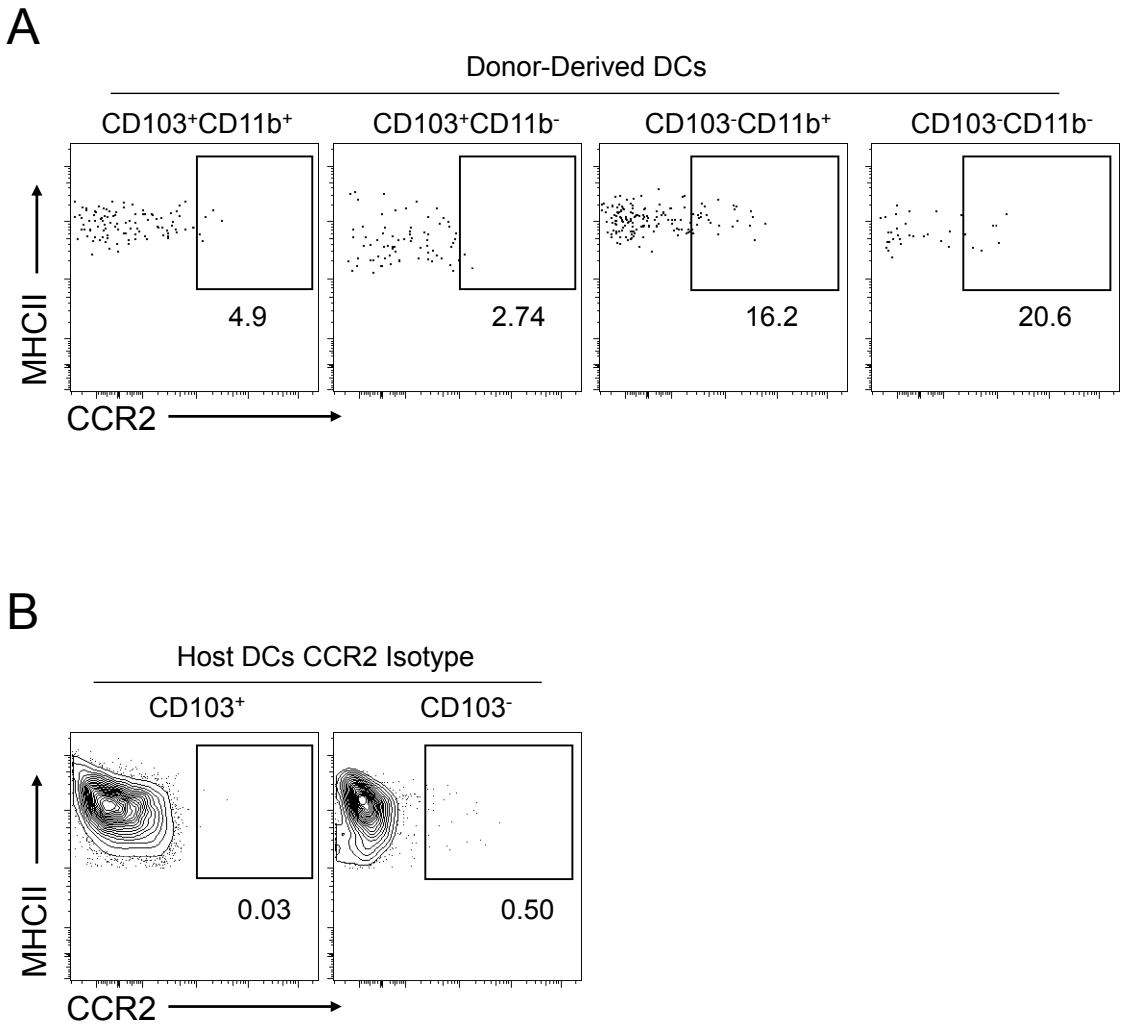

Figure 9.21: Pre-DC are heterogeneous for CCR2 expression and give rise to CCR2$^+$ CD103$^-$CD11b$^+$ DC

7x10^5 CD45.1$^+$/CD45.2$^+$ pre-DCs from WT mice that had been inoculated with Flt3L secreting B16 melanoma cells 10 days before, were FACS-purified, labelled with Cell Trace Violet dye and transferred i.v. into resting CD45.1$^+$ recipients and analysed for CCR2 expression 5 days later. **A.** CD45.2$^+$Violet$^+$CD11c$^+$MHCII$^+$CD64$^-$ donor-derived SI LP DCs were examined for CCR2 expression by flow cytometry. **B.** CCR2 isotype staining of endogenous host CD103$^+$ and CD103$^-$ CD11c$^+$MHCII$^+$CD64$^-$ DCs. Numbers represent proportion of each DC population expressing CCR2 or binding isotype. Data are from a single experiment with 1 recipient mouse.

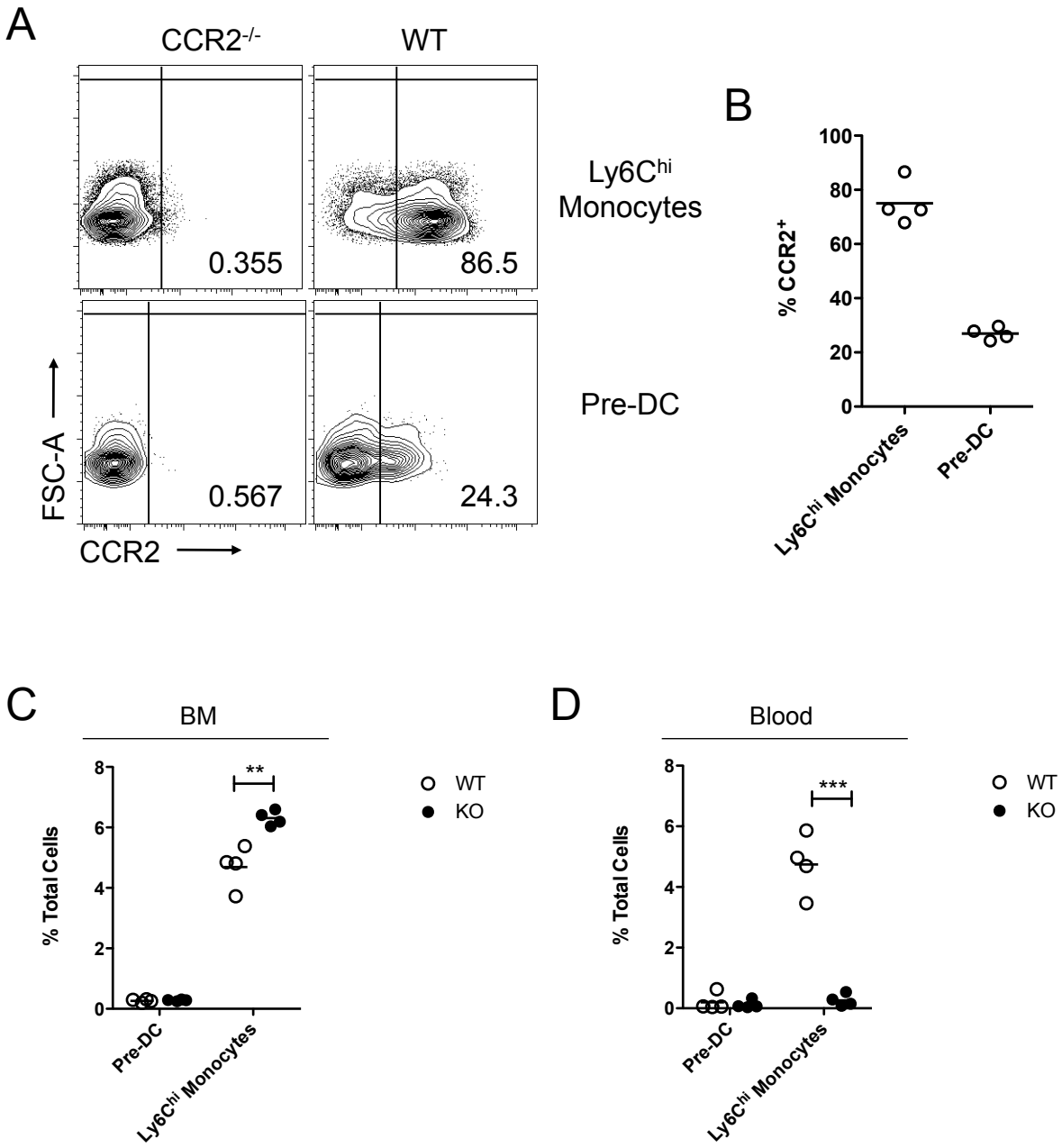

Figure 9.22: CCR2 expression and dependence by pre-DCs and Ly6C^{hi} monocytes

A. CCR2 expression was assessed on lin$^-$CD11c$^+$B220$^-$CCR9$^-$ pre-DCs and Ly6C^{hi} monocytes from WT and CCR2$^{-/-}$ BM by flow cytometry. Numbers represent the proportion of CCR2$^+$ cells. **B.** Proportions of CCR2$^+$ cells as a percentage of BM Ly6C^{hi} monocytes or pre-DCs. **C.** Proportion of pre-DCs and Ly6C^{hi} monocytes in WT and CCR2$^{-/-}$ BM as a percentage of total cells. **D.** Proportion of pre-DCs and Ly6C^{hi} monocytes in WT and CCR2$^{-/-}$ blood as a percentage of total cells. Data are from a single experiment with n=4. **p<0.01, ***p<0.001 Student's t test.

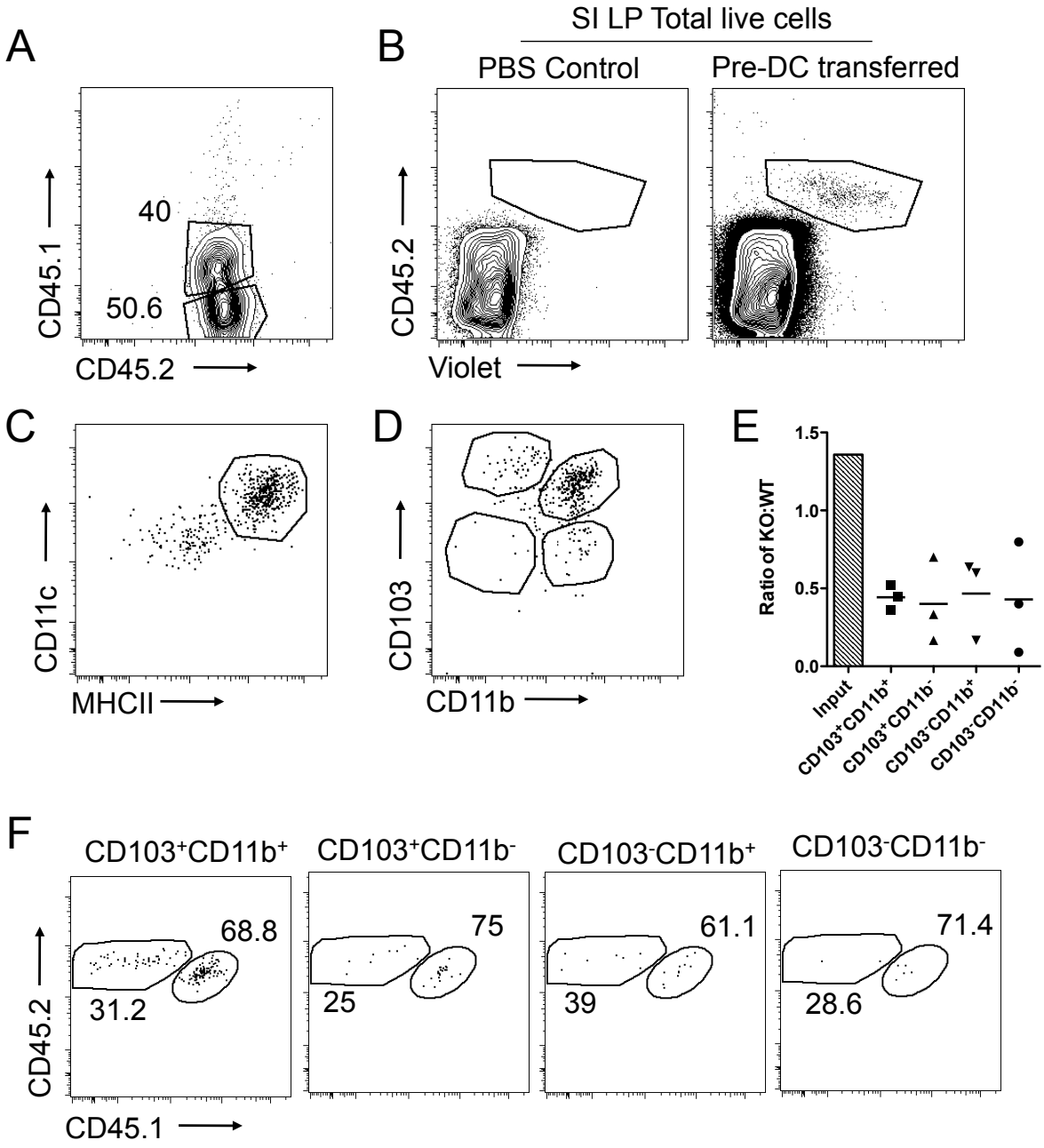

Figure 9.23: Comparative ability of WT and CCR2$^{-/-}$ pre-DCs to generate DCs in SI LP. 3.5x10^5 CD45.2$^+$ CCR2$^{-/-}$ pre-DCs and 3.5x10^5 CD45.1$^+$/CD45.2$^+$ WT pre-DCs from mice inoculated with Flt3L-secreting B16 melanoma cells 10 days before, were labelled with Cell Trace Violet dye, FACS-purified and adoptively transferred i.v. into resting CD45.1$^+$ WT mice. 7 days later tissues were harvested and examined for CCR2$^{-/-}$ and WT derived DC. **A.** CD45.1 and CD45.2 expression by transferred pre-DCs. **B.** Identification of donor-derived CD45.2$^+$Violet$^+$ cells in SI LP of recipient mice compared with non-injected control. **C.** Representative staining showing CD11c and MHCII expression on donor-derived cells identified in B. **D.** Representative staining showing CD103 and CD11b expression amongst donor-derived CD11c$^+$MHCII$^+$ DCs identified in C. **E.** Ratio of CCR2$^{-/-}$ CD45.2$^+$:WTCD45.1$^+$/CD45.2$^+$ derived DCs for each DC population in SI LP compared with the input ratio of transferred pre-DCs. **F.** Representative CD45.1 and CD45.2 staining by each donor-derived DC population in SI LP. Data are from a single experiment with 3 recipient mice.

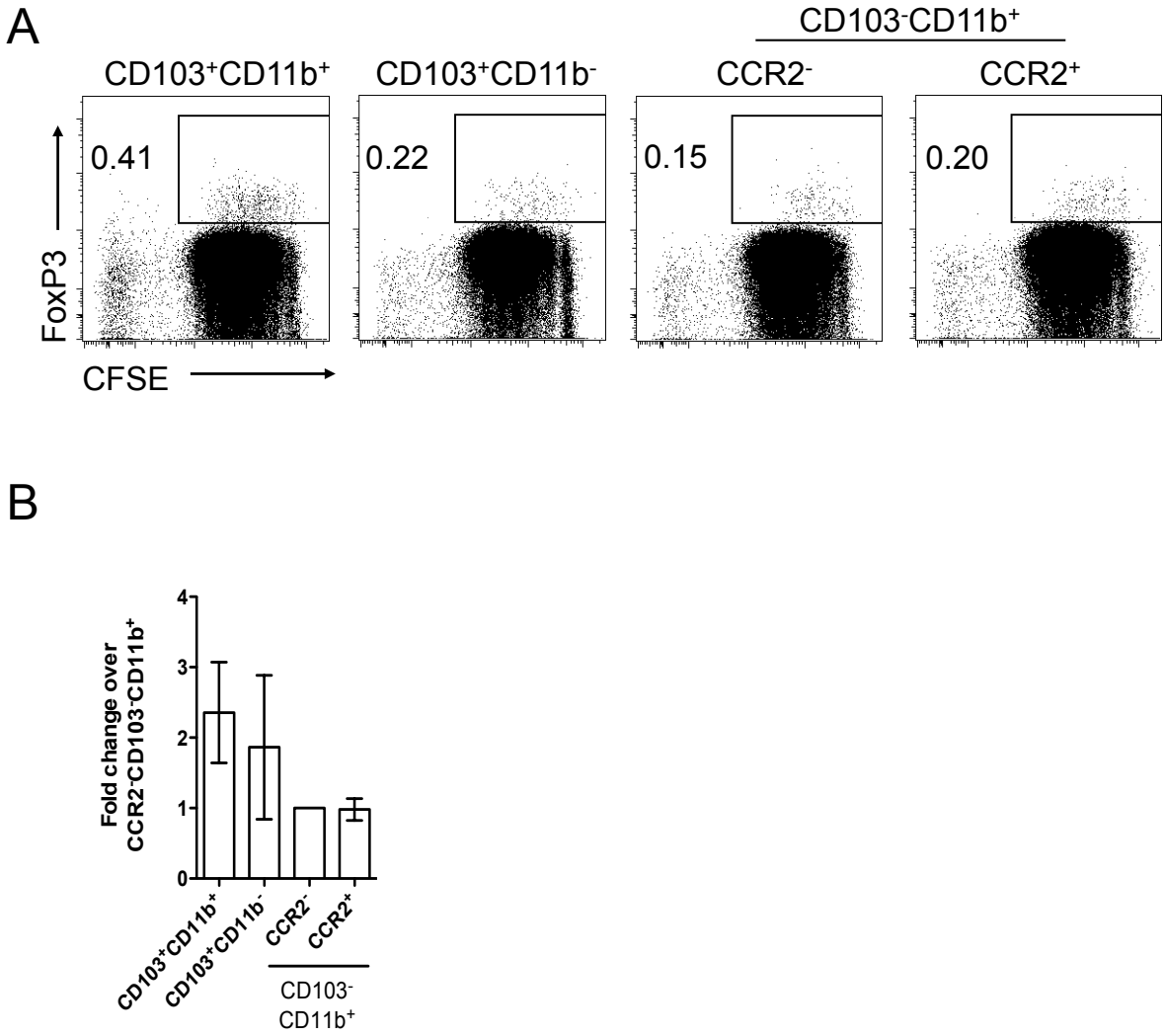

Figure 9.24: Induction of FoxP3 in naïve CD4⁺ T cells by DC subsets from SI LP

$3x10^4$ FACS-purified DC subsets from siLP were pulsed with 2mg/ml OVA protein and co-cultured for 4 days with $1x10^5$ FACS-purified CFSE labeled naïve OVA-specific $CD4^+$ (OTII) T cells before being assessed for CFSE dilution and FoxP3 expression by intracellular staining. **A.** Representative dilution of CFSE dye and FoxP3 expression by total T cells in culture with each DC subset. Numbers represent percentage of $FoxP3^+$ T cells. **B.** Scatter plots show fold change in FoxP3 induction by each DC population compared with that obtained using $CCR2^-CD103^-CD11b^+$ DCs. Data are shown as means ±1SD pooled from three independent experiments.

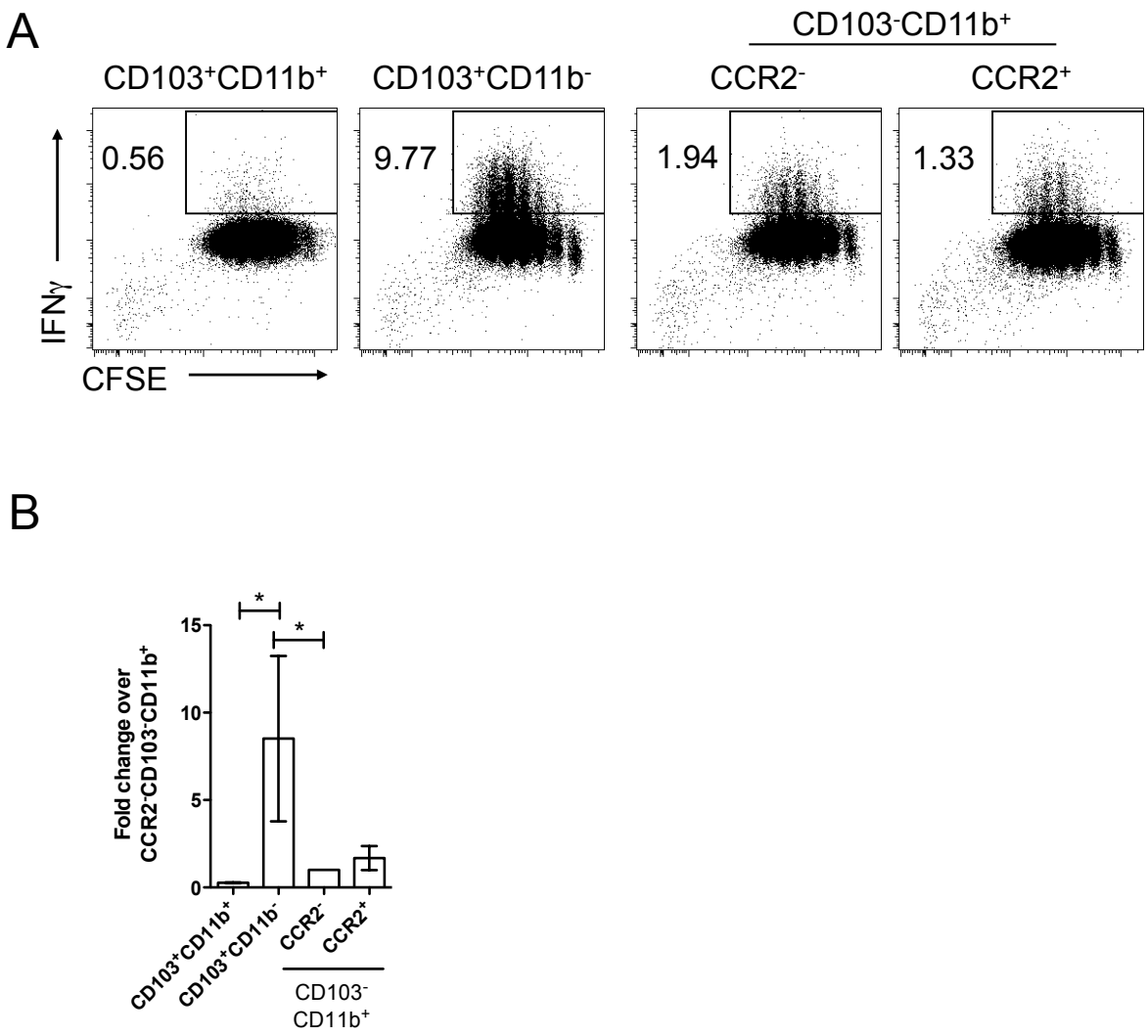

Figure 9.25: Induction of IFNγ in naïve CD4⁺ T cells by DC subsets from SI LP

3x10⁴ FACS-purified DC subsets from siLP were pulsed with 2mg/ml OVA protein and co-cultured for 4 days with 1x10⁵ FACS-purified CFSE labeled naïve OVA-specific CD4⁺ (OTII) T cells before being assessed for CFSE dilution and IFNγ expression by intracellular staining. **A.** Representative dilution of CFSE dye and IFNγ expression by total T cells in culture with each DC subset. Numbers represent percentage of IFNγ⁺ T cells. **B.** Scatter plots show fold change in IFNγ induction by each DC population compared with that obtained using CCR2⁻CD103⁻CD11b⁺ DCs. Data are shown as means ±1SD pooled from three independent experiments.

*p<0.05, one way ANOVA with Bonferroni post-test.

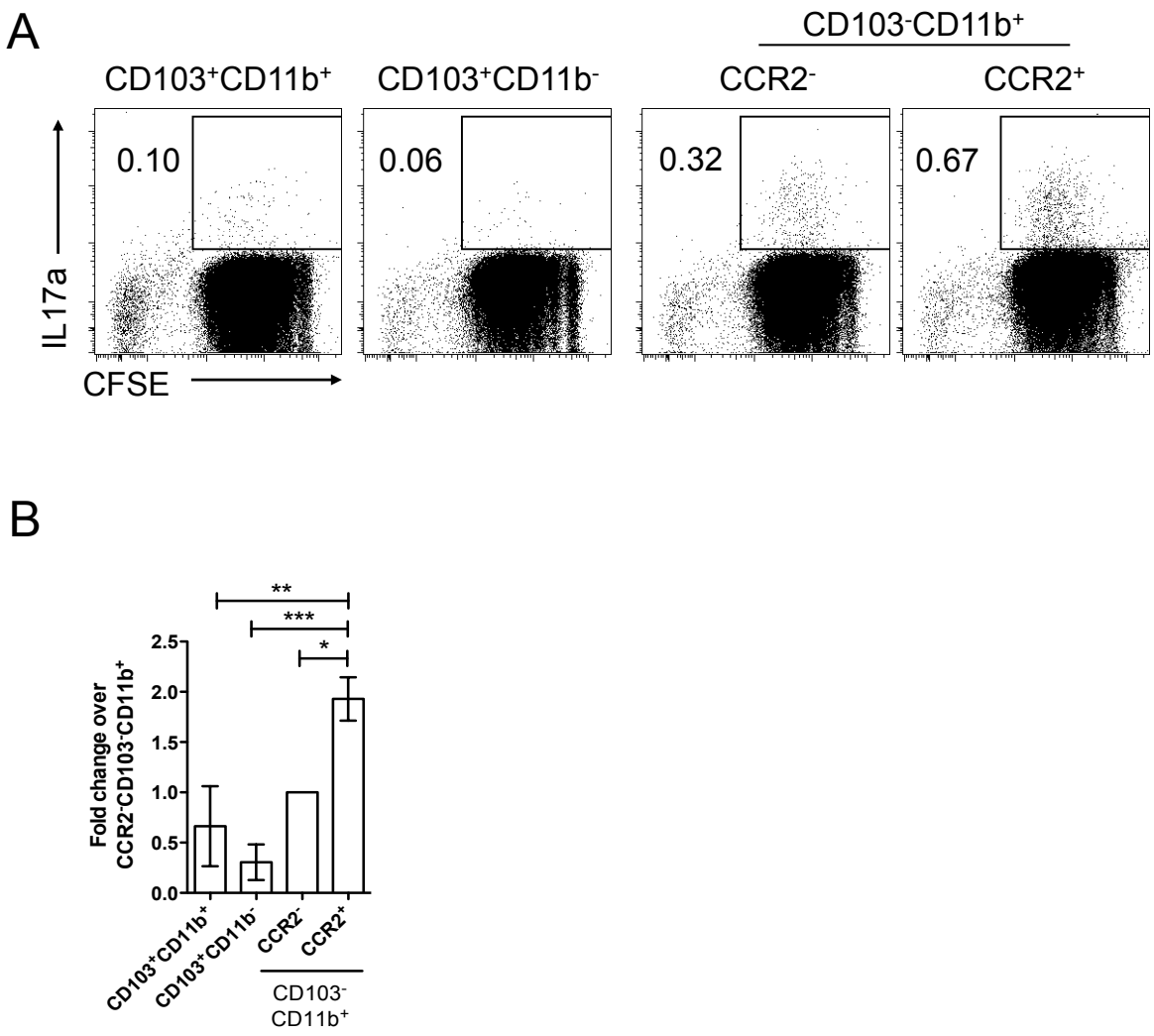

Figure 9.26: Induction of IL17a in naïve CD4⁺ T cells by DC subsets from SI LP

3x10⁴ FACS-purified DC subsets from siLP were pulsed with 2mg/ml OVA protein and co-cultured for 4 days with 1x10⁵ FACS-purified CFSE labeled naïve OVA-specific CD4⁺ (OTII) T cells before being assessed for CFSE dilution and IL17a expression by intracellular staining. **A.** Representative dilution of CFSE dye and IL17a expression by total T cells in culture with each DC subset. Numbers represent percentage of IL17a⁺ T cells. **B.** Scatter plots show fold change in IL17a induction by each DC population compared with that obtained using CCR2⁻CD103⁻CD11b⁺ DCs. Data are shown as means ±1SD pooled from three independent experiments. *p<0.05, **p<0.01, ***p<0.001, one way ANOVA with Bonferroni post-test.

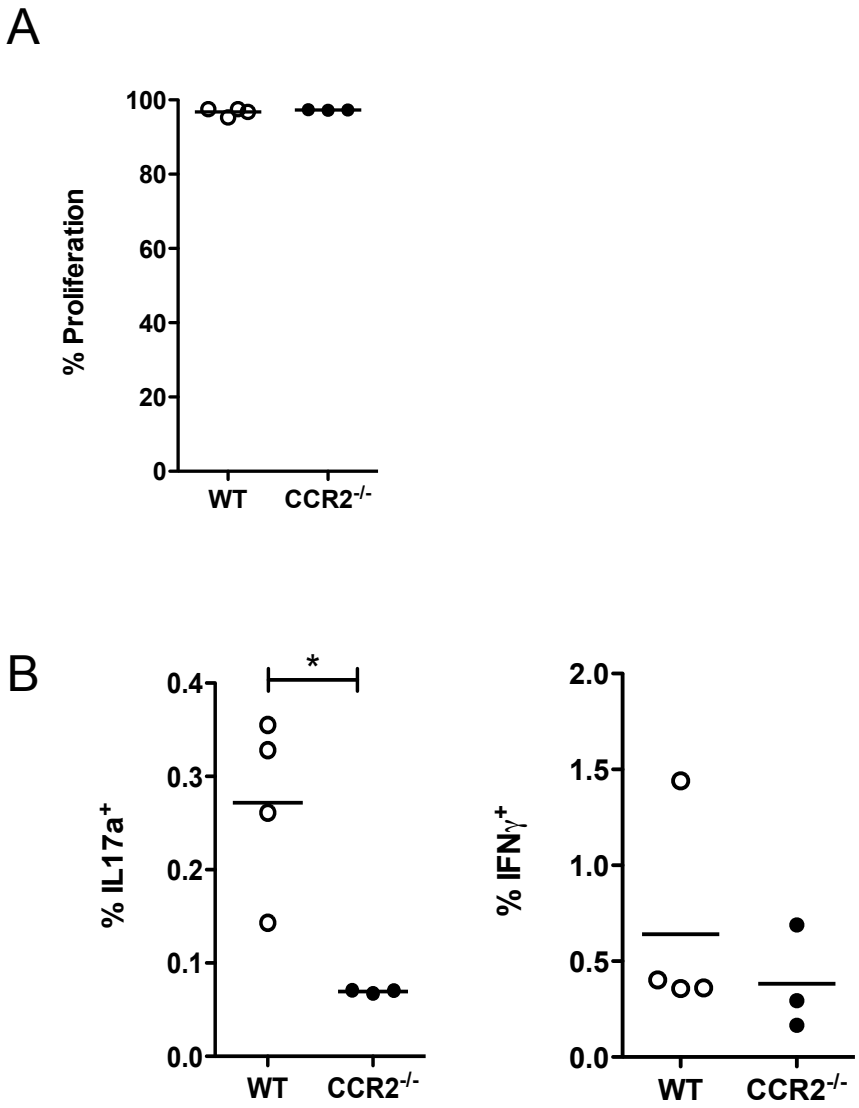

Figure 9.27: Role of CCR2 in generation of antigen-specific CD4⁺ effector T cells *in vitro*

$1.8x10^3$ $CD103^-CD11b^+$ DCs were FACS-purified from the SI LP of WT and $CCR2^{-/-}$ mice, pulsed with 2mg/ml OVA protein and co-cultured with naïve FACS-purified CFSE-labelled OTII cells for four days before IFNγ and IL17a production was assessed by intracellular cytokine staining. **A** Proportion of total T cells having gone through at least one round of proliferation as assessed by CFSE dilution following co-culture with WT or $CCR2^{-/-}$ $CD103^-CD11b^+$ DCs. **B.** Proportion of $IFN\gamma^+$ and $IL17a^+$ $CD4^+$ T cells following co-culture with WT or $CCR2^{-/-}$ $CD103^-CD11b^+$ DCs as a percentage of total live $CD4^+$ T cells. *$p<0.05$, Student's t test. Data are pooled from three independent experiments with 1-2 mice per group per experiment.

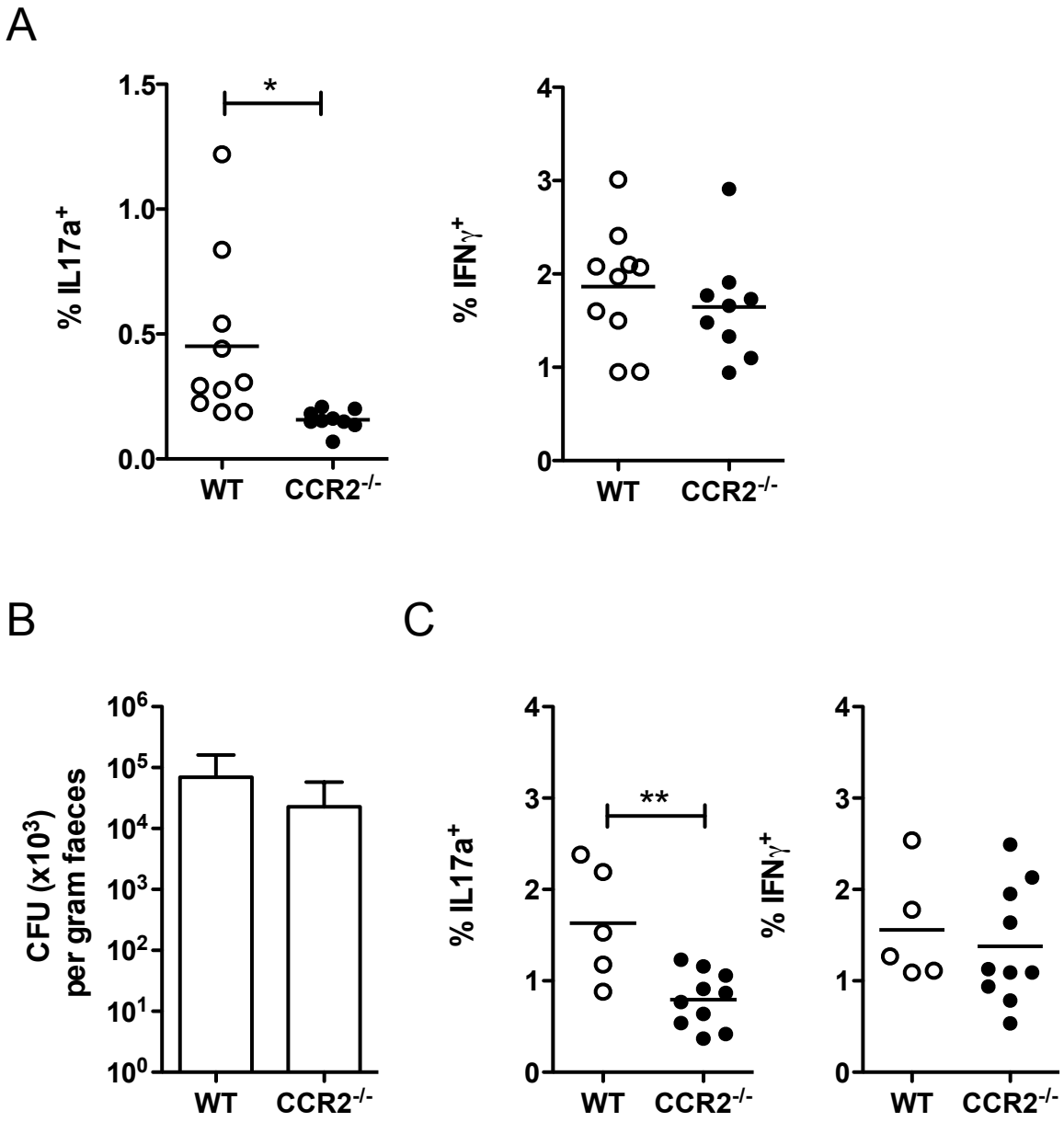

Figure 9.28: Role of CCR2 in generation of antigen-specific CD4⁺ effector T cells *in vivo*

A. WT and CCR2$^{-/-}$ mice received OTII cells i.v. and one day later were immunised i.p. with 0.5mg OVA, together with 25μg α-CD40 and 15μg LPS. One and three days later mice received 1mg/kg bodyweight FTY720 i.p. Mice were sacrificed four days after immunisation and IL17a$^+$ and IFNγ$^+$ T cells in the MLNs were identified by intracellular cytokine staining. Proportions of IL17a$^+$ and IFNγ$^+$ T cells in MLNs of WT and CCR2$^{-/-}$ mice. *p<0.05, Student's t test. Data are from a single experiment with n=9-10 per group. **B,C.** WT and CCR2$^{-/-}$ mice were infected with 1x10^9 *C. rodentium* CFUs and on day 6 of infection, bacteria levels were examined by faecal colony counts (B). (C) On day 7, IL17a$^+$ and IFNγ$^+$ T cells in the MLNs were identified by intracellular cytokine staining. Proportions of IL17a$^+$ and IFNγ$^+$ T cells in MLNs of WT and CCR2$^{-/-}$ mice. *p<0.05, Student's t test. Data are from a single experiment with n=5-10 per group.

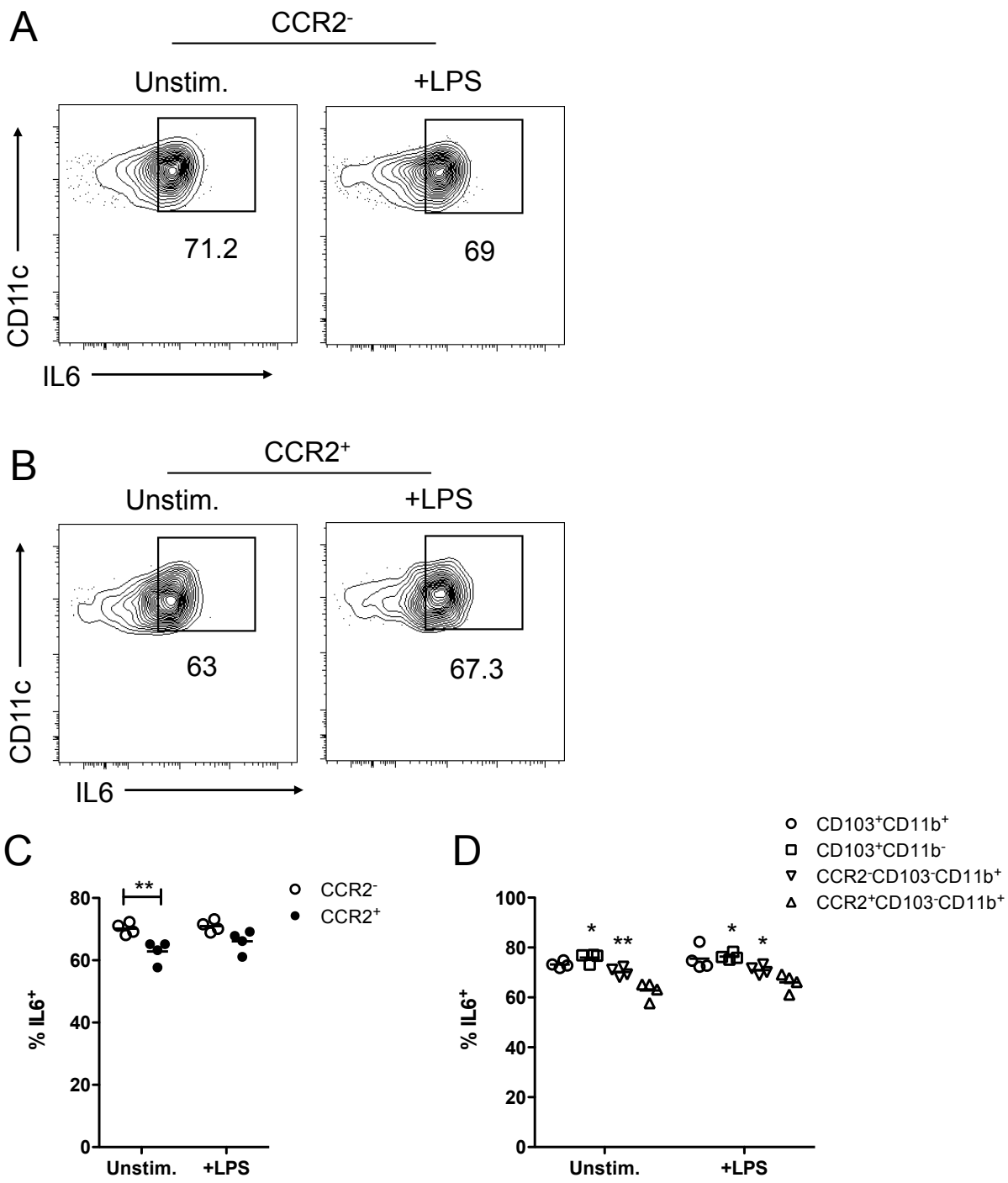

Figure 9.29: Production of IL6 by DC subsets from SI LP

Whole SI LP digests were incubated for 4.5hours in the presence of monensin and brefeldin A ± 100ng/ml LPS and IL6 expression by subsets of $CD11c^+MHCII^+CD64^-$ DCs was assessed by intracellular cytokine staining. **A,B.** Representative staining showing IL6 expression by (A) $CCR2^-CD103^-CD11b^+$ and (B) $CCR2^+CD103^-CD11b^+$ DC. **C.** Percentage of $IL6^+$ cells in $CCR2^-$ and $CCR2^+$ $CD103^-CD11b^+$ DC in the presence (+LPS) or absence (Unstim.) of LPS. Data are from a single experiment with n=4. **p<0.01 Student's t test. **D.** Percentage of $IL6^+$ cells amongst all populations of SI LP DCs in the presence (+LPS) or absence (Unstim.) of LPS. Data are from a single experiment with n=4. *p<0.05, **p<0.01, two way ANOVA with Bonferroni post-test. Asterisks denote different from $CCR2^+CD103^-CD11b^+$ DCs.

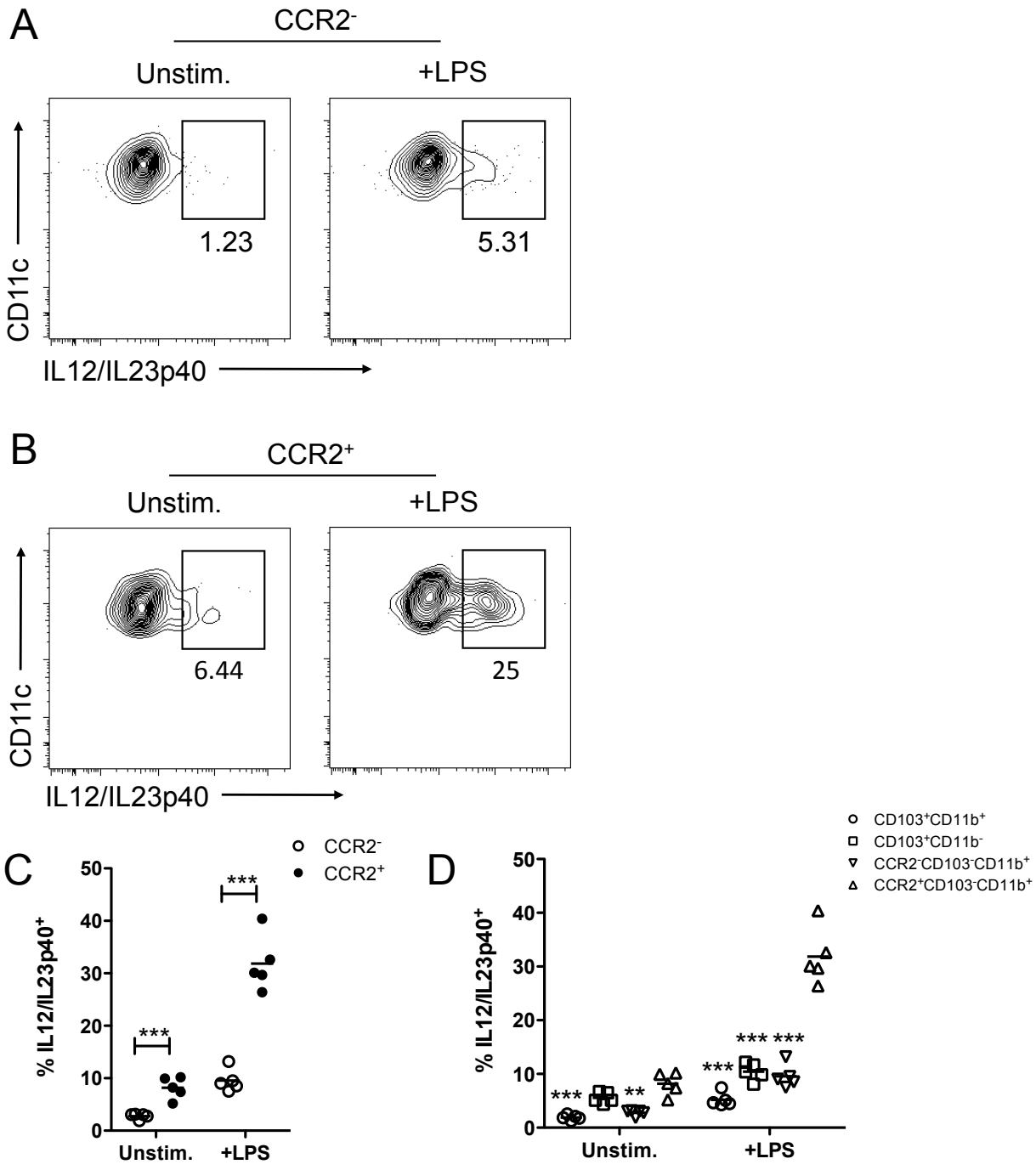

Figure 9.30: Production of IL12/IL23p40 expression by DC subsets from SI LP

Whole SI LP digests were incubated for 4.5hours in the presence of monensin and brefeldin A ± 100ng/ml LPS and IL12/IL23p40 expression by subsets of CD11c$^+$MHCII$^+$CD64$^-$ DCs was assessed by intracellular cytokine staining. **A,B.** Representative staining showing IL12/IL23p40 expression by (A) CCR2$^-$CD103$^-$CD11b$^+$ and (B) CCR2$^+$CD103$^-$CD11b$^+$ DC. **C.** Percentage of IL12/IL23p40$^+$ cells in CCR2$^-$ and CCR2$^+$ CD103$^-$CD11b$^+$ DC in the presence (+LPS) or absence (Unstim.) of LPS. Data are representative of 2 independent experiments with n=4-5 per experiment. ***p<0.001, Student's t test. **D.** Percentage of IL12/IL23p40$^+$ cells amongst all populations of SI LP DC in the presence (+LPS) or absence (Unstim.) of LPS. Data are representative of 2 independent experiments with n=4-5 per experiment. **p<0.01, ***p<0.001, two way ANOVA with Bonferroni post-test. Asterisks denote different from CCR2$^+$CD103$^-$CD11b$^+$ DCs.

Chapter 10 General Discussion

10.1 Introduction

The intestinal immune system is exposed continuously to a wide array of antigens including those from harmful pathogens, as well as harmless antigen deriving from commensal bacteria and dietary constituents. The immune system must respond appropriately by inducing active immunity against pathogens and tolerance to the harmless antigens. Dendritic cells (DCs), as sentinels of the immune system, are central to this process. However DCs in the intestine have been poorly characterised and often confused with other intestinal mononuclear phagocytes (MPs) such as mϕs, resulting from the use of non-specific and overlapping markers. This is not simply a semantic issue, as the correct identification of DCs and mϕs has important functional implications. Intestinal DCs acquire antigen and migrate to the MLNs, where they induce adaptive immune responses by presenting antigen to naïve T lymphocytes. In contrast intestinal mϕs are tissue resident cells, which maintain the local environment by scavenging bacteria and damaged cells, as well as regulating epithelial integrity. Thus the main aim of this thesis was to analyse intestinal MP populations properly, so that the phenotype, ontogeny and function of intestinal DCs could be characterised precisely. To do this, I used multi-parameter flow cytometric techniques in combination with genetically modified mice and precursor tracking focussing principally on the small intestine and their draining lymph nodes.

10.2 Identifying Dendritic Cells in the Intestine

When I began my PhD, the prevailing dogma was that intestinal DCs could be identified solely on the basis of their expression of CD11c and MHCII, and that they consisted of three distinct populations. Two of these were $CD103^{+}$ and derived from committed-DC precursors, while the third was $CD103^{-}$ and was thought to be monocyte-derived (Bogunovic et al., 2009; Varol et al., 2007; 2009). However, around the time I started, $CX3CR1^{+/GFP}$ mice (Jung et al., 2000) became widely available for the characterisation of myeloid cells and were used to identify a population of Flt3L-unresponsive, non-migratory CX3CR1-expressing cells which appeared to be the $CD103^{-}$ 'DCs' that had been found in previous studies (Schulz et al., 2009). This report suggested that the majority of these $CD103^{-}$ cells were mϕs rather than DCs and it was proposed that mutually exclusive expression of

CD103 and CX3CR1 could be used to identify intestinal DCs and mϕs respectively. Although I planned initially to employ this strategy, others in the lab had observed a population of CX3CR1^{int}CD103^{-} MPs which did not express the pan mϕ marker F4/80 (Bain et al., 2013). Indeed, a small population of cells with this phenotype had been noted by Schulz and they appeared to expand in response to exogenous Flt3L *in vivo,* albeit at a greatly reduced level compared with the CD103^{+} DCs (Schulz et al., 2009).

Together these results suggested that at least some CX3CR1-expressing MPs might be genuine DCs and therefore, I decided to develop a new gating strategy in which I made no *a priori* assumptions regarding the lineage restricted expression of CD103 and CX3CR1. Furthermore, as an important aim of my PhD was to determine the role of the signalling receptor SIRPα on intestinal DC function, using mice which lacked the CX3CR1 reporter gene and no antibody to CX3CR1 was available, I had to find an approach which could distinguish DCs and mϕs without relying on CX3CR1 expression. To do this, I first identified MPs as total CD11c^{+}MHCII^{+} live leukocytes in digests of lamina propria and examined them for their expression of CD103 and CD11b. This identified four populations, two of which were CD103^{+} and two of which were CD103^{-}, with the subsets being distinguished by their expression of CD11b. These four subsets were then examined for expression of F4/80 and CD64, a marker that Bernard Malissen's group at the CIML in Marseille had shown to be specific for mϕs in the intestine (Bain et al., 2013; Tamoutounour et al., 2012). This showed that both subsets of CD103^{+} MPs were CD64^{-}F4/80^{-}, as were the CD103^{-}CD11b^{-} MPs. In contrast, the CD103^{-}CD11b^{+} MPs were heterogeneous, consisting of a large number of CD64^{+}F4/80^{+} cells and a smaller population of CD64^{-}F4/80^{-} cells. Examination of CD8α and SIRPα expression, two markers commonly used to subset DCs, showed that the CD64^{-}CD103^{+}CD11b^{-} DCs expressed CD8α homogeneously and lacked SIRPα expression. It is important to note that although it has often been assumed that CD8α^{+} DCs found in preparations of the LP were contaminants from PPs or ILFs, recent work has shown they are present in LP preparations from RORγt$^{-/-}$ mice which lack these structures, demonstrating they are present in the LP itself (Cerovic et al., 2013). Both the CD103^{+}CD11b^{+} and putative CD103^{-} CD11b^{+} DCs expressed SIRPα and lacked CD8α. Interestingly, the CD103^{-}

CD11b$^-$ putative DCs were heterogeneous for these markers, suggesting they could be a mixed population.

Consistent with previous reports (Denning et al., 2011), I found the distribution of the two CD103$^+$ DC populations to change from the SI LP to the colonic LP, with CD103$^+$CD11b$^+$ DCs predominating in the SI, whereas CD103$^+$CD11b$^-$ DCs constituted the major population in the colon. The proportions of the two CD103$^-$ putative DC populations did not alter significantly in the two locations.

This initial analysis based on F4/80 and CD64 expression therefore appeared to confirm the DC nature of the CD103$^+$ MP populations, but also suggested that the CD103$^-$CD11b$^+$ MPs included both DCs and mϕs. However, although CD64 was described to be a mϕ-specific marker in the gut (Bain et al., 2013; Tamoutounour et al., 2012), it has also been reported to be present on monocyte-derived 'DCs' in the muscle and lung (Langlet et al., 2012; Plantinga et al., 2013). Thus, while the definition of these CD64$^+$ cells as 'DCs' is controversial and indeed a subsequent study has concluded that these 'monocyte-derived DCs' in the lung are in fact mϕs (Schlitzer et al., 2013), I thought it necessary to confirm my phenotypic classifications by examining the expression of a variety of genes and other surface markers. Consistent with their identification as DCs, all the CD64$^-$F4/80$^-$ MPs expressed mRNA for the recently described DC-specific transcription factor *Zbtb46* (zDC) (Meredith et al., 2012a; Satpathy et al., 2012), as well as the surface markers CD26 and CD272, which the Immunological Genome Consortium had reported to be DC-specific (Miller et al., 2012). In contrast, the CD64$^+$F4/80$^+$ MPs lacked these markers but instead expressed the mϕ-specific markers CD14 and MerTk, which were absent from the CD64$^-$ MPs (Gautier et al., 2012). Even more importantly, the CD64$^-$ MPs all expressed CD135, the receptor for the DC-specific growth factor Flt3L (Karsunky et al., 2003; Merad and Manz, 2009). In parallel, all these putative DCs were virtually absent from the LP of Flt3L$^{-/-}$ mice and their numbers were greatly expanded by administration of exogenous Flt3L *in vivo,* a characteristic of genuine DCs (Maraskovsky et al., 1996). This finding was consistent with earlier results in our lab, demonstrating the presence of a Flt3L responsive CD103$^-$ MP population in the colonic LP (Bain et al., 2013) and with studies performed simultaneously by the Milling lab on the subsets found migrating in pseudo-afferent lymph (Cerovic et al., 2013). In contrast, the

$CD64^+F4/80^+$ MPs lacked CD135 expression, but instead expressed high levels of CSF-1R (CD115), the receptor for the monocyte/macrophage specific growth factor, CSF-1 (Witmer-Pack et al., 1993; Yoshida et al., 1990). Although the $CD64^-$ $CD103^-$ MP populations also expressed CD115, this was at much lower levels than observed for the $CD64^+$ MPs. Unlike the $CD64^-$ MPs, the $CD64^+$ mϕs also had high phagocytic activity indicating that the CD64 defined subsets may be functionally distinct. Moreover, these populations had distinct kinetics *in vivo,* with all the DC populations showing 70-80% BrdU labelling following 3 days of feeding, compared with only approximately 20% of the $CD64^+F4/80^+$ mϕs being labelled in the same period. Together these findings confirm that CD64 and F4/80 are sufficient for discriminating DCs and mϕs amongst $CD11c^+MHCII^+$ intestinal MPs. At the time I carried out this work, my results were the only ones to identify genuine intestinal SI LP $CD103^-$ DCs (C.L. Scott et al., submitted for publication) however while I was preparing this thesis and manuscript, the presence of $CD103^-$ DCs in the SI LP was confirmed by three independent studies using either CD64 or DNGR-1 expression to discriminate between the two lineages (Schlitzer et al., 2013; Schraml et al., 2013; Tamoutounour et al., 2012).

In contrast to the distinct patterns of expression seen for Flt3 and CSF-1R, all intestinal MP populations expressed similar levels of the receptor for CSF-2 (GM-CSF). However only the $CD64^-$ DC populations increased in response to exogenous CSF-2 *in vivo,* while the numbers of mϕs were unaffected. However, as the distinction between $CD64^+$ and $CD64^-$ MPs in the intestinal LP observed in resting mice was lost following administration of CSF-2, it became difficult to accurately set the $CD64^-$ versus $CD64^+$ gates and hence it remains unclear if DC and mϕ populations were defined accurately in these studies. Interestingly, while this result seemed to contradict the expression pattern of CSF-2R, it is consistent with the findings of Schulz and co-workers who found that exogenous CSF-2 administration expanded $CD103^+$ DCs and not $CX3CR1^+$ mϕs (Schulz et al., 2009). Thus further experiments are required to validate these results and possibly define new markers to pull apart DCs and mϕs in non-steady state scenarios. One possible way to overcome this issue could be to perform these studies in Zbtb46-reporter mice, allowing DCs and mϕs to be distinguished. Interestingly, although all the DC populations appeared to respond to exogenous CSF-2 *in vivo*, I found that only the $CD103^+CD11b^+$ SI LP DCs were dependent upon this growth factor *in*

vivo, as CSF-2RKO mice had a reduction in this population. However, the correct interpretation of these results is also unclear, as I found a population of $CD103^{int}CD11b^{+}$ DCs in these mice that were absent from WT controls. Therefore these results could reflect the reported ability of CSF-2 to induce CD103 expression (Zhan et al., 2011) rather than indicating the dependence of specific MP subsets on this growth factor. Others have recently reported a similar reduction in $CD103^{+}CD11b^{+}$ LP DCs in CSF-2RKO mice using CD24 as a surrogate marker for CD103 and hence suggesting that the effects are not simply a result of the lack of CD103 expression (Greter et al., 2012). However, while preparing this thesis I have examined CD24 expression by the various subsets of intestinal MPs and found that it is present on all subsets and may not be an accurate marker of $CD103^{+}$ DCs, thus further investigation is warranted. Interestingly, despite a recent report that alveolar mϕs in the lung develop through a CSF-2 dependent pathway (Guilliams et al., 2013b), the intestinal mϕs appear to be CSF-2 independent as they were unaffected in the CSF-2RKO animals, suggesting a tissue-specific role for this growth factor.

Consistent with previous reports (Bogunovic et al., 2009; Schulz et al., 2009; Varol et al., 2009), I found that $CD103^{+}$ DCs lacked CX3CR1 expression, while the $CD103^{-}CD11b^{+}CD64^{+}F4/80^{+}$ mϕs expressed either high or intermediate levels of the chemokine receptor. Interestingly, I found that the $CD64^{-}CD103^{-}CD11b^{+}$ DCs also expressed intermediate levels of CX3CR1, consistent with earlier findings that Flt3L had some ability to expand a population of $CX3CR1^{int}$ MPs *in vivo* (Schulz et al., 2009). Similar findings have been made in our own laboratory, where a population of $CX3CR1^{int}$ non-mϕs in the colon (Bain et al., 2013) and the presence of CX3CR1-expressing genuine DCs in pseudo-afferent intestinal lymph (Cerovic et al., 2013) were identified. It is important to note that none of these studies, including my own, found evidence of DCs expressing high levels of CX3CR1 in the steady state intestine, lymph or MLN. This is in direct contrast to a recent study which proposed that $CX3CR1^{hi}$ MPs could migrate from the LP to the MLN (Diehl et al., 2013). The reasons for this discrepancy are unclear, but it seems likely that this reflects inaccurate gating of CX3CR1-expressing cells by Diehl et al., with the $CX3CR1^{int}$ cells I found likely being misidentified as $CX3CR1^{hi}$ (Diehl et al., 2013). All other work suggests that $CX3CR1^{hi}$ cells in the intestine are the sessile mϕs which comprise the majority of the phagocytic $F4/80^{+}CD64^{+}CD11b^{+}$ MPs I

identified. Contrary to the other intestinal DC populations, the $CD103^{-}CD11b^{-}$ DCs were heterogeneous for CX3CR1 expression, with some being $CX3CR1^{-}$ and others $CX3CR1^{int}$. This seems to confirm my results with CD8α and SIRPα that these are a mixed population.

10.3 Migratory DC Populations in the MLN

As the primary function of DCs is to migrate to the draining lymph nodes and present antigen, I explored the ability of the DC populations I had discovered in the LP to migrate to the draining MLN. Migratory DCs in the MLN were identified as $MHCII^{hi}$ (Henri et al., 2001; Persson et al., 2013b; Plantinga et al., 2013; Schlitzer et al., 2013) and all four populations of $CD64^{-}$ DCs were found in this gate. In contrast, the resident $CD11c^{+}MHCII^{int}$ gate contained only 3 populations of DCs, with the $CD103^{+}CD11b^{+}$ DCs being missing. As $CD103^{+}CD11b^{+}$ DCs are found almost exclusively in the intestinal mucosa, their absence from the $CD11c^{+}MHCII^{int}$ gate is consistent with these $CD11c^{+}MHCII^{int}$ cells being derived from the bloodstream rather than the mucosa. It should be noted that although I also identified a small population of $CD64^{+}F4/80^{+}$ mϕs within the 'migratory DC' compartment of the MLN, cells with this phenotype cannot be found in afferent lymph draining to the MLN ((Cerovic et al., 2013) and C.L. Scott, C.C. Bain, V. Cerovic and S.A. Houston, unpublished data). This could suggest that this gated population may be contaminated by some LN resident cells or by blood. Indeed the convention that this gate represents only migratory DCs is not backed up by much direct evidence and thus care must be taken when using this approach to identify migratory cells. Once these $CD64^{+}F4/80^{+}$ cells were excluded from the $CD11c^{+}MHCII^{hi}$ gate in MLN, the remaining four DC populations were present in similar proportions to those found in intestinal lymph (Cerovic et al., 2013), suggesting that this additional step allows migratory DCs to be identified in the MLN accurately. It is worth noting that the proportions of the DC populations in lymph and amongst migratory DCs in the MLNs differed slightly from those in the SI LP. In particular, the $CD103^{-}$ DCs make up a smaller population of DCs in the MLN than in the LP, perhaps reflecting the ontogeny of these cells (see below). My BrdU incorporation studies, further confirmed the migratory nature of $CD64^{-}F4/80^{-}$ cells within the $CD11c^{+}MHCII^{int}$ gate in the MLN, as they had distinct kinetics compared with those in both the resident DC population and in the LP. DCs in the LP were labelled maximally after 3 days of BrdU feeding, whereas most of the

migratory DC populations in the MLN did not show maximal labelling until 3 days after cessation of BrdU administration. The only exception to this was the migratory CD103$^-$CD11b$^-$ DCs, which, were labelled maximally after 3 days of feeding in both the LP and MLN. This result was surprising, given that the presence of this subset intestinal lymph suggests they can migrate from the intestine (Cerovic et al., 2013). However this population is unique in that it is significantly reduced in the LP of RORγt$^{-/-}$ mice which lack PP and isolated lymphoid follicles (ILFs) (Cerovic et al., 2013), suggesting that these DCs may arrive in the MLN from a distinct anatomical location, such as the ILFs or PPs, possibly explaining their distinct kinetics. My BrdU incorporation results appear to contradict an earlier report from Jaensson and colleagues, which suggested that CD103$^-$ DCs in MLN shared the population kinetics of DCs derived from the bloodstream. However, this study did not discriminate between migratory and resident DCs and as the latter constitute the majority of MLN DCs, most of the CD103$^-$ DCs would indeed have been blood-derived (Jaensson et al., 2008). Taken together, my studies clearly demonstrate the presence of previously unappreciated *bona fide* CD103$^-$ DCs in the intestine that are capable of migrating to the MLNs.

10.4 Ontogeny of Intestinal DC Populations

In adult animals DCs derive from DC-committed progenitors, while mϕs derive from monocytes (BM or foetal liver) or primitive yolk-sac macrophages and when I began my project, intestinal CD103$^+$ DCs were thought to be derived from DC-committed progenitors, while CD103$^-$ 'DCs', which I have now shown includes both DCs and mϕs, were thought be the progeny of BM-derived Ly6C^{hi} monocytes (Bogunovic et al., 2009; Varol et al., 2009). Given the heterogeneity I had uncovered amongst the SI LP CD103$^-$CD11b$^+$ MPs, I thought it important to re-examine the origin of CD103$^-$ intestinal MPs directly. To this end, I set up models to examine the fate of adoptively transferred precursors *in vivo.* My initial plan was to do this using recipient mice depleted of CD11c-expressing cells using the CD11c-DTR system, but my preliminary studies revealed that DCs were not depleted efficiently in these animals. Indeed, a greater proportion of CD11c$^+$ mϕs was ablated. Therefore I decided to attempt the transfers into WT recipients, which I hoped would also be a physiologically more relevant model of homeostatic DC

development. To the best of my knowledge this is the first study to examine the fate of pre-DCs in resting WT mice and therefore I decided to investigate DC development from pre-DCs over a time-course. However in order to perform these studies, a large number of progenitors was required and therefore I decided to first expand the numbers of pre-DCs in BM *in vivo* by inoculating donor mice with B16 melanoma cells secreting Flt3L. This is a standard method for expanding DCs and pre-DCs and there is no evidence that it alters the functions of the expanded cells (Maraskovsky et al., 1996; Naik, 2010; Naik et al., 2007; Viney et al., 1998; Zeng et al., 2013). BM monocytes were transferred into $CCR2^{-/-}$ recipients as these monocytopenic mice provide a partially empty niche without the need for additional manipulation and this model had been previously established in the laboratory, which demonstrated that unlike other tissues, gut mϕs derive from BM not foetal liver monocytes or primitive macrophages (Bain et al., 2013).

These approaches showed clearly that all the populations of $CD103^{+}$ and $CD103^{-}$ DCs, I had identified were derived only from DC-committed progenitors. In contrast, $Ly6C^{hi}$ monocytes could not give rise to any of the $CD64^{-}F4/80^{-}$ MPs, despite repopulating $CD64^{+}F4/80^{+}$ mϕs efficiently. By labelling the pre-DCs with CellTrace Violet dye and examining the time course of their appearance in the mucosa, I was able to obtain insights into the processes involved in the development of the DC subsets. 2-3 days after their arrival in the mucosa, the precursors acquired MHCII and upregulated CD11c before acquiring CD103 or CD11b. Interestingly however, $CD103^{+}CD11b^{+}$ DCs did not appear until days 5-7 after transfer indicating that these are a terminal stage of differentiation. Following acquisition of MHCII, the donor cells began to undergo cell division as assessed by dilution of the CellTrace dye. Previous studies have shown that mature DCs divide *in situ* (Ginhoux et al., 2009) but this has never been examined previously in the intestine. This proliferation was confirmed by short-term BrdU uptake and Ki67 staining which showed that up to 6% of all populations of intestinal DCs were dividing *in situ.* However putative pre-DCs in the LP were not dividing and nor were $CD64^{+}$ mϕs, underlining the different population kinetics of these cells.

Pre-DC development could also be observed in the colonic LP and also in the MLN where donor-derived cells first appeared in the resident ($CD11c^{+}MHCII^{int}$) gate. Importantly, donor cell progeny could not be found amongst the migratory ($CD11c^{+}MHCII^{hi}$) DC gate in the MLN until day 3-5, supporting the idea that these

had come from the mucosa. In the MLN and colonic LP, progeny of pre-DCs acquired the same pattern of subset distribution as the endogenous populations, with $CD103^+CD11b^-$ DCs for example being the predominant population in the colon. Transferred pre-DCs also gave rise to $CD103^+CD11b^+$ DCs only in the intestine, consistent with the absence of this DC population from non-intestinal tissues, such as the spleen, lung, liver and kidney. This ability to recapitulate the normal pattern of DC subset distribution in different tissues could reflect individual subsets of pre-DCs generating each mature DC populations as hypothesised by Naik and colleagues based on CD24 expression (Naik et al., 2006), tissue-specific subsets of pre-DCs or could also suggest the differential conditioning of the same progenitors by the local environment. It will be interesting to examine these possibilities directly in the future. Recently a population of gut-tropic DC progenitors has been described, suggesting that distinct precursors may be involved in the generation of intestinal DCs compared with those in other tissues (Zeng et al., 2013). However, it should be noted that these pre-mucosal DCs (pre-μDCs) were also capable of generating splenic DCs and appeared to generate $CD103^+CD11b^-$ DCs preferentially even in the SI (Zeng et al., 2013). These pre-μDCs expressed the β7 integrin and B220 and thus exactly how they relate classical pre-DCs, which are $B220^-$ is unclear. A proportion of the pre-DCs I used did express β7, suggesting there may be heterogeneity amongst the pre-DCs, I and others have used in transfer studies (Bogunovic et al., 2009; Liu et al., 2009; Naik et al., 2006; 2007) and hence there may be gut-specific precursors amongst them. An alternative possibility is that the DC progenitors are pre-programmed in the BM to become a distinct DC subset and this hypothesis is consistent with recent work which reported that HSCs in the BM are imprinted to become a specific cell type from an early stage, with clonally expanded HSCs giving rise to the same cell types in different mice (Naik et al., 2013). Thus the fate of DC progenitors needs to be examined at the single cell level, the feasibility of which is currently limited.

On the other hand, the idea that environmental conditioning might determine the fate of DC progenitors is supported by the fact that although pre-DCs could not generate $CD103^+CD11b^+$ DCs in any other steady state tissue, $CD103^+CD11b^+$ DCs are reported to appear in the inflamed lung (Guilliams et al., 2013a). Thus the presence of this population in the steady state gut may reflect the state of 'physiological inflammation' that characterises this tissue. That the development of

$CD103^+CD11b^+$ DCs in the gut requires specific signals from the local environment would be consistent with my finding that they were the last to appear after transfer of pre-DCs. In addition, they were the last subset to arrive in the intestine after birth, whereas $CD103^+CD11b^-$ DCs and both subsets of $CD103^-$ DCs could be identified from birth.

As discussed in Chapter 1, the nature of the local 'conditioning' factors that might drive the phenotype and function of intestinal DCs remains elusive, with a wide variety of different dietary, hormonal and cytokine-mediated processes having being proposed (Scott et al., 2011). Investigating this was beyond the scope of my project, but one factor I thought important to explore was the presence of the microbiota, especially as this could perhaps account for the changes in the neonatal period. Although previous studies have examined 'DC' populations in germ-free mice, these failed to distinguish accurately between the DC populations and included mϕs amongst the gated DCs, as well as gating $CD103^+CD11b^+$ with $CD103^-$ DCs and mϕs (Rivollier et al., 2012). However, I found that broad-spectrum antibiotics only affected $CD103^+CD11b^+$ DCs. Contrary to what I would have expected from my studies of neonatal mice, I found that the augmentation of the microbiota with antibiotics caused an increase in the numbers of $CD103^+CD11b^+$ DCs in the SI LP. There was also a proportional increase in this DC population amongst migratory DCs in the MLN. It is possible that this discrepancy reflects the need for specific bacterial species in the development of individual DC subsets and that these are differentially susceptible to the antibiotics I used. Additionally they may be differentially located in the small and large intestines explaining the differences in the number of $CD103^+CD11b^+$ DCs in these locations. To explore this, it will be necessary to study germ-free mice re-colonised with specific bacterial strains.

I also considered the possibility that CSF-2 might be involved in the development of $CD103^+CD11b^+$ DCs (Greter et al., 2012). Therefore, while preparing this thesis I tested the hypothesis that the levels of CSF-2 in different parts of the body and in the small versus large intestine would correlate with the frequency of $CD103^+CD11b^+$ DCs at each site. However, CSF-2 ELISAs showed that the levels of this growth factor were considerably lower in both the small and large intestine compared with a number of other tissues including the lung.

Irrespective of whether local conditioning factors or distinct precursors are involved, it is clear that the development of individual DC populations requires specific transcription factors. For example Batf3, Id2 and IRF8 are required for the homeostasis of CD8α^+ DCs in lymphoid tissues and their CD103$^+$CD11b$^-$ DC counterparts in non-lymphoid tissues, including the intestine (Aliberti, 2002; Edelson et al., 2010; Ginhoux et al., 2009; Hildner et al., 2008; Tailor et al., 2008). Despite this, I found Batf3 and Id2 to be expressed at similar levels by all intestinal MP populations. In addition, although CD103$^+$CD11b$^-$ DCs expressed IRF8 at higher levels than the other DCs, it was also expressed by mϕs. Similarly, while I and others have found IRF4 to be expressed by all intestinal DCs and mϕs, with the exception of CD103$^+$CD11b$^-$ DCs (Schlitzer et al., 2013), recent work indicates that IRF4 has a selective role in the homeostasis of CD103$^+$CD11b$^+$ DCs in the intestine (Persson et al., 2013b; Schlitzer et al., 2013). Although a role for IRF4 in CD103$^-$CD11b$^+$ DC development and/or homeostasis could also be argued from these data (Persson et al., 2013b; Schlitzer et al., 2013). However, this lack of a correlation between the expression of individual transcription factors and their requirement for homeostasis may support the idea that all DCs derive from a single precursor, whose subsequent fate is under the control of specific environmental cues. Importantly, the stage of DC development at which these transcription factors act is largely unknown, and indeed their role may not be in development at all. The effects of IRF4 on the homeostasis of CD103$^+$CD11b$^+$ DCs in the intestine appear to be due to its influence on their survival (Persson et al., 2013b), while IRF4 has also been implicated in regulating DC migration to the LNs (Bajaña et al., 2012). Further studies are thus required to examine these issues.

10.4.1 Role of CCR2 in Development of Intestinal DCs

My findings that intestinal CD103$^-$CD11b$^+$ DCs derive exclusively from DC-committed progenitors directly contradict previous studies which proposed that these DCs were generated from monocytes both in the steady state (Bogunovic et al., 2009; Varol et al., 2007; 2009) and during inflammation (Rivollier et al., 2012; Zigmond et al., 2012). Although I proposed that this was due to the imprecise gating strategies used in other studies to define DCs and mϕs, a recent study by Zigmond and colleagues, which discriminated CD103$^-$CD11b$^+$ DCs from mϕs accurately on the basis of zDC expression, also concluded that CD103$^-$ DCs were

monocyte-derived. This conclusion was based on their loss following *in vivo* administration of an anti-CCR2 antibody (Zigmond et al., 2012), a strategy which is usually considered to act by depleting Ly6C^{hi} monocytes. Therefore towards the end of my project, I assessed the role of CCR2 in the development and/or homeostasis of the intestinal DC populations I had defined in case I had missed some monocyte-derived DCs in my original transfer experiments. First I found there was a selective reduction in the proportion and number of CD103^{-}CD11b^{+} DCs in the SI LP and amongst migratory DCs in the MLN. This finding was replicated in WT:CCR2$^{-/-}$ competitive BM chimeras where the CD103^{-}CD11b^{+} DCs were less efficiently reconstituted by CCR2$^{-/-}$ cells than the other DC subsets or the eosinophils which were used as control myeloid cells. Notably, this defect was considerably less severe than that observed for the monocyte-derived mϕ population in the same mice, suggesting these may not be completely dependent upon CCR2-expressing cells, presumably monocytes, as is the case for intestinal mϕs (Bain et al., 2013; Tamoutounour et al., 2012). Interestingly, in preliminary parabiosis studies CCR2$^{-/-}$ mice had an enhanced population of CD103^{-}CD11b^{+} DCs in the SI LP deriving from their WT partner compared with the other DC subsets, further suggesting a dependence of these DCs on CCR2. Unfortunately it was not possible to examine the exchange between the DC-committed progenitors in the bloodstream of these animals and thus it is difficult to draw any conclusions from this experiment.

This novel finding of a CCR2 dependent population of DCs was not specific to the intestine, as the number of splenic DCs was also reduced in CCR2$^{-/-}$ mice although in this case, both CD11b^{+} and CD11b^{-} subsets were affected. A smaller defect was also occasionally seen with CD103^{+}CD11b^{-} DCs amongst migratory MLN DCs although this was not consistent and neither was it recapitulated in the chimeras or parabionts. For unknown reasons the resident DC populations in the MLN were largely unaffected in CCR2$^{-/-}$ mice despite the effects observed in the spleen. The reasons for these tissue-specific differences in CCR2 dependence remain unclear, although it seems clear that CCR2 is not restricted to the intestine. The cellular mechanism may also differ between tissues as although the defect in intestinal DCs was clearly cell intrinsic, this appeared not to be the case in the spleen, where WT and CCR2$^{-/-}$ BM reconstituted the splenic DCs in these mice equally as efficiently. This secondary defect could reflect the reduced population of mϕs in CCR2$^{-/-}$ mice and the known ability of mϕs to produce CCR2 ligands

(Tagliani et al., 2011). The exact reasons for these differences require further investigation.

Correlating with their selective and partial reduction in the $CCR2^{-/-}$ LP, a proportion of $CD103^{-}CD11b^{+}$ DCs in the LP expressed this receptor. Because of the reported technical difficulties associated with using a CCR2 antibody, I examined CCR2 expression using three distinct methods, antibody staining, a CCL2 uptake assay (Ford et al., 2013; McKimmie et al., 2008) and using $CCR2^{+/RFP}$ mice (Saederup et al., 2010). While all three methods identified a clear subset of CCR2-expressing $CD103^{-}CD11b^{+}$ DCs, the size of this population varied depending on the method used. While both the direct CCR2 antibody staining and CCL2 uptake assay indicated that approximately 25% of these DCs expressed CCR2, over 75% of them were $CCR2^{+}$ in $CCR2^{+/RFP}$ mice. This discrepancy is consistent with the original study of these animals, which identified RFP^{+} cells in the bloodstream that were not detected by CCR2 antibody staining (Saederup et al., 2010). I also obtained similar results amongst migratory DCs in the MLN, using CCR2 antibody staining or CCL2 uptake only approximately 12% of the $CD103^{-}CD11b^{+}$ migratory DCs expressed CCR2 however RFP expression was found in over 30% of these DCs in the $CCR2^{+/RFP}$ mice. It has been suggested that the explanation for this could be that CCR2 becomes internalised in some cells, due to constitutive or ligand induced recycling (Mack et al., 2001; Saederup et al., 2010; Volpe et al., 2012), thus preventing its detection on the cell surface by antibody or fluorescently-labelled ligand. Alternatively, although the RFP gene is under the control of the CCR2 promoter, the half-life of the RFP, which is thought to be 20-30 hours (Subach et al., 2011), may result in the extended presence of an RFP signal in the absence of CCR2 protein expression. Similar reasons may account for the fact that the $CD103^{+}CD11b^{+}$ DCs were also $CCR2^{+}$ in the $CCR2^{+/RFP}$ mice, but not when surface staining methods or ligand uptake was used. Additionally, $CD103^{+}CD11b^{-}$ LP DCs expressed low levels of CCR2 when antibody staining was used, but showed considerably more using both the CCL2-uptake assay and RFP expression. The reasons for this are unclear, but may represent issues with the CCL2-uptake assay, which had not previously been validated in the gut. Indeed migratory $CD103^{+}CD11b^{-}$ DCs in the MLN did not express CCR2 by either antibody staining or CCL2-uptake. Like the $CD103^{-}CD11b^{+}$ DCs, the $CD103^{-}CD11b^{-}$ DCs in the LP expressed CCR2 to some degree using all the methods, but the proportion of $CCR2^{+}$ cells amongst this population was highest when assessed

by the $CCR2^{+/RFP}$ mice. As in the LP, all migratory DC populations expressed some CCR2 when examined in $CCR2^{+/RFP}$ mice, however only the $CD103^{-}CD11b^{+}$ migratory DCs were $CCR2^{+}$ as assessed by antibody and CCL2 uptake. Despite these technical issues, it is important to note that using the antibody to define $CCR2^{+}$ DCs allowed a functionally distinct population of $CD103^{-}CD11b^{+}$ DCs in the LP to be identified (see below). Furthermore, in collaboration with Pamela Wright, I was able to identify a similar population of $CCR2^{+}CD103^{-}SIRP\alpha^{+}$ DCs in the human colonic LP, using an anti-CCR2 antibody. As SIRPα is believed to be a cross-species marker for the equivalent of $CD11b^{+}$ DCs found in mice, these cells may be analogous to the $CCR2^{+}$ subset of $CD103^{-}CD11b^{+}$ DCs found in mice. However, a larger proportion of $CD103^{-}SIRP\alpha^{+}$ DCs in humans expressed CCR2 than in mice, while a proportion of $CD103^{+}SIRP\alpha^{+}$ DCs in humans also expressed CCR2. This may reflect a technical issue, as the discrimination between $CD103^{+}$ and $CD103^{-}$ $SIRP\alpha^{+}$ DCs in the human LP was less discrete than in the mouse. Further optimisation of the staining panel may allow for greater resolution between the populations and a more detailed assessment of CCR2 expression on the different populations in humans. Alternatively, as discussed below, $CD103^{-}$ and $CD103^{+}$ $SIRP\alpha^{+}$ DCs may be developmentally linked, and, the upregulation of CD103 may occur prior to the loss of CCR2 in human but not mouse LP, evidently this requires direct investigation. Consistent with my findings in $CCR2^{-/-}$ mice, I found that CCR2 expression was not restricted to intestinal DCs, as a proportion of both splenic and lung $CD11b^{+}$ DCs were also found to express the chemokine receptor as assessed by antibody staining. This finding was supported by a report on splenic DC in $CCR2^{+/GFP}$ mice (Satpathy et al., 2013).

Because CCR2 is generally associated with the egress of monocytes from BM, as well as their accumulation in tissues (Serbina and Pamer, 2006), I thought it was important to examine directly if the $CCR2^{+}CD103^{-}CD11b^{+}$ DCs were *bona fide* pre-DC derived DCs. This was indeed the case, as not only did transferred pre-DCs generate $CCR2^{+}CD103^{-}CD11b^{+}$ DCs in the LP, but this subset expressed similar levels of mRNA for *Flt3, Zbtb46* and *Ccr7* as their $CCR2^{-}$ counterparts and the $CD103^{+}$ DC populations. I then investigated whether CCR2 might be expressed by pre-DCs in the BM and if this could be involved in their fate *in vivo*. Pre-DCs in the BM expressed heterogeneous levels of CCR2 as assessed using the CCR2 antibody, but unlike monocytes, their egress to the bloodstream was

unaffected in $CCR2^{-/-}$ mice, as was the numbers of pre-DCs in the BM. Unfortunately, I was unable to sort enough $CCR2^{+}$ pre-DCs to determine if they had a differential ability to generate LP DC subsets and this needs explored in the future. Instead I performed competitive adoptive transfers of pre-DCs from WT and $CCR2^{-/-}$ mice into WT recipients. Under these conditions, all the subsets of LP DC derived preferentially from WT progenitors, suggesting a role for CCR2 in the ability of the progenitors to gain access to the LP and leaving open the question of why there is a selective defect in the $CD103^{-}CD11b^{+}$ DCs in the $CCR2^{-/-}$ mouse. One explanation could be that those $CCR2^{-/-}$ DCs which do gain access to the mucosa undergo enhanced *in situ* proliferation to fill up the empty niche for most of the DC subsets. However, why this would not overcome the defect in $CD103^{-}$ $CD11b^{+}$ DCs is unclear and clearly further investigation is required to explain these results.

10.5 Function of Intestinal DC Populations

Having identified novel subsets of genuine DCs in the intestinal LP, I went on to investigate their functions. All four populations of DCs were equally efficient at inducing proliferation of naïve antigen-specific $CD4^{+}$ T cells when pulsed with ovalbumin (OVA) *in vitro.* Although all could also induce proliferation of naïve antigen-specific $CD8^{+}$ T cells when higher DC:T cell ratios were used, only the $CD103^{+}CD11b^{-}$ DCs were capable of inducing proliferation of naïve $CD8^{+}$ T cells when lower numbers of DCs were used and these were also the only DCs to drive the production of IFNγ under any conditions. The ability of the $CD8\alpha^{+}CD103^{+}CD11b^{-}$ DCs to cross-present antigen, coupled with their dependence on Batf3 and expression of XCR1 emphasises their relationship to the $CD8\alpha^{+}$ lineage in other tissues, which are often defined as $CD103^{+}$ (Bachem et al., 2010; 2012; Bedoui et al., 2009; Haniffa et al., 2012; Zhan et al., 2011). Interestingly, although they were inefficient at cross-presenting antigen, some $CD103^{-}CD11b^{-}$ intestinal DCs also expressed XCR1, perhaps indicating some relationship with the $CD8\alpha^{+}$ DC lineage. These cross-presentation results contrast with those of Fujimoto and colleagues, who showed that LP DC have little cross-presentation activity unless they have been stimulated via TLRs *in vitro* (Fujimoto et al., 2011). In addition these authors found that the $CD103^{+}CD11b^{+}$ DCs had equivalent cross presentation activity compared with their $CD11b^{-}$ counterparts

under these circumstances (Fujimoto et al., 2011). It is entirely possible that following the right signals multiple subsets of DCs may be capable of inducing cross-presentation, and indeed mature human lymphoid tissue DCs of multiple subtypes have been shown to be equally capable of cross-presenting antigen (Segura et al., 2013). Thus examination of the effects of distinct TLR ligation on the antigen presenting cell activity of the intestinal DC subsets represents an important avenue for investigation in the future.

Although all intestinal DC subsets were equally efficient at inducing proliferation of naïve $CD4^+$ T cells, my results showed that they had distinct effects on $CD4^+$ T cell polarisation. Consistent with earlier reports that $CD103^+$ DCs may be intrinsically tolerogenic (Annacker et al., 2005; Coombes et al., 2007; Jaensson et al., 2008; Scott et al., 2011; Siddiqui and Powrie, 2008; Sun et al., 2007), I found that the two subsets of $CD103^+$ DCs induced the differentiation of $FoxP3^+$ T_{Reg} cells better than the $CD103^-$ DC subsets. Although it needs to be confirmed with increased sample sizes, the $CD103^+CD11b^-$ DCs appeared to be slightly more efficient than the $CD103^+CD11b^+$ DCs in this respect. Interestingly this correlated with the finding that the $CD103^+CD11b^-$ DCs had increased ALDEFLUOR activity compared with the other DC subsets (Guilliams et al., 2010a), and were the only DC subset that expressed the TGFβ-activating integrin αvβ8 (Travis et al., 2007). Both TGFβ and RA are essential for the induction of T_{Reg} cells by DCs (Coombes et al., 2007; Jaensson et al., 2008; Sun et al., 2007) and it is interesting to note that my work and that of others shows that $CD103^+CD11b^-$ DCs predominate in the colonic LP where T_{Reg} cells are also most prominent (Denning et al., 2011). Furthermore, CD11c-driven conditional KOs of IRF4 and Notch2, as well as my SIRPα mt mice and mice expressing human langerin have normal T_{Reg} cells despite all displaying defects in the numbers of $CD103^+CD11b^+$ DCs (Lewis et al., 2011; Persson et al., 2013b; Welty et al., 2013). This apparent association between $CD103^+CD11b^-$ LP DCs and the generation of $FoxP3^+$ T_{Reg} cells contrasts with the study by Fujimoto and colleagues where $CD8\alpha^+$ LP DCs did not induce $FoxP3^+$ T_{Reg} cells *in vitro* (Fujimoto et al., 2011). In addition Batf3KO mice which lack $CD103^+CD11b^-$ DCs, have normal numbers of T_{Reg} cells in the intestine (Edelson et al., 2010). This may be because this study did not discriminate between populations of inducible (iT_{Reg}) versus natural (nT_{Reg}) cells on the basis of expression of neuropilin and Helios (Thornton et al., 2010;

Weiss et al., 2012; Yadav et al., 2012), which is important as intestinal mϕs have been shown to expand T_{Reg} cells locally (Hadis et al., 2011) and thus any defect in priming iT_{Reg} cells might be missed due to the increased local expansion of nT_{Reg} cells. Nevertheless, my findings showed that $CD103^+CD11b^+$ DCs were also capable of inducing T_{Reg} cells from naïve $CD4^+$ T cells *in vitro* and thus taken together these findings may suggest a level of redundancy in the ability of the $CD103^+$ DCs subsets to induce T_{Reg} cells. While I was finalising this discussion, a report was published demonstrating such redundancy where hu-LangerinDTAxBatF3 mice, which lack both $CD103^+CD11b^+$ and $CD103^+CD11b^-$ DCs were found to have reduced T_{Reg} cells in the LP despite the individual strains having normal numbers of these cells (Welty et al., 2013).

As well as their cross-priming activity and slightly enhanced ability to induce $FoxP3^+$ T_{Reg} cells, $CD103^+CD11b^-$ DCs were also the most efficient at priming IFNγ producing T_h1 cells *in vitro*, possibly due to their production of IL12p40. Although my initial studies shown in Chapter 6 did not reveal clear patterns of T_h1 generation by the other subsets, later experiments I carried out in Chapter 9, using optimised DC:T cell ratios and improved intracellular cytokine staining protocols showed that $CD103^+CD11b^+$ DCs did not induce significant T_h1 responses and the $CD103^-$ DC subsets were poor inducers of IFNγ production. Although this result is consistent with findings from my SIRPα mt mice and from CD11c-driven conditional KOs of IRF4 that $CD103^+CD11b^+$ DCs are dispensable for the presence of T_h1 cells in the intestine (Persson et al., 2013b), it contrasts with results using DCs isolated from intestinal lymph, which suggested $CD103^-CD11b^+$ DCs to be the main inducers of IFNγ from $CD4^+$ T cells *in vitro* (Cerovic et al., 2013). These differences may be due to the cells used in each study, and in particular, it may be that the $CD103^-CD11b^+$ DCs isolated from lymph are more activated than the equivalent subset in the LP. This could be because the DCs have received the signals needed to make them enter lymph, or because of inflammatory stimuli released during the surgical procedures needed to isolate DCs from intestinal lymph. Indeed my experiments on post-operative ileus show that even minor handling of the intestine can lead to an inflammatory infiltrate in the mucosa and therefore it would be interesting to examine how that might alter the T cell polarising functions of DCs. It would also be interesting to investigate

how migratory DC populations in the MLN polarise T cells *in vitro* in comparison with those I have isolated from the LP.

$CD103^+CD11b^+$ DCs have recently been associated with the induction of T_h17 responses *in vivo* (Lewis et al., 2011; Persson et al., 2013b; 2013a; Satpathy et al., 2013; Schlitzer et al., 2013; Welty et al., 2013) and consistent with this, I found this subset to be more effective than their $CD103^+CD11b^-$ counterparts at inducing T_h17 differentiation from naïve $CD4^+$ T cells *in vitro.* At first sight these results seem to contradict my experiments in which administration of a broad-spectrum antibiotic cocktail reduced the numbers of intestinal T_h17 cells but led to increased numbers of $CD103^+CD11b^+$ DCs in the LP. One possibility could be that the antibiotics had a selective effect on a certain bacterial strain which induce T_h17 responses such as segmented filamentous bacteria (SFB) (Denning et al., 2011; Gaboriau-Routhiau et al., 2009; Ivanov et al., 2008; 2009). Thus while more $CD103^+CD11b^+$ DCs are present, they may not receive the signals required for inducing T_h17 cells. Of course this does not explain why there are more $CD103^+CD11b^+$ DCs in the LP but as discussed earlier this could be a separate phenomenon where the presence of these DCs is also linked to a specific bacterial strain, which is perhaps resistant to the antibiotic regime. Alternative hypotheses also exist. It is possible that the antibiotic treatment affects more than just the intestinal DCs and perhaps may alter the presence or function of a number of innate cells such as mϕs and innate lymphoid cells (ILCs) which function in the maintenance of T_h17 cells in the LP (Hepworth et al., 2013; Shaw et al., 2012). Finally, $CD103^+CD11b^+$ DCs may not be the only DC subset involved in the induction of T_h17 cells *in vivo*. Consistent with this hypothesis, I found that $CD103^-CD11b^+$ DCs were more effective than $CD103^+CD11b^+$ DCs at inducing T_h17 cell polarisation *in vitro* and this was especially true of the $CCR2^+$ fraction of $CD103^-CD11b^+$ DCs. The presence of a pro-inflammatory $CD103^-$ 'DC' subset has been proposed on numerous occasions (Cerovic et al., 2013; Rivollier et al., 2012; Scott et al., 2011; Siddiqui et al., 2010; Varol et al., 2009; Zigmond et al., 2012) and although most of these previous studies used imprecisely gated populations of MPs, a recent study of intestinal lymph also found genuine $CD103^-$ DCs to be the most effective inducers of T_h17 cells *in vitro* (Cerovic et al., 2013). Importantly, I found that this was not just an *in vitro* phenomenon, as the defect in $CD103^-CD11b^+$ DCs in $CCR2^{-/-}$ mice was associated with impaired T_h17 priming in the MLNs following infection with *C. rodentium* or after priming of antigen-specific T

cells *in vivo* using LPS and α-CD40 as adjuvants. Although, infection with *C. rodentium* also correlated with a selective increase in the proportion of $CD103^-$ $CD11b^+$ DCs in the LP I did not examine specifically if there was a reduced population of T_h17 cells in the LP of infected $CCR2^{-/-}$ mice. This was because these animals are monocytopenic and thus have reduced populations of mϕs in the gut (Bain et al., 2013) and I was concerned that the lack of these cells might compromise the accumulation or maintenance of local T_h17 cells as has been described previously for both T_h17 and T_{Reg} cells (Hadis et al., 2011; Shaw et al., 2012).

To try and understand why $CD103^-CD11b^+$ DCs drove such robust T_h17 responses, I examined their expression of the cytokines IL6, TGFβ, IL1β and IL23, all of which are known to be involved in T_h17 polarisation (McGeachy and Cua, 2008; Shaw et al., 2012). I found all DC subsets from the LP to express mRNA for *Tgfβ*, but the significance of this is unclear as it does not measure the presence of bioactive TGFβ and several other cell types also make this cytokine. Recently it has been shown that IL6 production may be crucial for the induction of T_h17 cells by $CD103^+CD11b^+$ MLN DCs (Persson et al., 2013b), but I found that all subsets of LP DCs produced identical amounts of both mRNA and protein. If anything the $CCR2^+CD103^-CD11b^+$ DCs produced slightly less than the $CCR2^-$ fraction. It has been suggested that production of IL1β by mucosal mϕs may maintain previously primed T_h17 cells in the LP and that this is a mϕ-dependent process (Shaw et al., 2012), although the imprecise gating strategies employed in this study could not exclude a role for $CD103^-CD11b^+$ DCs. Consistent with their enhanced ability to induce T_h17 differentiation, $CD103^+CD11b^+$ and both $CD103^-$ DC subsets expressed similar levels of IL1β mRNA, and these were 10-fold more than produced by $CD103^+CD11b^-$ DCs. The one feature I did find was different for the $CCR2^+CD103^-CD11b^+$ DCs was that they expressed significantly more IL12/IL23p40 protein by intracellular cytokine staining than any other subset. This difference was maintained and greatly enhanced by *in vitro* stimulation with the TLR4 agonist LPS. As I hypothesised that this IL12/IL23p40 protein might represent production of IL23, I attempted to measure IL23p19 in steady state DC. Despite spending some time trying to optimise primers and protocols for detecting IL23p19, I was unable to detect any IL23p19 using either qPCR or intracellular cytokine staining from steady state LP DCs. I was also unable to measure IL12p35

by qPCR, but as $CCR2^{+}CD103^{-}CD11b^{+}$ DCs were poor inducers of IFNγ production by T cells, I would propose that the IL12/IL23p40 I detected reflected IL23, rather than IL12 production by the DCs and that this helps explain the T_h17 priming properties of these DCs. It would be important to prove this by blocking IL23 during the DC:T cell co-cultures.

10.6 Intestinal DC Subsets in Inflammation

Having identified distinct DC subsets in the steady state intestinal LP which appeared to function differentially in the induction of adaptive immune responses, I went on to examine how these subsets behaved during inflammation. To address this, I employed two models of sterile inflammation, DSS colitis and post-operative ileus (POI), together with *C. rodentium* infection. Although the two sterile models resulted in significant inflammation in the LP characterised by neutrophils and monocytes, these did not alter the balance between the DC populations in the LP. While it is possible that the POI model may be too acute to see changes in the DC populations, similar results were obtained in DSS colitis, which lasts for several days. Although it would be interesting to follow up these studies by examining events in the MLN and carrying out functional analyses of the DC subsets, I decided not to pursue these models because of the apparent lack of DC involvement.

However, an important result from the DSS model was that the lineage restriction of pre-DCs and monocytes remained faithful during inflammation. Thus adoptively transferred pre-DCs gave rise to all subsets of DCs I had identified previously, while previous work in the lab had demonstrated that monocytes solely generated mϕs under these conditions (Bain et al., 2013). Thus my work shows that a new population of monocyte-derived DCs does not appear to be recruited to the mucosa during inflammation, contrasting with previous studies (Rivollier et al., 2012; Serbina et al., 2003; Zigmond et al., 2012).

Unlike sterile inflammation, *C. rodentium* infection did alter the relative frequencies of the DC subsets in the LP with a selective increase in the number of $CD103^{-}CD11b^{+}$ DCs being observed. This further supports that these DCs may play a role in T_h17 cell induction as *C. rodentium* also increases the numbers of T_h17 cells selectively (Geddes et al., 2011; Satpathy et al., 2013). Again, it will be

necessary to examine the specific functions of the DC populations during infection with *C. rodentium*, especially in view of my later findings in SIRPα mt mice, which have reduced populations of $CD103^+CD11b^+$ DCs and T_h17 cells (see below).

10.7 Role of SIRPα Signalling in Intestinal DCs

My studies characterising intestinal DC subsets and their origins had indicated that their properties might be determined after the arrival of their precursors in the mucosa and thus it was of interest to try and identify the factors involved. When I began my PhD, SIRPα had been shown to discriminate between the two genuine intestinal DC subsets, $CD103^+CD11b^+$ and $CD103^+CD11b^-$ that were known at that time. As SIRPα is thought to be an inhibitory receptor, I hypothesised that the expression of SIRPα by $CD103^+CD11b^+$ DCs might contribute to their proposed tolerogenic function. Thus the original aim of my PhD was to characterise the DCs in the intestinal LP of mice with a point mutation in the cytoplasmic signalling domain of SIRPα, which abolishes intracellular signalling. It was while carrying out my initial studies into these mice that I found the four clear populations of *bona fide* DCs, whose characterisation became a substantial part of my project. In parallel, I continued my work on the SIRPα mt mice and found that the $CD103^+CD11b^+$ and $CD103^-CD11b^+$ DCs expressed SIRPα homogeneously, while the $CD103^-CD11b^-$ DCs were heterogeneous for this molecule and $CD103^+CD11b^-$ DCs were entirely negative. Mϕs and a host of other myeloid cells, including neutrophils, monocytes and eosinophils also expressed SIRPα.

A few months into my project, two studies reported that the SIRPα mt mice had a selective defect in $CD4^+CD11b^+$ DCs in the spleen (Saito et al., 2010), as well as a relative lack of a poorly characterised $CD11b^+CD11c^{int}$ cell in the SI LP (Kanazawa et al., 2010). Thus, to begin to examine the role of SIRPα in the intestine, I first enumerated the DC and mϕ populations in SIRPα mt mice using the precise gating strategies I had developed. Consistent with previous results, I found a considerable reduction in the proportions and number of $CD11b^+$ DCs in the spleen and amongst resident $CD11b^+$ DCs in the MLN. This was not unexpected, given that $CD11b^+$ cells in all tissues express SIRPα. However, the mt mice had a selective reduction in $CD103^+CD11b^+$ DCs in both the SI and

colonic LP as well as amongst $CD103^+CD11b^+$ migratory DCs in the MLN. In contrast, the $CD103^-CD11b^+$ DCs and other $SIRP\alpha^+$ myeloid populations were unaffected. This selective defect was probably not observed in the previous report because it used CD11c and CD11b to identify 'DCs' and thus they were unable discriminate between $CD103^+CD11b^+$ DCs, $CD103^-CD11b^+$ DCs and $F4/80^+$ mϕs (Kanazawa et al., 2010). Furthermore, the $CD11b^+CD11c^+$ 'DCs' identified in that paper would also include eosinophils, which were later shown to be defective in the intestine of SIRPα mt mice (Verjan Garcia et al., 2011). Interestingly, in my studies, SIRPα mt mice did not display any eosinophil phenotype. This may be a result of the different protocols used to isolate leukocytes from the intestine and the use of Percoll gradients by the other groups, or to differences in the microbiota in the different mice. I did not follow this up and therefore the role of SIRPα in the homeostasis of intestinal eosinophils needs further investigation.

The selective defect in $CD103^+CD11b^+$ DCs in the LP and amongst migratory DCs in the MLN was recapitulated in CD47KO mice, supporting previous results in the spleen (Saito et al., 2010) and suggesting that signalling through the SIRPα-CD47 axis is involved in regulating DC homeostasis. As CD47 is expressed ubiquitously in the intestine, it was unclear which CD47-expressing cells interact with $SIRP\alpha^+$ DCs, or at which stage of the DC lifespan this interaction occurs. I therefore set out to explore how SIRPα might act in the homeostasis of $CD103^+CD11b^+$ DCs by examining its role in their development, proliferation, migration and survival. As I had shown previously that all DC subsets arise from a common BM progenitor which uniformly expressed intermediate levels of SIRPα, it seemed unlikely that the lack of SIRPα signalling could affect the generation of these precursors, without having knock-on effects on all intestinal DC populations. Consistent with this hypothesis, I found WT and SIRPα mt mice had similar proportions of pre-DCs in the BM and there appeared to be no defect in the egress of progenitors from the BM into the bloodstream. Next, I investigated whether SIRPα mt pre-DCs could gain entry to the intestinal LP and develop normally into the various DC populations. Competitive adoptive transfers using a 50:50 mix of WT and SIRPα mt pre-DCs demonstrated that the pre-DCs from SIRPα mt mice could enter the LP and were capable of generating all DC subsets once there. However SIRPα mt pre-DCs generated $CD103^+CD11b^+$ DCs more rapidly than their WT counterparts, with a clear population of SIRPα mt BM-derived

$CD103^+CD11b^+$ DCs being present in the intestine 3 days after transfer, whereas this did not occur until day 5 for the WT-derived $CD103^+CD11b^+$ DCs. As I reasoned that these findings might indicate that SIRPα signalling might act as a brake on the maturation of $CD103^+CD11b^+$ DCs, including their acquisition of CD103. To investigate this further, I examined whether other facets of activation/maturation were affected in $CD103^+CD11b^+$ DCs from SIRPα mt mice. This showed that this population selectively expressed increased levels of the co-stimulatory molecule CD86 in the steady state compared with WT counterparts, consistent with the proposed role of SIRPα in dampening inflammatory responses (Braun et al., 2006).

Emigration from tissue to draining LN is a classical indicator of DC activation and a number of studies have implicated the SIRPα-CD47 axis in DC migration. However it is unclear whether SIRPα signalling induces or prevents this process (Hagnerud et al., 2006; Motegi et al., 2003; Van et al., 2006). Whereas one study demonstrated that ligation of SIRPα by an agonist antibody or CD47-Fc fusion protein impaired DC migration (Motegi et al., 2003), others have suggested that the reduction in DCs observed in the draining LNs of CD47KO mice reflects reduced migration (Hagnerud et al., 2006; Van et al., 2006). To explore this directly in the intestine, I collaborated with Dr. Simon Milling's group and examined the DC populations present in pseudo-afferent intestinal lymph from SIRPα mt mice. Interestingly, this demonstrated no differences in the proportions of any of the SIRPα-expressing DCs, but there was a slight increase in the proportion of $CD103^+CD11b^-$ DCs. At first sight this result seemed surprising in view of the sizeable reduction in the proportion of $CD103^+CD11b^+$ DCs in the LP, which is the main source of these DCs in intestinal lymph. However, putting these findings together could suggest that there is actually an underlying increase in the rate of migration of this DC population out of the mucosa into the lymph. Future studies will examine the DCs in both the LP and the lymph simultaneously allowing the severity of the defect in the LP to be assessed alongside the proportions of the DC subsets in lymph.

Despite the inconclusive nature of my experiments in lymph, my results so far suggested that the lack of SIRPα-CD47 signalling in the DCs may cause over-activation of $CD103^+CD11b^+$ DCs in LP. As a consequence the last stage of

mucosal DC development ($CD103^+CD11b^+$ DCs) occurs more quickly than normal and these are then triggered to migrate to the MLNs. As this idea would seem to be at odds with the defect in $CD103^+CD11b^+$ DCs in the MLN, I reasoned that the over-activated DCs might be more susceptible to death by apoptosis after their arrival in the MLN. Annexin V staining in the MLN supported this idea, by showing an increased proportion of apoptotic DCs in SIRPα mt MLN, which was selective for the $CD103^+CD11b^+$ subset. I did attempt to determine if a similar phenomenon occurred in the LP, but these studies were inconclusive perhaps because the extensive enzymatic digests, required to isolate the cells from the LP, kill any apoptotic cells and thus remaining cells appear to be normal. Alternatively, DCs arriving in the LN are known to die rapidly in the absence of cognate T cells, possibly explaining the increased apoptosis in the MLN. Additionally CD47 is expressed on T cells and the SIRPα/CD47 axis is proposed to be involved in the DC:T cell interaction in a manner analogous to the co-stimulatory molecule:CD28 interaction (Matozaki et al., 2009). Thus inefficient interactions between $CD103^+CD11b^+$ DCs and T cells might result in the induction of apoptosis in the DCs, although I would expect the latter to also induce apoptosis in the other SIRPα-expressing migratory DCs in the MLN.

Because these results might indicate that $CD103^+CD11b^+$ DCs in the LP of SIRPα mt mice are hyper-activated, I thought it important to assess whether these animals might develop spontaneous IBD. As my initial studies in young adult mice revealed no evidence of inflammation such as increased neutrophils or monocytes, I left a cohort of SIRPα mt mice to age for 11 months. Although this experiment was only performed once and hence requires further investigation, the mice displayed no clinical signs of IBD or ill-health during this time had no evidence of inflammatory infiltrates in the SI LP. However, I found that the aged SIRPα mt mice no longer had the defect in $CD103^+CD11b^+$ DCs seen in the 6-8 week old mt mice I had used previously. This was not due to significant changes in the DC populations in aged WT mice and therefore could suggest that regulatory mechanisms may come into play to prevent continued over-activation of $CD103^+CD11b^+$ DCs in the SIRPα mt intestine. This idea remains to be explored and intriguingly, the resolution of the DC defect was specific to the intestine and MLN, as the splenic defect remained in the aged SIRPα mt mice. The reasons for this discrepancy require further investigation, but could indicate a different role for

SIRPα in the different tissues, perhaps related to the distinct DC subtypes found in these locations. It is important to note that this effect of age on the DC defect in the intestine of SIRPα mt mice may have influenced the results obtained from the experiments on pseudo-afferent intestinal lymph. For technical reasons, the MLNx procedure needed for this protocol cannot be undertaken before 6 weeks of age and the mice then have to be left at least 6 weeks to allow reanastomosis of the lymphatics before the thoracic duct can be cannulated. Thus the mice used in this study were some 6-8 weeks older than those I normally used for phenotyping, raising the possibility that these mice had already overcome the DC defect and thus might explain why the DC subsets were normal in SIRPα mt lymph. As mentioned earlier, future studies will directly compare the lymph and LP from the same mice to determine the extent of the DC defect in these animals. As this finding came towards the end of my PhD, I did not have time to determine if this result was consistent between experiments or examine the exact time frame within which the SIRPα mt mice might overcome the DC defect. This is currently under investigation by a new PhD student in the lab.

To begin to understand how the SIRPα mutation was exerting its effects on the $CD103^+CD11b^+$ DCs, I wanted to address whether the requirement for SIRPα was intrinsic to the DCs. To examine this, I generated mixed BM chimeras in which WT mice were lethally irradiated before being reconstituted with WT and SIRPα mt BM in a 50:50 ratio. This showed no apparent defect in the ability of SIRPα mt BM to reconstitute haematopoietic cells in the intestine or MLN, including the $CD103^+CD11b^+$ DCs. This was not the case in the spleen, where the defect in $CD4^+CD11b^+$ DCs found in the SIRPα mt mouse was recapitulated by SIRPα BM, confirming a previous report (Saito et al., 2010). This result further highlights the differences between the requirements for SIRPα-CD47 signalling by DCs in the spleen and intestine. When I first carried out this experiment, I interpreted the result as showing that the DC defect in the intestine and MLNs of SIRPα mt mice was not cell intrinsic, however, again this conclusion may need to be reassessed in light of the possible age-related resolution of the DC defect in SIRPα mt mice as BM used to reconstitute the irradiated mice were from 8 week old animals and the chimeric mice were then left for a further 8 weeks to allow reconstitution. Thus it is possible that the defect had already been recovered by the time these mice were examined. To investigate this further it could be useful to

generate conditional SIRPα mt mice in which the SIRPα mutation has been specifically targeted to DCs, perhaps by using a Zbtb46cre-SIRPαflox system. Alternatively BM chimeras could be generated using BM from 1-2 week old animals. However first we will investigate the time course of the DC defect to ascertain at what age the mice recover the DC defect. If it turns out that the DC defect is not cell intrinsic, it will be interesting to examine the requirements for SIRPα in the non-haematopoietic compartment and I have made straight WT into SIRPα mt and SIRPα mt into WT chimeras to examine this in the near future.

Having identified a defect in intestinal $CD103^+CD11b^+$ DCs in SIRPα mt mice, I went on to explore its consequences for T cell function. These mice had normal numbers of T_h1 and T_{Reg} cells in the LP under steady state conditions, but had a selective reduction in the proportion and number of T_h17 cells. Although previous studies have observed a reduction in T_h17 cells in the spleen, lymph nodes and intestine of SIRPα mt mice (Kanazawa et al., 2010; Matozaki et al., 2009; Okuzawa et al., 2008; Tomizawa et al., 2007), this was not related to a DC defect and therefore I thought it important to rule out the possibility that the SIRPα mt mice had an intrinsic inability to generate T_h17 cells. This was not the case, as similar numbers of T_h17 cells could be generated *in vitro* from WT and SIRPα mt naïve $CD4^+$ T cells that were stimulated with α-CD3 and α-CD28 under T_h17 cell polarising conditions.

Interestingly, my finding that a defect in $CD103^+CD11b^+$ DCs in the SIRPα mt mice correlated with reduced T_h17 cells in the steady state mucosa is supported by five recent papers (Lewis et al., 2011; Persson et al., 2013b; Satpathy et al., 2013; Schlitzer et al., 2013; Welty et al., 2013). To explore this further, I next assessed the generation of antigen-specific $CD4^+$ T cells in SIRPα mt mice *in vivo* in response to oral or systemic administration of OVA. Consistent with the normal numbers of T_{Reg} cells in the SIRPα mt LP, the animals developed systemic tolerance as assessed by measurement of antigen-specific DTH responses after feeding OVA. However, OVA-specific $CD4^+$ TcR transgenic T cells showed defective proliferative responses in the MLNs of SIRPα mt mice after feeding OVA, suggesting the initial interaction between antigen-carrying DCs and transferred T cells in the MLNs may be impaired in these animals. This could be a result of the reduced total DC pool in the MLNs of these mice or alternatively due

to a poor interaction between SIRPα on the DCs and CD47 on the T cells. Despite this, similar proportions of antigen-specific T_{Reg} and T_h1 cells developed in SIRPα mt MLNs, but there was a trend towards fewer T_h17 cells. This experiment could be further optimised by blocking output of activated T cells to the LP using FTY720 as this might have obscured any differences in T cell priming. In addition, feeding OVA alone would not be expected to induce significant differentiation of T_h17 cells. To overcome these issues, I next transferred OTII cells into mice that were then immunised with OVA, together with LPS and α-CD40 as adjuvants to deliberately drive T_h17 polarisation (Persson et al., 2013b). Furthermore, the mice received two doses of FTY720 to block T cell egress from the MLN. Under these conditions, there was a clear reduction in the clonal expansion of donor T cells and defect in the generation of T_h17 cells in the MLNs of SIRPα mt mice, while the relative proportions of T_{Reg} and T_h1 cells were increased. These results suggest that the lack of $CD103^+CD11b^+$ DCs in the MLNs of SIRPα mt mice results in reduced T_h17 cell priming. Similarly, SIRPα mt mice demonstrated a reduced ability to clear the *C. rodentium* infection and this was associated with impaired T_h17 cell differentiation in the MLN. This is consistent with previous studies suggesting that SIRPα mt mice are less susceptible to T_h17-mediated CHS and EAE (Motegi et al., 2008; Tomizawa et al., 2007).

Although consistent with a number of reports which have suggested intestinal $CD103^+CD11b^+$ DCs to be the main inducers of mucosal T_h17 responses (Lewis et al., 2011; Persson et al., 2013b; Schlitzer et al., 2013), this finding contrasts with a recent report which demonstrated that $CD103^+CD11b^+$ DCs did not directly prime T_h17 cells as MHCII expression by these cells was not required for the presence of T_h17 cells in the LP (Welty et al., 2013). Thus an alternative explanation for this result, is that instead of $CD103^+CD11b^+$ DCs priming T_h17 cells and hence there being less of these T cells due to the reduction in this DC population in SIRPα mt mice, the interaction between SIRPα-expressing DCs and CD47-expressing T cells may be impaired in these mice and hence antigen-presentation by the SIRPα-expressing DCs is impaired. As my other studies found the $CCR2^+CD103^-CD11b^+$ intestinal DCs to be the main inducers of T_h17 cells and these DCs also express SIRPα, this is a valid second hypothesis. Additionally, this would be consistent with my findings that $CD103^+CD11b^+$ DCs FACS-purified from SIRPα mt LP were equally as capable of generating T_h17 cells *in vitro* as their WT

counterparts, while the $CD103^{-}CD11b^{+}$ DCs FACS-purified from SIRPα-mice appeared to be less efficient at inducing T_h17 cells than their WT controls. Although, this experiment requires repetition, it suggests that the defect in $CD103^{+}CD11b^{+}$ DCs and T_h17 cells in SIRPα mt mice may be a combined effect of reduced T_h17 cell priming in the MLNs by $CD103^{-}CD11b^{+}$ DCs and impaired maintenance of the T_h17 cell pool in the LP by the reduced population of $CD103^{+}CD11b^{+}$ DCs. This model would also begin to explain the discrepancies I had seen with T_h17 cell and $CD103^{+}CD11b^{+}$ DC numbers in the LP following antibiotic administration. That the effect on $CD103^{+}CD11b^{+}$ DCs may not explain fully the T cell phenotype in SIRPα mt mice is supported by my findings that SIRPα mt $CD103^{+}CD11b^{+}$ DCs from the SI LP produced normal amounts of the T_h17 polarising cytokines IL6 and IL1β. Conversely, there was a decrease in the overall levels of these cytokines when total SIRPα mt DCs were used and this slightly reduced IL6 and IL1β may demonstrate that the reduction in $CD103^{+}CD11b^{+}$ DCs leads to less overall T_h17 polarising cytokines within the DC pool as hypothesised in a recent study using a CD11c-driven conditional KO of IRF4 (Persson et al., 2013b). Again, these studies need to be repeated and $CD103^{-}CD11b^{+}$ DCs particularly the $CCR2^{+}$ fraction will also be examined for their cytokine profile. Performing similar *in vivo* priming experiments to those described above in CD47KO mice could also test the requirement for a SIRPα-CD47 interaction between DCs and T cells. These mice have a similar defect in $CD103^{+}CD11b^{+}$ DCs, however the remaining DCs have functional SIRPα. While the endogenous T cells lack CD47 expression in these mice, the transferred OTII cells will express this molecule and hence if normal priming occurs following OVA and adjuvant administration, it would suggest that it is the interaction between SIRPα on the DCs and CD47 on the T cells that contributes to this T_h17 phenotype rather than the correlative reduction in $CD103^{+}CD11b^{+}$ DCs. These experiments are currently ongoing in the lab. Moreover, it will be important to perform the *in vitro* co-culture assays using DCs FACS-purified from the MLNs rather than the LP of WT or SIRPα mt mice as these are the ones involved in T cell priming.

In addition to examining the DC defect, as well as its causes and consequences, I tried to connect the $CD103^{+}CD11b^{+}$ DC defect in the SIRPα mt mice to those reported in other models. Interestingly, my results indicate that

there may be a feedback loop between SIRPα and IRF4, as the expression of *Irf4* mRNA was increased amongst $CD103^+CD11b^+$ DCs in SIRPα mt mice. However, I could find no evidence for a direct link between SIRPα and IRF4 signalling pathways in the literature and nor could I find a link between SIRPα and Notch2 signalling, despite conditional CD11c-driven KOs of both these molecules causing a reduction in the numbers of $CD103^+CD11b^+$ DCs and T_h17 cells in the LP (Lewis et al., 2011; Persson et al., 2013b; Schlitzer et al., 2013).

As DCs are also essential for IgA production in the gut (Bergtold et al., 2005; Castigli et al., 2005; Massacand et al., 2008) and T_h17 cells are also implicated in this (Hirota et al., 2013), I also examined if the defects in these populations played any part in this process by assessing total faecal IgA levels in WT and SIRPα mt mice. While no differences were observed, it will be important to examine antigen-specific IgA responses in these animals, especially as it has been reported that CD47KO mice have decreased production of IgA following oral immunisation (Westlund et al., 2011).

Finally I examined the role played by SIRPα signalling and $CD103^+CD11b^+$ DCs during DSS colitis. When I began my PhD, others had reported that CD47KO mice were protected from TNBS-induced colitis due to a failure to recruit $CD103^-$ $SIRP\alpha^+$ monocyte-derived 'DCs' (Fortin et al., 2009). However as noted earlier, these were identified as 'DCs' solely on the basis of CD11c expression and so would have included macrophages and eosinophils. In my hands, the SIRPα mutation had no effects on disease progression or clinical score during DSS colitis. This may be due to the differences between these two models of IBD, but may also reflect a role for an additional ligand for CD47 such as surfactant proteins (Akiyama et al., 2002; Fournier et al., 2012; Gardai et al., 2003; Janssen et al., 2008; Madsen et al., 2000). Alternatively, the extracellular SIRPα region, which is still present in SIRPα mt mice, although expressed at lower levels, may enable active CD47 signalling which is required for protection from colitis. Indeed while preparing this thesis, I found CD47KO mice to be less susceptible to DSS colitis that WT controls.

My findings that SIRPα plays an important role in the activation of certain DCs and the generation of T_h17 responses may have therapeutic implications.

Indeed it has been shown ligating SIRPα with a CD47-Fc fusion protein can dampen IL1β and TNFα production (Baba et al., 2013). I did obtain CD47-Fc fusion protein to study this, but as it is a human homolog it did not bind murine SIRPα and these studies were unsuccessful. We are currently devising methods and applying for ethical approval to investigate this *in vitro* with human samples.

10.7.1 Proposed Model for the Role of SIRPα Signalling

My results suggest that SIRPα signalling may have a number of effects on intestinal DCs, the overall results culminating in a selective defect in the $CD103^+CD11b^+$ subset. Firstly, it appears to control their development, with $CD103^+CD11b^+$ DCs appearing in the mucosa more rapidly when pre-DCs lack the ability to signal via SIRPα. This suggests that SIRPα on arriving pre-DCs may interact with CD47 in the mucosa, acting as a brake on the differentiation of $CD103^+CD11b^+$ DCs (Fig. 10.1). Although it is possible that SIRPα ligands other than CD47 might be involved in this process, this seems unlikely, as the defect in $CD103^+CD11b^+$ DCs is phenocopied in CD47KO mice. The CD47-expressing cell responsible for the local ligation of SIRPα is unclear and given the complex strategies which will be needed to identify the relevant cell amongst the wide range that expresses CD47, this is a major challenge for the future.

The idea that SIRPα normally acts as an inhibitory factor for a specific subset of intestinal DCs is supported by the fact that those $CD103^+CD11b^+$ DCs that appear in SIRPα mutant mice appear to be more activated than WT DCs, as indicated by their expression of higher levels of CD86. Although not proven, it seems likely this role of SIRPα requires direct interaction with yet to be identified $CD47^+$ cells in the mucosa. If this increased activation of $CD103^+CD11b^+$ DCs can be confirmed, I hypothesise that it could be at least part of the explanation for the decreased population of $CD103^+CD11b^+$ DCs in the SIRPα mt LP, as it may lead to more rapid emigration of the $CD103^+CD11b^+$ DCs to the MLN and/or enhanced apoptosis of $CD103^+CD11b^+$ DCs in SIRPα mt intestine. As discussed above, although I tried to examine both these possibilities, further investigation is required before any conclusions can be drawn. However, despite being unable to obtain meaningful results from apoptosis assays using LP DCs, I was able to confirm that $CD103^+CD11b^+$ DCs from SIRPα mt MLNs are indeed more apoptotic than WT

counterparts. This increased susceptibility to apoptosis has also been suggested to control the $CD11b^+$ DC defect in the spleen (Saito et al., 2010) and more recently, the lack of IRF4 signalling in CD11c-expressing cells has also been suggested to cause the apoptosis of $CD103^+CD11b^+$ DCs (Persson et al., 2013b).

A universal feature of all the recent studies including my own in which there is a selective reduction in $CD103^+CD11b^+$ DCs is poor priming of T_h17 cells in the MLN and a smaller than normal population of T_h17 cells in steady state LP (Fig. 10.1). One possibility is that this reflects a specific role for the SIRPα - CD47 axis in co-stimulation of T_h17 cell differentiation, as was suggested by early studies of SIRPα function on DCs (Matozaki et al., 2009). My experiments attempting to explore these issues were relatively inconclusive, although my findings that the loss of $CD103^+CD11b^+$ DCs reduced IL6 production by the total intestinal DC pool are consistent with similar conclusions from CD11c-cre-IRF4 KO mice (Persson et al., 2013b). Together with the fact that the remaining $CD103^+CD11b^+$ DCs appear to function normally in both cases, this could suggest that the lower levels of T_h17 priming may simply reflect the lower numbers of the DCs, rather than a role for SIRPα in DC function. This idea would also be consistent with a very recent paper which shows that selective deletion of $CD103^+CD11b^+$ DCs in the LP by targeting them with diphtheria toxin A driven by the human langerin promoter also results in a reduced population of LP T_h17 cells (Welty et al., 2013). Interestingly however, this study also suggested that cognate interactions between $CD103^+CD11b^+$ DCs and T_h17 were not involved in the link between these cells, as the presence of T_h17 cells in the LP did not require MHCII expression on the $CD103^+CD11b^+$ DCs (Welty et al., 2013). Thus is it is possible that the absence of $CD103^+CD11b^+$ DCs influences the behaviour of other cells involved in priming of T_h17 cells, perhaps acting as sources of polarizing cytokines such as IL6 or IL23, or by providing a depot for antigen. Alternatively, the lack of SIRPα signalling may directly affect the function of the other SIRPα expressing DCs such as the $CCR2^+CD103^-CD11b^+$ DCs, which I have demonstrated to be the most potent inducers of mucosal T_h17 responses. Further studies are required to explore these issues.

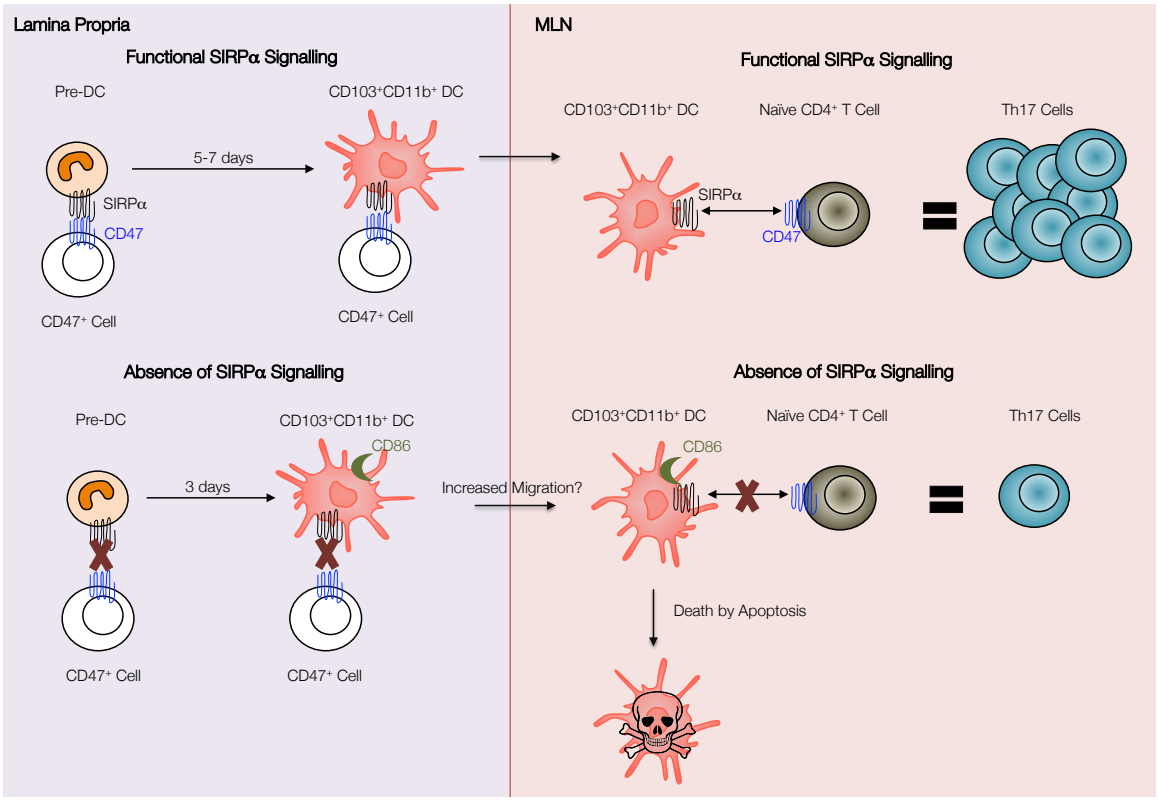

Figure 10.1: Working model for the role of the SIRPα-CD47 axis in CD103$^+$CD11b$^+$ DC homeostasis and function

10.8 An Overview of Intestinal DC Subsets

The results of my project have shown that DCs in the intestinal mucosa are much more heterogeneous than previously thought at least at the phenotypic level. An important question raised by this study is whether the intestinal DC subsets I identified are distinct populations or rather simply represent different maturation states of the same lineage. My findings confirm other work indicating that the CD103$^+$CD11b$^-$CD8α$^+$ DCs are a distinct population from the CD11b$^+$ DCs, having different behaviour and being dependent upon distinct transcription factors (Edelson et al., 2011; Schraml et al., 2013), as mentioned above, this raises the important question of distinct precursor subsets giving rise to these distinct DC lineages and this will be a focus of future studies, potentially using the barcoding system recently described by Naik and colleagues, in which the fate of transferred progenitors can be tracked at the single cell level (Naik et al., 2013).

The relationship between the CD103$^+$ and CD103$^-$ subsets of CD11b$^+$ DCs is less well defined, as is the position of the minor CD103$^-$CD11b$^-$ DCs in any

developmental scheme. While a recent report has suggested the presence of $CD103^-CD11b^-$ DCs in LP preparations is due to contamination by ILFs, these DCs were not completely absent from LP digests from RORγt-deficient animals (Cerovic et al., 2013), suggesting that a proportion may be also present in the LP. These cells are heterogeneous for many of the markers I examined, thus they may represent a mixture of follicle-derived and genuine mucosal DCs. Interestingly, they were the first to appear in the LP following adoptive transfer of pre-DCs. This could suggest that they are an intermediary phenotype in DC development and this may also explain their heterogeneity, as a proportion express markers consistent with the $CD103^+CD11b^-$ lineage, including CD8α and XCR1 (Bachem et al., 2012; Crozat et al., 2011; Edelson et al., 2010), while others express SIRPα, which is typically associated with $CD11b^+$ DCs (Persson et al., 2013b; Schlitzer et al., 2013). It could also be argued that the other subsets develop from a second wave of pre-DCs which take longer to enter the mucosa than the $CD103^-CD11b^-$ DC precursors, but this seems unlikely as I could not find donor cells in the bloodstream 24hours after injection, whereas the $CD103^-CD11b^+$ and $CD103^+CD11b^-$ DC subsets were not detected in the mucosa until days 3-5 post transfer. Intestinal $CD103^+CD11b^+$ DCs were found in the mucosa even later, with these cells not appearing until days 5-7 after transfer of pre-DCs, providing indirect evidence that a lineage relationship might exist between the $CD103^-CD11b^+$ and $CD103^+CD11b^+$ DC subsets. Additionally, these $CD103^+CD11b^+$ DCs do not appear in the intestine until day 7 of life while the other populations are present in neonatal animals from birth. While I was finalising this discussion, I received preliminary data from my microarray analyses, which demonstrated that only 127 genes are differentially regulated between these subsets, including CD103 and CCR2. This high degree of similarity between the two subsets further supports the hypothesis that these may be developmentally related. A recent report that loss of IRF4 on CD11c-expressing cells affects both the $CD103^+CD11b^+$ and $CD103^-CD11b^+$ DCs in the MLN also supports such a relationship (Persson et al., 2013b). Further evidence for a developmental link between these two $CD11b^+$ DC subsets comes from my functional studies which suggest both may be involved in the generation of mucosal T_h17 responses, albeit with the CD103-expressing $CD11b^+$ DCs also inducing $FoxP3^+$ T_{Reg} cells. Perhaps along this differentiation process the cells are imprinted with a tolerogenic phenotype, explaining their specificity in the gut, which is continuously exposed to a number of harmless antigens?

While there are a number of lines of evidence that suggest a developmental relationship may exist between the $CD103^-$ and $CD103^+$ $CD11b^+$ DCs, evidence also exists to the contrary. The main point against such a relationship is that all four mucosal DC populations are capable of migrating to the MLN, being present both in intestinal lymph (Cerovic et al., 2013) and amongst $MHCII^{hi}$ DCs in the MLN suggesting that at least some of them are terminally differentiated and ready to prime naïve T cells. Additional evidence against such a linear relationship comes from the studies of the $CCR2^{-/-}$ mice which have a selective reduction in $CD103^-CD11b^+$ DCs with $CD103^+CD11b^+$ DCs being unaffected. My BrdU studies also might argue against an ontogenical relationship between the subsets, as all the populations showed parallel uptake of BrdU at both 3 hours and 3 days after BrdU administration. However, this could reflect the rapid kinetics of DCs, meaning that the long term feeding protocol would achieve maximal labelling quickly and hence any differences at earlier points may be missed. This could potentially be examined by analysing a number of intermediate time points such as after 12 hours of feeding. However, the definitive proof that $CD103^-CD11b^+$ DCs could become $CD103^+CD11b^+$ DCs would need to involve transfer of $CD103^-CD11b^+$ DCs, which would then need to acquire CD103 *in vivo*. Such an experiment is technically challenging as it is unclear if these short-lived DCs would travel to the intestine and if enough cells could be transferred to allow a significant population to be identified in the LP enabling assessment of CD103 expression. Alternatively, the presence of a developmental relationship could be assessed using a novel fate mapping system in which a gene could be identified that is expressed by $CD103^-$ $CD11b^+$ DCs but not by pre-DCs (or earlier progenitors) and $CD103^+CD11b^+$ DCs. With such a gene, a fate mapping mouse could be generated using Cre recombinase-mediated excision with a ROSA26-reporter mouse (Luche et al., 2007; Mao et al., 2001). Thus any cell that has once expressed the gene will be labelled and hence any labelled $CD103^+CD11b^+$ DCs will have come through a $CD103^-CD11b^+$ intermediate step. This approach is obviously limited by our identification of a suitable gene, perhaps my microarray analyses of the distinct subsets coupled with previously analyses of pre-DCs might allow for such a gene to be identified. However, fate-mapping mice are not devoid of technical challenges, as these often have issues with the labelling efficiencies. This was recently demonstrated in the DNGR-1 fate mapping mouse where $CD11b^+$ DCs were only 50% labelled compared to the $CD11b^-$ DCs which were almost 100% labelled, despite progenitors being uniformly $DNGR\text{-}1^+$ (Schraml et al., 2013).

My identification of $CCR2^-$ and $CCR2^+$ fractions of $CD103^-CD11b^+$ DCs adds a further level of complexity to this maturation hypothesis. While pre-DCs in the BM are heterogeneous for CCR2, competitive adoptive transfers of pre-DCs from WT and $CCR2^{-/-}$ mice, showed that the $CCR2^{-/-}$ progenitors were outcompeted by their WT counterparts in generating all DC subsets, despite there only being a reduction in the $CD103^-CD11b^+$ DCs in the $CCR2^{-/-}$ mice LP. My functional data may shed some light on the relationship. The $CCR2^+$ fraction of $CD103^-CD11b^+$ DCs is more pro-inflammatory, being the most efficient at T_h17 cell priming. Although both the $CCR2^-CD103^-CD11b^+$ and $CD103^+CD11b^+$ DCs also appear to be capable priming T_h17 cells, they were less efficient than the $CCR2^+CD103^-CD11b^+$ DCs and recent data suggest that the $CD103^+CD11b^+$ DCs are in fact dispensable for T_h17 cell priming (Welty et al., 2013). It is possible that the DC progenitors enter the gut and first develop into $CCR2^+CD103^-CD11b^+$ pro-inflammatory DCs, these then lose CCR2 expression and acquire CD103 expression, as well as the ability to induce T_{Reg} cells. However, this hypothesis is purely speculative and experiments will need to be designed as described above to directly examine this.

While CCR2 and CD103 may be useful markers for delineating the differentiation process, a number of questions remain, for example little is known about the role of these markers. CCR2 is known to be involved in monocyte egress from the BM (Serbina and Pamer, 2006), however the $CCR2^+$ DCs are not monocyte-derived and my results to date suggest that CCR2 is not required on pre-DCs for their egress to the blood. While my data suggest CCR2 on pre-DCs may be involved in their ability to access tissues, this remains to be verified. Experiments examining the effects of exogenous CCL2 on the DC subsets could help to elucidate the role of this receptor and this will be examined in the future. Similarly the role of CD103 remains unclear. CD103 as it is expressed on T_{Reg} cells was originally thought to contribute to their function. Although demonstrating it was dispensable for this, Annacker and colleagues reported its presence on a CD11c-expressing cell and showed that these cells were required for protection from T-cell mediated colitis (Annacker et al., 2005). However, this probably does not require CD103 itself. Additionally although $CD103^+$ DCs are reported to drive the expression of the gut homing receptor, CCR9, on interacting naïve T cells and induce $FoxP3^+$ T_{Reg} cells (Coombes et al., 2007; Johansson-Lindbom et al., 2005; Siddiqui and Powrie, 2008; Sun et al., 2007), CD103 also appears dispensable for

this (Jaensson et al., 2008). Interestingly and consistent with $CD103^+$ DCs being more tolerogenic, it has recently been shown that CD103 is also dispensable on DCs for immunity against helminth infection (Mullaly et al., 2011).

Another important question is whether once the DCs acquire CD103 and their seemingly tolerogenic phenotype can they revert to their previous more pro-inflammatory phenotype if this is so desired? It has been previously been reported that intestinal inflammation can re-programme the tolerogenic nature of MLN $CD103^+$ DCs (Laffont et al., 2010) and thus it is possible that while the default property of steady state $CD103^+CD11b^+$ DCs is to drive $FoxP3^+$ T_{Reg} cell priming, exposure to pathogens can cause them to revert to a more pro-inflammatory phenotype inducing T_h17 cells (Satpathy et al., 2013). This would be consistent with a recent study by Kinnebrew and co-workers, which showed that following stimulation with the TLR5 agonist the $CD103^+CD11b^+$ DCs could be induced to produce IL23p19 (Kinnebrew et al., 2012). Single cell transfers, mature DC transfers, fate-mapping, transcriptome studies and *in vitro* cultures with various microbial-derived such as TLR ligands would help to investigate this in the future.

Regardless of whether a developmental relationship exists it will be interesting to elucidate the signals involved in the differentiation of $CD103^+CD11b^+$ DCs and why these are specific to the intestine in the steady state, but can also be found in the lung during inflammation (Guilliams et al., 2013a). Also it remains unclear if the same signal induces CD103 expression on both $CD11b^-$ and $CD11b^+$ DCs. It is possible that the microbiota are involved in the development of $CD103^+CD11b^+$ DCs, although then one might expect there to be more $CD103^+CD11b^+$ DCs in the colon given the higher microbial burden. Additionally, studies in germ-free animals, although inaccurately identifying intestinal MPs, have not reported on the absence of CD103-expressing DCs (Rivollier et al., 2012). As these studies did not discriminate between $CD11b^+$ and $CD11b^-$ $CD103^+$ DCs based on the gating strategies used, further experiments are required to directly investigate this possibility. Perhaps specific bacterial strains are involved in the generation of $CD103^+CD11b^+$ DCs. This may explain why administration of antibiotics appeared to affect their prevalence in the SI LP and why new-born mice lack these DCs. Another candidate is CSF-2 (Greter et al., 2012), but this also seems to affect $CD103^+CD11b^-$ DCs in other tissues and my studies using CSF-2RKO or exogenous administration of CSF-2 were inconclusive. Furthermore, as

discussed above my preliminary data have found CSF-2 levels to be quite low in the intestine in comparison to other tissues, such as the lung where $CD103^+CD11b^+$ DCs are usually absent. A recent study has suggested that retinoic acid may be the signal involved in $CD103^+CD11b^+$ DC development in the gut (Klebanoff et al., 2013), However, this report is in direct contrast to previously published studies which suggested RA to be dispensable for the phenotype of gut-derived DCs in the MLN (Jaensson-Gyllenbäck et al., 2011) and thus this requires further examination. Finally, my results using the SIRPα mt mice suggest a role for the SIRPα-CD47 axis in the generation of $CD103^+CD11b^+$ DCs, although whether this can be manipulated to generate or prevent the generation of $CD103^+CD11b^+$ DCs remains to be investigated.

Identifying the localisation of the distinct DC populations in the mucosa may help to delineate the factors involved in the generation of $CD103^+CD11b^+$ DCs, as it is possible that their phenotype and function is controlled by their location. It takes 8 fluorescent labels to identify accurately the different DC populations in the SI LP by flow cytometry, and thus as currently there has only been one report of immuno-histochemistry with this many fluorochromes (Gerner et al., 2012), this represents a long-term goal for the future. Interestingly, since completing my project, I have found that the $CD103^+$ DC subsets can also be isolated from the epithelial fraction of mucosal isolates. This is particularly the case for $CD103^+CD11b^+$ DCs, while $CD103^-$ DCs could not be found in these isolates. As the ligand for CD103 is E-cadherin, which is expressed by epithelial cells, this could suggest a preferential association between these cells and perhaps CD103 acts to keep the DCs in this location. However, the reasons for the presence of DCs in this location and hence the specific need for $CD103^+CD11b^+$ DCs in the intestine remains unclear. It is possible that the epithelial cell interaction might be responsible for the terminal differentiation of $CD103^+CD11b^+$ DCs as they produce a number of immunomodulatory molecules as discussed in Chapter 1. The specific compounds that may be involved however, requires direct investigation.

10.8.1 A Proposed Scheme

Taken together, it is clear that no definitive conclusions can be drawn regarding the inter-relationship between DC subsets at this time, largely because the techniques are not yet available to complete the analysis required to specifically address these issues. However based on the evidence available from my thesis and elsewhere a tentative scheme could be proposed, as shown in Fig. 10.2. In this scheme, pre-DCs enter the mucosa and first acquire CD11c and MHCII expression to become $CD103^{-}CD11b^{-}$ DCs. Following CD11c and MHCII acquisition, the DCs begin to divide *in situ* and continue to do so throughout their development. These may then subsequently acquire either CD11b or CD103 to become $CD103^{-}CD11b^{+}$ or $CD103^{+}CD11b^{-}$ DCs respectively. Alternatively, although not shown in the scheme, these phenotypes may develop from the pre-DCs without a $CD103^{-}CD11b^{-}$ intermediate step, as these DCs may be restricted to the ILFs and be contaminants of the LP digests as previously described (Cerovic et al., 2013). The next stage of differentiation sees the development of $CD103^{+}CD11b^{+}$ DCs presumably from the closely related $CD103^{-}CD11b^{+}$ DCs. This appears to be regulated through the SIRPα-CD47 axis, with more efficient generation of $CD103^{+}CD11b^{+}$ DCs in the absence of SIRPα signalling. Again, while not shown in the scheme, the development of $CD103^{+}CD11b^{+}$ DCs may occur independently of $CD103^{-}CD11b^{+}$ DCs.

As pre-DCs are heterogeneous for CCR2 expression, the $CCR2^{-}$ and $CCR2^{+}$ pre-DCs may preferentially generate $CCR2^{-}$ and $CCR2^{+}$ $CD103^{-}CD11b^{-}$ and $CCR2^{-}$ and $CCR2^{+}$ $CD103^{-}CD11b^{+}$ DCs respectively. The relationship between $CCR2^{-}$ and $CCR2^{+}$ pre-DCs and maturing DCs remains to be examined, but the $CCR2^{+}$ DCs may subsequently downregulate CCR2 to give rise to $CCR2^{-}$ counterparts. The $CD103^{+}CD11b^{+}$ DCs then develop from the $CD103^{-}CD11b^{+}$ DCs by downregulating CCR2 and upregulating CD103 expression also acquiring a more tolerogenic phenotype in the process. Additionally at each stage of differentiation some DCs may migrate to the MLN if they receive the correct signals, which remain to be identified. These could begin to be elucidated by examining the transcriptional differences between DCs in the LP, lymph and MLN.

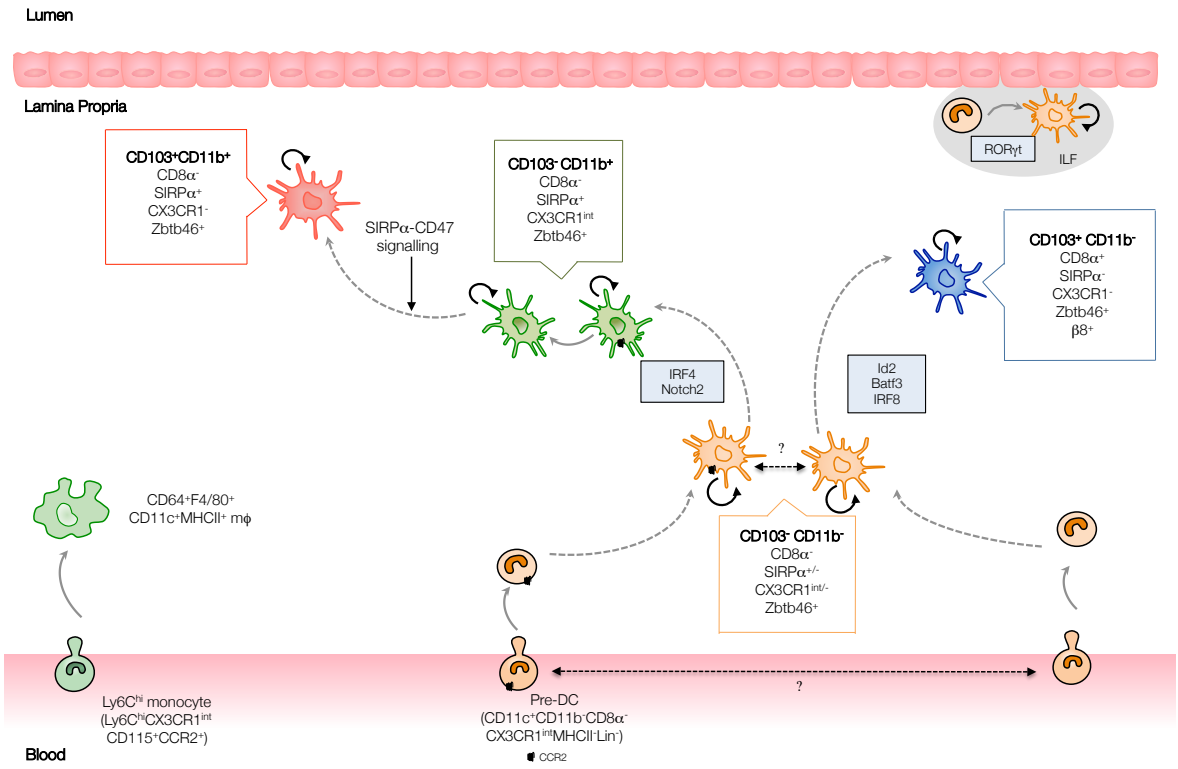

Figure 10.2: Inter-relationship between DC subsets

10.9 Concluding Remarks

While these studies have increased our understanding of intestinal DCs and their functions, a number of questions remain to be addressed. From my extensive phenotyping analysis, it is now clear that there are multiple populations of genuine DCs in the gut, including previously undescribed $CD103^-$ DCs, the presence of which has recently been confirmed in two separate studies while I was preparing this thesis (Schlitzer et al., 2013; Schraml et al., 2013). Interestingly I have uncovered a novel role for CCR2 in intestinal DCs with CCR2 expression delineating functionally distinct subsets. Furthermore, I have shown the SIRPα-CD47 axis to be involved in the development and maturation of $CD103^+CD11b^+$ DCs. As discussed above, one of the main questions arising from these studies is the nature of the relationship between the DCs subsets. If we can identify a gene from our microarray analyses that is expressed exclusively in the $CD103^-CD11b^+$ DCs but turned off in the $CD103^+CD11b^+$ DCs, it may be possible to generate a fate-mapping mouse system to directly investigate such a relationship.

In addition to the outstanding questions surrounding DC ontogeny, the role for SIRPα remains to be elucidated. My studies implicate the SIRPα-CD47 axis in the development of $CD103^+CD11b^+$ DCs, but how it functions in this regard remains to be seen. Moreover considerable work is required to elucidate if the SIRPα mutation affects the function of the $CD103^-CD11b^+$ DCs or if the T_h17 defect is a consequence of the reduced population of $CD103^+CD11b^+$ DCs seen in SIRPα mt mice. The ageing phenomenon in these mice also requires further investigation and this is currently underway in the laboratory.

The overall importance of my findings is that we can now accurately discriminate $CD103^-$ and $CD103^+$ DCs from other intestinal MPs and so we can begin to address their selective roles in regulating immune homeostasis. While I have begun to elucidate the functional specialisations of each DC population in the steady state gut and during *C. rodentium* infection, future studies can focus on identifying their functions in disease states. Furthermore, as I have shown in collaboration with Dr. Simon Milling's group that it might be possible to extrapolate these findings to the human gut and it would be interesting to compare these cells in healthy humans and in patients with IBD. As my findings suggest that the

SIRPα-CD47 axis may regulate at least one of these DC populations, future work could focus on targeting this pathway to enhance or retard $CD103^+CD11b^+$ DC development as appropriate in various disease settings. Given their apparent dual ability to induce T_{Reg} and T_h17 responses, manipulation of these DCs may be beneficial in both the development of oral vaccines and IBD therapeutics. As targeting SIRPα through the use of CD47-Fc fusion proteins has already been reported (Baba et al., 2013), this may be a viable therapeutic strategy in the near future.

References

Abbas, A.K., Murphy, K.M., and Sher, A. (1996). Functional diversity of helper T lymphocytes. Nature *383*, 787–793.

Abt, M.C., Osborne, L.C., Monticelli, L.A., Doering, T.A., Alenghat, T., Sonnenberg, G.F., Paley, M.A., Antenus, M., Williams, K.L., Erikson, J., et al. (2012). Commensal bacteria calibrate the activation threshold of innate antiviral immunity. Immunity *37*, 158–170.

Adams, S., van der Laan, L.J., Vernon-Wilson, E., Renardel de Lavalette, C., Döpp, E.A., Dijkstra, C.D., Simmons, D.L., and van den Berg, T.K. (1998). Signal-regulatory protein is selectively expressed by myeloid and neuronal cells. J Immunol *161*, 1853–1859.

Agace, W.W. (2008). T-cell recruitment to the intestinal mucosa. Trends Immunol. *29*, 514–522.

Agace, W.W., and Persson, E.K. (2012). How vitamin A metabolizing dendritic cells are generated in the gut mucosa. Trends Immunol. *33*, 42–48.

Agarwal, S., and Rao, A. (1998). Modulation of chromatin structure regulates cytokine gene expression during T cell differentiation. Immunity *9*, 765–775.

Aggarwal, S. (2002). Interleukin-23 Promotes a Distinct CD4 T Cell Activation State Characterized by the Production of Interleukin-17. Journal of Biological Chemistry *278*, 1910–1914.

Akashi, K., Traver, D., Miyamoto, T., and Weissman, I.L. (2000). A clonogenic common myeloid progenitor that gives rise to all myeloid lineages. Nature *404*, 193–197.

Akiyama, J., Hoffman, A., Brown, C., Allen, L., Edmondson, J., Poulain, F., and Hawgood, S. (2002). Tissue distribution of surfactant proteins A and D in the mouse. J. Histochem. Cytochem. *50*, 993–996.

Alblas, J., Honing, H., de Lavalette, C., Brown, M., Dijkstra, C., and van den Berg, T. (2005). Signal regulatory protein alpha ligation induces macrophage nitric oxide production through JAK/STAT- and phosphatidylinositol 3-kinase/Rac1/NAPDH oxidase/H2O2-dependent pathways. Mol Cell Biol *25*, 7181–7192.

Aliberti, J. (2002). Essential role for ICSBP in the in vivo development of murine CD8alpha + dendritic cells. Blood *101*, 305–310.

Allakhverdi, Z., Comeau, M.R., Jessup, H.K., Yoon, B.-R.P., Brewer, A., Chartier, S., Paquette, N., Ziegler, S.F., Sarfati, M., and Delespesse, G. (2007). Thymic stromal lymphopoietin is released by human epithelial cells in response to microbes, trauma, or inflammation and potently activates mast cells. J Exp Med *204*, 253–258.

Alpan, O., Rudomen, G., and Matzinger, P. (2001). The role of dendritic cells, B cells, and M cells in gut-oriented immune responses. J Immunol *166*, 4843–4852.

Anjuère, F., Martín, P., Ferrero, I., Fraga, M.L., del Hoyo, G.M., Wright, N., and Ardavín, C. (1999). Definition of dendritic cell subpopulations present in the spleen, Peyer's patches, lymph nodes, and skin of the mouse. Blood *93*, 590–598.

Anjuère, F., Luci, C., Lebens, M., Rousseau, D., Hervouet, C., Milon, G., Holmgren, J., Ardavin, C., and Czerkinsky, C. (2004). In vivo adjuvant-induced mobilization and maturation of gut dendritic cells after oral administration of cholera toxin. J Immunol *173*, 5103–5111.

Annacker, O., Coombes, J.L., Malmstrom, V., Uhlig, H.H., Bourne, T., Johansson-Lindbom, B., Agace, W.W., Parker, C.M., and Powrie, F. (2005). Essential role for CD103 in the T cell-mediated regulation of experimental colitis. J Exp Med *202*, 1051–1061.

Annes, J.P., Munger, J.S., and Rifkin, D.B. (2003). Making sense of latent TGFbeta activation. Journal of Cell Science *116*, 217–224.

Artis, D., Humphreys, N.E., Potten, C.S., Wagner, N., Muller, W., McDermott, J.R., Grencis, R.K., and Else, K.J. (2000). Beta7 integrin-deficient mice: delayed leukocyte recruitment and attenuated protective immunity in the small intestine during enteric helminth infection. Eur J Immunol *30*, 1656–1664.

Auffray, C., Fogg, D.K., Narni-Mancinelli, E., Senechal, B., Trouillet, C., Saederup, N., Leemput, J., Bigot, K., Campisi, L., Abitbol, M., et al. (2009). CX3CR1+ CD115+ CD135+ common macrophage/DC precursors and the role of CX3CR1 in their response to inflammation. J Exp Med. *206*, 595–606.

Axelsson, L.G., Landström, E., Goldschmidt, T.J., Grönberg, A., and Bylund-Fellenius, A.C. (1996). Dextran sulfate sodium (DSS) induced experimental colitis in immunodeficient mice: effects in CD4(+) -cell depleted, athymic and NK-cell depleted SCID mice. Inflamm. Res. *45*, 181–191.

Baba, N., Samson, S., Bourdet-Sicard, R., Rubio, M., and Sarfati, M. (2008). Commensal bacteria trigger a full dendritic cell maturation program that promotes the expansion of non-Tr1 suppressor T cells. J. Leukoc. Biol. *84*, 468–476.

Baba, N., Van, V.Q., Wakahara, K., Rubio, M., Fortin, G., Panzini, B., Soucy, G., Wassef, R., Richard, C., Tamaz, R., et al. (2013). CD47 fusion protein targets CD172a+ cells in Crohn's disease and dampens the production of IL-1β and TNF. J Exp Med *210,* 1251-1263.

Bachem, A., Güttler, S., Hartung, E., Ebstein, F., Schaefer, M., Tannert, A., Salama, A., Movassaghi, K., Opitz, C., Mages, H.W., et al. (2010). Superior antigen cross-presentation and XCR1 expression define human CD11c+CD141+ cells as homologues of mouse CD8+ dendritic cells. J Exp Med *207*, 1273–1281.

Bachem, A., Hartung, E., Güttler, S., Mora, A., Zhou, X., Hegemann, A., Plantinga, M., Mazzini, E., Stoitzner, P., Gurka, S., et al. (2012). Expression of XCR1 Characterizes the Batf3-Dependent Lineage of Dendritic Cells Capable of Antigen Cross-Presentation. Front Immunol *3*, 214.

Bain, C.C., Scott, C.L., Uronen-Hansson, H., Gudjonsson, S., Jansson, O., Grip, O., Guilliams, M., Malissen, B., Agace, W.W., and Mowat, A.M. (2013). Resident and pro-inflammatory macrophages in the colon represent alternative context-dependent fates of the same Ly6Chi monocyte precursors. Mucosal Immunology *6*, 498–510.

Bain, C.C., and Mowat, A.M. (2012). CD200 receptor and macrophage function in the intestine. Immunobiology *217*, 643–651.

Bajaña, S., Roach, K., Turner, S., Paul, J., and Kovats, S. (2012). IRF4 promotes cutaneous dendritic cell migration to lymph nodes during homeostasis and inflammation. The Journal of Immunology *189*, 3368–3377.

Banchereau, J., and Steinman, R.M. (1998). Dendritic cells and the control of immunity. Nature *392*, 245–252.

Barclay, A.N., and Brown, M.H. (2006). The SIRP family of receptors and immune regulation. Nat Rev Immunol *6*, 457–464.

Barnden, M.J., Allison, J., Heath, W.R., and Carbone, F.R. (1998). Defective TCR expression in transgenic mice constructed using cDNA-based alpha- and beta-chain genes under the control of heterologous regulatory elements. Immunol. Cell Biol. *76*, 34–40.

Baumgart, D.C., and Sandborn, W.J. (2007). Inflammatory bowel disease: clinical aspects and established and evolving therapies. The Lancet. *369,* 1641-1657.

Bedoui, S., Whitney, P.G., Waithman, J., Eidsmo, L., Wakim, L., Caminschi, I., Allan, R.S., Wojtasiak, M., Shortman, K., Carbone, F.R., et al. (2009). Cross-presentation of viral and self antigens by skin-derived CD103+ dendritic cells. Nat Immunol *10*, 488–495.

Beitnes, A.-C.R., Ráki, M., Lundin, K.E.A., Jahnsen, J., Sollid, L.M., and Jahnsen, F.L. (2011). Density of CD163+ CD11c+ dendritic cells increases and CD103+ dendritic cells decreases in the coeliac lesion. Scand J Immunol *74*, 186–194.

Belladonna, M.L., Grohmann, U., Guidetti, P., Volpi, C., Bianchi, R., Fioretti, M.C., Schwarcz, R., Fallarino, F., and Puccetti, P. (2006). Kynurenine pathway enzymes in dendritic cells initiate tolerogenesis in the absence of functional IDO. J Immunol *177*, 130–137.

Bellinger, D.L., Lorton, D., Brouxhon, S., Felten, S., and Felten, D.L. (1996). The significance of vasoactive intestinal polypeptide (VIP) in immunomodulation. Adv. Neuroimmunol. *6*, 5–27.

Bereswill, S., Muñoz, M., Fischer, A., Plickert, R., Haag, L.-M., Otto, B., Kühl, A.A., Loddenkemper, C., Göbel, U.B., and Heimesaat, M.M. (2010). Anti-inflammatory effects of resveratrol, curcumin and simvastatin in acute small intestinal inflammation. PLoS ONE *5*, e15099.

Bergtold, A., Desai, D.D., Gavhane, A., and Clynes, R. (2005). Cell surface recycling of internalized antigen permits dendritic cell priming of B cells. Immunity. *23,* 503-514.

Berlin, C., Berg, E.L., Briskin, M.J., Andrew, D.P., Kilshaw, P.J., Holzmann, B., Weissman, I.L., Hamann, A., and Butcher, E.C. (1993). Alpha 4 beta 7 integrin mediates lymphocyte binding to the mucosal vascular addressin MAdCAM-1. Cell *74*, 185–195.

Bettelli, E., Carrier, Y., Gao, W., Korn, T., Strom, T.B., Oukka, M., Weiner, H.L., and Kuchroo, V.K. (2006). Reciprocal developmental pathways for the generation of pathogenic effector TH17 and regulatory T cells. Nature *441*, 235–238.

Bevan, M.J. (1995). Antigen presentation to cytotoxic T lymphocytes in vivo. J Exp Med *182*, 639–641.

Bhat, P.V. (1998). Retinal dehydrogenase gene expression in stomach and small intestine of rats during postnatal development and in vitamin A deficiency. FEBS Lett. *426*, 260–262.

Bimczok, D., Sowa, E.N., Faber-Zuschratter, H., Pabst, R., and Rothkötter, H.-J. (2005). Site-specific expression of CD11b and SIRPalpha (CD172a) on dendritic cells: implications for their migration patterns in the gut immune system. Eur J Immunol *35*, 1418–1427.

Birnberg, T., Bar-On, L., Sapoznikov, A., Caton, M.L., Cervantes-Barragán, L., Makia, D., Krauthgamer, R., Brenner, O., Ludewig, B., Brockschnieder, D., et al. (2008). Lack of conventional dendritic cells is compatible with normal development and T cell homeostasis, but causes myeloid proliferative syndrome. Immunity *29*, 986–997.

Björck, P. (2001). Isolation and characterization of plasmacytoid dendritic cells from Flt3

ligand and granulocyte-macrophage colony-stimulating factor-treated mice. Blood *98*, 3520–3526.

Bogdan, C. (2001). Nitric oxide and the immune response. Nat Immunol *2*, 907–916.

Bogiatzi, S.I., Fernandez, I., and Bichet, J.C. (2007). Cutting edge: proinflammatory and Th2 cytokines synergize to induce thymic stromal lymphopoietin production by human skin keratinocytes. J Immunol. *178,* 3373-3377.

Bogunovic, M., Ginhoux, F., Helft, J., Shang, L., Hashimoto, D., Greter, M., Liu, K., Jakubzick, C., Ingersoll, M.A., Leboeuf, M., et al. (2009). Origin of the lamina propria dendritic cell network. Immunity *31*, 513–525.

Bonasio, R., Scimone, M.L., Schaerli, P., Grabie, N., Lichtman, A.H., and Andrian, von, U.H. (2006). Clonal deletion of thymocytes by circulating dendritic cells homing to the thymus. Nat Immunol *7*, 1092–1100.

Bonifaz, L., Bonnyay, D., Mahnke, K., Rivera, M., Nussenzweig, M.C., and Steinman, R.M. (2002). Efficient targeting of protein antigen to the dendritic cell receptor DEC-205 in the steady state leads to antigen presentation on major histocompatibility complex class I products and peripheral CD8+ T cell tolerance. J Exp Med *196*, 1627–1638.

Boring, L., Gosling, J., Chensue, S.W., Kunkel, S.L., Farese, R.V., Broxmeyer, H.E., and Charo, I.F. (1997). Impaired monocyte migration and reduced type 1 (Th1) cytokine responses in C-C chemokine receptor 2 knockout mice. J Clin Invest *100*, 2552–2561.

Bowman, E.P., Kuklin, N.A., Youngman, K.R., Lazarus, N.H., Kunkel, E.J., Pan, J., Greenberg, H.B., and Butcher, E.C. (2002). The intestinal chemokine thymus-expressed chemokine (CCL25) attracts IgA antibody-secreting cells. J Exp Med *195*, 269–275.

Brasel, K., De Smedt, T., Smith, J.L., and Maliszewski, C.R. (2000). Generation of murine dendritic cells from flt3-ligand-supplemented bone marrow cultures. Blood *96*, 3029–3039.

Braun, D., Galibert, L., Nakajima, T., Saito, H., Quang, V.V., Rubio, M., and Sarfati, M. (2006). Semimature stage: a checkpoint in a dendritic cell maturation program that allows for functional reversion after signal-regulatory protein-alpha ligation and maturation signals. J Immunol *177*, 8550–8559.

Brenan, M., and Puklavec, M. (1992). The MRC OX-62 antigen: a useful marker in the purification of rat veiled cells with the biochemical properties of an integrin. J Exp Med *175*, 1457–1465.

Brooke, G., Holbrook, J.D., Brown, M.H., and Barclay, A.N. (2004). Human lymphocytes interact directly with CD47 through a novel member of the signal regulatory protein (SIRP) family. J Immunol *173*, 2562–2570.

Brown, E.J., and Frazier, W.A. (2001). Integrin-associated protein (CD47) and its ligands. Trends in Cell Biology *11*, 130–135.

Brüstle, A., Heink, S., Huber, M., Rosenplänter, C., Stadelmann, C., Yu, P., Arpaia, E., Mak, T.W., Kamradt, T., and Lohoff, M. (2007). The development of inflammatory T(H)-17 cells requires interferon-regulatory factor 4. Nat Immunol *8*, 958–966.

Caminschi, I., Proietto, A.I., Ahmet, F., Kitsoulis, S., Shin Teh, J., Lo, J.C.Y., Rizzitelli, A., Wu, L., Vremec, D., van Dommelen, S.L.H., et al. (2008). The dendritic cell subtype-restricted C-type lectin Clec9A is a target for vaccine enhancement. Blood *112*, 3264–3273.

Carter, P.B., Woolcock, J.B., and Collins, F.M. (1975). Involvement of the upper

respiratory tract in orally induced salmonellosis in mice. J. Infect. Dis. *131*, 570–574.

Castigli, E., Wilson, S.A., Scott, S., Dedeoglu, F., Xu, S., Lam, K.-P., Bram, R.J., Jabara, H., and Geha, R.S. (2005). TACI and BAFF-R mediate isotype switching in B cells. J Exp Med *201*, 35–39.

Caton, M.L., Smith-Raska, M.R., and Reizis, B. (2007). Notch-RBP-J signaling controls the homeostasis of CD8- dendritic cells in the spleen. J Exp Med *204*, 1653–1664.

Caux, C., Dezutter-Dambuyant, C., Schmitt, D., and Banchereau, J. (1992). GM-CSF and TNF-alpha cooperate in the generation of dendritic Langerhans cells. Nature *360*, 258–261.

Cebula, A., Seweryn, M., Rempala, G.A., and Pabla, S.S. (2013). Thymus-derived regulatory T cells contribute to tolerance to commensal microbiota. Nature. *497,* 258-262.

Celada, A., Borràs, F.E., Soler, C., Lloberas, J., Klemsz, M., van Beveren, C., McKercher, S., and Maki, R.A. (1996). The transcription factor PU.1 is involved in macrophage proliferation. J Exp Med *184*, 61–69.

Cella, M., Sallusto, F., and Lanzavecchia, A. (1997). Origin, maturation and antigen presenting function of dendritic cells. Curr Opin Immunol *9*, 10–16.

Cella, M., Fuchs, A., Vermi, W., Facchetti, F., Otero, K., Lennerz, J.K.M., Doherty, J.M., Mills, J.C., and Colonna, M. (2009). A human natural killer cell subset provides an innate source of IL-22 for mucosal immunity. Nature *457*, 722–725.

Cerovic, V., Houston, S.A., Scott, C.L., Aumeunier, A., Yrlid, U., Mowat, A.M., and Milling, S.W.F. (2013). Intestinal CD103(-) dendritic cells migrate in lymph and prime effector T cells. Mucosal Immunology. *6,* 104-113.

Cerovic, V., Jenkins, C.D., Barnes, A.G.C., Milling, S.W.F., MacPherson, G.G., and Klavinskis, L.S. (2009). Hyporesponsiveness of Intestinal Dendritic Cells to TLR Stimulation Is Limited to TLR4. J Immunol. *182*, 2405–2415.

Cerutti, A., and Rescigno, M. (2008). The biology of intestinal immunoglobulin A responses. Immunity *28*, 740–750.

Chen, Y.H., and Weiner, H.L. (1996). Dose-dependent activation and deletion of antigen-specific T cells following oral tolerance. Ann. N. Y. Acad. Sci. *778*, 111–121.

Chen, Y., Inobe, J., Marks, R., Gonnella, P., Kuchroo, V.K., and Weiner, H.L. (1995). Peripheral deletion of antigen-reactive T cells in oral tolerance. Nature *376*, 177–180.

Chieppa, M., Rescigno, M., Huang, A.Y.C., and Germain, R.N. (2006). Dynamic imaging of dendritic cell extension into the small bowel lumen in response to epithelial cell TLR engagement. J Exp Med *203*, 2841–2852.

Chirdo, F., Millington, O., Beacock-Sharp, H., and Mowat, A. (2005). Immunomodulatory dendritic cells in intestinal lamina propria. Eur J Immunol *35*, 1831–1840.

Chmill, S., Kadow, S., Winter, M., Weighardt, H., and Esser, C. (2010). 2,3,7,8-Tetrachlorodibenzo-p-dioxin impairs stable establishment of oral tolerance in mice. Toxicol. Sci. *118*, 98–107.

Colonna, M. (2003). TREMs in the immune system and beyond. Nat Rev Immunol. *3,* 445-453.

Colonna, M., Trinchieri, G., and Liu, Y.-J. (2004). Plasmacytoid dendritic cells in immunity.

Nat Immunol *5*, 1219–1226.

Cong, Y., Wang, L., Konrad, A., and Schoeb, T. (2009). Curcumin induces the tolerogenic dendritic cell that promotes differentiation of intestine-protective regulatory T cells. Eur J Immunol. *39,* 3134-3146.

Coombes, J.L., Siddiqui, K.R.R., Arancibia-Cárcamo, C.V., Hall, J., Sun, C.-M., Belkaid, Y., and Powrie, F. (2007). A functionally specialized population of mucosal CD103+ DCs induces Foxp3+ regulatory T cells via a TGF-beta and retinoic acid-dependent mechanism. J Exp Med *204*, 1757–1764.

Cretney, E., Xin, A., Shi, W., Minnich, M., Masson, F., Miasari, M., Belz, G.T., Smyth, G.K., Busslinger, M., Nutt, S.L., et al. (2011). The transcription factors Blimp-1 and IRF4 jointly control the differentiation and function of effector regulatory T cells. Nat Immunol *12*, 304–311.

Crozat, K., Tamoutounour, S., Vu Manh, T.-P., Fossum, E., Luche, H., Ardouin, L., Guilliams, M., Azukizawa, H., Bogen, B., Malissen, B., et al. (2011). Cutting edge: expression of XCR1 defines mouse lymphoid-tissue resident and migratory dendritic cells of the CD8α+ type. The Journal of Immunology *187*, 4411–4415.

Cruickshank, S.M., Deschoolmeester, M.L., Svensson, M., Howell, G., Bazakou, A., Logunova, L., Little, M.C., English, N., Mack, M., Grencis, R.K., et al. (2009). Rapid Dendritic Cell Mobilization to the Large Intestinal Epithelium Is Associated with Resistance to Trichuris muris Infection. The Journal of Immunology *182*, 3055–3062.

D'Amico, A., and Wu, L. (2003). The early progenitors of mouse dendritic cells and plasmacytoid predendritic cells are within the bone marrow hemopoietic precursors expressing Flt3. J Exp Med *198*, 293–303.

Dai, X.-M., Ryan, G.R., Hapel, A.J., Dominguez, M.G., Russell, R.G., Kapp, S., Sylvestre, V., and Stanley, E.R. (2002). Targeted disruption of the mouse colony-stimulating factor 1 receptor gene results in osteopetrosis, mononuclear phagocyte deficiency, increased primitive progenitor cell frequencies, and reproductive defects. Blood *99*, 111–120.

De Becker, G., Moulin, V., Tielemans, F., De Mattia, F., Urbain, J., Leo, O., and Moser, M. (1998). Regulation of T helper cell differentiation in vivo by soluble and membrane proteins provided by antigen-presenting cells. Eur J Immunol *28*, 3161–3171.

DeKoter, R.P., Walsh, J.C., and Singh, H. (1998). PU.1 regulates both cytokine-dependent proliferation and differentiation of granulocyte/macrophage progenitors. The EMBO Journal *17*, 4456–4468.

Delgado, M., Chorny, A., Gonzalez-Rey, E., and Ganea, D. (2005a). Vasoactive intestinal peptide generates CD4+CD25+ regulatory T cells in vivo. J. Leukoc. Biol. *78*, 1327–1338.

Delgado, M., Gonzalez-Rey, E., and Ganea, D. (2005b). The neuropeptide vasoactive intestinal peptide generates tolerogenic dendritic cells. J Immunol *175*, 7311–7324.

Demeure, C.E., Tanaka, H., Mateo, V., Rubio, M., Delespesse, G., and Sarfati, M. (2000). CD47 engagement inhibits cytokine production and maturation of human dendritic cells. J Immunol *164*, 2193–2199.

Denning, T.L., Norris, B.A., Medina-Contreras, O., Manicassamy, S., Geem, D., Madan, R., Karp, C.L., and Pulendran, B. (2011). Functional specializations of intestinal dendritic cell and macrophage subsets that control Th17 and regulatory T cell responses are dependent on the T cell/APC ratio, source of mouse strain, and regional localization. The Journal of Immunology *187*, 733–747.

Denning, T.L., Wang, Y.-C., Patel, S.R., Williams, I.R., and Pulendran, B. (2007). Lamina propria macrophages and dendritic cells differentially induce regulatory and interleukin 17-producing T cell responses. Nat Immunol *8*, 1086–1094.

Derbinski, J., and Kyewski, B. (2010). How thymic antigen presenting cells sample the body's self-antigens. Curr Opin Immunol *22*, 592–600.

Diehl, G.E., Longman, R.S., Zhang, J.-X., Breart, B., Galan, C., Cuesta, A., Schwab, S.R., and Littman, D.R. (2013). Microbiota restricts trafficking of bacteria to mesenteric lymph nodes by CX(3)CR1(hi) cells. Nature *494*, 116–120.

Dietrich, J., Cella, M., Seiffert, M., Bühring, H.J., and Colonna, M. (2000). Cutting edge: signal-regulatory protein beta 1 is a DAP12-associated activating receptor expressed in myeloid cells. J Immunol *164*, 9–12.

Dieu, M.C., Vanbervliet, B., Vicari, A., Bridon, J.M., Oldham, E., Aït-Yahia, S., Brière, F., Zlotnik, A., Lebecque, S., and Caux, C. (1998). Selective recruitment of immature and mature dendritic cells by distinct chemokines expressed in different anatomic sites. J Exp Med *188*, 373–386.

Dillon, S., Agrawal, S., Banerjee, K., Letterio, J., Denning, T.L., Oswald-Richter, K., Kasprowicz, D.J., Kellar, K., Pare, J., van Dyke, T., et al. (2006). Yeast zymosan, a stimulus for TLR2 and dectin-1, induces regulatory antigen-presenting cells and immunological tolerance. J Clin Invest *116*, 916–928.

Duerr, R.H., Taylor, K.D., Brant, S.R., Rioux, J.D., Silverberg, M.S., Daly, M.J., Steinhart, A.H., Abraham, C., Regueiro, M., Griffiths, A., et al. (2006). A genome-wide association study identifies IL23R as an inflammatory bowel disease gene. Science *314*, 1461–1463.

Duester, G. (2000). Families of retinoid dehydrogenases regulating vitamin A function: production of visual pigment and retinoic acid. Eur. J. Biochem. *267*, 4315–4324.

Eberl, G., and Lochner, M. (2009). The development of intestinal lymphoid tissues at the interface of self and microbiota. Mucosal Immunology *2*, 478–485.

Edelson, B.T., Bradstreet, T.R., KC, W., Hildner, K., Herzog, J.W., Sim, J., Russell, J.H., Murphy, T.L., Unanue, E.R., and Murphy, K.M. (2011). Batf3-dependent CD11b(low/-) peripheral dendritic cells are GM-CSF-independent and are not required for Th cell priming after subcutaneous immunization. PLoS ONE *6*, e25660.

Edelson, B.T., KC, W., Juang, R., Kohyama, M., Benoit, L.A., Klekotka, P.A., Moon, C., Albring, J.C., Ise, W., Michael, D.G., et al. (2010). Peripheral CD103+ dendritic cells form a unified subset developmentally related to CD8alpha+ conventional dendritic cells. J Exp Med *207*, 823–836.

Elias, K.M., Laurence, A., Davidson, T.S., Stephens, G., Kanno, Y., Shevach, E.M., and O'Shea, J.J. (2008). Retinoic acid inhibits Th17 polarization and enhances FoxP3 expression through a Stat-3/Stat-5 independent signaling pathway. Blood *111*, 1013–1020.

Facchetti, F., Vermi, W., Mason, D., and Colonna, M. (2003). The plasmacytoid monocyte/interferon producing cells. Virchows Arch. *443*, 703–717.

Fallarino, F., Grohmann, U., You, S., McGrath, B.C., Cavener, D.R., Vacca, C., Orabona, C., Bianchi, R., Belladonna, M.L., Volpi, C., et al. (2006a). Tryptophan catabolism generates autoimmune-preventive regulatory T cells. Transpl. Immunol. *17*, 58–60.

Fallarino, F., Grohmann, U., You, S., McGrath, B.C., Cavener, D.R., Vacca, C., Orabona, C., Bianchi, R., Belladonna, M.L., Volpi, C., et al. (2006b). The combined effects of

tryptophan starvation and tryptophan catabolites down-regulate T cell receptor zeta-chain and induce a regulatory phenotype in naive T cells. J Immunol *176*, 6752–6761.

Farache, J., Koren, I., Milo, I., Gurevich, I., Kim, K.-W., Zigmond, E., Furtado, G.C., Lira, S.A., and Shakhar, G. (2013). Luminal bacteria recruit CD103+ dendritic cells into the intestinal epithelium to sample bacterial antigens for presentation. Immunity *38*, 581–595.

Finkelman, F.D., Katona, I.M., Urban, J.F., Holmes, J., Ohara, J., Tung, A.S., Sample, J.V., and Paul, W.E. (1988). IL-4 is required to generate and sustain in vivo IgE responses. J Immunol *141*, 2335–2341.

Fogg, D.K., Sibon, C., Miled, C., Jung, S., Aucouturier, P., Littman, D.R., Cumano, A., and Geissmann, F. (2006). A clonogenic bone marrow progenitor specific for macrophages and dendritic cells. Science *311*, 83–87.

Ford, L.B., Hansell, C.A.H., and Nibbs, R.J.B. (2013). Using fluorescent chemokine uptake to detect chemokine receptors by fluorescent activated cell sorting. Methods Mol. Biol. *1013*, 203–214.

Forster, R., Schubel, A., Breitfeld, D., Kremmer, E., Renner-Müller, I., Wolf, E., and Lipp, M. (1999). CCR7 coordinates the primary immune response by establishing functional microenvironments in secondary lymphoid organs. Cell *99*, 23–33.

Fortin, G., Raymond, M., Van, V.Q., Rubio, M., Gautier, P., Sarfati, M., and Franchimont, D. (2009). A role for CD47 in the development of experimental colitis mediated by SIRPalpha+CD103- dendritic cells. J Exp Med *206*, 1995–2011.

Fournier, B., Andargachew, R., Robin, A.Z., Laur, O., Voelker, D.R., Lee, W.Y., Weber, D., and Parkos, C.A. (2012). Surfactant Protein D (Sp-D) Binds to Membrane-proximal Domain (D3) of Signal Regulatory Protein (SIRP), a Site Distant from Binding Domain of CD47, while Also Binding to Analogous Region on Signal Regulatory Protein (SIRP). Journal of Biological Chemistry *287*, 19386–19398.

Fujihashi, K., Dohi, T., Rennert, P.D., Yamamoto, M., Koga, T., Kiyono, H., and McGhee, J.R. (2001). Peyer's patches are required for oral tolerance to proteins. Proceedings of the National Academy of Sciences of the United States of America *98*, 3310–3315.

Fujimoto, K., Karuppuchamy, T., Takemura, N., Shimohigoshi, M., Machida, T., Haseda, Y., Aoshi, T., Ishii, K.J., Akira, S., and Uematsu, S. (2011). A new subset of CD103+CD8alpha+ dendritic cells in the small intestine expresses TLR3, TLR7, and TLR9 and induces Th1 response and CTL activity. The Journal of Immunology *186*, 6287–6295.

Fujioka, Y., Matozaki, T., Noguchi, T., Iwamatsu, A., Yamao, T., Takahashi, N., Tsuda, M., Takada, T., and Kasuga, M. (1996). A novel membrane glycoprotein, SHPS-1, that binds the SH2-domain-containing protein tyrosine phosphatase SHP-2 in response to mitogens and cell adhesion. Mol Cell Biol *16*, 6887–6899.

Fukaura, H., Kent, S.C., Pietrusewicz, M.J., Khoury, S.J., Weiner, H.L., and Hafler, D.A. (1996). Induction of circulating myelin basic protein and proteolipid protein-specific transforming growth factor-beta1-secreting Th3 T cells by oral administration of myelin in multiple sclerosis patients. J Clin Invest *98*, 70–77.

Fukunaga, A., Nagai, H., Yu, X., Oniki, S., Okazawa, H., Motegi, S.-I., Suzuki, R., Honma, N., Matozaki, T., Nishigori, C., et al. (2006). Src homology 2 domain-containing protein tyrosine phosphatase substrate 1 regulates the induction of Langerhans cell maturation. Eur J Immunol *36*, 3216–3226.

Gaboriau-Routhiau, V., Rakotobe, S., Lécuyer, E., Mulder, I., Lan, A., Bridonneau, C.,

Rochet, V., Pisi, A., De Paepe, M., Brandi, G., et al. (2009). The key role of segmented filamentous bacteria in the coordinated maturation of gut helper T cell responses. Immunity *31*, 677–689.

Gallegos, A.M., and Bevan, M.J. (2004). Central tolerance to tissue-specific antigens mediated by direct and indirect antigen presentation. J Exp Med *200*, 1039–1049.

Gardai, S.J., Xiao, Y.-Q., Dickinson, M., Nick, J.A., Voelker, D.R., Greene, K.E., and Henson, P.M. (2003). By binding SIRPalpha or calreticulin/CD91, lung collectins act as dual function surveillance molecules to suppress or enhance inflammation. Cell *115*, 13–23.

Garrett, W.S., Lord, G.M., Punit, S., Lugo-Villarino, G., Mazmanian, S.K., Ito, S., Glickman, J.N., and Glimcher, L.H. (2007). Communicable ulcerative colitis induced by T-bet deficiency in the innate immune system. Cell *131*, 33–45.

Gautier, E.L., Shay, T., Miller, J., Greter, M., Jakubzick, C., Ivanov, S., Helft, J., Chow, A., Elpek, K.G., Gordonov, S., et al. (2012). Gene-expression profiles and transcriptional regulatory pathways that underlie the identity and diversity of mouse tissue macrophages. Nat Immunol *13*, 1118–1128.

Geddes, K., Rubino, S.J., Magalhaes, J.G., Streutker, C., Le Bourhis, L., Cho, J.H., Robertson, S.J., Kim, C.J., Kaul, R., Philpott, D.J., et al. (2011). Identification of an innate T helper type 17 response to intestinal bacterial pathogens. Nat Med *17*, 837–844.

Geissmann, F., Manz, M.G., Jung, S., Sieweke, M.H., Merad, M., and Ley, K. (2010). Development of monocytes, macrophages, and dendritic cells. Science *327*, 656–661.

Gerner, M.Y., Kastenmuller, W., Ifrim, I., Kabat, J., and Germain, R.N. (2012). Histo-cytometry: a method for highly multiplex quantitative tissue imaging analysis applied to dendritic cell subset microanatomy in lymph nodes. Immunity *37*, 364–376.

Ghigo, C., Mondor, I., Jorquera, A., Nowak, J., Wienert, S., Zahner, S.P., Clausen, B.E., Luche, H., Malissen, B., Klauschen, F., et al. (2013). Multicolor fate mapping of Langerhans cell homeostasis. J Exp Med. *210,* 1657-1664.

Ginhoux, F., Liu, K., Helft, J., Bogunovic, M., Greter, M., Hashimoto, D., Price, J., Yin, N., Bromberg, J., Lira, S.A., et al. (2009). The origin and development of nonlymphoid tissue CD103+ DCs. J Exp Med *206*, 3115–3130.

Ginhoux, F., Tacke, F., Angeli, V., Bogunovic, M., Loubeau, M., Dai, X.-M., Stanley, E.R., Randolph, G.J., and Merad, M. (2006). Langerhans cells arise from monocytes in vivo. Nat Immunol *7*, 265–273.

Gionchetti, P., Rizzello, F., Helwig, U., Venturi, A., Lammers, K.M., Brigidi, P., Vitali, B., Poggioli, G., Miglioli, M., and Campieri, M. (2003). Prophylaxis of pouchitis onset with probiotic therapy: a double-blind, placebo-controlled trial. Gastroenterology *124*, 1202–1209.

Glimcher, L.H., and Murphy, K.M. (2000). Lineage commitment in the immune system: the T helper lymphocyte grows up. Genes Dev. *14*, 1693–1711.

Gonnella, P.A., Chen, Y., Inobe, J., Komagata, Y., Quartulli, M., and Weiner, H.L. (1998). In situ immune response in gut-associated lymphoid tissue (GALT) following oral antigen in TCR-transgenic mice. J Immunol *160*, 4708–4718.

Gonzalez-Rey, E., and Delgado, M. (2006). Therapeutic treatment of experimental colitis with regulatory dendritic cells generated with vasoactive intestinal peptide. Gastroenterology *131*, 1799–1811.

Gorczynski, R.M. (2012). CD200: CD200R-Mediated Regulation of Immunity. ISRN Immunology.

Greter, M., Helft, J., Chow, A., Hashimoto, D., Mortha, A., Agudo-Cantero, J., Bogunovic, M., Gautier, E.L., Miller, J., Leboeuf, M., et al. (2012). GM-CSF controls nonlymphoid tissue dendritic cell homeostasis but is dispensable for the differentiation of inflammatory dendritic cells. Immunity *36*, 1031–1046.

Gubler, U., Chua, A.O., Schoenhaut, D.S., Dwyer, C.M., McComas, W., Motyka, R., Nabavi, N., Wolitzky, A.G., Quinn, P.M., and Familletti, P.C. (1991). Coexpression of two distinct genes is required to generate secreted bioactive cytotoxic lymphocyte maturation factor. Proceedings of the National Academy of Sciences of the United States of America *88*, 4143–4147.

Guermonprez, P., Valladeau, J., Zitvogel, L., Théry, C., and Amigorena, S. (2002). Antigen presentation and T cell stimulation by dendritic cells. Annu. Rev. Immunol. *20*, 621–667.

Guilliams, M., Lambrecht, B.N., and Hammad, H. (2013a). Division of labor between lung dendritic cells and macrophages in the defense against pulmonary infections. Mucosal Immunology *6*, 464–473.

Guilliams, M., Crozat, K., Henri, S., Tamoutounour, S., Grenot, P., Devilard, E., de Bovis, B., Alexopoulou, L., Dalod, M., and Malissen, B. (2010a). Skin-draining lymph nodes contain dermis-derived CD103(-) dendritic cells that constitutively produce retinoic acid and induce Foxp3(+) regulatory T cells. Blood *115*, 1958–1968.

Guilliams, M., De Kleer, I., Henri, S., Post, S., Vanhoutte, L., De Prijck, S., Deswarte, K., Malissen, B., Hammad, H., and Lambrecht, B.N. (2013b). Alveolar macrophages develop from fetal monocytes that differentiate into long-lived cells in the first week of life via GM-CSF. Journal of Experimental Medicine *210*, 1977–1992.

Guilliams, M., Henri, S., Tamoutounour, S., Ardouin, L., Schwartz-Cornil, I., Dalod, M., and Malissen, B. (2010b). From skin dendritic cells to a simplified classification of human and mouse dendritic cell subsets. Eur J Immunol *40*, 2089–2094.

Haan, den, J.M., Lehar, S.M., and Bevan, M.J. (2000). CD8(+) but not CD8(-) dendritic cells cross-prime cytotoxic T cells in vivo. J Exp Med *192*, 1685–1696.

Hacker, C., Kirsch, R.D., Ju, X.-S., Hieronymus, T., Gust, T.C., Kuhl, C., Jorgas, T., Kurz, S.M., Rose-John, S., Yokota, Y., et al. (2003). Transcriptional profiling identifies Id2 function in dendritic cell development. Nat Immunol *4*, 380–386.

Hadis, U., Wahl, B., Schulz, O., Hardtke-Wolenski, M., Schippers, A., Wagner, N., Müller, W., Sparwasser, T., Förster, R., and Pabst, O. (2011). Intestinal tolerance requires gut homing and expansion of FoxP3+ regulatory T cells in the lamina propria. Immunity *34*, 237–246.

Hagnerud, S., Manna, P., Cella, M., Stenberg, A., Frazier, W., Colonna, M., and Oldenborg, P. (2006). Deficit of CD47 results in a defect of marginal zone dendritic cells, blunted immune response to particulate antigen and impairment of skin dendritic cell migration. J Immunol *176*, 5772–5778.

Halle, S., Bumann, D., Herbrand, H., Willer, Y., Dähne, S., Förster, R., and Pabst, O. (2007). Solitary intestinal lymphoid tissue provides a productive port of entry for Salmonella enterica serovar Typhimurium. Infect. Immun. *75*, 1577–1585.

Hamada, H., Hiroi, T., Nishiyama, Y., Takahashi, H., Masunaga, Y., Hachimura, S., Kaminogawa, S., Takahashi-Iwanaga, H., Iwanaga, T., Kiyono, H., et al. (2002).

Identification of multiple isolated lymphoid follicles on the antimesenteric wall of the mouse small intestine. *168*, 57–64.

Hamann, A., Andrew, D.P., Jablonski-Westrich, D., Holzmann, B., and Butcher, E.C. (1994). Role of alpha 4-integrins in lymphocyte homing to mucosal tissues in vivo. J Immunol *152*, 3282–3293.

Hammerschmidt, S.I., Ahrendt, M., Bode, U., Wahl, B., Kremmer, E., Förster, R., and Pabst, O. (2008). Stromal mesenteric lymph node cells are essential for the generation of gut-homing T cells in vivo. Journal of Experimental Medicine *205*, 2483–2490.

Haniffa, M., Shin, A., Bigley, V., McGovern, N., Teo, P., See, P., Wasan, P.S., Wang, X.-N., Malinarich, F., Malleret, B., et al. (2012). Human tissues contain CD141hi cross-presenting dendritic cells with functional homology to mouse CD103+ nonlymphoid dendritic cells. Immunity *37*, 60–73.

Happel, K.I., Dubin, P.J., Zheng, M., Ghilardi, N., Lockhart, C., Quinton, L.J., Odden, A.R., Shellito, J.E., Bagby, G.J., Nelson, S., et al. (2005). Divergent roles of IL-23 and IL-12 in host defense against Klebsiella pneumoniae. J Exp Med *202*, 761–769.

Harrington, L.E., Hatton, R.D., Mangan, P.R., Turner, H., Murphy, T.L., Murphy, K.M., and Weaver, C.T. (2005). Interleukin 17-producing CD4+ effector T cells develop via a lineage distinct from the T helper type 1 and 2 lineages. Nat Immunol *6*, 1123–1132.

Harrison, O.J., and Maloy, K.J. (2011). Innate Immune Activation in Intestinal Homeostasis. J Innate Immun *3*, 585–593.

Hashimoto, C., Hudson, K.L., and Anderson, K.V. (1988). The Toll gene of drosophila, required for dorsal-ventral embryonic polarity, appears to encode a transmembrane protein. Cell. *52,* 269-279.

Hawiger, D., Inaba, K., Dorsett, Y., Guo, M., Mahnke, K., Rivera, M., Ravetch, J.V., Steinman, R.M., and Nussenzweig, M.C. (2001). Dendritic cells induce peripheral T cell unresponsiveness under steady state conditions in vivo. J Exp Med *194*, 769–779.

Håkansson, K., and Reid, K. (2000). Collectin structure: a review. Protein Science. *9,* 1607-1617.

Helft, J., Ginhoux, F., Bogunovic, M., and Merad, M. (2010). Origin and functional heterogeneity of non-lymphoid tissue dendritic cells in mice. Immunol Rev *234*, 55–75.

Henkel, G.W., McKercher, S.R., Yamamoto, H., Anderson, K.L., Oshima, R.G., and Maki, R.A. (1996). PU.1 but not ets-2 is essential for macrophage development from embryonic stem cells. Blood *88*, 2917–2926.

Henri, S., Vremec, D., Kamath, A., Waithman, J., Williams, S., Benoist, C., Burnham, K., Saeland, S., Handman, E., and Shortman, K. (2001). The dendritic cell populations of mouse lymph nodes. J Immunol *167*, 741–748.

Henry, S.C., Daniell, X.G., Burroughs, A.R., Indaram, M., Howell, D.N., Coers, J., Starnbach, M.N., Hunn, J.P., Howard, J.C., Feng, C.G., et al. (2009). Balance of Irgm protein activities determines IFN-gamma-induced host defense. J. Leukoc. Biol. *85*, 877–885.

Hepworth, M.R., Monticelli, L.A., Fung, T.C., Ziegler, C.G.K., Grunberg, S., Sinha, R., Mantegazza, A.R., Ma, H.-L., Crawford, A., Angelosanto, J.M., et al. (2013). Innate lymphoid cells regulate CD4+ T-cell responses to intestinal commensal bacteria. Nature *498*, 113–117.

Hildner, K., Edelson, B.T., Purtha, W.E., Diamond, M., Matsushita, H., Kohyama, M., Calderon, B., Schraml, B.U., Unanue, E.R., Diamond, M.S., et al. (2008). Batf3 deficiency reveals a critical role for CD8alpha+ dendritic cells in cytotoxic T cell immunity. Science *322*, 1097–1100.

Hirota, K., Turner, J.-E., Villa, M., Duarte, J.H., Demengeot, J., Steinmetz, O.M., and Stockinger, B. (2013). Plasticity of Th17 cells in Peyer's patches is responsible for the induction of T cell-dependent IgA responses. Nat Immunol *14*, 372–379.

Hoeffel, G., Wang, Y., Greter, M., See, P., Teo, P., Malleret, B., Leboeuf, M., Low, D., Oller, G., Almeida, F., et al. (2012). Adult Langerhans cells derive predominantly from embryonic fetal liver monocytes with a minor contribution of yolk sac-derived macrophages. Journal of Experimental Medicine *209*, 1167–1181.

Hogquist, K.A., Jameson, S.C., and Bevan, M.J. (1995). Strong agonist ligands for the T cell receptor do not mediate positive selection of functional CD8+ T cells. Immunity *3*, 79–86.

Holgate, S.T. (2007). The epithelium takes centre stage in asthma and atopic dermatitis. Trends Immunol. *28*, 248–251.

Holtschke, T., Löhler, J., Kanno, Y., Fehr, T., Giese, N., Rosenbauer, F., Lou, J., Knobeloch, K.P., Gabriele, L., Waring, J.F., et al. (1996). Immunodeficiency and chronic myelogenous leukemia-like syndrome in mice with a targeted mutation of the ICSBP gene. Cell *87*, 307–317.

Honma, K. (2005). Interferon regulatory factor 4 negatively regulates the production of proinflammatory cytokines by macrophages in response to LPS. Proceedings of the National Academy of Sciences *102*, 16001–16006.

Hooper, L.V., Stappenbeck, T.S., Hong, C.V., and Gordon, J.I. (2003). Angiogenins: a new class of microbicidal proteins involved in innate immunity. Nat Immunol *4*, 269–273.

Hori, S., Nomura, T., and Sakaguchi, S. (2003). Control of regulatory T cell development by the transcription factor Foxp3. Science *299*, 1057–1061.

Hsieh, C.-S., Lee, H.-M., and Lio, C.-W.J. (2012). Selection of regulatory T cells in the thymus. Nat Rev Immunol *12*, 157–167.

Huang, A.Y., Golumbek, P., Ahmadzadeh, M., and Jaffee, E. (1994). Role of bone marrow-derived cells in presenting MHC class I-restricted tumor antigens. Science. *264,* 961-965.

Hubert, F.-X., Kinkel, S.A., Davey, G.M., Phipson, B., Mueller, S.N., Liston, A., Proietto, A.I., Cannon, P.Z.F., Forehan, S., Smyth, G.K., et al. (2011). Aire regulates the transfer of antigen from mTECs to dendritic cells for induction of thymic tolerance. Blood *118*, 2462–2472.

Hume, D.A. (2008). Macrophages as APC and the dendritic cell myth. The Journal of Immunology *181*, 5829–5835.

Hurst, R.J.M., and Else, K.J. (2013). The retinoic acid-producing capacity of gut dendritic cells and macrophages is reduced during persistent T. muris infection. Parasite Immunol. *35*, 229–233.

Huysamen, C., Willment, J.A., Dennehy, K.M., and Brown, G.D. (2008). CLEC9A is a novel activation C-type lectin-like receptor expressed on BDCA3+ dendritic cells and a subset of monocytes. J Biol Chem *283*, 16693–16701.

Ichigotani, Y., Matsuda, S., Machida, K., Oshima, K., Iwamoto, T., Yamaki, K., Hayakawa, T., and Hamaguchi, M. (2000). Molecular cloning of a novel human gene (SIRP-B2) which encodes a new member of the SIRP/SHPS-1 protein family. J. Hum. Genet. *45*, 378–382.

Iliev, I.D., Mileti, E., Matteoli, G., Chieppa, M., and Rescigno, M. (2009a). Intestinal epithelial cells promote colitis-protective regulatory T-cell differentiation through dendritic cell conditioning. Mucosal Immunology *2*, 340–350.

Iliev, I., Spadoni, I., Mileti, E., Matteoli, G., Sonzogni, A., Sampietro, G., Foschi, D., Caprioli, F., Viale, G., and Rescigno, M. (2009b). Human intestinal epithelial cells promote the differentiation of tolerogenic dendritic cells. Gut *58*, 1481–1489.

Inaba, K., Inaba, M., Romani, N., Aya, H., Deguchi, M., Ikehara, S., Muramatsu, S., and Steinman, R.M. (1992). Generation of large numbers of dendritic cells from mouse bone marrow cultures supplemented with granulocyte/macrophage colony-stimulating factor. J Exp Med *176*, 1693–1702.

Ishigame, H., Kakuta, S., Nagai, T., Kadoki, M., Nambu, A., Komiyama, Y., Fujikado, N., Tanahashi, Y., Akitsu, A., Kotaki, H., et al. (2009). Differential Roles of Interleukin-17A and -17F in Host Defense against Mucoepithelial Bacterial Infection and Allergic Responses. Immunity *30*, 108–119.

Ivanov, I.I., Atarashi, K., Manel, N., Brodie, E.L., Shima, T., Karaoz, U., Wei, D., Goldfarb, K.C., Santee, C.A., Lynch, S.V., et al. (2009). Induction of intestinal Th17 cells by segmented filamentous bacteria. Cell *139*, 485–498.

Ivanov, I.I., Frutos, R. de L., Manel, N., Yoshinaga, K., Rifkin, D.B., Sartor, R.B., Finlay, B.B., and Littman, D.R. (2008). Specific microbiota direct the differentiation of IL-17-producing T-helper cells in the mucosa of the small intestine. Cell Host Microbe *4*, 337–349.

Ivanov, I.I., McKenzie, B.S., Zhou, L., Tadokoro, C.E., Lepelley, A., Lafaille, J.J., Cua, D.J., and Littman, D.R. (2006). The Orphan Nuclear Receptor RORγt Directs the Differentiation Program of Proinflammatory IL-17+ T Helper Cells. Cell *126*, 1121–1133.

Iwamura, H., Saito, Y., Sato-Hashimoto, M., Ohnishi, H., Murata, Y., Okazawa, H., Kanazawa, Y., Kaneko, T., Kusakari, S., Kotani, T., et al. (2011). Essential roles of SIRPα in homeostatic regulation of skin dendritic cells. Immunol Lett. *135,* 100-107.

Iwata, M., Hirakiyama, A., Eshima, Y., Kagechika, H., Kato, C., and Song, S.-Y. (2004). Retinoic acid imprints gut-homing specificity on T cells. Immunity *21*, 527–538.

Jackson, J.T., Hu, Y., Liu, R., Masson, F., D'Amico, A., Carotta, S., Xin, A., Camilleri, M.J., Mount, A.M., Kallies, A., et al. (2011). Id2 expression delineates differential checkpoints in the genetic program of CD8α+ and CD103+ dendritic cell lineages. The EMBO Journal *30*, 2690–2704.

Jaensson, E., Uronen-Hansson, H., Pabst, O., Eksteen, B., Tian, J., Coombes, J., Berg, P., Davidsson, T., Powrie, F., Johansson-Lindbom, B., et al. (2008). Small intestinal CD103+ dendritic cells display unique functional properties that are conserved between mice and humans. J Exp Med *205*, 2139–2149.

Jaensson-Gyllenbäck, E., Kotarsky, K., Zapata, F., Persson, E.K., Gundersen, T.E., Blomhoff, R., and Agace, W.W. (2011). Bile retinoids imprint intestinal CD103+ dendritic cells with the ability to generate gut-tropic T cells. Mucosal Immunology *4*, 438–447.

Jang, M.H., Kweon, M.-N., Iwatani, K., Yamamoto, M., Terahara, K., Sasakawa, C., Suzuki, T., Nochi, T., Yokota, Y., Rennert, P.D., et al. (2004). Intestinal villous M cells: an antigen entry site in the mucosal epithelium. Proceedings of the National Academy of

Sciences of the United States of America *101*, 6110–6115.

Jang, M.H., Sougawa, N., Tanaka, T., Hirata, T., Hiroi, T., Tohya, K., Guo, Z., Umemoto, E., Ebisuno, Y., Yang, B.-G., et al. (2006). CCR7 is critically important for migration of dendritic cells in intestinal lamina propria to mesenteric lymph nodes. J Immunol *176*, 803–810.

Janossy, G., Bofill, M., Poulter, L.W., Rawlings, E., Burford, G.D., Navarrete, C., Ziegler, A., and Kelemen, E. (1986). Separate ontogeny of two macrophage-like accessory cell populations in the human fetus. J Immunol *136*, 4354–4361.

Janssen, W.J., McPhillips, K.A., Dickinson, M.G., Linderman, D.J., Morimoto, K., Xiao, Y.-Q., Oldham, K.M., Vandivier, R.W., Henson, P.M., and Gardai, S.J. (2008). Surfactant proteins A and D suppress alveolar macrophage phagocytosis via interaction with SIRP alpha. Am. J. Respir. Crit. Care Med. *178*, 158–167.

Johansson-Lindbom, B., and Agace, W.W. (2007). Generation of gut-homing T cells and their localization to the small intestinal mucosa. Immunol Rev *215*, 226–242.

Johansson-Lindbom, B., Svensson, M., Pabst, O., Palmqvist, C., Marquez, G., Förster, R., and Agace, W.W. (2005). Functional specialization of gut CD103+ dendritic cells in the regulation of tissue-selective T cell homing. J Exp Med *202*, 1063–1073.

Jones, B.D., Ghori, N., and Falkow, S. (1994). Salmonella typhimurium initiates murine infection by penetrating and destroying the specialized epithelial M cells of the Peyer's patches. J Exp Med *180*, 15–23.

Jung, S., Aliberti, J., Graemmel, P., Sunshine, M.J., Kreutzberg, G.W., Sher, A., and Littman, D.R. (2000). Analysis of Fractalkine Receptor CX3CR1 Function by Targeted Deletion and Green Fluorescent Protein Reporter Gene Insertion. MCB. *20,* 4106-4114.

Jung, S., Unutmaz, D., Wong, P., Sano, G.-I., De los Santos, K., Sparwasser, T., Wu, S., Vuthoori, S., Ko, K., Zavala, F., et al. (2002). In vivo depletion of CD11c+ dendritic cells abrogates priming of CD8+ T cells by exogenous cell-associated antigens. Immunity *17*, 211–220.

Kanazawa, Y., Saito, Y., Supriatna, Y., Tezuka, H., Kotani, T., Murata, Y., Okazawa, H., Ohnishi, H., Kinouchi, Y., Nojima, Y., et al. (2010). Role of SIRPα in regulation of mucosal immunity in the intestine. Genes Cells *15*, 1189–1200.

Karsunky, H., Merad, M., Cozzio, A., Weissman, I.L., and Manz, M.G. (2003). Flt3 ligand regulates dendritic cell development from Flt3+ lymphoid and myeloid-committed progenitors to Flt3+ dendritic cells in vivo. J Exp Med *198*, 305–313.

Kato, A., Favoreto, S., Avila, P.C., and Schleimer, R.P. (2007). TLR3- and Th2 cytokine-dependent production of thymic stromal lymphopoietin in human airway epithelial cells. J Immunol *179*, 1080–1087.

Katona, I.M., Urban, J.F., Kang, S.S., Paul, W.E., and Finkelman, F.D. (1991). IL-4 requirements for the generation of secondary in vivo IgE responses. J Immunol *146*, 4215–4221.

Kawai, T., and Akira, S. (2009). The roles of TLRs, RLRs and NLRs in pathogen recognition. Int. Immunol.

Khan, K.J., Ullman, T.A., Ford, A.C., Abreu, M.T., Abadir, A., Marshall, J.K., Talley, N.J., and Moayyedi, P. (2011). Antibiotic Therapy in Inflammatory Bowel Disease: A Systematic Review and Meta-Analysis. Am J Gastroenterol *106*, 661–673.

Kharitonenkov, A., Chen, Z., Sures, I., Wang, H., Schilling, J., and Ullrich, A. (1997). A family of proteins that inhibit signalling through tyrosine kinase receptors. Nature *386*, 181–186.

Kilshaw, P.J. (1993). Expression of the mucosal T cell integrin alpha M290 beta 7 by a major subpopulation of dendritic cells in mice. Eur J Immunol *23*, 3365–3368.

Kim, S.V., Xiang, W.V., Kwak, C., Yang, Y., Lin, X.W., Ota, M., Sarpel, U., Rifkin, D.B., Xu, R., and Littman, D.R. (2013). GPR15-mediated homing controls immune homeostasis in the large intestine mucosa. Science *340*, 1456–1459.

King, I.L., Kroenke, M.A., and Segal, B.M. (2010). GM-CSF-dependent, CD103+ dermal dendritic cells play a critical role in Th effector cell differentiation after subcutaneous immunization. Journal of Experimental Medicine *207*, 953–961.

Kinnebrew, M.A., Buffie, C.G., Diehl, G.E., Zenewicz, L.A., Leiner, I., Hohl, T.M., Flavell, R.A., Littman, D.R., and Pamer, E.G. (2012). Interleukin 23 production by intestinal CD103(+)CD11b(+) dendritic cells in response to bacterial flagellin enhances mucosal innate immune defense. Immunity *36*, 276–287.

Klebanoff, C.A., Spencer, S.P., Torabi-Parizi, P., Grainger, J.R., Roychoudhuri, R., Ji, Y., Sukumar, M., Muranski, P., Scott, C.D., Hall, J.A., et al. (2013). Retinoic acid controls the homeostasis of pre-cDC-derived splenic and intestinal dendritic cells. J Exp Med. *210,* 1961-1976.

Klein, L., Hinterberger, M., Wirnsberger, G., and Kyewski, B. (2009). Antigen presentation in the thymus for positive selection and central tolerance induction. Nat Rev Immunol *9*, 833–844.

Kobayashi, K.S., Chamaillard, M., Ogura, Y., Henegariu, O., Inohara, N., Núñez, G., and Flavell, R.A. (2005). Nod2-dependent regulation of innate and adaptive immunity in the intestinal tract. Science *307*, 731–734.

Kobayashi, T., Okamoto, S., Hisamatsu, T., Kamada, N., Chinen, H., Saito, R., Kitazume, M.T., Nakazawa, A., Sugita, A., Koganei, K., et al. (2008). IL23 differentially regulates the Th1/Th17 balance in ulcerative colitis and Crohn's disease. Gut *57*, 1682–1689.

Kobayashi, T., Walsh, P.T., Walsh, M.C., Speirs, K.M., Chiffoleau, E., King, C.G., Hancock, W.W., Caamano, J.H., Hunter, C.A., and Scott, P. (2003). TRAF6 Is a Critical Factor for Dendritic Cell Maturation and Development. Immunity *19*, 353–363.

Kondo, M., Weissman, I.L., and Akashi, K. (1997). Identification of clonogenic common lymphoid progenitors in mouse bone marrow. Cell *91*, 661–672.

Krajina, T., Leithäuser, F., Möller, P., Trobonjaca, Z., and Reimann, J. (2003). Colonic lamina propria dendritic cells in mice with CD4+ T cell-induced colitis. Eur J Immunol *33*, 1073–1083.

Kunkel, E.J., Campbell, J.J., Haraldsen, G., Pan, J., Boisvert, J., Roberts, A.I., Ebert, E.C., Vierra, M.A., Goodman, S.B., Genovese, M.C., et al. (2000). Lymphocyte CC chemokine receptor 9 and epithelial thymus-expressed chemokine (TECK) expression distinguish the small intestinal immune compartment: Epithelial expression of tissue-specific chemokines as an organizing principle in regional immunity. J Exp Med *192*, 761–768.

Kurihara, T., Warr, G., Loy, J., and Bravo, R. (1997). Defects in Macrophage Recruitment and Host Defense in Mice Lacking the CCR2 Chemokine Receptor. J Exp Med. *186,* 1757-1562.

Kurts, C., Cannarile, M., Klebba, I., and Brocker, T. (2001). Dendritic cells are sufficient to cross-present self-antigens to CD8 T cells in vivo. J Immunol *166*, 1439–1442.

Kurts, C., Heath, W.R., Carbone, F.R., Allison, J., Miller, J.F., and Kosaka, H. (1996). Constitutive class I-restricted exogenous presentation of self antigens in vivo. J Exp Med *184*, 923–930.

Kusunoki, T., Sugai, M., Katakai, T., Omatsu, Y., Iyoda, T., Inaba, K., Nakahata, T., Shimizu, A., and Yokota, Y. (2003). TH2 dominance and defective development of a CD8+ dendritic cell subset in Id2-deficient mice. J Allergy Clin Immunol *111*, 136–142.

Lacy-Hulbert, A., Smith, A.M., and Tissire, H. (2007). Ulcerative colitis and autoimmunity induced by loss of myeloid αv integrins. PNAS. *104,* 15823-15828.

Laffont, S., Siddiqui, K.R.R., and Powrie, F. (2010). Intestinal inflammation abrogates the tolerogenic properties of MLN CD103+ dendritic cells. Eur J Immunol *40*, 1877–1883.

Lakatos, P.-L. (2006). Recent trends in the epidemiology of inflammatory bowel diseases: up or down? World J. Gastroenterol. *12*, 6102–6108.

Lampen, A., Meyer, S., Arnhold, T., and Nau, H. (2000). Metabolism of vitamin A and its active metabolite all-trans-retinoic acid in small intestinal enterocytes. J. Pharmacol. Exp. Ther. *295*, 979–985.

Langlet, C., Tamoutounour, S., Henri, S., Luche, H., Ardouin, L., Grégoire, C., Malissen, B., and Guilliams, M. (2012). CD64 expression distinguishes monocyte-derived and conventional dendritic cells and reveals their distinct role during intramuscular immunization. The Journal of Immunology *188*, 1751–1760.

Langrish, C.L., Chen, Y., Blumenschein, W.M., Mattson, J., Basham, B., Sedgwick, J.D., McClanahan, T., Kastelein, R.A., and Cua, D.J. (2005). IL-23 drives a pathogenic T cell population that induces autoimmune inflammation. J Exp Med *201*, 233–240.

Larsen, C.P., Ritchie, S.C., Pearson, T.C., Linsley, P.S., and Lowry, R.P. (1992). Functional expression of the costimulatory molecule, B7/BB1, on murine dendritic cell populations. J Exp Med. *176,* 1215-1220.

Latour, S., Tanaka, H., Demeure, C., Mateo, V., Rubio, M., Brown, E.J., Maliszewski, C., Lindberg, F.P., Oldenborg, A., Ullrich, A., et al. (2001). Bidirectional negative regulation of human T and dendritic cells by CD47 and its cognate receptor signal-regulator protein-alpha: down-regulation of IL-12 responsiveness and inhibition of dendritic cell activation. J Immunol *167*, 2547–2554.

Lee, H.-C., and Ziegler, S.F. (2007). Inducible expression of the proallergic cytokine thymic stromal lymphopoietin in airway epithelial cells is controlled by NFkappaB. Proceedings of the National Academy of Sciences of the United States of America *104*, 914–919.

Lennert, K., and Remmele, W. (1958). [Karyometric research on lymph node cells in man. I. Germinoblasts, lymphoblasts & lymphocytes]. Acta Haematol. *19*, 99–113.

Lenschow, D.J., Su, G.H., Zuckerman, L.A., Nabavi, N., Jellis, C.L., Gray, G.S., Miller, J., and Bluestone, J.A. (1993). Expression and functional significance of an additional ligand for CTLA-4. Proceedings of the National Academy of Sciences of the United States of America *90*, 11054–11058.

Lewis, K.L., Caton, M.L., Bogunovic, M., Greter, M., Grajkowska, L.T., Ng, D., Klinakis, A., Charo, I.F., Jung, S., Gommerman, J.L., et al. (2011). Notch2 receptor signaling controls functional differentiation of dendritic cells in the spleen and intestine. Immunity *35*, 780–

791.

Li, L., Jin, H., Xu, J., Shi, Y., and Wen, Z. (2011). Irf8 regulates macrophage versus neutrophil fate during zebrafish primitive myelopoiesis. Blood *117*, 1359–1369.

Li, M., Hener, P., Zhang, Z., Kato, S., Metzger, D., and Chambon, P. (2006). Topical vitamin D3 and low-calcemic analogs induce thymic stromal lymphopoietin in mouse keratinocytes and trigger an atopic dermatitis. Proceedings of the National Academy of Sciences of the United States of America *103*, 11736–11741.

Lin, Z., and Floros, J. (2002). Heterogeneous allele expression of pulmonary SP-D gene in rat large intestine and other tissues. Physiol. Genomics *11*, 235–243.

Lindberg, F.P., Bullard, D.C., Caver, T.E., Gresham, H.D., Beaudet, A.L., and Brown, E.J. (1996). Decreased resistance to bacterial infection and granulocyte defects in IAP-deficient mice. Science *274*, 795–798.

Lindstedt, M., Lundberg, K., and Borrebaeck, C.A.K. (2005). Gene family clustering identifies functionally associated subsets of human in vivo blood and tonsillar dendritic cells. J Immunol *175*, 4839–4846.

Liu, K., Victora, G.D., Schwickert, T.A., Guermonprez, P., Meredith, M.M., Yao, K., Chu, F.-F., Randolph, G.J., Rudensky, A.Y., and Nussenzweig, M. (2009). In vivo analysis of dendritic cell development and homeostasis. Science *324*, 392–397.

Liu, L.M., and MacPherson, G.G. (1991). Lymph-borne (veiled) dendritic cells can acquire and present intestinally administered antigens. Immunology *73*, 281–286.

Luche, H., Weber, O., Nageswara Rao, T., Blum, C., and Fehling, H.J. (2007). Faithful activation of an extra-bright red fluorescent protein in “knock-in” Cre-reporter mice ideally suited for lineage tracing studies. Eur J Immunol *37*, 43–53.

MacDonald, K.P.A., Munster, D.J., Clark, G.J., Dzionek, A., Schmitz, J., and Hart, D.N.J. (2002). Characterization of human blood dendritic cell subsets. Blood *100*, 4512–4520.

MacDonald, K.P.A., Palmer, J.S., Cronau, S., Seppanen, E., Olver, S., Raffelt, N.C., Kuns, R., Pettit, A.R., Clouston, A., Wainwright, B., et al. (2010). An antibody against the colony-stimulating factor 1 receptor depletes the resident subset of monocytes and tissue- and tumor-associated macrophages but does not inhibit inflammation. Blood *116*, 3955–3963.

Mack, M., Cihak, J., Simonis, C., Luckow, B., Proudfoot, A.E., Plachý, J., Brühl, H., Frink, M., Anders, H.J., Vielhauer, V., et al. (2001). Expression and characterization of the chemokine receptors CCR2 and CCR5 in mice. J Immunol *166*, 4697–4704.

Macpherson, A.J., Slack, E., and Geuking, M.B. (2009). The mucosal firewalls against commensal intestinal microbes - Springer. Seminars in Immunopathology. *31,* 145-149.

Macpherson, A.J., and Uhr, T. (2004). Induction of protective IgA by intestinal dendritic cells carrying commensal bacteria. Science *303*, 1662–1665.

Maden, M. (2002). Retinoid signalling in the development of the central nervous system. Nat. Rev. Neurosci. *3*, 843–853.

Madsen, J., Kliem, A., Tornoe, I., Skjodt, K., Koch, C., and Holmskov, U. (2000). Localization of lung surfactant protein D on mucosal surfaces in human tissues. J Immunol *164*, 5866–5870.

Maldonado-López, R., De Smedt, T., Michel, P., Godfroid, J., Pajak, B., Heirman, C.,

Thielemans, K., Leo, O., Urbain, J., and Moser, M. (1999). CD8alpha+ and CD8alpha- subclasses of dendritic cells direct the development of distinct T helper cells in vivo. J Exp Med *189*, 587–592.

Maloy, K.J., and Kullberg, M.C. (2008). IL-23 and Th17 cytokines in intestinal homeostasis. Mucosal Immunology *1*, 339–349.

Mangan, P.R., Harrington, L.E., O'Quinn, D.B., Helms, W.S., Bullard, D.C., Elson, C.O., Hatton, R.D., Wahl, S.M., Schoeb, T.R., and Weaver, C.T. (2006). Transforming growth factor-β induces development of the TH17 lineage. Nature *441*, 231–234.

Manicassamy, S., Ravindran, R., Deng, J., Oluoch, H., Denning, T.L., Kasturi, S.P., Rosenthal, K.M., Evavold, B.D., and Pulendran, B. (2009). Toll-like receptor 2-dependent induction of vitamin A-metabolizing enzymes in dendritic cells promotes T regulatory responses and inhibits autoimmunity. Nat Med *15*, 401–409.

Manz, M.G., Traver, D., Miyamoto, T., Weissman, I.L., and Akashi, K. (2001). Dendritic cell potentials of early lymphoid and myeloid progenitors. Blood *97*, 3333–3341.

Mao, X., Fujiwara, Y., Chapdelaine, A., Yang, H., and Orkin, S.H. (2001). Activation of EGFP expression by Cre-mediated excision in a new ROSA26 reporter mouse strain. Blood *97*, 324–326.

Maraskovsky, E., Brasel, K., Teepe, M., Roux, E.R., Lyman, S.D., Shortman, K., and McKenna, H.J. (1996). Dramatic increase in the numbers of functionally mature dendritic cells in Flt3 ligand-treated mice: multiple dendritic cell subpopulations identified. J Exp Med *184*, 1953–1962.

MartIn-Fontecha, A., Sebastiani, S., Höpken, U.E., Uguccioni, M., Lipp, M., Lanzavecchia, A., and Sallusto, F. (2003). Regulation of dendritic cell migration to the draining lymph node: impact on T lymphocyte traffic and priming. J Exp Med *198*, 615–621.

Mashimo, H., Wu, D.C., Podolsky, D.K., and Fishman, M.C. (1996). Impaired defense of intestinal mucosa in mice lacking intestinal trefoil factor. Science *274*, 262–265.

Massacand, J.C., Kaiser, P., Ernst, B., Tardivel, A., Bürki, K., Schneider, P., and Harris, N.L. (2008). Intestinal bacteria condition dendritic cells to promote IgA production. PLoS ONE *3*, e2588.

Matozaki, T., Murata, Y., Okazawa, H., and Ohnishi, H. (2009). Functions and molecular mechanisms of the CD47-SIRPalpha signalling pathway. Trends in Cell Biology *19*, 72–80.

Matteoli, G., Mazzini, E., Iliev, I.D., Mileti, E., Fallarino, F., Puccetti, P., Chieppa, M., and Rescigno, M. (2010). Gut CD103+ dendritic cells express indoleamine 2,3-dioxygenase which influences T regulatory/T effector cell balance and oral tolerance induction. Gut *59*, 595–604.

Mayrhofer, G., Holt, P.G., and Papadimitriou, J.M. (1986). Functional characteristics of the veiled cells in afferent lymph from the rat intestine. Immunology *58*, 379–387.

Mayrhofer, G., Pugh, C.W., and Barclay, A.N. (1983). The distribution, ontogeny and origin in the rat of Ia-positive cells with dendritic morphology and of Ia antigen in epithelia, with special reference to the intestine. Eur J Immunol *13*, 112–122.

Mazmanian, S.K., Liu, C.H., Tzianabos, A.O., and Kasper, D.L. (2005). An immunomodulatory molecule of symbiotic bacteria directs maturation of the host immune system. Cell *122*, 107–118.

McCaughtry, T.M., and Hogquist, K.A. (2008). Central tolerance: what have we learned from mice? Semin Immunopathol *30*, 399–409.

McDole, J.R., Wheeler, L.W., McDonald, K.G., Wang, B., Konjufca, V., Knoop, K.A., Newberry, R.D., and Miller, M.J. (2012). Goblet cells deliver luminal antigen to CD103+ dendritic cells in the small intestine. Nature *483*, 345–349.

McGeachy, M.J., and Cua, D.J. (2008). Th17 cell differentiation: the long and winding road. Immunity *28*, 445–453.

McKenna, H.J., Stocking, K.L., Miller, R.E., Brasel, K., De Smedt, T., Maraskovsky, E., Maliszewski, C.R., Lynch, D.H., Smith, J., Pulendran, B., et al. (2000). Mice lacking flt3 ligand have deficient hematopoiesis affecting hematopoietic progenitor cells, dendritic cells, and natural killer cells. Blood *95*, 3489–3497.

McKercher, S.R., Torbett, B.E., Anderson, K.L., Henkel, G.W., Vestal, D.J., Baribault, H., Klemsz, M., Feeney, A.J., Wu, G.E., Paige, C.J., et al. (1996). Targeted disruption of the PU.1 gene results in multiple hematopoietic abnormalities. The EMBO Journal *15*, 5647–5658.

McKimmie, C.S., Fraser, A.R., Hansell, C., Gutiérrez, L., Philipsen, S., Connell, L., Rot, A., Kurowska-Stolarska, M., Carreno, P., Pruenster, M., et al. (2008). Hemopoietic cell expression of the chemokine decoy receptor D6 is dynamic and regulated by GATA1. The Journal of Immunology *181*, 3353–3363.

Medzhitov, R. (2001). Toll-like receptors and innate immunity. Nat Rev Immunol *1*, 135–145.

Mellman, I., and Steinman, R.M. (2001). Dendritic cells: specialized and regulated antigen processing machines. Cell *106*, 255–258.

Merad, M., and Manz, M.G. (2009). Dendritic cell homeostasis. Blood. *113,* 3190-3197.

Merad, M., Sathe, P., Helft, J., Miller, J., and Mortha, A. (2013). The dendritic cell lineage: ontogeny and function of dendritic cells and their subsets in the steady state and the inflamed setting. Annu. Rev. Immunol. *31*, 563–604.

Meredith, M.M., Liu, K., Darrasse-Jeze, G., Kamphorst, A.O., Schreiber, H.A., Guermonprez, P., Idoyaga, J., Cheong, C., Yao, K.-H., Niec, R.E., et al. (2012a). Expression of the zinc finger transcription factor zDC (Zbtb46, Btbd4) defines the classical dendritic cell lineage. J Exp Med *209*, 1153–1165.

Meredith, M.M., Liu, K., Kamphorst, A.O., Idoyaga, J., Yamane, A., Guermonprez, P., Rihn, S., Yao, K.-H., Silva, I.T., Oliveira, T.Y., et al. (2012b). Zinc finger transcription factor zDC is a negative regulator required to prevent activation of classical dendritic cells in the steady state. J Exp Med *209*, 1583–1593.

Metlay, J.P., Witmer-Pack, M.D., Agger, R., Crowley, M.T., Lawless, D., and Steinman, R.M. (1990). The distinct leukocyte integrins of mouse spleen dendritic cells as identified with new hamster monoclonal antibodies. J Exp Med *171*, 1753–1771.

Miller, J.C., Brown, B.D., Shay, T., Gautier, E.L., Jojic, V., Cohain, A., Pandey, G., Leboeuf, M., Elpek, K.G., Helft, J., et al. (2012). Deciphering the transcriptional network of the dendritic cell lineage. Nat Immunol *13*, 888–899.

Milling, S., Yrlid, U., Cerovic, V., and MacPherson, G. (2010). Subsets of migrating intestinal dendritic cells. Immunol Rev *234*, 259–267.

Molenaar, R., Knippenberg, M., Goverse, G., Olivier, B.J., de Vos, A.F., O'Toole, T., and

Mebius, R.E. (2011). Expression of retinaldehyde dehydrogenase enzymes in mucosal dendritic cells and gut-draining lymph node stromal cells is controlled by dietary vitamin A. The Journal of Immunology *186*, 1934–1942.

Molodecky, N.A., Soon, I.S., Rabi, D.M., Ghali, W.A., and Ferris, M. (2012). Increasing Incidence and Prevalence of the Inflammatory Bowel Diseases With Time, Based on Systematic Review. Gastroenterology. *142,* 46-54.e42.

Monteleone, I., Platt, A.M., Jaensson, E., Agace, W.W., and Mowat, A.M. (2008). IL-10-dependent partial refractoriness to Toll-like receptor stimulation modulates gut mucosal dendritic cell function. Eur J Immunol *38*, 1533–1547.

Motegi, S.-I., Okazawa, H., Murata, Y., Kanazawa, Y., Saito, Y., Kobayashi, H., Ohnishi, H., Oldenborg, P.-A., Ishikawa, O., and Matozaki, T. (2008). Essential roles of SHPS-1 in induction of contact hypersensitivity of skin. Immunol Lett *121*, 52–60.

Motegi, S.-I., Okazawa, H., Ohnishi, H., Sato, R., Kaneko, Y., Kobayashi, H., Tomizawa, K., Ito, T., Honma, N., Bühring, H.-J., et al. (2003). Role of the CD47-SHPS-1 system in regulation of cell migration. The EMBO Journal *22*, 2634–2644.

Mowat, A. (2005). Dendritic cells and immune responses to orally administered antigens. Vaccine *23*, 1797–1799.

Mowat, A.M. (2003). Anatomical basis of tolerance and immunity to intestinal antigens. Nat Rev Immunol *3*, 331–341.

Mowat, A.M., and Bain, C.C. (2010). The curious case of the intestinal eosinophil. Mucosal Immunology *3*, 420–421.

Mowat, A.M., and Viney, J.L. (1997). The anatomical basis of intestinal immunity. Immunol Rev *156*, 145–166.

Mu, D., Cambier, S., Fjellbirkeland, L., Baron, J.L., Munger, J.S., Kawakatsu, H., Sheppard, D., Broaddus, V.C., and Nishimura, S.L. (2002). The integrin alpha(v)beta8 mediates epithelial homeostasis through MT1-MMP-dependent activation of TGF-beta1. J Cell Biol *157*, 493–507.

Mucida, D., Park, Y., Kim, G., Turovskaya, O., Scott, I., Kronenberg, M., and Cheroutre, H. (2007). Reciprocal TH17 and regulatory T cell differentiation mediated by retinoic acid. Science *317*, 256–260.

Mudter, J., Yu, J., Zufferey, C., Brüstle, A., Wirtz, S., Weigmann, B., Hoffman, A., Schenk, M., Galle, P.R., Lehr, H.A., et al. (2011). IRF4 regulates IL-17A promoter activity and controls RORγt-dependent Th17 colitis in vivo. Inflamm Bowel Dis *17*, 1343–1358.

Mullaly, S.C., Burrows, K., Antignano, F., and Zaph, C. (2011). Assessing the role of CD103 in immunity to an intestinal helminth parasite. PLoS ONE *6*, e19580.

Murata, T., Ohnishi, H., Okazawa, H., Murata, Y., Kusakari, S., Hayashi, Y., Miyashita, M., Itoh, H., Oldenborg, P.-A., Furuya, N., et al. (2006). CD47 promotes neuronal development through Src- and FRG/Vav2-mediated activation of Rac and Cdc42. J. Neurosci. *26*, 12397–12407.

Naik, S.H. (2010). Generation of large numbers of pro-DCs and pre-DCs in vitro. Methods Mol. Biol. *595*, 177–186.

Naik, S.H., Metcalf, D., van Nieuwenhuijze, A., Wicks, I., Wu, L., O'Keeffe, M., and Shortman, K. (2006). Intrasplenic steady-state dendritic cell precursors that are distinct from monocytes. Nat Immunol *7*, 663–671.

Naik, S.H., Perié, L., Swart, E., Gerlach, C., van Rooij, N., de Boer, R.J., and Schumacher, T.N. (2013). Diverse and heritable lineage imprinting of early haematopoietic progenitors. Nature *496*, 229–232.

Naik, S.H., Sathe, P., Park, H.-Y., Metcalf, D., Proietto, A.I., Dakic, A., Carotta, S., O'Keeffe, M., Bahlo, M., Papenfuss, A., et al. (2007). Development of plasmacytoid and conventional dendritic cell subtypes from single precursor cells derived in vitro and in vivo. Nat Immunol *8*, 1217–1226.

Nakaishi, A., Hirose, M., Yoshimura, M., Oneyama, C., Saito, K., Kuki, N., Matsuda, M., Honma, N., Ohnishi, H., Matozaki, T., et al. (2008). Structural insight into the specific interaction between murine SHPS-1/SIRP alpha and its ligand CD47. J Mol Biol *375*, 650–660.

Nakano, H., Yanagita, M., and Gunn, M.D. (2001). CD11c(+)B220(+)Gr-1(+) cells in mouse lymph nodes and spleen display characteristics of plasmacytoid dendritic cells. J Exp Med *194*, 1171–1178.

Nenci, A., Becker, C., Wullaert, A., Gareus, R., van Loo, G., Danese, S., Huth, M., Nikolaev, A., Neufert, C., Madison, B., et al. (2007). Epithelial NEMO links innate immunity to chronic intestinal inflammation. Nature *446*, 557–561.

Neutra, M.R., Frey, A., and Kraehenbuhl, J.P. (1996). Epithelial M cells: gateways for mucosal infection and immunization. Cell *86*, 345–348.

Newberry, R.D., and Lorenz, R.G. (2005). Organizing a mucosal defense. Immunol Rev *206*, 6–21.

Niess, J.H., Brand, S., Gu, X., Landsman, L., Jung, S., McCormick, B.A., Vyas, J.M., Boes, M., Ploegh, H.L., Fox, J.G., et al. (2005). CX3CR1-mediated dendritic cell access to the intestinal lumen and bacterial clearance. Science *307*, 254–258.

Norbury, C.C. (2006). Drinking a lot is good for dendritic cells. Immunology *117*, 443–451.

O'Garra, A. (1998). Cytokines induce the development of functionally heterogeneous T helper cell subsets. Immunity *8*, 275–283.

O'Neill, L.A.J., Golenbock, D., and Bowie, A.G. (2013). The history of Toll-like receptors — redefining innate immunity. Nat Rev Immunol *13*, 453–460.

Ohl, L., Mohaupt, M., Czeloth, N., Hintzen, G., Kiafard, Z., Zwirner, J., Blankenstein, T., Henning, G., and Förster, R. (2004). CCR7 governs skin dendritic cell migration under inflammatory and steady-state conditions. Immunity *21*, 279–288.

Ohnishi, H., Kubota, M., Ohtake, A., Sato, K., and Sano, S.I. (1996). Activation of protein-tyrosine phosphatase SH-PTP2 by a tyrosine-based activation motif of a novel brain molecule. J Biol Chem *271*, 25569–25574.

Okuzawa, C., Kaneko, Y., Murata, Y., Miyake, A., Saito, Y., Okajo, J., Tomizawa, T., Okazawa, H., Ohnishi, H., Matozaki, T., et al. (2008). Resistance to collagen-induced arthritis in SHPS-1 mutant mice. Biochem Biophys Res Commun *371*, 561–566.

Oldenborg, P., Zheleznyak, A., Fang, Y., Lagenaur, C., Gresham, H., and Lindberg, F. (2000). Role of CD47 as a marker of self on red blood cells. Science *288*, 2051–2054.

Olsson, M., Nilsson, A., and Oldenborg, P. (2007). Dose-dependent inhibitory effect of CD47 in macrophage uptake of IgG-opsonized murine erythrocytes. Biochem Biophys Res Commun *352*, 193–197.

Onai, N., Obata-Onai, A., Schmid, M.A., and Manz, M.G. (2007a). Flt3 in regulation of type I interferon-producing cell and dendritic cell development. Ann. N. Y. Acad. Sci. *1106*, 253–261.

Onai, N., Obata-Onai, A., Schmid, M.A., Ohteki, T., Jarrossay, D., and Manz, M.G. (2007b). Identification of clonogenic common Flt3+M-CSFR+ plasmacytoid and conventional dendritic cell progenitors in mouse bone marrow. Nat Immunol *8*, 1207–1216.

Oppmann, B., Lesley, R., Blom, B., Timans, J.C., Xu, Y., Hunte, B., Vega, F., Yu, N., Wang, J., Singh, K., et al. (2000). Novel p19 Protein Engages IL-12p40 to Form a Cytokine, IL-23, with Biological Activities Similar as Well as Distinct from IL-12. Immunity *13*, 715–725.

Oshima, K., Ruhul Amin, A.R.M., Suzuki, A., Hamaguchi, M., and Matsuda, S. (2002). SHPS-1, a multifunctional transmembrane glycoprotein. FEBS Lett. *519*, 1–7.

Ouellette, A.J., and Bevins, C.L. (2001). Paneth Cell Defensins and Innate Immunity of the Small Bowel. Inflammatory Bowel Diseases *7*, 43–50.

P Pavli, C.E.W.W.F.D.D.A.H. (1990). Isolation and characterization of antigen-presenting dendritic cells from the mouse intestinal lamina propria. Immunology *70*, 40.

Pabst, O., and Mowat, A.M. (2012). Oral tolerance to food protein. Mucosal Immunology *5*, 232–239.

Pabst, O. (2012). New concepts in the generation and functions of IgA. Nat Rev Immunol *12*, 821–832.

Pabst, O., and Bernhardt, G. (2010). The puzzle of intestinal lamina propria dendritic cells and macrophages. Eur J Immunol *40*, 2107–2111.

Pabst, O., Ohl, L., Wendland, M., Wurbel, M.-A., Kremmer, E., Malissen, B., and Förster, R. (2004). Chemokine receptor CCR9 contributes to the localization of plasma cells to the small intestine. J Exp Med *199*, 411–416.

Parham, C., Chirica, M., Timans, J., Vaisberg, E., Travis, M., Cheung, J., Pflanz, S., Zhang, R., Singh, K.P., Vega, F., et al. (2002). A receptor for the heterodimeric cytokine IL-23 is composed of IL-12Rbeta1 and a novel cytokine receptor subunit, IL-23R. J Immunol *168*, 5699–5708.

Park, H., Li, Z., Yang, X.O., Chang, S.H., Nurieva, R., Wang, Y.-H., Wang, Y., Hood, L., Zhu, Z., Tian, Q., et al. (2005). A distinct lineage of CD4 T cells regulates tissue inflammation by producing interleukin 17. Nat Immunol *6*, 1133–1141.

Persson, E.K., Scott, C.L., Mowat, A.M., and Agace, W.W. (2013a). Dendritic cell subsets in the intestinal lamina propria: Ontogeny and function. Eur J Immunol. *43,* 3098-3107.

Persson, E.K., Uronen-Hansson, H., Semmrich, M., Rivollier, A., Hägerbrand, K., Marsal, J., Gudjonsson, S., Håkansson, U., Reizis, B., Kotarsky, K., et al. (2013b). IRF4 Transcription-Factor-Dependent CD103(+)CD11b(+) Dendritic Cells Drive Mucosal T Helper 17 Cell Differentiation. Immunity *38*, 958–969.

Picarella, D., Hurlbut, P., Rottman, J., Shi, X., Butcher, E., and Ringler, D.J. (1997). Monoclonal antibodies specific for beta 7 integrin and mucosal addressin cell adhesion molecule-1 (MAdCAM-1) reduce inflammation in the colon of scid mice reconstituted with CD45RBhigh CD4+ T cells. J Immunol *158*, 2099–2106.

Pinet, V., Vergelli, M., Martini, R., Bakke, O., and Long, E.O. (1995). Antigen presentation

mediated by recycling of surface HLA-DR molecules. Nature. *375,* 603-606.

Plantinga, M., Guilliams, M., Vanheerswynghels, M., Deswarte, K., Branco-Madeira, F., Toussaint, W., Vanhoutte, L., Neyt, K., Killeen, N., Malissen, B., et al. (2013). Conventional and Monocyte-Derived CD11b(+) Dendritic Cells Initiate and Maintain T Helper 2 Cell-Mediated Immunity to House Dust Mite Allergen. Immunity *38*, 322–335.

Platt, A.M., Bain, C.C., Bordon, Y., Sester, D.P., and Mowat, A.M. (2010). An independent subset of TLR expressing CCR2-dependent macrophages promotes colonic inflammation. J Immunol *184*, 6843–6854.

Pooley, J.L., Heath, W.R., and Shortman, K. (2001). Cutting edge: intravenous soluble antigen is presented to CD4 T cells by CD8- dendritic cells, but cross-presented to CD8 T cells by CD8+ dendritic cells. J Immunol *166*, 5327–5330.

Postigo, A.A., Corbí, A.L., Sánchez-Madrid, F., and de Landázuri, M.O. (1991). Regulated expression and function of CD11c/CD18 integrin on human B lymphocytes. Relation between attachment to fibrinogen and triggering of proliferation through CD11c/CD18. J Exp Med *174*, 1313–1322.

Poulin, L.F., Reyal, Y., Uronen-Hansson, H., Schraml, B.U., Sancho, D., Murphy, K.M., Håkansson, U.K., Moita, L.F., Agace, W.W., Bonnet, D., et al. (2012). DNGR-1 is a specific and universal marker of mouse and human Batf3-dependent dendritic cells in lymphoid and nonlymphoid tissues. Blood *119*, 6052–6062.

Poulin, L.F., Salio, M., Griessinger, E., Anjos-Afonso, F., Craciun, L., Chen, J.-L., Keller, A.M., Joffre, O., Zelenay, S., Nye, E., et al. (2010). Characterization of human DNGR-1+ BDCA3+ leukocytes as putative equivalents of mouse CD8alpha+ dendritic cells. Journal of Experimental Medicine *207*, 1261–1271.

Proietto, A.I., van Dommelen, S., Zhou, P., Rizzitelli, A., D'Amico, A., Steptoe, R.J., Naik, S.H., Lahoud, M.H., Liu, Y., Zheng, P., et al. (2008). Dendritic cells in the thymus contribute to T-regulatory cell induction. Proceedings of the National Academy of Sciences *105*, 19869–19874.

Pugh, C.W., MacPherson, G.G., and Steer, H.W. (1983). Characterization of nonlymphoid cells derived from rat peripheral lymph. J Exp Med *157*, 1758–1779.

Pulendran, B., Banchereau, J., Burkeholder, S., Kraus, E., Guinet, E., Chalouni, C., Caron, D., Maliszewski, C., Davoust, J., Fay, J., et al. (2000). Flt3-ligand and granulocyte colony-stimulating factor mobilize distinct human dendritic cell subsets in vivo. J Immunol *165*, 566–572.

Pulendran, B., Smith, J.L., Caspary, G., Brasel, K., Pettit, D., Maraskovsky, E., and Maliszewski, C.R. (1999). Distinct dendritic cell subsets differentially regulate the class of immune response in vivo. Proceedings of the National Academy of Sciences of the United States of America *96*, 1036–1041.

Rakoff-Nahoum, S., Paglino, J., Eslami-Varzaneh, F., Edberg, S., and Medzhitov, R. (2004). Recognition of commensal microflora by toll-like receptors is required for intestinal homeostasis. Cell *118*, 229–241.

Raymond, M., Rubio, M., Fortin, G., Shalaby, K.H., Hammad, H., Lambrecht, B.N., and Sarfati, M. (2009). Selective control of SIRP-alpha-positive airway dendritic cell trafficking through CD47 is critical for the development of T(H)2-mediated allergic inflammation. J Allergy Clin Immunol *124*, 1333–42.e1.

Reis e Sousa, C., and Germain, R.N. (1995). Major histocompatibility complex class I presentation of peptides derived from soluble exogenous antigen by a subset of cells

engaged in phagocytosis. J Exp Med *182*, 841–851.

Rescigno, M., Urbano, M., Valzasina, B., Francolini, M., Rotta, G., Bonasio, R., Granucci, F., Kraehenbuhl, J.P., and Ricciardi-Castagnoli, P. (2001). Dendritic cells express tight junction proteins and penetrate gut epithelial monolayers to sample bacteria. Nat Immunol *2*, 361–367.

Rimoldi, M., Chieppa, M., Salucci, V., and Avogadri, F. (2005a). Intestinal immune homeostasis is regulated by the crosstalk between epithelial cells and dendritic cells. Nature. *6,* 507-514.

Rimoldi, M., Chieppa, M., Larghi, P., Vulcano, M., Allavena, P., and Rescigno, M. (2005b). Monocyte-derived dendritic cells activated by bacteria or by bacteria-stimulated epithelial cells are functionally different. Blood. *106*, 2818–2826.

Rivollier, A., He, J., Kole, A., Valatas, V., and Kelsall, B.L. (2012). Inflammation switches the differentiation program of Ly6Chi monocytes from antiinflammatory macrophages to inflammatory dendritic cells in the colon. J Exp Med. *209,* 139-155.

Robb, L., Drinkwater, C.C., Metcalf, D., Li, R., Köntgen, F., Nicola, N.A., and Begley, C.G. (1995). Hematopoietic and lung abnormalities in mice with a null mutation of the common beta subunit of the receptors for granulocyte-macrophage colony-stimulating factor and interleukins 3 and 5. Proceedings of the National Academy of Sciences of the United States of America *92*, 9565–9569.

Robbins, S.H., Walzer, T., Dembélé, D., Thibault, C., Defays, A., Bessou, G., Xu, H., Vivier, E., Sellars, M., Pierre, P., et al. (2008). Novel insights into the relationships between dendritic cell subsets in human and mouse revealed by genome-wide expression profiling. Genome Biol. *9*, R17.

Rogler, G., Hausmann, M., Vogl, D., Aschenbrenner, E., Andus, T., Falk, W., Andreesen, R., Schölmerich, J., and Gross, V. (1998). Isolation and phenotypic characterization of colonic macrophages. Clin. Exp. Immunol. *112*, 205–215.

Ruane, D., Brane, L., Reis, B.S., Cheong, C., Poles, J., Do, Y., Zhu, H., Velinzon, K., Choi, J.-H., Studt, N., et al. (2013). Lung dendritic cells induce migration of protective T cells to the gastrointestinal tract. Journal of Experimental Medicine *210*, 1871–1888.

Saederup, N., Cardona, A.E., Croft, K., Mizutani, M., Cotleur, A.C., Tsou, C.-L., Ransohoff, R.M., and Charo, I.F. (2010). Selective chemokine receptor usage by central nervous system myeloid cells in CCR2-red fluorescent protein knock-in mice. PLoS ONE *5*, e13693.

Saito, Y., Iwamura, H., Kaneko, T., Ohnishi, H., Murata, Y., Okazawa, H., Kanazawa, Y., Sato-Hashimoto, M., Kobayashi, H., Oldenborg, P.-A., et al. (2010). Regulation by SIRPα of dendritic cell homeostasis in lymphoid tissues. Blood *116*, 3517–3525.

Sallusto, F., and Lanzavecchia, A. (1994). Efficient presentation of soluble antigen by cultured human dendritic cells is maintained by granulocyte/macrophage colony-stimulating factor plus interleukin 4 and downregulated by tumor necrosis factor alpha. J Exp Med *179*, 1109–1118.

Sallusto, F., Cella, M., Danieli, C., and Lanzavecchia, A. (1995). Dendritic cells use macropinocytosis and the mannose receptor to concentrate macromolecules in the major histocompatibility complex class II compartment: downregulation by cytokines and bacterial products. J Exp Med *182*, 389–400.

Sallusto, F., Schaerli, P., Loetscher, P., Schaniel, C., Lenig, D., Mackay, C.R., Qin, S., and Lanzavecchia, A. (1998). Rapid and coordinated switch in chemokine receptor

expression during dendritic cell maturation. Eur J Immunol *28*, 2760–2769.

Sancho, D., Mourão-Sá, D., Joffre, O.P., Schulz, O., Rogers, N.C., Pennington, D.J., Carlyle, J.R., and Reis E Sousa, C. (2008). Tumor therapy in mice via antigen targeting to a novel, DC-restricted C-type lectin. J Clin Invest *118*, 2098–2110.

Sanos, S.L., Bui, V.L., Mortha, A., Oberle, K., Heners, C., Johner, C., and Diefenbach, A. (2009). RORgammat and commensal microflora are required for the differentiation of mucosal interleukin 22-producing NKp46+ cells. Nat Immunol *10*, 83–91.

Sarra, M., Pallone, F., Macdonald, T.T., and Monteleone, G. (2010). IL-23/IL-17 axis in IBD. Inflammatory Bowel Diseases *16*, 1808–1813.

Satpathy, A.T., Briseño, C.G., Lee, J.S., Ng, D., Manieri, N.A., KC, W., Wu, X., Thomas, S.R., Lee, W.-L., Turkoz, M., et al. (2013). Notch2-dependent classical dendritic cells orchestrate intestinal immunity to attaching-and-effacing bacterial pathogens. Nat Immunol. *14,* 937-948.

Satpathy, A.T., KC, W., Albring, J.C., Edelson, B.T., Kretzer, N.M., Bhattacharya, D., Murphy, T.L., and Murphy, K.M. (2012). Zbtb46 expression distinguishes classical dendritic cells and their committed progenitors from other immune lineages. J Exp Med *209*, 1135–1152.

Schiavoni, G., Mattei, F., Sestili, P., Borghi, P., Venditti, M., Morse, H.C., Belardelli, F., and Gabriele, L. (2002). ICSBP is essential for the development of mouse type I interferon-producing cells and for the generation and activation of CD8alpha(+) dendritic cells. J Exp Med *196*, 1415–1425.

Schlitzer, A., Heiseke, A.F., Einwächter, H., Reindl, W., Schiemann, M., Manta, C.-P., See, P., Niess, J.H., Suter, T., Ginhoux, F., et al. (2012). Tissue-specific differentiation of a circulating CCR9- pDC-like common dendritic cell precursor. Blood. *119,* 6063-6071.

Schlitzer, A., Loschko, J., Mair, K., Vogelmann, R., Henkel, L., Einwächter, H., Schiemann, M., Niess, J.H., Reindl, W., and Krug, A. (2011). Identification of CCR9- murine plasmacytoid DC precursors with plasticity to differentiate into conventional DCs. Blood *117*, 6562–6570.

Schlitzer, A., McGovern, N., Teo, P., Zelante, T., Atarashi, K., Low, D., Ho, A.W.S., See, P., Shin, A., Wasan, P.S., et al. (2013). IRF4 Transcription Factor-Dependent CD11b(+) Dendritic Cells in Human and Mouse Control Mucosal IL-17 Cytokine Responses. Immunity *38*, 970–983.

Schraml, B.U., van Blijswijk, J., Zelenay, S., Whitney, P.G., Filby, A., Acton, S.E., Rogers, N.C., Moncaut, N., Carvajal, J.J., and Reis E Sousa, C. (2013). Genetic Tracing via DNGR-1 Expression History Defines Dendritic Cells as a Hematopoietic Lineage. Cell *154*, 843–858.

Schulz, C., Gomez Perdiguero, E., Chorro, L., Szabo-Rogers, H., Cagnard, N., Kierdorf, K., Prinz, M., Wu, B., Jacobsen, S.E.W., Pollard, J.W., et al. (2012). A lineage of myeloid cells independent of Myb and hematopoietic stem cells. Science *336*, 86–90.

Schulz, O., Jaensson, E., Persson, E.K., Liu, X., Worbs, T., Agace, W.W., and Pabst, O. (2009). Intestinal CD103+, but not CX3CR1+, antigen sampling cells migrate in lymph and serve classical dendritic cell functions. J Exp Med *206*, 3101–3114.

Schwartz, R.H. (2003). T cell anergy. Annu. Rev. Immunol. *21*, 305–334.

Scott, C.L., Aumeunier, A.M., and Mowat, A.M. (2011). Intestinal CD103+ dendritic cells: master regulators of tolerance? Trends Immunol. *32*, 412–419.

Segura, E., Durand, M., and Amigorena, S. (2013). Similar antigen cross-presentation capacity and phagocytic functions in all freshly isolated human lymphoid organ-resident dendritic cells. Journal of Experimental Medicine *210*, 1035–1047.

Seiffert, M., Brossart, P., Cant, C., Cella, M., Colonna, M., Brugger, W., Kanz, L., Ullrich, A., and Buhring, H. (2001). Signal-regulatory protein alpha (SIRPalpha) but not SIRPbeta is involved in T-cell activation, binds to CD47 with high affinity, and is expressed on immature CD34(+)CD38(-) hematopoietic cells. Blood *97*, 2741–2749.

Sellon, R.K., Tonkonogy, S., Schultz, M., Dieleman, L.A., Grenther, W., Balish, E., Rennick, D.M., and Sartor, R.B. (1998). Resident enteric bacteria are necessary for development of spontaneous colitis and immune system activation in interleukin-10-deficient mice. Infect. Immun. *66*, 5224–5231.

Serbina, N.V., and Pamer, E.G. (2006). Monocyte emigration from bone marrow during bacterial infection requires signals mediated by chemokine receptor CCR2. Nat Immunol *7*, 311–317.

Serbina, N., Salazar-Mather, T., Biron, C., Kuziel, W., and Pamer, E. (2003). TN/iNOS-producing dendritic cells mediate innate immune defense against bacterial infection. Immunity *19*, 59–70.

Shaw, M.H., Kamada, N., Kim, Y.-G., and Núñez, G. (2012). Microbiota-induced IL-1β, but not IL-6, is critical for the development of steady-state TH17 cells in the intestine. J Exp Med *209*, 251–258.

Shen, Z., Reznikoff, G., Dranoff, G., and Rock, K.L. (1997). Cloned dendritic cells can present exogenous antigens on both MHC class I and class II molecules. J Immunol. *158,* 2723-2730.

Shortman, K., and Liu, Y. (2002). Mouse and human dendritic cell subtypes. Nat Rev Immunol *2*, 151–161.

Shurin, M.R., Pandharipande, P.P., Zorina, T.D., Haluszczak, C., Subbotin, V.M., Hunter, O., Brumfield, A., Storkus, W.J., Maraskovsky, E., and Lotze, M.T. (1997). FLT3 ligand induces the generation of functionally active dendritic cells in mice. Cell Immunol *179*, 174–184.

Siddiqui, K.R.R., and Powrie, F. (2008). CD103+ GALT DCs promote Foxp3+ regulatory T cells. Mucosal Immunology *1 Suppl 1*, S34–S38.

Siddiqui, K.R.R., Laffont, S., and Powrie, F. (2010). E-cadherin marks a subset of inflammatory dendritic cells that promote T cell-mediated colitis. Immunity *32*, 557–567.

Sixt, M., Kanazawa, N., Selg, M., Samson, T., Roos, G., Reinhardt, D.P., Pabst, R., Lutz, M.B., and Sorokin, L. (2005). The conduit system transports soluble antigens from the afferent lymph to resident dendritic cells in the T cell area of the lymph node. Immunity *22*, 19–29.

Smith, R.E., Patel, V., Seatter, S.D., Deehan, M.R., Brown, M.H., Brooke, G.P., Goodridge, H.S., Howard, C.J., Rigley, K.P., Harnett, W., et al. (2003). A novel MyD-1 (SIRP-1alpha) signaling pathway that inhibits LPS-induced TNFalpha production by monocytes. Blood *102*, 2532–2540.

Snapper, C.M., Finkelman, F.D., and Paul, W.E. (1988a). Differential regulation of IgG1 and IgE synthesis by interleukin 4. J Exp Med *167*, 183–196.

Snapper, C.M., Peschel, C., and Paul, W.E. (1988b). IFN-gamma stimulates IgG2a secretion by murine B cells stimulated with bacterial lipopolysaccharide. J Immunol *140*,

2121–2127.

Soerensen, C.M., Nielsen, O.L., and Willis, A. (2005). Purification, characterization and immunolocalization of porcine surfactant protein D. Immunol. *114,* 72-82.

Sonnenberg, G.F., Monticelli, L.A., Elloso, M.M., Fouser, L.A., and Artis, D. (2011). CD4(+) lymphoid tissue-inducer cells promote innate immunity in the gut. Immunity *34*, 122–134.

Sonnenburg, J.L., Angenent, L.T., and Gordon, J.I. (2004). Getting a grip on things: how do communities of bacterial symbionts become established in our intestine? Nat Immunol *5*, 569–573.

Sozzani, S., Allavena, P., D'Amico, G., Luini, W., Bianchi, G., Kataura, M., Imai, T., Yoshie, O., Bonecchi, R., and Mantovani, A. (1998). Differential regulation of chemokine receptors during dendritic cell maturation: a model for their trafficking properties. J Immunol *161*, 1083–1086.

Spadoni, I., Iliev, I.D., Rossi, G., and Rescigno, M. (2012). Dendritic cells produce TSLP that limits the differentiation of Th17 cells, fosters Treg development, and protects against colitis. Mucosal Immunology *5*, 184–193.

Spahn, T.W., Fontana, A., Faria, A.M., Slavin, A.J., Eugster, H.P., Zhang, X., Koni, P.A., Ruddle, N.H., Flavell, R.A., Rennert, P.D., et al. (2001). Induction of oral tolerance to cellular immune responses in the absence of Peyer's patches. Eur J Immunol *31*, 1278–1287.

Spahn, T.W., Weiner, H.L., Rennert, P.D., Lügering, N., Fontana, A., Domschke, W., and Kucharzik, T. (2002). Mesenteric lymph nodes are critical for the induction of high-dose oral tolerance in the absence of Peyer's patches. Eur J Immunol *32*, 1109–1113.

Spencer, J., MacDonald, T.T., and Isaacson, P.G. (1987). Heterogeneity of non-lymphoid cells expressing HLA-D region antigens in human fetal gut. Clin. Exp. Immunol. *67*, 415–424.

Steinman, R.M. (1973). Identification of a novel cell type in peripheral lymphoid organs of mice: I. Morphology, quantitation, tissue distribution. J Exp Med. *137*, 1142–1162.

Steinman, R.M., and Cohn, Z.A. (1974). Identification of a novel cell type in peripheral lymphoid organs of mice. II. Functional properties in vitro. J Exp Med *139*, 380–397.

Steinman, R.M., Lustig, D.S., and Cohn, Z.A. (1974). Identification of a novel cell type in peripheral lymphoid organs of mice. 3. Functional properties in vivo. J Exp Med *139*, 1431–1445.

Steinman, R.M., Hawiger, D., and Nussenzweig, M.C. (2003). Tolerogenic dendritic cells. Annu. Rev. Immunol. *21*, 685–711.

Subach, F.V., Piatkevich, K.D., and Verkhusha, V.V. (2011). Directed molecular evolution to design advanced red fluorescent proteins. Nat. Methods *8*, 1019–1026.

Subramanian, S., Parthasarathy, R., Sen, S., Boder, E.T., and Discher, D.E. (2006). Species- and cell type-specific interactions between CD47 and human SIRPalpha. Blood *107*, 2548–2556.

Sun, C.-M., Hall, J.A., Blank, R.B., Bouladoux, N., Oukka, M., Mora, J.R., and Belkaid, Y. (2007). Small intestine lamina propria dendritic cells promote de novo generation of Foxp3 T reg cells via retinoic acid. J Exp Med *204*, 1775–1785.

Suzuki, S., Honma, K., Matsuyama, T., Suzuki, K., Toriyama, K., Akitoyo, I., Yamamoto, K., Suematsu, T., Nakamura, M., Yui, K., et al. (2004). Critical roles of interferon regulatory factor 4 in CD11bhighCD8alpha- dendritic cell development. Proceedings of the National Academy of Sciences of the United States of America *101*, 8981–8986.

Svensson, M., Johansson-Lindbom, B., Zapata, F., Jaensson, E., Austenaa, L.M., Blomhoff, R., and Agace, W.W. (2008). Retinoic acid receptor signaling levels and antigen dose regulate gut homing receptor expression on CD8+ T cells. Mucosal Immunology *1*, 38–48.

Swidsinski, A., Weber, J., Loening-Baucke, V., Hale, L.P., and Lochs, H. (2005). Spatial organization and composition of the mucosal flora in patients with inflammatory bowel disease. J. Clin. Microbiol. *43*, 3380–3389.

Szabo, S.J., Kim, S.T., Costa, G.L., Zhang, X., Fathman, C.G., and Glimcher, L.H. (2000). A novel transcription factor, T-bet, directs Th1 lineage commitment. Cell *100*, 655–669.

Szatmari, I., Pap, A., Rühl, R., Ma, J.-X., Illarionov, P.A., Besra, G.S., Rajnavolgyi, E., Dezso, B., and Nagy, L. (2006). PPARgamma controls CD1d expression by turning on retinoic acid synthesis in developing human dendritic cells. J Exp Med *203*, 2351–2362.

Tagliani, E., Shi, C., Nancy, P., Tay, C.-S., Pamer, E.G., and Erlebacher, A. (2011). Coordinate regulation of tissue macrophage and dendritic cell population dynamics by CSF-1. Journal of Experimental Medicine *208*, 1901–1916.

Tailor, P., Tamura, T., Morse, H.C., and Ozato, K. (2008). The BXH2 mutation in IRF8 differentially impairs dendritic cell subset development in the mouse. Blood *111*, 1942–1945.

Tamoutounour, S., Henri, S., Lelouard, H., de Bovis, B., de Haar, C., van der Woude, C.J., Woltman, A.M., Reyal, Y., Bonnet, D., Sichien, D., et al. (2012). CD64 distinguishes macrophages from dendritic cells in the gut and reveals the Th1-inducing role of mesenteric lymph node macrophages during colitis. Eur J Immunol. *42,* 3150-3166.

Tamura, T., Tailor, P., Yamaoka, K., Kong, H.J., Tsujimura, H., O'Shea, J.J., Singh, H., and Ozato, K. (2005). IFN regulatory factor-4 and -8 govern dendritic cell subset development and their functional diversity. J Immunol *174*, 2573–2581.

Thery, C., and Amigorena, S. (2001). The cell biology of antigen presentation in dendritic cells. Curr Opin Immunol *13*, 45–51.

Thomson, A.W., and Knolle, P.A. (2010). Antigen-presenting cell function in the tolerogenic liver environment. Nat Rev Immunol *10*, 753–766.

Thornton, A.M., Korty, P.E., Tran, D.Q., Wohlfert, E.A., Murray, P.E., Belkaid, Y., and Shevach, E.M. (2010). Expression of Helios, an Ikaros transcription factor family member, differentiates thymic-derived from peripherally induced Foxp3+ T regulatory cells. The Journal of Immunology *184*, 3433–3441.

Tomizawa, T., Kaneko, Y., Saito, Y., Ohnishi, H., Okajo, J., Okuzawa, C., Ishikawa-Sekigami, T., Murata, Y., Okazawa, H., Okamoto, K., et al. (2007). Resistance to experimental autoimmune encephalomyelitis and impaired T cell priming by dendritic cells in Src homology 2 domain-containing protein tyrosine phosphatase substrate-1 mutant mice. J Immunol *179*, 869–877.

Travis, M.A., Reizis, B., Melton, A.C., Masteller, E., Tang, Q., Proctor, J.M., Wang, Y., Bernstein, X., Huang, X., Reichardt, L.F., et al. (2007). Loss of integrin alpha(v)beta8 on dendritic cells causes autoimmunity and colitis in mice. Nature *449*, 361–365.

Tsujimura, H., Tamura, T., and Ozato, K. (2003). Cutting edge: IFN consensus sequence binding protein/IFN regulatory factor 8 drives the development of type I IFN-producing plasmacytoid dendritic cells. J Immunol *170*, 1131–1135.

Turnbull, E.L., Yrlid, U., Jenkins, C.D., and MacPherson, G.G. (2005). Intestinal dendritic cell subsets: differential effects of systemic TLR4 stimulation on migratory fate and activation in vivo. J Immunol *174*, 1374–1384.

Tussiwand, R., Lee, W.-L., Murphy, T.L., Mashayekhi, M., Wumesh, K.C., Albring, J.C., Satpathy, A.T., Rotondo, J.A., Edelson, B.T., Kretzer, N.M., et al. (2012). Compensatory dendritic cell development mediated by BATF-IRF interactions. Nature *490*, 502–507.

Tussiwand, R., Onai, N., Mazzucchelli, L., and Manz, M.G. (2005). Inhibition of natural type I IFN-producing and dendritic cell development by a small molecule receptor tyrosine kinase inhibitor with Flt3 affinity. J Immunol *175*, 3674–3680.

Uematsu, S., Fujimoto, K., Jang, M.H., Yang, B.-G., Jung, Y.-J., Nishiyama, M., Sato, S., Tsujimura, T., Yamamoto, M., Yokota, Y., et al. (2008). Regulation of humoral and cellular gut immunity by lamina propria dendritic cells expressing Toll-like receptor 5. Nat Immunol *9*, 769–776.

Vaishnava, S., Behrendt, C.L., Ismail, A.S., Eckmann, L., and Hooper, L.V. (2008). Paneth cells directly sense gut commensals and maintain homeostasis at the intestinal host-microbial interface. Proceedings of the National Academy of Sciences *105*, 20858–20863.

Vallon-Eberhard, A., Landsman, L., Yogev, N., Verrier, B., and Jung, S. (2006). Transepithelial pathogen uptake into the small intestinal lamina propria. J Immunol *176*, 2465–2469.

Van der Sluis, M., and van Seuningen, I. (2006). Important role for Mucin 2 in colonic protection against dextran sulfate sodium. European Journal of Gastroenterology and Hepatology. *18,* A65.

Van der Sluis, M., de Koning, B., and Velcich, A. (2006). Spontaneous development of colitis in mice deficient for Mucin 2. European Journal of Gastroenterology and Hepatology. *18,* A27.

Van der Sluis, M., De Koning, B.A.E., De Bruijn, A.C.J.M., Velcich, A., Meijerink, J.P.P., Van Goudoever, J.B., Büller, H.A., Dekker, J., Van Seuningen, I., Renes, I.B., et al. (2006). Muc2-deficient mice spontaneously develop colitis, indicating that MUC2 is critical for colonic protection. Gastroenterology *131*, 117–129.

Van Furth, R., Cohn, Z.A., Hirsch, J.G., Humphrey, J.H., Spector, W.G., and Langevoort, H.L. (1972). The mononuclear phagocyte system: a new classification of macrophages, monocytes, and their precursor cells. Bull. World Health Organ. *46*, 845–852.

Van, V.Q., Lesage, S., Bouguermouh, S., Gautier, P., Rubio, M., Levesque, M., Nguyen, S., Galibert, L., and Sarfati, M. (2006). Expression of the self-marker CD47 on dendritic cells governs their trafficking to secondary lymphoid organs. The EMBO Journal *25*, 5560–5568.

Varga, T., and Nagy, L. (2008). Nuclear receptors, transcription factors linking lipid metabolism and immunity: the case of peroxisome proliferator-activated receptor gamma. European Journal of Clinical Investigation *38*, 695–707.

Varol, C., Landsman, L., Fogg, D.K., Greenshtein, L., Gildor, B., Margalit, R., Kalchenko, V., Geissmann, F., and Jung, S. (2007). Monocytes give rise to mucosal, but not splenic, conventional dendritic cells. J Exp Med *204*, 171–180.

Varol, C., Vallon-Eberhard, A., Elinav, E., Aychek, T., Shapira, Y., Luche, H., Fehling, H.J., Hardt, W.-D., Shakhar, G., and Jung, S. (2009). Intestinal Lamina Propria Dendritic Cell Subsets Have Different Origin and Functions. Immunity *31*, 502–512.

Veillette, A., Thibaudeau, E., and Latour, S. (1998). High expression of inhibitory receptor SHPS-1 and its association with protein-tyrosine phosphatase SHP-1 in macrophages. J Biol Chem *273*, 22719–22728.

Veldhoen, M., Hocking, R.J., Atkins, C.J., Locksley, R.M., and Stockinger, B. (2006). TGFbeta in the context of an inflammatory cytokine milieu supports de novo differentiation of IL-17-producing T cells. Immunity *24*, 179–189.

Verjan Garcia, N., Umemoto, E., Saito, Y., Yamasaki, M., Hata, E., Matozaki, T., Murakami, M., Jung, Y.-J., Woo, S.-Y., Seoh, J.-Y., et al. (2011). SIRPα/CD172a regulates eosinophil homeostasis. The Journal of Immunology *187*, 2268–2277.

Vernon-Wilson, E.F., Kee, W.J., Willis, A.C., Barclay, A.N., Simmons, D.L., and Brown, M.H. (2000). CD47 is a ligand for rat macrophage membrane signal regulatory protein SIRP (OX41) and human SIRPalpha 1. Eur J Immunol *30*, 2130–2137.

Viney, J.L., Mowat, A.M., O'Malley, J.M., Williamson, E., and Fanger, N.A. (1998). Expanding dendritic cells in vivo enhances the induction of oral tolerance. J Immunol *160*, 5815–5825.

Volpe, S., Cameroni, E., Moepps, B., Thelen, S., Apuzzo, T., and Thelen, M. (2012). CCR2 acts as scavenger for CCL2 during monocyte chemotaxis. PLoS ONE *7*, e37208.

Vremec, D., Lieschke, G.J., Dunn, A.R., Robb, L., Metcalf, D., and Shortman, K. (1997). The influence of granulocyte/macrophage colony-stimulating factor on dendritic cell levels in mouse lymphoid organs. Eur J Immunol *27*, 40–44.

Vremec, D., Pooley, J., Hochrein, H., Wu, L., and Shortman, K. (2000). CD4 and CD8 expression by dendritic cell subtypes in mouse thymus and spleen. J Immunol *164*, 2978–2986.

Vremec, D., Zorbas, M., Scollay, R., Saunders, D.J., Ardavin, C.F., Wu, L., and Shortman, K. (1992). The surface phenotype of dendritic cells purified from mouse thymus and spleen: investigation of the CD8 expression by a subpopulation of dendritic cells. J Exp Med *176*, 47–58.

Waclavicek, M., Majdic, O., Stulnig, T., Berger, M., Baumruker, T., Knapp, W., and Pickl, W.F. (1997). T cell stimulation via CD47: agonistic and antagonistic effects of CD47 monoclonal antibody 1/1A4. J Immunol *159*, 5345–5354.

Wagner, N., Löhler, J., Kunkel, E.J., Ley, K., Leung, E., Krissansen, G., Rajewsky, K., and Muller, W. (1996). Critical role for beta7 integrins in formation of the gut-associated lymphoid tissue. Nature *382*, 366–370.

Wang, H., VerHalen, J., Madariaga, M., Xiang, S., Wang, S., Lan, P., Oldenborg, P., Sykes, M., and Yang, Y. (2007). Attenuation of phagocytosis of xenogeneic cells by manipulating CD47. Blood *109*, 836–842.

Wang, S., Villablanca, E.J., De Calisto, J., Gomes, D.C.O., Nguyen, D.D., Mizoguchi, E., Kagan, J.C., Reinecker, H.-C., Hacohen, N., Nagler, C., et al. (2011). MyD88-dependent TLR1/2 signals educate dendritic cells with gut-specific imprinting properties. The Journal of Immunology *187*, 141–150.

Waskow, C., Liu, K., Darrasse-Jeze, G., Guermonprez, P., Ginhoux, F., Merad, M., Shengelia, T., Yao, K., and Nussenzweig, M. (2008). The receptor tyrosine kinase Flt3 is

required for dendritic cell development in peripheral lymphoid tissues. Nat Immunol *9*, 676–683.

Watanabe, N., Wang, Y.H., Lee, H.K., Ito, T., and Wang, Y.H. (2005). Hassall's corpuscles instruct dendritic cells to induce CD4+ CD25+ regulatory T cells in human thymus. Nature. *436,* 1181-1185.

Weber, B., Saurer, L., Schenk, M., Dickgreber, N., and Mueller, C. (2011). CX3CR1 defines functionally distinct intestinal mononuclear phagocyte subsets which maintain their respective functions during homeostatic and inflammatory conditions. Eur J Immunol *41*, 773–779.

Wehkamp, J., Salzman, N.H., Porter, E., Nuding, S., Weichenthal, M., Petras, R.E., Shen, B., Schaeffeler, E., Schwab, M., Linzmeier, R., et al. (2005). Reduced Paneth cell alpha-defensins in ileal Crohn's disease. Proceedings of the National Academy of Sciences of the United States of America *102*, 18129–18134.

Wehner, S., Behrendt, F.F., Lyutenski, B.N., and Lysson, M. (2007). Inhibition of macrophage function prevents intestinal inflammation and postoperative ileus in rodents. Gut. *56,* 176-185.

Weiss, J.M., Bilate, A.M., Gobert, M., and Ding, Y. (2012). Neuropilin 1 is expressed on thymus-derived natural regulatory T cells, but not mucosa-generated induced Foxp3+ T reg cells. J Exp Med. *209,* 1723-1742.

Welty, N.E., Staley, C., Ghilardi, N., Sadowsky, M.J., Igyártó, B.Z., and Kaplan, D.H. (2013). Intestinal lamina propria dendritic cells maintain T cell homeostasis but do not affect commensalism. Journal of Experimental Medicine *210*, 2011–2024.

Weng, Y., Sun, J., Wu, Q., and Pan, J. (2007). Regulatory effects of vasoactive intestinal peptide on the migration of mature dendritic cells. Journal of Neuroimmunology. *182,* 48-54.

Westlund, J., Livingston, M., Fahlén-Yrlid, L., Oldenborg, P.-A., and Yrlid, U. (2011). CD47-deficient mice have decreased production of intestinal IgA following oral immunization but a maintained capacity to induce oral tolerance. Immunology. *135,* 236-244.

Wilson, N.S., Young, L.J., Kupresanin, F., Naik, S.H., Vremec, D., Heath, W.R., Akira, S., Shortman, K., Boyle, J., Maraskovsky, E., et al. (2008). Normal proportion and expression of maturation markers in migratory dendritic cells in the absence of germs or Toll-like receptor signaling. Immunol. Cell Biol. *86*, 200–205.

Witmer-Pack, M.D., Hughes, D.A., Schuler, G., Lawson, L., McWilliam, A., Inaba, K., Steinman, R.M., and Gordon, S. (1993). Identification of macrophages and dendritic cells in the osteopetrotic (op/op) mouse. Journal of Cell Science *104 (Pt 4)*, 1021–1029.

Worbs, T., Bode, U., Yan, S., Hoffmann, M.W., Hintzen, G., Bernhardt, G., Förster, R., and Pabst, O. (2006). Oral tolerance originates in the intestinal immune system and relies on antigen carriage by dendritic cells. J Exp Med *203*, 519–527.

Worthington, J.J., Czajkowska, B.I., Melton, A.C., and Travis, M.A. (2011). Intestinal dendritic cells specialize to activate transforming growth factor-β and induce Foxp3+ regulatory T cells via integrin αvβ8. Gastroenterology *141*, 1802–1812.

Wu, L., D'Amico, A., Hochrein, H., O'Keeffe, M., Shortman, K., and Lucas, K. (2001). Development of thymic and splenic dendritic cell populations from different hemopoietic precursors. Blood *98*, 3376–3382.

Wu, L., D'Amico, A., Winkel, K.D., Suter, M., Lo, D., and Shortman, K. (1998). RelB is essential for the development of myeloid-related CD8alpha- dendritic cells but not of lymphoid-related CD8alpha+ dendritic cells. Immunity *9*, 839–847.

Xavier, R.J., and Podolsky, D.K. (2007). Unravelling the pathogenesis of inflammatory bowel disease. Nature *448*, 427–434.

Yadav, M., Louvet, C., Davini, D., Gardner, J.M., Martinez-Llordella, M., Bailey-Bucktrout, S., Anthony, B.A., Sverdrup, F.M., Head, R., Kuster, D.J., et al. (2012). Neuropilin-1 distinguishes natural and inducible regulatory T cells among regulatory T cell subsets in vivo. Journal of Experimental Medicine *209*, 1713–22–S1–19.

Yamao, T., Matozaki, T., Amano, K., Matsuda, Y., Takahashi, N., Ochi, F., Fujioka, Y., and Kasuga, M. (1997). Mouse and human SHPS-1: molecular cloning of cDNAs and chromosomal localization of genes. Biochem Biophys Res Commun *231*, 61–67.

Yanagihara, S., Komura, E., Nagafune, J., Watarai, H., and Yamaguchi, Y. (1998). EBI1/CCR7 is a new member of dendritic cell chemokine receptor that is up-regulated upon maturation. J Immunol *161*, 3096–3102.

Yang, X.O., Chang, S.H., Park, H., Nurieva, R., Shah, B., Acero, L., Wang, Y.H., Schluns, K.S., Broaddus, R.R., Zhu, Z., et al. (2008). Regulation of inflammatory responses by IL-17F. Journal of Experimental Medicine *205*, 1063–1075.

Yokota, A., Takeuchi, H., Maeda, N., Ohoka, Y., Kato, C., Song, S.-Y., and Iwata, M. (2009). GM-CSF and IL-4 synergistically trigger dendritic cells to acquire retinoic acid-producing capacity. Int. Immunol. *21*, 361–377.

Yona, S., Kim, K.-W., Wolf, Y., Mildner, A., Varol, D., Breker, M., Strauss-Ayali, D., Viukov, S., Guilliams, M., Misharin, A., et al. (2013). Fate mapping reveals origins and dynamics of monocytes and tissue macrophages under homeostasis. Immunity *38*, 79–91.

Yoshida, H., Hayashi, S., Kunisada, T., Ogawa, M., Nishikawa, S., Okamura, H., Sudo, T., Shultz, L.D., and Nishikawa, S. (1990). The murine mutation osteopetrosis is in the coding region of the macrophage colony stimulating factor gene. Nature *345*, 442–444.

You, Q., Cheng, L., Kedl, R.M., and Ju, C. (2008). Mechanism of T cell tolerance induction by murine hepatic Kupffer cells. Hepatology *48*, 978–990.

Yrlid, U., Cerovic, V., Milling, S., Jenkins, C.D., Klavinskis, L.S., and MacPherson, G.G. (2006a). A distinct subset of intestinal dendritic cells responds selectively to oral TLR7/8 stimulation. Eur J Immunol *36*, 2639–2648.

Yrlid, U., Milling, S.W.F., Miller, J.L., Cartland, S., Jenkins, C.D., and MacPherson, G.G. (2006b). Regulation of Intestinal Dendritic Cell Migration and Activation by Plasmacytoid Dendritic Cells, TNF-α and Type 1 IFNs after Feeding a TLR7/8 Ligand. *176,* 5205-5212.

Zaph, C., Troy, A.E., Taylor, B.C., Berman-Booty, L.D., Guild, K.J., Du, Y., Yost, E.A., Gruber, A.D., May, M.J., Greten, F.R., et al. (2007). Epithelial-cell-intrinsic IKK-beta expression regulates intestinal immune homeostasis. Nature *446*, 552–556.

Zelenay, S., Keller, A.M., Whitney, P.G., Schraml, B.U., Deddouche, S., Rogers, N.C., Schulz, O., Sancho, D., and Reis E Sousa, C. (2012). The dendritic cell receptor DNGR-1 controls endocytic handling of necrotic cell antigens to favor cross-priming of CTLs in virus-infected mice. J Clin Invest *122*, 1615–1627.

Zeng, R., Oderup, C., Yuan, R., Lee, M., Habtezion, A., Hadeiba, H., and Butcher, E.C. (2013). Retinoic acid regulates the development of a gut-homing precursor for intestinal

dendritic cells. Mucosal Immunology. *6,* 847-856.

Zeuthen, L.H., Fink, L.N., and Frokiaer, H. (2008). Epithelial cells prime the immune response to an array of gut-derived commensals towards a tolerogenic phenotype through distinct actions of thymic stromal lymphopoietin and transforming growth factor-beta. Immunology *123*, 197–208.

Zhan, Y., Carrington, E.M., van Nieuwenhuijze, A., Bedoui, S., Seah, S., Xu, Y., Wang, N., Mintern, J.D., Villadangos, J.A., Wicks, I.P., et al. (2011). GM-CSF increases cross-presentation and CD103 expression by mouse $CD8^+$ spleen dendritic cells. Eur J Immunol *41*, 2585–2595.

Zhang, D.H., Cohn, L., Ray, P., Bottomly, K., and Ray, A. (1997). Transcription factor GATA-3 is differentially expressed in murine Th1 and Th2 cells and controls Th2-specific expression of the interleukin-5 gene. J Biol Chem *272*, 21597–21603.

Zheng, W., and Flavell, R.A. (1997). The transcription factor GATA-3 is necessary and sufficient for Th2 cytokine gene expression in CD4 T cells. Cell *89*, 587–596.

Zheng, Y., Valdez, P.A., Danilenko, D.M., Hu, Y., Sa, S.M., Gong, Q., Abbas, A.R., Modrusan, Z., Ghilardi, N., de Sauvage, F.J., et al. (2008). Interleukin-22 mediates early host defense against attaching and effacing bacterial pathogens. Nat Med *14*, 282–289.

Zheng, Y., Chaudhry, A., Kas, A., deRoos, P., Kim, J.M., Chu, T.-T., Corcoran, L., Treuting, P., Klein, U., and Rudensky, A.Y. (2009). Regulatory T-cell suppressor program co-opts transcription factor IRF4 to control T(H)2 responses. Nature *458*, 351–356.

Zhou, L., Nazarian, A.A., and Smale, S.T. (2004). Interleukin-10 inhibits interleukin-12 p40 gene transcription by targeting a late event in the activation pathway. Mol Cell Biol *24*, 2385–2396.

Zigmond, E., Varol, C., Farache, J., Elmaliah, E., Satpathy, A.T., Friedlander, G., Mack, M., Shpigel, N., Boneca, I.G., Murphy, K.M., et al. (2012). Ly6C(hi) Monocytes in the Inflamed Colon Give Rise to Proinflammatory Effector Cells and Migratory Antigen-Presenting Cells. Immunity *37*, 1076–1090.